Ceramic and mixed construction and demolition wastes (CDW): A technically viable and environmentally friendly source of coarse aggregates for the concrete manufacture

Residuos de la construcción y demolición (RCD) cerámicos y mixtos: Una fuente de áridos gruesos técnicamente viable y medioambientalmente respetuosa para la producción de hormigón

Keramisch en gemengd bouw- en sloopafval: Een technisch haalbare en milieuvriendelijke bron van grove granulaten voor betonproductie

Desirée Rodríguez Robles

Andrés Juan Valdés
Julia Mª Morán del Pozo

Nele De Belie

Ceramic and mixed construction and demolition wastes (CDW)

A technically viable and environmentally friendly source of coarse aggregates for the concrete manufacture

Desirée Rodríguez Robles

Marzo 2016

Andrés Juan Valdés (Universidad de León)
Julia Mª Morán del Pozo (Universidad de León)
Nele De Belie (Ghent University)

UNIVERSITEIT GENT

Acknowledgements
Agradecimientos

Me gustaría agradecer en estas líneas a todas aquellas personas que, de alguna forma, me han ayudado durante la realización de la presente tesis doctoral.

En primer lugar me gustaría agradecer a Andrés Juan Valdés y Julia Mª Morán del Pozo, mis directores de tesis en la Universidad de León, por toda la confianza que siempre han depositado en mí y por su inestimable ayuda y consejos. I would also like to express my sincere gratitude to my Belgian co-supervisor, Prof. Nele De Belie, for offering me the opportunity to stay at the Magnel Laboratoy for Concrete Research during 6 months and all her help through the joint PhD between the Ghent University and the University of León.

También me gustaría agradecer al Ministerio de Educación por la financiación en concepto de beca predoctoral de Formación al Profesorado Universitario (FPU AP2010-0613) que ha hecho posible el desarrollo de esta tesis.

A Eloína Panero Pérez y al Departamento de Ingeniería y Ciencias Agrarias por facilitar en todo lo posible la consecución del doctorado conjunto. Besides, I would like to acknowledge all the help received by the administrative staff (Christel Malfait, Marijke Reunes and Viviane Van Gaver) and technical staff (Nicolas Coppieters, Stefan De Bock, Sandra De Buck, Tommy De Ghein, Bart De Waele, Dieter Hillewaere, Peter Lampaert, Nathan Lampens, Jan Lesage, Marc Scheerlinck, and Tom Stulemeijer) at the Magnel Laboratory.

A María Isabel Sánchez de Rojas, Moisés Frías Rojas y Eloy Asensio de Lucas por abrirme las puertas al Instituto de Ciencias de la Construcción Eduardo Torroja y su ayuda con los ensayos microestructurales.

A mis compañeros de la Universidad de León (Julia, Sara, Álvaro, Óscar y Paulo) por compartir el día a día de la elaboración de nuestras tesis. Thanks should be also extended to the whole Concrete & Environment group (Mathias Maes, Didier Snoeck Hugo Egüez, Arn Mignon, João Feiteira, Yusuf Cagatay Ersan, Adelalide Gomes De Araújo, Romy Suryaningrat Edwin, Ali Behnood, Benoît Hilloulin, Bjorn Van Belleghem, Elke Gruyaert, Kim Van Tittelboom, Jianyun Wang, Mieke De Schepper, Philip Van den Heede and Yury Villagrán) and the rest of colleagues at the Magnel Laboratory, especially to Florent Forest and Lijie Wang. I am grateful for all the help and good times in Ghent. Thank you all for making my stay in Belgium unforgettable.

Finalmente, pero no por ello menos importante, me gustaría agradecer a mi familia, amigos y, en especial, a Jorge por la comprensión y apoyo brindados.

Summary

The role of industry in the growth of modern society and economy is indisputable, as is its contribution to the degradation of the environment. Amongst its negative impacts, land depletion and deterioration, energy consumption, solid waste generation, dust and gas emission, noise pollution, and consumption of non-renewable natural resources could be cited. Experts consider the overconsumption of resources and the elevated generation of wastes as two of the most important environmental challenges of the 21st century. In this regard, just in the in the European Union, yearly around 1.15 billion tonnes of aggregates directly extracted from the earth lithosphere are employed as raw materials in the concrete production and approximately 821 million tonnes of construction and demolition wastes (CDW) were produced in 2012, which accounts for one third of the total waste generation.

Traditionally, natural resources and wastes are found, respectively, at the start and ending point of the linear model of production. However, the growing social concern about the protection and conservation of the environment is shifting the take-use-dispose attitude towards a circular economy model that promotes the exploitation of wastes as secondary resources. Due to the large quantities of concrete consumed annually, around 1 tonne per inhabitant and year, concrete is the most employed material worldwide, and therefore the perfect receptor of large quantities of residual products as recycled aggregates which concurrently solves the waste generation problem and reduces the consumption of natural resources, which alleviates the pressure on the carrying capacity of the environment and contribute to a more sustainable future by closing the concrete production loop.

Over the last years, the recycling potential of CDW as total or partial replacement of the natural coarse aggregates has become an important target of interest among scientist. However, the majority of the research works carried out have been focused on the use of aggregates recovered from concrete rubble. Nevertheless, the typical building and demolition practice, as well as the waste management systems, employed in Mediterranean countries such as Spain, result in CDW of mixed nature with average ceramic contents of 54%. Thus, mixed and ceramic recycled aggregates represent 70% of the total recycled aggregates produced in the waste management plants. The aforementioned figures convey the importance of the treatment and recycling of this kind of waste beyond low level applications such as unbound materials in earthworks, backfilling and road constructions, which constitutes a down-cycling of the material.

The general objective of the present thesis is twofold; first, the analysis of the engineering properties of the commercially available recycled aggregates from CDW with varying percentages of ceramic waste and, secondly, the assessment of recycled concrete mixtures made with a partial substitution (50%) of the natural coarse aggregates by the aforementioned recycled aggregates when compared with a conventional concrete mixture used as a reference.

Materials and methods

For all the concrete mixtures, regular tap water was employed and CEM III/A 42.5 N SR and CEM III/B 42.5 N SR LH LA were used in the first and second phase respectively. Regarding the natural aggregates, both river sand and gravel were of siliceous nature, and the recycled aggregates, which were collected from Spain and Belgium, presented different proportions (low, medium and high) of the ceramic materials. A 50% replacement in weight of the natural coarse aggregate was selected for the design of the concretes with 25 MPa target strength at 28 days according to De la Peña method and the Fuller parabola. The experimental program was based on fixing both the cement content (390.91 Kg/m^3) and the total water/cement ratio (0.55) to be used as comparison parameters among concrete mixtures.

Despite the lack of standardization for the mixed and ceramic recycled aggregates in the manufacture in Spain, the recycled materials were analysed according to the requirements set in the Spanish Code on structural concrete (EHE-08) in order justify the feasibility of this type of recycled aggregates from CDW in concrete applications. Thus, the testing program was comprised of a physical and mechanical characterization (constituents, particle size distribution, geometry, fines assessment, density and water absorption, mechanical resistance and adhered mortar). Moreover, a microstructural characterization (X-ray powder diffraction -XRD-, X-ray fluorescence -XRF-, scanning electron microscopy, mercury intrusion porosimetry -MIP-) was performed to achieve a better understanding of the heterogeneity of their origin.

In order to assess the influence of such substitution several concrete mixed were batched conforming to separate research phases. In the first stage of the investigation, the tests performed on a conventional concrete mix and three recycled concrete mixtures made with recycled aggregates collected from Spanish CDW management plants were focused on physical (consistency, air content, bulk density), mechanical (compressive, flexural and splitting-tensile strength tests, the elasticity modulus and the stress-strain behaviour) and microstructural (morphology of the interfacial transition zone (ITZ) and porosity) properties of the fresh and hardened concrete, although some durability properties were analysed in accordance to the equipment possibilities. In addition, an environmental performance analysis of those concrete mixtures was carried out by means of a life cycle assessment (LCA). The second research phase included a mixed recycled aggregate collected from a Belgian CDW management plant, and consequently a fourth recycled concrete sample. Furthermore, the number of characterization assays was expanded by including calorimetric and ultrasonic wave transmission tests on fresh concrete, long-term performance of the hardened concrete and the study of several durability indicators (gas permeability, carbonation, water absorption by capillarity and under vacuum, water penetration under pressure, frost resistance, chloride ingress, electrical resistivity, alkali-silica reaction and resistance to organic acids).

Characterization of the recycled aggregates

The characteristics of the aggregates used in the manufacture of concrete largely determine the properties of the final product.

As the aim of this research work is to characterize the suitability of mixed recycled aggregates with significant contents of ceramic in the concrete manufacture, the limits in the standards regarding ceramic materials were ignored, and the applied aggregates had a ceramics content of 34% and 38% (low), 66% (medium) and 100% (high). In any case, the requirements regarding the presence of impurities were generally complied, except for the sample with low ceramic from the TEC-REC management plant, which suggests some failure in the separation procedure. At particle size level, the D/d ratio is greater than the limit stipulated of 1.40 for all samples. Although comparatively higher than the flakiness index of conventional coarse aggregates, all recycled aggregates comply with the 35% limit established in the EHE-08. In terms of quantity of fines (<0.063 mm), the limit for coarse aggregates is up to 1.50%, value not exceed by any of the recycled aggregates. However, special attention should be paid to mixing time to avoid an excessive production of fines due to the friability of the ceramic materials, as well as the significant amounts of attached mortar that were identified. Higher absorption coefficients were observed with the increase in the percentage of masonry that prevented the compliance of the 7% limit in the Spanish specification, but would be within the allowable intervals in other international legislations such as DIN 4226-100 (2002) and the RILEM recommendation. Finally, the Los Angeles performance requirements were satisfied by all the recycled aggregates, despite that the sample from the TEC-REC plant would only be apt for concrete with target strength up to 30 MPa, in part due to the faulty cleaning procedure.

The XRF tests found a majority chemical composition of silicon oxide (SiO_2), aluminium oxide (Al_2O_3) and calcium oxide (CaO), followed by high loss on ignition (LOI) values. As both aluminium and silicon oxides are typical components of brick and tiles, their content in the sample directly alluded to the ceramic content, while the CaO percentage refers to the presence of both adhered mortar and old concrete particles. Hence, the results easily distinguished between mixed and pure recycled aggregates. Based on these results it was possible to conclude that the use of the recycled materials entails an additional risk for alkali-silica reactions (ASR), as the alkali content was 23-34 and 3-6 times higher than the gravel and the cement respectively. However, recycled aggregates did not present problems to comply with the sulphates or chlorides constraints imposed by the EHE-08, when indirectly assessed by the XRF tests. Complementary, the results of the XRD tests showed quartz and calcite as the main minerals for mixed recycled aggregates, while quartz was the main phase of the ceramic aggregate, since a lower presence of adhered mortar was observed in this sample. Mineralogical compounds such as anorthite, dolomite, hematite, orthoclase, muscovite or illite, associated with the presence of ceramic materials, were also identified in significant amounts in all recycled aggregates. Finally, the determination of the total porosity by MIP showed increasing figures for rising ceramic incorporations with average values 23 times higher than that of the gravel. Nonetheless, recycled aggregates displayed higher levels of ink-bottle porosity, which is indicative of an elevated non-accessible porosity, and a high amount of pores lower than 0.10 μm, which also is indicative of a finer microstructure.

Fresh properties

Since no correction on the amount of water was carried out to the original proportioning method, a reduction of slump ensued due to water absorption presented by the recycled aggregates. Anyhow, no problems in workability were detected when casting or compacting the test specimens.

The results showed that recycled concrete presented air content values between 40% and 80% higher than the conventional concrete due to presence of more porous aggregates and the influence that their grading and shape have on the percentage of air entrapped in concrete. In addition, the fresh density of recycled concrete mixes was also lower than the conventional concrete (1.62%-5.41%).

The differences between the semi-adiabatic temperature curves revealed that the use of recycled aggregates containing varying percentages of ceramic waste resulted in lower initial temperature values (9%-17%) and higher temperature values at the end of the experiment (1%-4%). Hence, the heat production growth was between 5% and 15% higher than that of the conventional concrete and the peak occurrence in the heat production rate curve was both advanced to a maximum 3% and delayed up to 8% compared to conventional concrete. Regarding to the setting time, both determined by calorimetric and ultrasonic methods, the use of recycled aggregates was responsible for a significant delay in the hardening of concrete. In any case, problems were not identified in the demoulding of specimens after 24 hours.

Microstructure

The morphological study suggested a similar microstructure between conventional and recycled concretes. In the recycled mixtures, the interfaces were fairly dense and continuous due to the lower effective water/cement ratio, the internal curing effect produced as the recycled aggregates return part of the water absorbed to the cement matrix, the use of a blended slag cement and the additional pozzolanic activity of the recycled aggregates. In addition, it was observed that ceramic aggregates without adhered mortar exhibited a denser ITZ bonding. Moreover, the chemical composition of the cement paste was found to be similar, i.e. calcium and silicon as major elements, magnesium and aluminium as consequence of the slag particles and sulphur coming from the hydration retardant agent in the cement and the Ca/Si ratio was is in the range for normal concretes.

The MIP values showed that the rising ceramic content in the recycled concrete entailed an increase in the total porosity for 28 days of curing, However, after the refinement of the porous network of concrete with time, which was greater for recycled concretes with lower ceramic contents, the results suggested an inverse relationship between the total porosity of the recycled concretes and the percentage of ceramic waste included as aggregate after 56 days of curing. Therefore, the recycled concretes acquired a significant decrease in porosity, up to a 41% for I-RC-L(S), 26% for I-RC-M(S) and 31% for I-RC-H(S).

Analogously to the results of air content for the fresh mixtures, all recycled concrete mixtures presented higher air content values than the conventional concrete. However, none of the concrete mixtures complied with the recommendations for frost-resistant concrete regarding to air content, specific surface or spacing factor, but the use of air entrainment agents would significantly improve this property.

Mechanical behaviour

It is widely recognized that the density of concrete is mainly influenced by the density of the aggregates employed. Thus, recycled concrete mixtures displayed density reductions ranging from 2.06% to 7.52%. It was observed that the conventional and recycled mixtures exhibited compressive strengths over 25 MPa targeted in the mixture dosage and would be expected to continue to rise with age due to cement hydration.

Compared to the conventional concrete, the maximum reduction in the compression strength at 28 days is around 11%, while the differences are lower for 91 curing days. Increasing ceramic content did not proportionally decrease the compressive resistance of concrete. In general, recycled concrete mixtures suffered a decrease in the flexural strength between 8% and 22%. Similarly, the splitting tensile strength was reduced by 1% to 13%. Notwithstanding the observed declines, the use of recycled aggregates from CDW did not pose a problem in the mechanical performance of concrete. Several factors were identified behind the good performance results: the decrease of the aggregate/cement ratio with rising ceramic ratios, the use of recycled aggregates in in air-dried condition that reduced the effective water/cement ratio, the mixture procedure, the use of slag blended cement, the pozzolanic activity of the CDW fines, the superficial roughness of the recycled aggregates and their ability to return the water absorbed during the mixing to produce an internal curing effect enhancing the ITZ bond.

Regarding the toughness performance of the material, maximum 8% declines in the elastic modulus were observed compared to the conventional concrete when mixed or ceramic recycled aggregates were applied The study of the stress-strain curves suggested a similar behaviour in the first part of the curve regardless of the ceramic content incorporated, whereas the parabolic stage presented noticeable differences. While the recycled mixtures with low ceramic content exhibited lower deformations than the conventional concrete, the recycled mixtures with medium and high ceramic contents displayed higher deformations than their respective reference mixtures.

For long-term deformations, both conventional and recycled mixtures presented a parallel shrinkage and creep behaviour as a hyperbolic curve that tends to an asymptotic value. Due to the lower restraining properties of the recycled aggregates, the total shrinkage and creep strains experienced by recycled concretes were greater than those of the conventional concrete. While rising ceramic contents were not linked to higher shrinkage strains, it became apparent that the use of increasing amounts of ceramic aggregates had a beneficial influence in the creep behaviour among the recycled concretes.

Durability performance

The transport properties of concrete were evaluated to assess the durability behaviour of the recycled concrete mixtures compared to the conventional concrete. In term of gas permeability, recycled concretes exhibited both lower and higher values than the reference mixture with the porosity values being the main controlling factor instead of the ceramic content. However, the results obtained for all concrete mixtures suggested a good performance regarding this property. For the analysis of the penetration of CO_2 of concrete exposed to a natural outdoor experiment, recycled concrete exhibited a worse behaviour (around 70-75%) after 1 year of exposure, strongly associated to the increase in the pore sizes higher than 0.067 μm. When the recycled concrete samples were tested in a 10% CO_2 artificial environment, an average decline of 30% in the penetration depth was observed for 1 month of exposure that progressively transformed in higher penetration values (up to 5% higher than the reference) after 3 months of exposure. Both the lower water/cement ratio and the higher alkalinity of recycled mixtures hinder the early penetration but the higher porosity leads to worse performances in long instances.

The water absorption of concrete was performed by means of several tests. Recycled concretes presented lower capillary absorption as consequence of a lower effective water/cement ratio that entailed an improvement in the quality of the cement paste. Moreover, the comparison among the recycled mixtures showed better durability for increasing ceramic incorporations, partly due to a higher pozzolanic activity, with primary sorptivity values between 22% and 63% lower than that of the conventional concrete. Similarly, the water penetration depth under pressure declined for rising amounts of ceramic aggregates, with 2% to 32% and 1% to 56% in phase I and II, respectively. Therefore, according to the requirements laid down in EHE-08, sufficient impermeability was ensured for reinforced concrete in environmental classes IIIa, IIIb, IV, Qa, E, H, F and Qb. Contrarily, the results of water absorption under vacuum showed increases in the accessible capillary porosity between 10% and 40%, values which were strongly influenced by the ceramic content, which indicated a worse performance of the recycled concretes with respect to the conventional mixture.

The deterioration of concrete due to freeze-thaw cycles in presence of de-icing salts showed that recycled concretes presented a worse performance than the conventional concrete. Nonetheless, the ultrasonic pulse velocity (UPV) results at the end of the test in phase I were indicative of a good quality concrete. In phase II, it became apparent that trowelled surfaces were more susceptible to the frost-salt action and mass loses between 2.71% and 26.12% were observed without correlation with the ceramic content. Nevertheless, it is worth remarking that no air entrainment agent was employed in this research work and that the use of such admixture would considerably improve the frost resistance of all concrete mixtures.

Regarding the chloride penetration, the electrical migration test indicated that the non-steady state migration coefficient of the recycled mixtures was between 17% and 42% higher than that of the conventional concrete for increasing ceramic contents, which also suggested a moderate resistance against the penetration of chlorides. Both the lower water/cement ratio and the pozzolanic activity of the slag blended cement and the CDW were identified as beneficial for this property.

The electrical resistivity results for the recycled mixtures are within the range of values (10-100 Ω·m) commonly reported conventional concrete. Whereas mixed recycled aggregates exhibited an electrical resistivity comparable to that of a conventional mixture, the recycled concrete made with ceramic aggregates displayed a 6.68% lower value as consequence of a higher release of ions to the pore solution.

Despite the higher ASR risk, none of the recycled aggregates caused a length variation higher than 0.10% after 20 days of the Oberholster testing and therefore were deemed as non-reactive. Nonetheless, it should be noted that these results occurred under the specific conditions favoured by the use of slag blended cements, which are responsible for reducing the ASR risk.

Finally, the concrete mixtures were exposed to a simulated farm environment by means of a lactic-acetic acid solution. While the maximum reduction in radius of the cylindrical specimens was lower than 2 mm for the conventional concrete at the end of the test, none of the recycled mixtures presented a decline in radius higher than 1 mm. Similarly, the surface roughness of recycled concrete was between 40% and 74% smoother for rising ceramic content. The improved performance of concrete against acidic attacks was explained by the beneficial effect of pozzolanic materials, the presence of secondary elements in the cement matrix, the lower effective cement/ratio as well as the refinement in the porous network that use of recycled aggregates causes.

Environmental performance

The environmental credit due to the decrease in the demand for natural resources and the avoidance of CDW landfilling are the basis of the environmental benefits associated to the production of recycled concrete made with 50% secondary aggregates from CDW. The main advantages were found in the reduction of the ozone depletion potential and the abiotic resource depletion for the CML 2001 assessment and the decrease in the damage to mineral and fossil resources for the Eco-indicator 99 evaluation. Despite these benefits, when Eco-indicator 99 is employed, recycled concrete presented a worse environmental performance in terms of damage to the human health than the conventional mixture.

In conclusion, this research demonstrated that untreated recycled aggregates from CDW with varying ceramic contents present acceptable physical and mechanical properties according to the current Spanish standard. Despite that recycled aggregates present a low quality when compared to natural aggregates, the differential performance level shall not definitively exclude the use of these materials since their use as a blend with virgin materials could meet the more strict requirements resulting for high level applications such as the concrete manufacture. For instance, a 50% blend of natural gravel and the coarse fraction of mixed and ceramic recycled aggregates led to recycled concretes with good physical, mechanical and durability properties and were furthermore environmentally responsible.

Samenvatting

De rol van de industrie voor de groei van de moderne samenleving en economie staat buiten kijf, zowel als haar bijdrage aan de degradatie van onze leefomgeving. Als negatieve impact kunnen onderscheiden worden: landverbruik, energieverbruik, afvalproductie, stof en gasemissies, lawaaihinder en consumptie van niet-hernieuwbare grondstoffen. Experten beschouwen de overconsumptie van grondstoffen en de toenemende productie van afval als de twee belangrijkste uitdagingen voor het leefmilieu in de 21ste eeuw. Aansluitend hierbij, kan vermeld worden dat enkel in de Europese unie jaarlijks ongeveer 1,15 miljard ton granulaten direct onttrokken worden aan de lithosfeer voor gebruik als basismaterialen voor betonproductie. Ongeveer 821 miljoen ton bouw- en sloopafval werd geproduceerd in 2012, wat overeenkomt met een derde van de totale afvalproductie.

Traditioneel bevinden natuurlijke grondstoffen en afval zich respectievelijk aan start- en eindpunt van een lineair productiemodel. Het groeiende sociaal besef in verband met bescherming en behoud van het leefmilieu doet echter de "neem-gebruik-werp weg" attitude wijzigen in de richting van een circulaire economie, die de exploitatie van afval als secundaire grondstof promoot. Door de grote hoeveelheden beton die jaarlijks verbruikt worden, ongeveer 1 ton per inwoner per jaar (beton is het meest gebruikte materiaal wereldwijd), is beton het ideale materiaal om grote hoeveelheden gerecycleerde granulaten in te verwerken. Dit kan helpen om het afvalprobleem op te lossen en de consumptie van natuurlijke grondstoffen te verminderen, wat de druk op de draagcapaciteit van het milieu vermindert en bijdraagt tot een meer duurzame toekomst door sluiting van de betonkringloop.

In de afgelopen jaren is het recyclagepotentieel van bouw- en sloopafval als gehele of gedeeltelijke vervanging van de natuurlijke grove granulaten een belangrijk onderzoeksonderwerp geworden. De meeste onderzoeksprojecten hebben zich hierbij gericht op granulaten herwonnen uit betonpuin. Nochtans leiden de typische bouw- en slooppraktijken, zowel als de afvalverwerkingssystemen, in de mediterrane landen zoals Spanje tot gemengd bouw- en sloopafval, met een gemiddeld gehalte aan keramische materialen van 54%. Zodoende maken gemende en keramische gerecycleerde granulaten 70% uit van het geheel aan gerecycleerde granulaten geproduceerd. Dit geeft aan dat de behandeling en recyclage van dit type afval van belang is, en dit niet enkel in laagwaardige toepassingen zoals ongebonden materialen voor grondwerken, opvullingen en wegconstructies, wat een "down-cycling" van het materiaal inhoudt.

De doelstellingen van de deze thesis zijn tweevoudig: vooreerst de analyse van de ingenieurseigenschappen van de commercieel beschikbare gerecycleerde granulaten uit bouw- en sloopafval; ten tweede, de beoordeling van gerecycleerd beton met een partiële vervanging (50%) van de natuurlijke grove granulaten door de hogergenoemde gerecycleerde granulaten, vergeleken met een conventioneel referentiebeton.

Materialen en methoden

Voor alle betonmengsels werd leidingwater gebruikt en de cementen CEM III/A 42.5 N SR en CEM III/B 42.5 N SR LH LA in respectievelijk de eerste en tweede fase van het onderzoek. Als natuurlijke granulaten werden silicieus rivierzand en grind gebruikt. De gerecycleerde granulaten, die verzameld werden in Spanje en België, bevatten verschillende proporties keramische materialen (laag, medium of hoog). De natuurlijke granulaten werden voor 50% op gewichtsbasis vervangen door de gerecycleerde granulaten, voor het ontwerp van beton met 25 MPa ontwerpsterkte op 28 dagen, volgens de methode van De la Peña en de Fuller parabool. In het experimentele programma werden het cementgehalte (390,91 kg/m^3) en de totale water/cement-verhouding (0,55) constant gehouden.

Ondanks het gebrek aan standaardisering voor gemengde en keramische gerecycleerde granulaten in Spanje, werden de gerecycleerde materialen geanalyseerd volgens de eisen van de Spaanse code voor structureel beton (EHE-08) om de haalbaarheid van het gebruik van dit type granulaten voor betontoepassingen aan te tonen. Het testprogramma bestond uit een fysische en mechanische karakterisering (bestanddelen, korrelverdeling, geometrie, gehalte aan fijnen, dichtheid, waterabsorptie, mechanische weerstand, gebonden mortel). Bovendien werd een microstructurele karakterisering uitgevoerd om hun heterogeniteit beter te begrijpen (X-straal diffractie (XRD), X-straal fluorescentie (XRF), rasterelektronenmicroscopie (SEM), kwikporosimetrie (MIP)).

Om het effect van een dergelijke substitutie te onderzoeken, werden verschillende betonmengsels vervaardigd in de opeenvolgende onderzoeksfasen. In de eerste fase werden de inspanningen geconcentreerd op een conventioneel betonmengsel en drie mengsels met gerecycleerde granulaten van Spaanse fabrieken voor verwerking van bouw- en sloopafval. Hierbij werden de fysische (consistentie, luchtgehalte, dichtheid), mechanische (druksterkte, buig- en splijttreksterkte, elasticiteitsmodulus en het krachtvervormingsverband) en microstructurele eigenschappen (morfologie van de transitiezone en porositeit) van het verse en verharde beton onderzocht. Ook werden enkele duurzaamheidseigenschappen geanalyseerd met de voorhanden zijnde apparatuur. Bovendien werd een milieu-impact analyse uitgevoerd van deze mengsels met behulp van een levenscyclusanalyse (LCA). In de tweede fase van het onderzoek werd daarenboven een gemengd gerecycleerd granulaat van een Belgisch bedrijf meegenomen, en dus ook een vierde betonsamenstelling onderzocht. Bovendien werden de karakteriseringsproeven uitgebreid met calorimetrie en transmissie van ultrasoongolven voor vers beton, lange-duur performantie van verhard beton, en de studie van verschillende duurzaamheidsparameters (gaspermeabiliteit, carbonatatie, water absorptie door capillariteit en onder vacuüm, waterindringing onder druk, vorstweerstand, chloriden-indringing, elektrische resistiviteit, alkali-silica reactie en weerstand tegen organische zuren).

Karakterisering van de gerecycleerde granulaten

De karakteristieken van de granulaten gebruikt voor de vervaardiging van het beton, bepalen in hoge mate de eigenschappen van het eindproduct.

Omdat de doelstelling is om de geschiktheid van gemengde gerecycleerde granulaten met een significant gehalte aan keramisch materiaal voor gebruik in beton te onderzoeken, werd de limiet in de normen m.b.t. keramische materialen genegeerd, en de keramische gehalten van de gebruikte materialen bedroegen 34% en 38% (laag), 66% (gemiddeld) en 100% (hoog). In elk geval werden de vereisten met betrekking tot de afwezigheid van onzuiverheden over het algemeen vervuld, behalve voor het monster met een laag gehalte aan keramische bestanddelen van de TEC-REC fabriek, wat duidt op gebreken in het afscheidingsproces. Op deeltjesniveau is de D/d verhouding groter dan de grenswaarde van 1,4 voor alle monsters. Alhoewel het schilferig karakter hoger is dan bij conventionele granulaten, vallen alle gerecycleerde granulaten onder de limiet van 35% vermeld in EHE-08. Wat de hoeveelheid fijnen (<0.063 mm) betreft, ligt de grens voor grove granulaten op 1,5%, een grenswaarde die niet overschreden wordt door de gerecycleerde granulaten. Nochtans moet de mengtijd beperkt worden om een buitensporige vorming van fijnen in deze broze keramische materialen en o.w.v. de significante hoeveelheid aanhechtende mortel te vermijden. Er werden hogere absorptiecoëfficiënten opgemeten bij stijgende percentages metselwerk en dit verhinderde een overeenstemming met de 7% grens in de Spaanse specificaties; nochtans zouden de gemeten waarden binnen de intervallen liggen die in andere regelgeving is opgenomen, zoals DIN 4226-100 (2002) en de RILEM aanbeveling. Tenslotte werd de vereiste performantie bereikt in de Los Angeles test door alle gerecycleerde granulaten, onafgezien van het feit dat het monster van de TEC-REC fabriek enkel zou geschikt zijn voor beton met een richtsterkte van 30 MPa, gedeeltelijk door de gebreken in de reinigingsprocedure.

Bij de XRF metingen werd een chemische samenstelling gevonden met overheersende hoeveelheden siliciumdioxide (SiO_2), aluminiumoxide (Al_2O_3) en calciumoxide (CaO), gevolgd door een hoge waarde voor het gloeiverlies (LOI). Vermits aluminium- en siliciumoxide typische componenten zijn van stenen en tegels, was hun aanwezigheid in direct verband te brengen met het gehalte keramisch materiaal, terwijl het CaO gehalte verwees naar de aanwezigheid van aangehechte mortel en oud beton. Daardoor kon gemakkelijk een onderscheid gemaakt worden tussen gemengde en niet gemengde granulaten. Gebaseerd op deze resultaten kon besloten worden dat de gerecycleerde granulaten een bijkomend risico op alkali-silica reacties (ASR) met zich meebrengen, omdat het alkaligehalte 23-24 en 3-6 keer hoger was dan in grind en cement respectievelijk. Anderzijds voldeden de gerecycleerde granulaten zonder probleem aan de beperkingen m.b.t. sulfaten of chloriden opgelegd door de EHE-08, bij indirecte analyse via XRF. Aanvullende metingen via XRD toonden kwarts en calciet als de belangrijkste mineralen bij gemengde gerecycleerde granulaten, terwijl kwarts de belangrijkste fase was van de keramische granulaten omdat deze een lager percentage aanhechtende mortel vertoonden. Mineralogische componenten zoals anortiet, dolomiet, hematiet, orthoklaas, muscoviet, of illiet, geassocieerd met de aanwezigheid van keramische materialen, werden ook gedetecteerd in significante hoeveelheden in alle gerecycleerde granulaten. De totale porositeit bepaald via kwikporosimetrie vertoonde een toename met toenemende hoeveelheden keramische deeltjes, met gemiddelde waarden die 23 keer hoger lagen dan bij natuurlijk grind. Nochtans vertoonden de gerecycleerde granulaten wel een hogere "inktfles" porositeit, die wijst op minder-toegankelijke poriën, en een hoog gehalte aan poriën kleiner dan 0,10 µm, wat ook wijst op een fijnere microstructuur.

Eigenschappen in verse toestand

Omdat er geen correctie van de waterhoeveelheid werd uitgevoerd t.o.v. de originele methode voor mengselontwerp, werd een vermindering van de zetting vastgesteld o.w.v. de waterabsorptie door de gerecycleerde granulaten. Nochtans werden geen problemen met verwerkbaarheid vastgesteld tijdens het gieten en compacteren van de proefstukken.

De resultaten gaven aan dat beton met gerecycleerde granulaten een luchtgehalte vertoonde dat tussen de 40% en 80% hoger was dan bij conventioneel beton door de aanwezigheid van meer poreuze granulaten en het effect van hun korrelverdeling en vorm op de ingesloten lucht in het beton. Bovendien was de dichtheid in verse toestand lager dan bij conventioneel beton (1,62%-5,41%).

De verschillen tussen de temperatuurcurves bij semi-adiabatische calorimetrie onthulden dat het gebruik van gerecycleerde granulaten met variërende hoeveelheden keramisch afval resulteerde in initieel lagere temperaturen (9%-17%), en in hogere temperaturen op het einde van het experiment (1%-4%). De snelheid van warmteproductie was 5 tot 15% lager dan deze van traditioneel beton en de piek in de temperatuurcurve varieerde rond deze van het traditioneel beton (van 3% eerder tot 8% later in de tijd). Wat betreft de bindingstijd, bepaald uit calorimetrische en ultrasone resultaten, zorgden de gerecycleerde granulaten voor een significante vertraging. Nochtans konden de proefstukken wel zonder problemen na 24 u ontkist worden.

Microstructuur

De morfologische studie suggereerde een gelijkaardige microstructuur voor conventioneel beton en beton met gerecycleerde granulaten. In de gerecycleerde mengsels waren de interfasen vrij dicht en continu, door de lagere effectieve water/cement verhouding, de interne nabehandeling doordat de gerecycleerde granulaten een deel van het geabsorbeerde water afgeven aan de cementmatrix, het gebruik van een slakhoudend cement en de bijkomende puzzolane activiteit van de gerecycleerde granulaten. Er werd geobserveerd dat keramische granulaten zonder aanhechtende mortel een dichtere transitiezone vertoonden. Bovendien was de chemische samenstelling van de cementpasta gelijkaardig, d.w.z. met calcium en silicium als belangrijkste elementen, magnesium en aluminium afkomstig van de slakdeeltjes en zwavel afkomstig van de bindingsvertrager in het cement; en de Ca/Si verhouding was in het bereik van deze voor gewoon beton.

De waarden van de kwikporosimetrie toonden dat een toenemend gehalte aan keramische materialen in de gerecycleerde granulaten, leidde tot een toename van de totale porositeit van het beton na 28 dagen nabehandeling. Echter, de verfijning van de poriënstructuur met de tijd, was meer uitgesproken voor beton met gerecycleerde granulaten met een beperkt gehalte aan keramisch materiaal, dan bij conventioneel beton. Daardoor suggereerden de resultaten een inverse relatie tussen de totale porositeit van het gerecycleerde beton en het percentage keramische granulaten na 56 dagen nabehandeling. De gerecycleerde betontypes verwierven een significante daling van de porositeit, met tot 41% voor I-RC-L(S), 26% voor I-RC-M(S) en 31% voor I-RC-H(S).

Analoog aan de resultaten voor het luchtgehalte in het vers beton, hadden alle betonsoorten met gerecycleerde granulaten een hoger luchtgehalte dan het conventioneel beton. Geen enkele van de betonmengsels voldeed echter aan de aanbevelingen voor vorstresistent beton betreffende luchtgehalte, specifieke oppervlakte of afstandsfactor; maar het gebruik van een luchtbelvormer zou deze eigenschappen kunnen verbeteren.

Mechanisch gedrag

Het is algemeen erkend dat de dichtheid van beton sterk beïnvloed wordt door de dichtheid van de granulaten. De betonmengsels met gerecycleerde granulaten vertoonden een vermindering van de dichtheid tussen 2,06 en 7,52%. Zowel de conventionele als gerecycleerde mengsels hadden een druksterkte hoger dan de 25 MPa die vooropgesteld werd bij de dosering; een sterkte die nog verondersteld wordt om toe te nemen met de ouderdom dankzij de voortschrijdende cementhydratatie.

In vergelijking met conventioneel beton was de maximale reductie in sterkte op 28 dagen ongeveer 11%, terwijl het verschil kleiner is na 91 dagen nabehandeling. Een toenemend gehalte keramische granulaten deed de druksterkte van het beton niet proportioneel afnemen. Over het algemeen onderging het gerecycleerd beton een vermindering van de buigtreksterkte met 8 tot 22%. De splijttreksterkte werd gereduceerd met 1 tot 13%. Onafgezien van de geobserveerde dalingen, stelde het gebruik van gerecycleerde granulaten uit bouw- en sloopafval geen probleem voor de mechanische performantie van het beton. Verschillende factoren werden geïdentificeerd als redenen voor deze goede performantie: de afname van de granulaat/cement verhouding met toenemend gehalte keramisch materiaal, het gebruik van gerecycleerde granulaten in de luchtdroge toestand waardoor de effectieve water/cement verhouding afnam, de mengprocedure, het gebruik van cement met hoogovenslak, de puzzolane activiteit van de fijnen, de oppervlakkige ruwheid van de gerecycleerde granulaten en hun mogelijkheid om geabsorbeerd mengwater terug af te geven leidend tot een effect van interne nabehandeling waardoor de binding in de transitiezone verbeterde.

Betreffende de stijfheid van het materiaal, werd een vermindering van maximum 8% van de elasticiteitsmodulus vastgesteld wanneer gemengde of keramische granulaten gebruikt werden. Onderzoek van de spannings-vervormingsdiagrammen leerde dat het eerste deel van de curve gelijkaardig was als bij traditioneel beton, terwijl er opmerkelijke verschillend optraden in het parabolisch deel. Terwijl de mengsels met een laag gehalte aan keramische granulaten een meer beperkte vervorming vertoonden dan het conventioneel beton, gaven de mengsels met een gemiddeld of hoog gehalte aan keramische granulaten hogere vervormingen dan de referentie.

Wat betreft de lange duur vervormingen toonden conventionele en gerecycleerde mengsels een parallel krimp- en kruipgedrag volgens een hyperbolische curve die naar een asymptotische waarde evolueert. De gerecycleerde granulaten hadden een beperkter verhinderend effect op de totale rek veroorzaakt door krimp of kruip, leidend tot hogere waarden voor deze rek. Terwijl de toenemende gehaltes aan keramische materialen niet in verband konden gebracht worden met hogere krimprekken, werd het duidelijk dat ze een positief effect hadden op het kruipgedrag.

Duurzaamheid

De transporteigenschappen van het beton werden geëvalueerd om de duurzaamheid van het gerecycleerde beton te vergelijken met het conventioneel beton. Wat gaspermeabiliteit betreft, kon het gerecycleerd beton zowel een lagere als een hogere waarde vertonen, met de porositeit als belangrijkste controlerende factor i.p.v. het gehalte aan keramisch materiaal. De resultaten bekomen voor alle betonmengsels wezen op een goede prestatie voor deze eigenschap. Het gerecycleerd beton vertoonde een slechter gedrag voor de CO_2 indringing (ongeveer 70-75% meer indringing) wanneer blootgesteld aan een natuurlijke buitenomgeving gedurende 1 jaar, wat sterk geassocieerd was met het aantal poriën groter dan 0,067 µm. Wanneer het gerecycleerd beton getest werd in een kunstmatige omgeving met 10% CO_2, werd een gemiddelde afname van 30% vastgesteld t.o.v. traditioneel beton voor de indringingsdiepte na 1 maand blootstelling; een waarde die progressief omgezet werd in hogere waarden, tot 5% hoger dan de referentie na 3 maanden blootstelling. Zowel de lagere water/cement verhouding als de hogere alkaliniteit van het gerecycleerd beton verhinderen de indringing in de beginfase, maar de hogere porositeit leidt tot een minder goed gedrag op langere termijn.

De waterabsorptie van het beton werd met verschillende testen bepaald. Gerecycleerd beton vertoonde een lagere capillaire absorptie als gevolg van een lagere effectieve water/cement verhouding die een verbetering in kwaliteit van de cementpasta met zich meebracht. Bovendien wees een vergelijking binnen de gerecycleerde mengsels op een betere duurzaamheid bij toenemende gehaltes aan keramisch materiaal, gedeeltelijk door de hogere puzzolane activiteit, met waarden voor de primaire sorptiviteit die 22 tot 63% lager waren dan voor conventioneel beton. Eveneens nam de waterindringing onder druk af voor toenemende hoeveelheden keramische granulaten, met 2 tot 32 % en 1 tot 56% in fase I en II respectievelijk. Daarom, volgens de voorschriften van de EHE-08, is voldoende ondoorlatendheid verzekerd voor gewapend beton in de omgevingsklassen IIIa, IIIb, IV, Qa, E, H, F en Qb. Daarentegen toonden de resultaten van waterabsorptie onder vacuüm toenames in de open capillaire porositeit met 10 tot 40%, die sterk beïnvloed werden door het gehalte keramisch materiaal, en wezen op een minder goede prestatie van het gerecycleerde beton.

De aantasting van beton door vorst-door cycli met dooizouten toonde aan dat het gerecycleerd beton minder goed presteerde dan het conventioneel beton. Nochtans wezen de metingen van de ultrasoonsnelheid op het einde van de proef in fase I op een beton van goede kwaliteit. In fase II werd duidelijk dat afstrijkvlakken meer gevoelig waren aan de vorst en de inwerking van dooizouten en er werden massaverliezen van 2,7 tot 26,1 % vastgesteld zonder correlatie met het gehalte keramisch materiaal. Er moet wel opgemerkt worden dat geen luchtbelvormer werd gebruikt in dit onderzoek, en dat gebruik van deze hulpstof de vorstweerstand van alle betonmengsels aanzienlijk zou verhogen.

In de tweede fase gaf de elektrische migratieproef aan dat de migratiecoëfficiënt van de gerecycleerde mengsels tussen de 17 en 42% hoger was dan deze van traditioneel beton voor toenemende gehaltes keramisch materiaal, wat een matige resistentie tegen de penetratie van chloriden suggereerde. Zowel de lagere water/cement verhouding als de aanwezigheid van hoogovenslak en de puzzolane activiteit van het bouw- en sloopafval werden geïdentificeerd als factoren met een positief effect.

De elektrische resistiviteit van het gerecycleerd beton had dezelfde grootteorde als gerapporteerde waarden voor conventioneel beton (10-100 Ω·m). Terwijl de gemengde gerecycleerde granulaten leidden tot een resistiviteit die vergelijkbaar was met deze van een conventioneel mengsel, gaf het gerecycleerd beton met keramische granulaten een 7% lagere waarde als gevolg van een hogere vrijstelling van ionen in de poriënoplossing.

Ondanks het hogere risico op alkali-silica-reactie (ASR), veroorzaakte geen enkele van de gerecycleerde granulaten een lengtetoename van meer dan 0,10% na 20 dagen in de Oberholster test en daarom werden ze geklasseerd als niet-reactief. Nochtans moet hierbij wel opgemerkt worden dat deze resultaten bekomen werden voor mengsels met hoogovenslak in het cement, die ervoor gekend staan het ASR risico te reduceren.

Tot slot werden de mengsels blootgesteld aan een gesimuleerde agrarische omgeving, met name aan een oplossing van melk- en azijnzuur. Terwijl de maximale vermindering van de straal van de cilindrische referentieproefstukken kleiner bleef dan 2 mm op het einde van de proef, vertoonde geen van de gerecycleerde mengsels een vermindering van de straal hoger dan 1 mm. Ook was de oppervlakteruwheid van het gerecycleerde beton zo'n 40-74% lager bij toenemend gehalte keramisch materiaal. De verbeterde performantie kon uitgelegd worden door het positieve effect van de puzzolane materialen, de aanwezigheid van secundaire elementen in de cementmatrix, de lagere effectieve water/cement verhouding en de verfijning van het poriënnetwerk door gebruik van de gerecycleerde granulaten.

Milieu-effecten

De positieve effecten op het milieu liggen vooral in een vermindering van de vraag naar natuurlijke grondstoffen en het vermijden van storten van bouw- en sloopafval, bij productie van gerecycleerd beton met 50% secundaire granulaten uit bouw- en sloopafval. De belangrijkste voordelen werden gezien ter hoogte van een reductie van de effecten op de ozonlaag en gebruik van abiotische grondstoffen bij de CML 2001 beoordeling, en voor de schade aan minerale en fossiele voorraden bij de Eco-indicator 99. Ondanks deze voordelen had het gerecycleerd beton een hogere milieu-impact wat betreft schade aan de menselijke gezondheid wanneer de Eco-indicator 99 methode werd aangewend.

Als besluit kan gesteld worden dat dit onderzoek heeft aangetoond dat niet-behandelde granulaten uit bouw- en sloopafval met variërend gehalte aan keramisch materiaal aanvaardbare fysische en mechanische eigenschappen vertoonden volgens de huidige Spaanse norm. Ondanks het feit dat gerecycleerde granulaten een lagere kwaliteit bezitten in vergelijking met natuurlijke granulaten, zal het verschil in performantie het gebruik van deze materialen niet uitsluiten. Met een mengsel van gerecycleerde en natuurlijke materialen kunnen zelfs de meer strikte voorwaarden voor hoogwaardige toepassingen, zoals de productie van beton, voldaan worden. Een 50% mengsel van natuurlijk grind en de grove fractie van gemengde of keramische gerecycleerde granulaten, leidde tot beton met goede fysische, mechanische en duurzaamheidseigenschappen, dat ook nog milieuvriendelijk is.

Resumen

En los últimos 50 años, la sociedad mundial ha desarrollado una creciente preocupación por la protección y conservación del medio ambiente. En general, el libro "Primavera Silenciosa" de Rachel Carson (1962) es considerado como el catalizador del despertar de la conciencia ambiental en la población general.

En cualquier caso, la década de 1970 también ha sido considerada un período crucial en el desarrollo de la conciencia ambiental. En primer lugar, la creación del Club de Roma y la posterior publicación de sus preocupaciones ambientales sobre el carácter limitado de los recursos naturales, en el llamado Informe de Meadows, también jugaron un papel importante al resaltar las interdependencias entre el medio ambiente y la economía. Asimismo, en 1972, la celebración de la Conferencia de las Naciones Unidas sobre el Medio Humano o Conferencia de Estocolmo, fue la primera señal de reconocimiento global de que la protección y mejora del medio ambiente es un problema importante que afecta al bienestar humano y al desarrollo económico.

No obstante, el principal hito en este sentido se produjo a finales de 1980 con la publicación del Informe Brundtland, que definió el concepto de desarrollo sostenible como aquél que satisface las necesidades del presente sin comprometer la capacidad de las generaciones futuras para satisfacer sus propias necesidades.

El papel de la industria de la construcción en el crecimiento de la sociedad y la economía es indiscutible. A pesar de los efectos de la última crisis económica, el sector europeo de la construcción genera una facturación anual de aproximadamente 1600 mil millones de euros, constituye alrededor del 10% del producto interno bruto (PIB) de la Unión Europea y ofrece 13 millones de puestos de trabajo directos en cerca de 3 millones de empresas.

No obstante, también es incuestionable su contribución a la degradación del medio ambiente. Entre sus impactos negativos, el agotamiento de la tierra y su deterioro, el consumo de energía, la generación de residuos sólidos, el polvo y las emisiones de gases, la contaminación acústica, y el consumo de los recursos naturales no renovables pueden ser citados.

Los expertos consideran que el consumo excesivo de recursos y la elevada generación de residuos son dos de los retos ambientales más importantes del siglo 21. En este sentido, sólo en la Unión Europea, alrededor de 1,15 millones de toneladas de áridos directamente extraídos de la litosfera terrestre se emplean como materia prima en la producción de hormigón y aproximadamente 821 millones de toneladas de residuos de construcción y demolición (RCD) se produjeron en el año 2012, lo que representa un tercio de la generación total de residuos (Figura 1). En este escenario, solamente en base a la producción total de residuos, España fue el sexto mayor productor de RCD de la Unión Europea en 2012, aunque ocupó la vigésimo quinta posición cuando se tienen en cuenta la producción per cápita.

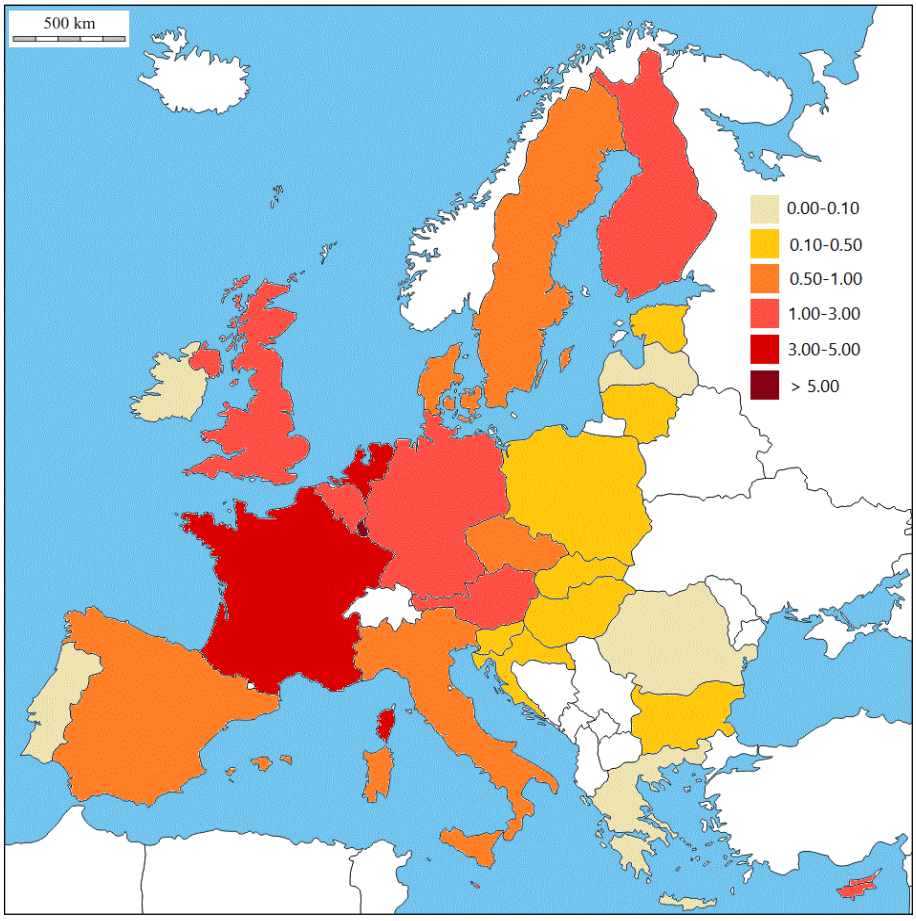

Figura 1: Producción de RCD por habitante en la UE durante 2012

Dichos RCD son substancias indeseadas generadas durante el transcurso de las actividades de construcción, rehabilitación y demolición de un bien inmueble (edificio, carretera, puerto, aeropuerto, ferrocarril, canal, presa, instalación deportiva o de ocio, así como cualquier otro análogo de ingeniería civil), tal como recoge la legislación vigente en España.

De una forma más detallada, los RCD están compuestos por hormigón, ladrillos, tejas y otros materiales cerámicos, madera, vidrio, plástico, materiales bituminosos, carbón, asfalto, metales y aleaciones, basura, suelo contaminado, materiales aislantes y materiales que contengan amianto o yeso. No obstante, en ningún caso, deben considerarse RCD las tierras y piedras no contaminadas por sustancias peligrosas reutilizadas en la misma obra, en una obra distinta o en una actividad de restauración, acondicionamiento o relleno, siempre y cuando pueda acreditarse de forma fehaciente su destino a reutilización; y los residuos que se generen en obras de construcción o demolición y estén regulados por legislación específica.

La estrategia para la gestión de los residuos en la Unión Europea responde a un esquema jerárquico conocido como el principio de las 3R (Figura 2), en el que la mejor opción de tratamiento de los residuos es aquella que causa un menor impacto ambiental.

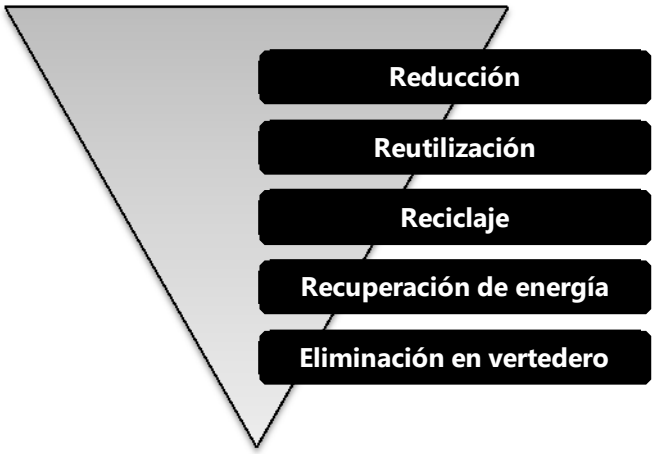

Figura 2: Jerarquía en la gestión de residuos

De este modo, la reducción en la generación de residuos es siempre la mejor alternativa tanto por la minimización de la producción como por la reducción de los costes asociados por transporte, tratamiento y eliminación. Seguidamente, la reutilización es preferida al reciclaje, pues aunque este último también consigue una reducir el consumo de los recursos naturales, requiere de una serie de operaciones de procesado que llevan asociados sus propios costes medioambientales. Para algunos tipos de residuos, la incineración puede representar la mejor opción de tratamiento ya que posibilita una recuperación energética como combustibles alternativos o por la producción de calor o energía. Finalmente, la eliminación de residuos en vertederos debe considerarse como la última opción de tratamiento debido a los altos impactos ambientales asociados con este método de gestión.

Pese a la ausencia de una legislación específica para los RCD, la Unión Europea los considera como uno de los seis flujos prioritarios, debido tanto a las ingentes cantidades producidas como a su alto potencial para la reutilización y reciclaje.

Como Estado Miembro de la Unión Europea, España está obligada a cumplir con los principios y objetivos estipulados a nivel supranacional en materia de medio ambiente, a la vez que ostenta la principal responsabilidad a la hora de abordar problemas en materia de residuos. De este modo, la actual Directiva europea de residuos se encuentra transpuesta al ordenamiento español mediante la Ley 22/2011 de residuos y el Real Decreto 1481/2001 de eliminación de residuos mediante depósito en vertedero, el marco legislativo de residuos en España también cuenta con el Real Decreto 105/2008, que específicamente regula la producción y tratamiento de RCD, a la vez que establece las obligaciones de los distintos agentes involucrados en la producción y gestión de RCD.

Como tal, los diferentes agentes deben seguir una serie de procedimientos obligatorios conducentes a una gestión de los RCD respetuosa con el medio ambiente. La Figura 3 ilustra sucintamente el modelo de gestión de estos residuos en España. El promotor (1), que inicia el ciclo, ha de contratar a un proyectista (2) para que desarrolle tanto el proyecto de ingeniería como un estudio de gestión de RCD, que tiene que incluir una estimación de la generación de RCD así como las medidas previstas para su minimización mediante una planificación racional de los trabajos de construcción y demolición, el almacenaje y la separación de residuos, así como su posterior gestión para satisfacer los requisitos establecidos en el Real Decreto 105/2008. Una vez aprobados por el ayuntamiento (3), se conceden los oportunos permisos de obra que permiten el inicio de la actividad. No obstante, el inicio de la actividad está supeditado al pago de una fianza con el objetivo de desalentar el vertido en favor del reciclaje (4). Una vez cumplidos todos los trámites administrativos, el contratista (5) puede comenzar los trabajos, que han de desarrollarse de acuerdo al plan inicial de gestión de residuos y han de culminar con el transporte de los residuos una planta de gestión de RCD (6) donde serán sometidos a una serie de tratamientos que permitan su posterior reutilización y reciclaje como materiales secundarios de construcción. Como justificante del correcto manejo de los RCD, el promotor recibirá un certificado de gestión (7) que presentado ante el ayuntamiento le servirá para recuperar el depósito (8). Aunque es esencial que todos los agentes implicados sean conscientes de la importancia de su papel, asuman las nuevas obligaciones legales de acuerdo con los principios de sostenibilidad, la realidad aun refleja la reticencia de los diferentes profesionales a la hora de implementar estas medidas por considerarlas un gasto innecesario de tiempo y dinero.

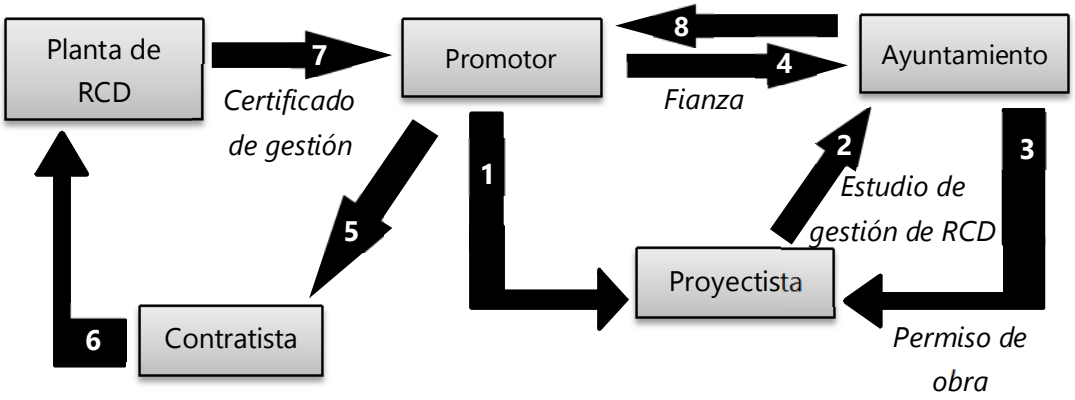

Figura 3: Modelo de gestión de RCD en España

Satisfaciendo los objetivos de la Directiva 2008/98/CE, España ha desarrollado dos planes de gestión de residuos implantando las estrategias generales con el fin de cumplir con los objetivos mínimos de prevención, reutilización, reciclaje, valorización y eliminación de los RCD. Actualmente, una nueva versión está siendo preparada para el periodo 2015-2020 con el fin de promover un mejor desempeño ambiental de acuerdo con los objetivos legales de la Unión Europea y establecer los objetivos cuantitativos de la valorización de los RCD, que en 2020 tienen que alcanzar, como mínimo, un 70% del total. A pesar del interés legislativo en la gestión de RCD, España aún carece de normativa específica respecto a la reutilización o reciclaje de los áridos reciclados procedentes de RCD en la industria de la construcción. Si bien es cierto que, la Instrucción de hormigón estructural (EHE-08) y el pliego de prescripciones técnicas generales para obras de carreteras y puentes recogen algunos aspectos en este sentido.

Tradicionalmente, los recursos naturales y los residuos se encuentran, respectivamente, en el inicio y final del modelo lineal de la producción. Sin embargo, la creciente preocupación social por la protección y conservación del medio ambiente está cambiando la actitud de uso y desecho de los recursos hacia un modelo de economía circular que promueve la explotación de los residuos como recursos secundarios. Bajo este principio de circularidad (Figura 4), los recursos se mantienen dentro de los límites de la economía durante varios ciclos de vida, ya que pueden ser utilizados de forma repetitiva al final de cada período de utilidad. Entonces, el balance general representa el uso de menos recursos naturales para producir el mismo producto, siendo ésta la base de la eco-eficiencia, y una interrupción en la relación entre el uso de las materia prima y la producción económica, conocido como el desacoplamiento.

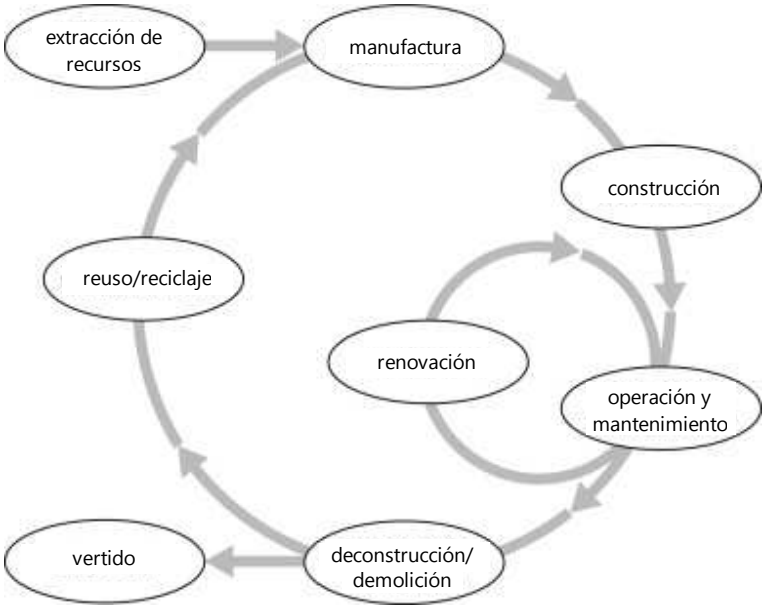

Figura 4: Ciclo cerrado de los materiales de construcción

En general, las plantas de gestión de residuos reciben los RCD como residuos limpios de un componente individual (hormigón o cerámico) o residuos como mixtos. Dado que las operaciones de procesamiento para cada categoría son diferentes, la tasa de entrada de los residuos se establece en consecuencia, es decir, precios más bajos para los flujos de residuos individuales que sólo requieran operaciones de trituración y cribado.

Por el contrario, los RCD mixtos requieren de un mayor nivel de procesado que comienza con su extendido en la playa de recepción con el fin de facilitar la separación de los grandes y más pesados contaminantes por medio de retroexcavadoras. Posteriormente, los residuos son alimentados a un tamiz vibratorio denominado tromel que separa los residuos de menor tamaño (<4 mm) para su almacenado de forma independiente. Entonces, el resto del material en la criba vibratoria es reconducido por medio de cintas transportadoras y alimenta las máquinas trituradoras responsables de la reducción de tamaño de los RCD. Después se llevan a cabo varias operaciones de separación con el fin de eliminar las impurezas que acompañan al material granular (vidrio, metal, madera, plástico, papel y otros). Por último, una operación de cribado clasifica los RCD tratados en varias fracciones. Por lo general tres tipos de áridos reciclados son producidos en función de su composición: hormigón, mixto o cerámico. La Figura 5 ilustra esquemáticamente los procedimientos llevados a cabo en una planta de gestión de RCD para la producción de áridos reciclados.

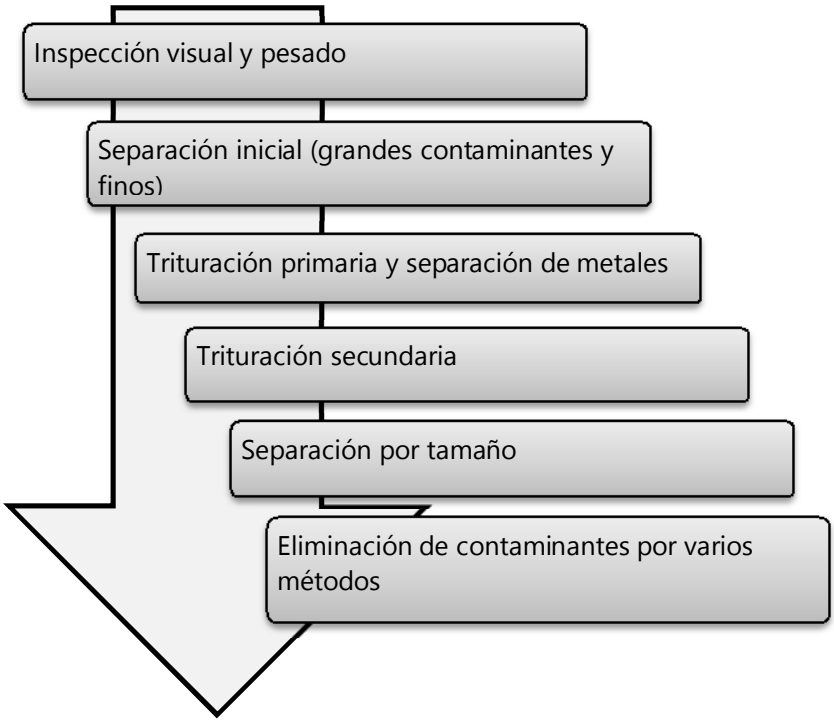

Figura 5: Proceso de producción en una planta de tratamiento de RCD

Debido a las grandes cantidades de hormigón consumido anualmente, alrededor de una tonelada por habitante y año, es el material más empleado en todo el mundo, y por lo tanto el receptor perfecto de grandes cantidades de productos residuales como áridos reciclados, lo que al mismo tiempo soluciona el problema de la generación de residuos y reduce el consumo de los recursos naturales, aliviando la presión sobre la capacidad de carga del medio ambiente y contribuyendo a un futuro más sostenible al cerrar el bucle de la producción de hormigón.

En los últimos años, el potencial de reciclaje de RCD como reemplazo total o parcial de los áridos gruesos naturales se ha convertido en un objetivo importante de interés entre los científicos. Sin embargo, la mayoría de los trabajos de investigación llevados a cabo se han centrado en el uso de áridos recuperados de los escombros de hormigón. Sin embargo, las prácticas constructivas y de demolición convencionales, así como los sistemas de gestión de residuos, empleados en los países mediterráneos como España, dan lugar a RCD de carácter mixto con un contenido medio de cerámica de 54% (Figura 6). Por lo tanto, los áridos reciclados cerámicos y mixtos representan el 70% del total de los áridos reciclados producidos en las plantas de gestión de residuos. Las cifras citadas transmiten la importancia del tratamiento y reciclaje de este tipo de residuos más allá de las aplicaciones de bajo nivel tales como materiales no consolidados en movimientos de tierras, rellenos y construcción de carreteras, lo que constituye una depreciación del potencial reciclaje del material.

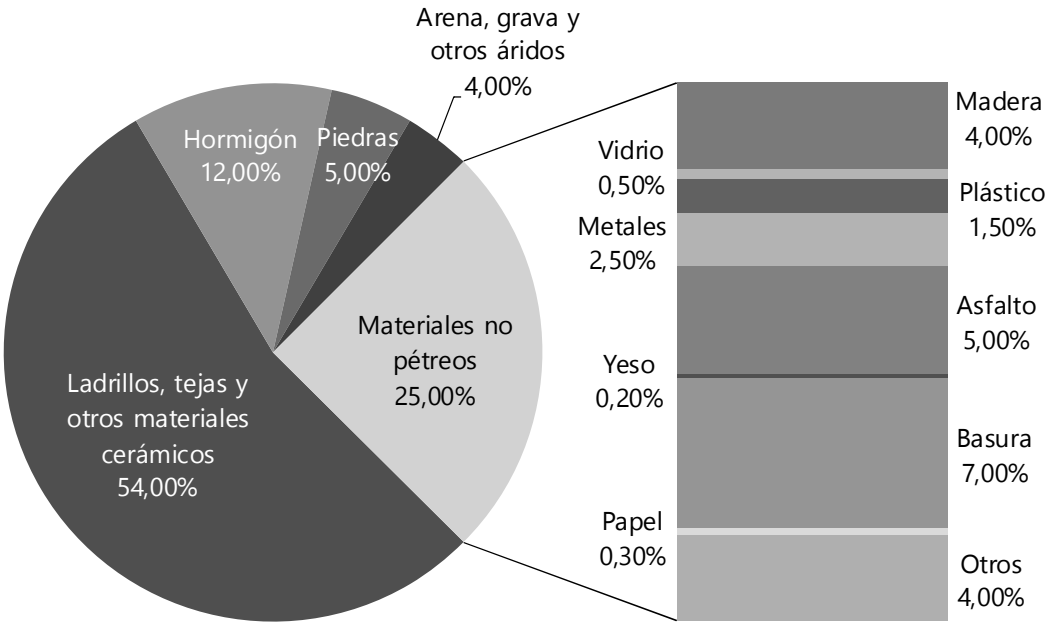

Figura 6: Composición típica de los RCD en España

Programa experimental

El objetivo general de la presente tesis es doble. Primero, el análisis de las propiedades de los áridos reciclados disponibles comercialmente procedentes de RCD con diferentes porcentajes de residuos cerámicos y, en segundo lugar, la evaluación de las características de los hormigones reciclados incorporando una sustitución parcial de los áridos gruesos naturales por los áridos reciclados antes mencionados tal cual fueron obtenidos de la planta de gestión de RCD sin ningún tratamiento específico que modificase sus propiedades características comparado con una mezcla de hormigón convencional utilizado como referencia. El porcentaje de reemplazo fue fijado en un 50%, ya que varios investigadores han sugerido este valor como el límite de sustitución en la que el hormigón reciclado tiene propiedades físicas y mecánicas comparables a una mezcla convencional, sin la necesidad de aumentar drásticamente el contenido de cemento.

Desde un punto de vista de la calidad, la caracterización de los áridos reciclados juega un papel importante en las propiedades del hormigón resultante. A pesar de la falta de estandarización de los áridos reciclados cerámicos y mixtos para la fabricación de hormigón estructural en España, los materiales secundarios seleccionados fueron analizados de acuerdo a los requisitos establecidos en la Instrucción de Hormigón Estructural (EHE-08) a fin de evaluar sus propiedades físicas, mecánica, químicas, mineralógicas y micro estructurales como medio para justificar la viabilidad de este tipo de áridos reciclados de RCD en aplicaciones estructurales de hormigón.

Por lo tanto, el programa experimental se compuso de una caracterización física y mecánica (constituyentes, distribución de tamaño de partícula, geometría, evaluación de los finos, densidad y absorción de agua, resistencia mecánica y mortero adherido). Por otra parte, se realizó una caracterización microestructural (difracción de rayos X -DRX-, fluorescencia de rayos X -FRX-, microscopía electrónica de barrido, porosimetría por intrusión de mercurio -PIM-) para lograr una mejor comprensión de la heterogeneidad de su origen.

Además, con el fin de evaluar la influencia de dicha sustitución, varias dosificaciones de hormigón fueron ensayadas. En una primera etapa de la investigación, se estudió un hormigón convencional y tres mezclas de hormigón reciclado hechos con áridos reciclados obtenidos de plantas de gestión de RCD. Los ensayos realizados sobre estas muestras se centraron en las propiedades físicas (consistencia, contenido de aire ocluido y densidad), mecánicas (resistencia a la compresión, tracción y flexión, módulo de elasticidad, curvas de tensión-deformación) y microestructurales (morfología de la interfase árido-pasta y la porosidad) del hormigón fresco o endurecido, aunque también se analizaron algunas propiedades de durabilidad (permeabilidad al oxígeno, carbonatación, penetración de iones cloruro en ambientes de niebla salina, penetración de agua bajo presión, resistencia a los ciclos de hielo-deshielo y resistividad eléctrica), de acuerdo a las posibilidades de acceso a máquinas de ensayo en la Universidad de León. Finalmente, se llevó a cabo un análisis de rendimiento medioambiental de los hormigones reciclados en esta fase de la investigación mediante la metodología del análisis del ciclo de vida con el fin de evaluar los beneficios de la incorporación de árido grueso reciclado en la fabricación de hormigón.

La segunda fase de la investigación coincide con el inicio del acuerdo de doctorado conjunto entre la Universidad de León y la Universidad de Gante, lo que permitió ampliar el número de ensayos de caracterización, así como la incorporación de un árido reciclado mixto procedente de una planta de tratamiento de RCD belga. Por lo tanto, cuatro hormigones reciclados fueron comparados con la mezcla de hormigón convencional diseñada como referencia para esta fase de la investigación. Además de algunas pruebas ya realizadas en la etapa anterior (consistencia, densidad, aire ocluido, resistencia a la compresión, tracción y flexión, módulo de elasticidad, curvas de tensión-deformación, retracción y fluencia), la investigación incluyó pruebas de transmisión de la onda ultrasónica y análisis calorimétrico y se centró en el efecto que la sustitución de los áridos gruesos naturales por los áridos reciclados mixtos y de cerámica tiene en la durabilidad y rendimiento a largo plazo del hormigón endurecido (permeabilidad al oxígeno, carbonatación, absorción de agua por capilaridad y bajo vacío, penetración de agua bajo presión, resistencia al hielo-deshielo en presencia de sales de deshielo, penetración de iones cloruro mediante ensayos acelerados de migración, resistividad eléctrica, reacción álcali-sílice y resistencia a los ácidos orgánicos mediante un ensayo acelerado con mezclas de ácido acético y láctico).

Materiales

Para todas las mezclas de hormigón, se utilizó agua potable, cemento con escorias de alto horno (CEM III/A 42.5 N SR y CEM III/B 42.5 N SR LH LA en las fases I y II de la investigación, respectivamente), arena y grava de naturaleza silícea. Además, un 50% del árido grueso convencional fue sustituido en las dosificaciones de hormigón reciclado por áridos reciclados procedentes de RCD.

Cuatro muestras de áridos reciclados fueron utilizadas en la presente investigación. Mientras que tres de ellas (RA-L(S), RA-L(B) y RA-H(S)) fueron directamente obtenidas del material comercializado en una planta de gestión de RCD, -TEC-REC, ARC y Bierzo Recicla, respectivamente-, la cuarta muestra (RA-M(S)) fue creada artificialmente mediante la mezcla de los áridos reciclados españoles de acuerdo con los objetivos de la investigación (
Figura 7). Cabe destacar que la notación de las muestras hace referencia tanto al nivel de cerámica (L-bajo-, M-medio- y H-alto-) como a la procedencia de los residuos (S-España- y B-Bélgica-).

Figura 7: Áridos reciclados empleados en la investigación

Caracterización de los áridos reciclados

Los resultados mostraron una composición mayoritaria de hormigón (44% y 37%, respectivamente) seguida por materiales de naturaleza cerámica (34% y 38%, respectivamente) en las muestras RA-L(S) y RA-L(B), mientras que la situación se invirtió en la muestra RA-M(S), con un componente cerámico mayoritario (66%), seguido por la ocurrencia de materiales a base de cemento (17%). En la muestra RA-H(S), solo materiales cerámicos (ladrillos y azulejos principalmente) formaron parte del árido reciclado.

En términos impurezas, RA-L(B) excedió el límite de 1% de asfalto, que es más estricto que en otros estándares europeos, y RA-L(S) superó el límite del 1% de otras impurezas (vidrio, metal, plástico y madera entre otros), lo que sugiere un cierto grado de fracaso en el procedimiento de separación en la planta de gestión. Respecto al contenido de materia orgánica, todos los áridos presentaron valores inferiores a 0,80%, evitando así los efectos nocivos en la fabricación de hormigón. Además, los resultados de los ensayos de remojo en ácido clorhídrico 1M y los daños por heladas indicaron contenidos similares de mortero adherido, 34%, 23% y 6% para RA-L(S), RA-L(B) y RA-H(S) respectivamente.

La granulometría de los áridos reciclados siguió una curva continua y no uniforme y presentó una relación D/d superior al límite estipulado de 1,40. Tanto los componentes como la gestión de los RCD resultaron en un índice de lajas más alto para los áridos reciclados que, en todos los casos, cumplió con el límite del 35% establecido en la EHE-08. También dependiente del tratamiento en la planta de gestión RCD, el contenido de finos de todas las muestras se mantuvo por debajo del límite de 1,50%. Sin embargo, se debe prestar especial atención a la generación de más finos durante el mezclado debido al auto-desgate de los materiales. A pesar de que el equivalente arena indicó una calidad cuestionable de los finos al no cumplir ninguna muestra los requisitos de 70-75%, la difracción de rayos X no detectó arcillas expansivas que pudieran afectar negativamente al hormigón reciclado.

Pese a que la EHE-08 no establece ninguna limitación para la densidad de los áridos de hormigón, los áridos reciclados presentaron una densidad significativamente menor que la de los áridos naturales (entre 18% y 29% para aumentos del contenido cerámico). Por el contrario, la absorción de agua está estrictamente limitada a 7%, mientras el estándar alemán o las recomendaciones RILEM son más permisivos. Por lo tanto, ninguno de los áridos reciclados cumplió las especificaciones nacionales. En cuanto a las prestaciones mecánicas de los áridos reciclados, todos ellos fueron considerados adecuados bajo las restricciones de la EHE-08, aunque la muestra RA-L(S) solo sería apta para hormigón hasta 30 MPa ya que el coeficiente de Los Ángeles estuvo entre 40% y 50%.

La composición química, principalmente óxido de silicio y óxido de aluminio, indicó la presencia de minerales de arcilla y cuarzo en los áridos reciclados. Además, el contenido de álcali de los áridos reciclados fue aproximadamente 23-34 veces mayor que la grava. Mientras que el límite de contenido de cloruro (0,05%) no fue alcanzado por ninguno de los áridos reciclados, la muestra de la RA-L(S) superó el límite de 0,80% de contenido en sulfatos, principalmente debido a la alta presencia de yeso.

La composición mineralógica de las muestras coincidió con los resultados químicos de fluorescencia de rayos X. El principal mineral en el árido reciclado cerámico (RA-H(S)) fue el cuarzo; mientras que para los áridos reciclados mixtos (RA-L(S) y RA-M(S)), además del de cuarzo, el porcentaje de calcita también fue importante debido a la presencia de hormigón y mortero. El resto de los componentes apuntó al contenido relativo de cerámica, por ejemplo feldespato (anortita, ortoclasa), dolomita, hematita, moscovita, illita y cristobalita.

Hoy en día, se sabe muy poco acerca de la porosidad de los áridos reciclados mixtos y cerámicos, más allá de que es un valor relativamente alto en comparación con la de los áridos naturales. Aunque los resultados apoyaron este hecho (18%, 21% y 26% para la RA-L(S), RA-M(S) y RA-H(S) respectivamente, es decir, alrededor de 23 veces mayores), también proporcionaron una visión más amplia de la estructura porosa de los áridos reciclados. Por ejemplo, la porosidad no efectiva para la grava (0,23%) es el componente minoritario de la porosidad total, mientras que lo contrario ocurre en los áridos reciclados (15% para RA-L(S), 15% para RA-M(S) y 19% para RA-H(S)). Estos valores son indicativos de una porosidad no accesible elevada, que sugiere que las diferencias entre ambos áridos no son tan extremas como se consideró inicialmente.

Aunque que el uso de áridos reciclados mixtos o cerámicos aún no está permitido por la legislación española, los resultados obtenidos en la caracterización física, mecánica y microestructural realizada (Figura 8) revelaron que las muestras de áridos reciclados con diferente contenido cerámico exhiben prometedores resultados de calidad para su aplicación en la fabricación de hormigón.

Sin embargo, basado en la caracterización experimental, la absorción de agua, pérdida por abrasión de Los Ángeles y las impurezas son las principales limitaciones para el uso de estos tipos de áridos reciclados en la fabricación de hormigón, ya que presentaron incumplimientos con respecto a los límites legales.

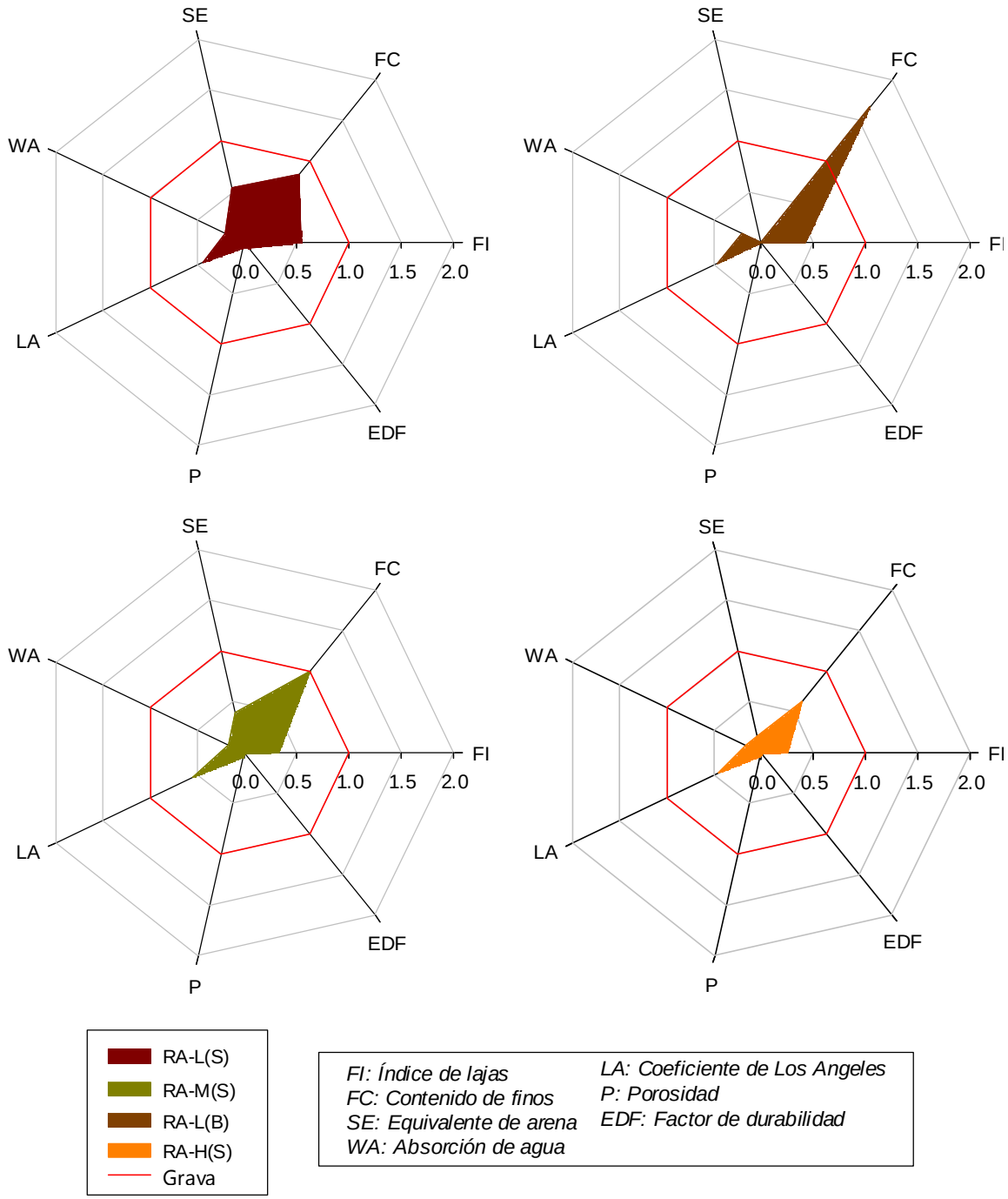

Figura 8: Caracterización de los áridos reciclados

Dosificación

Al igual que la calidad de los componentes usados en la elaboración del hormigón, su dosificación y mezcla también influyen en las propiedades finales del hormigón, tanto en estado fresco (trabajabilidad) como endurecido (resistencia y durabilidad).

En esta investigación, hormigones convencionales y reciclados con diferentes porcentajes cerámicos fueron dosificados para evaluar la influencia que un reemplazo parcial (50%) del árido grueso natural tiene en las propiedades del hormigón. Para la dosificación, se seleccionó el método De la Peña y se estableció una resistencia característica mínima a la compresión de 25 MPa a los 28 días, consistente con un uso estructural. Otros parámetros de diseño adoptados fueron un tamaño de árido máximo de 20 mm y asentamiento S2 para el hormigón convencional según lo establecido en la EHE-08. Puesto que la dosificación de los áridos se basó en la parábola de Fuller y la densidad de la grava de río es mayor que la de los áridos gruesos reciclados, los hormigones reciclados contienen mayores cantidades de arena a medida que aumenta el contenido cerámico. Finalmente, para cumplir con los requisitos de durabilidad, la relación total de agua/cemento se estableció en 0,55. Por lo tanto, el contenido de cemento y agua fue fijado en 391 kg/m^3 y 215 l/m^3. Dado que no se añadió agua adicional, la absorción por parte de los áridos reciclados causó que la relación efectiva de agua/cemento se redujera a 0,50 en los hormigones reciclados. En la Tabla 1 pueden observarse las distintas dosificaciones ensayadas.

Tabla 1: Composición de las mezclas de hormigón convencional y reciclado en las dos fases de la investigación

	CC	**RC-L(S)**	**RC-L(B)**	**RC-M(S)**	**RC-H(S)**
Fase I					
Agua (l/m^3)	215.00	215.00	-	215.00	215.00
Cemento (kg/m^3)	390.91	390.91	-	390.91	390.91
Arena (kg/m^3)	650.49	715.89	-	734.20	751.88
Grava (kg/m^3)	1030.71	446.97	-	425.89	405.54
Árido reciclado (kg/m^3)	0.00	446.97	-	425.89	405.54
Fase II					
Agua (l/m^3)	215.00	215.00	215.00	215.00	215.00
Cemento (kg/m^3)	390.91	390.91	390.91	390.91	390.91
Arena (kg/m^3)	480.48	703.46	736.08	766.73	821.06
Grava 2-8 mm (kg/m^3)	1000.30	368.32	356.90	335.93	307.79
Grava 8-16 mm	250.07	92.08	89.23	83.98	76.95
Árido reciclado (kg/m^3)	0.00	460.40	446.13	419.92	384.74

Asimismo, un ejemplo de la sección transversal de cada una de las diferentes dosificaciones de hormigón es mostrado en la Figura 9, donde claramente puede observarse el paulatino incremento del porcentaje de árido grueso cerámico procedente de RCD.

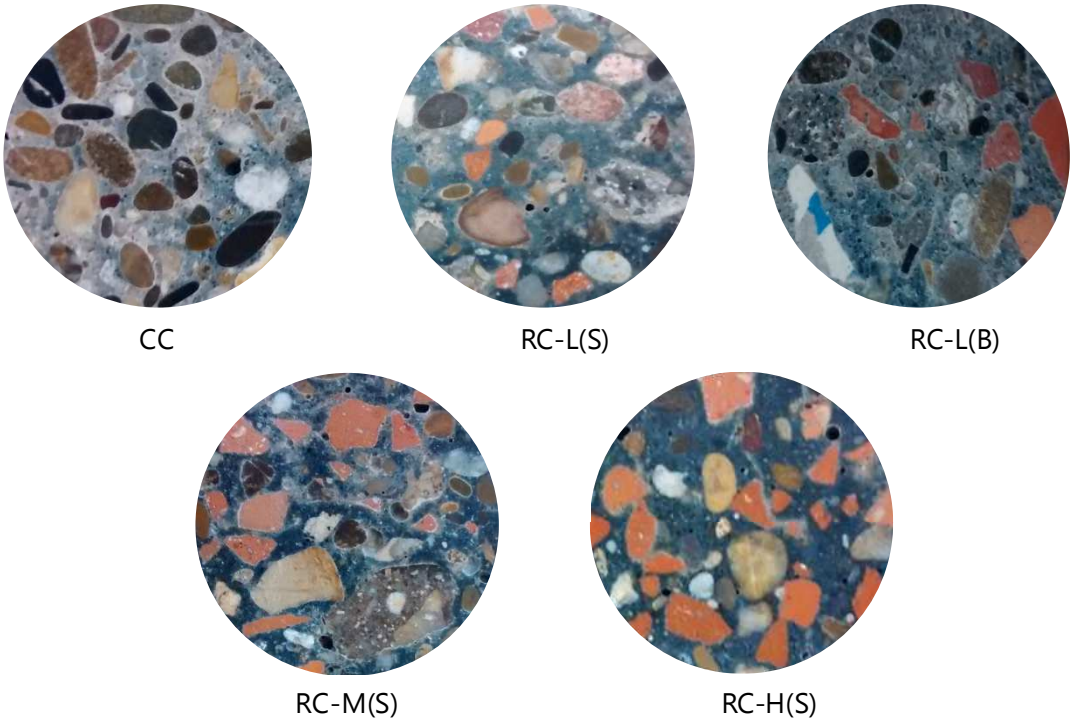

Figura 9: Sección transversal de las diferentes dosificaciones de hormigón

Propiedades del hormigón fresco

Dado que la cantidad de agua respecto al método de dosificación original no fue corregida, el asentamiento de los hormigones reciclados fue menor. En la primera fase, el hormigón reciclado presentó reducciones inferiores de la consistencia, hasta un 28% para bajos contenidos de cerámica (I-RC-L(S)), alrededor de 41% para un contenido medio (I-RC-M (S)) y entorno al 69% para un contenido alto de cerámica (I-RC-H (S)). En la fase II, las reducciones de asentamiento fueron mayores ya que el hormigón convencional presentó una consistencia más alta, oscilando entre 20% y 29% para un bajo contenido cerámico (II-RC-L(S) y II-RC-L(B)), alrededor de 75% para un contenido medio (II-RC-M(S)) y casi 91% para un contenido alto de cerámica (II-RC-H (S)). Sin embargo, no se detectaron problemas en la trabajabilidad en ninguna de las fases de la investigación.

Debido a la presencia de mortero y cerámica, el contenido de aire de los hormigones reciclados fue mayor y osciló entre un 40% en II-RC-L(S) y un 80% en II-RC-L(B), II-RC-M(S) y II-RC-H(S) pues mayores porosidades favorecen la oclusión de aire en los poros. Por el contrario, ya que la densidad de los áridos reciclados mixtos y cerámicos es menor que la de los áridos naturales, la densidad en fresco de los hormigones reciclados también fue inferior que en el hormigón convencional, entre 5% y 2%, para incorporaciones crecientes de cerámica.

A pesar de que todas las materias primas estuvieron a la misma temperatura ambiente, los hormigones reciclados presentaron valores de temperatura iniciales (tras no más de 12 minutos después la mezcla de los materiales) más bajas, entre un 9% (II-RC-L (S)) y 17% (II-RC-M (S)) respecto al hormigón convencional. Por el contrario, también registraron valores de temperatura final más alta, oscilando entre un 1% (II-RC-L (S)) y un 4% (II-RC-H (S)).

Por lo tanto, los hormigones reciclados mostraron liberación total de calor entre el 5% y 15% superior que el hormigón convencional a medida que aumentaba el contenido de cerámica incorporado. A pesar de la mayor probabilidad en la formación de grietas a edad temprana, se espera que el menor coeficiente de expansión térmica de los materiales cerámicos contrarreste el mayor calor de hidratación.

En general, el uso de áridos reciclados en la fabricación de hormigón fue responsable del retraso en los tiempos iniciales y finales de fraguado. Sin embargo, algunos resultados extremos y la falta de coincidencia entre los métodos evidenciaron la necesidad de un mayor número de investigaciones con el fin de asegurar la exactitud de algunos de los criterios propuestos para hormigones convencionales. En cualquier caso, todas las muestras fueron desmoldadas tras 24 horas sin que surgiera ningún problema de fraguado.

Propiedades del hormigón endurecido: Microestructura

El estudio de la microestructura mostró resultados comparables entre el hormigón convencional y reciclado, ya que las interfaces observadas entre los áridos reciclados de hormigón y cerámicos con la matriz de cemento fueron bastante densas y continuas. La buena calidad de ITZ fue debida a la menor relación efectiva agua/cemento, el efecto de curado interno producido por la devolución de parte del agua absorbida en los áridos reciclados, el uso de un cemento con escorias, la actividad puzolánica adicional de los RCD, y la superficie rugosa y contornos más nítidos de los áridos reciclados. Por otra parte, la incorporación de áridos reciclados no cambió la composición química de la pasta de cemento (es decir, calcio y silicio como elementos principales, magnesio y aluminio como consecuencia de las partículas de escoria, y azufre procedente del agente retardante del cemento) ni la relación Ca/Si.

Los hormigones reciclados presentaron una porosidad total mayor que el hormigón convencional a los 28 días. En particular, se encontraron diferencias más altas para incorporaciones de cerámica inferiores, que fueron desde 28% para bajo contenido cerámico (I-RC-L(S)) y 15% para contenido medio (I-RC-M(S)) a 3% para altos porcentajes de cerámica, lo que sugiere una relación inversa entre ambas variables.

Sin embargo, la situación se invirtió después de 56 días de curado y hormigones reciclados presentaron una porosidad menor que la del hormigón convencional, alrededor de 29% para I-RC-L(S), 11% para I-RC-M(S) y 17% para I-RC-H(S). Por lo tanto, los hormigones reciclados experimentaron una disminución significativa en la porosidad, hasta de un 41% para I-RC-L(S), 26% para I-RC-M(S) y 31% para I-RC-H(S). Además, en general, los áridos reciclados presentan tamaños de poro crítico entre 20% y 36% inferiores al del hormigón convencional, lo que es indicativo de estructuras con poros más finos.

Análogamente al contenido de aire en estado fresco, el hormigón convencional presentó la menor cantidad de aire ocluido (1%), mientras que los hormigones reciclados presentaron valores entre 1,6 y 2,5 veces mayores para contenido de cerámica crecientes. Sin embargo, los hormigones reciclados mostraron una peor distribución del aire ocluido en comparación con el hormigón convencional, con una disminución del factor de separación entre un 21% y un 39%, y longitud media de cuerda entre 1,7 y 2 veces superior. Sin embargo, ninguno de los hormigones reciclados cumplió las recomendaciones establecidas para hormigones resistentes a heladas en ausencia de agentes incorporadores de aire.

Propiedades del hormigón endurecido: Resistencia

Al igual que en el estado fresco, la densidad del hormigón reciclado está principalmente influenciada por la densidad de los áridos empleadas y, por lo tanto, fueron observadas reducciones entre 2% y 8% para contenidos de cerámica crecientes.

En cuanto a la resistencia a la compresión, todos los hormigones reciclados mostraron valores superiores a los 25 MPa establecidos en la dosificación para 28 días. Sin embargo, se registraron reducciones máximas de hasta 22% para I-RC-L(S) a los 7 días y 11% para I-RC-M(S) a los 28 días. Cabe destacar que la pérdida de resistencia fue más pronunciada a los 7 días y se redujo progresivamente con la edad del hormigón. Es decir, los hormigones reciclados desarrollaron más rápidamente su resistencia mecánica debido a la presencia de partículas de cemento no hidratadas y finos de cerámica que contribuyeron a la ganancia de resistencia.

Sin embargo, vale la pena mencionar que los resultados obtenidos para los hormigones reciclados con alto contenido cerámico (I-RC-H(S) y II-RC-(S)) indicaron una influencia positiva de los áridos reciclados en esta propiedad. En base a los índices de resistencia a la compresión, la sustitución de los áridos naturales con áridos reciclados tuvo un efecto favorable en I-RC-H(S) y II-RC-H(S) en todas las edades de curado y en las muestras II-RC-L(S) y II-RC-L(B) a los 90 días de curado. En consecuencia, se confirmó el efecto adverso de la sustitución para el resto de hormigones dado que la contribución a la resistencia es algo inferior que la cantidad de árido grueso natural reemplazado.

Del mismo modo, el uso de áridos reciclados causó una reducción de la resistencia a la flexión alrededor de 8% en la fase I, mientras que las disminuciones de la fase II estuvieron en el rango 20% para II-RC-L(S), II-RC-L(B) y II-RC-M(S), y 13% para II-RC-H(S). En cuanto a la resistencia a la tracción, las disminuciones respecto al hormigón convencional disminuyeron con el aumento de cerámica. En promedio, se registraron reducciones del 11%, 7% y el 2% para áridos reciclados con bajo, medio o alto contenido cerámico. Para ambas propiedades, la curva Eurocódigo-2 produjo un ajuste aceptable para especímenes cúbicos y el ensayo de punto central.

En cuanto a la tenacidad del material, cuando se emplean áridos reciclados mixtos o cerámicos, descensos máximos de un 8% en el módulo elástico se observaron en comparación con el hormigón convencional. En este caso, la fórmula propuesta por el ACI 318-14 produjo el mejor ajuste debido a la incorporación del parámetro de densidad a la predicción.

El análisis de las curvas de tensión-deformación mostró que los hormigones convencionales y reciclados presentan un comportamiento lineal similar en la primera parte de la curva, independientemente del contenido de cerámica incorporado. Sin embargo, las diferencias fueron notables en la zona parabólica.

Para un mismo nivel de esfuerzo, los hormigones con bajo contenido de cerámica (I-RC-L(S), II-RC-L(S) y II-RC-L(B)) exhibieron deformaciones más bajas que el hormigón convencional, mientras que aquellas muestras con contenido medio y alto (I-RC-M(S), II-RC-M(S), I-RC-H(S) y II-RC-H(S)) mostraron deformaciones superiores. En promedio, los hormigones reciclados con contenidos cerámicos bajas (I-RC-L(S), II-RC-L(S) y II-RC-L(B)) presentaron una deformación 4% inferior. Por el contrario, la deformación para contenidos de cerámica medios (I-RC-M(S) y II-RC-M(S)) y altos (I-RC-H(S) y II-RC-H(S)) fueron hasta 12% y 6% superiores respectivamente.

En cuanto a la evolución de la retracción con el tiempo, tanto los hormigones convencionales como los reciclados presentaron comportamientos paralelos como curvas hiperbólicas que tienden a un valor asintótico. A pesar de que el hormigón II-RC-M(S) experimentó una retracción inferior durante los 10 primeros días de ensayo, el uso de áridos reciclados produjo un aumento general de las deformaciones por retracción en comparación con la del hormigón convencional independientemente del tipo de árido reciclado empleado. Por lo tanto, después de 91 días, los hormigones reciclados presentaron deformaciones totales entre 12% y 745% superiores a las del hormigón convencional.

Análogamente, es posible concluir que los áridos reciclados de RCD, tanto mixtos como cerámicos, ocasionaron un comportamiento de fluencia paralelo al de un hormigón convencional, aunque con un peor rendimiento general. Por ello, los hormigones reciclados exhibieron deformaciones de fluencia total entre 24% y 46% más altas, para contenidos decrecientes de cerámica.

Pese a todo, el comportamiento mecánico exhibido por los hormigones reciclados puede ser considerado como bueno y se explica por la disminución de la relación de árido/cemento con el aumento de las proporciones de cerámica, el uso de áridos reciclados secados al aire que reduce la relación efectiva agua/cemento, el proceso de mezclado, el uso de cemento con escorias, la actividad puzolánica de los finos de RCD, la rugosidad superficial de los áridos reciclados y su capacidad para devolver parte del agua absorbida durante el mezclado, produciendo un efecto de curado interno que mejora el vínculo de la ITZ.

Propiedades del hormigón endurecido: Durabilidad

En términos de permeabilidad al oxígeno, los hormigones reciclados exhibieron valores inferiores (hasta 15%) y superiores (hasta 71%) a los del hormigón convencional, siendo la porosidad la principal responsable en lugar del contenido de cerámica. Sin embargo, los resultados de todas las muestras sugirieron un buen comportamiento.

La penetración de CO_2 fue evaluada para un ambiente natural exterior (0,06%) y uno acelerado (10%) en las fases I y II respectivamente. Los hormigones reciclados de la fase I exhibieron una peor durabilidad después de 1 año de exposición (alrededor de 70-75%) debido al aumento del tamaño de poro mayor que 0,067 micras. A pesar de observarse un descenso del 30% en la profundidad de penetración tras un 1 mes de exposición acelerada, ya que la menor relación agua/cemento y la mayor alcalinidad de los hormigones reciclados dificultaron la penetración, estos valores aumentaron progresivamente (hasta un 5% superior a II-CC) después de 3 meses.

El hormigón reciclado mostró una absorción de agua por capilaridad inferior al hormigón convencional debido a la mejor calidad de la matriz de cemento, es decir, menor relación agua/cemento y refinamiento poroso. Por lo tanto, los valores de absorción primarios fueron más bajos que los del hormigón convencional, oscilando entre 22% y 63% para contenidos de cerámica crecientes.

El ensayo de absorción de agua bajo vacío permitió la evaluación de la porosidad accesible. Los resultados indicaron que la porosidad capilar accesible fue mayor, entre 10% y 40%, en los hormigones reciclados en función del contenido de cerámica, lo que sugirió un peor rendimiento de los hormigones reciclados.

Respecto a la penetración de agua bajo presión, los hormigones reciclados generalmente exhibieron un mejor comportamiento que el convencional. La máxima profundidad de penetración se redujo un máximo de 32% y 56% en la fase I y II, respectivamente. En términos de profundidad media, se observaron reducciones de 36% y 62% para I-RC-L(S) y I-RC-M(S), mientras que la muestra I-RC-H(S) mostró un profundidad un 17% mayor. No obstante, los resultados garantizaron una durabilidad suficiente para clases ambientales IIIa, IIIb, IV, Qa, E, H, F y Qb.

El deterioro del hormigón debido a ciclos hielo-deshielo en presencia de sales de deshielo mostró que los hormigones reciclados se comportan peor que el hormigón convencional. Sin embargo, las velocidades de pulso ultrasónico (VPU) al final de la prueba en la fase I indicaron su buena calidad a pesar de que las pérdidas de masa fueron 13% superiores después de 25 ciclos. En la fase II, la pérdida de masa relativa aumentó hasta un 26% sin correlación con el contenido de cerámica pero con una mayor incidencia en las superficies de fratasado. Sin embargo, vale la pena comentar que el uso de aditivos mejoraría estos resultados.

En el ensayo de penetración de cloruros, Respecto a la penetración de cloruros, las profundidades de migración fueron más bajas para los hormigones reciclados, lo que conllevó a que el coeficiente de la migración no estacionario fuera un 37%, 25% y 43% menor en las superficies de moldeo de las muestras II-RC-L(S), II-RC-L(B) y II-RC-H(S), y variase hasta un 3%, -19% y -37% en las caras de frasatado de los hormigones II-RC-L(S), II-RC-L(B) y II-RC-H(S), respectivamente. Es así que las superficies de fratasado mostraron valores más altos que la cara de acabado, entre 17% y 56%. El buen comportamiento exhibido se debió a la baja relación agua/cemento efectiva, el cemento con escorias y la actividad puzolánica de los RCD.

Los resultados de resistividad eléctrica se encontraron dentro del rango de los hormigones convencionales (10-100 Ω·m). Mientras que los áridos reciclados mixtos exhibieron una resistividad eléctrica comparable a un hormigón convencional, el hormigón reciclado hecho con áridos cerámicos mostró un valor 7% inferior como consecuencia de una mayor liberación de iones. No obstante, los hormigones convencionales y reciclados presentaron valores de resistividad eléctrica asociados a un mal desempeño contra la corrosión.

Como se mencionó anteriormente, los áridos reciclados son susceptibles de liberar álcalis y pueden aumentar el riesgo de ASR. Sin embargo, ninguno de los áridos reciclados utilizados en esta tesis fue identificado como reactivo pues la variación de la longitud del prisma de hormigón reciclado en una prueba Oberholster durante 20 días fue inferior a 0,10%. Por otra parte, no se apreciaron grietas en la inspección visual de los cilindros de hormigón tras el ensayo. No obstante, cabe señalar que estos resultados se produjeron favorecidos por el uso de cementos con escorias.

Por último, la resistencia a los ácidos orgánicos fue probada mediante una mezcla de solución de ácido láctico-acético simulando las condiciones típicas de un alojamiento de animales y/o silo. Mientras que la reducción máxima en el radio fue inferior a 2 mm para el hormigón convencional, ninguno de los hormigones reciclados presentó una disminución superior a 1 mm. La degradación fue progresiva durante los 6 ciclos y terminó con un comportamiento un 46%, 63%, 69% y 87% mejor para porcentajes cerámicos crecientes. Análogamente, la rugosidad superficial al final del ensayo resultó entre un 40% y 74% más suave a medida que aumentó el contenido de cerámica incorporado en el peso total de los áridos. La mejora del rendimiento del hormigón frente a los ataques ácidos se explica por el efecto beneficioso de los materiales puzolánicos, la presencia de elementos secundarios en la matriz de cemento, la relación agua/cemento efectiva más baja, así como el refinamiento de la red porosa causada por el uso de áridos reciclados.

A modo de resumen, la Figura 10 esquematiza el comportamiento en materia de durabilidad de los hormigones en la segunda fase de la investigación.

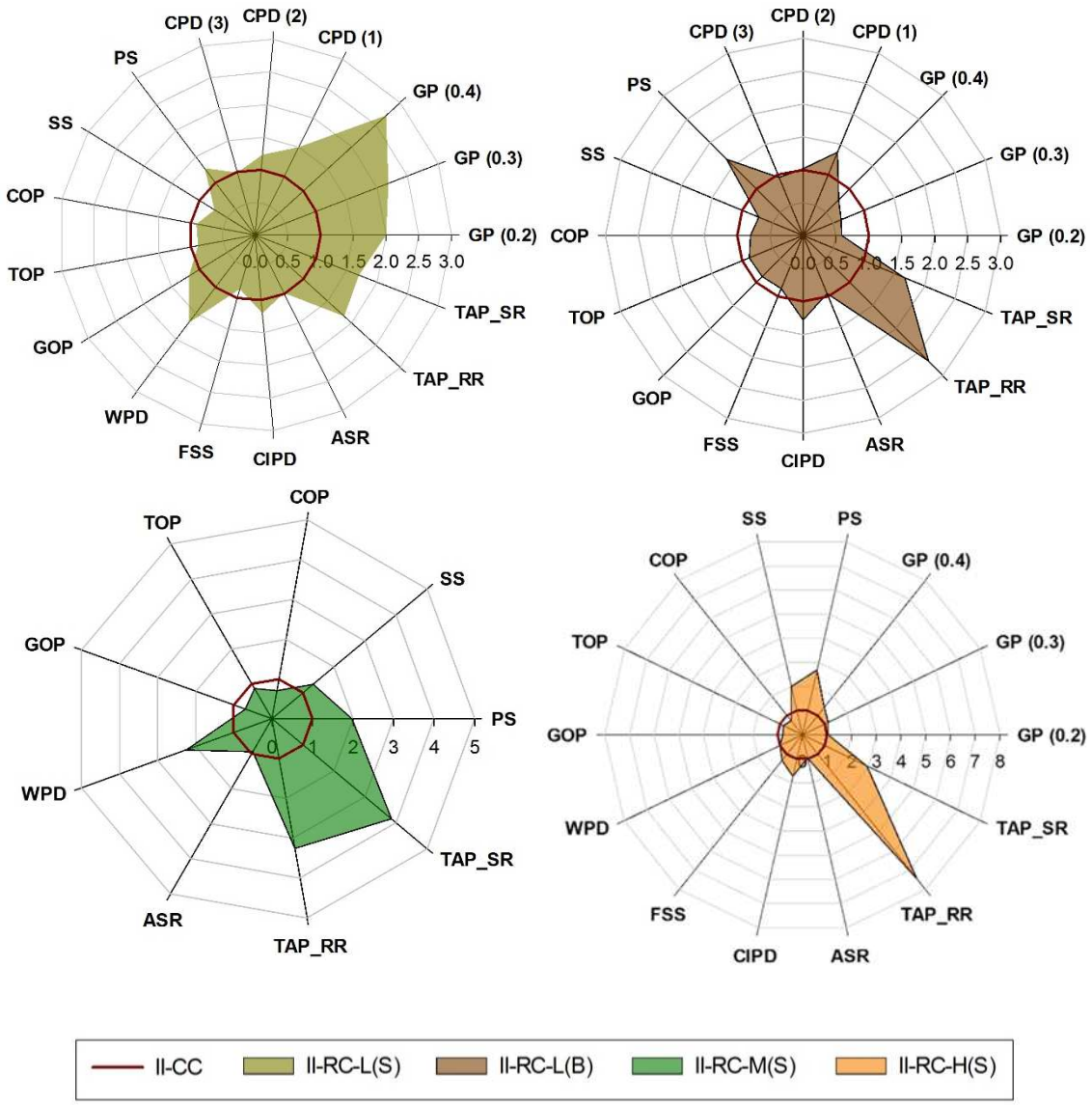

GP: Permeabilidad al O_2 a 0.20, 0.30 y 0.40 MPa
CDP: Profundidad de carbonatación acelerada
PS: Absorción por capilaridad primaria
SS: Absorción por capilaridad secundaria
COP: Poros capilares accesibles
TOP: Porosidad total accesible
GOP: Poros de gel accesibles
WPD: Profundidad de penetración de agua
FSS: Pérdida de masa por hielo-deshielo
ClPD: Profundidad de penetración de cloruros
ASR: Reacción álcali-sílice
TAP_RR: Reducción en radio por ataque ácido
TAP_SR: Textura superficial por ataque ácido

Figura 10: Índices de durabilidad del hormigón elaborado en la fase II

Desempeño medioambiental

A pesar de la vasta relevancia del sector de la construcción en la economía de los países desarrollados, cada vez es más aparente que el futuro desarrollo de la sociedad debe estar limitado por la capacidad de carga del planeta y no en las posibilidades técnicas y económicas de la humanidad. Las cifras apuntan a que la industria de la construcción consume aproximadamente un 50% de los recursos naturales, un 40% de la energía y es responsable de la producción de un 34% de los residuos de la Unión Europea.

Los niveles de consumo del hormigón, lo convierten en el material de construcción más usado en todo el mundo, por lo que los esfuerzos llevados a cabo para paliar el daño medioambiental causado por este subsector tienen especial repercusión a nivel global. La producción de 1 tonelada de áridos y cemento ocasiona un consumo de agua alrededor de 500 litros, a los que han de sumarse otros 300 litros aproximadamente para la elaboración de 1 metro cúbico de mezcla de hormigón. Además, la producción de 1 tonelada de cemento requiere alrededor de 1.46 toneladas de materias primas como piedra caliza, arcilla, pizarra, marga, yeso y adiciones minerales. Sin embargo, las emisiones de dióxido de carbono (CO_2) y otros gases de efecto invernadero son los mayores causantes del daño medioambiental de su manufactura. Expertos apuntan a que la fabricación de cemento, en especial del clínker, es responsable por el 5% de las emisiones de CO_2 y el 3% de los gases de efecto invernadero. Respecto al consumo de materias primas no renovables, al representar un 80% en peso de los componentes del hormigón, los volúmenes requeridos de arena y grava para satisfacer las necesidades mundiales los ponen en riesgo de agotamiento si no se producen cambios en la tendencia actual de su utilización. Finalmente, la producción de residuos en la fase de manufactura puede alcanzar máximos de un 5-9% de la producción total de hormigón, pudiendo ser limitada a un 0.45% con los controles adecuados. No obstante, es la producción de residuos al final de su vida útil la que ocasiona un mayor perjuicio medioambiental, no tanto por su poder contaminante, sino por los grandes volúmenes generados (alrededor de 821 millones de toneladas).

Es así que, desde el punto de vista medioambiental, el uso los RCD en la producción de hormigones reciclados está considerado como una de las mejores opciones en el camino hacia la sostenibilidad del sector de la construcción ya que reduce el consumo de energía y recursos naturales no renovables, a la vez que disminuye la necesidad del vertido de residuos al final de la vida útil de edificios e infraestructuras. Sin embargo, el uso de áridos reciclados procedentes de RCD en la manufactura de hormigón solo representar un 5% del total de áridos usados en la Unión Europea.

El uso de técnicas como el análisis del ciclo de vida (ACV) resulta una herramienta indispensable en el análisis de los impactos ambientales asociados con la reutilización de los RCD como áridos en la manufactura de hormigón. Los límites del estudio se establecieron en la cuna y la puerta del proceso, lo que corresponde a la producción de materias primas -es decir, extracción y proceso de áridos naturales, el procesamiento de RCD en áridos reciclados, la explotación del agua y la producción de cemento-, su transporte a la planta de hormigón y las operaciones de transformación.

Tanto para el inventario como para el análisis, se emplearon la base de datos Ecoinvent y el software SimaPro LCA, aunque se hicieron las modificaciones precisas para la situación española. Sin embargo, inventarios específicos fueron creados para la producción de áridos reciclados incluyendo las cargas ambientales de la generación y gestión de los RCD y los créditos ambientales alcanzados al evitar las operaciones de vertido y la extracción de recursos naturales.

En términos generales, salvo la emisión de partículas que aumentó casi un 50% cuando se utilizaron los áridos reciclados debido a la generación de polvo en el manejo de los RCD, la producción de hormigón reciclado supone una mejora medioambiental. El beneficio más notable es el ahorro en agua (33% de media) y la disminución en la energía acumulada (8% de media). En términos de emisiones, el NOx presenta la reducción más alta (10% de media) debido a la reducción en el consumo de combustible como resultado de los impactos evitados, y las emisiones de CO_2 son las menos afectadas (3%) ya que el principal responsable de su generación, es decir, la producción de cemento, se mantuvo constante para todas las composiciones de hormigón.

La principal ventaja de utilizar hormigón reciclado hecho de áridos secundarios de RCD se encuentra en la reducción del potencial de agotamiento de ozono y el agotamiento de los recursos abiótico de acuerdo a la evaluación CML 2001 y la disminución en el daño a los recursos minerales y fósiles según el Eco-indicador 99. A pesar de estas ventajas, cuando se emplea Eco-indicador 99, el hormigón reciclado presentó un peor comportamiento ambiental en términos de daños a la salud humana. Sin embargo, dado que la generación de partículas es el parámetro responsable de esta deficiencia, podrían aplicarse algunas medidas técnicas con el fin de prevenir o reducir las emisiones.

En conclusión, esta investigación demostró que los áridos reciclados procedentes de RCD con diferentes contenidos de cerámica presentan propiedades físicas y mecánicas aceptables de acuerdo con la actual normativa española. A pesar de que estos áridos presentaron una menor calidad en comparación con la grava natural, su nivel de rendimiento no los excluye definitivamente como áridos secundarios para la producción de hormigón, ya que su uso como una mezcla con materiales vírgenes les permite cumplir con los requisitos más estrictos que resultan para aplicaciones de alto nivel, tales como la fabricación de hormigón. Por ejemplo, una mezcla de 50% de grava natural y la fracción gruesa de los áridos reciclados mixtos y cerámicos produjeron hormigones reciclados con buenas propiedades físicas, mecánicas y de durabilidad, así como económicamente viables y ambientalmente responsables.

Table of contents/Índice

ABBREVIATIONS AND ACRONYMS

ACI	American concrete institute
ADP	Abiotic depletion
AP	Acidification
ASR	Alkali-silica reaction
BFS	Blast-furnace slag
BSE	Backscattered electron
$C\bar{S}H_2$	Gypsum
C_2S	Belite
C_3A	Aluminate
C_3S	Alite
$C_3S_2H_3$	Calcium silicate hydrate
C_4AF	Ferrite
C_4AH_{13}	Tetracalcium aluminate hydrate
$C_6AFS_2H_8$	Hydrogarnet
$C_6A\bar{S}_3H_{32}$ or AFt	Ettringite
CDW	Construction and demolition wastes
CEDEX	Spanish centre for studies and experimentation of public works
CFC	Chlorofluorocarbon
CH	Calcium hydroxide
CH	Switzerland
CML	Centre of environmental science of Leiden University
COPRO	Impartial organization for the control of construction products
CTE	Coefficient of thermal expansion
CUR	Dutch committee for applied research
DAQ	Data acquisition system
DB	Dichlorobenzene
DVR	Direct volume replacement
DWR	Direct weight replacement
EBC	European building confederation
EDF	Expected durability factor
EDS	Energy dispersive spectroscopy
EHE-08	Spanish Code on structural concrete
EMV	Equivalent mortar volume
EP	Eutrophication
EPD	Environmental product declarations
ERMCO	European ready mixed concrete organization
ES	Spain
EU	European Union
FAETP	Fresh water aquatic ecotoxicity
FI	Flakiness index
FIB	International federation for structural concrete
GBFS	Ground granulated blast-furnace slag
GERD	Spanish association of managers of construction and demolition wastes
GIS	Geographic information system
GLO	Global
GVA	Gross value added
GWP100	Global warming
HTP	Human toxicity
ICDD	International centre for diffraction data
ITZ	Interfacial transition zone
IUPAC	International union of pure and applied chemistry
LA	Los Angeles test
LA	Low alkali
LCA	Life cycle assessment
LH	Low heat
LOI	Loss on ignition
M_5AH_{13}	Hydrotalcite
MAETP	Marine aquatic ecotoxicity
MIP	Mercury intrusion porosimetry
NACE	Statistical classification of economic activities in the european community
NMVOC	Non-methane volatile organic compounds

OD Oven-dried density
ODP Ozone layer depletion
OPI Oxygen permeability index
PMMA Poly-methyl-methacrylate
POCP Photochemical oxidation
PVC Polyvinyl chloride
RAWA Real-time assessment of water absorption
RCA Recycled concrete aggregates
RDME Relative dynamic modulus of elasticity
RER Europe
RILEM International union of laboratories and experts in construction materials, systems, and structures
SD Saturation degree
SE Sand equivalent
SE Secondary electron
SEM Scanning electron microscopy
SR Sulphate resistant
SSD Saturated surface-dried density
SWOT Strengths, weaknesses, opportunities and threats
TAP Accelerated degradation tests
TEM Transmission electron microscopy
TETP Terrestrial ecotoxicity
TM Triple mixing method
TSMA Two-stage mixing approach
U Unit process
UCTE Union for the co-ordination of transmission of electricity
UEPG European aggregates association
UNEP United nations environment programme
UPV Ultrasonic pulse velocity
WA Water absorption
WBCSD World business council for sustainable development
WF Water footprint
XRD X-ray powder diffraction
XRF X-ray fluorescence

SYMBOLS

a calorimeter calibration constant [J/K/h]
A cross-sectional area [mm^2]
Ac air content [%]
A_p area of the tracing paper sheet [mm^2]
A_{pf} wet area [mm^2]
b calorimeter calibration constant [$J/K^2/h$]
b Van Genuchten parameter [-]
c set-up thermal capacity [J/K]
c_a aggregates thermal capacity [J/kg/K]
c_c cement thermal capacity [J/kg/K]
c_{Cc} container thermal capacity [J/kg/K]
c_w water thermal capacity [J/kg/K]
C_{acc} CO_2 concentration in accelerated conditions [%]
C_b basic creep [µm/mm]
C_{nat} CO_2 concentration in natural conditions [%]
C_{tot} total creep at a certain age [µm/mm]
d minimum aggregate size [mm]
d_1, d_2 lateral dimensions [mm]
d_{ap} average depth of water penetration [mm]
d_i intruded pore diameter [nm]
d_s interplanar spacing [nm]
D diameter [mm]
D maximum aggregate size [mm]
D/d aggregate size ratio [-]
D_{nssm} non-steady-state migration coefficient [10^{-12} m^2/s]
E energy [eV]

- E_a activation energy [J/mol]
- EDF expected durability factor [-]
- E_s secant modulus of elasticity [MPa]
- f_c compressive strength [MPa]
- f_{ck} characteristic compressive strength [MPa]
- f_{cm} average compressive strength [MPa]
- f_{cst} splitting tensile strength [MPa]
- f_{ct} flexural strength [MPa]
- f_{ct} direct tensile strength [MPa]
- F maximum load [N]
- $F(x)$ cumulative particle distribution function (Weibull or Log-logistic) [%]
- g_i p-wave acceleration [m/s^2]
- G gauge length [mm]
- h height of the specimen [m]
- I intensity crossing the circuit [A]
- I_r span [mm]
- k Spectral series constant [eV]
- K constant [m/s]
- K measure of particle size spread [-]
- K_{app} apparent gas permeability coefficient [m^2]
- Kb positive integer as a function of the type of binder and aggregates [-]
- K_c capillary water absorption coefficient [kg/m^2·√s]
- K_{CO2} carbonation rate at certain CO_2 concentration [mm/√years]
- $K_{corr,CO2}$ corrected carbonation rate at certain CO_2 concentration [mm/√years]
- K_r relative gas permeability coefficient [-]
- Ks specific strength ratio [-]
- L length of the specimen [mm]
- L_0 length comparator reading of the reference bar [µm]
- L_i length comparator reading of the specimen at certain age [µm]
- L_m average chord length [mm]
- L_s spacing factor [µm]
- m_a mass of the aggregates [kg]
- m_c mass of the cement [kg]
- m_{Cc} mass of the container [kg]
- m_w mass of the water [kg]
- MD median diameter of intruded pores larger than 4.50 nm [µm]
- M_{dry} mass of the oven dry sample [g]
- M_p mass of the tracing paper sheet [g]
- M_{pf} mass of the wet area reproduction in the tracing paper [g]
- M_{pyk} mass of the pyknometer full of water [g]
- M_{rd} mass of the oven dried aggregates [g]
- M_{sat} mass of saturated aggregates inside the pyknometer [g]
- M_{sat} mass of the vacuum saturated sample weighed in air [g]
- M_{ssd} mass of the saturated aggregates with dry surface [g]
- M_x mass of the sample at certain age [g]
- n_r order of reflection
- N total number of air void chord lengths [-]
- p paste content [%]
- P pressure [N/nm^2 or Pa]
- P_{atm} atmospheric pressure [Pa]
- Ps strength contribution in percentage [%]
- PV total intruded pore volume down to a diameter of 4.50 nm [ml/g]
- q heat production [J/g/h]
- q_{nat} percentage of natural aggregates [%]
- Q cumulative heat production [J/g]
- Q_0 mass prior to the test [kg]
- Q_g gas flow rate [m^3/s]
- Q_n mass at saturation point [kg]
- R universal gas constant [J/mol/K]
- R_a asphalt [%]
- R_a surface roughness [mm]
- R_b ceramic particles [%]
- R_c concrete and mortar [%]
- R_g glass [%]

R_n contribution to strength of the natural aggregates [MPa]
R_r contribution to strength of the recycled aggregates [-]
R_s electrical resistance of the sponges [Ω]
R_u unbound natural aggregates [%]
S_a autogenous shrinkage before the loading [µm/mm]
SD saturation degree of the sample [%]
SL sampling length [mm]
S_t total shrinkage before the loading [µm/mm]
S_x shrinkage at certain age [µm/mm]
t exposure period [s, h, year]
t_e equivalent age [h]
T temperature [°C]
T_a total chord length of air voids [mm]
T_c temperature under semi-adiabatic conditions [K]
T_p total chord length of paste [mm]
T_r temperature of reference [K]
T_{tot} total surface distance traversed [mm]
U applied voltage [V]
v p-wave velocity [m/s]
v_i asymptotic p-wave velocity [m/s]
V potential difference between electrodes [V]
w/c water/cement ratio [%],
WA_{24} 24 hours water absorption [%]
W_d weight of the dried specimen weighed in air [g]
W_s weight of the saturated specimen [g]
W_w weight of the saturated specimen measured under water [g]
x percentage of particles passing a specific sieve [%]
x_d average penetration depth [mm]
X_1 gypsum [%]
X_2 other impurities [%]
$y(x)$ profile height function [mm]
Z atomic number [-]

α heat loss [J/K/h]
α_s specific surface [mm^{-1}]
δ standard deviation [-]
ΔT temperature rise [K]
Δt time interval [h]
ε_a average strain on the last loading[-]
ε_c strain caused at a certain load [‰]
ε_{c1} peak strain [‰].
ε_e effective porosity [-]
ε_p average strain on the last unloading [-]
ε_s strain in the sealed specimen under load at a certain age [µm/mm]
ε_u strain in the unsealed specimen under load at a certain age [µm/mm]
γ mercury surface tension of [N/nm]
η dynamic viscosity [Pa·s]
φ_T open porosity after drying at a certain temperature [%]
λ mean particle size [mm]
λ_x X-ray wavelength [nm]
μ empty calorimeter thermal capacity [J/kg/K]
θ angle of X-ray incidence [º]
θ_i mercury intrusion angle [º]
ρ density [kg/m^3]
ρ_a apparent specific gravity [Mg/m^3]
ρ_c electrical resistivity [Ωm]
ρ_{rd} dry bulk specific gravity [Mg/m^3]
ρ_{ssd} saturated with surface dried bulk specific gravity [Mg/m^3]
ρ_w density of water [kg/m^3]
σ shielding constant [-]
σ/E elastic strain [-]
σ_a stress corresponding to one third of the compressive strength [MPa]
σ_c/f_{cm} relative stress [-]
σ_p stress corresponding to the preload stress [MPa]

Chapter 1

General introduction

1. PROBLEM STATEMENT

Although human activities have always had an impact on the environment, after the industrial revolution, the technological development achieved has not only meant that humankind has a greater capacity for economic growth but also a greater negative impact on the environment.

In the last 50 years, a growing social concern about the protection and conservation of the environment has developed among worldwide society. Generally, the book "Silent spring" by Rachel Carson (1962) is considered as the catalyst of the awakening of the environmental awareness in the general public. In any case, the 1970s was a crucial time period in the development of the environmental conscience. Firstly, the creation of the Club of Rome and the subsequent publication of their environmental concerns on the limited nature of the natural resources in the so-called Meadows Report (Meadows et al., 1972) played an important role highlighting the interdependences between environment and economy despite all the criticism received regarding the adopted assumptions and methodologies. And later that same year, the celebration of the United Nations Conference on the Human Environment was the first sign of worldwide recognition that the protection and improvement of the environment is a major issue affecting the human well-being and the economic development.

Nonetheless, the major milestone in this regard occurred in the late 1980s by the publication of the Brundtland report (World Commission on Environment and Development, 1987) that defined the concept of sustainable development as the forms of progress that meets the needs of the present without compromising the ability of future generations to meet their own needs. Despite this definition has been criticised due to its ambiguity (Wackernagel and Rees, 1996; Mawhinney, 2002), it is unequivocally, the most popular explanation for sustainable development and represents a shift in the understanding of the relationship between mankind and environment (Hopwood et al., 2005).

Although the traditional representation of the sustainable development concept involves three circles of the same size corresponding to the so-called pillars of sustainability, i.e. environment, economy and society, interlocked in a symmetrical interconnection, the conceptual scheme shown in Figure 1.1 builds upon the typical depiction in order to offer a more comprehensive vision of the real extension of the key measures across the environmental, economic and social spheres that should be adopted to achieve the sustainable development.

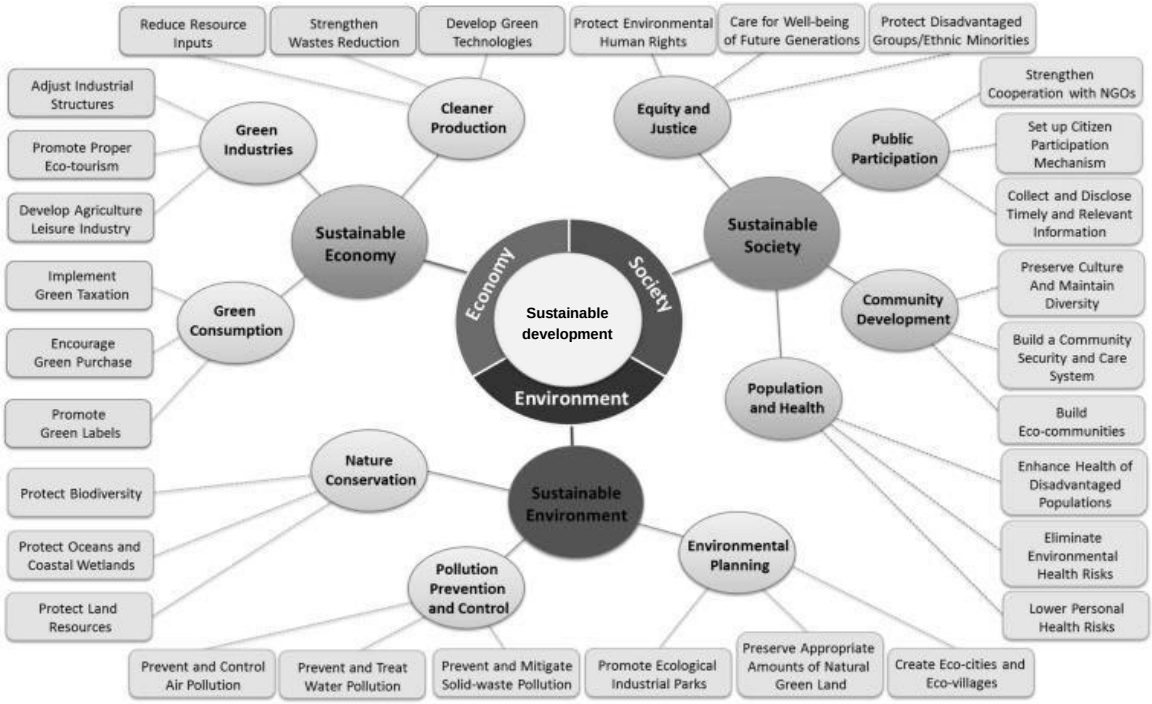

Figure 1.1: Conceptual scheme of the three pillars of sustainable development (Li et al., 2015)

The role of industry in the growth of modern society and economy is indisputable, as is its contribution to the degradation of the environment. The notion of sustainable development is leading to a fundamental reassessment of the contribution that industries have beyond economic aspects such as profits and sales. For example, the application of the principles of sustainable development in the construction sector has resulted in the creation of the term of sustainable construction to reflect that the built environment should be generated and maintained under social and ecological principles (Kibert, 1994).

While the typical archetype of construction is based upon achieving the maximum quality at the minimum cost and time, the implementation of the sustainability concept has led to the development of a new paradigm of construction which includes aspects such as the avoidance of negative environment impacts, the resource efficiency and the human satisfaction (Figure 1.2).

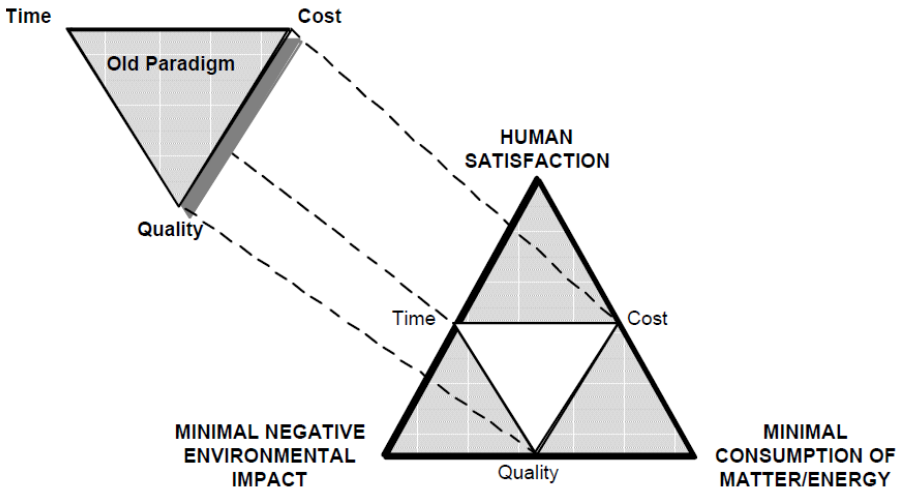

Figure 1.2: New paradigm of construction (Vanegas et al., 1996)

The construction sector has a great relevance in the growth of Europe's economic and social activities. Despite the effects of the last economic crisis, the European construction sector generates an annual turnover of around € 1600 billion of euros and contributes around 10% of the gross domestic product (GPD) in the European Union, with the construction of buildings (residential and non-residential) accounting for 78% of the production output and the remaining 22% corresponding to the construction of civil engineering works (e.g. railways, roads, bridges, airport runways, dams), and provides 13 million direct jobs in around 3 million enterprises (EBC, 2015).

By contrast, the construction industry is not an environmentally friendly activity, indeed it is a major contributor in the degradation of the environment (Bossink and Brouwers, 1996). Amongst its negative impacts, land depletion and deterioration, energy consumption, solid waste generation, dust and gas emission, noise pollution, and consumption of non-renewable natural resources could be cited (Ofori, 1992). In fact, the European construction industry is the largest consumer of raw materials as it exhausts more than the 50% of the total European natural resources (Schultmann et al., 2010). For instance, the European Aggregates Association (UEPG, 2015) reported that the annual demand of aggregates in the European Union is up to 2.70 billion tonnes, being aggregates directly extracted from the earth lithosphere (roughly 95%) and recycled aggregates (5%), of which 45% end up as raw materials in the concrete production (Figure 1.3). Despite that no signs of a worldwide shortage of sand and gravel have been perceived yet, some regions (e.g. Sweden) have already reported some scarcity (EEA, 2008) and the United Nations Environment Programme (UNEP, 2014) has alerted of the actual depletion risk that the continued trend in the consumption of aggregates could cause.

Furthermore, the construction industry is the economic activity with the highest rate of waste generation in the European Union, accounting for one third of the total waste generated, which represented 821 million tonnes in 2012 (Eurostat, 2012). Moreover, the waste generation problem also exacerbates the depletion of natural resources since the current trends of management mainly entail the disposal of waste in landfills.

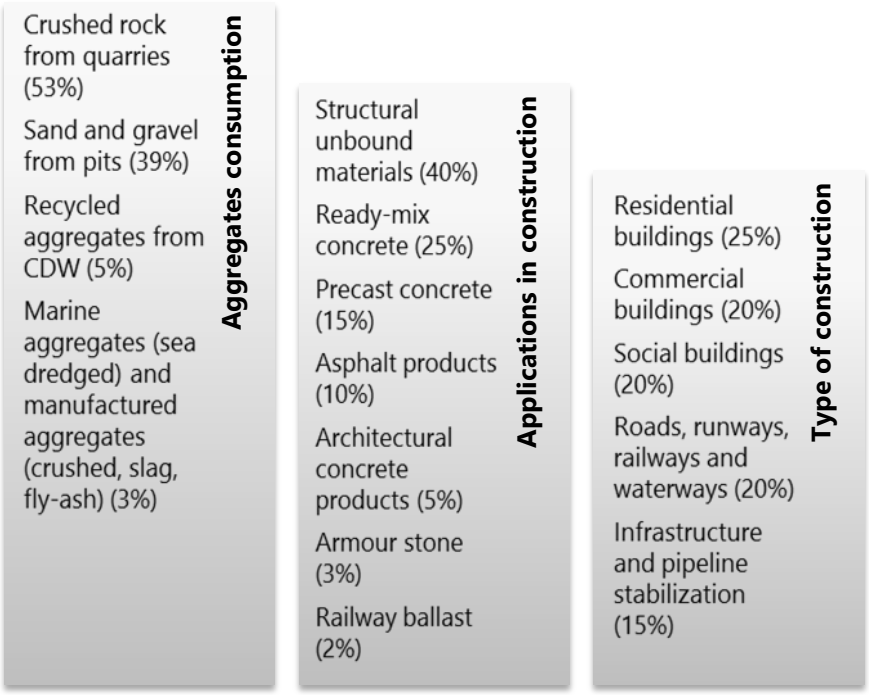

Figure 1.3: European aggregate sector in 2013-2014 (UEPG, 2015)

Experts consider the overconsumption of resources and the elevated generation of wastes as two of the most important environmental challenges of the 21st century. Traditionally, natural resources and wastes are found, respectively, at the start and ending point of the linear model of production, i.e. the material life cycle, which encourage the take-use-dispose attitude responsible for the problems in the first place. Hence, the European Union has proposed the adoption of a circular economy model in order to transform the production chains and consumption habits by means of turning waste into resources in order to close the production loop (European Commission, 2014). Under this circularity principle, the resources stay within the limits of the economy during several life cycles since they can be repetitively used at the end of each lifespan. Then, the overall balance is the use of fewer natural resources to produce the same output, which is the core of the resource efficiency, and a disruption in the relationship between raw material use and economic output, also known as decoupling (Van Ewijk and Stegemann, 2014).

Given the level of consumption and wastage, the idea of closing the production loops results particularity useful among construction activities to alleviate their pressure on the carrying capacity of the environment and contribute to a more sustainable future. Figure 1.4 illustrates a closed cycle of construction materials, in which the "materials" resulting from the deconstruction or demolition activities at the end of life of a building are reincorporated in the manufacture of new products, avoiding both the waste disposal and the use of raw materials.

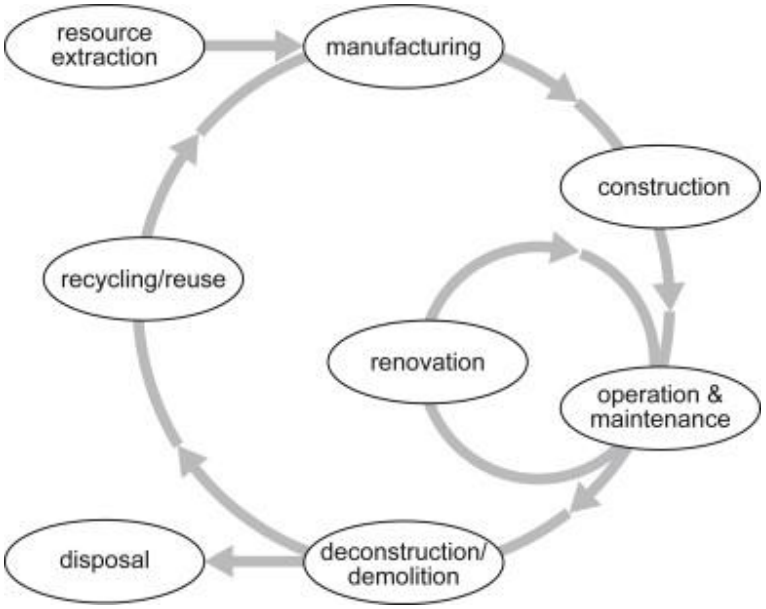

Figure 1.4: Construction materials closed cycle (Melià et al., 2014)

Among construction materials, estimates indicate that concrete is the most employed material worldwide with around 1 tonne per inhabitant and year (Van den Heede and De Belie, 2012). For instance, in 2013, the total production of concrete, both ready mix and precast, was estimated as 338 million cubic meters in Europe (ERMCO, 2014). Up to 45% of the aggregates employed in Europe are used in concrete and since this materials represents 80% by mass of the total weight of a concrete structure, the concrete production consumes around 1.2 billion tonnes of concrete in Europe (UEPG, 2015). Both facts made concrete the perfect receptor of large quantities of residual products as recycled aggregates which concurrently solves the waste generation problem and reduces the consumption of natural resources (Damtoft et al., 2008). Unquestionably, this measure incorporates a sustainability aspect to the production of recycled concrete, which also could be considered as an eco-efficient material, since the final product satisfies the human necessities at a competitive price while reducing the environmental impacts resulting from its production (Keffer et al., 1999).

In the path towards the sustainability in the construction sector, several studies have been carried out to assess the feasibility to employ different industrial wastes or by-products (glass (Topçu and Canbaz, 2004; de Castro and de Brito, 2013), plastic (Siddique et al., 2008), tyres (Bignozzi and Sandrolini, 2006; Bravo and de Brito, 2012)…) in the concrete manufacture. However, over the last years, the recycling potential of construction and demolition waste (CDW) has become the main target of interest as it concurrently solves the two problems of the construction industry, namely the resource intensiveness and the waste generation through the life cycle of buildings and infrastructures.

Numerous studies have investigated the possibilities of using recycled aggregates from CDW in concrete mixes as total or partial replacement of the natural coarse aggregates in order to prove this practice as technically and economically viable and environmentally responsible for a range of concrete applications.

However, the majority of them have been focused on the use of aggregates recovered from concrete rubble (Limbachiya et al., 2000; Gómez-Soberón, 2002; Lin et al., 2004; Tabsh and Abdelfatah, 2009; Fathifazl et al., 2011; Gokce et al., 2011; Ismail and Ramli, 2013, 2014; Manzi et al., 2013; Mazzotti et al., 2013; Safiuddin et al., 2013) since this type of recycled aggregate presents properties similar to those of virgin materials and most countries have already specifications allowing and regulating their use.

Nonetheless, in Spain, recycled concrete aggregates only represent up to a 30% of the total production at CDW management plants, while the remaining 70% corresponds to recycling aggregates containing varying percentages of ceramic wastes (mixed and ceramic recycled aggregates) (Güell-Ferré et al., 2012). The explanation for this production scheme could be found both in the typical building practice of the country, which is also common in other Mediterranean countries such as Portugal, Italy or Greece (de Brito et al., 2005), and the implanted waste management systems. On the one hand, the Spanish typical building constructive practice is based upon concrete materials in conjunction with ceramic materials; thus, the resulting CDW at the end of life of a building includes high percentages of brick, tiles and other ceramic materials. Hence figures up to 54% of ceramic waste are common in the CDW composition (Spanish Ministry of Environment, 2001), which is well above the 30% average for the European Union (Böhmer et al., 2008). On the other hand, the current regulations regarding CDW management, namely Royal Decree 105/2008 (Spanish Ministry of Presidency, 2008), do not establish the requirement for on-site sorting unless it is forecasted that more than 80 tonnes of concrete rubble or 40 tonnes of masonry rubble are going to be generated, in which case this fraction is separately collected. Therefore, the most common situation entails the CDW management plant receiving mixed CDW that are not subjected to further sorting and end up as mixed recycled aggregates.

The aforementioned figures convey the importance of the treatment and recycling of this kind of waste. Nowadays, mixed and ceramic recycled aggregates are used as unbound materials in earthworks, backfilling and road constructions, which constitutes a down-cycling of the material in lower-grade technical application. While down-cycling is still an environmental improvement, taking advantage of the full potential of recycled materials is more in line with the sustainability concept and high-grade applications should be sought for the reutilization of recycled aggregates. Thus, some investigations have been developed to first describe the properties of mixed and ceramic recycled aggregates and verify the influence that has their incorporation in the concrete production (de Brito et al., 2005; Correia et al., 2006; Gomes and Brito, 2008; Mas Gracia and Cladera Bohigas, 2009; Pacheco-Torgal and Jalali, 2010a, 2010b; Agrela et al., 2011; Ihobe and CEDEX, 2011; Yang et al., 2011; Mas et al., 2012a, 2012b; Geraldes, 2013; Medina et al., 2014; Rodríguez-Robles et al., 2014; Sadek and Nouhy, 2014). Nonetheless, mixed and ceramic recycled aggregates are still considered with suspicion as a reliable source of secondary aggregates for the concrete manufacture, their use may be acceptable as a blend of virgin and recycled aggregates in order to meet more strict requirements resulting from high level applications such as concrete for structural purposes. Thus, further research on the feasibility of the use of recycled aggregates from CDW incorporating varying ceramic wastes percentages in the concrete manufacture is necessary to reduce the uncertainty linked to a future field application besides unbound material.

2. SCOPE AND OBJECTIVES

The general objective of the present thesis is twofold; first, the analysis of the engineering properties of both the commercially available recycled aggregates from CDW with varying percentages of ceramic waste and, secondly, the assessment of recycled concrete mixtures made with a partial substitution of the natural coarse aggregates by the aforementioned recycled aggregates as directly obtained from the CDW management plant and without any specific treatment that modifies their characteristic properties when compared with a conventional concrete mixture used as a reference. A 50% replacement ratio has been selected since several researchers have suggested this value as the substitution limit in which the recycled concrete has comparable physical and mechanical properties to a conventional mixture without the need to drastically increase the cement content (González-Fonteboa and Martinez-Abella, 2005; Gomes and Brito, 2008; González-Fonteboa and Martínez-Abella, 2008).

From a quality point of view, the characterization of the recycled aggregates becomes an important objective. Despite the lack of standardization for mixed and ceramic recycled aggregates for the manufacture of structural concrete in Spain, the selected secondary materials were analysed according to the requirements set in the Spanish Code on structural concrete (EHE-08) (Permanent Commission on Concrete, 2008) in order to evaluate their physical, chemical, mineralogical and microstructural properties as a means to justify the feasibility of this type of recycled aggregates from CDW in structural concrete applications.

Lately, in order to assess the influence of such substitution several concrete mixed were batched conforming to separate research phases. In the first stage of the investigation, a conventional concrete mix and three recycled concrete mixtures made with recycled aggregates collected from Spanish CDW management plants was planned. The tests performed on these samples were focused on physical, mechanical and microstructural properties of the fresh and hardened concrete, although some durability properties were analysed in accordance to the equipment possibilities. In addition, an environmental performance analysis of the concrete mixtures conforming this research phase was carried out by means of a life cycled assessment (LCA) in order to evaluate the benefits of the incorporation of recycled coarse aggregate in the concrete manufacture. The second phase of the investigation coincides with the start of the joint PhD agreement between the University of León and Ghent University, which made it possible to expand the number of characterization tests, as well as the incorporation of a forth mixed recycled aggregate and the subsequent recycled concrete. Thus, four recycled concrete mixtures where compared with a conventional concrete mixture designed as reference for this research phase. In addition to some tests already carried out in the previous stage, the investigation included calorimetric and ultrasonic wave transmission tests and was focussed on the effect that the replacement of the natural coarse aggregates by the mixed and ceramic recycled aggregates has on the durability and long-term performance of the hardened concrete.

3. STRUCTURE OF THE THESIS

The research works encompassed in this PhD dissertation combine both theoretical and experimental components that have been carried out in two universities (Universidad de León and Ghent University) under a joint PhD agreement. Following the clauses of this doctoral contract, the thesis includes a Dutch, English and Spanish summary, and both the table of content and the conclusions are written in English and Spanish.

A general introduction on the topic of the PhD dissertation has been offered in the present chapter focusing on the significance of the research on the reutilization of mixed and ceramic recycled aggregates as an alternative of the natural coarse aggregates in the manufacture of concrete. In addition, Chapter 1 includes the scope and objectives of the investigation.

Since literature review plays a significant role in research, a theoretical background on the CDW and the derived recycled aggregates is presented in chapter 2 involving an examination of the legal framework, an overview of their generation and possibilities for recycling including current challenges and specifications. However, the literature review concerning to the contextualization of the different properties subjected to evaluation in this dissertation was not included in this chapter but placed at the beginning of the corresponding section in order to provide the basis for for justifying the research and the results obtained when compared to the investigations carried out by other researchers.

Chapter 3 describes the procedures and experimental methods employed in the development of the research comprising the PhD thesis. Each research methodology is followed by a statement of the adopted methods, and their applicability and benefits.

In chapter 4, the specific characteristics of the raw materials employed in the manufacture of concrete are explained. Special attention was paid to the selection and definition of the recycled aggregates employed in the research, as well as their characterization according to the current Spanish legislation on natural aggregates for the concrete manufacture, namely the EHE-08 (Permanent Commission on Concrete, 2008). Thus, the testing program on aggregates was comprised of a physical and mechanical characterization (constituents of coarse recycled aggregate, particle size distribution, geometry of coarse aggregates, fines assessment, density and water absorption, mechanical resistance and adhered mortar) in order to prove their suitability as replacement of the coarse natural aggregate in the recycled concrete manufacture. Moreover, a microstructural characterization (X-ray powder diffraction, X-ray fluorescence, scanning electron microscopy, mercury intrusion porosimetry) was performed to achieve a better understanding of the heterogeneity of their origin.

Chapter 5 includes a literature review on the specifics concerning the proportioning of concrete dosages incorporating recycled aggregates, as well as the assumptions and calculations performed in order to proportion the different conventional and recycled concrete mixtures employed for the experimental program of the thesis.

Subsequently, the designed concrete mixtures were tested in order to assess the influence that the replacement of half of the conventional coarse aggregate by mixed or ceramic aggregates has on their behaviour and performance. In chapter 6, the analysis was focus on the fresh state (consistency, air content, bulk density, hydration heat and setting time). Chapter 7 shows the results regarding the microstructure of the different conventional and recycled concrete mixtures by assessing the interfacial transition zone (ITZ) by X-ray scanning microscopy and the porosity through mercury intrusion porosimetry, X-ray scanning microscopy and air void analysis. In chapter 8, the mechanical behaviour of concrete is explained by means of the results arising from compressive, flexural and splitting-tensile strength tests, the determination of the elasticity modulus and the stress-strain behaviour, and the shrinkage and creep properties under different circumstances. The influence of the replacement on the durability properties of concrete was analysed in chapter 9 by testing the gas permeability, carbonation, water absorption by capillarity and under vacuum, water penetration under pressure, frost resistance, chloride ingress, electrical resistivity, alkali-silica reaction and resistance to organic acids.

Chapter 10 studies the environmental performance of the use of recycled aggregates from CDW with varying percentages of ceramic waste as a partial (50%) substitution of natural coarse aggregates in the manufacture of concrete. The LCA methodology was employed in order to evaluate the benefits that the three concrete mixtures used in phase I of this research have in comparison with the reference concrete mixture.

Finally, chapter 11 gathers the general conclusions obtained from the experimental works carried out in the framework of the present PhD.

Several appendixes have been included at the end of the dissertation in order to provide more detailed information regarding to several issues.

4. REFERENCES

Agrela, F., Sánchez de Juan, M., Ayuso, J., Geraldes, V.L., Jiménez, J.R., 2011. Limiting properties in the characterisation of mixed recycled aggregates for use in the manufacture of concrete. *Construction and Building Materials* 25 (10): 3950–3955.

Bignozzi, M.C., Sandrolini, F., 2006. Tyre rubber waste recycling in self-compacting concrete. *Cement and Concrete Research* 36 (4): 735–739.

Böhmer, S., Moser, G., Neubauer, C., Peltoniemi, M., Schachermayer, E., Tesar, M., Walter, B., Winter, B., 2008. Aggregates case study (No. 150787-2007 F1SC-AT). Institute for Prospective Technological Studies, Vienna, Austria.

Bossink, B.A.G., Brouwers, H.J.H., 1996. Construction waste: quantification and source evaluation. *Journal of Construction Engineering and Management* 122 (1): 55–60.

Bravo, M., de Brito, J., 2012. Concrete made with used tyre aggregate: durability-related performance. *Journal of Cleaner Production* 25: 42–50.

Carson, R., 1962. Silent spring. Houghton Mifflin ; Riverside Press, Boston; Cambridge, Mass.

Correia, J.R., Brito, J. de, Pereira, A.S., 2006. Effects on concrete durability of using recycled ceramic aggregates. *Materials and Structures* 39 (2): 169–177.

Damtoft, J.S., Lukasik, J., Herfort, D., Sorrentino, D., Gartner, E.M., 2008. Sustainable development and climate change initiatives. *Cement and Concrete Research*, Special Issue: The 12th International Congress on the Chemistry of Cement. Montreal, Canada, July 2007 38 (2): 115–127.

de Brito, J., Pereira, A.S., Correia, J.R., 2005. Mechanical behaviour of non-structural concrete made with recycled ceramic aggregates. *Cement and Concrete Composites* 27 (4): 429–433.

de Castro, S., de Brito, J., 2013. Evaluation of the durability of concrete made with crushed glass aggregates. *Journal of Cleaner Production* 41: 7–14.

EBC, 2015. Annual report 2014-2015 of the European Building Confederation. European Building Confederation, Brussels, Belgium.

EEA, 2008. Effectiveness of Environmental Taxes and Charges for Managing Sand, Gravel and Rock Extraction in Selected EU Countries. European Environment Agency, Copenhagen, Denmark.

ERMCO, 2014. European ready mixed concrete industry statistics based on the production data on 2013. European Ready Mixed Concrete Organization, Brussels, Belgium.

European Commission, 2014. Towards a circular economy: A zero waste programme for Europe (COM 398(2014)). European Commission, Brussels, Belgium.

Eurostat, 2012. European Statistics. Statistical Office of the European Communities.

Fathifazl, G., Ghani Razaqpur, A., Burkan Isgor, O., Abbas, A., Fournier, B., Foo, S., 2011. Creep and drying shrinkage characteristics of concrete produced with coarse recycled concrete aggregate. *Cement and Concrete Composites* 33 (10): 1026–1037.

Geraldes, V.L., 2013. Study on non-structural recycled concretes with mixed recycled aggregate: Mechanical properties and expansion due to sulphates [in Spanish]. Universidad Politécnica de Madrid, Madrid, Spain.

Gokce, A., Nagataki, S., Saeki, T., Hisada, M., 2011. Identification of frost-susceptible recycled concrete aggregates for durability of concrete. *Construction and Building Materials* 25 (5): 2426–2431.

Gomes, M., Brito, J. de, 2008. Structural concrete with incorporation of coarse recycled concrete and ceramic aggregates: durability performance. *Materials and Structures* 42 (5): 663–675.

Gómez-Soberón, J.M.V., 2002. Porosity of recycled concrete with substitution of recycled concrete aggregate: An experimental study. *Cement and Concrete Research* 32 (8): 1301–1311.

González-Fonteboa, B., Martinez-Abella, F., 2005. Recycled aggregates concrete: aggregate and mix properties. *Materiales de Construcción* 55 (279): 53–66.

González-Fonteboa, B., Martínez-Abella, F., 2008. Concretes with aggregates from demolition waste and silica fume. Materials and mechanical properties. *Building and Environment* 43 (4): 429–437.

Güell-Ferré, A., Váquez-Ramonich, E., Varela-Pinto, E., Serna-Ros, P., Martínez-Abella, F., López-Gayarre, F., Barra-Bizinotto, M., Tirado-Alonso, A., Romero-Casado, A., Girbés-Clari, I., 2012. Spanish handbook on recycled aggregates from construction and demolition wastes (CDW) [in Spanish], Fueyo Editores. ed. Madrid, Spain.

Hopwood, B., Mellor, M., O'Brien, G., 2005. Sustainable development: mapping different approaches. *Sustainable Development* 13 (1): 38–52.

Ihobe, CEDEX, 2011. Uses of mixed recycled aggregates from construction and demolition wastes [in Spanish] (Pre-normative investigation). Ihobe.

Ismail, S., Ramli, M., 2013. Engineering properties of treated recycled concrete aggregate (RCA) for structural applications. *Construction and Building Materials* 44: 464–476.

Ismail, S., Ramli, M., 2014. Effect of different moisture states of surface-treated recycled concrete aggregate on properties of fresh and hardened concrete. *International Journal of Civil, Architectural, Structural and Construction Engineering* 8: 65–71.

Keffer, C., Shimp, R., Lehni, M., 1999. Eco-efficiency indicators and reporting. World Business Council for Sustainable Development (WBCSD), London, UK.

Kibert, C.J., 1994. Establishing principles and a model for sustainable construction, in: Proceedings of the First International Conference on Sustainable Construction. Florida, USA, 6–9.

Li, J., Pan, S.-Y., Kim, H., Linn, J.H., Chiang, P.-C., 2015. Building green supply chains in eco-industrial parks towards a green economy: Barriers and strategies. *Journal of Environmental Management* 162: 158–170.

Limbachiya, M.C., Leelawat, T., Dhir, R.K., 2000. Use of recycled concrete aggregate in high-strength concrete. *Materials and Structures* 33 (9): 574–580.

Lin, Y.-H., Tyan, Y.-Y., Chang, T.-P., Chang, C.-Y., 2004. An assessment of optimal mixture for concrete made with recycled concrete aggregates. *Cement and Concrete Research* 34 (8): 1373–1380.

Manzi, S., Mazzotti, C., Bignozzi, M.C., 2013. Short and long-term behavior of structural concrete with recycled concrete aggregate. *Cement and Concrete Composites* 37: 312–318.

Mas, B., Cladera, A., Bestard, J., Muntaner, D., López, C.E., Piña, S., Prades, J., 2012a. Concrete with mixed recycled aggregates: Influence of the type of cement. *Construction and Building Materials* 34: 430–441.

Mas, B., Cladera, A., del Olmo, T., Pitarch, F., 2012b. Influence of the amount of mixed recycled aggregates on the properties of concrete for non-structural use. *Construction and Building Materials* 27 (1): 612–622.

Mas Gracia, B., Cladera Bohigas, A., 2009. Effect of the incorporation of mixed recycled aggregate on the properties of non-structural concretes [in Spanish]. *Hormigón y acero* 253: 83–94.

Mawhinney, M., 2002. Sustainable Development: Understanding the Green Debates. Blackwell, Science, Oxford.

Mazzotti, C., Manzi, S., Bignozzi, M.C., 2013. Role of recycled concrete aggregates on the long-term behavior of structural concrete, in: Mechanics and Physics of Creep, Shrinkage, and Durability of Concrete: A Tribute to Zden? K P. Ba Ant: Proceedings of the Ninth International Conference on Creep, Shrinkage, and Durability Mechanics (CONCREEP-9), September 22-25, 2013 Cambridge, Massachusetts. ASCE Publications, 388.

Meadows, D.H., Meadows, D.., Randers, J., Behrens III, W.., 1972. The limits to growth. Universe Books, New York.

Medina, C., Zhu, W., Howind, T., Sánchez de Rojas, M.I., Frías, M., 2014. Influence of mixed recycled aggregate on the physical – mechanical properties of recycled concrete. *Journal of Cleaner Production* 68: 216–225.

Melià, P., Ruggieri, G., Sabbadini, S., Dotelli, G., 2014. Environmental impacts of natural and conventional building materials: a case study on earth plasters. *Journal of Cleaner Production* 80: 179–186.

Ofori, G., 1992. The environment: the fourth construction project objective? *Construction Management and Economics* 10 (5): 369–395.

Pacheco-Torgal, F., Jalali, S., 2010a. Reusing ceramic wastes in concrete. *Construction and Building Materials* 24 (5): 832–838.

Pacheco-Torgal, F., Jalali, S., 2010b. Compressive strength and durability properties of ceramic wastes based concrete. *Materials and Structures* 44 (1): 155–167.

Permanent Commission on Concrete, 2008. Code on structural concrete (EHE-08) [in Spanish]. Spanish Ministry of Public Works, Madrid.

Rodríguez-Robles, D., García-González, J., Juan-Valdés, A., Morán-del Pozo, J.M., Guerra-Romero, M.I., 2014. Effect of mixed recycled aggregates on mechanical properties of recycled concrete. *Magazine of Concrete Research* 67 (5): 247–256.

Sadek, D.M., Nouhy, H.A. El, 2014. Properties of paving units incorporating crushed ceramic. *HBRC Journal* 10 (2): 198–205.

Safiuddin, M., Alengaram, U.J., Rahman, M.M., Salam, M.A., Jumaat, M.Z., 2013. Use of recycled concrete aggregate in concrete: a review. *Journal of Civil Engineering and Management* 19 (6): 796–810.

Schultmann, F., Hiete, M., Kuehlen, A., Ludwig, J., Schulte Beerbuehl, S., Stengel, J., Vannieuwenhuyse, M., 2010. Collection of background information for the development of EMAS pilot reference sectoral documents: The construction sector. French-German Institute for Environmental Research (DFIU), Karlsruhe Institute of Technology (KIT), Karlsruhe, Germany.

Siddique, R., Khatib, J., Kaur, I., 2008. Use of recycled plastic in concrete: A review. *Waste Management* 28 (10): 1835–1852.

Spanish Ministry of Environment, 2001. Resolution of 14 June, that approves the National National Plan of Construction and Demolition Waste 2001-2006 [in Spanish], BOE 166, 25305-25313.

Spanish Ministry of Presidency, 2008. Royal Decree 105/2008, of 1 February, that regulates the production and management of construction and demolition waste [in Spanish], BOE 38, 7724-7730.

Tabsh, S.W., Abdelfatah, A.S., 2009. Influence of recycled concrete aggregates on strength properties of concrete. *Construction and Building Materials* 23 (2): 1163–1167.

Topçu, İ.B., Canbaz, M., 2004. Properties of concrete containing waste glass. *Cement and Concrete Research* 34 (2): 267–274.

UEPG, 2015. A sustainable industry for a sustainable Europe (Annual Review 2013-2014). European Aggregates Association, Brussels, Belgium.

UNEP, 2014. Sand, rarer than one thinks. UNEP Global Environmental Alert Service.

Van den Heede, P., De Belie, N., 2012. Environmental impact and life cycle assessment (LCA) of traditional and "green" concretes: Literature review and theoretical calculations. *Cement and Concrete Composites* 34 (4): 431–442.

Vanegas, J.A., DuBose, J.R., Pearce, A.R., 1996. Sustainable technologies for the building construction industry, in: Proceedings, Symposium on Design for the Global Environment, Atlanta, GA. Atlanta, USA.

Van Ewijk, S., Stegemann, J.A., 2014. Limitations of the waste hierarchy for achieving absolute reductions in material throughput. *Journal of Cleaner Production* (In press): 10.1016/j.jclepro.2014.11.051.

Wackernagel, M., Rees, W., 1996. Our Ecological Footprint: Reducing Human Impact on the Earth. New Society Publishers, Canada.

World Commission on Environment and Development, 1987. Our Common Future. Oxford University Press, Oxford.

Yang, J., Du, Q., Bao, Y., 2011. Concrete with recycled concrete aggregate and crushed clay bricks. *Construction and Building Materials* 25 (4): 1935–1945.

Chapter 2

Theoretical background

1. INTRODUCTION

This chapter presents an overview regarding construction and demolition aggregates (CDW) with a focus on the Spanish situation. Information on the relevant waste legislation in Europe and Spain is provided as a theoretical background to understand the current CDW scenario both in terms of management and field applications. In the first section, the last available figures on generation, composition and recycling rates of CDW are discussed. The second section is centred on the recycled aggregates that could be derived from CDW, examining the treatment process resulting in their production, the recycled aggregate market, the limitations identified in their use, as well as the available instruments to promote the recycling practice, and their application, in particular for concrete manufacturing.

2. CONSTRUCTION AND DEMOLITION WASTES

Any substance or object which the holder discards or intends or is required to discard is considered as a waste if the material is not intended for reuse, obtained as a by-product to be used in another production process without previous transformation, or is a defective product which will be returned (European Parliament and Council, 2008).

Thus, in general, CDW could be regarded as undesirable substances arising from construction, rehabilitation and demolition activities (Kofoworola and Gheewala, 2009).

In Spain, the legal definition employed for this waste stream was set in the Royal Decree 105/2008 as "any type of waste that is generated from construction and demolition works … which consists of activities within the context of construction, demolition, and renovation of any building, road, port, airport, railroad, canal, dam, sports zone, leisure area, or any other type of engineered structure" (Spanish Ministry of Presidency, 2008). In a more detailed manner, CDW could consist of concrete, bricks, tiles and ceramic material, wood, glass, plastic, bituminous mixes, coal, tar, metals and alloys, dirt, contaminated excavation soils, rocks and sewage, insulating materials and construction materials that contain asbestos, and construction materials sourcing from plaster. However, excluded from the CDW definition are non-contaminated earth and stones, and wastes regulated by other specific legislation, such as the Directive 2006/21/EC (European Parliament and Council, 2006).

2.1. WASTE POLICY IN THE EUROPEAN UNION

Despite that the environment was not an explicit objective in the creation of the current European Union (EU) in the 1950s, environmental matters were regulated under economic justifications and from the 1970s the EU has been implementing a wide range of policies aiming to ensure the sensible use of natural resources, to minimise adverse environmental impacts of production and consumption, and to protect biodiversity and natural habitats.

In terms of waste management, the first Directive on Waste (75/442/EEC) was adopted in 1975 (European Council, 1975) to harmonize the waste related laws in the Member States. Since then, EU regulations implemented to address this environmental problem have grown to form a legislative framework that includes both general and specific legislation that address different waste treatment options and several waste streams.

Nowadays, the Waste Framework Directive 2008/98/EC (European Parliament and Council, 2008) establishes a legal context for managing waste in the European Union in order to prevent and/or mitigate the adverse environmental impacts caused by its generation and, in the end, to allow the decoupling between economic growth and waste production. Complementing the general body of waste laws, the European Waste Catalogue (EWC) (European Commission, 2000) conforms a comprehensive classification of different types of waste. For instance, chapter 17 is a collection of waste sourcing from construction and demolition works, including excavated soil.

In terms of waste treatment options, Directive 2000/76/EC (European Parliament and Council, 2000a) regulates the incineration of waste, Directive 2000/59/EC (European Parliament and Council, 2000b) controls the shipment of waste and Directive 1999/31/EC (European Council, 1999) establishes the specifications for the landfilling of materials. Regarding the specific management of different waste streams, only 8 types of waste are specifically regulated (end of life vehicles, electrical and electronic equipment, polychlorinated biphenyls and polychlorinated terphenyls, wastes from the titanium dioxide industry, batteries and accumulators, packaging and packaging waste, sewage sludge for agricultural use and waste oils).

Albeit the lack of specific legislation addressing the waste stream generated from construction and demolition activities, in 1991, the European Union included construction and demolition wastes as one of the six priority waste streams to be assessed in the Priority Waste Stream Programme due to the large volumes generated and their high potential for reuse and recycling. After eight years of work, the CDW project group drafted the renowned Symonds report (Symonds Group Ltd, 1999) analysing the CDW management practices and the associated legislative measures; furthermore, the report presented the first estimates of CDW production and recycling rates in Europe.

Besides the aforementioned regulations, the European Union periodically issues environmental action programmes, which could be dated back to 1972, to set out environmental concerns that are discussed in a broader perspective and serve as proposals for forthcoming regulations. The fifth environmental action program "Towards sustainability" (European Council, 1993) addressed, for the first time, waste management as a key area on the EU environmental agenda. Following this path, the sixth environmental action program "Our future, our hands" (European Parliament and Council, 2000a) defined the need for an efficient use of natural resources in a framework that both protects the environment and conserves the economic prosperity and social development by means of a decoupling of natural resources and waste from economic growth and promoting eco-efficient practices in the industry sector. Nowadays, under the Seventh environmental action program "Living well, within the limits of our planet" (European Parliament and Council, 2013) continues the effort towards a resource-efficient economy through the transformation of wastes into resources.

2.1.1. SPANISH REGULATORY FRAMEWORK

Despite the existence of legislation at supranational level, the primary responsibility for addressing waste-related problems falls into the Member States of the European Union, which are required to comply with the principles and objectives stipulated in EU waste management legislation through transposition into its own legal system. It is interesting to mention that environmental policy is the area with higher number of infringements both in terms of late or incorrect transposition and bad applications. For instance, the last available report on the monitoring of the application of EU policy (European Commission, 2015) showed 322 cases of infringement, which represent a 24% of the total cases, in 2014.

The current framework for waste legislation in Spain, Law 22/2011 (Spanish Head of State, 2011), is in fact an example of this type of transgression, since the EU legislation was transposed into the national legal acquis out of the 12/12/2010 deadline imposed by the EU. It is worth mentioning that this law, as its now repelled predecessor Law 10/1998 (Spanish Head of State, 1998), also contains the legal regulation of contaminated soils, an environmental area not required in the Directive 2008/98/EC (European Parliament and Council, 2008). In the same manner, the legislation regulating the disposal of wastes on landfills, i.e. Royal Decree 1481/2001 (Spanish Ministry of Environment, 2002), is a direct transposition of the EU landfill directive.

Conversely to the EU situation, Spain possesses a specific legislative framework for regulating the generation and management of CDW set forth in the Royal Decree 105/2008 (Spanish Ministry of Presidency, 2008). Within this legislation, the responsibilities of the different agents involved are established; thus, the producer of waste is obliged to include a waste management study in the engineering project that has to be followed by the contractor, who also has to ensure the proper management of the waste by the redaction of a waste management plan as the waste holder, and finally the waste manager, who is responsible for the final waste treatment or disposal. The Royal Decree also establishes the conditions that the CDW management plants should meet for the treatment of the CDW, as well as the requirements for the different waste management options.

Moreover, as one of the requirements of the Waste Framework Directive 2008/98/EC (European Parliament and Council, 2008), Member States are also obliged to develop waste management plans that contain the general waste policy and strategies in order to meet the minimum objectives of prevention, reuse, recycling, recovery and disposal. In 2001, Spain began to pay special attention to the CDW stream by adopting the first National waste Plan of Construction and Demolition Waste (Spanish Ministry of Environment, 2001). Coinciding with the end of effect of the first National Plan of CDW (Spanish Ministry of Environment, 2001) and the approval of the Royal Decree (Spanish Ministry of Presidency, 2008), a second National Plan of Construction and Demolition Waste came in force (Spanish Ministry of Environment, 2009). Both documents were aimed to delineate the national guidelines for the management of CDW. Currently, a new version for the national plan on construction and demolition wastes is being prepared for the 2015-2020 time period under the State Waste Framework Plan (Spanish Ministry of Agriculture, Food and Environment, 2015). The chapter corresponding to the CDW management is based upon the European Communication "Resource efficiency opportunities in the building sector" (European Commission, 2014), and aims to improve the deficiencies detected in previous plans, as well as to promote a better environmental performance in line with the legal objectives of the EU and establishing the quantitate objectives for the CDW treatment (Table 2.1).

Table 2.1: Requirements proposed in the current draft of the State Waste Framework Plan 2015-2020 (Spanish Ministry of Agriculture, Food and Environment, 2015)

Requirement	**2016**	**2018**	**2020**
Minimum percentage of CDW (excluded non-contaminated soil and stones) destined to preparation for reuse, recycling or other valorisation activities	60	65	70
Maximum percentage of CDW disposed in landfills	40	35	30
Minimum percentage of non-contaminated soil and stones destined to backfilling or remodelling activities	75	85	90
Maximum percentage of non-contaminated soil and stones disposed in landfills	25	15	10

Despite the legislative interest in the management of construction and demolition waste, Spain still lacks of any specific end of waste status regulations. However, recently, the Basque country has approved regional legislation (Regional Environment and Territorial Policy Department of the Basque country, 2015) regulating the end of waste criteria for the use of recycled aggregates from CDW, which outlined limits and allowed areas for their use, as well as the conditions in which the wastes obtain the status of product to be used in construction applications.

Similarly, a lack of specific policies on the reuse or recycling of recycled aggregates from CDW could be noticed in Spain. Nonetheless, some aspects of the use of recycled aggregates for the production of concrete are included in the EHE-08 (Permanent Commission on Concrete, 2008), and in the current General Technical Specifications on Road and Bridge Construction Works (PG-4) (Spanish Ministry of Public Works, 2014) in the case of road construction.

2.2. WASTE MANAGEMENT

The European Union waste management policy set with the Directive 2008/98/EC (European Parliament and Council, 2008) lays down a priority order in which wastes should be managed at the least environmental impact. The waste hierarchy (Figure 2.1), also known as the 3R principle, establish the desirability in which CDW management should be based on the avoidance of environmental impacts.

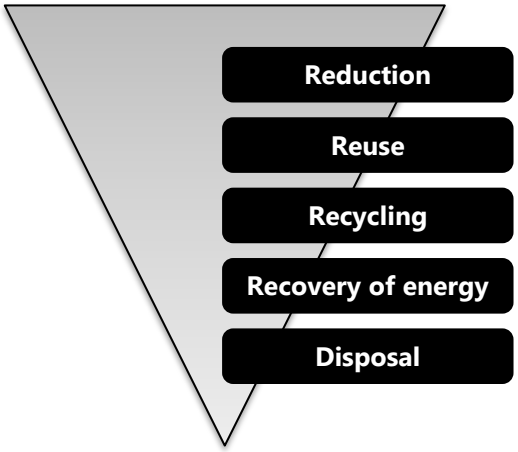

Figure 2.1: Waste hierarchy

Reduction should always be the first effort as it is the best option (Peng et al., 1997), not only to minimize CDW production, but also the associated cost of transport, recycling and disposal (Tam and Tam, 2008). The reduction of waste through government legislation, careful design, effective waste management systems, use of low waste technologies such as the use of prefabricated elements and improving the practitioners' attitudes towards waste reduction are regarded as key measures (Seydel et al., 2002; Begum et al., 2007). The reuse, second option in appropriateness, implies the repetitive use of a material for the same or a different purpose for which it was designed. Those materials that could not be directly reused should be recycled into new materials to reduce the consumption of natural resources, the energy costs derived from transport and production and the need for landfilling (Tam, 2008a). For some type of wastes, incineration could serve to recover energy as alternative fuels or by means of heat or electricity production. Finally, due to the related environmental impacts, disposal should be, at all times, considered as the less preferred option.

Despite being one of the ruling principles of the waste policies in the European Union and the United States, the waste hierarchy has been subjected to criticism, since the waste hierarchy does not contemplate the possibility that a CDW management option not following the 3R prioritization could result in the best solution under a particular set of conditions (Schall, 1992; Van Ewijk and Stegemann, 2014).

2.2.1. SPANISH CDW MANAGEMENT PROCEDURES

As previously mentioned, the Royal Decree 105/2008 (Spanish Ministry of Presidency, 2008) established the mandatory procedures to follow in the management of the CDW. In order to achieve a successful management, the aforementioned legislation implicates all agents involved by means of interrelated responsibilities. Briefly, the Spanish management model of CDW is shown in Figure 2.2.

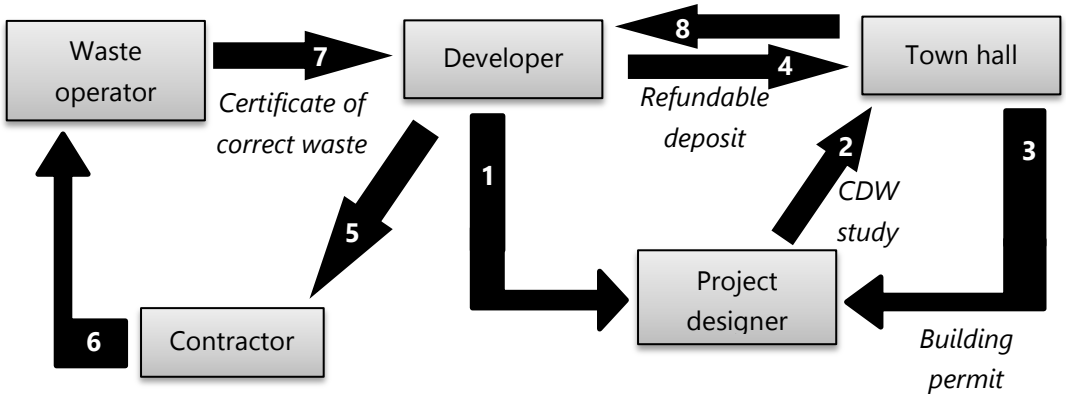

Figure 2.2: CDW management model in Spain

The property developer initiates the CDW management cycle by hiring a project designer (1) that must present the corresponding engineering project in the town hall for its approval (2). As part of the engineering project, a waste management study has to be included to satisfy the requirements set down in the Royal Decree 105/2008 (Spanish Ministry of Presidency, 2008). This document should be aimed at waste minimization, rational planning of building work, storage of materials and waste sorting. Among other information, the inclusion of the data regarding the estimated amount of CDW generated during the construction works and the measures envisaged for its management are compulsory. Figure 2.3 illustrates the guidelines for construction and demolition waste quantification followed by the project designer. Once the local authorities deem that the documents comply with all current regulations (both national and regional), a building permit is issued (3). Nonetheless, the construction activities could not begin until the developer pays a deposit fee aiming to discourage landfilling in favour of recycling (4). When all the administrative procedures are met, the contractor can start the construction or demolition works ensuring the proper management of the waste by the redaction of a waste management plan (5). Usually, the CDW are only separated on the work site when the generation exceeds certain quantities (i.e. 80 tonnes of concrete, 40 tonnes of brick, tiles and other ceramic materials, 2 tonnes of metals, 1 tonne of wood, 1 tonne of glass, 0.5 tonnes of plastic and 0.5 tonnes of paper and cardboard) as per requirements of the Royal Decree 105/2008 (Spanish Ministry of Presidency, 2008).

In spite of the separate or mixed nature of the wastes, the contractor has to deliver them to an authorised waste management facility for comprehensive recovery assessment (6). After the treatment of the CDW, the waste operator issues a certificate of correct waste management (7) to be presented in the town hall in order to recover the financial guaranty previously deposited (8). Failure to complete any of these phases will halt the process and render it ineffective. Therefore, it is essential that all the agents involved in each phase are aware of the importance of their role, assume the new legal obligations and act according to the principles of sustainability.

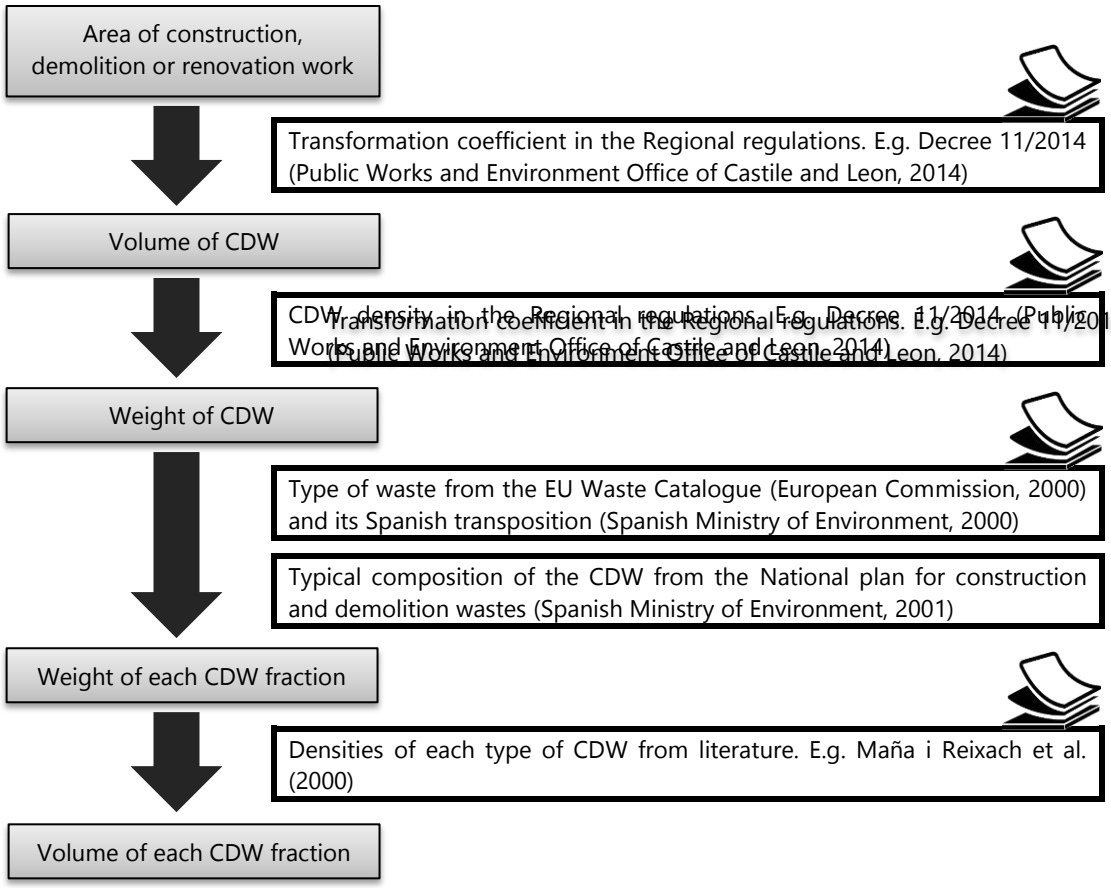

Figure 2.3: Guidelines for construction and demolition waste quantification

Despite that change in practitioners' attitudes regarding the benefits of waste management could represent a significant contribution (Teo and Loosemore, 2001), the need for a defined waste management plan in the construction works is regarded as an administrative nuisance instead of a measure of environmental protection. Nowadays, some Spanish professionals are still reluctant to implement waste management practices in construction (de Guzmán Báez et al., 2012).

According to Morán del Pozo et al. (2011) the agents involved in the waste management process may present in some cases behaviours that hinder a correct completion of the task at hand:

- The property developer considers obligatory waste management to be a costly requirement, the benefits of which do not directly accrue to him.

- The project designer deems waste management a time-consuming formality which increases the project work-load and which can be accomplished by the inclusion of a generic study.

- The project designer disregards the importance of a proper waste quantification and carries out a "bottom to top" calculation process - based on estimates of how much waste can be generated before it becomes obligatory to sort the waste - in order to evade the obligatory waste separation.

- The project designer has problems in order to estimate the quantity and the composition of the construction and demolition wastes that will arise. This difficulty constitutes one of the most serious deficiencies of the current legislation, which requires waste volume to be determined, but does not provide the essential indicators for such calculations, which however could be found in the literature as some Spanish researches (Maña i Reixach et al., 2000; Ramírez de Arellano-Agudo et al., 2002; Pascual and Cladera, 2004; Solís-Guzmán et al., 2009; Martínez-Lage et al., 2010; Llatas, 2011; Villoria-Sáez et al., 2011; de Guzmán Báez et al., 2012; Mercader-Moyano and Ramírez-de-Arellano-Agudo, 2013) have focused on addressing this drawback. Note that section 2.3.2 offers a more detailed approach to some of the quantification models developed worldwide.

- The constructor rejects deconstruction practices since they represent higher costs and labour times (Klang et al., 2003; Dantata et al., 2005; da Rocha and Sattler, 2009). However, some investigations carried out by Tam (2008a, 2008b) indicate that CDW management does not necessarily represent an additional cost.

- The construction workers do not get any specific formation regarding to waste management, and frequently seek to evade their obligations and solve the problem in the easiest way possible rather than in the most efficient and sustainable manner. By improving the skills of the construction workers (Wang et al., 2004a) and getting them involved in a reward-punishment system (Chen et al., 2002; Osmani et al., 2008), the actual material wastage could be reduced and a correct waste management could be encouraged.

- Local authorities do not really enforce compliance with the law in terms of landfill fees or fines, or the environmental law is enforced to a different extent by the various Autonomous Regions.

Nevertheless, it is important to highlight that the aim of this rather new legislation on CDW, goes much further than the mere legal obligation to draw up complicated documents or be in compliance with a bureaucratic procedure. The ultimate goal is to eliminate the traditional approach to waste management, which was based on the use of a product until the end of its service life and subsequent disposal in a landfill, and replace it with a hierarchical approach to waste management.

2.3. GENERATION OF CONSTRUCTION AND DEMOLITION WASTES

According to Bossink and Brouwers (1996), between 1% and 10% by mass of the building materials used in construction end up as a waste, being the incorrect decisions at the project design stage responsible for around 33% of the total CDW generated on-site (Osmani et al., 2008). Since the relevance of the environmental problem posed by the CDW is linked to the elevated generation figures, Figure 2.4 shows the waste generation per economic activity in the European Union. Quantitatively, the construction sector accounts for one third of the total waste generated, representing 821 million tonnes in 2012 (Eurostat, 2012). The wastes generated by the construction activities stand for the largest waste stream, closely followed by the wastes arising from the mining and quarrying activities (29%). Half of the Member States echo this tendency, as the wastes produced in the construction sector constitute the major waste stream in the country (Spain, Denmark, Hungary, Italy, Belgium, Czech Republic, United Kingdom, Cyprus, Germany, Austria, Netherlands, France, Malta and Luxembourg), ranging from 22% to 84% in Spain and Luxembourg respectively. However, mining and quarrying activities constitute the major waste stream in Poland, Estonia, Finland, Greece Sweden, Romania and Bulgaria, oscillating between 42% in Poland and 88% in Bulgaria. For countries such as Slovenia, Slovakia, Ireland and Lithuania, the wastes arising from the manufacture of goods represent the highest waste stream ranging from 30% and 45% in Slovenia and Lithuania respectively. Finally, Portugal (33%), Croatia (35%) and Latvia (53%) report households as the principal economic activity in terms of waste generation.

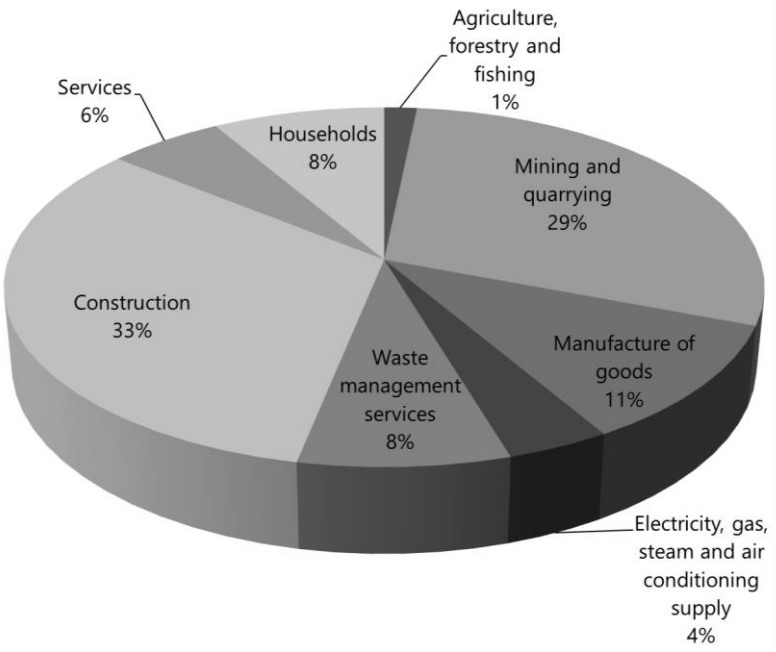

Figure 2.4: Waste generation per economic activity in the European Union (Eurostat, 2012)

Although the large volumes of CDW produced are stated as the obvious problem, the identification of the exact figures is complex, as the data of CDW generation and treatment are scarce, mismatched and sometimes extremely outdated. Furthermore, the lack of a consolidated definition for the CDW stream amongst countries causes that the data analysis and comparison becomes a problem (Sonigo et al., 2010; Rodríguez-Robles et al., 2014a).

For instance, the current information provided by Eurostat (2012) does not allow an accurate CDW quantification according to the recommended theoretical approach which takes into account both the nature (building materials) and the activities that originate them (construction and demolition) regardless of who performs these activities. Thus, despite all the legislative efforts, the unawareness of this basic information implies the impossibility of a correct assessment and remedy of the situation. Nonetheless, according Monier et al. (2011), the quantities of wastes generated under the construction -NACE code F- from Eurostat is an adequate framework to collect information regarding the CDW production in the EU Member States despite the inclusion of small quantities of non CDW generated in the construction sector such as packaging and the exclusion of small quantities of CDW generated by households or other industries. Table 2.2 shows the figures of CDW generation in all Member States expressed in total weight, in weight per capita and weight per million euros of gross value added (GVA) by the construction sector in 2012, which are also illustrated in Figure 2.5, Figure 2.6 and Figure 2.7, respectively.

Table 2.2: CDW generation in the European Union in 2012 (Eurostat, 2012)

Country	CDW (t)	CDW (t/capita)	Waste factor (t/million € GVA)
Austria	19,470,934	2.310	1080.90
Belgium	24,570,406	2.208	1234.57
Bulgaria	1,032,651	0.141	494.00
Croatia	682,058	0.160	331.16
Cyprus	965,177	1.117	1018.66
Czech Republic	8,592,900	0.818	1011.68
Denmark	3,867,209	0.692	397.33
Estonia	657,089	0.497	572.58
Finland	16,033,874	2.962	1414.42
France	246,702,428	3.771	2233.71
Germany	197,527,868	2.456	1763.89
Greece	812,519	0.073	183.47
Hungary	4,038,081	0.407	1288.19
Ireland	365,723	0.080	132.23
Italy	52,965,743	0.890	679.81
Latvia	7,509	0.004	6.36
Lithuania	419,136	0.140	234.67
Luxembourg	7,079,473	13.334	3403.27
Malta	1,040,846	2.481	3715.98
Netherlands	81,354,111	4.856	2923.67
Poland	15,367,995	0.404	589.40
Portugal	928,394	0.088	129.46
Romania	1,325,341	0.066	117.10
Slovakia	806,184	0.149	136.72
Slovenia	535,154	0.260	294.27
Spain	26,129,151	0.559	429.90
Sweden	7,655,935	0.804	368.60
United Kingdom	100,230,495	1.573	916.11
EU-28 total	*821,164,384*	-	-
EU-28 average	*29,327,299*	*1.546*	*967.93*

In terms of total production (Figure 2.5), there are five countries (France, Germany, United Kingdom, Netherlands and Italy) with a CDW generation above the European Union (EU-28) average. In addition, these five countries account for 82.66% of the CDW generation in the EU-28, while hosting the 56% of the population. Another five countries, namely Spain, Belgium, Austria, Finland and Poland, present a high CDW production without surpassing the EU-28 average, ranging between 15 and 26 millions of tonnes and representing 12.37% of the total waste. Note that the countries with higher waste generation are five out of the six founding Member States, while the rest of them where incorporated in the expansions of 1973 (United Kingdom), 1986 (Spain), 1995 (Austria and Finland) and 2004 (Poland). The rest of the counties have a CDW generation inferior to 9 million of tonnes (Czech Republic, Sweden, Luxembourg, Hungary, Denmark, Romania, Malta, Bulgaria, Cyprus, Portugal, Greece, Slovakia, Croatia, Estonia, Slovenia, Lithuania, Ireland and Latvia, in decreasing order of production) and conjointly roughly embody a 5% of the total CDW generation in the EU-28.

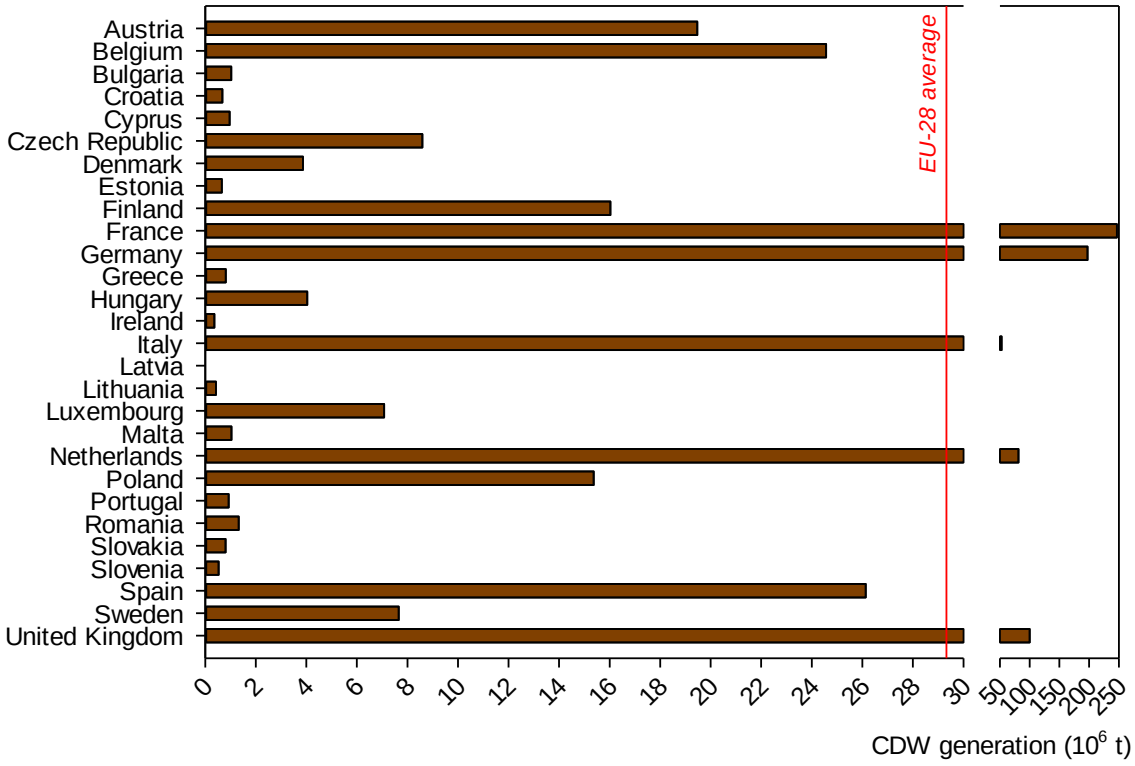

Figure 2.5: Generation of CDW in the European Union in 2012 (Eurostat, 2012)

Provided that the waste generation has a strong dependence with the size of the territory studied, the data is also presented as a function of mass of waste per inhabitant (Figure 2.6). The figures show important differences among Member States, with the CDW generation per capita ranging from 0.004 tonnes in Latvia to 13.334 in Luxembourg. This trend was also observed by Monier et al. (2011) when studying data of CDW generation from previous years. The countries with the lowest CDW generation are Latvia, Romania, Greece, Ireland and Portugal with values below 0.10 tonnes per capita. The generation of CDW in a second group of countries, consisting of Lithuania, Bulgaria, Slovakia, Croatia, Slovenia, Poland, Hungary and Estonia, oscillate between 0.10 and 0.50 tonnes per capita. There are still five countries (Spain, Denmark, Sweden, Czech Republic and Italy)

under the milestone of 1 tonne per capita; while seven countries (Cyprus, United Kingdom, Belgium, Austria, Germany, Malta, Finland, France and The Netherlands) have a waste generation ranging between 1 and 3 tonnes per inhabitant. France and The Netherlands report quantities of CDW generation between 3 and 5 tonnes per capita; and undeniably, Luxembourg is the Member State with the highest CDW generation level, almost 2.8 times higher than the second top producer. The five countries with high generation per capita generate close to 43% of the total CDW reported in the EU-28; and this percentage increases up to almost 85% when the top 10 producers per capita are observed.

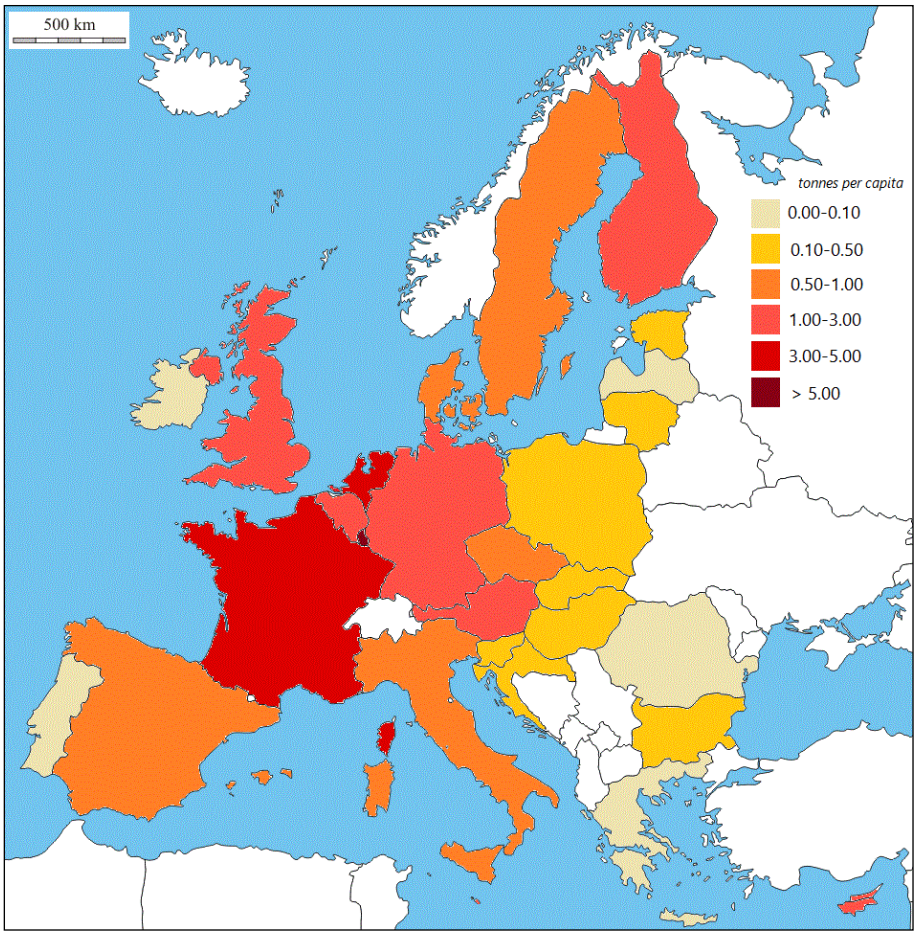

Figure 2.6: Generation of CDW per capita in the European Union in 2012 (Eurostat, 2012)

Since CDW is intrinsically linked to construction activity, a cross-analysis of the waste generation with an economic indicator of the construction sector such as the gross value added (GVA) results interesting (Figure 2.7). Once again the geographical differences are important, oscillating between 3715.98 and 6.36 tonnes of CDW per million euros added value in the construction sector, respectively, in Malta and Latvia. The countries with the lowest CDW generation per million euros of GVA are Latvia, Romania, Portugal, Ireland, Slovakia and Greece, with figures lower than 200 tonnes per million of euros. Ranging from 200 to 500 tonnes per million euros of GVA, there are seven countries (Lithuania, Slovenia, Croatia, Sweden, Denmark, Spain and Bulgaria), while Estonia, Poland, Italy and United Kingdom are below 1000 tonnes per million of euros of added value in the construction sector. Among the countries with higher CDW production, there are seven in the 1000-2000 tonnes per million euros (Czech Republic, Cyprus, Austria, Belgium,

Hungary, Finland and Germany) and only two surpassing the 2000 tonnes per million added (France and The Netherlands). Finally, under this economic criterion, Malta and Luxembourg are the highest waste generators with figures over 3000 tonnes per million euros of GVA in the construction sector.

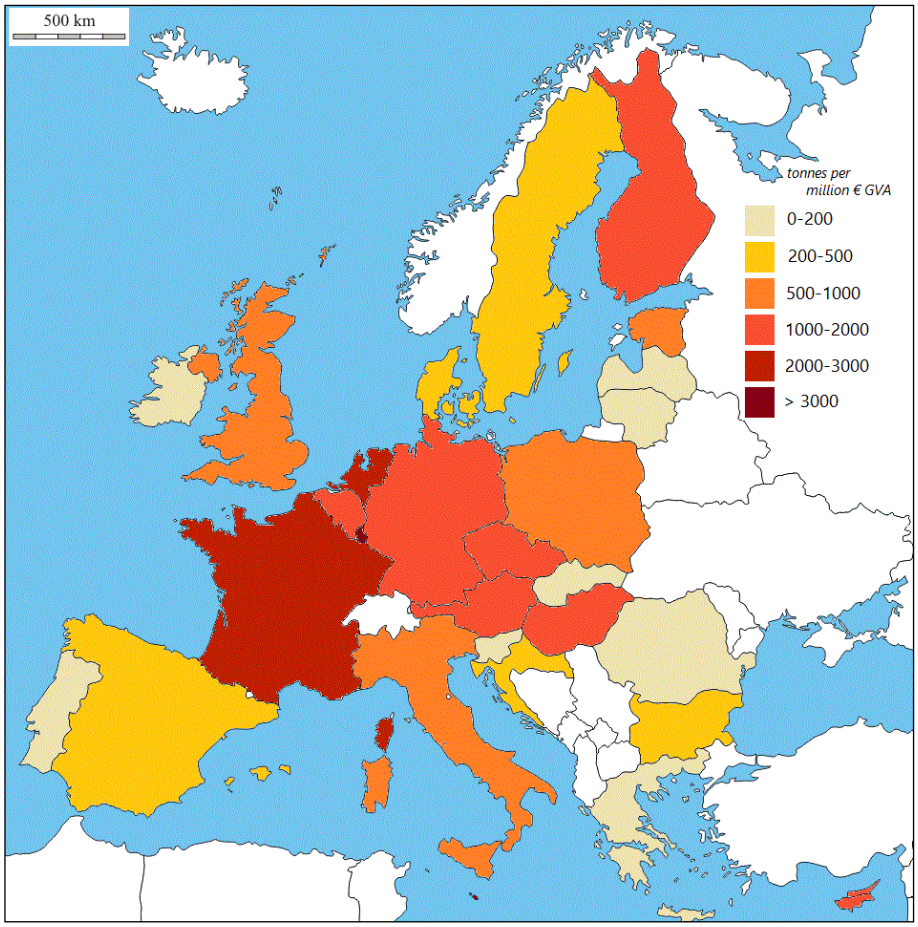

Figure 2.7: Generation of CDW millions euros gross value added (GVA) in the European Union in 2012 (Eurostat, 2012)

From the previous analysis, important differences among Member States could be observed when comparing to the CDW generation in terms of different parameters. Table 2.3 illustrates the order of the different countries forming the European Union in terms of CDW generation according to the three parameters of study, as well as, a visual indication of the relative change when compared to the total weight generated. For instance, the top 5 waste generators are France, Germany, United Kingdom, Netherlands and Italy. However, if waste generation per capita is observed, countries such as Luxembourg, Finland and Malta gain a place among the top 5 along the Netherlands and France. A similar effect occurs when contemplating the economic interrelation between CDW generation and GVA in the construction sector, with Malta, Luxembourg, the Netherlands, France and Germany as the five greatest CDW generators in the EU-28. Focusing solely on the Spanish figures, the country is placed sixth for total generation of CDW, fifteenth for the generation per capita and seventeenth for the generation linked to the GVA of the construction sector.

Table 2.3: Differences in the order of countries regarding the CDW generation according to the studied parameters

Country	CDW (t)	CDW (t/capita)		Waste factor (t/million € GVA)	
Austria	8	7	▲	9	▼
Belgium	7	8	▼	8	▼
Bulgaria	18	22	▼	16	▲
Croatia	23	20	▲	20	▲
Cyprus	19	10	▲	10	▲
Czech Republic	11	12	▼	11	=
Denmark	15	14	▲	18	▼
Estonia	24	16	▲	15	▲
Finland	9	4	▲	6	▲
France	1	3	▼	4	▼
Germany	2	6	▼	5	▼
Greece	21	26	▼	23	▼
Hungary	14	17	▼	7	▲
Ireland	27	25	▲	25	▲
Italy	5	11	▼	13	▼
Latvia	28	28	=	28	=
Lithuania	26	23	▲	22	▲
Luxembourg	13	1	▲	2	▲
Malta	17	5	▲	1	▲
Netherlands	4	2	▲	3	▲
Poland	10	18	▼	14	▼
Portugal	20	24	▼	26	▼
Romania	16	27	▼	27	▼
Slovakia	22	21	▲	24	▼
Slovenia	25	19	▲	21	▲
Spain	6	15	▼	17	▼
Sweden	12	13	▼	19	▼
United Kingdom	3	9	▼	12	▼

In terms of reliability, these figures should be regarded with caution as some shortcomings have been reported. For example, it has been recognised that some countries report excavated soil as part of the CDW which hinders the comparison among Member States (Monier et al., 2011; Rodríguez-Robles et al., 2014a). Monier et al. (2011) analysed the effect of this inclusion in the CDW generation of six countries (Denmark, Finland, France, Germany, Ireland and Luxembourg) which resulted in reductions between 62% and 88% of the total per capita generation. In addition, very low levels of CDW generation could suggest a lack of control and incomplete reporting by some Member States (Monier et al., 2011). Finally, note that the illegal dumping of this type of waste has been a common practice (Esin and Cosgun, 2007; Zygouras et al., 2009), and thus all these estimates should be regarded as the best case scenario.

2.3.1. EVOLUTION OF THE CDW GENERATION

In Figure 2.8, the evolution of the generation of CDW between 2004 and 2012 - which is the available data range from Eurostat (2012) - is represented for 10 EU Member States. If the obvious differences in terms of amount of CDW produced among the EU countries are left out of consideration, the bi-annual variations show a change of generation pattern in 2006 and a reduction in the levels produced from 2008 onwards for most countries due to the onset of the economic crisis and the period of recession as the generation of waste is intrinsically linked to the economic growth. Figure 2.9 illustrates the evolution of the economic climate in the Euro area within the 2006-2015 period. From 2006 onwards, the economic situation in the euro area pointed to a downswing that in 2008 materialized in economic crisis. With a period of economic recession almost lasting for seven years, 2014 was considered as the beginning of a new economic cycle. Nowadays, although some countries such as Greece, Finland, France, Italy, Spain, Austria, Portugal and Cyprus are still reporting negative balances, according to experts the EU economic sector is on its path towards recovery, despite the recent loss in momentum, with improving figures around most Member States with the exception of Germany, Finland and Lithuania (Ifo Institute, 2015).

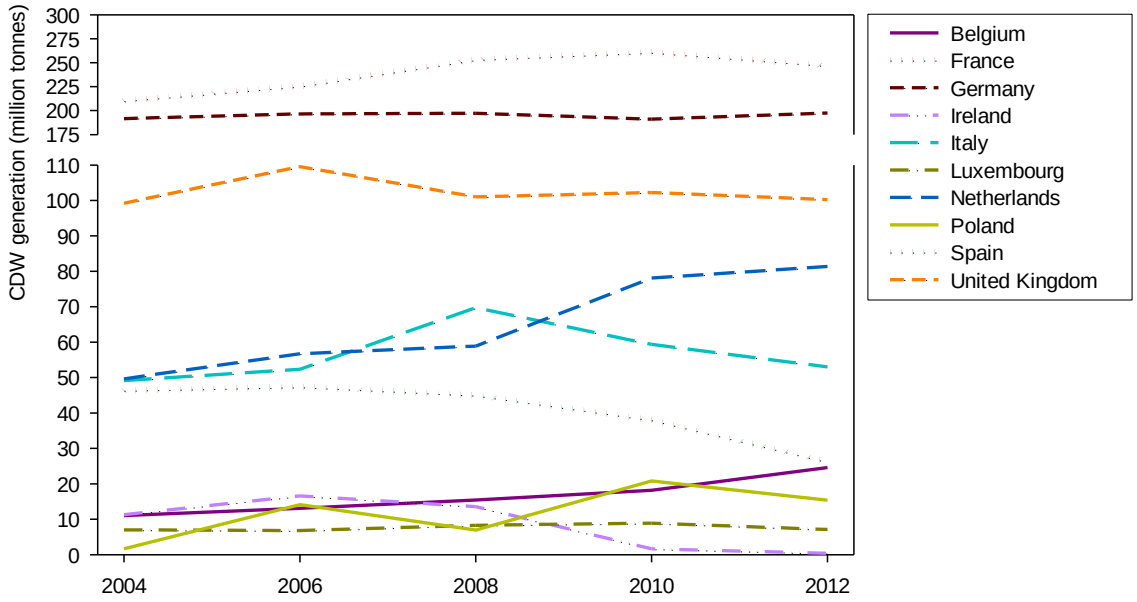

Figure 2.8: Evolution of the CDW generation in selected EU Member States

Nonetheless, in a more detailed analysis of Figure 2.8, the evolution of the CDW generation for some countries does not perfectly reflect the previous explanation. For example, France, the Netherlands and Belgium just showed a deceleration in the production of CDW between 2006 and 2008 but later displayed an increase in the generation figures. The generation of CDW in Germany and Luxembourg barely was affected and remained significantly stable through the analysed period. The varying scenarios displayed by the different countries are due to the unequal force of the crisis among the Member States, in particular with respect to its influence in the construction sector, which is the main responsible for the generation of CDW.

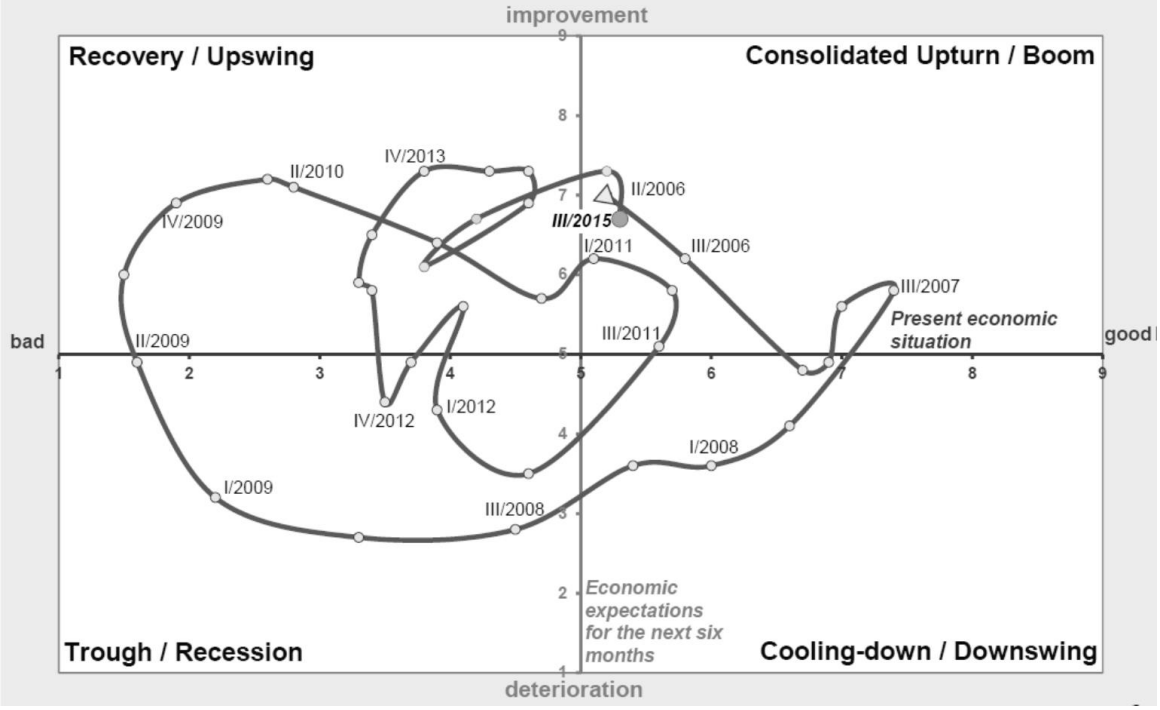

Figure 2.9: Evolution of the economic climate in the Euro area (Ifo Institute, 2015)

Focusing on the Spanish case, over the period 2004-2006, the generation pattern in Spain was characterized by a rise around 2% (Eurostat, 2012). Since the construction sector was the driver of the economy in Spain, the collapse of the denominated housing bubble in 2008 has meant a significant setback in numerous construction-related matters. For instance, between 2008 and 2014, the number of employees in the construction sector was reduced with 60%, the public tender fell down 76% and the new construction, rehabilitation and demolition activities decreased with 82%, 67% and 69%, respectively (Spanish Ministry of Public Works, 2015). According to the generalised reduction in the construction sector outcome CDW generation levels dropped almost a 42% in the 2008-2012 time interval, almost a 11% below the EU-28 average production (Eurostat, 2012). However, in any case, the reduction in the generation of CDW due to the economic crisis should not be perceived as positive, since the fewer amounts do not correlate with a better management of the CDW, neither are they in line with an actual trend in the CDW minimization.

Although the forecasting regarding CDW is a complicated matter, a general correlation between the amount of waste and the growth of the construction sector is to be expected. Despite that the economic crisis lasted longer in the construction sector than in the rest of the European economy, the end of the recession period in the construction sector could be pinpointed to 2014 and a moderate growth ranging between 1.9% and 2.6% could be expected within the 2015-2017 period (Euroconstruct, 2015). Figure 2.10 shows the latest forecast for the construction sector in selected Member States of the European Union. Thus, in the short term, an increase in the generation of CDW could be also expected for most EU Member States, with the exception of Denmark, Slovakia, Hungary, Sweden and Poland that present reduction in the growth of the construction sector between 2015 and 2017.

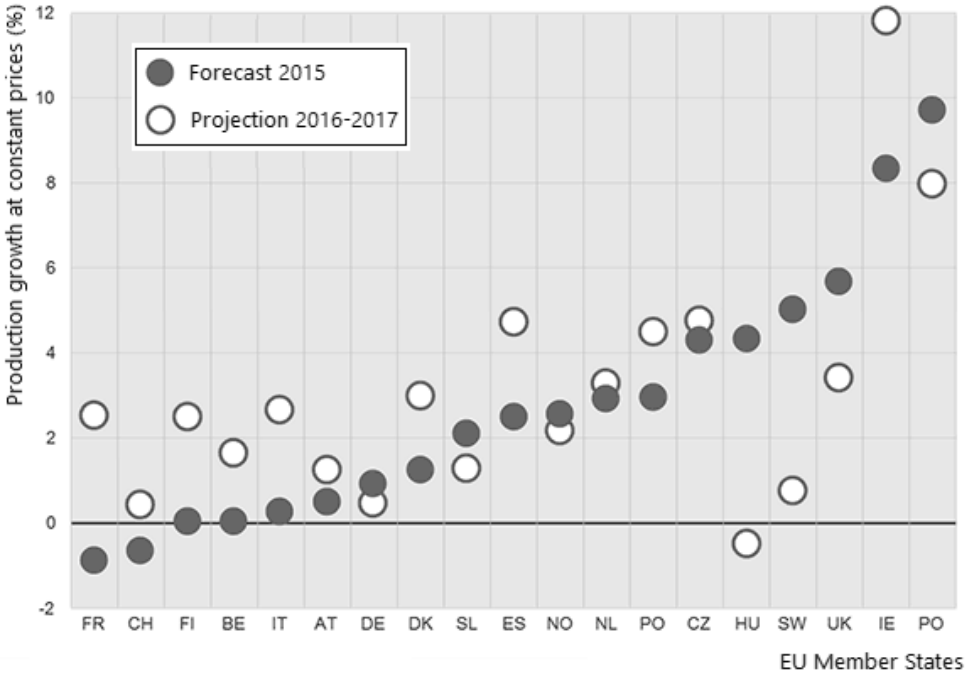

Figure 2.10: Forecast of the construction sector in selected EU countries (Euroconstruct, 2015)

2.3.2. CDW QUANTIFICATION MODELS

As the figures of generation are often cited as the trigger in the consideration of the environment problems posed by the CDW, several quantification methods have been proposed to estimate the waste generated from construction and demolition works, and thus facilitate their proper control and management (Solís-Guzmán et al., 2009).

The first quantification model in Europe dates from 1976, the waste management rate of 37 categories of residues was calculated by comparing contractors' records (Skoyles, 1976). Also in the United Kingdom, a software was developed (SMARTWaste, 2010) that enables the CDW estimation from the collected reference values of waste generation in new construction projects. In the Netherlands, Bossink and Brouwers (1996) assessed the wastes arising from 184 buildings to propose a waste material rate of 9 waste fractions (debris piles, bricks, concrete, blocks, tiles, mortars, aggregates, packages and others), and Müller (2006) simulated the CDW generation as a function of the population and its life style until 2100. Another forecasting of CDW generation was carried out by Bergsdal et al. (2007) in Norway with 2020 as time horizon. Jalali (2007) gathered data from construction sites to develop indexes covering the typical CDW generation as a total or separate fractions in Portugal.

The topic of CDW quantification has received a plethora of attention in Spain since the current legislation, namely the Royal Decree 105/2008 (Spanish Ministry of Presidency, 2008) set the obligation to include a CDW management study in all engineering projects. Initially, an index for CDW generation based on the area of the construction, renovation or demolition works was proposed for different construction projects by the Institute of Technological Construction in Catalonia (Maña i Reixach et al., 2000).

Martínez Lage et al. (2010), Villoria Saez et al. (2011) and Mercader-Moyano and Ramírez-de-Arellano-Agudo (2013) also carried out waste quantifications based on the range of waste generated in each type of construction activity. In the Autonomous Community of Andalusia, the CDW generation was estimated from the budget for waste management of the construction projects and the expected wastage rate of each type of building material (Ramírez de Arellano-Agudo et al., 2002; Solís-Guzmán et al., 2009; Llatas, 2011). Similarly, de Guzmán Báez et al. (2012) determined CDW generation in rail works based on budget records. Pascual and Cladera (2004) resorted to the annual cement consumption per inhabitant to estimate the CDW production assuming a linear relationship between the two variables.

By assessing the economic value reflected in the building permit, Yost and Halstead (1996) were the first researchers to estimate the CDW generated in the United States of America (USA). Later on, the methodology adopted by the USA Environmental Protection Agency was drafted by Franklin Associates (1998), who calculated the waste generation as a function of the area of construction, demolition or renovation works. More recently, the mass balance principle has been employed for estimating CDW generation taking into account the consumption and the typical waste factors of construction materials (Wang et al., 2004b; Cochran and Townsend, 2010). In Canada, a simulation model based on the schedule of work activities was employed to estimate CDW generation in five separate categories (Chandrakanthi et al., 2002).

In China, estimates have been produced based upon the annual figures of cement consumption and the area of the construction works (Shi and Xu, 2006). In addition, Li et al. (2013) modelled the waste generation per gross floor area employing a mass balance between the purchased amount of each type of building material and their typical waste material rate. Centred on building permits data, Hsiao et al. (2002) designed a CDW quantification and forecasting model for Taiwan. A similar approach was followed in Thailand by Kofoworola and Gheewala (2009), who also based the quantification on data relevant to the type of building activity and the number and area of construction permits. In Malaysia, the CDW generation was estimated according the typical layouts of waste on the construction site (stockpiled, gathered, scattered and stacked), its estimated volume and unit weight (Lau et al., 2008). A much more accurate model was employed in Hong Kong by using building information modelling (BIM) technology (Cheng and Ma, 2013).

Recently, more complicated methods have been used to better reflect the future generation of CDW. While Wu et al. (2015) employed gene expression programming, the majority of the studies using more advanced methods (Hsiao et al., 2002; Elshkaki, 2005; Hao et al., 2007, 2010; Hu et al., 2010; Chinda et al., 2013) are based upon the use of system dynamic approaches in order to build CDW generation models integrating all the variables and the relationships among variables influencing the production of CDW by means of causal loops diagrams.

2.4. COMPOSITION OF CONSTRUCTION AND DEMOLITION WASTES

CDW includes a wide range of inert materials, making important the knowledge of its composition since it would largely determine the waste treatment and its end-use. On the one hand, wastes arising from new construction, renovation or demolition are expected to have a different composition.

For example, wastes from a new construction are expected to be more homogenous and less contaminated than those originating from rehabilitation or demolition works, in which hazardous substances (such as lead or asbestos) could be present if the building demolished was constructed under past less restrictive regulations. On the other hand, the composition of CDW is affected by numerous factors, including the raw materials and building products, the building typology and architectural techniques and the local construction and demolition practices employed (Pacheco Torgal et al., 2013).

Thus, several EU Member states have carried out studies on the typical composition of the CDW generated within their borders in an attempt to favour their proper control and management. For instance, there is available compositional data at national level for Austria and Hungary (Fischer and Werge, 2009), Czech Republic, Estonia and Finland (Böhmer et al., 2008), Denmark (Danish Ministry of the Environment., 2011), Ireland (Irish Environmental Protection Agency, 1995), Germany (Basten et al., 2015), the Netherlands (Government of the Netherlands, 2012) and Spain (Spanish Ministry of Environment, 2001). In general, the data shown in this compilation dates several years back, which compromises its reliability. Although some countries such as the Netherlands and Germany have been updating the available information in this regard, commonly the countries just report total quantities without differentiation by waste stream. Besides, albeit the existence the European Catalogue of Waste (European Commission, 2000) as a common model for waste identification for comparison of waste statistics across all member states, the great quantity of types of substances considered and the different definitions and considerations of CDW within each country renders it difficult to compare values between different countries with any accuracy,

2.4.1. SPANISH CDW COMPOSITION

The typical composition for the Spanish CDW was reported in the first National waste Plan of Construction and Demolition Waste (Spanish Ministry of Environment, 2001). The composition of the CDW is predominantly of stony nature, of which 54% presents a ceramic nature, 12% corresponds to concrete rubble and the remaining 9% are natural aggregates (stone, sand and gravel). It is interesting to mention that the high ceramic percentage is explained by the fact that, as in other Mediterranean countries such as Portugal, Italy or Greece, the construction of buildings in Spain is usually based on ceramic elements combined with mortar and concrete (de Brito et al., 2005). Studies show that the average content of ceramic in the European Union is about 30% (Böhmer et al., 2008) and ranges between 8% and 54% according to Monier et al. (2011), which places Spain in the high range for the production of ceramic and mixed recycled aggregates. The rest of the materials (25%) comprising the CDW are non-stony, consist of the so-called impurities and include a wide diversity of materials such as asphalt (5%), wood (4%), metals (2.5%), plastic (1.5%), glass (0.5%), paper (0.5%), gypsum (0.2%) and varied rubbish (11%).

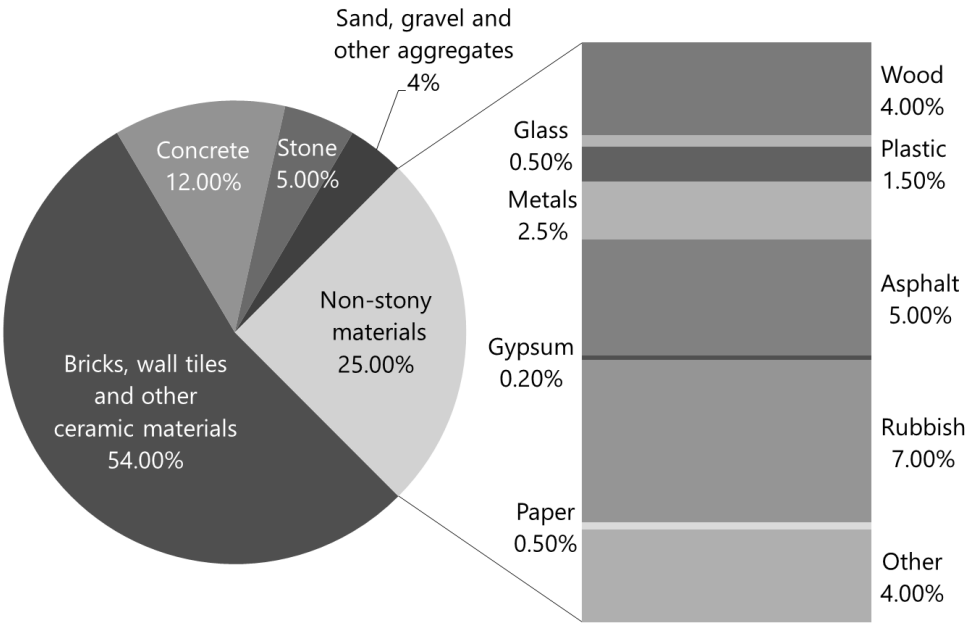

Figure 2.11: Typical composition of CDW in Spain (Spanish Ministry of Environment, 2001)

As occurring in other countries, the information on CDW composition has not been updated in Spain since 2001. Nonetheless, with the approval of the standard UNE-EN 933-11 (2009), most of the scientific works carried out in Spain incorporate a classification of the components of the CDW recycled aggregates as a part of the experimental research programme; thus, more recent composition data could be observed through the review of the relevant literature. In chapter 4, as part of the characterization of the recycled aggregates to be used in the research works of this dissertation, a detailed literature review on the constituents of the CDW both from Spain and other countries in collected in Table 4.5.

2.5. RECYCLING RATES

Besides waste generation, Eurostat (2012) registers the treatment of wastes by waste category. Although, there is no grouping for CDW as mentioned before, the analysis of the management options of the mineral wastes derived from CDW followed by the EU-28 countries is a useful indicator (Figure 2.12). At first glance, landfilling is still the most used option in 5 countries (Greece (100%), Bulgaria (86%), Finland (84%), Malta (81%) and Slovakia (61%)); while 15 countries (the Netherlands, Ireland, Luxembourg, Belgium, Italy, Estonia, Latvia, Denmark, Germany, United Kingdom, Slovenia, Poland, Austria, Czech Republic and Lithuania) show values inferior to the EU-28 average of 14%. The percentages corresponding to the other management options (incineration, energy recovery, backfilling and other recovery) seem to be in agreement with the waste hierarchy, with lower preference for incineration and energy recovery. In this regard, it is interesting to note that incineration is only a significant option in Bulgaria (2%); while the countries with relevant energy recovery are Denmark (8%), Sweden (6%) and Finland (4%), i.e. all Nordic countries, which points to a common pattern both in the composition of CDW and building construction practices.

Meanwhile, the EU-28 average is 6% for backfilling and 67% for other ways of recovering (reuse and recycling). It is worth mentioning that the category representing other recovery is the only option followed in the Netherlands, since there is a ban in the landfilling of these types of materials; while in countries such as Austria, Belgium, Croatia, Latvia, Luxembourg, Malta, Portugal, Romania and Slovakia there is a dichotomy between landfill and other recovery. Moreover, Ireland is the only Member State in which the alternation among significant management options includes backfilling and other recovery. As Eurostat (2012) has been carrying out this type of data collection since 2010, it is possible to assess the evolution in the way in which the Member States undertake the management of the mineral fraction of CDW. In general, a positive trend towards the amount of material landfilled has been observed for most countries, while Bulgaria suffered an increase up to 47% at the expense of the category of reuse and recycling. However, this data does not offer an actual representation of the recycling rates as it does not consider the management of all the materials comprising the CDW, just the mineral fraction.

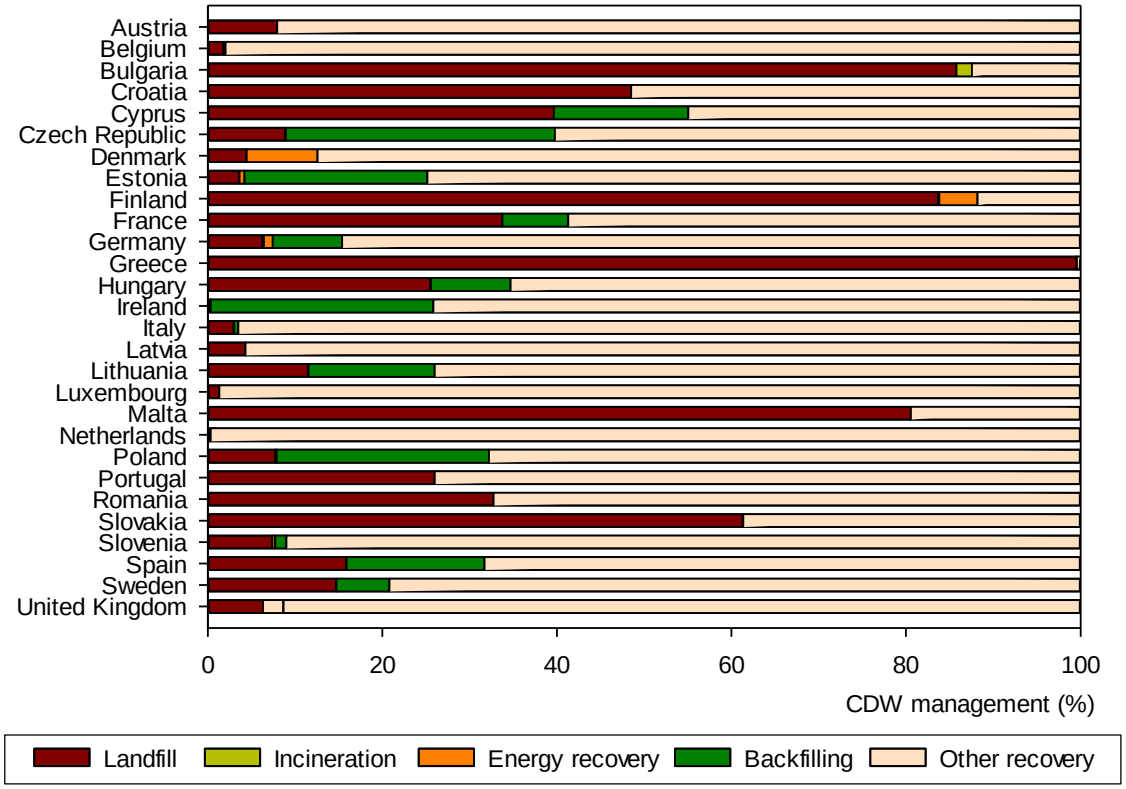

Figure 2.12: Management options of the mineral wastes derived from CDW followed by the EU-28 countries in 2012 (Eurostat, 2012)

Another shortcoming in the research about recovery and recycling rates relates to the inclusion of non-contaminated earth and stones in the calculations of some European Union countries, which contravenes the requirement of the Waste Framework Directive 2008/98/EC (European Parliament and Council, 2008) to exclude both hazardous materials, and soil and stones not containing dangerous substances - category 170504 in the European Waste Catalogue (European Commission, 2000) - in the calculation of the recycling rates employed to assess the achievement of the 70% recycling target established by the aforementioned directive in 2020.

It is worth mentioning that countries such as Denmark, Germany and the Netherlands, which present the highest recycling ratios among the European Union, include soil in their calculations (Fischer and Werge, 2009). This fact represents an important bias when comparing the values of the recycling ratios achieved to other EU countries such as Spain which does not include excavated material in their figures. For example, Table 2.4 gathers the information of several German reports monitoring the recycling rates of a typical composition of German CDW within the 2006-2012 period (Basten et al., 2011a, 2011b, 2013, 2015) with figures above the 70% target for all years. Nonetheless, the breakdown of the German CDW according to its composition indicates that an average of the 57% of the total CDW consists of soil and stones that contribute, on average, up to a 49% into the total recycling rate of Germany.

Table 2.4: German CDW composition and recycling rates within the 2006-2012 period (Basten et al., 2011a, 2011b, 2013, 2015)

	German CDW	**Soil and stones**		**"Core" CDW**	
	Recycling rate (%)	**Composition (%)**	**Recycling rate (%)**	**Composition (%)**	**Recycling rate (%)**
2006	89.80	56.20	48.40	43.80	41.50
2008	89.50	55.90	47.70	44.10	41.80
2010	91.70	56.70	50.00	43.30	41.70
2012	91.20	57.20	50.30	42.80	40.90

Aware of the unreliability of the statistics available in the CDW management literature, Monier (2011) reinterpreted the recycling rates arising from two European reports by excluding the non-contaminated excavation figures and assuming the worst case scenario for countries without reported data (Bulgaria, Italy, Malta, Romania, Slovakia and Sweden). The authors estimated a 46% recycling rate for EU-27 in 2009. Moreover, in view of the results, Member States were classified according to their fulfilment of the 2020 objective, with 6 countries (Denmark, Estonia, Germany, Ireland, United Kingdom and the Netherlands) surpassing the 70% target, 3 countries (Austria, Belgium and Lithuania) ranging between 60% to 70% recycling rates, 4 countries (France, Latvia, Luxembourg and Slovenia) presenting recycling levels between 40% and 60% and 8 countries (Cyprus, Czech Republic, Finland, Greece, Hungary, Poland, Portugal and Spain) with recycling figures inferior to 40%.

2.5.1. SPANISH RECYCLING RATE

The Spanish CDW recycling rate is always been well below of the figures presented by the leading EU recycling countries such as Denmark, Germany and the Netherlands, where recycling is less expensive than dumping (Lauritzen, 2004), and even beneath the average recycling values of the European Union. In 1999, Spain recycled less than 5% of the total CDW generated while in the EU the average recycling rate was around 28 % (Symonds Group Ltd, 1999). However, considerable progress has been achieved since those figures. In 2011, the average recycling rate in the European Union was up to 47% (Monier et al., 2011) and, not that far below, a recycling rate up to 30% was achieved in Spain (Güell-Ferré et al., 2012), although with notable differences between the recycling values accomplished in each Autonomous Community, as shown in Figure 2.13 (Rodríguez-Robles et al., 2014a).

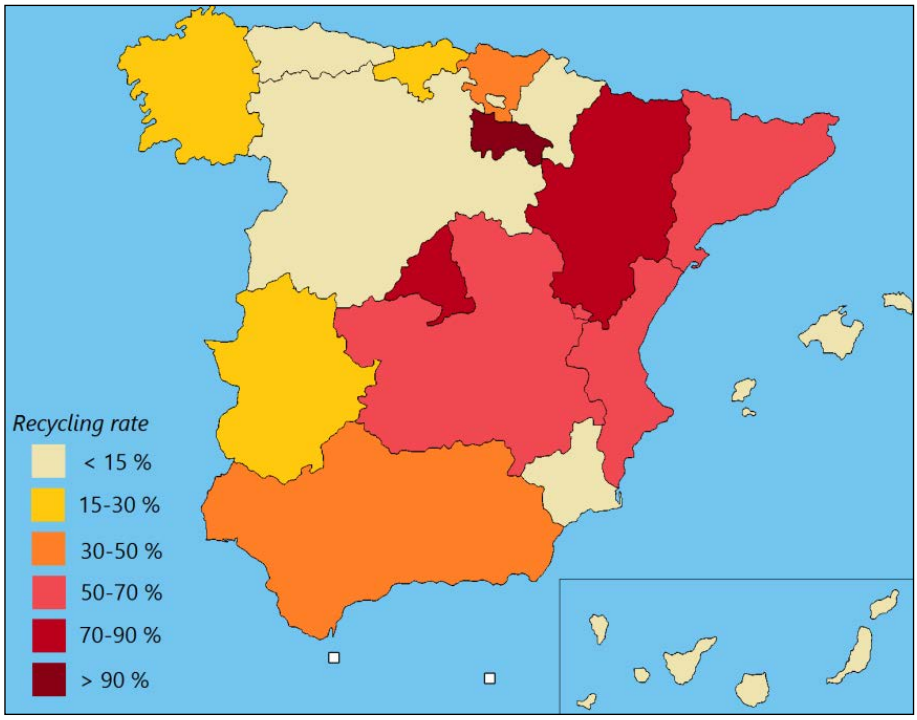

Figure 2.13: Level of CDW recycling in the Spanish Autonomous Communities

The last available information regarding recycling rates has been presented in a country factsheet of an European project (BIO et al., 2015) and estimates that from the 27 million tonnes of CDW generated in 2012, 19 million tonnes (68%) were recycled, 4 million tonnes (16%) were backfilled and the remaining 4 million tonnes (16%) were landfilled, which puts Spain on the correct path to achieve the 70% EU target.

3. RECYCLED AGGREGATES

Recycled aggregates are products obtained from the treatment of CDW. Generally three types of recycled aggregates could be distinguished according to their composition: recycled concrete aggregate, mixed recycled aggregates and ceramic recycled aggregates, being the use of these two last types in the production of concrete the object of this dissertation. While the classification as recycled concrete aggregate is mostly unambiguous, i.e. the concrete rubble must represent a minimum percentage of 90%, some controversy exists when classifying mixed and ceramic aggregates. For example, Agrela et al. (2011) suggested that recycled aggregates should be considered as ceramic if the percentage of this material surpassed the 30%, meanwhile the Spanish guide on recycled aggregates from CDW (Güell-Ferré et al., 2012) is more strict in the classification of ceramic recycled aggregates and established that ceramic recycled aggregates have to possess a minimum of 70% of ceramic waste. In the framework of this dissertation, the latter approach has been adopted and recycled aggregates are considered as mixed if the percentage of ceramic waste was inferior to 70%, otherwise they were classified as ceramic aggregates.

3.1. PRODUCTION PROCESS

3.1.1. DEMOLITION

Currently, complete demolition is the typical end-of-life scenario for buildings. However, since the cleanliness of the CDW is considered one factor in its potential recovery, operations favouring a separate collection are to be promoted. For example, the current CDW management legislation in Spain (Spanish Ministry of Presidency, 2008) enforces a compulsory on-site separation of the individual fractions of CDW when the estimated generation quantities in the waste management study included in the engineering project exceed the previsions in the Royal Decree 105/2008 (Spanish Ministry of Presidency, 2008).

Regarding the field application, selective demolition (Figure 2.14), also known as deconstruction, aims to the separate collection of materials from a building in order to directly reuse some of them and facilitate the reuse of the rest of them. Deconstruction is often described as a reversed construction process, and it consist of the selective removal of accessible materials with obvious sales value (e.g. copper pipes and wiring, windows, doors, roof tiles…), followed by the selective removal of accessible materials which, if not removed, will cause the CDW to be treated as hazardous (e.g. asbestos) or will decrease the value of the remaining CDW when crushed (e.g. plaster, plastic…) (Symonds Group Ltd, 1999). Thus, a first stage of sorting and processing wastes occurs at the demolition site in order to separate the two streams of wastes. It was estimated that up to a 65% of the total wastes arising from selective demolition could be reused directly (Working group 2/5, 2006).

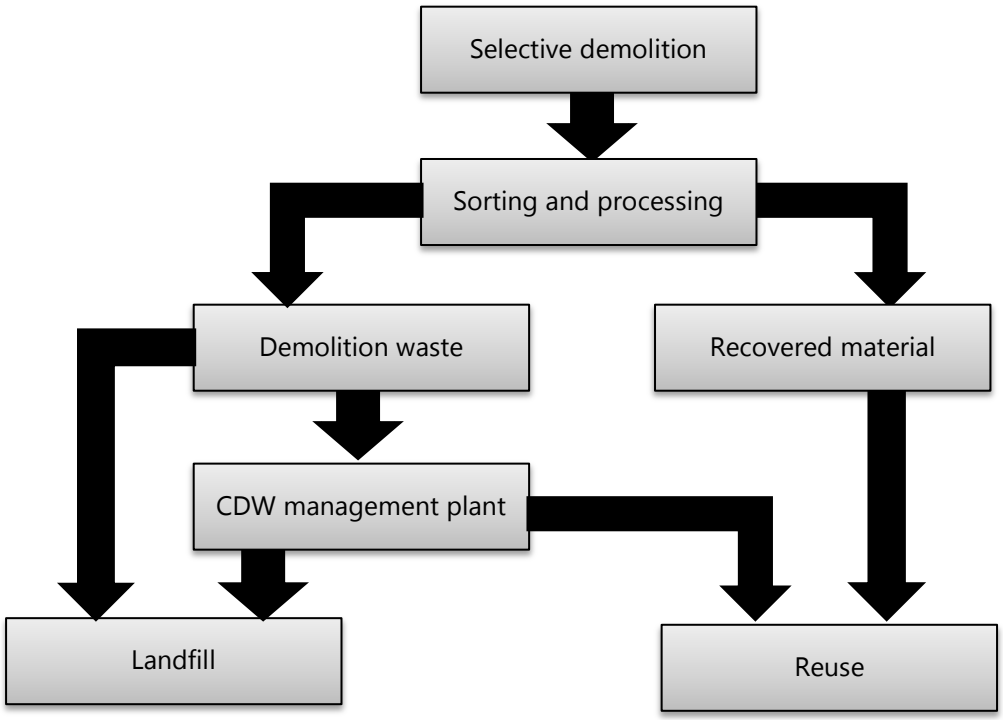

Figure 2.14: Management scheme in selective demolition activities

Some studies on the technical, economic and environmental implications of selective demolition have reported that while the environmental benefits of this approach are unquestionable due to the reduction in landfilled material, the economic feasibility depends on the labour cost, landfill fee and prices of recovered wastes (Dantata et al., 2005; Roussat et al., 2009; Coelho and de Brito, 2011). Nowadays, waste operators charge cheaper entrance fee for sorted waste streams than mixed wastes what could counteract the cost of the deconstruction activities, which is estimated around 17% and 25% higher than congenital demolition (Dantata et al., 2005). In addition, the accessibility of the materials to be recovered, the need for more space in the demolition site and time restriction are often cited as barriers to the application of this method (Pacheco Torgal et al., 2013). Nonetheless, in the future, the design for deconstruction approach could solve the problem of an effective material recovery since the structure is designed having in mind the reutilization of the materials in a new construction cycle under reasonable labour work and investment conditions (Hechler et al., 2010).

3.1.2. CDW MANAGEMENT PLANTS

CDW treatment plants, which could be fixed or mobile, classify and valorise the different fractions of CDW to be reused or recycled. In addition, CDW could be temporally stored (less than 2 years if intended for reutilization and 1 year when destined to landfill according to Spanish regulations) in transference plants where the owner must ensure hygienic conditions and secure measures.

One of the most common classifications, distinguishes the CDW management plants in three levels according to the technology employed and the processing activities carried out (Symonds Group Ltd, 1999). Figure 2.15 illustrates this classification, as well as the limits for technical and economic viability in function of the processing activities and type of CDW that is prepared to efficiently treat. Hence, level 1 plants provide a crushing and sieving operation in a mobile plant, level 2 facilities are fixed and include metal separation besides the crushing and sieving operations and level 3 plants incorporate crushing and sieving operations and more thorough separation techniques for several impurities (metal, paper, plastic, gypsum…).

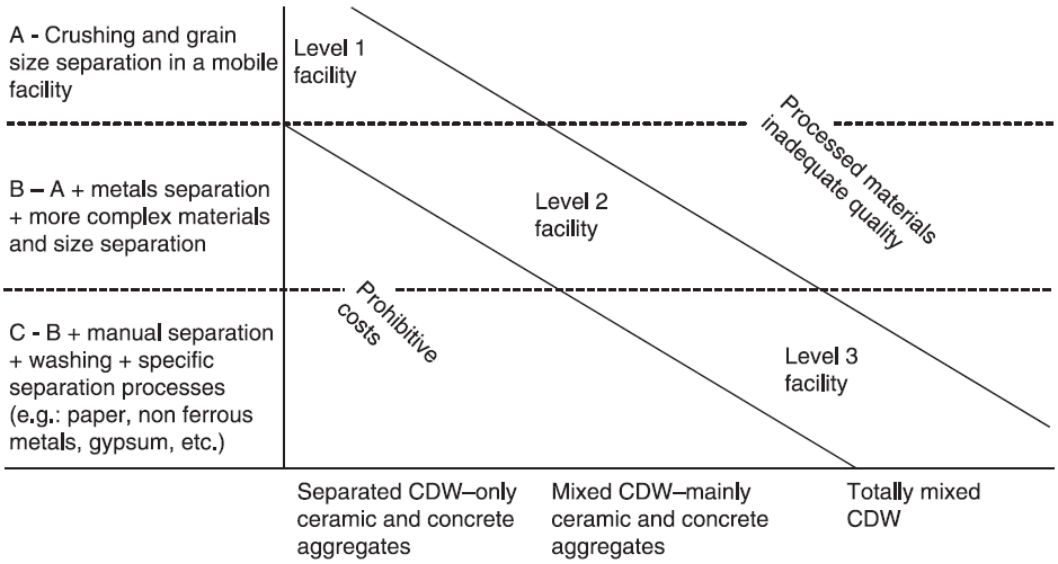

Figure 2.15: Types of CDW facilities according to the Symonds Group Ltd. (1999)

Several investigations have focused on the operations at CDW management plants from diverse points of view, while some research works have studied the technical aspects (Xing et al., 2004; Tam and Tam, 2006; Mulder et al., 2007), other studies have investigated the economic performance of the CDW treatment plants in order to verify their profitability (Duran et al., 2006; Nunes et al., 2007; Tam, 2008b; Zhao et al., 2010; Coelho and de Brito, 2013a). Finally, some investigations have revised the environmental impact of this type of waste management (Weil, 2006; Blengini and Garbarino, 2010; Chong and Hermreck, 2010; Marinković et al., 2010; Ortiz et al., 2010; Hiete et al., 2011; Coelho and de Brito, 2013b, 2013c).

Generally, CDW management plants receive the CDW as clean waste of an individual component (e.g. concrete or masonry) or as mixed wastes. Since the processing operations for each category are different, the gate fee for the residues is established accordingly, i.e. lower prices for individual waste streams that would only require crushing and screening operations. On the contrary, mixed CDW are spread out in order to facilitate the separation of the large and heavier contaminants by means of grab cranes. Afterwards, bulk waste is fed to a vibrating screen by a front-end loader to separate the initial fine fraction (<4mm) that would be stockpiled independently. Then, the upper part of the vibrating screen feeds the crusher machines responsible for the size reduction of the material. Afterwards, several separation operations take place in order to remove the impurities accompanying the granular material. Finally, a screening operation classifies the CDW in several size fractions of recycled aggregates. Figure 2.16 schematically illustrates the unit procedures carried out in a CDW management plant for the production of recycled aggregates.

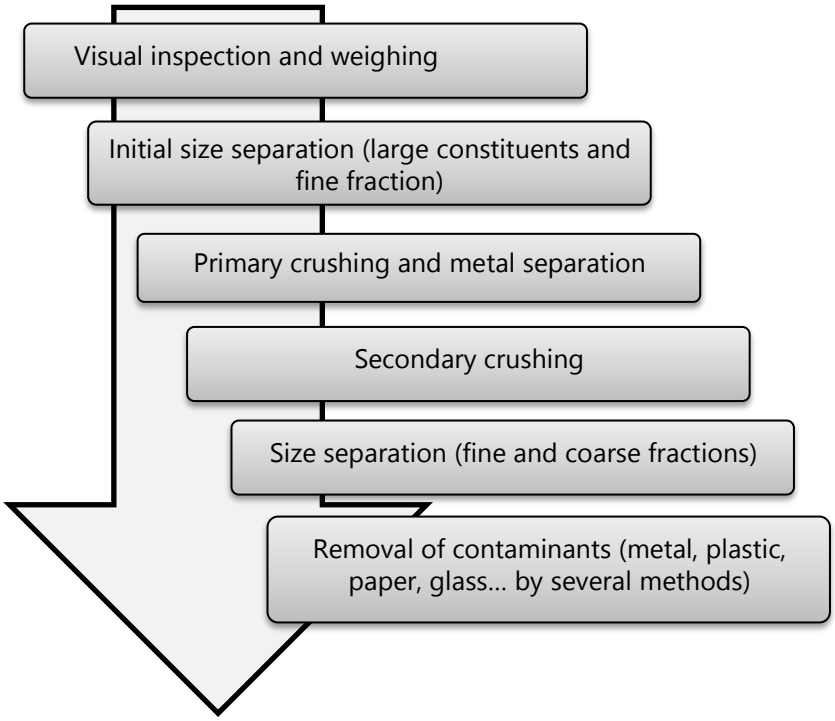

Figure 2.16: Production process at a CDW management plant

Commonly, the crushing operation in a CDW management plant is carried out in a two-stage process, which is beneficial for the overall quality of the recycled aggregates since sequential crushing operations have been identified as cleaning method of the mortar adhered to the CDW, with reductions ranging between 10% and 40% (Akbarnezhad et al., 2013). The machines employed for these operations are impact, jaw and cone crushers (Figure 2.17). A jaw crusher consists of a moving plate against a fixed one; these crushers are used for primary crushing stages and achieve a good particle size distribution with a low content of fines (<10%), but on the other hand they usually generate a high percentage of flaky-like particles. An impact crusher consists of a shaft fitted with hammers turning in a sealed chamber, which allows a greater reduction in particle size, but at the expense of the generation of a high (approximately 40%) content of fines. A cone crusher consists of an eccentrically rotating shaft turning in a fixed conic liner called concave, its principal disadvantage is the size of the input material which limits its use for secondary crushing stages, but this type of crusher is able to achieve a good particle size reduction with a low content of fines (around 20%).

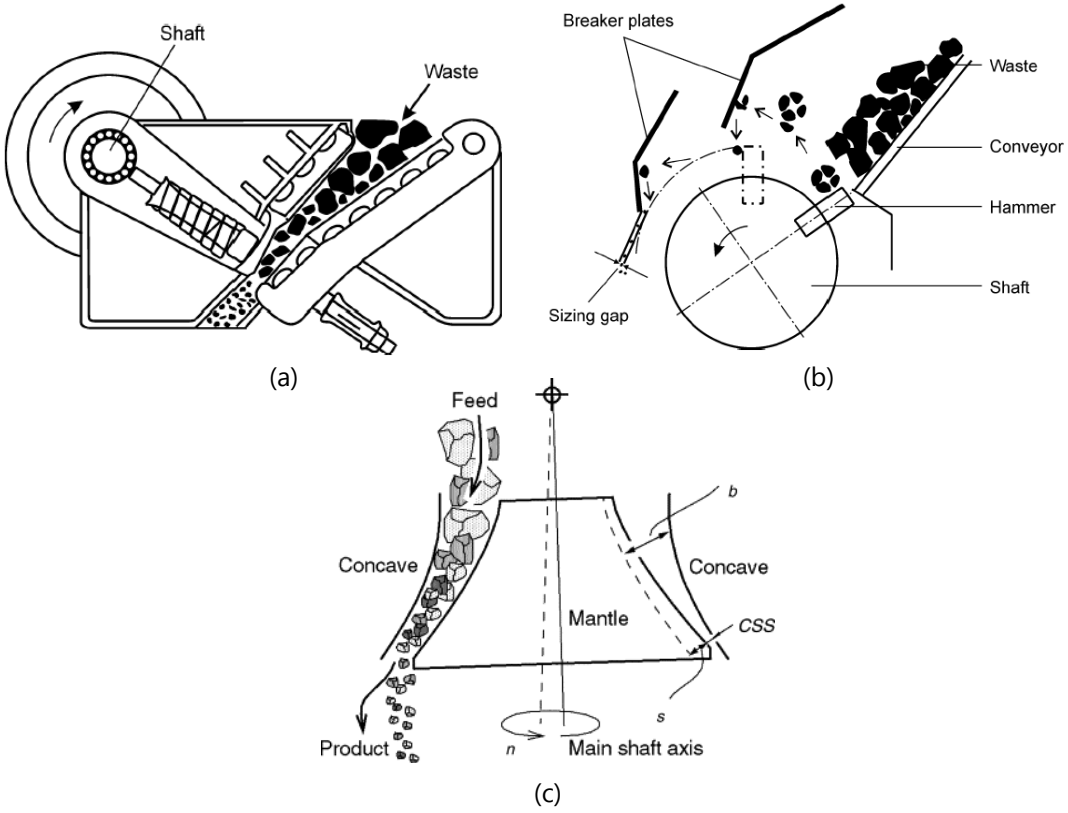

Figure 2.17: Type of crushers employed in CDW management plants. Jaw crusher (a), impact crusher (b) and cone crusher (c). (Lindqvist and Evertsson, 2006; Bilitewski, 2010)

In the processing of mixed CDW, the separation stage is of great importance in order to produce recycled aggregates with high quality, which is strongly influenced by the amount of impurities in the final product. Nonetheless, the cost of the separation process would limit the extent of the cleaning operations (Mulder et al., 2007). There are several types of separations to be employed based on the different properties (size, shape, density, magnetism, electrical conductivity…) of the individual wastes composing the CDW.

- Manual sorting: Two different stages of this operation could be distinguished. First, the mixed waste arriving at the CDW facility is assessed and the large and heavier contaminants are removed by means of a grab crane. Secondly, after the crushing stage and other separation techniques (Figure 2.16), other contaminants are removed by hand as the materials are transported in a conveyor belt.

- Size separation: The particle size is used to classify the CDW, being the screening the most common technique. Vibrating screens are considered an inexpensive technique, and rotary drum screens, also known as trommel, are also employed in CDW management plants.

- Density separation: Currently, this method is used to separate light materials such as plastic or paper from the bulk CDW. On one hand, pneumatic classification is used by means of air blowers at the discharge end of conveyor belts transporting the CDW; while the heavy material is unaffected, the light material is carried along the air stream. On the other hand, water is employed to separate the lightweight materials (<1000 kg/m^3) that float in the fluidised bed.

- Metals separation: Magnetic separation is one of the most common methods due to the economic benefits represented by the recycling of metals with a small investment. The mixed CDW are transported along moving conveyor belts to the mediations of magnets that remove the ferrous metals with an efficiency of about 95% to 99% (Kreith and Tchobanoglous, 1994). Afterwards, an eddy current separation method could be employed to recover non-ferrous materials at the end of conveyor belts. This technique is based on the induction of a secondary magnetic in the metal particle that would be repelled by the magnetic field of the rotor. Despite that the separation forces would depend on the type of material, a recovery efficiency ranging between 80 % and 95% could be expected (Lund, 2001).

Despite that the aforementioned separation techniques are the most commonly employed in CDW management plants, several investigations have pointed out the feasibility to implement alternative methods to separate the fractions comprising the mixed CDW. However, notwithstanding the potential shown by this technology at research level, its technological transfer to field applications is still a distant reality.

Among the investigations on wet separation techniques, Hendricks and Xing (2004a) used wet jigging to efficiently separate concrete and masonry particles, especially those greater than 19 mm. Conversely, Müller and Wienke (2004) obtained better results for the separation of gypsum than for the separation of masonry from concrete. For example, Schnellert et al. (2011) reported a 4 to 5 times reduction of the gypsum content when using this method. Nevertheless, wet methods are not considered the best technical option due to the high water usage, the cost derived from the slurry treatment and the soaking of the sorted aggregates.

Within the dry separation techniques, de Jeong and Fabrizi (2004) reported that dry sand fluidised bed has good efficiency, similar to a wet jigging system, for the separation of impurities in the 20-40 mm fraction on a pilot-scale base. Although the method has the disadvantage of sand loss to the final product, the authors argue that the sand incorporation is within the tolerated content in aggregates. More research efforts have been carried out about air jigging, which is based on the stratification of the particles by density due to vertical pulsations of air. Hendricks and Xing (2004b) suggested jigging as an alternative to vibrating screens or wind-shifting for particles greater than 4 mm and Coelho and de Brito (2013a) proposed a two-stage air jigging operation for the separation of the ceramic and gypsum particles greater than 4 mm from recycled concrete aggregates. Recently, Cazacliu et al. (2014) separated a ternary sample of CDW into its three constituent fractions: concrete (with 0.97% of gypsum and 8.35% of bricks remaining), brick (with 30.42% of concrete and 11.04% of gypsum remaining) and gypsum (with 3.39% of concrete and 18.06% brick remaining) by an air jigging operation lasting less than a minute, which speaks of the efficiency of this method for the improvement of quality of recycled aggregates, especially regarding to the cleaning of the concrete fraction. Furthermore, in his PhD thesis, Xing (2004) was able to efficiently separate brick and concrete rubble through magnetic separators, since the content of Fe_2O_3 in the bricks is more than twice of that in the concrete waste, by adapting the current and the tilting angle of the machine.

Finally, several investigations have focused on the optoelectronic separation of components with different colouring. The results from the study performed by de Jeong and Fabrizi (2004) indicated a good efficiency for the separation of wood, gypsum and glass. Another attempt in the use of the colour separation technique was performed by Xing (2004) as a means to separate brick (red and yellow) from concrete (grey) rubble. In spite of the high efficiency of the method, the higher process cost and the requirement of clean enough material in order to show the original colour are important disadvantages that hinder the current applicability of this technique.

3.1.3. CDW MANAGEMENT PLANTS IN SPAIN

The level of technology employed at the CDW management plants is relatively simple (Figure 2.16), as it basically consists of sequential phases of sieving, crushing and sorting. According to its technological level, the majority of Spanish CDW management plants could be classified as level 2 (55%), followed by level 3 plants (34%) and level 1 plants (11%) (Güell-Ferré et al., 2012). In addition, based on the mobility level of the equipment, 61% are stationary plants, 11% are mobile and the remaining 28% could be considered semi-mobile (Güell-Ferré et al., 2012).

A comprehensive survey on the characterization of Spanish CDW recycling plants' management models was performed by Rodríguez et al. (2015). The authors indicated that a typical Spanish CDW recycling facility is privately funded, has an intra-provincial operation level (reception and commercialization), which is carried out from a permanent site despite the possibility of incorporating mobile equipment.

Current information on the number of CDW management facilities has been reported in the draft of the State Waste Framework Plan (Spanish Ministry of Agriculture, Food and Environment, 2015). Table 2.5 shows the CDW management plants and landfills reported in the aforementioned draft for 2015 as well as the last available data for those Autonomous Communities without information in the State Waste Framework Plan (Spanish Ministry of Agriculture, Food and Environment, 2015). Hence, at least 571 CDW management plants are operating in Spain nowadays.

Table 2.5: Number and geographic distribution of transference plants, CDW treatment facilities and landfills in Spain (Spanish Ministry of Agriculture, Food and Environment, 2015)

Autonomous Community	Stationary plants	Mobile plants	Landfills
Andalusia	119	21	71
Aragon	6	1	5
Asturias	4	5	1
Balearic islands	5[a]		2[a]
Basque country	n/a	11	2[a]
Canary islands	23	n/a	7
Cantabria	4	12	2
Castile la Mancha	28	27	12
Castile and Leon	45	0	3
Catalonia	50	0	57
Ceuta	1[a]		1[a]
Extremadura	21	1	0
Galicia	43	21	5
La Rioja	16	0	2
Madrid	14	0	4
Melilla	1[a]		1[a]
Murcia	4	32	19
Navarra	7	3	7
Valencia	46[a]		9[a]

[a]*Data for 2013*

In spite of the high number of CDW management facilities, their geographical distribution is not homogenous which hampers the real treatment capabilities of the arising CDW. Since a sufficient number and an adequate spatial distribution of the CDW treatment plants is a key factor in the consecution of an efficient waste management (Kawano, 2002; Rao et al., 2007), local governments are including clauses regulating the location of waste management facilities in order to provide the tools necessary to implement the compulsory waste management process. For example, the Autonomous Community of Castile and León, Decree 11/2014 (Public Works and Environment Office of Castile and Leon, 2014) envisages the creation of primary waste sorting plants in provincial capitals, secondary plants in other towns, all of them with a 35 km radius of operation and containment zones or landfill sites for non-hazardous waste in isolated areas.

Furthermore, notwithstanding the number of CDW recycling facilities, Spain has always been characterized by high level of CDW disposal, both in authorized and illegal landfills. For instance, up to 64.30% of the total CDW produced in 2003 ended in uncontrolled disposal sites.

Nowadays, the illegal dumping is more controlled but the high availability for disposal in authorized landfills also influences the national CDW management model. In 2015, at least 210 authorized landfilling sites were available in Spain (Table 2.5). Furthermore, the landfill cost is relative cheaper, about 5 and 40 euros per tonne depending on the region, which is well below the actual cost of the process and comparatively lower than the cost of other management techniques that are more environmentally friendly. In addition, currently, only five Autonomous Communities (Cantabria, Catalonia, Madrid, Murcia and Valencia) incorporate landfill tax for CDW oscillating between 3 € and 7 € per tonne.

3.2. MARKET FOR RECYCLED AGGREGATES

The commercialization of recycled aggregates has been identified as one of the weakest links in the CDW recycling scenario (Kartam et al., 2004). In in any free market economy, price plays a major role in the purchase decision of any product, thus recycled aggregates have to be cheaper than natural aggregates with similar mechanical, physical and chemical properties (Klang et al., 2003; Duran et al., 2006; Rodríguez et al., 2007; Lu and Yuan, 2011). Nonetheless, in order to be economically advantageous, the price of recycled aggregates has to cover the production and transport cost as well as include a profit for the waste operator. For example, the estimated cost per tonne of processing CDW in stationary and mobile management plants was estimated, respectively, at 1.43 € and 2.61 € in Germany (Maurer, 2002), while Garbarino's (2005) calculations rendered a cost per tonne among 3.4 € and 5 € for CDW managed in Italian stationary plants and Zhao et al. (2010) obtained cost per tonne of 5.44 € in the Netherlands, where labour cost almost represented 55% of the total. Since virgin aggregates are a low-cost product due to their high availability in most EU countries, with average prices ranging between 5 and 10 euros per tonne in Europe (Böhmer et al., 2008), the selling prices for recycled aggregates should be kept below those figures. For example, prices of 2.75€ and 9 € per tonne have been reported for recycled concrete aggregates in Portugal and the Netherlands, respectively (Pacheco Torgal et al., 2013). These low prices mean that the sales of recycled aggregates only account for 14% of the benefits originating from a CDW management plant in Portugal, while the remaining 86% corresponds to the entrance fee applied to the CDW (Coelho and de Brito, 2013a).

Through different legislative efforts such as regulations, specifications, guidelines, taxation and public procurement (Karavezyris, 2007; Jaillon and Poon, 2008), the government plays a major role in the promotion of the CDW reutilization and the competitiveness of the recycled aggregates. First, waste framework policies and CDW policies, which usually transpose the EU waste legislation, could serve as a useful tool for tailoring the CDW management general guidelines to the specific characteristics of the country. Moreover, the creation of standards regulating the use of secondary aggregates from CDW in several construction applications is recognised as a key factor for promotion by establishing clear quality requirements putting at bay the current performance concerns that provoke the use of recycled materials. Also, by regulating environmental performances of building beyond energy issues, the use of secondary materials could be encouraged, as well as the building design favouring its future deconstruction.

Furthermore, the adoption of economic instruments such as the implementation of a taxation scheme on natural resources (Dahlbo et al., 2015) and landfill operations (Fatta et al., 2003; Dantata et al., 2005; Duran et al., 2006) that reflect the environmental externalities of their production under the polluter pays principle serves to counteract the imbalances between natural and recycled aggregates prices. In practice, countries such as Sweden, Denmark and United Kingdom imposing taxes on the landfill disposal and the primary aggregates extraction have some of the highest figures of recycled aggregate usage (Delgado et al., 2009). Finally, it is also within the power of the administration to stimulate the demand of recycled aggregates by means of green clauses in the public procurement.

Although the actual quality of the recycled aggregates influences its marketability (Kartam et al., 2004; Lu and Yuan, 2011), the consumer perception of secondary aggregates is one of the key factors in the competitiveness of recycled against natural aggregates (Klang et al., 2003; Kartam et al., 2004; Osmani et al., 2008). Despite that the undeniable environmental problem is forcing a change in the way people see waste, recycled aggregates are still been regarded as a waste, which for the general society is associated with unwanted things that suppose a cost, a problem or a source of contamination. Although all the different measures implemented by the government to foster the use of recycling aggregates indirectly serve to promote the acceptability of recycled aggregates among consumers, the incorporation of end of waste criteria status in the country regulations and the creation of certification systems based on performance criteria are the measures with the higher potential to counteract the current quality misconception of recycled aggregates and improve the confidence of consumers in the idea that waste can be a resource to be exploited.

Finally, the inconsistency of the supply of recycled aggregates was identified as a constraint of the recycled market by da Rocha and Sattler (2009). Although, a study carried out by Coelho (2015) proved the feasibility of self-sufficiency of construction materials in the Evora region (Portugal) through maintenance and retrofitting of the building stock, and the reuse and recycling of the CDW, recycled aggregates should not be considered as a substitute of the natural aggregates but an alternative in the aggregate supply chain and thus should not represent a limitation in their marketability.

3.2.1. SPANISH RECYCLING MARKET

Despite the interest in identifying the barriers and suggesting incentives to promote the use of recycled aggregates in Europe, the implementation of the proposed measures, as well as their effectiveness, vary greatly among the different Member States (Tojo et al., 2011). The case of Spain is characterized by a comprehensive waste framework (see section 2.1.1), the lack of national regulations for the use of recycled aggregates from CDW but the existence of guidelines developed by private initiatives (Güell-Ferré et al., 2012), an unequal enforcement on the taxation of the disposal at landfills among regions (see section 3.1.3) and a lack of taxation on the extraction of the natural aggregates. Table 2.6 illustrates the results from the SWOT analysis conducted to assess the factors influencing the actual possibilities of reuse of recycled aggregates from the CDW in the Spanish scenario from a strategic perspective.

Table 2.6: SWOT analysis for the use of recycled aggregates

Strengths	Weaknesses
1. Conservation of raw materials by substitution with secondary aggregates from CDW 2. Reduction of the need for landfill disposal 3. Interest of the research community 4. Interest of the government by means of investments on R&D projects (e.g. RECHINOR, CLEAM…)	1. CDW management as a reactive measure, not proactive 2. High availability and low cost of natural aggregates 3. Consumer perception 4. Quality linked to investment in CDW management 5. Quality inconsistencies 6. Lack of on-site separation 7. Higher times and costs for deconstruction
Opportunities	**Threats**
1. Taxation on natural resources 2. Taxation on landfilling 3. Ban of inert wastes in landfills 4. Economic incentives to selective demolition or deconstruction 5. Certification systems based upon performance criteria 6. Support from government by means of green procurement	1. Resistance to change 2. Supply inconsistences 3. Immature market for recycled aggregates 4. Unequal application in the Autonomous Communities

Consequently, the market of recycled aggregates in Spain is among the less developed in the European Union. It has been estimated that in the 2013-2014 period, Spain produced less than a million tonnes of recycled aggregate, whereas Germany and the UK were the biggest producers in the EU with values of 68 and 44 million tonnes, respectively (UEPG, 2015). Given the CDW typical composition in Spain, there are basically three types: recycled concrete aggregates, which despite having received most attention only accounts for 15% of the CDW generated and 30% of the CDW marketed (Güell-Ferré et al., 2012), and recycled aggregates comprising a mix of components that could be considering mixed or ceramic recycled aggregates depending on the percentages of the ceramic material. As regards market prices, the values range between 1.8 € and 5 € per tonne depending the region and the type of recycled aggregate.

3.3. APPLICATIONS

Once processed, the recycled aggregates can be used in backfilling, earthwork and road works, which imply the down-cycling of the residue, i.e. their transformation into new products of lower quality and reduced functionality; or can be reintroduced into the manufacturing of concrete. Since concrete is the most used material worldwide with an estimated consumption around 10 km^3 annually (Gartner and Macphee, 2011), which approximately constitutes 1 tonne per person (Van den Heede and De Belie, 2012), the use of recycled aggregates as total or partial substitution of the conventional coarse aggregate offers a solution for the environmental problem posed by the elevated figures of CDW while taking advantage of the full potential of the recycled aggregates. Thus, this dissertation will be focused on their use in the concrete manufacture.

Historical information dates the first use of construction and demolition wastes in the production of concrete to the end of World War II (Nixon, 1978), since Europe was partly reconstructed using the building rubble left behind after the bombings. Furthermore, Glushge (1946) is often cited as the first researcher to conduct an investigation on the recycling of concrete waste as secondary aggregates in the production of new concrete. Regarding the use of ceramic aggregates in the production of concrete, the origin dates back even further to the Roman era (Hewlett, 2003).

Nevertheless, it has been reported that just 2.2% of the recycled aggregates reused in the European Union are employed in the production of concrete (Geraldes, 2013). High quality recycling of concrete waste as secondary aggregate for concrete production is more common in Asia, specifically Japan, than Europe (Tam et al., 2010), even when it still could be considered down-cycling since the resulting product has lower strength than the parent concrete and it is usually employed in non-structural applications.

Nowadays, the scientific efforts are focused in proving the feasibility of recycled aggregates as substitutes of the natural coarse aggregates in the production of concrete in order to bolster this type of application. Hence, research employing the different types of recycled aggregates, namely concrete, mixed and ceramic, is based on the study of the influence of their quality and composition on the properties of the fresh and hardened recycled concrete. Among the three types of recycled aggregates, recycled concrete aggregates have received the main attention (Limbachiya et al., 2000; Gómez-Soberón, 2002; Lin et al., 2004; Tabsh and Abdelfatah, 2009; Fathifazl et al., 2011; Gokce et al., 2011; Ismail and Ramli, 2013, 2014; Manzi et al., 2013; Mazzotti et al., 2013; Safiuddin et al., 2013), since their properties are the most similar to those of virgin materials and most countries have specifications allowing and regulating their use. However, since mixed aggregates comprise great part of the CDW production in countries such as Spain, some investigations have been developed to first describe the properties of these types of recycled aggregates and verify the influence that has their incorporation in the concrete production (Mas Gracia and Cladera Bohigas, 2009; Agrela et al., 2011; Ihobe and CEDEX, 2011; Mas et al., 2012a, 2012b; Geraldes, 2013; Medina et al., 2014; Rodríguez-Robles et al., 2014b). Regarding ceramic aggregates, the number of research works is more limited (de Brito et al., 2005; Correia et al., 2006; Gomes and Brito, 2008; Pacheco-Torgal and Jalali, 2010a, 2010b; Yang et al., 2011; Sadek and Nouhy, 2014), and while many types of ceramic wastes have been incorporated as alternative aggregates in concrete, those recycled aggregates were not necessarily from CDW but rejects from production (Senthamarai and Devadas Manoharan, 2005; Medina et al., 2012a, 2012b; Halicka et al., 2013; Silvestre et al., 2013a, 2013b).

3.3.1. USES OF RECYCLED AGGREGATES IN SPAIN

Table 2.7 recreates the CDW valorisation options mentioned in the 2008-2015 Spanish national plan on CDW (Spanish Ministry of Environment, 2009). Although the table was created having in mind all possible alternatives for the application of these wastes, the current situation of the legislation and the constructive practice in Spain make that earthworks, roads and backfilling are the principal applications for the recycled products instead of the concrete manufacture (Jiménez et al., 2011; Mas et al., 2012a). Thus, around 90% of the recycled aggregates commercialized in Spain is employed as unbound aggregates (Güell-Ferré et al., 2012).

Table 2.7: Valorisation options for CDW according to the 2008-2015 Spanish national plan on CDW (Spanish Ministry of Environment, 2009)

Waste	**Product/Application**
Concrete	Aggregates/Unbound material for roads, pipeline stabilization and soil stabilization, mortar, mass and reinforced concrete, and manufacture of cement and other construction materials
Bricks	Lightweight aggregates/ Lightweight concrete and mortar, mass and reinforced concrete, manufacture of construction materials, pipeline stabilization and filling for sport, gardening or landscaping activities
Roof tiles and other ceramics	Lightweight aggregates/ Lightweight concrete and mortar, pipeline stabilization and filling for sport, gardening or landscaping activities
Mixed waste of concrete and ceramics without contaminants	Aggregates/Earthworks, backfilling, sealing of landfills and mass concrete for low level applications
Mixed waste of concrete and ceramics with contaminants	Waste/Landfill

3.3.2. SPECIFICATIONS FOR RECYCLED COARSE AGGREGATES IN CONCRETE

As the lack of standardization on the use of recycled aggregates is recognized as a barrier in their application; several countries have adopted specifications or guides in order to regulate, as well as promote, the use of recycled coarse aggregates in the production of concrete.

Despite the worldwide existence of specifications regarding requirements and limits for applications (e.g. Brazil (NBR 15116, 2004), Hong Kong (HKWB, 2002) and Japan (JIS A 5021, 2011; JIS A 5022, 2012; JIS A 5023, 2012), in the following sections, only a more detailed approach to the specifications over several Member States of the European Union is offered.

3.3.2.1. *RILEM recommendation*

A recommendation from the International union of laboratories and experts in construction materials, systems and structures (RILEM) proposed some specifications to classify recycled aggregates (RILEM TC 121-DRG, 1994). Three categories were suggested: type I aggregates originating from masonry rubble, type II aggregates originating from concrete rubble and type III aggregates which consist of a blend of natural and recycled aggregates satisfying a minimum content of natural aggregates (80%) and a maximum content of type I aggregates (10%). In addition, the recommendation also specifies some mandatory requirements for the use of different types of recycled aggregates in the concrete manufacture (Table 2.8). Besides, the recycled aggregate cannot contain any substance that delays the setting time up to a 15% of that of a reference concrete.

Table 2.8: Technical requirements of recycled coarse aggregates according to RILEM (RILEM TC 121-DRG, 1994)

	Type I	Type II	Type III
Dry particle density (kg/m^3)	≥1500	≥2000	≥2400
Water Absorption (%)	≤20	≤10	≤3
Content of material with SSD < 2200 kg/m^3 (%)	-	≤10	≤10
Content of material with SSD < 1800 kg/m^3 (%)	≤10	≤1	≤1
Content of material with SSD < 1000 kg/m^3 (%)	≤1	≤0.5	≤0.5
Content of impurities -metals, glass, bitumen…- (%)	≤5	≤1	≤1
Content of metals (%)	≤1	≤1	≤1
Content of organic material (%)	≤1	≤0.5	≤0.5
Content of sand (< 4 mm) (%)	≤5	≤5	≤5
Content of filler (< 0.063 mm) (%)	≤3	≤2	≤2
Content of sulphate (%)	≤1	≤1	≤1

SSD: saturated surface dried density

In terms of applications, the specification suggests that a total replacement ratio is possible, but under certain strength limitations and additional testing (Table 2.9) depending on the type of recycled aggregates and the exposure class if used in reinforced concrete.

Table 2.9: Provisions for the use of recycled concrete

	Type I	Type II	Type III
Maximum strength class	C16/20[a]	C50/60	No limit
Additional testing for dry exposure class[b]	None	None	
Additional testing for humid exposure class[b]	Alkali-silica test if allowed	Alkali-silica test	
Additional testing for marine exposure class[b]	Not allowed	Alkali-silica test Bulk freeze-thaw test	
Additional testing for chemical aggressive exposure class[b]	Not allowed	Alkali-silica test Bulk freeze-thaw test De-icing salt test	

[a] C20/37 if the saturated surface dry (SSD) density is ≥ 2000 kg/m^3; [b] The exposure classes in the original standard do not represent the current legislation (EN 206-1, 2013), hence the corresponding modifications have been made

3.3.2.2. *European Union*

In 2008, the modifications in the European standard EN 12620 (2002) included the topic of recycled aggregates. The specification addresses the need for specific testing methods of the recycled aggregates such as tests for chloride content due to the presence of attached mortar (UNE EN 1744-5, 2007), organic substances that can alter the rate of setting and hardening of concrete (UNE EN 1744-6, 2007) and resistance to freeze-thaw cycles (UNE EN 1367-1, 2008). In addition, the standard establishes that all recycled aggregates should be considered as potentially reactive for alkali-silica reactions. Moreover, a procedure for the identification of constituents of recycled coarse aggregates due to their typical heterogeneity was included to classify them.

Furthermore, the CEN/TC 104/SC 1 has been preparing an amendment to the EN 206-1 (2013) in order to include some general recommendations (such as limitations in the replacement ratio, the strength class or the environmental exposure) for the use of recycled aggregates in concrete, that is currently under enquiry but will be permissibly adopted in 2016.

3.3.2.3. *Belgium*

A working group (Vyncke and Rousseau, 1993) issued a recommendation for the use of two types of recycled aggregates in concrete; GBSB-I with masonry as major component and GBSB-II which mostly consisted of concrete rubble, covering the requirements for aggregates (Table 2.10) and the conditions for application of concrete made of recycled aggregates. While concrete mixtures made of GBSB-I aggregates were restricted to a maximum C16/20 strength, when employing GBSB-II aggregates for concrete the maximum permitted strength increased up to C30/37. Nonetheless, both types of concrete mixes were circumscribed to elements in the inside of a building or non-aggressive and dry environments.

Table 2.10: Technical requirements of recycled coarse aggregates according to Vyncke and Rousseau (1993)

	GBSB-I	**GBSB-II**
Dry density (kg/m^3)	≥1600	≥2100
Water absorption (%)	≤18	≤9
Content of material with density < 2100 kg/m^3 (%)	-	≤10
Content of material with density < 1600 kg/m^3 (%)	≤10	≤1
Content of material with density < 1000 kg/m^3 (%)	≤1	≤0.5
Content of minerals (%)	≥95	≥95
Content of non-minerals (%)	≤1	≤1
Content of organic materials (%)	≤0.5	≤0.5
Content of fines (<0.080 mm) (%)	≤5	≤3
Content of chlorides (%)	≤0.06	≤0.06
Content of sulphates (%)	≤1	≤1

Later on, the Impartial organization for the control of construction products (COPRO, 2003) proposed technical prescriptions for three types of recycled aggregates (concrete, masonry, and mixed waste). Table 2.11 shows the compositional requirements established in the standard. Conversely, no specifications for water absorption, density or maximum content of chlorides are included in the standard.

Lastly, in this regard, a Belgian annex to European regulations (NBN B 15-001, 2012) defines the requirements regarding quality and percentages for the use of recycled aggregates in concrete and limits up to 20% by volume the replacement ratio for indoor applications.

Table 2.11: Technical requirements of recycled coarse aggregates according to PTV 406 (COPRO, 2003)

	Concrete waste	Mixed waste	Masonry waste
Content of concrete and natural materials (%)	≥90	≥40	≤40
Content of masonry (%)	≤10	≥10	≥60
Content of other minerals such as shingles, tiles, ceramics, cellular and lightweight concrete… (%)	≤5	- ≤10	- ≤10
Content of bituminous materials (%)	≤5	≤5	≤5
Content of non-minerals such as gypsum, plastic, glass, metals… (%)	≤0.5	≤1	≤1
Content of organic materials (%)	≤0.5	≤0.5	≤0.5

3.3.2.4. *Denmark*

The Danish Concrete association (1990) was among the first developers of technical specifications for the use of crushed recycled concrete as aggregate in new concrete. Three types of aggregates were identified. On one hand, GP1 tested and GP1 untested, being both concrete wastes originating from recycling plants or other sources, respectively, and presenting a dry density higher than 2200 kg/m^3. On the other hand, GP2 are recycled aggregates mixed from concrete and masonry wastes that present a dry density over 1800 kg/m^3. This specification allowed a total replacement ratio for coarse recycled aggregates but restricted the use of concrete mixes made with GP1 and GP2 up to 40 MPa in low to moderate aggressive conditions and 20 MPa in a low aggressive medium, respectively.

Nowadays, standard DS 2426 (2011) includes the additional requirements and clarifications to the EN 206-1 (2013).

3.3.2.5. *Germany*

Almost two decades ago, the German Committee for reinforced concrete (1998) proposed a standard establishing guidelines for the use of recycled aggregates in concrete applications. The specification allowed a maximum C30/37 strength class while restraining the replacement ratio in function of the concrete application, ranging from 30% to 40% of total volume of coarse aggregate content for exterior and interior elements, respectively. Moreover, up to 50% replacement ratio was permitted for interior elements with strength class lower than C20/25.

Currently, the standard DIN 4226-100 (2002) classifies recycled aggregates in four categories: type 1 mainly composed by concrete waste, type 2 originating from demolition works (concrete as a major constituent but also masonry), type 3 involves masonry waste and type 4 which originates from mixed CDW, and establishes the requirements for their use in the concrete and mortar manufacture (Table 2.12).

Table 2.12: Technical requirements of recycled coarse aggregates according to DIN 4226-100 (2002)

	Type 1	Type 2	Type 3	Type 4
Dry particle density[a] (kg/m^3)	≥2000		≥1800	≥1500
Water absorption[b] (%)	≤10	≤15	≤20	No limit
Content of concrete (%)	≥90	≥70	≤20	
Content of clinker and solid brick (%)	≤10	≤30	≥80	≥80
Content of calcareous sandstone (%)			≤5	
Content of brick with pores, light or porous concrete, stucco, cement, pumice (%)	≤2	≤3	≤5	
Content of asphalt (%)	≤1	≤1	≤1	≤20
Content of mineral impurities such glass, plaster of stucco… (%)	≤2	≤2	≤2	
Content of non-mineral impurities such plastic, metal, wood… (%)	≤0.5	≤0.5	≤0.5	≤1
Content de fines (< 0.063 mm) (%)	≤4	≤4	≤4	≤4
Content of sulphate (%)	0.8	0.8	0.8	-
Content of chlorides (%)	≤0.04	≤0.04	≤0.04	≤0.15

[a] Allowable deviation of ±150 kg/m^3 for types 1, 2 and 3; [b] Determination after 10 minutes

In general, the replacement is allowed up to 5% without any additional restrictions. For higher percentages (maximum of 45% for type 1 and 25% for type 2), different uses are established together with the need to conduct additional tests. It is noteworthy that the use of type 3 or 4 aggregates is not permitted in structural concrete.

3.3.2.6. *The Netherlands*

Since 1984, the Dutch Committee for applied research (CUR) has issued several recommendations (Table 2.13) regarding the use of recycled concrete aggregates and crushed masonry on concrete (CUR, 1984a, 1984b, 1986). It is noteworthy that the Dutch specification recommends different size requirements for concrete aggregate and masonry aggregate, allowing greater quantity of fines in recycled aggregates originating from concrete. Regarding the application of these recycled aggregates in concrete (plain, reinforced or pre-stressed), substitutions up to 20% could be considered equivalent to conventional concrete and the total replacement of the conventional coarse aggregate is allowed. However, special measures such as the compensation for the water absorption by means of pre-saturation or addition of additional water or the increase up to 10% of the height or thickness of the structural element to increase stiffness should be applied for substitution values higher than 20%.

Currently, the NEN 5905 (2010) supplements the European standard for concrete aggregates, classifying coarse recycled aggregates into three types: recycled concrete aggregate (1), mixture of recycled brickwork and concrete aggregate (2) and recycled brickwork aggregate (3). In terms of applications, a substitution is permitted up to 100% and 20% for recycled aggregates type 1 and 2 respectively.

Table 2.13: Technical requirements for recycled coarse aggregates according to Dutch recommendations (CUR, 1984a, 1984b, 1986)

	Concrete waste	Masonry waste
Content of concrete and mortar (%)	≥95	≤55
Content of masonry (%)	≤5	≥65
Content of non-minerals such as bitumen, metals, wood, glass… (%)	≤1.5	≤2
Content of lamellar particles (%)	≤30	≤30
Content of calcium carbonate (%)	≤25	-
Content of dispersible fines (%)	-	≤4
Content of chlorides (%)	≤-/0.1/0.015[a]	≤1/0.1/0.015[a]
Content of sulphates (%)	≤1	≤1
Freeze-thaw weight loss (%)	≤3	≤3

[a] *Values for plan, reinforced and pre-stressed concrete respectively*

3.3.2.7. *Portugal*

The standard LNEC E-471 (2009) classifies recycled coarse aggregates into three groups: ARB1 and ARB2 - mainly concrete - and ARC - mixed wastes of concrete, unbound aggregates and masonry - and establishes their requirements for the production of concrete (Table 2.14).

Table 2.14: Technical requirements for recycled coarse aggregates according to LNEC E-471 (2009)

	ARB1	ARB2	ARC
Density (kg/m^3)	≥2200	≥2200	≥2000
Water absorption (%)	≤7	≤7	≤7
Content of concrete (%)	≥90	≥70	≥90
Content of unbound aggregates (%)			
Content of masonry (%)	≤10	≤30	
Content of bituminous materials (%)	≤5	≤5	≤10
Content of particles with density < 1000 kg/m^3 [a] (%)	≤1	≤1	≤1
Content of impurities such as glass, clay, plastic, metals… (%)	≤0.2	≤0.5	≤1
Content of fines (%)	≤4	≤4	≤3
Content of acid soluble sulphates (%)	≤0.8	≤0.8	≤0.8

[a] *If the particles are from mineral origin and non-harmful for concrete the limit is increased up to 3%*

Whilst for mass concrete, total substitution with ARB1 or AB2 aggregates is permitted; their use in structural concrete is subjected to a maximum replacement ratio in function of the concrete strength class. The substitution is allowed for X0, XC1, XC2, XC3, XC4, XS1, XA1 environmental exposures in conformance with EN 206-1 (2013), up to a 25% replacement with ARB1 aggregates in concrete mixtures of up to C40/50 strength class and up to a 20% replacement with ARB2 aggregates in concrete mixtures of up to C35/45 strength class. Nevertheless, higher percentages are acceptable if specific studies are conducted. In terms of the ARC aggregates, up to 100% substitution is permitted, but only for non-structural concrete and in non-aggressive environments.

3.3.2.8. *Spain*

In Spain, the recommendations for the use of recycled concrete aggregates were first proposed by the Spanish Scientific-technical association for structural concrete (ACHE) (Working group 2/5, 2006) and were the ground for the inclusion of this topic in the current legislation. The updated version of the Spanish Code on structural concrete (EHE-08) (Permanent Commission on Concrete, 2008) includes recommendations for the use of recycled aggregates in structural concrete (annex 15), which permits a substitution percentage of 20% for concrete with a maximum compressive strength of 40 MPa, and non-structural concrete (annex 18), which allows up to a 100% replacement. However, the current legislation only contemplates the use of recycled concrete aggregates that comply with the requirements shown in Table 2.15, as well as the general requirements of the standard for natural aggregates.

Table 2.15: Technical requirements for recycled coarse aggregates according to EHE-08 (Permanent Commission on Concrete, 2008)

	Recycled concrete aggregate
Water absorption[a] (%)	≤7
Content of ceramic (%)	≤5
Content of lightweight particles (%)	≤1
Content of asphalt (%)	≤1
Content of glass, plastic, metals… (%)	≤1
Content of sand (<4 mm) (%)	≤5
Content of clay for 20% substitutions (%)	≤0.15
Content of clay for 100% substitutions (%)	≤0.25

[a] Besides the natural aggregate should not exceed a 4.5% value and if the substitution is higher than 20%, the water absorption of the aggregates combined should not exceed 5%

Recently, the Spanish Association of CDW (GERD) carried out a national project in order to set the guidelines for the use of recycled aggregates in order to strengthen the recycling activities by means of technical recommendations (Güell-Ferré et al., 2012). Despite most suggestions refer to applications as unbound materials, specifications are also set for the manufacture of precast elements (concrete blocks, kerbs, slabs and benches), mass concrete and roller-compacted concrete with recycled aggregates from concrete and mixed wastes with ceramic depending on the demands of the final application.

3.3.2.9. *United Kingdom*

Initially, the British Research Establishment (BRE, 1998) classified recycled aggregates in three classes: masonry wastes (RCA I), concrete wastes with a maximum content of brick up to 10% (RCA II) and a combination of natural and recycled aggregates with a maximum content of brick up to 50% (RCA III), which are comparable to those of RILEM. Although the technical specifications were mostly limited to maximum commended levels of impurities (Table 2.16), recommendations were issued regarding the maximum grade of concrete in which these types of aggregates were suitable.

For RCA I, the density was a conditioning factor; thus, the maximum strength classes permitted were C20 and C35 for density values lower and higher than 2000 kg/m^3, respectively. And, while RCA II was limited to C50 concrete mixtures; no restrictions were suggested when using a combination of natural (80%) and recycled RCA III (20%) aggregates.

Table 2.16: : Technical requirements for recycled coarse aggregates according to BRE Digest 433 (1998)

	RCA I	RCA II	RCA III
Content of wood (%)	≤1	≤0.5	≤2.5
Content of glass, metals, plastics, asphalt, clay lumps… (%)	≤5	≤1	≤5
Content of sulphates (%)	≤1	≤1	≤1
10% fines value (kN)	≥70	≥100	≥70

Nowadays, the standard BS 8500-2 (2015) establishes the general specifications (Table 2.17), mostly related to the composition of the aggregates, and prescribes the limitations on their use in the production of recycled concrete. This specification only distinguishes between aggregate obtained from concrete (RCA) or from ceramic or mixed materials (RA). A limit up to a 20% replacement of RCA is established for C20/25 and C40/50 concrete classes in structural applications, although it leaves open the possibility to modifications under the responsibility of the prescriber. In addition, for non-structural concrete, total substitution of RCA or RA is permitted for lower strength classes under moderate exposure classes.

Table 2.17: Technical requirements for recycled coarse aggregates according to BS 8500-2 (2015)

	RCA	RA
Content of masonry (%)	≤5	≤100
Content of fines (%)	≤5	≤3
Content of lightweight materials (%)	≤0.5	≤1
Content of asphalt (%)	≤5	≤10
Content of wood, glass, plastic… (%)	≤1	≤1
Content of acid soluble sulphite (%)	≤1	- [a]

[a] *The limit should be determined in each case*

3.3.2.10. *Summary of the specifications for recycled coarse aggregates in concrete*

A similar pattern could be observed among the requirements for recycled aggregates and the specifications for their use in the manufacture of concrete. On one hand, the classification of the recycled aggregates mostly responds to their composition, specifically to the presence of ceramic materials; thus, the existence of three types of recycled aggregates originating from concrete rubble, masonry rubble and the mix of the previous waste is the typical scenario. On the other hand, the requirements established by these standards focus mostly on density, water absorption, and content of impurities, fines, sulphates and chlorides. Nonetheless, it is worth mentioning the English standard (BS 8500-2, 2015) as exception, since the requirements regarding composition are considered sufficient to classify and ensure the quality of aggregates.

In general, the density and water absorption values are used to classify the recycled aggregates. Usually, these parameters are consistent with the composition of the various types of aggregates, i.e. decreasing values of density and increasing values of water absorption as the ceramic content increases. However, in the Portuguese standard (LNEC E-471, 2009), different density limits correspond to the same water absorption constraint, which is expected to hinder the compliance of recycled aggregates with higher ceramic contents. Density limits vary between 2000-2400 kg/m^3 for concrete aggregates, between 1800-2000 kg/m^3 for mixed aggregates and between 1500-1800 kg/m^3 for masonry aggregates. Although density and water absorption can be calculated on the basis of each other, excluding in the Spanish standard (Permanent Commission on Concrete, 2008), the standards provide values for both requirements. Except for the Portuguese specification (LNEC E-471, 2009) that limits water absorption for all types of recycled aggregates up to a 7%, the absorption limits range between 3% and 10% for concrete aggregates, between 10% and 15% for mixed aggregates and between 18% and 20% for ceramic aggregates. Nevertheless, attention should be paid to the water absorption limits in the German standard (DIN 4226-100, 2002), since the limit for water absorption is based upon a 10 minutes determination. This fact, in conjunction with the allowable values, made the standard one of the most permissible in this regard. In addition, the lack of limit for the water absorption for type 4 recycled aggregates indicates that its allowable uses are to be not demanding and not quite dependent on this property.

The concept of impurities includes a wide range of materials, which is not identical in all specifications, and usually ranges between 1% and 5%. The content of fines oscillates between 2% and 5%, although particle sizes inferior to 0.080 mm and 0.063 mm are considered as fines in different specifications. In terms of chemical requirements, all countries have established maximum values for sulphates of between 0.8% and 1%. Regarding to the limit of chlorides, some countries (Portugal, Spain and United Kingdom) do not establish a specific restriction; hence, recycled aggregates should comply with the limitations imposed for natural aggregates; while the rest of the analysed standards enforce constraints ranging from 0.04% to 1%. It is of interest to note on this subject that in the Netherlands (CUR, 1984a, 1984b, 1986) several limit values with higher restriction levels are included for different concrete applications (mass, reinforced and pre-stressed), which lessen the excessive requirement imposed in other countries for mass concrete applications.

Finally, respecting the specifications on the application of the recycled aggregates for the concrete manufacture, the allowed ratios of replacement of natural aggregates by recycled aggregates for concrete production are relatively low, which hampers the use of high volumes. A replacement ratio of 20% seems to be commonly accepted for structural purposes without excessively compromising the concrete strength class since small modifications in the performance of concrete are expected for such low level of substitution with recycled aggregates derived from concrete rubble, which could be considered of good quality according to the requirements that they must meet in order to be used in the concrete manufacture. Thus, standards enforcing this replacement ratio (Permanent Commission on Concrete, 2008; LNEC E-471, 2009; BS 8500-2, 2015) could be regarded as conservative. Contrarily, total substitution levels are allowed for masonry and mixed recycled aggregates, but only for non-structural applications and under a moderate environment.

4. REFERENCES

Agrela, F., Sánchez de Juan, M., Ayuso, J., Geraldes, V.L., Jiménez, J.R., 2011. Limiting properties in the characterisation of mixed recycled aggregates for use in the manufacture of concrete. *Construction and Building Materials* 25 (10): 3950–3955.

Akbarnezhad, A., Ong, K., Tam, C., Zhang, M., 2013. Effects of the Parent Concrete Properties and Crushing Procedure on the Properties of Coarse Recycled Concrete Aggregates. *Journal of Materials in Civil Engineering* 25 (12): 1795–1802.

Basten, M., Pahl, G., Schäfer, B., 2011a. Monitoring of construction and demolition waste in 2008 [in German]. Bundesverband Baustoffe - Steine und Erden e.V, Berlin, Germany.

Basten, M., Pahl, G., Schäfer, B., 2011b. Monitoring of construction and demolition waste in 2006 [in German]. Bundesverband Baustoffe - Steine und Erden e.V, Berlin, Germany.

Basten, M., Pahl, G., Schäfer, B., 2013. Monitoring of construction and demolition waste in 2010 [in German]. Bundesverband Baustoffe - Steine und Erden e.V, Berlin, Germany.

Basten, M., Pahl, G., Schäfer, B., 2015. Monitoring of construction and demolition waste in 2012 [in German]. Bundesverband Baustoffe - Steine und Erden e.V, Berlin, Germany.

Begum, R.A., Siwar, C., Pereira, J.J., Jaafar, A.H., 2007. Implementation of waste management and minimisation in the construction industry of Malaysia. *Resources, Conservation and Recycling* 51 (1): 190–202.

Bergsdal, H. avard, Bohne, R.A., Brattebø, H., 2007. Projection of construction and demolition waste in Norway. *Journal of Industrial Ecology* 11 (3): 27–39.

Bilitewski, B., 2010. Mechanical Treatment: Unit Processes, in: Christensen, T.H. (Ed.), Solid Waste Technology & Management. John Wiley & Sons, Ltd, 319–348.

BIO, Deloitte, BRE, ICEDD, VTT, RPS, FCT of NOVA University of Lisbon, 2015. Construction and demolition waste management in Spain, Resource efficient use of mixed wastes.

Blengini, G.A., Garbarino, E., 2010. Resources and waste management in Turin (Italy): The role of recycled aggregates in the sustainable supply mix. *Journal of Cleaner Production* 18 (10-11): 1021–1030.

Böhmer, S., Moser, G., Neubauer, C., Peltoniemi, M., Schachermayer, E., Tesar, M., Walter, B., Winter, B., 2008. Aggregates case study (No. 150787-2007 F1SC-AT). Institute for Prospective Technological Studies, Vienna, Austria.

Bossink, B.A.G., Brouwers, H.J.H., 1996. Construction waste: quantification and source evaluation. *Journal of Construction Engineering and Management* 122 (1): 55–60.

BRE, 1998. Recycled aggregates (BRE Digest 433). BRE, London, UK.

BS 8500-2, 2015. Concrete. Complementary British standard to BS EN 206. Specification for constituent materials and concrete. BSI, London.

Chandrakanthi, M., Hettiaratchi, P., Prado, B., Ruwanpura, J.Y., 2002. Optimization of the waste management for construction projects using simulation, in: Proceedings of the 2002 Winter Simulation Conference. San Diego, California, 1771–1777.

Cheng, J.C.P., Ma, L.Y.H., 2013. A BIM-based system for demolition and renovation waste estimation and planning. *Waste Management* 33 (6): 1539–1551.

Chen, Z., Li, H., Wong, C.T.C., 2002. An application of bar-code system for reducing construction wastes. *Automation in Construction* 11 (5): 521–533.

Chinda, T., Engpanyalert, W., Tananoo, A., Chaikong, J., Methawachananont, A., 2013. The development of the construction and demolition waste dynamic model. *International Journal of Engineering and Technology* 5 (5): 617–621.

Chong, W.K., Hermreck, C., 2010. Understanding transportation energy and technical metabolism of construction waste recycling. *Resources, Conservation and Recycling* 54 (9): 579–590.

Cochran, K.M., Townsend, T.G., 2010. Estimating construction and demolition debris generation using a materials flow analysis approach. *Waste Management*, Special Thematic Section: Sanitary Landfilling 30 (11): 2247–2254.

Coelho, A., 2015. Preliminary study for self-sufficiency of construction materials in a Portuguese region – Évora. *Journal of Cleaner Production* (In press): 10.1016/j.jclepro.2015.06.113.

Coelho, A., de Brito, J., 2011. Economic analysis of conventional versus selective demolition—A case study. *Resources, Conservation and Recycling* 55 (3): 382–392.

Coelho, A., de Brito, J., 2013a. Economic viability analysis of a construction and demolition waste recycling plant in Portugal – part I: location, materials, technology and economic analysis. *Journal of Cleaner Production* 39: 338–352.

Coelho, A., de Brito, J., 2013b. Environmental analysis of a construction and demolition waste recycling plant in Portugal – Part II: Environmental sensitivity analysis. *Waste Management* 33 (1): 147–161.

Coelho, A., de Brito, J., 2013c. Environmental analysis of a construction and demolition waste recycling plant in Portugal – Part I: Energy consumption and CO2 emissions. *Waste Management* 33 (5): 1258–1267.

COPRO, 2003. Recycled aggregates from construction and demolition waste [in French] (Technical prescriptions PTV 406). Impartial organization for the control of construction products, Brussels, Belgium.

Correia, J.R., Brito, J. de, Pereira, A.S., 2006. Effects on concrete durability of using recycled ceramic aggregates. *Materials and Structures* 39 (2): 169–177.

CUR, 1984a. Crushed concrete as aggregate for concrete [in Dutch] (Recommedation 4). Dutch Committee for applied research, Netherlands.

CUR, 1984b. Crushed masonry as aggregate for concrete [in Dutch] (Recommedation 5). Dutch Committee for applied research, Netherlands.

CUR, 1986. Crushed concrete rubble and masonry rubble as aggregate for concrete [in Dutch] (Report 125). Dutch Committee for applied research, Netherlands.

Dahlbo, H., Bachér, J., Lähtinen, K., Jouttijärvi, T., Suoheimo, P., Mattila, T., Sironen, S., Myllymaa, T., Saramäki, K., 2015. Construction and demolition waste management – a holistic evaluation of environmental performance. *Journal of Cleaner Production* (In press): 10.1016/j.jclepro.2015.02.073.

Danish Concrete association, 1990. Recommendations for the use of recycled aggregates for concrete in passive environmental class (No. 34). Copenhagen, Denmark.

Danish Ministry of the Environment., 2011. Waste Statistics 2009 and projections of waste 2011–2050 [in Danish]. Danish Ministry of the Environment.

Dantata, N., Touran, A., Wang, J., 2005. An analysis of cost and duration for deconstruction and demolition of residential buildings in Massachusetts. *Resources, Conservation and Recycling* 44 (1): 1–15.

da Rocha, C.G., Sattler, M.A., 2009. A discussion on the reuse of building components in Brazil: An analysis of major social, economical and legal factors. *Resources, Conservation and Recycling* 54 (2): 104–112.

de Brito, J., Pereira, A.S., Correia, J.R., 2005. Mechanical behaviour of non-structural concrete made with recycled ceramic aggregates. *Cement and Concrete Composites* 27 (4): 429–433.

de Guzmán Báez, A., Sáez, P.V., del Río Merino, M., Navarro, J.G., 2012. Methodology for quantification of waste generated in Spanish railway construction works. *Waste management* 32 (5): 920–924.

de Jong, T.P.., Fabrizi, L., 2004. Dry separation of mixed construction and demolition waste. *Recycling International* (December): 24–27.

Delgado, L., Catarino, A.S., Eder, P., Litten, D., Luo, Z., Villanueva, A.V., 2009. End-of-Waste Criteria (JRC 53238). Institute for Prospective and Technological Studies, Joint Research Centre, Luxembourg.

DIN 4226-100, 2002. Aggregates for mortar and concrete. Part 100: recycled aggregates. DIN, Berlin.

DS 2426, 2011. Concrete – Materials – Rules for application of EN 206-1 in Denmark. DS, Copenhagen, Denmark.

Duran, X., Lenihan, H., O'Regan, B., 2006. A model for assessing the economic viability of construction and demolition waste recycling—the case of Ireland. *Resources, Conservation and Recycling* 46 (3): 302–320.

Elshkaki, A., 2005. Dynamic stock modelling: A method for the identification and estimation of future waste streams and emissions based on past production and product stock characteristics. *Energy* 30 (8): 1353–1363.

EN 206-1, 2013. Concrete. Part 1: Specification, performance, production and conformity. CEN, Brussels.

EN 12620, 2002. Aggregates for concrete. CEN, Brussels, Belgium.

Esin, T., Cosgun, N., 2007. A study conducted to reduce construction waste generation in Turkey. *Building and Environment* 42 (4): 1667–1674.

Euroconstruct, 2015. Latest European construction trends and forecasts 2015-2017. Presented at the 79th Euroconstruct Conference, Warsaw, Poland.

European Commission, 2000. Decision 2000/532/EC, of 3 May 2000, replacing Decision 94/3/EC establishing a list of wastes pursuant to Article 1(a) of Council Directive 75/442/EEC on waste and Council Decision 94/904/EC establishing a list of hazardous waste pursuant to Article 1(4) of Council Directive 91/689/EEC on hazardous waste (notified under document number C(2000) 1147), Official Journal of the European Communities, L 226, 3-24.

European Commission, 2014. Resource efficiency opportunities in the building sector (COM 445(2014)). European Commission, Brussels, Belgium.

European Commission, 2015. Monitoring the application of Union law. 2014 Annual Report (COM 329 (2015)). Brussels, Belgium.

European Council, 1975. Directive 75/442/EEC, of 15 July, on waste, Official Journal of the European Communities,L 194, 39–41.

European Council, 1993. Resolution of the Council and the Representatives of the Governments of the Member States, of 1 February, on a Community programme of policy and action in relation to the environment and sustainable development, Official Journal of the European Communities, C 138, 1-4.

European Council, 1999. Directive 1999/31/EC, of 26 April, on the landfill of waste, Official Journal of the European Communities, L 182, 1-19.

European Parliament and Council, 2000a. Directive 2000/76/EC, of 4 December, on the incineration of waste, Official Journal of the European Communities, L 332, 91-111.

European Parliament and Council, 2000b. Directive 2000/59/EC, of 27 November, on port reception facilities for ship-generated waste and cargo residues, Official Journal of the European Communities, L 332, 81-90.

European Parliament and Council, 2006. Directive 2006/21/EC, of 15 March 2006, on the management of waste from extractive industries and amending Directive 2004/35/EC, Official Journal of the European Communities, L 102,15–34.

European Parliament and Council, 2008. Directive 2008/98/EC of 19 November 2008 on waste and repealing certain directives, Official Journal of the European Communities, L 312, 3-30.

European Parliament and Council, 2013. Decision 1386/2013/EU, of 20 November, on a General Union Environment Action Programme to 2020 "Living well, within the limits of our planet," Official Journal of the European Communities, L 354, 171-200.

Eurostat, 2012. European Statistics. Statistical Office of the European Communities.

Fathifazl, G., Ghani Razaqpur, A., Burkan Isgor, O., Abbas, A., Fournier, B., Foo, S., 2011. Creep and drying shrinkage characteristics of concrete produced with coarse recycled concrete aggregate. *Cement and Concrete Composites* 33 (10): 1026–1037.

Fatta, D., Papadopoulos, A., Avramikos, E., Sgourou, E., Moustakas, K., Kourmoussis, F., Mentzis, A., Loizidou, M., 2003. Generation and management of construction and demolition waste in Greece—an existing challenge. *Resources, Conservation and Recycling* 40 (1): 81–91.

Fischer, C., Werge, M., 2009. EU as a recycling society: present recycling levels of municipal waste and construction & demolition waste in the EU. European Topic Centre on Sustainable Consumption and Production, Copenhagen, Denmark.

Franklin Associates, 1998. Characterization of building-related construction and demolition debris in the United States (EPA530-R-98-010). US Environmental Protection Agency, Washington DC.

Garbarino, E., 2005. State of the art and results of an experimental research on beneficiation of recycled aggregate and concrete production. Politecnico di Torino, Torino, Italy.

Gartner, E.M., Macphee, D.E., 2011. A physico-chemical basis for novel cementitious binders. *Cement and Concrete Research* 41 (7): 736–749.

Geraldes, V.L., 2013. Study on non-structural recycled concretes with mixed recycled aggregate: Mechanical properties and expansion due to sulphates [in Spanish]. Universidad Politécnica de Madrid, Madrid, Spain.

German Committee for reinforced concrete, 1998. Guideline, concrete with recycled aggregates [in German]. German Committee for reinforced concrete, Germany.

Glushge, P., 1946. The work of the Scientific Research Institute. *Gidrotskhnicheskoge Stroitelstvo* 4 (10): 27–28.

Gokce, A., Nagataki, S., Saeki, T., Hisada, M., 2011. Identification of frost-susceptible recycled concrete aggregates for durability of concrete. *Construction and Building Materials* 25 (5): 2426–2431.

Gomes, M., Brito, J. de, 2008. Structural concrete with incorporation of coarse recycled concrete and ceramic aggregates: durability performance. *Materials and Structures* 42 (5): 663–675.

Gómez-Soberón, J.M.V., 2002. Porosity of recycled concrete with substitution of recycled concrete aggregate: An experimental study. *Cement and Concrete Research* 32 (8): 1301–1311.

Government of the Netherlands, 2012. Annexes to the Secretary of Infrastructure and the Environment on waste management [in Dutch]. Government of the Netherlands, Netherlands.

Güell-Ferré, A., Váquez-Ramonich, E., Varela-Pinto, E., Serna-Ros, P., Martínez-Abella, F., López-Gayarre, F., Barra-Bizinotto, M., Tirado-Alonso, A., Romero-Casado, A., Girbés-Clari, I., 2012. Spanish handbook on recycled aggregates from construction and demolition wastes (CDW) [in Spanish], Fueyo Editores. ed. Madrid, Spain.

Halicka, A., Ogrodnik, P., Zegardlo, B., 2013. Using ceramic sanitary ware waste as concrete aggregate. *Construction and Building Materials* 48: 295–305.

Hao, J.L., Hills, M.J., Huang, T., 2007. A simulation model using system dynamic method for construction and demolition waste management in Hong Kong. *Construction Innovation: Information, Process, Management* 7 (1): 7–21.

Hao, J.L.J., Tam, V.W.Y., Yuan, H.P., Wang, J.Y., Li, J.R., 2010. Dynamic modeling of construction and demolition waste management processes: An empirical study in Shenzhen, China. *Engineering, Construction and Architectural Management* 17 (5): 476–492.

Hechler, O., Larsen, O.P., Nielsen, S., 2010. Design for deconstruction (Final Report COST C25 WG3). European Cooperation in Science and Technology.

Hendriks, C.F., Xing, W., 2004a. Suitable separation treatment of stony components in construction and demolition waste (CDW), in: Proceedings of the International RILEM Conference on the Use of Recycled Materials in Building and Structures. RILEM Publications SARL, 166–172.

Hendriks, C.F., Xing, W., 2004b. Quality improvement of granular wastes by separation techniques, in: International RILEM Conference on the Use of Recycled Materials in Building and Structures. RILEM Publications SARL, 142–149.

Hewlett, P. (Ed.), 2003. Lea's chemistry of cement and concrete. Butterworth-Heinemann.

Hiete, M., Stengel, J., Ludwig, J., Schultmann, F., 2011. Matching construction and demolition waste supply to recycling demand: a regional management chain model. *Building Research & Information* 39 (4): 333–351.

HKWB, 2002. Specifications facilitating the use of recycled aggregates (Technical Circular 12). Hong Kong Works Bureau, Hong Kong, RP China.

Hsiao, T., Huang, Y., Yu, Y., Wernick, I., 2002. Modeling materials flow of waste concrete from construction and demolition wastes in Taiwan. *Resources Policy* 28 (1): 39–47.

Hu, M., Van Der Voet, E., Huppes, G., 2010. Dynamic material flow analysis for strategic construction and demolition waste management in Beijing. *Journal of Industrial Ecology* 14 (3): 440–456.

Ifo Institute, 2015. Ifo Economic climate for the Euro area (Ifo Wordld economic survey of the third quarter of 2015). Munich, Germany.

Ihobe, CEDEX, 2011. Uses of mixed recycled aggregates from construction and demolition wastes [in Spanish] (Pre-normative investigation). Ihobe.

Irish Environmental Protection Agency, 1995. National waste database – report for 1995. Irish Environmental Protection Agency.

Ismail, S., Ramli, M., 2013. Engineering properties of treated recycled concrete aggregate (RCA) for structural applications. *Construction and Building Materials* 44: 464–476.

Ismail, S., Ramli, M., 2014. Effect of different moisture states of surface-treated recycled concrete aggregate on properties of fresh and hardened concrete. *International Journal of Civil, Architectural, Structural and Construction Engineering* 8: 65–71.

Jaillon, L., Poon, C.S., 2008. Sustainable construction aspects of using prefabrication in dense urban environment: a Hong Kong case study. *Construction Management and Economics* 26 (9): 953–966.

Jalali, S., 2007. Quantification of construction waste amount, in: 6th International Technical Conference of Waste. Viseu, Portugal.

Jiménez, J.R., Agrela, F., Ayuso, J., López, M., 2011. A comparative study of recycled aggregates from concrete and mixed debris as material for unbound road sub-base. *Materiales de Construcción* 61 (302): 289–302.

JIS A 5021, 2011. Recycled aggregate for concrete-class H. Japan Concrete Institute, Tokyo, Japan.

JIS A 5022, 2012. Recycled aggregate for concrete-class M. Japan Concrete Institute, Tokyo, Japan.

JIS A 5023, 2012. Recycled aggregate for concrete-class L. Japan Concrete Institute, Tokyo, Japan.

Karavezyris, V., 2007. Report: treatment of commercial, construction and demolition waste in North Rhine-Westphalia: policy-making and operation options. *Waste Management & Research* 25 (2): 183–189.

Kartam, N., Al-Mutairi, N., Al-Ghusain, I., Al-Humoud, J., 2004. Environmental management of construction and demolition waste in Kuwait. *Waste Management* 24 (10): 1049–1059.

Kawano, H., 2002. The state of using by-products in concrete in Japan and outline of JIS/TR on recycled concrete using recycle aggregate, in: The First Fib Congress on Concrete Structures in the 21st Century. Osaka, Japan.

Klang, A., Vikman, P.-Å., Brattebø, H., 2003. Sustainable management of demolition waste—an integrated model for the evaluation of environmental, economic and social aspects. *Resources, Conservation and Recycling* 38 (4): 317–334.

Kofoworola, O.F., Gheewala, S.H., 2009. Estimation of construction waste generation and management in Thailand. *Waste Management* 29 (2): 731–738.

Kreith, F., Tchobanoglous, G., 1994. Handbook of solid waste management. McGraw-Hill, New York, USA.

Lau, H.H., Whyte, A., Law, P., 2008. Composition and characteristics of construction waste generated by residential housing project. *International Journal of Environmental Research* 2 (3): 261–268.

Lauritzen, E.K., 2004. Recycling concrete-an overview of development and challenges, in: International RILEM Conference on Use of Recycled Materials in Buildings. Barcelona, Spain, 9–11.

Li, J., Ding, Z., Mi, X., Wang, J., 2013. A model for estimating construction waste generation index for building project in China. *Resources, Conservation and Recycling* 74: 20–26.

Limbachiya, M.C., Leelawat, T., Dhir, R.K., 2000. Use of recycled concrete aggregate in high-strength concrete. *Materials and Structures* 33 (9): 574–580.

Lindqvist, M., Evertsson, C.M., 2006. Development of wear model for cone crushers. *Wear* 261 (3–4): 435–442.

Lin, Y.-H., Tyan, Y.-Y., Chang, T.-P., Chang, C.-Y., 2004. An assessment of optimal mixture for concrete made with recycled concrete aggregates. *Cement and Concrete Research* 34 (8): 1373–1380.

Llatas, C., 2011. A model for quantifying construction waste in projects according to the European waste list. *Waste Management* 31 (6): 1261–1276.

LNEC E-471, 2009. Guide for the use of recycled coarse aggregates in concretes with hydraulic binder [in Portuguese]. LNEC, Lisbon.

Lund, H.F., 2001. Recycling handbook. McGraw-Hill, New York, USA.

Lu, W., Yuan, H., 2011. A framework for understanding waste management studies in construction. *Waste Management* 31 (6): 1252–1260.

Maña i Reixach, F., González i Barroso, J.M., Sagrera i Cuscó, A., 2000. Management plan on construction and demolition works [in Spanish]. Institut de Tecnología de la Construcció de Catalunya (ITeC), Barcelona, Spain.

Manzi, S., Mazzotti, C., Bignozzi, M.C., 2013. Short and long-term behavior of structural concrete with recycled concrete aggregate. *Cement and Concrete Composites* 37: 312–318.

Marinković, S., Radonjanin, V., Malešev, M., Ignjatović, I., 2010. Comparative environmental assessment of natural and recycled aggregate concrete. *Waste Management*, Special Thematic Section: Sanitary Landfilling 30 (11): 2255–2264.

Martínez-Lage, I., Martínez-Abella, F., Vázquez-Herrero, C., Ordóñez, J.L.P., 2010. Estimation of the annual production and composition of C&D debris in Galicia (Spain). *Waste management* 30: 636–645.

Mas, B., Cladera, A., Bestard, J., Muntaner, D., López, C.E., Piña, S., Prades, J., 2012a. Concrete with mixed recycled aggregates: Influence of the type of cement. *Construction and Building Materials* 34: 430–441.

Mas, B., Cladera, A., del Olmo, T., Pitarch, F., 2012b. Influence of the amount of mixed recycled aggregates on the properties of concrete for non-structural use. *Construction and Building Materials* 27 (1): 612–622.

Mas Gracia, B., Cladera Bohigas, A., 2009. Effect of the incorporation of mixed recycled aggregate on the properties of non-structural concretes [in Spanish]. *Hormigón y acero* 253: 83–94.

Maurer, H., 2002. Economic issues in the mobile recycling of building materials. *Aufbereitungs-Technik* 43 (12): 26–31.

Mazzotti, C., Manzi, S., Bignozzi, M.C., 2013. Role of recycled concrete aggregates on the long-term behavior of structural concrete, in: Mechanics and Physics of Creep, Shrinkage, and Durability of Concrete: A Tribute to Zden? K P. Ba Ant: Proceedings of the Ninth International Conference on Creep, Shrinkage, and Durability Mechanics (CONCREEP-9), September 22-25, 2013 Cambridge, Massachusetts. ASCE Publications, 388.

Medina, C., Frías, M., Sánchez de Rojas, M.I., 2012a. Microstructure and properties of recycled concretes using ceramic sanitary ware industry waste as coarse aggregate. *Construction and Building Materials* 31: 112–118.

Medina, C., Sánchez de Rojas, M.I., Frías, M., 2012b. Reuse of sanitary ceramic wastes as coarse aggregate in eco-efficient concretes. *Cement and Concrete Composites* 34 (1): 48–54.

Medina, C., Zhu, W., Howind, T., Sánchez de Rojas, M.I., Frías, M., 2014. Influence of mixed recycled aggregate on the physical – mechanical properties of recycled concrete. *Journal of Cleaner Production* 68: 216–225.

Mercader-Moyano, P., Ramírez-de-Arellano-Agudo, A., 2013. Selective classification and quantification model of C&D waste from material resources consumed in residential building construction. *Waste Management & Research* 31 (5): 458–474.

Monier, V., Hestin, M., Trarieux, M., Mimid, S., Domröse, L., van Acoleyen, M., Hjerp, P., Mudgal, S., 2011. Study on the management of construction and demolition waste in the EU. BIO Intelligence Service.

Morán del Pozo, J.M., Juan Valdés, A., Aguado, P.J., Guerra, M.I., Medina, C., 2011. State of the art on construction and demolition wastes management: limitations [in Spanish]. *Informes de la Construcción* 63 (521): 89–95.

Mulder, E., de Jong, T.P.R., Feenstra, L., 2007. Closed cycle construction: An integrated process for the separation and reuse of C&D waste. *Waste Management*, Wascon 2006 6th International Conference: Developments in the re-use of mineral waste 27 (10): 1408–1415.

Müller, A., Wienke, L., 2004. Measurements and models for the gravity concentration of C&D waste through jigging, in: International RILEM Conference on the Use of Recycled Materials in Building and Structures. RILEM Publications SARL, 115–122.

Müller, D.B., 2006. Stock dynamics for forecasting material flows—case study for housing in The Netherlands. *Ecological Economics* 59 (1): 142–156.

NBN B 15-001, 2012. Concrete - Specification, properties, production and conformity - National supplement to NBN EN 206-1: 2001 [in Dutch]. NBN, Brussels, Belgium.

NBR 15116, 2004. Recycled aggregate of solid residue of building constructions. Requirements and methodologies [in Portuguese]. ABNT, Sao Paulo, Brazil.

NEN 5905, 2010. Dutch supplement to NEN-EN 12620+A1 "Aggregates for concrete" [in Dutch]. NEN, Netherlands.

Nixon, P.J., 1978. Recycled concrete as an aggregate for concrete—a review. *Materials and Structures* 11 (5): 371–378.

Nunes, K.R.., Mahler, C.., Valle, R., Neves, C., 2007. Evaluation of investments in recycling centres for construction and demolition wastes in Brazilian municipalities. *Waste Management* 27 (11): 1531–1540.

Ortiz, O., Pasqualino, J.C., Castells, F., 2010. Environmental performance of construction waste: Comparing three scenarios from a case study in Catalonia, Spain. *Waste Management* 30 (4): 646–654.

Osmani, M., Glass, J., Price, A.D.F., 2008. Architects' perspectives on construction waste reduction by design. *Waste Management* 28 (7): 1147–1158.

Pacheco-Torgal, F., Jalali, S., 2010a. Compressive strength and durability properties of ceramic wastes based concrete. *Materials and Structures* 44 (1): 155–167.

Pacheco-Torgal, F., Jalali, S., 2010b. Reusing ceramic wastes in concrete. *Construction and Building Materials* 24 (5): 832–838.

Pacheco Torgal, F., Tam, V.W.Y., Labrincha, J.A., Ding, Y., de Brito, J. (Eds.), 2013. Handbook of recycled concrete and demolition waste. Woodhead Publishing, Cambridge.

Pascual, M., Cladera, A., 2004. Demolition waste management in Majorca: the particular case of an Island, in: Proceedings of the Internactional RILEM Conference on the Use of Recycled Materials in Buildings Structures, Barcelona.

Peng, C.-L., Scorpio, D.E., Kibert, C.J., 1997. Strategies for successful construction and demolition waste recycling operations. *Construction Management and Economics* 15 (1): 49–58.

Permanent Commission on Concrete, 2008. Code on structural concrete (EHE-08) [in Spanish]. Spanish Ministry of Public Works, Madrid.

Public Works and Environment Office of Castile and Leon, 2014. Decree 11/2014, of 20 March, that approves the Castile and Leon Integrated plan on wastes, BOCYL 57, 18777-18783.

Ramírez de Arellano-Agudo, A., Llatas-Oliver, C., García-Torres, I., Linares-Romero, P., García-Caraballo, E., Escobar-García, M., Carnerero-Moya, M., Hernández-Juárez, R., 2002. Selective Waste Disposal: Estimate Model [in Spanish]. Building Engineers Foundation, Seville, Spain.

Rao, A., Jha, K.N., Misra, S., 2007. Use of aggregates from recycled construction and demolition waste in concrete. *Resources, Conservation and Recycling* 50 (1): 71–81.

Regional Environment and Territorial Policy Department of the Basque country, 2015. Order 12/01/2015 on the use of recycled aggregates from the recovery of CDW [in Spanish], BOPV 22, 507 1-10.

RILEM TC 121-DRG, 1994. Specifications for concrete with recycled aggregates. *Materials and Structures* 27 (9): 557–559.

Rodríguez, G., Alegre, F.J., Martínez, G., 2007. The contribution of environmental management systems to the management of construction and demolition waste: The case of the Autonomous Community of Madrid (Spain). *Resources, Conservation and Recycling* 50 (3): 334–349.

Rodríguez, G., Medina, C., Alegre, F.J., Asensio, E., Sánchez de Rojas, M.I., 2015. Assessment of construction and demolition waste plant management in Spain: in pursuit of sustainability and eco-efficiency. *Journal of Cleaner Production* 90: 16–24.

Rodríguez-Robles, D., García-González, J., Juan-Valdés, A., Morán-del Pozo, J.M., Guerra-Romero, M.I., 2014a. Overview regarding construction and demolition waste in Spain. *Environmental technology* (Ahead-of-print): 10.1080/09593330.2014.957247.

Rodríguez-Robles, D., García-González, J., Juan-Valdés, A., Morán-del Pozo, J.M., Guerra-Romero, M.I., 2014b. Effect of mixed recycled aggregates on mechanical properties of recycled concrete. *Magazine of Concrete Research* 67 (5): 247–256.

Roussat, N., Dujet, C., Méhu, J., 2009. Choosing a sustainable demolition waste management strategy using multicriteria decision analysis. *Waste Management* 29 (1): 12–20.

Sadek, D.M., Nouhy, H.A. El, 2014. Properties of paving units incorporating crushed ceramic. *HBRC Journal* 10 (2): 198–205.

Safiuddin, M., Alengaram, U.J., Rahman, M.M., Salam, M.A., Jumaat, M.Z., 2013. Use of recycled concrete aggregate in concrete: a review. *Journal of Civil Engineering and Management* 19 (6): 796–810.

Schall, J., 1992. Does the solid waste management hierarchy make sense? A technical, economic and environmental justification for the priority of source reduction and recycling. School of Forestry and Environmental Studies, Yale University.

Schnellert, T., Kehr, K., Müller, A., 2011. Development of a separation process for gypsum-contaminated concrete aggregates, in: Second International RILEM Conference on Progress of Recycling in the Built Environment. RILEM Publications SARL, 477 – 482.

Senthamarai, R., Devadas Manoharan, P., 2005. Concrete with ceramic waste aggregate. *Cement and Concrete Composites* 27 (9–10): 910–913.

Seydel, A., Wilson, O.D., Skitmore, R.M., 2002. Financial evaluation of waste management methods: a case study. *Journal of Construction Research* 03 (01): 167–179.

Shi, J., Xu, Y., 2006. Estimation and forecasting of concrete debris amount in China. *Resources, Conservation and Recycling* 49 (2): 147–158.

Silvestre, R., Medel, E., García, A., Navas, J., 2013a. Using ceramic wastes from tile industry as a partial substitute of natural aggregates in hot mix asphalt binder courses. *Construction and Building Materials* 45: 115–122.

Silvestre, R., Medel, E., García, A., Navas, J., 2013b. Utilizing recycled ceramic aggregates obtained from tile industry in the design of open graded wearing course on both laboratory and in situ basis. *Materials & Design* 50: 471–478.

Skoyles, E.R., 1976. Materials wastage – a misuse of resources. *Batiment International, Building Research and Practice* 4 (4): 232–232.

SMARTWaste, 2010. SMARTWaste Plan. Building Research Establishment, http://www.smartwaste.co.uk.

Solís-Guzmán, J., Marrero, M., Montes-Delgado, M.V., Ramírez-de-Arellano, A., 2009. A Spanish model for quantification and management of construction waste. *Waste Management* 29 (9): 2542–2548.

Sonigo, P., Hestin, M., Mimid, S., 2010. Management of construction and demolition waste in Europe, in: Stakeholders Workshop. Brussels, Belgium.

Spanish Head of State, 1998. Law 10/1998, of 21 April, on waste [in Spanish], BOE 96, 13372-13384.

Spanish Head of State, 2011. Law 22/2011, of 28 July, on waste and contaminated soils [in Spanish], BOE 181, 85650-85705.

Spanish Ministry of Agriculture, Food and Environment, 2015. State Waste Framework Plan 2015-2020 [in Spanish].

Spanish Ministry of Environment, 2000. Order MAM/304/2002, of 8 February, that publishes the recovery and disposal waste operations and the European list of wastes, BOE 49, 6494-6515.

Spanish Ministry of Environment, 2001. Resolution of 14 June, that approves the National National Plan of Construction and Demolition Waste 2001-2006 [in Spanish], BOE 166, 25305-25313.

Spanish Ministry of Environment, 2002. Royal Decree 1481/2001, of 27 December, that regulates the disposal of wastes in landfills [in Spanish], BOE 25, 3507-3521.

Spanish Ministry of Environment, 2009. Resolution of 20 January, that approves the second National Plan of Construction and Demolition Waste 2008-2015 [in Spanish], BOE 49, 19893-20016.

Spanish Ministry of Presidency, 2008. Royal Decree 105/2008, of 1 February, that regulates the production and management of construction and demolition waste [in Spanish], BOE 38, 7724-7730.

Spanish Ministry of Public Works, 2014. Order FOM/2523/2014, of 12 December, that amends certain articles of the General Technical Specifications on Road and Bridge Construction Works relating to basic materials, firms and pavements, and signals, markings and vehicle contention [in Spanish], BOE 3, 584-1096.

Spanish Ministry of Public Works, 2015. Annual statistical report 2014 [in Spanish]. Spanish Ministry of Public Works, Madrid, Spain.

Symonds Group Ltd, 1999. Construction and demolition; waste management practices, and their economic impacts, Report to DGXI. European Commission.

Tabsh, S.W., Abdelfatah, A.S., 2009. Influence of recycled concrete aggregates on strength properties of concrete. *Construction and Building Materials* 23 (2): 1163–1167.

Tam, V.W., Tam, C.M., 2008. Waste reduction through incentives: a case study. *Building Research & Information* 36 (1): 37–43.

Tam, V.W.Y., 2008a. On the effectiveness in implementing a waste-management-plan method in construction. *Waste Management* 28 (6): 1072–1080.

Tam, V.W.Y., 2008b. Economic comparison of concrete recycling: A case study approach. *Resources, Conservation and Recycling* 52 (5): 821–828.

Tam, V.W.Y., Tam, C.M., 2006. A review on the viable technology for construction waste recycling. *Resources, Conservation and Recycling* 47 (3): 209–221.

Tam, V.W.Y., Tam, L., Le, K.N., 2010. Cross-cultural comparison of concrete recycling decision-making and implementation in construction industry. *Waste Management* 30 (2): 291–297.

Teo, M.M.M., Loosemore, M., 2001. A theory of waste behaviour in the construction industry. *Construction Management and Economics* 19 (7): 741–751.

Tojo, N., Fischer, C., Saki, O., 2011. Europe as a recycling society. European recycling policies in Relation to the actual recycling achieved. European Topic Centre on Sustainable Consumption and Production, Copenhagen, Denmark.

UEPG, 2015. A sustainable industry for a sustainable Europe (Annual Review 2013-2014). European Aggregates Association, Brussels, Belgium.

UNE EN 933-11, 2009. Tests for geometrical properties of aggregates. Part 11: Classification test for the constituents of coarse recycled aggregate [in Spanish]. AENOR, Madrid.

UNE EN 1367-1, 2008. Tests for thermal and weathering properties of aggregates. Part 1: Determination of resistance to freezing and thawing. AENOR, Madrid, Spain.

UNE EN 1744-5, 2007. Tests for chemical properties of aggregates. Part 5: Determination of acid soluble chloride salts. AENOR, Madrid, Spain.

UNE EN 1744-6, 2007. Tests for chemical properties of aggregates. Part 6: Determination of the influence of recycled aggregate extract on the initial setting time of cement. AENOR, Madrid, Spain.

Van den Heede, P., De Belie, N., 2012. Environmental impact and life cycle assessment (LCA) of traditional and "green" concretes: Literature review and theoretical calculations. *Cement and Concrete Composites* 34 (4): 431–442.

Van Ewijk, S., Stegemann, J.A., 2014. Limitations of the waste hierarchy for achieving absolute reductions in material throughput. *Journal of Cleaner Production* (In press): 10.1016/j.jclepro.2014.11.051.

Villoria-Sáez, P., del Río Merino, M., Porras-Amores, C., 2011. Estimation of construction and demolition waste volume generation in new residential buildings in Spain. *Waste Management & Research* 30 (2): 137–46.

Vyncke, J., Rousseau, E., 1993. Recycling of construction and demolition waste in Belgium: actual situation and future evolution, in: Third International RILEM Symposium on Demolition and Reuse of Concrete and Masonry. RILEM Publications SARL.

Wang, J.Y., Kang, X., Shen, L., Tam, V.W.Y., 2004a. Research on management measures for reducing construction waste. *Architecture Technology* 35 (10): 732–734.

Wang, J.Y., Touran, A., Christoforou, C., Fadlalla, H., 2004b. A systems analysis tool for construction and demolition wastes management. *Waste Management* 24 (10): 989–997.

Weil, M., 2006. Closed-loop recycling of construction and demolition waste in Germany in view of stricter environmental threshold values. *Waste Management & Research* 24 (3): 197–206.

Working group 2/5, 2006. Use of recycled aggregates in the manufacture of structural concrete [in Spanish] (No. M-11). ACHE, Madrid, Spain.

Wu, Z., Fan, H., Liu, G., 2015. Forecasting construction and demolition waste using gene expression programming. *Journal of Computing in Civil Engineering* 29 (5): 04014059.

Xing, W., 2004. Quality improvement of granular secondary raw building materials by separation and cleansing techniques. Delft University, Netherlands.

Xing, W., Hendriks, C.F., Fraaij, A., Rem, P., 2004. Quality improvement of granular wastes. The effective way to recycle secondary raw building materials. *Journal of Wuhan University of Technology Materials Science* 19 (4): 87–90.

Yang, J., Du, Q., Bao, Y., 2011. Concrete with recycled concrete aggregate and crushed clay bricks. *Construction and Building Materials* 25 (4): 1935–1945.

Yost, P.A., Halstead, J.M., 1996. A methodology for quantifying the volume of construction waste. *Waste Management & Research* 14 (5): 453–461.

Zhao, W., Leeftink, R.B., Rotter, V.S., 2010. Evaluation of the economic feasibility for the recycling of construction and demolition waste in China—The case of Chongqing. *Resources, Conservation and Recycling* 54 (6): 377–389.

Zygouras, M., Karagiannidis, A., Malamakis, A., 2009. Construction and demolition waste processing in Athens, Greece: A pilot demonstration. *International Journal of Environment and Waste Management* 3 (1-2): 177–192.

Chapter 3

Experimental program

1. INTRODUCTION

In this chapter, the experimental methodology employed in order to characterize both the recycled aggregates and the recycled concretes is reviewed (Figure 3.1).

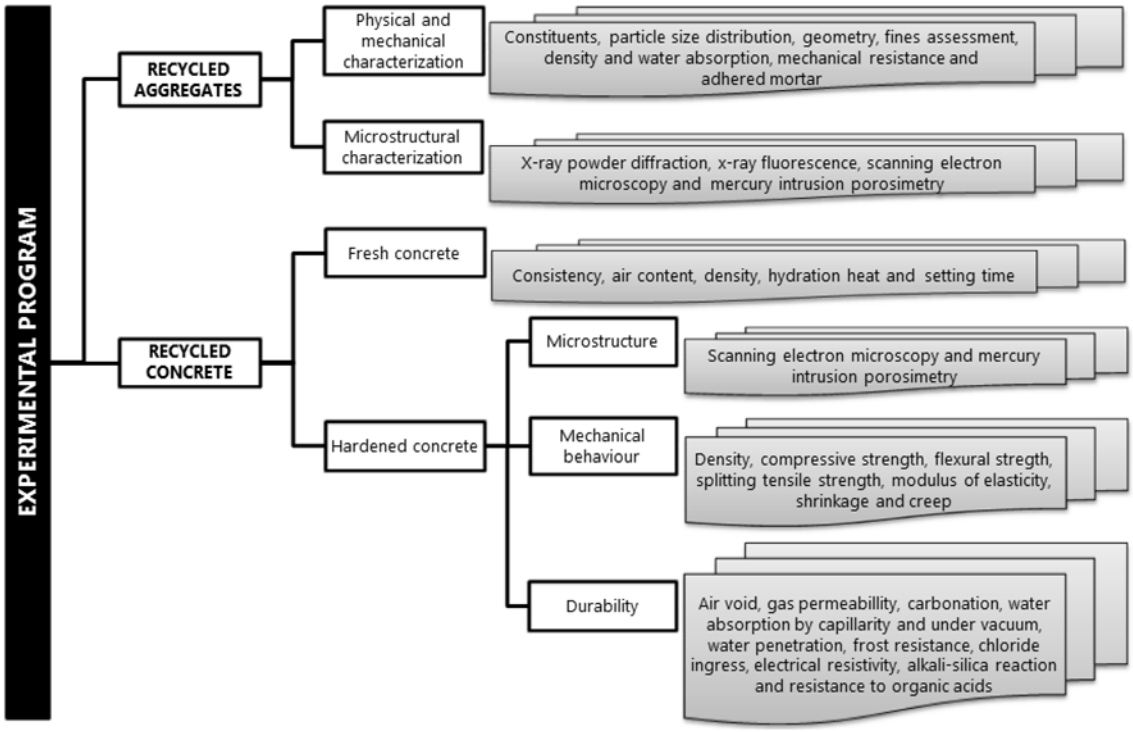

Figure 3.1: Summary of the experimental program followed in this dissertation

2. PHYSICAL AND MECHANICAL CHARACTERIZATION OF AGGREGATES

2.1. CONSTITUENTS

Recycled aggregates stand out by their heterogeneity, and as such the determination of the different components becomes highly relevant. For the recycled coarse aggregates, the identification of constituents were performed following the procedure described in UNE EN 933-11 (2009).

A sample in keeping with the requirements described in UNE EN 932-1 (1997) and UNE EN 932-2 (1999) was selected per each type of recycled aggregate and dried (40±5 ºC) until constant mas. Then, by means of a manual classification seven fractions were separated: concrete, mortar and natural aggregates with mortar attached (Rc), unbound natural aggregates without mortar attached (Ru), ceramics such as brick, or tiles (Rb), glass (Rg), asphalt (Ra), gypsum (X_1) and other impurities such as wood, plastic or metals (X_2). Lastly, the estimation of the relative weight proportion of each fraction was determined as a percentage by mass.

This test not only made possible to detect the different components of a recycled aggregate but also, when used in conjunction with the results arising from other tests, to determine the influence of their presence on the physical, mechanical and chemical behaviour of the recycled aggregates and the recycled concrete.

2.2. PARTICLE SIZE DISTRIBUTION

A granulometric analysis was carried out with an electromechanical sieve shaker (Figure 3.2) for all natural and recycled aggregates. The testing procedure was performed in consonance with UNE EN 933-1 (2012). The maximum (D) and minimum (d) sizes of aggregates were calculated respectively as the minimum and maximum opening in a UNE EN 933-2 (1996) sieve which satisfies the general requirements set out in the Spanish Code on Structural Concrete (EHE-08) (Permanent Commission on Concrete, 2008), and their relationship known as the D/d ratio was evaluated within the limitations (<1.40) of the EHE-08 (Permanent Commission on Concrete, 2008).

Figure 3.2: Sieve shaker

In addition, the results were represented graphically as grading curves to easily verify the compliance with the upper and lower limits of the optimal particle size distribution of coarse and fine aggregate specified in the requirements of the EHE-08 (Permanent Commission on Concrete, 2008).

2.3. GEOMETRY

Although the geometrical differences between natural and recycled coarse aggregates were apparent to the naked eye, a more thorough analysis was performed. The shape of coarse aggregates was determined through the flakiness index (FI) expressed as the percentage of flaky or needle-like particles in the total of the sample (UNE EN 933-3, 2012).

The determination comprised two screening steps, a sample selected according to UNE EN 932-2 (1999) was first sieved in accordance to UNE EN 933-1 (2012), and each retained granulometric fraction was subsequently manually sieved with the corresponding rectangular slot sieve (Figure 3.3) as indicated in UNE EN 933-3 (2012). Thereby, the FI value was calculated as the percentage in mass of the particles that pass through from the total tested in the second sieving operation. Finally, the obtained values were assessed according to the 35 wt% upper limit stipulated by EHE-08 (Permanent Commission on Concrete, 2008).

Figure 3.3: Rectangular slot sieve for flakiness index determination

2.4. FINES ASSESSMENT

A fines assessment, comprising both quantity and quality parameters, was carried out based on the requirements stipulated in the EHE-08 (Permanent Commission on Concrete, 2008). In the first place, the percentage of fines passing through a 0.063 mm sieve was determined and compared with the limits of 1.50 wt% for coarse aggregates and 6.00 wt% for fine aggregate; and if this limit was exceeded, compliance with the limitation for the total fines of concrete - coming both from the aggregates and the cement - (<175 kg/m^3) was sought (Permanent Commission on Concrete, 2008).

In terms of quality, a sand equivalent (SE) test was performed according to UNE EN 933-8 (2012) in order to determine the presence of clay-like fines. The equipment consisted of a sand equivalent shaker, 2 measuring cylinders with rubber stoppers, a weighted foot, a solution with flocculent properties in a bottle assembled with a siphon and an irrigator tube, and a graduated rule (Figure 3.4).

For the determination, two samples selected according to UNE EN 932-2 (1999) and within the 0/2 mm size range were air dried (<2.00% saturation degree) and then flocculated with a solution of calcium chloride ($CaCl_2$), glycerol ($C_3H_8O_3$), formaldehyde (CH_2O) and distilled water in the proportions indicated in UNE EN 933-8 (2012) to promote the release and suspension of the clay coatings. After a waiting time of 20 minutes in the measuring cylinder, the SE value was calculated as the percentage of the total height of flocculated material (Figure 3.5).

The evaluation of this index was made depending on the concrete general class of exposure, having in mind that the SE values should exceed 70 vol% for I, IIa or IIb general exposures or 75 vol% for the remaining classes of exposure (Permanent Commission on Concrete, 2008). Appendix A can be consulted for equivalence between Spanish and European environmental exposures classes.

(a) **(b)**

Figure 3.4: Sand equivalent equipment (a) automatic shaker and (b) measuring cylinders, weighted foot, and solution bottle.

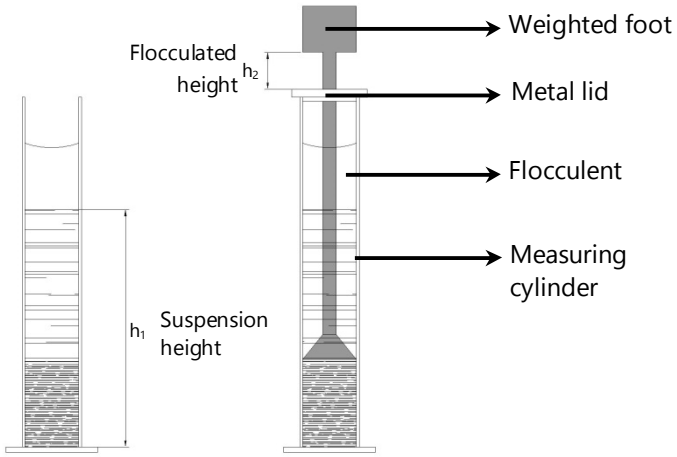

Figure 3.5: Sand equivalent determination

Finally, if some uncertainty arose as to whether the fines contained any clay, its presence was identified and qualitatively calculated using an X-ray diffraction test (described in section 3.1 of this chapter) allowing the use of the fine material if the clays were of the kaolinite or illite type (Permanent Commission on Concrete, 2008).

2.5. DENSITY AND WATER ABSORPTION

Density and water absorption (WA) values were determined simultaneously by means of a pycnometer (Figure 3.6) according to UNE EN 1097-6 (2014) standard. The pycnometer method is a well-known method for determining the volume of irregularly formed samples based on Archimedes' Principle.

Figure 3.6: Pycnometer

A sample in accordance with UNE EN 932-2 (1999) was submerged in water inside a pycnometer taking care that no air bubbles were present. After 24 hours in a thermostatic bath (22±3 ºC), the existing air bubbles were eliminated before refilling with water and weighing the pycnometer with stopper (M_{sat}). Afterwards for coarse aggregates, the test portion was cloth-dried in order to get a moisture state of saturation with dried surface and then was weighed (M_1) and oven-dried (110±5 ºC) to constant mass (M_{rd}). In the case of fine aggregates, the test portion was air-dried and the collapse behaviour (Figure 3.7) after removing from a conical mould (D_{bottom}=90 mm, D_{top}=40 mm, H=75 mm) was used to assess the moisture condition until a saturation state with dried surface was reached, and at this moment it was weighed (M_{ssd}) and oven-dried (110±5 ºC) to constant mass (M_{rd}). Finally, the pycnometer with stopper completely filled with water was weighed (M_{pyk}).

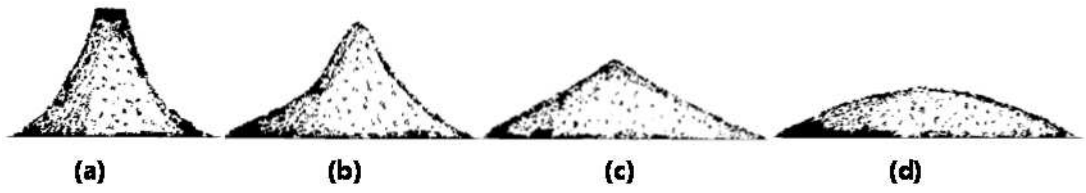

Figure 3.7: Collapse criterion for fine aggregates (a) wet aggregates, (b) slightly wet aggregates, (c) saturated with dried surface aggregates and (d) oven dried aggregates (UNE EN 1097-6, 2014)

Following this procedure three main specific gravities were determined: apparent specific gravity (3.1), dry bulk specific gravity (3.2) and saturated with dry surface bulk specific gravity (3.3), and also water saturation (3.4) was obtained.

$$\rho_a = \rho_w \cdot \frac{M_{rd}}{M_{rd} - (M_{sat} - M_{pyk})} \quad (3.1)$$

$$\rho_{rd} = \rho_w \cdot \frac{M_{rd}}{M_{ssd} - (M_{sat} - M_{pyk})} \quad (3.2)$$

$$\rho_{ssd} = \rho_w \cdot \frac{M_{ssd}}{M_{ssd} - (M_{sat} - M_{pyk})} \quad (3.3)$$

$$WA_{24} = \frac{100 \times (M_{ssd} - M_{rd})}{M_{rd}} \quad (3.4)$$

with ρ_a the apparent specific gravity [Mg/m^3], ρ_{rd} the dry bulk specific gravity [Mg/m^3], ρ_{ssd} the saturated with surface dried bulk specific gravity [Mg/m^3], WA_{24} the water absorption after 24 hours of immersion [wt%], ρ_w the density of the water at test temperature (0.9982 Mg/m^3 at 20ºC) [Mg/m^3], M_{ssd} the mass of the saturated aggregates with dry surface [g], M_{sat} the mass of the pycnometer with the test sample - saturated aggregates - and the water [g], M_{pyk} the mass of the pycnometer only with water [g] and M_{rd} the mass of the test sample -oven dried aggregates- [g].

Although the EHE-08 (Permanent Commission on Concrete, 2008) does not establish any limitation for the density of aggregates, strict specifications are laid down for water absorption. Natural and recycled aggregates shall not exceed 5 wt% and 7 wt% respectively, while the combination of natural and recycled coarse aggregate shall obey the 5 wt% limit for recycled concrete with more than 20 wt% of recycled aggregates.

2.6. MECHANICAL RESISTANCE

The mechanical resistance of the aggregates to degradation by abrasion and impact was determined in accordance with UNE EN 1097-2 (2010) by means of the Los Angeles test (LA) as recommended by EHE-08 (Permanent Commission on Concrete, 2008).

The tested sample was produced in accordance to UNE EN 932-2 (1999) and as specified in the Los Angeles test standard presented a 10/14 mm size with a 65 wt% proportion of the total sample passing through the 12.50 mm sieve. After drying (110±5 ºC) to constant mass and cooling down in a desiccator, the coarse aggregates were introduced in the testing machine (Figure 3.8) with 11 steel balls of 400 g and were subjected to 500 revolutions at a constant speed between 31 and 33 rpm. The resulting material was screened through a 1.60 mm sieve and the retained portion was dried (110±5 ºC) until constant mass was achieved. Finally, the LA coefficient was calculated as the percentage of the test portion passing a 1.60 mm sieve after completion of the test.

Figure 3.8: Los Angeles test machine

Regarding the evaluation of this property, EHE-08 (Permanent Commission on Concrete, 2008) sets a 40 wt% upper limit but also extends the previous limitation to 50 wt% for those aggregates whose previous field experience deemed them as suitable for mass or reinforced concrete with a characteristic strength not exceeding 30 MPa.

2.7. ADHERED MORTAR

The presence of adhered mortar is a common occurrence in coarse recycled aggregates coming from construction and demolition, as certain amount of paste from the original concrete inevitably remains attached to natural aggregates or other particles present (mostly bricks) after the demolition occurs.

Currently, there is no standardized method for assessing the amount of adhered mortar in recycled aggregates. Thus, two experimental methods previously described in the literature have been employed.

One of the research techniques conducted in this PhD involved the immersion of recycled aggregates in different acidic environments in order to dissolve the attached mortar. In the first test implemented, a coarse recycled aggregate sample was washed with demineralized water to remove fine particles and dried at 75±5 ºC for 24 hours. Then, the recycled aggregate was submerged and carefully stirred in a hydrochloric acid solution (HCl) at 0.10 M at 20±2 ºC. After 24 hours, the sample was washed with demineralized water and dried at 75±5 ºC for 24 hours. In the same conditions, a second treatment was performed to verify the level of efficacy of the method. The mortar attached was then calculated as the percentage of total weight loss. The second test employed was also based on the dissolution of the cement paste in a hydrochloric acid solution. However, the aforementioned procedure was slightly adjusted to increase the treatment aggressiveness, in such a way that made it more relatable to methods found in the literature (Duan and Poon, 2014). First, the temperature of drying was risen up to 105±5 ºC. Moreover, the HCl concentration was modified up to 1.00 M and the immersion period was reduced to 8 hours. To conclude, the particles presenting adhered mortar were gently brushed and the sample was sieved though a 4 mm sieve to ensure that only the recycled coarse aggregates were weighed.

Additionally, the mortar evaluation method based on daily freeze-thaw cycles of soaked coarse recycled aggregates in a salt solution was also performed. This technique combines mechanical stresses and chemical degradation to remove the mortar from the aggregate surface. The procedure was first employed by (Abbas et al., 2008) as a modification of (ASTM C88-13, 2013). The sample was washed with demineralized water and dried at 105±5 ºC for 48 hours. Then, the aggregates were immersed in a 26 wt% sodium sulphate solution (Na_2SO_4) for 24 hours. After that time period, the still immersed samples were subjected to five daily freeze-thaw cycles, i.e. 16 hours at -15 ºC and 8 hours at 80 ºC. Lastly, the sample was drained, washed again with demineralized water, sieved though a 4 mm sieve and dried at 105±5 ºC for 24 hours before weighing. The ratio of attached mortar was calculated as percentage of differential weight before and after the treatment.

3. MICROSTRUCTURAL CHARACTERIZATION OF AGGREGATES AND CONCRETE

3.1. X-RAY POWDER DIFFRACTION

X-ray powder diffraction (XRD) is a non-destructive technique generally employed for phase identification of polycrystalline samples. Currently, it is one of the most applied methods for mineralogical material characterization.

Diffraction methods are based on the phenomenon of wave interferences, and the prerequisite that X-ray wavelengths are of the same order of magnitude as interplanar spacing in crystal lattices (Klockenkämper and Bohlen, 2014). Monochromatic X-ray beams incident on a crystalline solid will be diffracted according to Bragg's law (3.5) as illustrated in Figure 3.9.

$$n_r \cdot \lambda_x = 2 \cdot d_s \cdot \sin\theta \tag{3.5}$$

with n_r a positive integer, also called order of reflection, which is conventionally established as the unity (Fultz and Howe, 2013) [-], λ_x the wavelength of the incident X-ray beam [nm], d_s the interplanar spacing in the ionic lattice [nm], and θ the angle of incidence of the X-ray on the crystal [º].

By continuously changing the incident angle of the X-ray beam, information on the spacing between atomic planes is gathered and a spectrum of diffraction is recorded. Various intensity peaks located at different angles 2θ provide the "fingerprint" for a crystalline solid which enables the mineral phase identification among known patterns from a standard sample or from a calculation (Leng, 2013a).

The analysis was performed on the aggregates and conducted through the Debye–Scherrer method, as is the most appropriate for polycrystalline samples. Sample preparation consisted of a particle size reduction to grain sizes smaller than 88 μm by means of an agate mortar. Then, the homogeneous powder was placed on an aluminium sample holder and pressed at 0.60 MPa in order to ensure a flat surface.

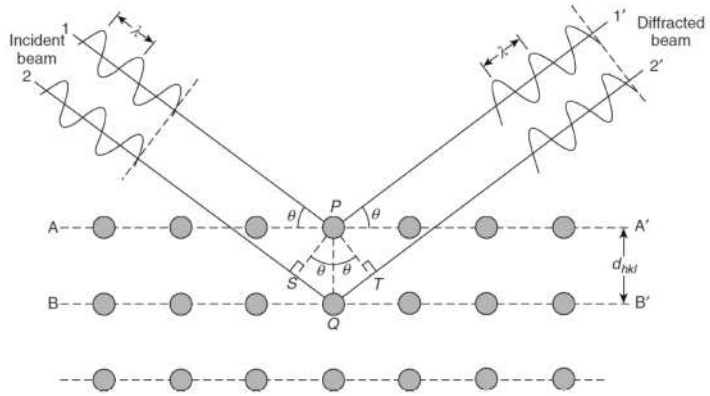

Figure 3.9: Schematic explanation of Bragg's Law (Callister, 2007)

XRD tests were performed on a Bruker D8 Advanced (Theta/Theta) non-monochromator diffractometer (Figure 3.10). The operating parameters used for X-ray generation were tungsten cathode, 2.2 kW copper anode ($CuK\alpha_1$: 1.5406 Å; $CuK\alpha_2$: 1.5444 Å), 30 mA intensity, 40 kV voltage and a 6 mm slit. Radiation data were gathered over the angular 2θ range of 5–60° with a step size of 0.019° and a count time per step of 0.5 s.

Finally, the mineralogical phase identification was determined by the comparison of the positions of the diffraction peak maxima and the relative peak intensities of the powder diffraction patterns obtained and the ones indexed on the Powder Diffraction File (PDF) of the International Centre for Diffraction Data (ICDD, 2015) via the search-match DiffracPlus Evaluation software.

Figure 3.10: X-ray powder diffraction spectrometer

3.2. X-RAY FLUORESCENCE

An X-ray fluorescence (XRF) analysis, a non-destructive technique employed for chemical material characterization, was carried out for both the aggregates and the concrete mixtures pertaining to the first research phase.

Fluorescence occurs when a sample is irradiated by X-rays. The high energy photons emitted induce an ionization of inner shell electrons (K, L, M) of the atoms in the specimen creating electron vacancies leading to the emission of secondary radiation. The spectrum is then dispersed by a single crystal of known interplanar spacing (d) causing that each wavelength detected will diffract at a specific angle given by Bragg's law (3.5). And, as stated by Moseley's law (3.6), there is a relationship between the energy - or reciprocal wavelength - of the secondary X-ray emitted and the atomic number of the element present in the sample. Therefore, the measurement of wavelength or energy and intensity of the characteristic photons emitted from the sample allows the identification of the elements present and the determination of their mass or concentration (Jenkins, 2001; Janssens, 2003; Klockenkämper and Bohlen, 2014)

$$E = {}^{1241}/_{\lambda} = k \times (Z-\sigma)^2 \tag{3.6}$$

with E the energy of the photons emitted by the sample [eV], λ the wavelength of the radiation released by the sample [nm], k a constant that takes different values for each spectral series [eV] (values of different transition energies can be found in Deslattes et al. (2003)), Z the atomic number of the absorbing element [-] and σ a shielding constant [-] (different values can be found in Klockenkämper and von Bohlen (2014)).

Figure 3.11: X-ray fluorescence spectrometer

XRF tests were performed on a Bruker S8 Tiger wavelength dispersive X-ray fluorescent spectrometer (Figure 3.11) with tungsten tube, lithium fluoride (LiF) crystal analyser and generator of 4 kW. As specimen preparation is an all-important factor in the ultimate accuracy of any X-ray determination, to obtain quantitatively correct results, the sample was crushed and the powder was pressed into tablets by fusion with lithium tetraborate ($Li_2B_4O_7$) in a platinum/gold crucible to form a stable glass bead. The analysis was carried out using Quant Express standardless calibration software (SpectraPlus package) and taking into account the resulting data from a loss on ignition (LOI) analysis determined in conjunction with the XRF.

3.3. SCANNING ELECTRON MICROSCOPY

The scanning electron microscopy (SEM) is positively one of the most used non-destructive methods as it allows simultaneous morphological and chemical characterization by raster-scanning the surface of the specimen. The polyvalence of this technique is based on the different manners in which the focused beam of electrons interacts with the matter in the sample, producing diverse electromagnetic responses. The most frequently detected signals are high-energy backscattered electrons, low-energy secondary electrons and X-rays, while less common detections include Auger electrons, cathodoluminescence, and measurements of beam-induced current (Scheu and Kaplan, 2012).

The information gathered from the most usual detected signals allows a profound knowledge (imaging, qualitative and quantitative analysis) of the microstructure related to the relative position in the specimen surface. On one hand, signals of secondary electrons (SE) - due to inelastic electron scattering and with low energies (<50 eV) - are used to obtain SEM images that provide a topographical representation of the sample surface. On the other hand, the detection of backscattered electrons (BSE) - due to elastic electron scattering and with high energies (>50 eV) - is associated with the atomic number of the elements present in the sample. As such, a BSE image displays a compositional contrast - on a greyscale ranging from 0 (black) to 255 (white) - where brighter areas correspond to heavier elements. Consequently, the different phases can be distinguished by their differential brightness. Finally, an energy dispersive spectroscopy (EDS) could be performed based on the measurements of the characteristic intensity of the X-rays leaving the sample which, based on Mosely's law equation (3.6), allows obtaining the chemical composition in a point analysis or over a much broader raster area to create an element map (Kristiansen, 1997; Wang and Petrova, 2012; Leng, 2013b).

The microstructural studies were conducted on the aggregates and the concrete mixture of phase I using a Hitachi S-4800 scanning electron microscope (Figure 3.12) with tungsten as X-ray source, a Si/Li detector and a Brucker XFlash 5030 EDS analyser. In order to preserve the features of the specimen surface, samples used for SEM were subjected to minimal preparation, which involved their placement in a metallic holder by means of a bi-adhesive graphite film and a subsequent carbon coating to ensure conductivity and avoid signal masking.

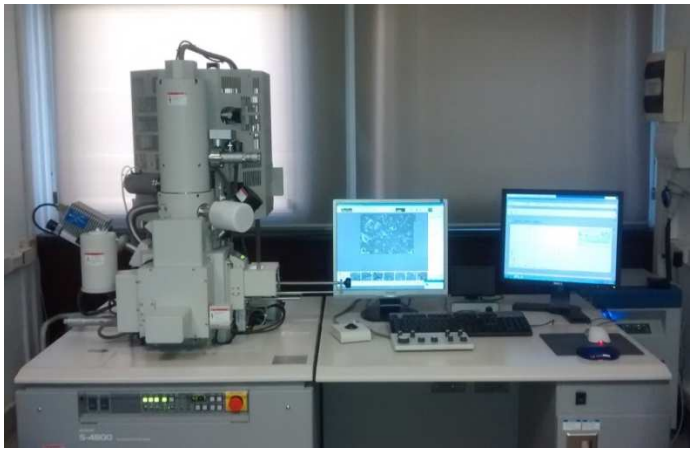

Figure 3.12: Scanning electron microscope

3.4. MERCURY INTRUSION POROSIMETRY

Mercury intrusion porosimetry (MIP) is an extremely valuable characterization procedure for porous materials. The method is based on the behaviour of mercury with respect to most solids. As a non-wetting liquid - one having a contact angle greater than 90º, the application of an external pressure is required to force the mercury into the specimen pores. Washburn's equation (3.7) states that the pressure needed for the intrusion of a non-wetting liquid into a circular cross-section pore is inversely proportional to its diameter and directly proportional to the surface tension of the liquid and the angle of contact with the solid surface (Washburn, 1921).

$$d_i = \frac{-4 \cdot \gamma \cdot \cos\theta}{P} \tag{3.7}$$

with d_i the equivalent diameter of the intruded pores [nm], γ the surface tension of mercury [N/nm], θ_i the contact angle between mercury and the pore walls [º] and P the pressure at which a given increment of mercury intrudes into de pore system [N/nm^2]. The values established for the surface tension of mercury and the contact angle - both, advancing and receding angle - were here set at $485 \cdot 10^{-12}$ N/nm and 141.3° respectively.

In a MIP analysis, the test specimen is placed in a glass cell of a sealed penetrometer that is filled with mercury which is forced to successively intrude in smaller pores of the sample by gradually increasing the setup pressure or to sequentially extrude of pores by progressively decreasing the pressure at the end of the test (Giesche, 2002).

The results obtained with this technique provide a wide range of information, such as the average pore diameter, the porosity, the skeletal and apparent density, the threshold pressure, the tortuosity, and the specific surface area of a sample among others. Although the determination of the pore size distribution is also possible, the reliability of this method for cement-based materials has been profoundly discussed (Abell et al., 1999; Diamond, 2000, 2003; Gallé, 2001, 2003; Kumar and Bhattacharjee, 2003) to finally be accepted as a reasonable estimate (Bermejo et al., 2010).

The test was conducted to ASTM D4404-10 (2010) on a Micromeritics Autopore IV 9500 mercury intrusion porosimeter (Figure 3.13) capable of operating at up to 33,000 psia (227.5 MPa). The operating parameters were mercury filling pressure of 0.45 psia (~3.10 Pa), maximum intrusion volume of 0.50 ml/g and equilibration time of 10 seconds.

The effect of sample preconditioning has been thoroughly investigated (Winslow and Diamond, 1970; Konecny and Naqvi, 1993; Gallé, 2001, 2003; Rübner et al., 2002; Diamond, 2003; Kumar and Bhattacharjee, 2003). However, there is no agreement in the method specimens should be prepared before undergoing MIP (Bermejo et al., 2010). In the framework of this PhD, samples were dried to constant weight at 40 ºC and degassed with a vacuum pump for 30 minutes in order to ensure moisture removal. Moreover, for recycled concrete characterizations, samples were selected guaranteeing the presence of at least one ceramic coarse aggregate with enough quantity of mortar adhered.

Figure 3.13: Mercury intrusion porosimeter

3.5. AIR VOID ASSESSMENT

The assessment of the air void system of the concretes mixtures from phase II was performed through the linear traverse method described in ASTM C457 (2012) Procedure A. By means of a RapidAir 457 apparatus (Figure 3.14), which allows an automatic image analysis of the samples, the air content, void frequency, spacing factor, specific surface, chord length and paste-air ratio were determined for hardened concrete specimens at 28 days.

Figure 3.14: RapidAir 457 apparatus

For each concrete mixture, four slices were cut from the same 100x100 mm cube specimen. A concrete saw with diamond edge was employed to cut four slices of approximately 2.5 mm in thickness in the perpendicular direction of the trowelled surface of the cube.

Since scratches must be avoided for this determination, the sawn surface of the sample was mechanically flattened and polished with a sequence of wet diamond polishing pads (grit 50, 100, 200, 400, 800, 1500, 3000 and 8000). The polishing pad was switched when the raster chalk applied to control the smoothing process was completely erased from the surface. After the polishing procedure, each slice was further cut to remove the unavoidable unpolished part due to the holding configuration of the test machine, and specimens of 65x100 mm were finally used for the air void examinations.

In order to ensure a proper detection with the air void analyser, a contrast enhancement process was also followed. The samples were coloured black with a broad tipped black marker, taking care of overlapping two consecutive ink lines. After air-drying for a few seconds, the same colouring process was repeated in the perpendicular direction to guarantee a perfect coating and the sample was allowed to dry. Next, a barium sulphate ($BaSO_4$) white powder, with average grain size of 2 μm, was poured in the black-coated surface. To fill the air voids, the powder was tamped with a rubber stopper until all the voids were completely occupied and the excess powder was removed by pressing and dragging a steel blade over the sample surface. Then, the fine dust was cleaned in a circular motion with soft paper. The final step consisted of the colouring of the voids or cracks present in the aggregates, in which the white powder also penetrated, by means of a fine tipped black marker. Finally, the quality of the sample preparation was verified under microscope, and the enhancement process was repeated.

Once the treatment was deemed satisfactory, the sample was mounted and levelled in the sample holder of the RapidAir apparatus. After adjusting the light and focus, the sample was automatically analysed using 5 traverse lines per frame and a total traverse length of 2413.1 mm. Two analyses were performed per sample, by turning the sample over 90° and an average of the two readings of the sample was reported. As the examination was based on a white and black image analysis, a threshold value was implemented in order to distinguish between colours.

However, this value varies with light/contrast settings of the system and general room lighting among others (Jacobsen and Arntsen, 2007), and a proper threshold value needed to be chosen for each sample.

During the test, the total chord length traversed, the chord length traversed through air voids, the chord length traversed through paste and the number of air voids intersected by the traverse line were automatically gathered by the RapidAir software. To avoid any lack of representativeness between the sample and the concrete batch, the paste content in the original mix was manually determined and input in the software to be factored in the automatic analysis. Lately, all this parameters were used to fully characterize the air void system parameters, i.e. the air content (3.8), the specific surface (3.9), the spacing factor (3.10) and the average chord length (3.11).

$$Ac = \frac{T_a}{T_{tot}} \cdot 100 \tag{3.8}$$

$$\alpha_s = \frac{4N}{T_a} \tag{3.9}$$

$$L_s = \frac{T_p}{4N} \quad \text{for } p/Ac \leq 4.33$$
$$L_s = \frac{3}{\alpha_s}\left[1.4 \cdot \left(1 + \frac{p}{Ac}\right)^{1/3} - 1\right] \quad \text{for } p/Ac > 4.33 \tag{3.10}$$

$$L_m = \frac{T_a}{N} \tag{3.11}$$

with *Ac* the air content [%], T_a the total chord length of air voids [mm], T_{tot} the total surface distance traversed [mm], α_s the specific surface [mm^{-1}], *N* the total number of air void chord lengths [-], L_s the spacing factor [µm], T_p the total chord length of paste [mm], *p* the paste content [%], L_m the average chord length [mm].

4. FRESH PROPERTIES OF CONCRETE

4.1. CONSISTENCY

The consistency of each fresh batch of concrete was measured by means of a slump test (Figure 3.15) commonly known as Abrams cone (UNE EN 12350-2, 2009). This test was performed on a sample obtained in accordance with UNE EN 12350-1 (2009) immediately after the mixing stopped. The fresh concrete was poured into a conical mould (D_{bottom}=200 mm, D_{top}=100 mm, L=300 mm) in three layers of equal volume. After filling each layer, the concrete was compacted 25 times by strokes of a standardized steel rod (D=16 mm, L=600 mm). Next, the cone was withdrawn upwards and the vertical settlement of the unsupported fresh concrete compared with the height of the mould, which is known as slump, was measured.

Figure 3.15: Abrams cone

Then, the workability was evaluated in accordance to the five classes (Table 3.1) specified by EHE-08 (Permanent Commission on Concrete, 2008). As the values stipulated by the EHE-08 greatly differ from those of other European Standards, comparison with EN 206-1 (2005) is also shown in Table 3.1.

Table 3.1: Slump classes according to EN 206-1 (2005) and EHE-08 (Permanent Commission on Concrete, 2008).

Class	EHE-08 Slump range (mm)	EN 206-1 Slump range (mm)
S1	0-20	10-40
S2	30-50	50-90
S3	60-90	100-150
S4	100-150	160-210
S5	≥ 150	≥ 220

4.2. AIR CONTENT

The entrapped air in the concrete mix was determined by pressure gauge method described in UNE EN 12350-7 (2010) immediately after mixing. A remixed sample obtained according to UNE EN 12350-1 (2009) was placed in the testing container in three layers of equal depth, and each one of them was compacted 25 times with a steel rod (D=16 mm, L=600 mm). Then by introducing a known volume of air at a known pressure in a TESTING Air entrainment meter (Figure 3.16) and based on the Boyle-Mariotte's principle, the air content of each concrete batch was determined.

Figure 3.16: Air entrainment meter

4.3. DENSITY

The mathematical concept of density, i.e. mass divided by volume, was employed for the determination of fresh concrete density in accordance with UNE EN 12350-6 (2009). A sample obtained as indicated in UNE EN 12350-1 (2009) was remixed before testing. A vessel of known mass and volume, in this case the TESTING Air container of 8 litres of capacity, was employed for the mass determination of the fresh concrete. A specific sequence of filling was followed, and the concrete was poured in three layers of equal depth, each one was compacted through 25 strokes of a standardized steel rod (D=16 mm, L=600 mm). After the compaction of the upper layer, the surface was trowelled and the filled container was weighed.

4.4. HYDRATION HEAT

The Langavant method was employed for the automatic monitoring of the hydration heat development of phase II concrete mixtures during hardening (UNE EN 196-9, 2011). In a temperature controlled room (20±2 ºC and 65±5 % relative humidity), two semi-adiabatic calorimeters, i.e. a calorimeter with a maximum heat loss inferior to 100J/K·h (RILEM TC 119-TCE, 1997), were employed for this test in accordance with UNE EN 196-9 (2011). Each calorimeter (Figure 3.17) consisted of a heat insulated flask, e.g. Dewar flask, sealed with an insulated stopper incorporating a thermocouple connected with a data acquisition system (DAQ card) connected to a computer and enclosed in a rigid case for protection. One of the calorimeters was used as a reference and contained an inert sample, i.e. a fully hydrated concrete specimen, with a thermocouple that monitored possible temperature variations throughout all the experiment; while the other accommodated the test sample.

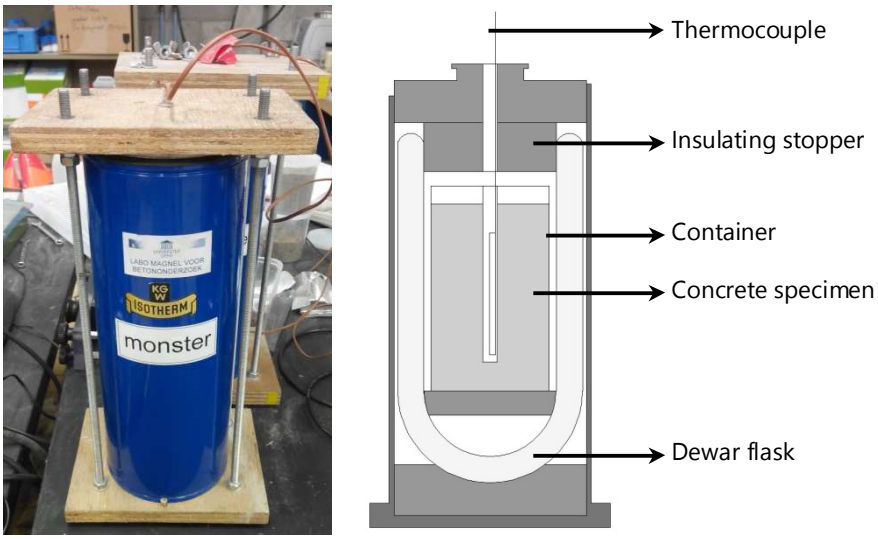

Figure 3.17: Semi-adiabatic calorimeter

Preceding the testing procedure, a calibration of the Langavant calorimeter was performed as specified in NT BUILD 480 (1997). In such way, the coefficient of heat loss of the calorimeter (3.12) and the thermal capacity of the setup (3.13) was determined.

$$\alpha = a + b \times \Delta T \tag{3.12}$$

with α the heat loss [J/K/h], a the calorimeter calibration constant [J/K/h], b the other calorimeter calibration constant [J/K^2/h] and ΔT the temperature rise [K]. The calibration constants of the calorimeter are displayed in Table 3.2.

$$c = c_C \times m_c + c_a \times m_a + c_w \times m_w + c_{Cc} \times m_{Cc} + \mu \tag{3.13}$$

with c the thermal capacity of the setup [J/K], c_c the thermal capacity of cement [J/kg/K], m_c the mass of the cement in the sample [kg], c_a the thermal capacity of the aggregates [J/kg/K], m_a the mass of aggregates in the sample [kg], c_w the thermal capacity of the water [J/kg/K], m_w the mass of water in the sample [kg], c_{Cc} the thermal capacity of the cylindrical container [J/kg/K], m_{Cc} the mass of the cylindrical container [kg], and μ the thermal capacity of the empty calorimeter [J/kg/K]. The values used for these parameters are tabulated in Table 3.2.

Table 3.2: Calibration parameters (Robeyst, 2009; UNE EN 196-9, 2011)

	Calibration parameters	Value
a	Constant for heat loss determination	58 J/K/h
b	Constant for heat loss determination	0.28 J/K^2/h
c_c	Thermal capacity of the cement	800 J/kg/K
c_a	Thermal capacity of the aggregates	800 J/kg/K
c_w	Thermal capacity of the water	3800 J/kg/K [a]
c_{cc}	Thermal capacity of the cylindrical container	500 J/kg/K
μ	Thermal capacity of the empty calorimeter	355 J/K

[a] *average of bound and unbound water*

Once the calorimeter was calibrated, and just after the concrete mixing finalized, a sample of fresh concrete was poured into a cylindrical tinplate container of known weight and fitted with a lid. Then, after being compacted by means of a vibration table and weighed, the container was introduced in the semi-adiabatic calorimeter with an embedded thermocouple in the centre of the concrete sample. Not more 15 minutes elapsed between the water incorporation to the mixture and the beginning of the recording process; nonetheless the time of the addition of water was taken as the start of timing. The temperature evolution of the sample was registered for at least 48 hours, as most of the heat release occurs within the first days, to calculate its hydration heat.

Knowing the specific parameters of the Langavant calorimeter, the cumulative heat production was estimated with equation (3.14), where the first term represents the heat accumulated in the calorimeter while the second term exemplifies the heat loss into the atmosphere.

$$Q = \frac{c}{m_c} \cdot \Delta T + \frac{1}{m_c} \sum_{i=0}^{i=n} \alpha_i \cdot \Delta T_i \cdot \Delta t_i \tag{3.14}$$

with Q the cumulative heat production [J/g], c the thermal capacity of the setup, computed according to equation (3.13) [J/K], m_c the mass of cement contained in the test sample [g], ΔT the temperature rise [K], α_i the mean coefficient of heat loss [J/K·h], ΔT_i the temperature rise of the test sample [K] and Δt_i the hydration time [h].

Additionally, the heat production rate was calculated as the derivative of the cumulative heat production in function of time. To facilitate comparison with the results obtained by means of a FreshCon system (section 4.5 in this chapter), the heat production rate was also determined applying the maturity concept, which was used to transform the actual age of the concrete sample to its equivalent age at 20ºC. The Arrhenius equation (3.15), as first suggested by Freiesleben-Hansen and Pederson (1977), was used as the transforming maturity function.

$$t_e = \sum_0^t e^{\frac{E_a}{R}\left(\frac{1}{273+T_r}-\frac{1}{273+T_c}\right)} \tag{3.15}$$

with t_e the equivalent age at a specified temperature [h], E_a the activation energy [J/mol], R the universal gas constant [8.314 J/mol/K], T_r the temperature at which the equivalent age is calculated [K], T_c the average temperature of the concrete during a time interval and Δt the time interval during which temperature was measured [h].

4.5. SETTING TIME

Simultaneously to the semi-adiabatic calorimetric tests (described in the section 4.4 of the present chapter), the determination of the initial and final setting time of phase II concrete mixtures was carried out in a controlled temperature room at 20±2 ºC and 65±5 % relative humidity. A FreshCon system developed by the Institute of Construction Materials (IWB) at the University of Stuttgart (Reinhardt et al., 2001) was used to automatically monitor the early behaviour, i.e. setting and hardening, of concrete based on the through-transmission ultrasonic wave principle (Reinhardt and Grosse, 2004)

The system (Figure 3.18) consisted of a computer equipped with a DAQ card responsible for the collection of the ultrasonic velocity, the energy and the frequency spectrum evolution, a high voltage pulse generator (with an amplifier up to 800 V) of pulse signals with a width of 5 µs and frequency band of approximately 400 kHz, a specific container of 450 cm^3 with piezoelectric sensors and a pre-amplifier. The container used in this test was composed of a U-shaped rubber foam centrally enclosed between two poly-methyl-methacrylate (PMMA) walls separated 59 mm and held together by four screws with spacers. Both, the configuration and materials employed, avoid the wave propagation around the sample or through the mould. Coupled in each PMMA wall and merely separated from the sample by a protective wear cap, a piezoelectric sensor (25.4 mm) of 0.5 MHz central frequency was used to achieve a good wave directionality and signal-to-noise ratio (Robeyst, 2009).

Preceding each test, the control parameters (transmission distance, test interval, input voltage and zero time) were configured in the computer and a layer of petroleum jelly was applied to all the parts susceptible of entering in contact with the sample. This is especially important for the protective wear cap of the sensors, as the treatment has a double purpose. On one hand, it prevents the creation of air bubbles in the contact surface due to its viscosity, and on the other avoids the absorption of part of the water in the mixture, what otherwise could happen due to the hydrophilic nature of the nylon used as material in the protective wear caps.

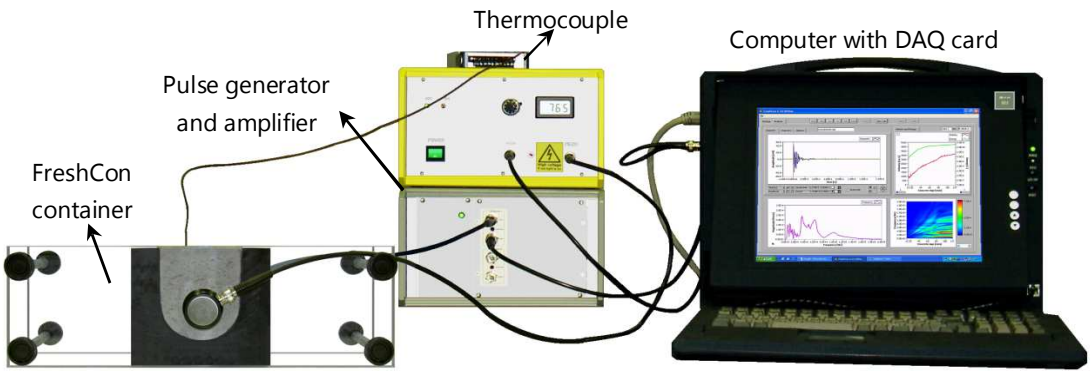

Figure 3.18: FreshCon system (Robeyst, 2009)

Afterwards, a fresh concrete sample was poured in the FreshCon container and was compacted by means of a vibrating table during approximately 30 seconds to remove entrapped air. The container was immediately covered with a plastic film to avoid any water evaporation that could lead to the shrinkage of the concrete, which could cause a deficient coupling between the sensor and the sample. As well as in the calorimetric test, not more 15 minutes elapsed between the water incorporation to the mixture and the beginning of the recording process; nonetheless the time of the addition of water was taken as the start of timing.

Once the FreshCon software was triggered, the DAQ card controlled the sending of electric pulses in a 5 minute sequence from the amplifier towards one of the ultrasonic sensors of the FreshCon container. At this point, a piezoelectric broadband transmitter in the sensor transformed the electrical signal into a mechanical one, in the form of vibration, responsible for the creation of an ultrasonic longitudinal or compression wave (p-wave). After travelling though the hardening concrete sample, said ultrasonic wave was detected by the piezoelectric receiver of the ultrasonic sensor situated in the opposite wall of the container and reconverted into an electrical signal that was sent back to the pre-amplifier and the DAQ card of the computer closing the through transmission process. During the test, the FreshCon software recorded the ultrasonic velocity, energy and frequency spectrum evolution.

Although the measurement capacities of the FreshCon system are far more extensive, the focus of this study was the ultrasonic p-wave velocity and the frequency spectra. The evaluation of the data recorded was carried out by the offline version of the FreshCon software. Even though it is a mostly automatic process implemented by algorithms, the onset time was manually picked as the point of the first wave arrival for the first hours of the test - beginning of the stiffening process - when the signal-to-noise ratio was too low for a good automatic detection. Then, the Akaike Information Criterion (AIC) algorithm was applied since studies by Kurz et al. (2005) demonstrate the reliability of this method.

Since the ultrasonic velocity was calculated as the travel distance between transmitter and receiver in each side of the FreshCon container divided by the travel time at 5 minutes steps, the measured velocity curves were smoothed using a 3-point moving average algorithm and modelled using the multi-logistic function in equation (3.16), which describes an S-shaped curve (Robeyst, 2009).

Finally for the practical application of the results, the initial setting was calculated as the first inflection point (maximum on the derivative of the velocity curve) and the final setting time was determined as the point at which the derivative of the velocity curve decreased to 20% of its maximum value (Robeyst, 2009).

$$v = \sum_i \frac{v_i}{1+e^{(\Delta t - t_i)/g_i}} + K \tag{3.16}$$

with v the velocity of the ultrasonic p-wave [m/s], v_i the asymptotic value of velocity of one logistic function [m/s], Δt the time elapsed since the beginning of the test [s], t_i the point of inflection of one logistic function [s], g_i the slope – acceleration - of one logistic function [m/s^2] and K a constant [m/s].

Regarding the frequency spectra, the Fast Fourier Transformation (FFT) has been employed to identify the dominant components in the 0-200 kHz frequency bandwidth (Grosse and Reinhardt, 2000; Robeyst et al., 2009; Trtnik and Gams, 2013) that have been used as indicators of the stiffening of the concrete. In addition, the TG parameter (3.17) proposed by Trtnik and Gams (2013) was employed as means to compare the frequency and ultrasonic results.

$$TG = \frac{a_H - a_L}{a_H + a_L} \tag{3.17}$$

with TG the ratio between the maximum amplitude of the wavelength in the two frequency domains [-], a_H the maximum amplitude of the high frequency range and a_L the maximum amplitude of the low frequency range.

5. MECHANICAL BEHAVIOUR OF CONCRETE

5.1. DENSITY

Hardened density of concrete at 28 days was determined according to UNE EN 12390-7 (2009). After demoulding, three 100 mm cube specimen in phase II were immersed in water for each mixture (20±2 ºC). After 28 days of curing, the specimen surface was wiped in order to remove any water excess using a damp cloth and then the cube was weighed. Afterwards, the volume was determined by actual measurements with a calliper in accordance with UNE EN 12390-1 (2013). Finally, using the determined values, i.e. the saturated mass of the specimen divided by its volume the hardened density of concrete in water saturation condition was calculated.

5.2. COMPRESSIVE STRENGTH

Cylindrical and cubical specimens meeting with the shape and size requirements of UNE EN 12390-1 (2013) were employed in the determination of compressive strength in accordance with UNE EN 12390-3 (2009). Cylindrical specimens (n=3, 150x300 mm) were used in phase I for determinations at 7 and 28 days and cubical specimens (n=3, 100 mm or 150 mm) were used in phase II for concretes at 7, 28 and 90 days of curing.

The compressive test on cylindrical specimens was always preceded by a capping process with pure sulphur into the trowelled surface, and trimming when necessary, in order to achieve a smooth surface for uniform distribution of the load during testing. In the case of cube specimens, the testing was performed without any conditioning and in such way that the load is applied perpendicularly to the direction of casting.

(a) **(b)**

Figure 3.19: Compressive strength test hydraulic machines used in phase I (a) and phase II (b)

The loading was performed at a constant rate of 0.6 MPa per second by means of a hydraulic press (Figure 3.19) conforming to UNE EN 12390-4 (2001). The form of failure of the specimen was verified and if satisfactory the maximum load was recorded and the compressive strength was calculated by dividing the maximum load by the cross-sectional area of the specimen (3.18).

$$f_c = \frac{F}{A} \tag{3.18}$$

with f_c the compressive strength [MPa], F the maximum load at failure [N] and A the cross-sectional area of the specimen on which the compressive force acted [mm^2].

The three specimens were individually tested and their average value was used for the determination of the characteristic compressive strength using equation (3.19).

$$f_{ck} = f_{cm} \cdot (1\text{-}1.64 \cdot \delta) \tag{3.19}$$

with f_{ck} the characteristic compressive strength [MPa], f_{cm} the average value of three compressive strength tests [MPa] and δ the standard deviation of the three compressive strength tests [-].

5.3. FLEXURAL STRENGTH

The determination of the flexural strength was carried out in accordance to UNE EN 12390-5 (2009). A special testing device for four-point bending tests (Figure 3.20) was coupled to the hydraulic press (Figure 3.19a) in phase I tests. The test specimen rested on two steel roller supports (20x40 mm) - one of them capable of inclination and rotation - while the two superior steel rollers (20x40 mm) - both of them capable of rotation and inclination and situated in such way that the loading span equals one third of the supporting span - were accountable for the load application. However, for phase II tests, a hydraulic press for three-point bending tests (Figure 3.21), conforming to UNE EN 12390-4 (2001), was employed. In this test arrangement, the test specimen rested on two steel roller supports (20x40 mm) - one of them capable of inclination and rotation - while a third steel roller of the same dimensions, capable of rotation and inclination and located at mid-span was responsible for the load application of the bending moment.

Figure 3.20: Testing device for four-point bending tests

Figure 3.21: Hydraulic press for three-point bending tests

The test was performed on three 100x100x400 mm prismatic specimens of phase I mixtures and on three prismatic specimens of 150x150x600 mm for mixtures belonging to phase II at the age of 28 days. In all cases, the direction of loading was perpendicular to the direction of casting with a loading rate of 0.05 MPa per second, and the span between the two supporting rollers was three times the width of the specimen tested, i.e. 300 mm in phase I and 450 mm in phase II.

After checking that the fracture plane occurred within the space between the roller supports, the maximum load at failure was recorded and the flexural strength was calculated using equation (3.20) for the four-point test arrangement and equation (3.21) for the three-point test arrangement.

$$f_{cf}=\frac{F\cdot l_r}{d_1\cdot d_2^{\,2}} \tag{3.20}$$

$$f_{cf}=\frac{3\cdot F\cdot l_r}{2\cdot d_1\cdot d_2^{\,2}} \tag{3.21}$$

with f_{ct} the flexural strength [MPa], F the maximum load at failure [N], l_r the distance between the supporting rollers, i.e. span [mm], d_1 and d_2 the lateral dimensions of the specimen [mm].

5.4. SPLITTING TENSILE STRENGTH

The tensile strength of concrete was determined though indirect testing by the determination of the splitting tensile strength according to UNE EN 12390-6 (2010) on 28 days old concrete specimens.

In phase I, splitting tensile strength was determined on cylindrical specimens (n=3, 150x300 mm). A jig (Figure 3.22) was employed to ensure the positioning of the specimen in the hydraulic testing machine (Figure 3.19a) and a correct application of a compressive force, with a loading rate 0.05 MPa per second, along the opposite generators of the cylinder.

In phase II, the determination of splitting tensile strength was performed by a manually controlled testing machine (Figure 3.23) on two concrete specimens resulting from a prism (150x150x600 mm) previously subjected to a bending test (described in section 5.3 in the present chapter). Accordingly, the specifications in annex A (UNE EN 12390-6, 2010) were followed. Appropriately placed hardboard strips were employed in the plane of loading - perpendicular to the trowelled surface - in order to create an orthogonal tensile force that caused the specimen to fail in tension under a loading rate of approximately 0.05 MPa per second.

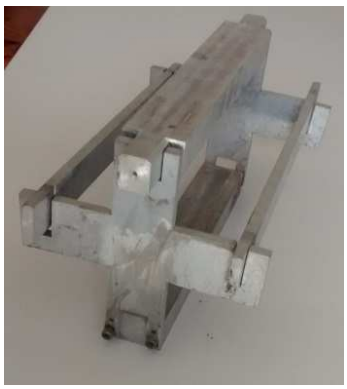

Figure 3.22: Jig employed for splitting tensile strength tests

Figure 3.23: Manually controlled press for splitting tensile strength tests

Each fractured specimen was examined to check that the failure occurred along the load plane. In both cases, the splitting tensile strength was calculated by the formula (3.22).

$$f_{cst} = \frac{2 \cdot F}{\pi \cdot L \cdot d_1} \tag{3.22}$$

with f_{cst} the splitting tensile strength [MPa], F the maximum load at failure (N), L the length of the line of contact of the specimen [mm] and d_1 the cross-sectional dimension of the specimen [mm].

5.5. MODULUS OF ELASTICITY

The modulus of elasticity in compression, also called the stabilized secant modulus, was determined from a 28 days cured cylindrical specimen (150x300 mm) in accordance with UNE EN 12390-13 (2014).

Before performing the test, the specimens were capped and instrumented with two 100 mm resistive strain gauges situated in two diametrically opposed generators of the cylinder using a bi-component adhesive. Additionally, in order to set the upper strength of the loading cycles, three specimens pertaining to the same batch were tested to determine the compressive strength of the concrete (UNE EN 12390-3, 2009). The test specimen was centrally placed in the lower platen of one of the hydraulic presses, depending on the phase of analysis (Figure 3.19), and subjected to an adjusting loading cycle, which lately was not employed for calculations. Afterwards, several loading cycles were performed with a maximum load corresponding to one third of the compressive strength previously determined and at a loading rate of 0.60 MPa per second. During the test, the loading values applied and the strain values that the specimen correspondingly suffered at each one of the cycles were registered through a DAQ card connected to a computer. Moreover, when all measurements were completed, the compressive strength of the specimen was determined (UNE EN 12390-3, 2009) and the obtained value compared with the characteristic compressive strength of the concrete mixture.

The modulus of elasticity was calculated as the slope of the stress stain curve of the material with equation (3.23).

$$E_s = \frac{\sigma_a - \sigma_p}{\varepsilon_a - \varepsilon_p} \tag{3.23}$$

with E_s the stabilized secant modulus of elasticity [MPa], σ_a the measured stress corresponding to one third of the compressive strength or upper strength [MPa], σ_p the measured stress corresponding to the preload stress or lower strength [MPa], ε_a the average strain at the upper stress on the last loading [-] and ε_p the average strain at lower stress on the last unloading [-].

5.6. SHRINKAGE

Shrinkage was measured on three specimens with a cross-sectional area of 150x150 mm^2 and 600 mm of height from concrete mixtures of phase II in accordance with the recommendation of RILEM TC 107-CSP (1998). Immediately after demoulding, two pre-drilled stainless steel discs were glued 300 mm apart on the four longitudinal sides. Then, the samples were placed in a controlled temperature room (20±2 ºC and 65±5 % relative humidity) for the remaining time of the experiment.

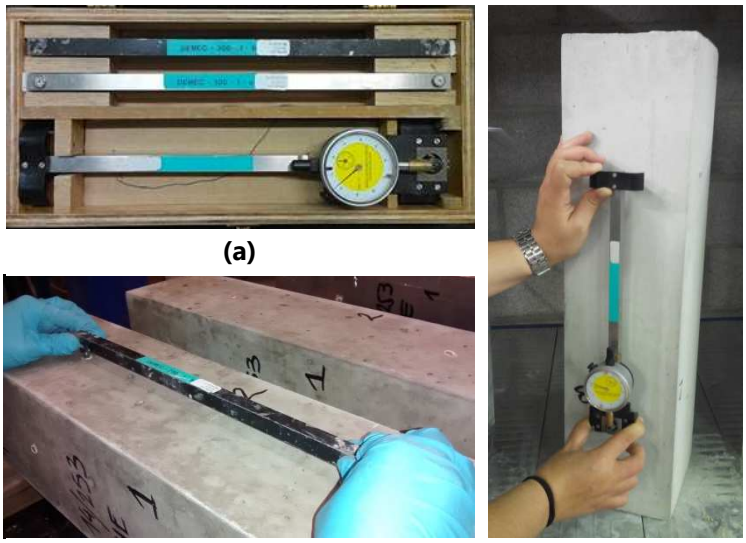

(a) **(b)** **(c)**

Figure 3.24: Shrinkage: DEMEC-300-1 gauge (a), placing of the two pre-drilled stainless steel discs (b) and measurement of the shrinkage

Length changes between the measuring studs were employed for monitoring the expansion or contraction phenomena occurring in the concrete specimen during the test. The measurements were performed with a mechanical strain gauge (DEMEC-300-1) by inserting the pins from the device into the holes of the glued studs and reading the strain indicated by the dial gauge (Figure 3.24).

The first reading was performed immediately after placing the specimens in the controlled temperature room, i.e. at 1 day of age, and follow up measurements were recorded when the samples reached the age of 3, 7, 14, 28, 42, 63 and 91 days.

The shrinkage was determined as the length changes of the specimen using equation (3.24).

$$S_x = \frac{L_i - L_0}{G} \tag{3.24}$$

with S_x the shrinkage at certain age [µm/mm], L_i the length comparator reading of the specimen at certain age [µm], L_0 the length comparator reading of the reference bar [µm], G the gauge length [300 mm].

5.7. CREEP

The creep determination was carried out in specimens pertaining to phase II concrete mixtures in a temperature controlled room (20±2 ºC and 65±5 % relative humidity) following the procedure described in the Belgian standard NBN B 15-278 (1976). The test was performed on two prim-shaped specimens of 150x150x500 mm. After 24 hours, the specimens were demoulded and one of them was immediately sealed with aluminium tape, in order to prevent evaporation of water and both samples were equipped with two pre-drilled stainless steel discs 300 mm apart on the four longitudinal sides. Then, the samples were placed in a controlled temperature room (20±2 ºC and 65±5 % relative humidity) for the remaining time of the experiment. After 28 days, the top and the bottom of the specimens were prepared to achieve a flattened surface suitable for the uniform application of the compressive force.

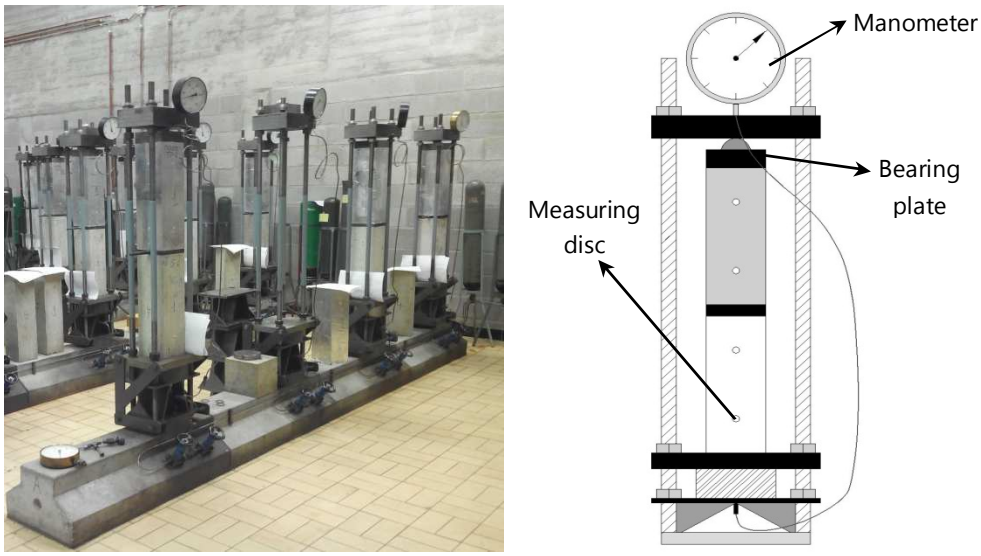

Figure 3.25: Compressive creep devices

The compressive creep devices employed (Figure 3.25) consisted of a rigid frame with two bearing plates, a hydraulic jack with a pump able to apply a load up to 25 MPa, and a hydro-pneumatic system with a nitrogen accumulator was used to maintain the pressure over time. The configuration of the device allowed the simultaneous testing of two concrete specimens from the same concrete composition in the same apparatus by stacking one on top the other with a steel bearing plate between both samples to eliminate any surface roughness influence.

The specimens were placed in the compressive creep device at 28 days of age to begin the sustained loading procedure. The load was applied on the top-plate and corresponded to one third of the compressive strength calculated for three specimens from the same concrete batch (UNE EN 12390-3, 2009).

Similarly to the shrinkage test, the longitudinal deformations were periodically measured on the four longitudinal sides of each specimen by means of a strain gauge (DEMEC 300-1) and the initially fixed measuring studs as per equation (3.24). The strains were recorded 10 minutes, 2 and 6 hours after applying the force in the first day of testing. Thereafter, the measurements were registered daily for the first week and then weekly for the rest of the experiment.

The experimental program allowed the determination of the basic creep from the measurements obtained from the sealed specimen, and the drying creep as the difference between the measurements obtained from the sealed and unsealed specimens. The basic creep and the total creep were calculated using equations (3.25) and (3.26) respectively.

$$C_b = \varepsilon_s - \frac{\sigma}{E} - S_a \tag{3.25}$$

$$C_{tot} = \varepsilon_u - \frac{\sigma}{E} - S_t \tag{3.26}$$

with C_b the basic creep at a certain age [µm/mm], ε_s the strain in the sealed specimen under load at a certain age calculated as a length change [µm/mm], σ/E the elastic strain [-], S_a the autogenous shrinkage before the loading [µm/mm], C_{tot} the total creep at a certain age [µm/mm], ε_u the strain in the unsealed specimen under load at a certain age calculated as a length change [µm/mm] and S_t the total shrinkage before the loading [µm/mm].

6. DURABILITY CHARACTERIZATION OF CONCRETE

6.1. GAS PERMEABILITY

Gas permeability of concrete mixtures pertaining to phase I was evaluated in accordance to the Spanish standard UNE 83981 (2008) by means of a permeability system patented by researchers of the University of Cantabria (Thomas-García et al., 2014). Figure 3.26 shows a schematic of the setup employed, consisting of a gas supply bottle, a pressure regulator (up to 0.60 MPa), a permeability cell and a patented digital flow meter (Thomas-García et al., 2013).

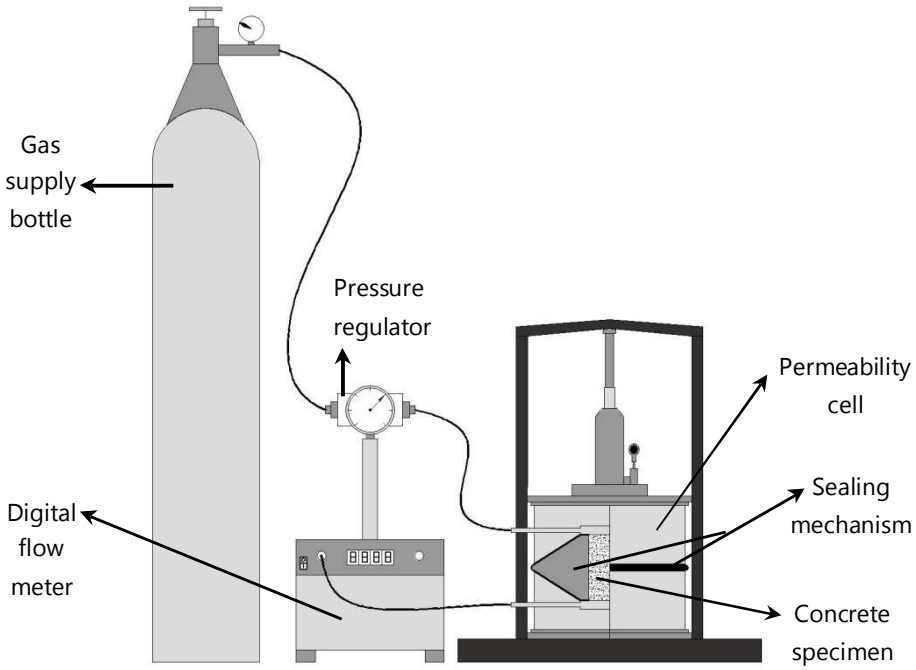

Figure 3.26: Gas permeability setup based on the University of Cantabria test procedure

Cylindrical samples (n=3, 100x100 mm) coming from the central third of a 100x200 mm standardized cylindrical specimen were used to analysed the gas permeability. Test specimens were preconditioning in accordance to UNE 83966 (2008) to obtain a saturation degree between 65% and 75%. To attain this moisture state, samples were dried (50±2 ºC) during 4 days, then sealed in a polyethylene film and dried again (50±2 ºC) during 3 days in order to redistribute the moisture content and finally, specimens were preserved in a controlled environment (20±2 ºC and 65-75% relative humidity) during 21 days. Finally, the circumferential surface of the specimens are coated with a silicone layer to improve the further sealing as recommended by ASTM C577-07 (2014) standard.

The sample was surrounded with a rubber collar to prevent lateral leakage of gas and introduced into a permeability cell. The permeability test itself involved the measurement of a unidirectional flow rate of gas through a specimen exposed to the gas at a known pressure (0.15 and 0.20 MPa respectively) in the top surface while the bottom surface remained at atmospheric pressure. The patented flow meter is a digital mass flow detector configured to convert the amount of gas flow (registered as an electric current) into a flow value in m^3/s. With this change in flow meter, a real-time graphical flow evolution over time can be obtained and thus recognize when the system is stabilized to begin the automatized data acquisition.

For phase II concrete mixtures, the gas permeability test was conducted using a constant head permeameter, commonly known as the CEMBUREAU permeameter (Kollek, 1989; RILEM TC 116-PCD, 1999). As schematically represented in Figure 3.27, the equipment consisted essentially of a gas supply bottle with a precision pressure regulation (0.10 to 0.60 MPa), 3 pressure cells, 4 calibrated soap bubble volumetric gas flow meters (1.50 ml, 5 ml, 20 ml and 160 ml) and a stop-watch.

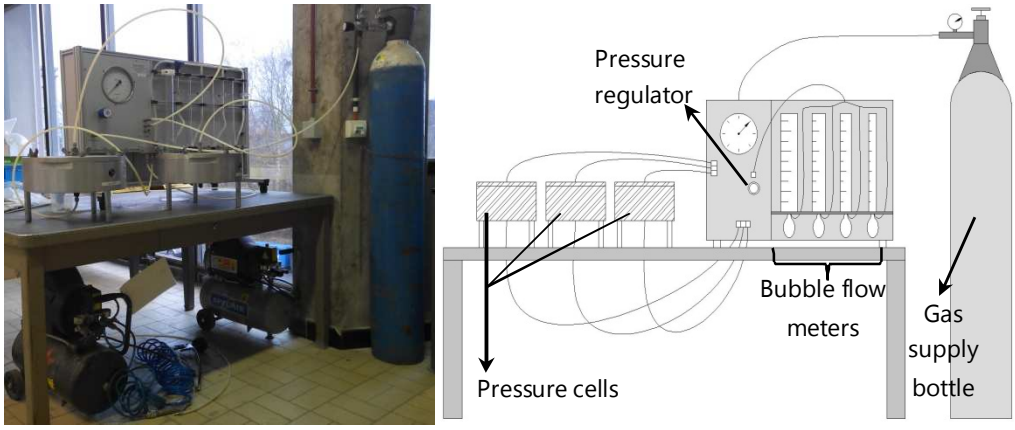

Figure 3.27: CEMBUREAU permeameter

The samples studied (n=3, 150x50 mm) were taken from the middle third of 28 days cured cylindrical specimens drilled from a concrete slab (400x400x100 mm). This is a standard disc specimen, presenting a similar volume as a 100 mm cube and a thickness approximately twice the typical cover to reinforcement (Kollek, 1989).

To obtain meaningful and comparable results all the test specimens were preconditioned to ensure a same moisture sate condition. Towards this end, after the end of the curing period, the samples were first dried (80±5 ºC) until constant mass - less than 0.10 wt% of evaporated water loss during 24 hours -, which required approximately 14 days. Afterwards, specimens were vacuuming at 2.70 kPa for 2.50 hours and subsequently, still under vacuum, immersed under water at a 50 mm/h rate until complete coverage. Finally, the samples were kept under water for 24 hours at atmospheric pressure. At that point, concrete specimens were fully saturated - which impeded any gas flow - and by further sequential drying (at 80±5 ºC and 105±5 ºC respectively), moisture redistributing and cooling (20±2 ºC and 60±5 % relative humidity), three different saturation degrees were attained, the last of them corresponding with the completely dry state of the sample. The weighing of the samples at each preconditioning step allows the determination of the saturation degree using equation (3.27).

$$SD = \frac{M_x - M_{dry}}{M_{sat} - M_{dry}} \cdot 100 \qquad (3.27)$$

with *SD* the saturation degree of the sample at a certain gas permeability measurement [%], M_x the mass of the sample at the corresponding gas permeability measurement [g], M_{dry} the mass of the oven dry sample measured at the last gas permeability measurement [g], M_{sat} the mass of the vacuum saturated sample weighed in air [g].

Figure 3.28 summarizes both the preconditioning and measurement steps followed in the gas permeability determination, which are mainly based on the preparing procedure suggested by Carcases et al. (2002).

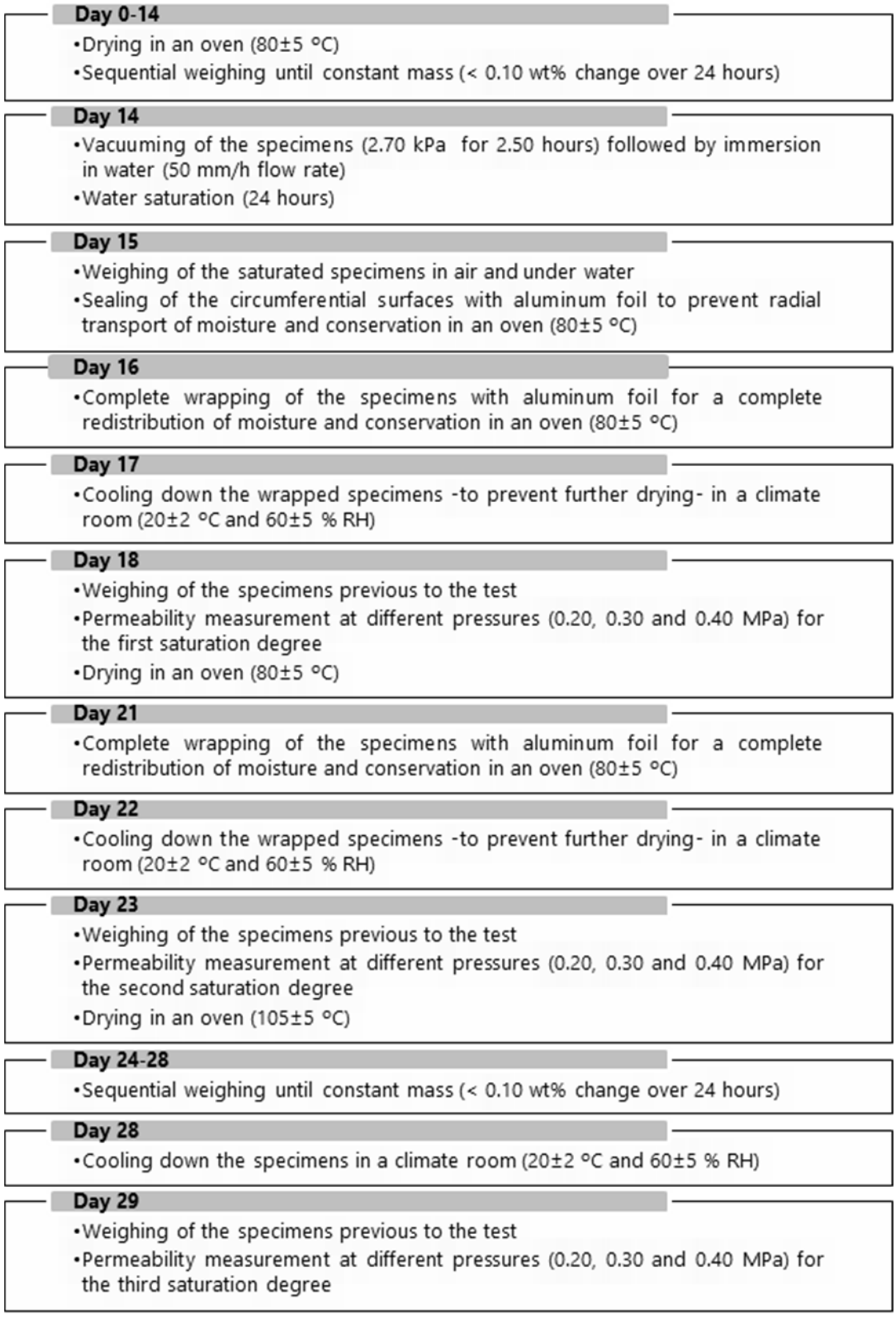

Figure 3.28: Gas permeability preconditioning and test procedure

All permeability measurements followed RILEM TC 116-PCD (1999) recommendations. The specimens were situated in the pressure cells inside of a rubber ring and were tightly fitted by pumping the rubber tube pressing against the curved surface of the concrete specimen up to a pressure of 0.80 MPa to guarantee a uniaxial flow and prevent leakage of oxygen gas. Details of the experimental setup can be seen in Figure 3.29. After assembling all the pressure cells, the oxygen pressure was set according to the pressure stage of the test (0.20, 0.30 and 0.40 MPa respectively) and the bottom face was exposed to the pressurized oxygen while the top face remained at atmospheric pressure in order to generate the pressure gradient that governs permeability transport. The gas flow was allow to stabilize (±30 minutes) to a steady-state regime before an actual measurement was taken using the appropriate flow meter.

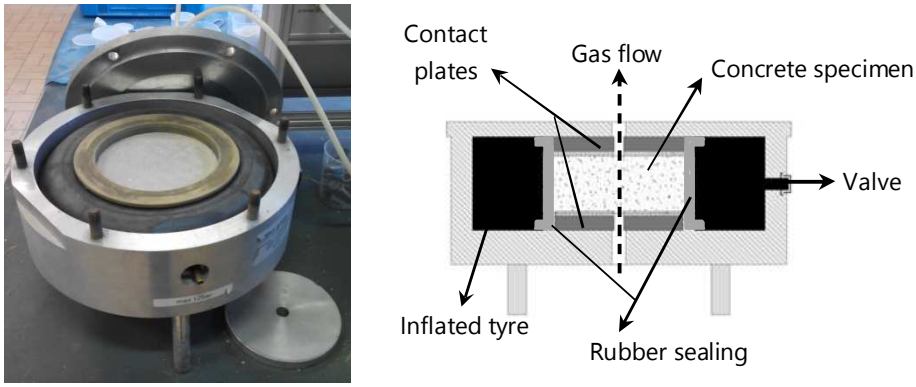

Figure 3.29: Pressure cell in the CEMBUREAU method

For each saturation degree and applied pressure of both methods, the apparent permeability coefficient was calculated according to Darcy's law and the Hagen-Poiseuille equation (3.28) for laminar flow of a compressible fluid through a porous medium with small capillaries under steady-state conditions.

$$K_{app} = \frac{2Q_g P_{atm} L\eta}{A\left(P^2 - P_{atm}^{\ 2}\right)} \tag{3.28}$$

with K_{app} the apparent gas permeability coefficient [m^2], Q_g the measured gas flow rate through the sample [m^3/s], P_{atm} the atmospheric pressure [101300 Pa], L the sample thickness in the flow direction [m], η the dynamic viscosity of the fluid at test temperature [Pa·s], A the cross-sectional area of the specimen [m^2] and P the inlet pressure applied during test [Pa]. Given that the employed gas should not react chemically with concrete to prevent pore structure changes during the test (Hilsdorf and Kropp, 2004), oxygen was used as the permeating medium and a dynamic viscosity of 2.02×10^{-5} Pa·s was assumed.

6.2. CARBONATION

The natural carbonation test described in UNE 83993-1 (2013) was carried out on specimens from phase I in order to determine the carbon dioxide (CO_2) penetration rate of the different concrete compositions. After 28 days of curing, two cylindrical concrete specimens (100x200 mm) pertaining to the same concrete batch were exposed to the natural outdoor environment with a 0.06 vol% CO_2, while being protected from the rain, for a testing period of 1 year.

However, for phase II specimens an accelerated carbonated testing procedure was followed. The original specimens, 10 mm cubes, were sawn into two 50 mm thick slices and coated to obtain one-dimensional carbon dioxide ingress. Except the casting surface, all other sides were painted with two epoxy resin layers with a 24 hour delay just before the start of the test. At 28 days of age, nine concrete specimens of each mix were introduced in a chamber with an atmosphere with a carbon dioxide content of 10 vol% at 20±2 °C and 60±5 % relative humidity (Figure 3.30). The regular exposure period under accelerated conditions was 1, 2 and 3 months for three samples of each concrete mixture.

Figure 3.30: Carbonation chamber employed in Phase II

Once the testing age was reached, specimens were broken by means of a Brazilian tests (UNE EN 12390-6, 2010). Immediately, the broken surfaces were cleaned and sprayed with a solution of 1 g of phenolphthalein indicator in 70 % ethanol. Since pH values of 8.0-9.5 are the point of transition for phenolphthalein, non-carbonated concrete turned purple while carbonated concrete remained uncoloured. Then, the carbonation front depth was determined as the average distance from the surface to the purple colour boundary measured every 10 mm as outlined in the Spanish standard UNE 112011(2011).

The measured carbonation depth was plotted against the square root of the exposure time and Fick's first law of diffusion was employed for the determination of the carbonation coefficient as shown in equation (3.29). In addition, as the accelerated method was carried out at an unrealistic CO_2 concentration, the obtained values for the carbonation coefficient were corrected for natural conditions by means of equation (3.30).

$$K_{CO_2} = \frac{x_d}{\sqrt{t}} \tag{3.29}$$

$$K_{corr,\,CO_2} = K_{CO_2} \cdot \frac{\sqrt{C_{nat}}}{\sqrt{C_{acc}}} \tag{3.30}$$

with K_{CO2} the carbonation rate at certain CO_2 concentration [mm/√years], x_d the mean carbonation depth [mm], t the exposure period [years], $K_{corr,CO2}$ the corrected carbonation rate at certain CO_2 concentration [mm/√years], C_{nat} the CO_2 concentration in natural conditions [0.06 vol%] and C_{acc} the CO_2 concentration in accelerated conditions [vol%].

6.3. WATER ABSORPTION BY CAPILLARITY

The capillary water absorption tests were performed on four prismatic (100x100x50 mm) concrete specimens from phase II at 28 days based on Spanish standard UNE 83982 (2008) in a temperature controlled room at 20±2 °C and 60±5 % of relative humidity.

Test specimens were preconditioned in accordance to UNE 83966 (2008) in order to obtain an average moisture concentration. Samples were dried (50±2 ºC) during 4 days, then sealed in a polyethylene film and dried again (50±2 ºC) during 3 days in order to redistribute the moisture content and finally, specimens were preserved in a controlled environment (20±2 ºC and 65-75% relative humidity) during 21 days.

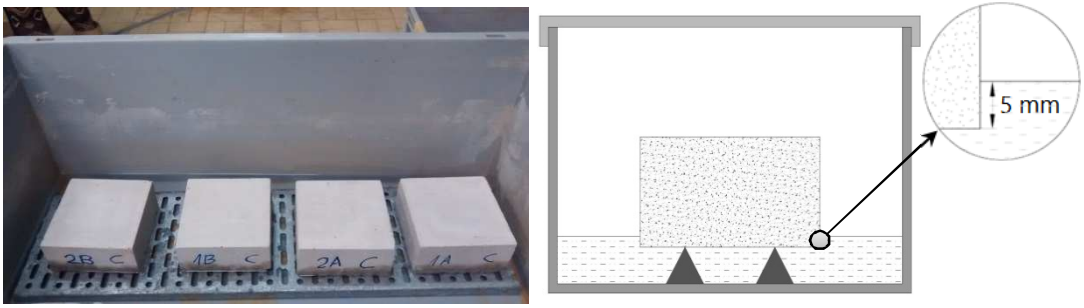

Figure 3.31: Capillary water absorption test setup

In this test method, the rate of absorption was determined by measuring the increase in the mass of four samples. Figure 3.31 displays the capillary water absorption test setup. The bottom face of each specimen was put in contact with water, taking special care that the samples were only submerged 5±1 mm at all moments. The water uptake was measured as the differential weight of the specimen at controlled intervals (5, 10, 15 and 30 minutes and 1, 2, 3, 4, 6, 24, 48, 72 and 96 hours) until the specimen achieved a constant mass. Before each weighing, the bottom part of the specimen was dried with a wet cloth to remove any water excess, and immediately after the measurement, samples were placed again in the container.

The aforementioned Spanish standard (UNE 83982, 2008) establishes equations (3.31) and (3.32) to respectively calculate the effective porosity and the capillary water absorption coefficient.

$$\varepsilon_e = \frac{Q_n - Q_0}{A \cdot h \cdot \rho_w} \tag{3.31}$$

with ε_e the effective porosity of the concrete specimen [-], Q_n the weight of the specimen when the saturation was achieved [kg], Q_0 the weight of the specimen prior to the test [kg], A the cross-sectional area of the specimen in contact with water [m^2], h the height of the specimen [m] and ρ_w the density of water [1000 kg/m^3].

$$K_c = \frac{\rho_w \cdot \varepsilon_e}{10 \cdot \sqrt{\frac{t_n}{h^2}}} \tag{3.32}$$

with K_c the capillary water absorption coefficient [kg/$m^2 \cdot \sqrt{s}$], ρ_w the density of water [1000 kg/m^3], ε_e the effective porosity of the concrete specimen -equation (3.31)- [-], t_n the time elapsed until the saturation of the specimen was achieved [s], h the height of the specimen [m].

In general, this determination of the capillary water absorption coefficient is rather uncommon in literature. Thus, in order to determine the sorptivity coefficient, the cumulative amount of water absorbed per unit area was plotted against the square root of time and the best-fit curve was obtained by regression analysis. Graphically, two separate components were identified, the initial sorptivity corresponding with the slope of the fitted curve during the first six hours of testing and the secondary sorptivity determined as the slope of the fitted curve using the measurements obtained from the first day to the end of the testing period (ASTM C1585-13, 2013).

6.4. WATER ABSORPTION UNDER VACUUM

The accessible porosity was determined according to the water absorption under vacuum test described in paragraph 6.1 of the Belgium standard NBN B 05-201 (1976). Figure 3.32 displays the vacuum saturation setup employed for the assessment of concrete specimens from phase II.

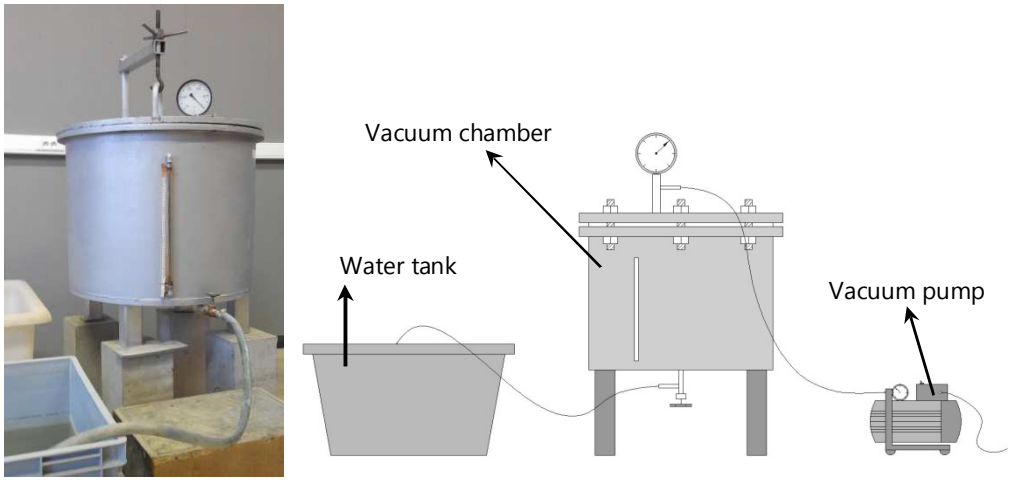

Figure 3.32: Vacuum saturation setup

At 28 days of curing, two cores with a diameter of 100 mm were drilled from a concrete slab (400x400x100 mm) and equally sawn in two halves to obtain four cylindrical specimens (100x50 mm) for testing. The experimental program for this test consisted of two consecutive vacuum saturation steps of the same specimens after two different drying temperatures. The samples were dried until constant mass was achieved - differential weight loss in 24 hours less than 0.1 wt% - in a ventilated oven at 40±5 ºC in the first step and 105±5 ºC in the second step, corresponding with the temperature of evaporation of free capillary water and gel water respectively.

After measuring the oven dry masses in each step of the procedure, the specimens were vacuum saturated in a tank where a residual pressure of 2.70 kPa was maintained for 2.50 hours. Then, water was introduced at a 50 mm/h rate. When completely covered, approximately after 2 hours as the cylinders were standing on their circumferential surface to minimize the contact surface with the bottom of the tank, the atmospheric air pressure was re-established and the specimens were kept into water for 24 hours before their weighing in air and under water.

Based on the different weight recorded, the open porosity at each one of the drying temperatures was calculated with equation (3.33) as the percentage of pores filled with water. Hence, capillary water porosity was computed from the difference in water content of saturated samples and samples dried at 40 ºC and gel porosity was determined from the difference in water content of samples dried at 40 ºC and 105 ºC.

$$\varphi_T = \frac{W_s - W_d}{W_s - W_w} \cdot 100 \tag{3.33}$$

with φ_T the open porosity after drying at a certain temperature [wt%], W_s the weight of the saturated specimen [g], W_d the weight of the dried specimen weighed in air [g], W_w the weight of the saturated specimen measured under water [g].

6.5. WATER PENETRATION UNDER PRESSURE

The evaluation of the permeability of the concrete was assessed through the water penetration test outlined in UNE EN 12390-8 (2009).

Different test specimens and sample preparation were employed for the determination of water penetration under pressure in each research stage. In phase I, three standardized cylindrical specimens (150x300 mm) were tested for each concrete composition. Immediately after demoulding, the specimens were brushed to roughen the surface to be exposed to the water pressure and cured under water for 28 days. However, concrete specimens from phase II were subjected to a more thorough sample conditioning. Subsequent to the 28 days of curing in a saturated atmosphere, one 150 mm cubical specimen of each concrete mixture was drilled to obtain a cylinder of 100 mm diameter. This core was carefully resin-bonded to a dummy concrete specimen in order to ensure a unidirectional flow of water. Finally, the surface to be exposed to the water pressure was roughened in order to eliminate any possible resin residue. Before the beginning of the testing procedure, a 7 days immersion period under water was imposed to achieve the saturation state required in the standard, given that these specimens were not cured under water.

The test consisted of the application of a 0.50 MPa upward water pressure on the roughened face of the specimen within a 100 mm diameter watertight rubber seal. Figure 3.33 displays the equipment employed in phase I and phase II respectively. After 72 hours of maintained pressure, the specimens were split in half by means of a Brazilian test (UNE EN 12390-6, 2010) and the maximum height achieved in the penetration of the water was measured with a calliper.

(a)

(b)

Figure 3.33: Water penetration test machines used in phase I (a) and phase II (b)

Moreover, the complete water penetration profile was marked for further analysis. The EHE-08 (Permanent Commission on Concrete, 2008) also establishes requirements for the average penetration depth. The Spanish standard UNE EN 12390-8 (2009) includes a national annex that proposes a method for this determination. This parameter was calculated as the ratio between the wet area and the diameter of the specimen using equation (3.34).

$$d_{ap} = \frac{A_{pf}}{D} = \frac{A_p \times M_{pf}}{D \times M_p} \tag{3.34}$$

with d_{ap} the average depth of water penetration [mm], A_{pf} the wet area [mm^2], D the diameter of the specimen [mm], A_p the area of the whole tracing paper sheet [mm^2], M_{pf} the mass of the wet area reproduction in the tracing paper [g] and M_p the mass of the whole tracing paper sheet [g].

For phase I research works, the measure of the wet enclosed area was determined according the UNE EN 12390-8 (2009) recommended technique. The water penetration profile was obtained as the weight difference between the mass of an untouched sheet of tracing paper and that of the reproduction of the wet area on the tracing paper with an accuracy of 0.1 g (Figure 3.34).

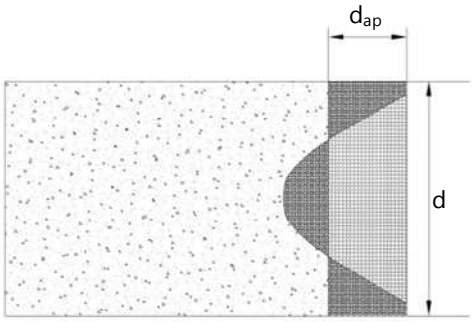

Figure 3.34: Average depth of water penetration as defined by EHE-08

So as to assess the penetration depth results, the EHE-08 (Permanent Commission on Concrete, 2008) establishes requirements for both the maximum and average penetration depth as a function of the environmental exposure classes. The limit for mass or reinforced concrete is established at 30 mm for average penetration depth and 50 mm for maximum penetration depth when subjected to IIIa, IIIb, IV, Qa, Qb, H, F or E exposure classes. Appendix A can be consulted for the equivalent nomenclature used in EN 206-1 (2005) for the environmental exposure classes.

6.6. FROST-SALT RESISTANCE

Concrete exposed to low temperatures could be subjected to two types of frost damage: surface scaling resulting in the loss of mortar or even coarse aggregates due to the presence of de-icing agents; and internal micro-cracking caused by the expansion of freezing moisture, which reduces the mechanical properties - strength and stiffness - of the element.

The internal damage of freeze-thaw cycles of phase I concrete mixtures was evaluated on three 100 mm cubical specimens according to ASTM C666M-03 (2008), Procedure B: Rapid freezing in air and thawing in water. Test specimens were subjected to 25 freeze-thaw cycles. In the freezing period, dried samples (105 ºC) were placed in a temperature controlled chest at -23±2 ºC during 16 hours; while in the thawing period, test specimens were submerged in containers with a salt solution at 20±2 ºC during 8 hours. In this study, a salt solution of sodium chloride (NaCl) at 3 wt% was chosen as de-icing agent due to the literature reports stating this concentration as the most prejudicial (Marchand et al., 1999; Valenza II and Scherer, 2007).

In each cycle, the transmission time of p-waves was measured in the axial direction -perpendicular to the casting direction- in order to accurately pinpoint the beginning of the internal degradation process. Samples were superficially dried before both transducer probes of a Portable Ultrasonic Non-destructive Digital Indicating Tester (PUNDIT) were firmly held in contact with opposite sides of the specimen (cross-probing) and coupled with the concrete surface with a water-based ultrasound gel (Figure 3.35).

Electric-acoustic pulses were emitted and received after passing through the known length of the specimen and the time lapse was measured. The ultrasonic pulse velocity was then determined dividing the travel distance by the elapsed time (UNE EN 12504-4, 2006).

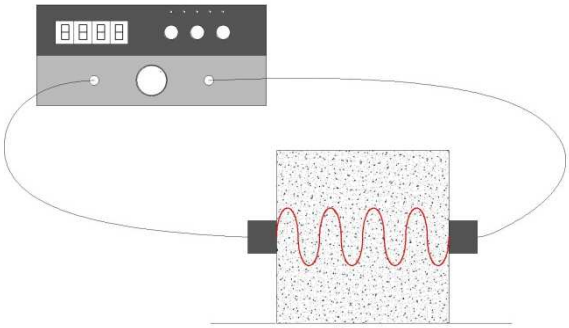

Figure 3.35: Ultrasonic pulse velocity testing

Finally, the weight change measured as a mass change after the 25 freeze-thaw cycles, was used to gauge the internal structural damage.

Moreover, surface scaling of concrete mixes in phase II was evaluated based on the appendix D of UNE EN 1339 (2004) on 28 days cured cylinders, drilled from a concrete slab (400x400x100 mm) and sawn in half to allow the differential characterization of both casting and trowelled surfaces. Figure 3.36 shows the specific configuration followed in the sample preparation.

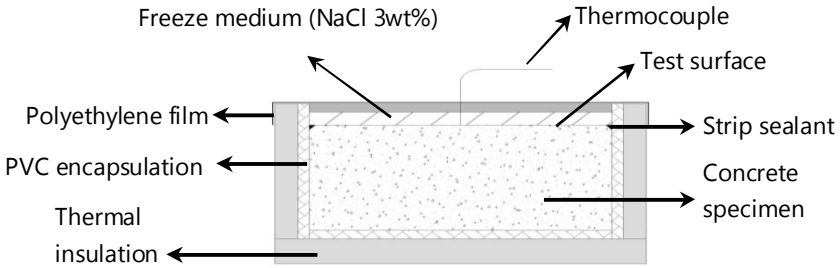

Figure 3.36: Test specimen for freeze-thaw attack with de-icing agents

The test specimens (n=6, 100x50 mm) were glued into a polyvinyl chloride (PVC) tube to ensure continued exposure to the freezing medium. After a leakage test to guarantee a correct sealing, a 5 mm thick layer of freezing medium was placed on each specimen. As in the first method, sodium chloride (NaCl) with a 3 wt% concentration was chosen as de-icing agent. Lastly, to maintain the salt solution at a constant height and concentration throughout the experiment a plastic film was used to cover each sample.

Subsequently, the specimens were introduced in a freezing chamber at the beginning of a freeze-thaw cycle with temperatures ranging from -18 ºC to 20 ºC in 24 hours following the pattern established in UNE EN 1339 (2004) (Figure 3.37). A temperature-time graph obtained during the experiments is given in Figure 3.38 showing the compliance with the aforementioned standard.

Figure 3.37: Freezing chamber employed in Phase II

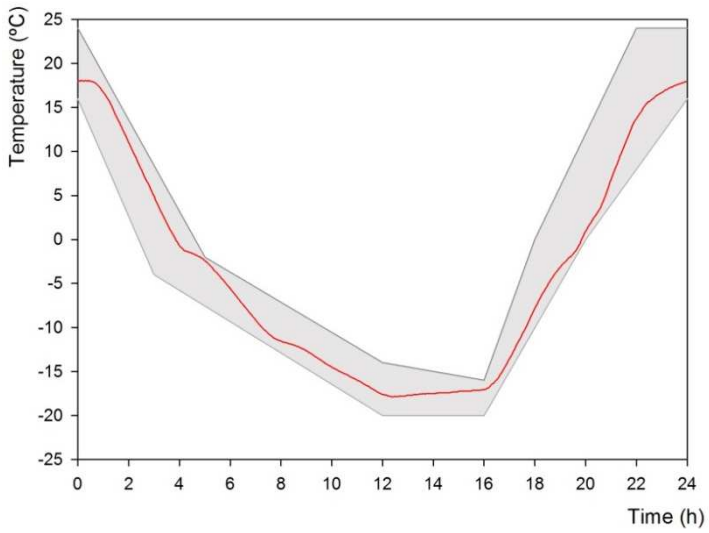

Figure 3.38: Temperature regime log for one cycle of freezing and thawing

During the thawing phase of the 7th, 14th, 21th and 28th cycle, each specimen was rinsed with tap water into a filter paper in order to collect the scaled material that afterwards was dried a 105 ºC during at least 24 hours. Finally, the same quantity of freezing medium was poured again onto the test surface and the specimen was returned to the freezing chamber at the beginning of a new freeze-thaw cycle.

Salt scaling resistance was assessed by subsequently weighing of surface mass loss per unit area, with a limit of 1 kg/m^2 mass loss at 28 cycles established in European standard (UNE EN 1339, 2004). Moreover, visual observations were also employed to evaluate the extent of the frost attack using the criterion displayed in Table 3.3.

Table 3.3: Salt scaled criterion for the visual examination

Rating	Description
0	No scaling
1	Slight scaling (small flakes)
2	Moderate scaling (small flakes and some coarse aggregate visible)
3	Severe scaling (chunks coming out of the surfaces and/or coarse aggregate visible over the entire surface)

6.7. CHLORIDE INGRESS

The rapid chloride migration test defined in the NT BUILD 492 (1999) standard was performed on concrete specimens from phase II. Six cylindrical specimens (100x50 mm) were obtained by drilling 3 cores of 100 mm diameter from a concrete slab (400x400x100 mm) and subsequently the cylinders were sawn in half in the perpendicular direction of casting, which enabled the differential characterization of the casting and trowelled surfaces of the sample.

After 28 days of curing, the test specimens were vacuumed (2.50 KPa) for three hours. Then, the samples were submerged in a calcium hydroxide ($Ca(OH)_2$) solution (4 g/l) and further vacuumed for an additional hour. After recovery of the atmospheric pressure, the specimens were kept in the $Ca(OH)_2$ solution for 18±2 hours before the beginning of the testing procedure. This process ensures the complete saturation of the samples and therefore a pure migration mechanism of the chloride ions through the concrete.

Once preconditioned, each specimen was tightly fitted in a silicone rubber sleeve with two stainless steel clamps to avoid any leakage and 300 ml of the anolyte solution, i.e. a sodium hydroxide (NaOH) solution (0.30 N) in distilled water, was poured in top of the samples. Taking care to avoid any spill, the sample was introduced in the catholyte reservoir, i.e. a 10 wt% sodium chloride (NaCl) solution in distilled water, and the electrodes were placed, such as the cathode was connected to the positive pole and the anode was connected to the negative pole (Figure 3.39). Then, the procedure consisted of the forced migration of the chloride ions from the reservoir into the specimen by the application of an electrical current.

Figure 3.39: Chloride migration set up (NT BUILD 492, 1999)

Initially, the voltage was established at 30 V and adjusted for each concrete composition after the indications in the Appendix 2 of NT BUILD 492 (1999) in order to determine the appropriate duration of the test. After the prescribed period - usually 24 hours - the specimens were washed and split by means of the Brazilian method (UNE EN 12390-6, 2010) and the resulting sections were sprayed with a silver nitrate ($AgNO_3$) solution (0.10 M). The colour change boundary due to the white silver chloride (AgCl) precipitation, visible after approximately 15 minutes of the application, served as indicator of the chloride ions penetration depth, which was measured at 10 mm intervals.

From the chloride ingress penetration depths a non-steady-state migration coefficient was calculated according to simplified equation (3.35) (NT BUILD 492, 1999). Although this formula was initially proposed for concrete made with ordinary Portland cement, its validity for blast furnace slag concrete has been proven (Gruyaert, 2011; Gruyaert et al., 2013; Maes et al., 2013).

$$D_{nssm} = \frac{0.0239 \cdot (273+T) \cdot L}{(U-2) \cdot t} \left(x_d - 0.0238 \sqrt{\frac{(273+T) \cdot L \cdot x_d}{(U-2)}} \right) \quad (3.35)$$

with D_{nssm} the non-steady-state migration coefficient [10^{-12} m^2/s], T the average value of the initial and final temperature in the anolyte solution [°C], L the length of the specimen [mm], U the applied voltage [V], t the duration of the test [h] and x_d the average penetration depth [mm].

6.8. ELECTRICAL RESISTIVITY

The electrical resistivity of concrete was determined at 20 ºC in 28 days saturated surface-dry specimens of phase I according to UNE 83988-1 (2008). A schematic of the setup employed for the measurement of the electrical resistivity is provided in Figure 3.40.

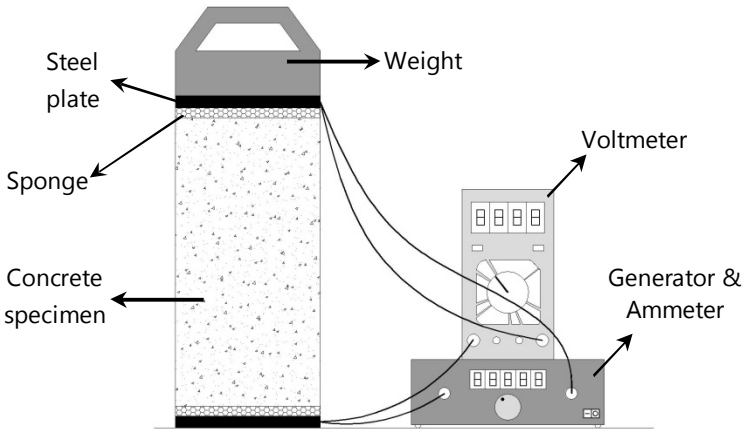

Figure 3.40: Schematic of the electrical resistivity setup

In this procedure, an electrical field was applied to two electrodes (steel plates) pressed to the two parallel faces of three 100x200 mm cylindrical specimens. To ensure a proper electrical contact, two wetted sponges (5 mm thickness) of known electrical resistance were inserted in between. Then, the electrical resistance of the hardened concrete was measured by means of a hand-held resistance meter, as the ratio between the applied voltage and the resulting intensity of current passing through the specimen based on Ohm's Law. Lastly, the electrical resistivity was calculated, as per equation (3.36), multiplying the electrical resistance of the concrete by the geometrical cell constant of the setup.

$$\rho_c = \frac{A}{h} \cdot \left(\frac{V}{I} - R_s \right) \tag{3.36}$$

with ρ_c the electrical resistivity of the concrete specimen [Ωm], A the area [m^2], h the height of the specimen [m], V the potential difference between the electrodes [V], I the intensity crossing the circuit [A] and R_s the electrical resistance of the sponges [Ω].

6.9. ALKALI-SILICA REACTION

The susceptibility for expansive alkali-silica reaction in all concrete mixtures from phase II was assessed by means of a modification of the South-African NBRI-method or Oberholster test (Oberholster and Davies, 1986).

At the age of 28 days, three cylindrical test specimens of 50x150 mm were drilled from a standardized cubical specimen of each mixture. The samples and a stainless steel reference cylinder were carefully arranged on the supporting rods inside the machine shown in Figure 3.41. Moreover, a stainless steel pin was placed on top of each sample to allow the measurements - changes in length of the specimen - during the experiment. After covering the setup, a length dial gauge was installed for each sample.

Figure 3.41: Alkali-silica measurement setup

On the first day of testing, the tank was filled with water and heated up to 80 ºC. One day later, a 1 M sodium hydroxide (NaOH) solution was used to replace the water and the tank was heated up to 80 ºC. This solution was replenished throughout the test to compensate volume loses due to evaporation. The first test measurement was performed one hour after the temperature stabilization of the setup, and subsequently measures were registered on a daily basis for the 20 following days.

Although the length expansion after 20 days was used as the alkali-silica susceptibility test indicator, the daily values were employed as a validation of the method, i.e. the final result was considered correct if not more than 15% deviation from the mean between daily measures was recorded. In addition, the expansion measurements performed on the reference sample were used to monitor possible change in length due to external factors, e.g. temperature. Finally, in order to evaluate the alkali-silica susceptibility, the concrete mixes were considered non-reactive when the final expansion was below 0.10% (Oberholster and Davies, 1986) or 0.15 % (Davies and Oberholster, 1987).

6.10. RESISTANCE TO ORGANIC ACIDS

In order to examine the resistance to acidic solution of the different concrete compositions, an accelerated degradation test was carried out employing the apparatus developed by De Belie et al. (2002). The accelerated test procedure was based on the combination of a chemical action (wetting in an acid solution and drying in air) and a mechanical action (brushing).

Three toroid specimens were casted in a special mould for testing each concrete batch. The mould presented an internal diameter of 40 mm, an external diameter of 270 mm and a height of 70 mm. In addition, the mould contained the anchoring mechanisms needed for the attachment of the specimen into one axle of the apparatus and for the metallic piece serving as the trigger for the beginning of the laser measurements.

The testing machine (Figure 3.42a) consisted of four horizontal rotating stainless steel axles, each one able to contain two sets of three samples turning through their own container and covered by a shared case to avoid evaporation. A switch gear manually actioned made possible the variation in the rotating speed between 1.04 and 24.41 revolutions per hour. The equipment also permitted the coupling of the brushing device (Figure 3.42b) and laser device (Figure 3.42c) to a fixed position on the frame of the apparatus by use of two stop pieces and two bolts. A more detailed description of the apparatus can be found in De Belie et al. (2002).

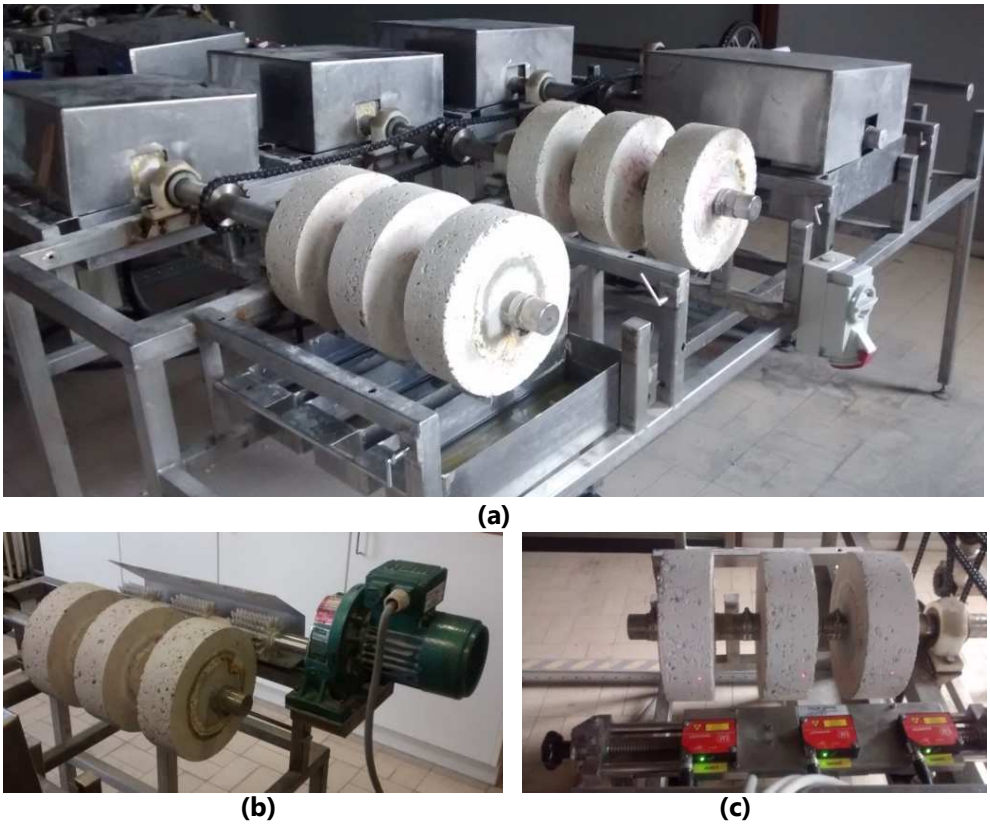

Figure 3.42: TAP apparatus

After 28 days of curing, the concrete specimens were installed into the accelerated degradation tests (TAP) apparatus with two clamping rings, and a stainless steel angle (10x10 mm) was screwed by means of two bolts into each sample. Each test container was filled with two litres of acid solution composed of 30 g/l of acetic acid and 30 g/l lactic acid, which affected only to the outer bottom part of each specimen.

One accelerated degradation cycle consisted of the immersion of the samples in a fresh acid solution during 7 days, followed by a 2 hours air-drying period before 3 brushing steps - in alternate direction of rotation - to remove the degraded concrete weakened by the chemical attack. Whilst the low rotating speed was selected during the acid immersion, the brushing step was performed with the samples rotating at high speed by means of three rotary brushes with 20 mm long white nylon hairs turning at 394 rpm. This testing sequence was repeated until 6 attack cycles were completed. Previous to the testing procedure and after each attack cycle, the distance between the samples and the laser sensors was determined by means of optical triangulation and registered as a means to evaluate the change in radius due to the degradation process. All the measurements - 4 contour parallel lines separated 0.50 mm per specimen - were performed in steps of 0.24 mm with the samples turning at high speed. In addition, the evolution of the degradation was evaluated visually and the pH of the solution was measured at the beginning and at the end of each attack cycle.

The laser measurements were employed to calculate the degradation depth by comparing the radius change through the experiment. Moreover, the surface roughness (3.37) was calculated as the arithmetical average value of the departure y(x) (mm) of the profile above and below the centre line throughout a prescribed sample length, based on ISO 4287 (1997).

$$R_a = \frac{1}{SL} \cdot \int_0^{SL} |y(x)| dx \tag{3.37}$$

with R_a the surface roughness [mm], SL the prescribed sampling length [mm] and $y(x)$ the profile height function [mm]. Given that a 50 mm sampling length was chosen (De Belie et al., 2002), thirteen Ra values were obtained per contour profile.

7. REFERENCES

Abbas, A., Fathifazl, G., Isgor, O.B., Razaqpur, A., Fournier, B., Foo, S., 2008. Proposed method for determining the residual mortar content of recycled concrete aggregates. *Journal of ASTM International* 5 (1): 12.

Abell, A.B., Willis, K.L., Lange, D.A., 1999. Mercury intrusion porosimetry and image analysis of cement-based materials. *Journal of Colloid and Interface Science* 211 (1): 39–44.

ASTM C88-13, 2013. Test method for soundness of aggregates by use of sodium sulfate or magnesium sulfate. ASTM International, Pennsylvania.

ASTM C457-12, 2012. Test Method for Microscopical Determination of Parameters of the Air-Void System in Hardened Concrete. ASTM International, Pennsylvania.

ASTM C577-07, 2014. Test method for permeability of refractories. ASTM International, Pennsylvania.

ASTM C666M-03, 2008. Test method for resistance of concrete to rapid freezing and thawing. ASTM International, Pennsylvania.

ASTM C1585-13, 2013. Test method for measurement of rate of absorption of water by hydraulic-cement concretes. ASTM International, Pennsylvania.

ASTM D4404-10, 2010. Test method for determination of pore volume and pore volume distribution of soil and rock by mercury intrusion porosimetry. ASTM International, Pennsylvania.

Bermejo, E.B., Moragues, A., Gálvez, J.C., Fernández Cánovas, M., 2010. Permeability and pore size distribution in medium strength self-compacting concrete. *Materiales de Construcción* 60 (299): 37–51.

Callister, W.D.J., 2007. Materials science and engineering: An introduction. John Wiley & Sons, Hoboken, New Jersey.

Carcasses, M., Abbas, A., Ollivier, J.-P., Verdier, J., 2002. An optimised preconditioning procedure for gas permeability measurement. *Materials and Structures* 35 (1): 22–27.

Davies, G., Oberholster, R.E., 1987. An interlaboratory test programme on the NBRI accelerated test to determine the alkali reactivity of aggregates (Special Report No. BOU 92-1987). National Building Research Institute, Council for Scientific and Industrial Research, Pretoria.

De Belie, N., Monteny, J., Taerwe, L., 2002. Apparatus for accelerated degradation testing of concrete specimens. *Materials and Structures* 35 (7): 427–433.

Deslattes, R.D., Kessler, E.G., Indelicato, P., de Billy, L., Lindroth, E., Anton, J., 2003. X-ray transition energies: new approach to a comprehensive evaluation. *Reviews of Modern Physics* 75 (1): 35–99.

Diamond, S., 2000. Mercury porosimetry: An inappropriate method for the measurement of pore size distributions in cement-based materials. *Cement and Concrete Research* 30 (10): 1517–1525.

Diamond, S., 2003. A discussion of the paper "Effect of drying on cement-based materials pore structure as identified by mercury porosimetry: a comparative study between oven, vacuum, and freeze-drying" by C. Gallé. *Cement and Concrete Research* 33 (1): 169–170.

Duan, Z.H., Poon, C.S., 2014. Properties of recycled aggregate concrete made with recycled aggregates with different amounts of old adhered mortars. *Materials & Design* 58: 19–29.

EN 206-1, 2005. Concrete. Part 1: Specification, performance, production and conformity. CEN, Brussels.

Freiesleben Hansen, P., Pedersen, J., 1977. Maturity computer for controlled curing and hardening of concrete. *Nordisk Betong* 1: 19–34.

Fultz, P.D.B., Howe, P.D.J., 2013. Diffraction and the x-ray powder diffractometer, in: Transmission Electron Microscopy and Diffractometry of Materials. Springer Berlin Heidelberg, 1–57.

Gallé, C., 2001. Effect of drying on cement-based materials pore structure as identified by mercury intrusion porosimetry: A comparative study between oven, vacuum, and freeze-drying. *Cement and Concrete Research* 31 (10): 1467–1477.

Gallé, C., 2003. Reply to the discussion by S. Diamond of the paper "Effect of drying on cement-based materials pore structure as identified by mercury intrusion porosimetry: a comparative study between oven, vacuum and freeze-drying." *Cement and Concrete Research* 33 (1): 171–172.

Giesche, H., 2002. Mercury porosimetry, in: Schüth, F., Sing, K.S.W., Weitkamp, J. (Eds.), Handbook of Porous Solids. Wiley-VCH Verlag GmbH, 309–351.

Grosse, C.U., Reinhardt, H.W., 2000. Ultrasound technique for quality control of cementitious materials. Presented at the Proceedings of the 15th Conference on Nondestructive Testing.

Gruyaert, E., 2011. Effect of blast-furnace slag as cement replacement on hydration, microstructure, strength and durability of concrete. Ghent University, Ghent, Belgium.

Gruyaert, E., Maes, M., De Belie, N., 2013. Performance of BFS concrete: k-value concept versus equivalent performance concept. *Construction and Building Materials* 47: 441–455.

Hilsdorf, H., Kropp, J. (Eds.), 2004. Performance criteria for concrete durability, RILEM Report. CRC Press.

ICDD, 2015. International Centre for Diffraction Data [http://www.icdd.com/].

ISO 4287, 1997. Geometrical Product Specifications (GPS). Surface texture: Profile method. Terms, definitions and surface texture parameters. ISO, Geneva.

Jacobsen, S., Arntsen, B., 2007. Aggregate packing and void saturation in mortar and concrete proportioning. *Materials and Structures* 41 (4): 703–716.

Janssens, K., 2003. X-ray fluorescence analysis, in: Gauglitz, G., Vo-Dinh, T. (Eds.), Handbook of Spectroscopy. Wiley-VCH Verlag GmbH & Co. KGaA, 363–420.

Jenkins, R., 2001. X-ray fluorescence spectrometry, in: Günzler, H., Williams, A. (Eds.), Handbook of Analytical Techniques. Wiley-VCH Verlag GmbH, 753–766.

Klockenkämper, R., Bohlen, A. von (Eds.), 2014. Fundamentals of x-ray fluorescence, in: Total-Reflection X-Ray Fluorescence Analysis and Related Methods. John Wiley & Sons, Inc., 1–78.

Kollek, J.J., 1989. The determination of the permeability of concrete to oxygen by the Cembureau method—a recommendation. *Materials and Structures* 22 (3): 225–230.

Konecny, L., Naqvi, S.J., 1993. The effect of different drying techniques on the pore size distribution of blended cement mortars. *Cement and Concrete Research* 23 (5): 1223–1228.

Kristiansen, K., 1997. Scanning electron microscope with energy-and wavelength-dispersive spectrometry, in: Brune, D., Hellborg, R., Whitlow, H.J., Hunderi, O. (Eds.), Surface Characterization. Wiley-VCH Verlag GmbH, 111–128.

Kumar, R., Bhattacharjee, B., 2003. Study on some factors affecting the results in the use of MIP method in concrete research. *Cement and Concrete Research* 33 (3): 417–424.

Kurz, J.H., Grosse, C.U., Reinhardt, H.-W., 2005. Strategies for reliable automatic onset time picking of acoustic emissions and of ultrasound signals in concrete. *Ultrasonics* 43 (7): 538–546.

Leng, Y., 2013a. X-Ray diffraction methods, in: Materials Characterization. Wiley-VCH Verlag GmbH & Co. KGaA, 47–82.

Leng, Y., 2013b. Scanning electron microscopy, in: Materials Characterization. Wiley-VCH Verlag GmbH & Co. KGaA, 127–161.

Maes, M., Gruyaert, E., Belie, N.D., 2013. Resistance of concrete with blast-furnace slag against chlorides, investigated by comparing chloride profiles after migration and diffusion. *Mater Struct* 46 (1-2): 89–103.

Marchand, J., Pigeon, M., Bager, D., Talbot, C., 1999. Influence of chloride solution concentration on de-icer salt scaling deterioration of concrete. *ACI Materials Journal* 96 (4).

NBN B 05-201, 1976. Resistance of materials to freezing - Water absorption by capillarity. NBN, Brussels.

NBN B 15-278, 1976. Testing of concrete. Creep [in French]. NBN, Brussels.

NT BUILD 480, 1997. Cement. Heat of hydration. NORDTEST, Espoo.

NT BUILD 492, 1999. Concrete, mortar and cement-based repair materials: Chloride migration coefficient from non-steady-state migration experiments. NORDTEST, Espoo.

Oberholster, R.E., Davies, G., 1986. An accelerated method for testing the potential alkali reactivity of siliceous aggregates. *Cement and Concrete Research* 16 (2): 181–189.

Permanent Commission on Concrete, 2008. Code on Structural Concrete (EHE-08) [in Spanish]. Spanish Ministry of Public Works, Madrid.

Reinhardt, H.W., Grosse, C.U., 2004. Continuous monitoring of setting and hardening of mortar and concrete. *Construction and Building Materials*, 3rd Kumamoto International Workshop on Fracture, Acoustic Emission and NDE in Concrete (KIFA-3) 18 (3): 145–154.

Reinhardt, H.W., Grosse, C.U., Herb, A., Weiler, B., Schmidt, G., 2001. Method for examining a solidifying and/or hardening material using ultrasound, receptacle and ultrasound sensor for carrying out the method. Patent n^{o} 09/857, 536.

RILEM TC 107-CSP, 1998. Measurement of time-dependent strains of concrete. *Materials and Structures* 31: 507–512.

RILEM TC 116-PCD, 1999. Permeability of concrete as a criterion of its durability. Recommendations. *Materials and Structures* 32: 174–179.

RILEM TC 119-TCE, 1997. TCE1: Adiabatic and semi-adiabatic calorimetry to determine the temperature increase in concrete due to hydration heat of the cement. *Materials and Structures* 30 (8): 451–464.

Robeyst, N., 2009. Monitoring setting and microstructure development in fresh concrete with the ultrasonic through-transmission method. Ghent University, Ghent, Belgium.

Robeyst, N., Grosse, C.U., De Belie, N., 2009. Monitoring fresh concrete by ultrasonic transmission measurements: Exploratory multi-way analysis of the spectral information. *Chemometrics and Intelligent Laboratory Systems* 95 (1): 64–73.

Rübner, K., Fritz, T., Jacobs, F., 2002. Precision of porosity measurements on cementitious mortars, in: F. Rodriguez-Reinoso, B.M. J. Rouquerol and K. Unger (Ed.), Studies in Surface Science and Catalysis, Characterization of Porous Solids VI Proceedings of the 6th International Symposium on the Characterization of Porous Solids (COPS-VI). Elsevier, 459–466.

Scheu, C., Kaplan, W.D., 2012. Introduction to scanning electron microscopy, in: Dehm, G., Howe, J.M., Zweck, J. (Eds.), In-Situ Electron Microscopy. Wiley-VCH Verlag GmbH & Co. KGaA, 1–37.

Thomas-García, C., Polanco-Madrazo, J.A., Setien-Marquínez, J., 2013. Flow meter for the gas permeability determination of a material [in Spanish]. Patent nº ES2400592B1.

Thomas-García, C., Polanco-Madrazo, J.A., Setien-Marquínez, J., 2014. System for the gas permeability determination of a material [in Spanish]. Patent nº ES2406386B1.

Trtnik, G., Gams, M., 2013. The use of frequency spectrum of ultrasonic P-waves to monitor the setting process of cement pastes. *Cement and Concrete Research* 43: 1–11.

UNE 83981, 2008. Concrete durability. Test methods. Determination to gas permeability of hardened concrete [in Spanish]. AENOR, Madrid.

UNE 83982, 2008. Concrete durability. Test methods. Determination of the capillar suction in hardened concrete. Fagerlund method [in Spanish]. AENOR, Madrid.

UNE 83988-1, 2008. Concrete durability. Test methods. Determination of the electrical resistivity. Part 1: Direct test (reference method). [in Spanish]. AENOR, Madrid.

UNE 83993-1, 2013. Durability of concrete. Test method. Measurement of carbonation penetration rate in hardened concrete. Part 1: Natural method [in Spanish]. AENOR, Madrid.

UNE 112011, 2011. Corrosion of concrete reinforcement steel. Determination of the carbonatation depht for in-service concrete [in Spanish]. AENOR, Madrid.

UNE EN 196-9, 2011. Methods of testing cement. Part 9: Heat of hydration - Semi-adiabatic method [in Spanish]. AENOR, Madrid.

UNE EN 932-1, 1997. Test for general properties of aggregates. Part 1: Methods for sampling [in Spanish]. AENOR, Madrid.

UNE EN 932-2, 1999. Tests for general properties of aggregates. Part 2: Methods for reducing laboratory samples [in Spanish]. AENOR, Madrid.

UNE EN 933-1, 2012. Tests for geometrical properties of aggregates. Part 1: Determination of particle size distribution - Sieving method [in Spanish]. AENOR, Madrid.

UNE EN 933-2, 1996. Test for geometrical properties of aggregates. Part 2: Determination of particle size distribution. Test sieves, nominal size of apertures [in Spanish]. AENOR, Madrid.

UNE EN 933-3, 2012. Tests for geometrical properties of aggregates. Part 3: Determination of particle shape - Flakiness index [in Spanish]. AENOR, Madrid.

UNE EN 933-8, 2012. Tests for geometrical properties of aggregates. Part 8: Assessment of fines - Sand equivalent test [in Spanish]. AENOR, Madrid.

UNE EN 933-11, 2009. Tests for geometrical properties of aggregates. Part 11: Classification test for the constituents of coarse recycled aggregate [in Spanish]. AENOR, Madrid.

UNE EN 1097-2, 2010. Tests for mechanical and physical properties of aggregates. Part 2: Methods for the determination of resistance to fragmentation [in Spanish]. AENOR, Madrid.

UNE EN 1097-6, 2014. Tests for mechanical and physical properties of aggregates. Part 6: Determination of particle density and water absorption [in Spanish]. AENOR, Madrid.

UNE EN 1339, 2004. Concrete paving flags - Requirements and test methods [in Spanish]. AENOR, Madrid.

UNE EN 12350-1, 2009. Testing fresh concrete. Part 1: Sampling [in Spanish]. AENOR, Madrid.

UNE EN 12350-2, 2009. Testing fresh concrete. Part 2: Slump-test [in Spanish]. AENOR, Madrid.

UNE EN 12350-6, 2009. Testing fresh concrete. Part 6: Density [in Spanish]. AENOR, Madrid.

UNE EN 12350-7, 2010. Testing fresh concrete. Part 7: Air content. Pressure methods [in Spanish]. AENOR, Madrid.

UNE EN 12390-1, 2013. Testing hardened concrete. Part 1: Shape, dimensions and other requirements for specimens and moulds [in Spanish]. AENOR, Madrid.

UNE EN 12390-3, 2009. Testing hardened concrete. Part 3: Compressive strength of test specimens [in Spanish]. AENOR, Madrid.

UNE EN 12390-4, 2001. Testing hardened concrete. Part 4: Compressive strength - Specification for testing machines [in Spanish]. AENOR, Madrid.

UNE EN 12390-5, 2009. Testing hardened concrete. Part 5: Flexural strength of test specimens [in Spanish]. AENOR, Madrid.

UNE EN 12390-6, 2010. Testing hardened concrete. Part 6: Tensile splitting strength of test specimens [in Spanish]. AENOR, Madrid.

UNE EN 12390-7, 2009. Testing hardened concrete. Part 7: Density of hardened concrete [in Spanish]. AENOR, Madrid.

UNE EN 12390-8, 2009. Testing hardened concrete. Part 8: Depth of penetration of water under pressure [in Spanish]. AENOR, Madrid.

UNE EN 12390-13, 2014. Testing hardened concrete. Part 13: Determination of secant modulus of elasticity in compression [in Spanish]. AENOR, Madrid.

UNE EN 12504-4, 2006. Testing concrete - Part 4: Determination of ultrasonic pulse velocity [in Spanish]. AENOR, Madrid.

Valenza II, J.J., Scherer, G.W., 2007. A review of salt scaling: I. Phenomenology. *Cement and Concrete Research* 37 (7): 1007–1021.

Wang, Y., Petrova, V., 2012. Scanning electron microscopy, in: Padua, G.W., Wang, Q. (Eds.), Nanotechnology Research Methods for Foods and Bioproducts. Wiley-Blackwell, 103–126.

Washburn, E.W., 1921. Note on a method of determining the distribution of pore sizes in a porous material, in: Proceedings of the National Academy of Sciences of the United States of America. 115–116.

Winslow, D.N., Diamond, S., 1970. A mercury porosimetry study of the porosity in Portland cement. *Journal of Materials (ASTM)* 5 (3): 564–585.

Chapter 4

Concrete raw materials

1. INTRODUCTION

The emergence of the use of recycled materials in the construction industry, specifically in the production of concrete, has met with varying degrees of success due to the barriers that the market for recycled products has still to overcome. Since to a large extent, the quality of the concrete mixture depends upon the properties of the raw materials used in its manufacture; the quality of the recycled aggregates is perceived as an obstacle in the recycling of construction and demolition wastes (CDW) as secondary aggregates for concrete. Nonetheless, numerous scientific studies show that it is possible to obtain good quality, economic and environmentally friendly building materials when the coarse fraction of CDW recycled aggregates is used appropriately.

This chapter presents an overview of the significant characteristics of the different constituents to be used in the conventional and recycled concrete mixtures. From a quality point of view, special attention was paid to the recycled coarse aggregates since their heterogeneous nature strongly affects their quality. Thus, a thorough physical, mechanical and microstructural characterization was carried out in order to assess the suitability of their use in the concrete manufacture in accordance with the requirements set for natural aggregates in the current Spanish legislation. Nevertheless, note that the Spanish Code on Structural Concrete (EHE-08) (Permanent Commission on Concrete, 2008) does not take into account the use of mixed recycled aggregates in the concrete manufacture, not even in a non-structural capacity.

2. MATERIAL SELECTION

2.1. WATER

For all the concrete mixtures, regular tap water was employed conforming to the requirements established in the Spanish Code on Structural Concrete (EHE-08) (Permanent Commission on Concrete, 2008).

2.2. CEMENT

Granulated blast furnace slag (GBFS) is one major by-product of the iron and steel production (approximately 13% of the total input of raw materials) (Lee and Park, 2005) resulting from the rapid cooling of the slag melt by spraying high-pressurized water or immersion in water. Conforming to UNE EN 197-1 (2011), GBFS consist of at least two-thirds by mass of CaO, MgO and SiO_2 ($(CaO+MgO)/SiO_2 > 1$) while the remaining proportion contains mostly Al_2O_3.

In 1774, the first use of slag cement was reported; but more than a century had to pass before the production of Portland slag cement happened in 1892 (ACI Committee 233, 2003). Since then, most (90%) of the GBFS is used as cementitious material (Lee and Park, 2005) since it has been proven that the use of blast furnace slag enhances some of the concrete properties when compared to pure Portland cement.

Studies about the fresh properties of concrete suggest that the use of slag improves the workability (Fulton, 1974; Meusel and Rose, 1983; Wan et al., 2004), delays the setting (Fulton, 1974; Hogan and Meusel, 1981; Wainwright and Ait-Aider, 1995), and increases the bleeding (Wainwright and Ait-Aider, 1995; Olorunsogo, 1998; Wainwright and Rey, 2000). At microstructural level, the use of GBFS in conjunction with Portland cement refines the pore structure (Nakamura et al., 1992; Luo et al., 2003) which reduces the overall permeability of concrete. In terms of mechanical strength, the gaining of strength is slower but the long term resistance is higher (Hogan and Meusel, 1981); moreover, the content of alumina influences the strength of concrete with an optimum at 13% alumina content (Smolczyk, 1980). Regarding the shrinkage and creep behaviour of blended cement, a tendency towards lower values has been reported by Tazawa et al. (1989) and Sivasundaran and Malhotra (1992).

The blending of GBFS with Portland cement also influences the durability properties of the concrete; for instance, it reduces the potential expansion by the alkali-silica reaction (Hogan and Meusel, 1981; Frigione, 1986), increases the sulphate resistance when more than 50% of GBFS is used (Hogan and Meusel, 1981; Frearson, 1986; Cao et al., 1997) and the chloride resistance (Dhir et al., 1996; Zhang et al., 1999; Luo et al., 2003). However, higher GBFS contents (70-80%) may cause higher salt scaling (Virtanen, 1983; Pigeon and Pleau, 1995; Panesar and Chidiac, 2007) or carbonation problems (Osborne, 1999).

Besides the technological motives associated to the use of Portland cement incorporating blast furnace slag, the recycling of GBFS is in line with the sustainability principles since it avoids waste disposal and reduces the consumption of virgin materials and energy and the production of greenhouse gasses. According to Lee and Park (2005), recycling GBFS as slag cement or Portland slag cement presents important environmental benefits with a reduction of more than 850 g CO_2 equivalent by substituted kilogram of GBFS in the cement production. Finally, the use of blast furnace slag also involves economic motives as the cost of cement production is lower due to the use of a by-product as a raw material.

Furthermore, the study of Mas et al. (2012b) suggests that the use of blend cements including blast furnace slag or fly ash could be beneficial to the behaviour and performance of recycled concrete, since one of the main problems associated to the use of recycled aggregates rests in the sulphate content incorporated to the mixture by the replacement of the natural aggregates.

Thus, blast furnace slag (BFS) cements were used as binder to take advantage of the sulphate resistance and the environmental advantages provided by the BFS addition compared to ordinary Portland cement. In this PhD, two BFS cements were employed, and CEM III/A 42.5 N SR and CEM III/B 42.5 N SR/LA/LH in phase I and II of the research works respectively, complying with the UNE EN 197-1 (2011). Moreover, both products are generally used in construction works and are readily available in the markets of the European Union, which presents an advantage for an easy access to the product and the manufacture of a recycled concrete as similar as possible to that of the ordinary concrete. Table 4.1 displays the results of an X-ray diffraction test performed on both cements employed in the research of the PhD thesis in order to compare their chemical compositions.

Table 4.1: XRF analysis of the cements

	CEM III/A 42.5 N SR	**CEM III/B 42.5 N SR LH LA**
CaO (%)	51.330	45.100
SiO_2 (%)	25.080	28.000
Al_2O_3 (%)	7.590	9.840
MgO (%)	3.870	7.290
SO_3 (%)	2.540	4.560
Fe_2O_3 (%)	2.040	1.300
K_2O (%)	0.600	0.450
TiO_2 (%)	0.390	0.840
Mn_2O_3 (%)	0.220	0.190
Na_2O (%)	0.140	0.350
SrO (%)	0.105	0.100
P_2O_5 (%)	0.060	0.120
ZnO (%)	0.036	-
Cl (%)	0.020	0.059
BaO (%)	0.018	0.070
Cr_2O_3 (%)	0.005	0.020
Loss on ignition (%)	3.930	0.810

2.3. NATURAL AGGREGATES

Siliceous river sand (0-4 mm) was used to manufacture all concrete mixtures in conjunction with a single fraction (4-16 mm) of siliceous gravel in the production of concretes pertaining to the first phase of research works and two fractions (2-8 mm) and (8-16 mm) of siliceous gravel for the concretes from phase II studies.

2.4. RECYCLED AGGREGATES

Numerous studies have investigated the possibilities of using recycled aggregates in diverse applications as a solution to the environmental problem caused by the construction sector. The investigations regarding the use of construction and demolition wastes (CDW) as secondary building materials in the concrete manufacture have been notoriously focused on recycled aggregates recovered form crushed concrete (Hansen and Narud, 1983; Ravindrarajah and Tam, 1985; Padmini et al., 2009; Sánchez de Juan and Alaejos Gutiérrez, 2009; Tabsh and Abdelfatah, 2009; Cabral et al., 2010; Ferreira et al., 2011; Soares et al., 2014) since their properties do not differ as much from the natural aggregates and their use as partial substitution is supported by most standards; for instance, the Spanish Code on structural concrete (Permanent Commission on Concrete, 2008) allows up to a 20% replacement.

Nonetheless, mixed recycled aggregates are the secondary material most produced (70%) at the Spanish CDW management plants (Güell-Ferré et al., 2012), since the construction works highly rely on the use of ceramic materials (mainly bricks and tiles for buildings) and the demolition practices are not selective which means that usually different types of wastes are conjointly sent for valorization. Hence, this thesis aims to study the quality of recycled aggregates with different percentages of ceramic waste and their influence when used as a partial substitution of the gravel in the concrete manufacture.

2.4.1. SELECTED SAMPLES

To make an informed material selection, a list of all the CDW management plants operating in Spain was collected in the first place. After an inquiry to the initial 127 processing companies, 12 recycling plants were selected based upon their willingness to participate in the research works and the reported level of ceramic wastes in the produced recycled aggregates. As the objective regarding the recycled aggregates was the evaluation of recycled aggregates with significant percentages of ceramic fraction (brick, tiles, sanitary waste…), only recycled aggregates containing a significant amount of ceramic were taken into account in this investigation. Moreover, in order to avoid any territorial bias, the plants selected were spread out across the national territory (Figure 4.1) in seven Autonomous Communities: Galicia (2), Asturias (1), Castile and Leon (3), Catalonia (1), Madrid (2), Castile-La Mancha (1), Andalusia (2).

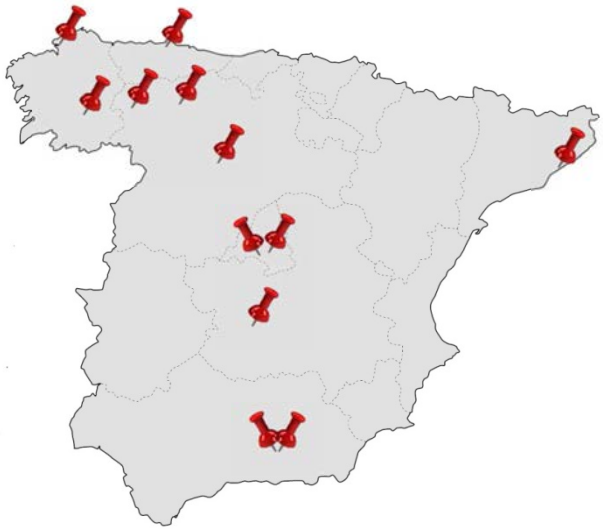

Figure 4.1: CDW management plants subjected to study

For all the selected CDW management plants, a field trip was programed in which the characteristics of the productive procedure were examined in detail and a representative sample of the recycled aggregates produced was collected for further analysis according to the Spanish Code on structural concrete (Permanent Commission on Concrete, 2008) with included the study of the particle size distribution, flakiness index, fines assessment, mechanical resistance trough Los Angeles abrasion test, density and water absorption. The results arising from these investigations were published (Rodríguez-Robles et al., 2014) and used as a means to select the recycled aggregates employed in the research works included in the framework of this thesis dissertation.

Figure 4.2: TEC-REC construction and demolition management plant (Madrid, Spain)

First, in the light of the results from the preliminary investigations, the recycled aggregates produced at TEC-REC (Madrid) (Figure 4.2) were selected for further analysis. However, this choice did not rely on the characterization results only, but also on the recycling procedure followed that could be considered standard and the ceramic level within the mean values of the Spanish recycled aggregates. Lately, since the CDW recycling plants knew about the subject of the study, Bierzo Recicla (Figure 4.3) located in Castile and Leon offered the possibility to supply a 100% ceramic recycled aggregate. This recycled aggregate was derived from the demolition of a building construction and was completely comprised of bricks, stoneware tiles, roof tiles, … with and without adhered mortar. In this way, the mean and extreme values of the spectrum of recycled aggregates with varying percentages of ceramic waste were incorporated into the research.

Figure 4.3: Bierzo Recicla construction and demolition management plant (Castile and Leon, Spain)

Given that the objective was to study the influence of the ceramic percentage on the quality and performance of the recycled aggregates in the concrete manufacture, a new sample of recycled aggregates was artificially crafted in the laboratory. In order to achieve an intermediate ceramic content, the recycled aggregates retrieved from the two Spanish CDW management plants were mixed in the same proportion by weight. Note that, this option was preferred to the selection of a new sample of recycled aggregates from another recycling plant to avoid the inclusion of new variables in the study.

Finally, during the investigation period at Ghent University, a CDW management plant in Belgium (ARC sited in the port of Antwerp) agreed to a visit and to facilitate a sample of recycled aggregates (Figure 4.4). Although upon visual identification, the ceramic content of the sample was in the lower range of the considered spectrum, it was decided that it could make a good comparison point with the results arising from the recycled aggregates collected at the TEC-REC site with similar ceramic content.

Figure 4.4: ARC construction and demolition management plant (Antwerp, Belgium)

To fulfil the experimental program, around 1 tonne of recycled aggregates was collected from outdoor stockpiles at the three CDW recycling plants. The samples were gathered in accordance with UNE EN 932-1 (1997), screened to a particle size <20 mm and reduced in the laboratory as outlined in UNE EN 932-2 (1999). After the artificial sample was created, all the recycled aggregates were classified by their ceramic content -low (L) or lower than 40%, medium (M) or lower than 70% and high (H) around 100%- which was used to designate the different samples in conjunction with their origin - Spain (S) or Belgium (B) - (Figure 4.5).

Figure 4.5: Recycled aggregates subjected to study

Nonetheless, it is necessary to emphasize that the reproducibility over time within the same CDW management plant is not ensured since the samples were collected at a specific day of sampling and highly depend on the origin of the processed wastes; although when testing recycled aggregates with similar origin or composition, similar results should be expected.

As one objective was to assess the treatment and production at the CDW management plants, it is worth mentioning that the recycling process basically consisted of a selection process to get rid of large impurities, a crushing step in order to drastically reduce the aggregate size followed by a screening step to discard the fines and cleaning procedures in order to remove other impurities such as fines, metals, glass, asphalt, wood, plastic, … by different means of separation, and a final crushing and screening process to achieve the desired recycled aggregate fraction. Table 4.2 summarizes the specific characteristics of the management procedure followed at each one of the recycling companies. Figure 4.2, Figure 4.3 and Figure 4.4 illustrate the facilities and equipment employed in the production process of the recycled aggregates in each of the selected CDW management plants.

Table 4.2: CDW management at the selected recycling plants

	TEC-REC	**Bierzo Recicla**	**ARC**
First crushing stage	Jaw crusher	Jaw crusher	Jaw crusher
Second crushing stage	Impact crusher	Impact crusher	Cone crusher
Methods for the removal of impurities	Electromagnet Air-blower Manual separation	Electromagnet Air-blower Manual separation	Electromagnet Non-ferrous separator Air-blower Manual separation Aqua screen
Recycled aggregates produced	0/4 mm 4/25 mm 40/80 mm	0/30 mm 30/60 mm	0/4 mm 4/20 mm

3. CHARACTERIZATION OF THE AGGREGATES

The characteristics of the aggregates used in the manufacture of concrete largely determine the properties of the final product. Since fine and coarse aggregates generally comprise the majoritarian volume (approximately 60-75%) in a concrete composition, the effects that these raw materials have on the final characteristics of the concrete are significant and thus the material selection of the aggregates is of great importance when planning the final dosage and performance of the concrete mixture. General knowledge indicates that recycled aggregates present a low quality when compared to natural aggregates. However, the differential performance level shall not definitively exclude the use of these materials. On the contrary, a more specific and case by case study should be carried out in order to assess their quality in the framework of a specific application.

Conventionally, the characterization of coarse recycled aggregates is based upon the determination of the macroscopic composition, several key properties depending on their final use and some chemical analysis on harmful substances for the intended application or the environment. Although less frequently, some investigations include specific testing bearing in mind the particular nature of the recycled aggregates, such as the determination of the attached mortar (Sánchez de Juan and Alaejos Gutiérrez, 2009; Quan et al., 2010; Duan and Poon, 2014; Seo and Choi, 2014) or the presence of clay mineral and micas (Limbachiya et al., 2007; Angulo et al., 2009) that are known to negatively affect the quality and performance of this secondary material.

In addition, unless otherwise indicated, coarse recycled aggregates are tested by means of the traditional methods used for the characterization of conventional aggregates. Currently, alternative tests are only required for chloride content due to the presence of attached mortar (UNE EN 1744-5, 2007), organic substances that can alter the rate of setting and hardening of concrete (UNE EN 1744-6, 2007) and resistance to freeze-thaw cycles (UNE EN 1367-1, 2008) since the traditional magnesium sulphate test (UNE EN 1367-2, 2010) is not suitable for due to the presence of adhered mortar. Nonetheless, some researchers have expressed the necessity to use alternative testing methods when sieving or measuring the water absorption in order to contemplate the peculiar features of secondary building materials.

Schouenborg et al. (2004b) observed that recycled aggregates are sensitive to traditional mechanical sieving leading to particle size distributions with an excess of fines due to the rapid abrasion of the adhered mortar. In addition, as sieving is a common pre-treatment process in several characterization methods this negative effect would be detrimental in the assessment of other properties as well (e.g. flakiness index, Los Angeles test…). Thus, in order to alleviate the influence of the sieving, reducing the sieving time (2 minutes) and load (one fifth of the traditional load) was recommended.

Regarding the determination of the water absorption, the current standards present several problems when applied to recycled aggregates since the compulsory pre-drying at 105ºC involves the removal of the crystallized water in the mortar attached (Tam et al., 2008), the attainment of a saturated surface-dried surface by means of a cloth could detach the adhered mortar (Tam et al., 2008) and the proposed time period of 24 hours is insufficient to reach the complete saturation

(Schouenborg et al., 2004a, 2004b; Tam et al., 2008; García-González et al., 2014); all of these facts resulting in an inaccurate water absorption value. Hence, several novel techniques have been proposed. Tamura et al. (2001) recommended a rapid test method for water absorption of recycled aggregates based upon the use of hot water and pressure able to achieved results within two hours; the investigations of Schouenborg et al. (2004a, 2004b) also suggested that the solution relies on an enhanced vacuum absorption method at 5 kPa during 5 hours, but dismissed the possibility of boiling as a quick approach to the water absorption determination since the saturated surface-dried measurements were difficult and some of the adhered mortar was disintegrated. Later on, Tam et al. (2008) proposed a method for the real-time assessment of water absorption (RAWA in short) which consisted of a pre-drying of the recycled aggregate at 75ºC and the use of a pycnometer to control the water level and the weight of the set-up at different time intervals in order to calculate the water absorption as the ratio between mass difference of the set-up at a certain time interval and the oven-dried mass of the aggregate in air. However, none of these techniques have had any further application in other research works or in order to develop new standards.

3.1. PHYSICAL AND MECHANICAL CHARACTERIZATION

3.1.1. CONSTITUENTS

Given that the recycled aggregates used in this research work came from construction and demolition wastes (CDW), their common composition is a mixture of unbound aggregates (Ru), cement based materials (Rc), ceramics (Rb), asphalt (Ra), glass (Rg), gypsum (X_1) and other impurities (X_2) such as wood, plastic, and metal in varying proportions.

- Unbound aggregates: Apart from their natural origin, the crushing procedure at the CDW management plant causes not only the reduction in size of the concrete lumps but also serves as a cleaning procedure for the adhered mortar on the surface of some natural aggregates appearing in the recycled aggregate. It is generally acknowledged that this fraction has the same behaviour as natural aggregates; and as such, no investigation on their effect on the quality of mixed recycled aggregates has ever been performed.

- Cement based materials: Concrete rubble and particles with attached mortar are one of the most generated materials in the demolition works. This fraction has been identified as responsible of the increased porosity in comparison with the natural aggregates and the derived variation in physical (density and water absorption) and mechanical properties of the mixed recycled aggregates (Katz, 2003; Etxeberria et al., 2007; Padmini et al., 2009; Sánchez de Juan and Alaejos Gutiérrez, 2009; Paine and Dhir, 2010; Silva et al., 2014).

- Ceramic: The clay based fraction is composed by different ceramic materials such as bricks, tiles, stoneware and sanitary ware. Except for sanitary ware waste (Medina et al., 2012), the ceramic component is as well recognised as accountable for the higher porosity of the mixed and ceramic recycled aggregates (Khalaf and DeVenny, 2005; Silva et al., 2014)

- Asphalt: Because of the predominant use of this material in road construction works, the likelihood of this component in the mixed recycled aggregates is associated to the origin of the construction and demolition wastes. Moreover, given its high potential for reuse, the recovered material is generally taken to an asphalt plant instead to a CDW plant in order to be reused in road base layers or even the wearing course of pavements. Medina et al. (2015) studied the effect of asphalt on the quality of the mixed recycled aggregates and two recycled concrete mixes (30 MPa) with a 25% and 50% substitution of the natural coarse aggregate, and their results showed a higher density and lower water absorption of the mixed recycled aggregates without asphalt content and therefore a higher density and compressive strength of the recycled concrete.

- Glass: In order to facilitate its reuse and recycling, the common practice dictates removing this material before the demolition of the building; thus, the quantities of glass in the CDW are usually not significant. In addition, research works indicate that the negative effect of using glass waste as coarse recycled aggregate in concrete increases with the substitution rate; for instance, Topçu and Canbaz (2004) registered decreases in compressive, flexural and indirect tensile strength for concrete with recycled glass aggregates up to 15% and Shayan and Xu (2004) concluded that no deleterious alkali-silica reaction (ASR) effects were detected up to a 30% replacement of the conventional coarse aggregate.

- Gypsum: As the construction industry uses gypsum for stucco, plasterwork, cardboard-plaster panels, etc. its occurrence in the mixed recycled aggregates as an independent component or associated to other particles is fairly common. The presence of gypsum has a negative effect on the quality of mixed recycled aggregates due to its solubility, low density and hardness (Vrancken and Laethem, 2000); moreover, as gypsum is a source of sulphates its incorporation could cause expansions in the recycled concrete due to the delayed formation of ettringite (Neville, 1995; Odler and Colán-Subauste, 1999) and contaminate the environment through the leaching of water soluble sulphate (Barbudo et al., 2012b).

- Other impurities: In general terms, the separation process depends on the simplicity of the procedure and the economic benefits achieved. Paper, wood and plastic are normally separated by air blowers after the crushing step and by hand-picking during their transport in the conveyor belt. Likewise, magnetic belts and eddy currents are used to remove ferrous (steel) and non-ferrous (aluminium, stainless steel and cooper) metals after the crushing procedure and the aforementioned hand-picking step is also employed to separate this component from the final recycled aggregate. Hence, the occurrence of these impurities in the mixed recycled aggregate is low and it is associated to the level of effectiveness of the treatment process in the CDW management plant. The research conducted by Medina et al. (2015) also studied the influence of the floating particles on the quality of the mixed recycled aggregates and the recycled concrete, and their results showed that the floating particles were accountable for lower density and higher water absorption of the recycled aggregate and lower density and a decline in the compressive strength of the recycled concrete.

Table 4.3 and Figure 4.6 display the proportion in weight of the different components being part of the selected recycled aggregates. The results show that the predominant component was concrete (44.11% and 37.05% respectively) followed by materials of ceramic nature (33.56% and 38.44% respectively) in RA-L(S) and RA-L(B) samples, while in RA-M(S) the situation was reversed with a majoritarian ceramic component (66.38%) followed by the occurrence of cement based materials (17.31%). For these three, unbound aggregates was the third most common component with values ranging between 15.07% and 22.46%., In regard to sample RA-H(S), the recycled aggregate was solely composed by ceramic materials (bricks and tiles principally) as expected

Table 4.3: Composition of the recycled aggregates

	RA-L(S)	RA-L(B)	RA-M(S)	RA-H(S)
Ru	17.51	22.46	15.07	0.00
Rc	44.11	37.05	17.31	0.00
Rb	33.56	38.44	66.38	100.00
Ra	0.44	1.74	0.43	0.00
Rg	0.75	0.00	0.19	0.00
X_1	3.48	0.30	0.22	0.00
X_2	0.16	0.00	0.41	0.00

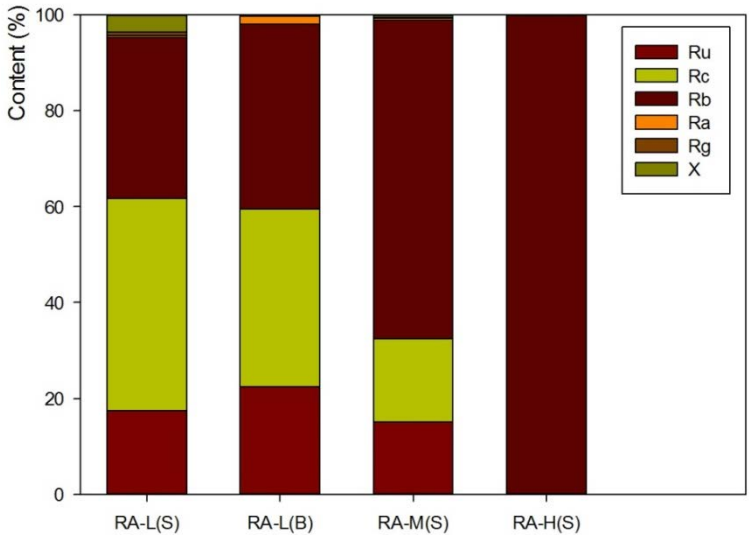

Figure 4.6: Composition of the recycled aggregates

As the Spanish EHE-08 (Permanent Commission on Concrete, 2008) only allows the use of crushed concrete as recycled aggregate for structural and non-structural applications of concrete, the standard considers the ceramic component as an impurity, and as such it is limited up to 5%. However, as the aim of this research work is to characterize the suitability of mixed recycled aggregates with significant contents of ceramic in the concrete manufacture, this requirement would be ignored. Nonetheless, based on the aforementioned objective, the determination of the component proportions allows the classification of the recycled aggregates according to their ceramic content. Hence in this context, the sample RA-H(S) is considered as ceramic recycled aggregate and the rest of the samples, (RA-L(S), RA-L(B) and RA-M(S)), are classified as mixed recycled aggregates due to the variability in their composition.

A more detailed analysis of the existing classifications of the recycled aggregates in function of their ceramic percentages was discussed in Chapter 2. Concerning to the rest of impurities, EHE-08 (Permanent Commission on Concrete, 2008) lays down a 1% limit for asphalt and the so-called other impurities (glass, metals, plastic, wood…). On one hand, for the asphalt limitation, only sample RA-L(B) exceeded the requirement; however, the Spanish limit is stricter when compared to other European requirements (LNEC E-471, 2009; CEN/TC 104/SC 1/TG 19, 2013; BS 8500-2, 2015). In this regard, the Spanish Association of CDW management plants (GERD) carried out a national wide study on the quality and performance of 65 CDW treatment plants and recommended a 5% limit for the asphalt constrain in mixed recycled aggregates (Güell-Ferré et al., 2012). On the other hand, the content requirement for the other impurities (glass, metal, plastic and wood among others) was only not complied by the sample RA-L(S), which suggests some failure in the separation procedure at the TEC-REC management plant. Special mention should be made of the high gypsum content of samples RA-L(S), as Agrela et al. (2011) recommended the rejection of recycled aggregates containing more than 1.67% of gypsum due to lack of compliance with the EHE-08 sulphate requirements (Permanent Commission on Concrete, 2008). Section 3.2.1.2 deals with the results and discussion of the sulphate content of the analysed samples.

In addition, the content of so-called other impurities (wood, paper, plastic) is considered to provide a good estimation of the content of organic substances in mixed recycled aggregates (Vegas et al., 2011). Despite that the Spanish Code on structural concrete (Permanent Commission on Concrete, 2008) appoints the UNE EN 1744-1 (2010) as the reference method for the determination of organic matter, the suitability of this technique is further on criticized in the annex 15 of recommendations for the use of recycled aggregates in concrete. Likewise, the effectiveness of other recognised methods for the determination of organic matter, such as the potassium permanganate ($KMnO_4$) method and the loss on ignition at 500°C have also been questioned when applied to recycled aggregates (Vegas et al., 2011).

Hence, the aforementioned approach was used to evaluate the organic matter content of the four samples (Table 4.3). All the recycled aggregates exhibited contents inferior to 0.80%, which falls in line with the recommendation of Sherwood (1995) to avoid the deleterious effects of this component in the concrete manufacture, and within the normal range of values found in the literature (Table 4.4). In the previous fashion, the data from the literature review is expressed by the average and interval values of all the recycled aggregates assessed in each research work.

Table 4.4: Literature review on the organic matter content of the mixed recycled aggregates

	Organic matter (%)
Vegas et al. (2011)	0.76 (0.59-1.17)
	0.87 (0.82-0.95)
	0.39 [a]
Agrela et al. (2012)	0.25 (0.24-0.26)
Barbudo et al. (2012a)	0.43 (0.24-0.95)
	0.45 (0.21-0.89)
Jiménez et al. (2012a)	0.50
Jiménez et al. (2012b)	0.40

[a] 100% ceramic recycled aggregate

Nevertheless, as organic substances were detected in some samples (RA-L(S) and RA-M(S)), their influence on the setting time and the compression strength of the recycled concrete was further assessed and will be discussed in chapter 6 and 8, respectively, in accordance with the requirements laid down in the EHE-08 (Permanent Commission on Concrete, 2008).

Since the approval of the standard for the classification of the constituents of coarse recycled aggregates (UNE EN 933-11, 2009), scientific works not only incorporate the components classification but try to infer quality properties of the recycled aggregate based on the proportions of a determined constituent. Further details of such attempts will be discussed in this chapter for each one of the properties analysed.

Although comparatively inferior to the attention received by the recycled aggregates from crushed concrete, several studies on the composition of the mixed recycled aggregates were found in the literature. The compositional data of 146 mixed recycled aggregates pertaining to 29 research works can be consulted in Table 4.5, where the mean value and the interval range of each set of recycled aggregates are presented. Nonetheless, in all further analysis the data of each individual sample of recycled aggregates was employed. Note that, although the categories of components outlined in UNE EN 933-11 (2009) were followed, some studies presented together the content of cement based materials and unbound aggregates (Rc+Ru).

Table 4.5: Literature review on the composition of mixed recycled aggregates

	Rc	**Ru**	**Rc+Ru**	**Rb**	**Ra**	**Rg**	**X_1**	**X_2**
Chen et al. (2003)	-	-	70.47 (67.55-75.37)	29.12 (24.21-32.00)	-	-	-	0.41 (0.36-0.45)
Sani et al. (2005)	45.00	29.00	74.00	25.00	0.50	-	-	0.50
Poon et al. (2009)	43.90 (13.40-74.40)	46.05 (11.20-80.90)	89.95 (85.60-94.30)	8.75 (4.50-13.00)	-	-	-	1.30 (1.20-1.40)
Agrela et al. (2011)	-	-	77.90 (70.01-88.90)	16.63 (6.00-28.90)	4.03 (0.00-16.70)	0.28 (0.00-1.53)	0.78 (0.00-3.20)	-
	-	-	49.00 (36.38-65.08)	44.34 (30.08-53.90)	2.58 (0.00-6.90)	0.61 (0.00-2.30)	3.11 (0.00-9.90)	-
Jiménez et al. (2011)	34.60 (15.20-51.00)	37.40 (22.00-53.00)	71.98 (67.90-78.90)	21.90 (19.00-27.00)	3.83 (0.80-9.20)	-	0.95 (0.40-1.50)	0.85 (0.30-2.30)
Leite et al. (2011)	55.00	12.00	67.00	30.00	-	-	-	3.00
Vegas et al. (2011)	52.70 (42.00-79.00)	14.40 (4.00-20.00)	67.10 (53.00-83.00)	27.40 (12.00-43.00)	4.20 (0.00-12.00)	0.30 (0.00-0.70)	0.61 (0.00-1.00)	0.33 (0.00-0.80)
	66.40 (56.00-73.00)	20.40 (16.00-29.00)	21.90 (19.00-26.00)	3.00 (1.00-5.00)	10.20 (8.00-14.00)	0.00	0.00	0.00
Yang et al. (2011)	-	-	84.10	14.50	-	-	-	1.40

Table 4.4: Literature review on the composition of mixed recycled aggregates (continued)

	Rc	Ru	Rc+Ru	Rb	Ra	Rg	X_1	X_2
Agrela et al. (2012)	65.67 (63.14-68.20)	15.02 (13.96-16.08)	80.69 (77.10-84.28)	18.78 (15.13-22.42)	0.06 (0.00-0.11)	-	0.39 (0.35-0.42)	0.10 (0.06-0.13)
Barbudo et al. (2012a)	-	-	78.40 (67.80-90.30)	16.40 (5.50-24.50)	3.50 (0.00-9.60)	-	0.60 (0.00-1.60)	0.50 (0.00-2.20)
	-	-	63.40 (41.80-74.30)	33.10 (24.50-46.70)	1.10 (0.00-4.40)	-	1.10 (0.10-5.20)	1.30 (0.00-9.30)
Barbudo et al. (2012b)	42.30 (25.65-60.08)	18.91 (8.14-41.49)	61.21 (42.23-79.13)	35.68 (12.67-56.12)	2.17 (0.00-6.78)	-	0.82 (0.00-2.13)	0.12 (0.00-0.62)
Galvín et al. (2012)	44.23 (15.20-76.00)	32.23 (20.80-52.70)	76.45 (67.90-96.80)	17.93 (3.10-26.60)	4.03 (0.00-9.20)	-	0.88 (0.10-1.50)	0.75 (0.00-2.30)
Güell-Ferré et al. (2012)	-	-	79.15 (69.00-87.45)	18.15 (8.45-30.00)	1.77 (0.00-5.00)	-	-	0.63 (0.00-1.00)
	-	-	50.30 (30.90-65.00)	43.84 (32.00-60.30)	2.52 (0.00-4.70)	-	-	0.76 (0.20-1.00)
Jiménez et al. (2012a)	34.80	33.40	68.20	26.60	4.40	-	0.40	0.30
Jiménez et al. (2012b)	15.20	52.70	67.90	21.00	9.20	-	1.5	0.40
Mas et al. (2012a)	40.00 (35.00-45.00)	33.00 (22.00-47.00)	75.33 (69.00-82.00)	21.00 (15.00-25.00)	0.83 (0.64-1.00)	0.42 (0.10-0.88)	0.77 (0.47-0.94)	1.77 (0.13-4.80)
Mas et al. (2012b)	40.00 (30.00-47.00)	33.00 (22.00-46.00)	75.00 (69.00-80.00)	23.38 (18.00-32.00)	0.70 (0.30-1.00)	0.38 (0.10-0.90)	1.28 (0.30-3.50)	1.73 (0.50-4.80)
Martínez-Lage et al. (2012)	43.00 (42.00-44.00)	19.00 (18.00-20.00)	62.00	36.50 (36.00-37.00)	0.25 (0.00-0.50)	-	0.55 (0.10-1.00)	0.70 (0.40-1.00)
Galvín et al. (2013)	51.26 (38.12-59.82)	24.03 (11.02-39.36)	75.29 (70.84-77.56)	21.00 (14.34-26.21)	2.99 (0.00-7.00)	-	0.72 (0.06-1.13)	-
Geraldes (2013)	35.87 (28.80-43.60)	20.93 (12.6-29.1)	56.80 (56.20-57.90)	38.10 (32.60-41.20)	1.77 (0.40-2.60)	0.87 (0.00-2.40)	1.90 (0.40-3.90)	0.67 (0.20-1.00)
López-Gayarre et al. (2013)	9.33	69.00	78.33	17.67	1.33	-	-	2.67
Sheen et al. (2013)	-	-	71.46 (67.55-75.37)	28.11 (24.21-32.00)	-	-	-	0.44 (0.42-0.45)
Galvín et al. (2014)	29.60 (15.20-38.10)	40.65 (33.10-52.70)	70.25 (66.40-77.40)	24.80 (21.00-28.70)	4.15 (0.00-9.20)	-	0.55 (0.10-1.50)	0.25 (0.00-0.40)

Table 4.4: Literature review on the composition of mixed recycled aggregates (continued)

	Rc	Ru	Rc+Ru	Rb	Ra	Rg	X_1	X_2
Gómez-Meijide and Pérez (2014)	62.50	32.50	95.00	3.90	-	-	0.06	1.30
González-Corominas and Etxeberria (2014)	22.20	9.80	32.00	67.30	0.00	0.10	-	0.70
Medina et al. (2014b)	45.64	28.06	73.70	5.30	19.33	0.07	-	1.59
Rodríguez-Robles et al. (2014)	36.23 (12.76-56.41)	28.17 (9.33-45.44)	64.40 (34.14-78.61)	32.30 (16.51-64.75)	1.33 (0.17-4.38)	0.14 (0.00-0.75)	1.59 (0.09-4.12)	0.24 (0.10-0.45)
Vegas et al. (2015)	52.34 (32.40-81.40) 44.76 (28.80-71.60)	15.44 (2.50-27.40) 22.46 (3.90-55.20)	67.78 (52.30-87.50) 67.22 (36.50-91.40)	27.12 (6.30-44.90) 29.10 (8.50-62.90)	0.88 (0.00-2.80) 0.94 (0.00-4.70)	1.42 (0.00-6.10) 1.92 (0.00-8.20)	- -	2.80 (1.40-3.40) 0.82 (0.10-1.40)
Mean	*43.04*	*27.94*	*70.30*	*25.06*	*2.77*	*0.27*	*0.86*	*0.58*
Minimum	*9.33*	*2.50*	*32.00*	*1.00*	*0.00*	*0.00*	*0.00*	*0.00*
Maximum	*81.40*	*80.90*	*96.80*	*67.30*	*19.33*	*8.20*	*9.90*	*9.30*

Figure 4.7 illustrates the margin in which the compiled compositional results fluctuate. The percentage of cement based materials (concrete lumps and natural aggregate with attached mortar) ranged between 9.33% and 81.40% with a mean value of 43.04%, the natural aggregates without mortar attached present an average of 27.94% ranging between 2.50% and 80.90%, and the ceramic particles content ranged between 1% and 67.30% with an average of 25.06%. Regarding to the asphalt, this component constituted on average 2.77%, which is in keep with other European less strict standards. However, approximately the 20% and the 5% of the mixed recycles aggregates surpassed the 5% (LNEC E-471, 2009; CEN/TC 104/SC 1/TG 19, 2013) and 10% (LNEC E-471, 2009; CEN/TC 104/SC 1/TG 19, 2013; BS 8500-2, 2015) limit respectively; the asphalt content reaching a maximum of 19.33% for one of the samples.

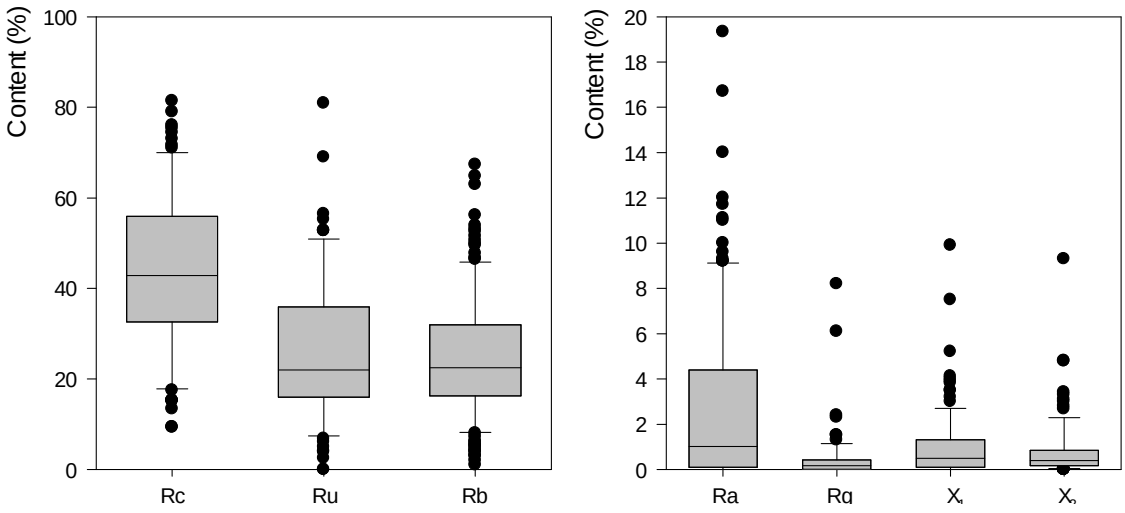

Figure 4.7: Literature review on the composition of mixed recycled aggregates

Similar results can be seen for the rest of impurities (glass, gypsum and others), and approximately 56% of the samples exceeded the 1% conjoint limit established in the EHE-08 (Permanent Commission on Concrete, 2008). Nonetheless, the RILEM TC 121-DRG (1994) recommended less severe limitations that depend on the type of waste materials generating the recycled aggregates; for example, the restriction of foreign materials for aggregates with a ceramic origin (Type I) is fixed at 5%, which translates in roughly 8% of samples not complying with the recommendation. These results suggest the necessity to implement more strict separation methods in order to remove impurities that could hinder the quality of the mixed recycled aggregates.

A Pearson product-moment correlation analysis was performed in order to detect possible linear correlation between the different components present in the recycled aggregates of the experimental study and the literature review. Table 4.6 and Table 4.7 show the Pearson coefficient (top row) and the p-value (bottom row) for each pair of variables evaluated. Significant linear correlations (p-value<0.05) are displayed in grey coloured cells.

Table 4.6: Pearson correlation results for the components of the recycled aggregates (correlation coefficient (top row) and p-value (bottom row))

	Rc	**Rb**	**Ra**	**Rg**	**X_1**	**X_2**
Ru	10.882	-0.9340	0.7930	0.2970	0.3310	0.2020
	0.1180	0.0660	0.2070	0.7030	0.6690	0.7980
Rc		-0.9920	0.6000	0.6230	0.7050	0.0106
		0.0082	0.4000	0.3770	0.2950	0.9890
Rb			-0.6560	-0.5600	-0.6280	-0.0779
			0.3440	0.4400	0.3720	0.9220
Ra				-0.2510	-0.1230	-0.2860
				0.7490	0.8770	0.7140
Rg					0.9700	0.3100
					0.0302	0.6900
X_1						0.0799
						0.9200

The quantity of natural unbound aggregates shows a linear dependence with the ceramic content in the sample and as the natural aggregates tend to decrease the ceramic materials tend to increase, a normal tendency when dealing with mixed recycled aggregates. In addition, a linear relationship became apparent between the glass and gypsum content of the samples. This connection suggests that both contaminants increase simultaneously with a decrease in the cleanliness of the sample or the effectiveness of the CDW treatment process.

In addition to the already established relationships between concrete/mortar and ceramic content and glass and gypsum content from the experimental data, five more linear interrelations were detected when analysing the results of the literature review. An almost perfect correlation (p-value=0.00) was found for two pairs of compositional variables, unbound aggregates and concrete/mortar content and asphalt and ceramic content.

In the first case, an inverse relationship is evident since the amount of unbound aggregates tends to decrease when the concrete/mortar content increases, which responds to a substitution between two of the main components of the mixed recycled aggregates. The same reasoning applies to the correlation found between the content of unbound aggregates and the ceramic presence in the recycled aggregates. For the dependency between the asphalt and ceramic content, although the previous argument is also valid, the correlation is also explained by the fact that the presence of these components in the sample responds to two opposed origins of the CDW, since the ceramic is associated to the demolition of buildings and the asphalt is linked to maintenance works of roads.

Table 4.7: Pearson correlation results for the literature review

	Rc	**Rb**	**Ra**	**Rg**	**X_1**	**X_2**
Ru	-0.6960 0.0000	-0.3110 0.0039	0.0904 0.4140	0.0599 0.6920	0.2300 0.0659	-0.1480 0.2160
Rc		-0.4340 0.0000	0.0387 0.7270	-0.1420 0.3450	-0.3570 0.0036	0.1860 0.1180
Rb			-0.3660 0.0000	0.0474 0.6830	0.2810 0.0020	0.0534 0.5960
Ra				-0.0064 0.9560	0.0592 0.5220	-0.0346 0.7310
Rg					0.3900 0.0011	0.2010 0.1920
X_1						-0.0525 0.6400

All the remaining correlations connected the gypsum content with the relative presence of other materials (concrete/mortar, ceramic and glass) in the recycled aggregates sample. Based on the absolute value of the Pearson coefficient of the different relationships, it is possible to identify the glass content and the ceramic content as the variables with higher and lower influence respectively. While the association gypsum-glass has been explained as a matter of effectiveness in the CDW treatment process, the positive correlation of gypsum with the ceramic is due to the common constructive practice of plastering the masonry walls and finally the negative correlation of gypsum with the concrete/mortar content could be justified by the underlying fact previously stated between the concrete/mortar and ceramic content substitution.

In spite of the detected dependencies between compositional variables, the regression analysis performed showed low R^2 values (Figure 4.8) for the pairs of variables selected from the Pearson correlation analysis in order to fit the results from the literature into a straight line, due to the wide dispersion of the results found in the literature.

However, other authors have found stronger linear regressions within a smaller set of data, in the same way as the results obtained for the experimental data of this research work. For instance, Agrela et al. (2011) identified a good correlation index (R^2=0.93) for the relationship between the cement based materials and unbound aggregates mix with the ceramic content arising from 35 recycled aggregate samples (y=95.312-1.0304x). Nonetheless, ignoring this fact and only focusing on the tendency of the results from the experimental work and those from the literature, the regression lines illustrated in Figure 4.8 show a similar behaviour for both set of results.

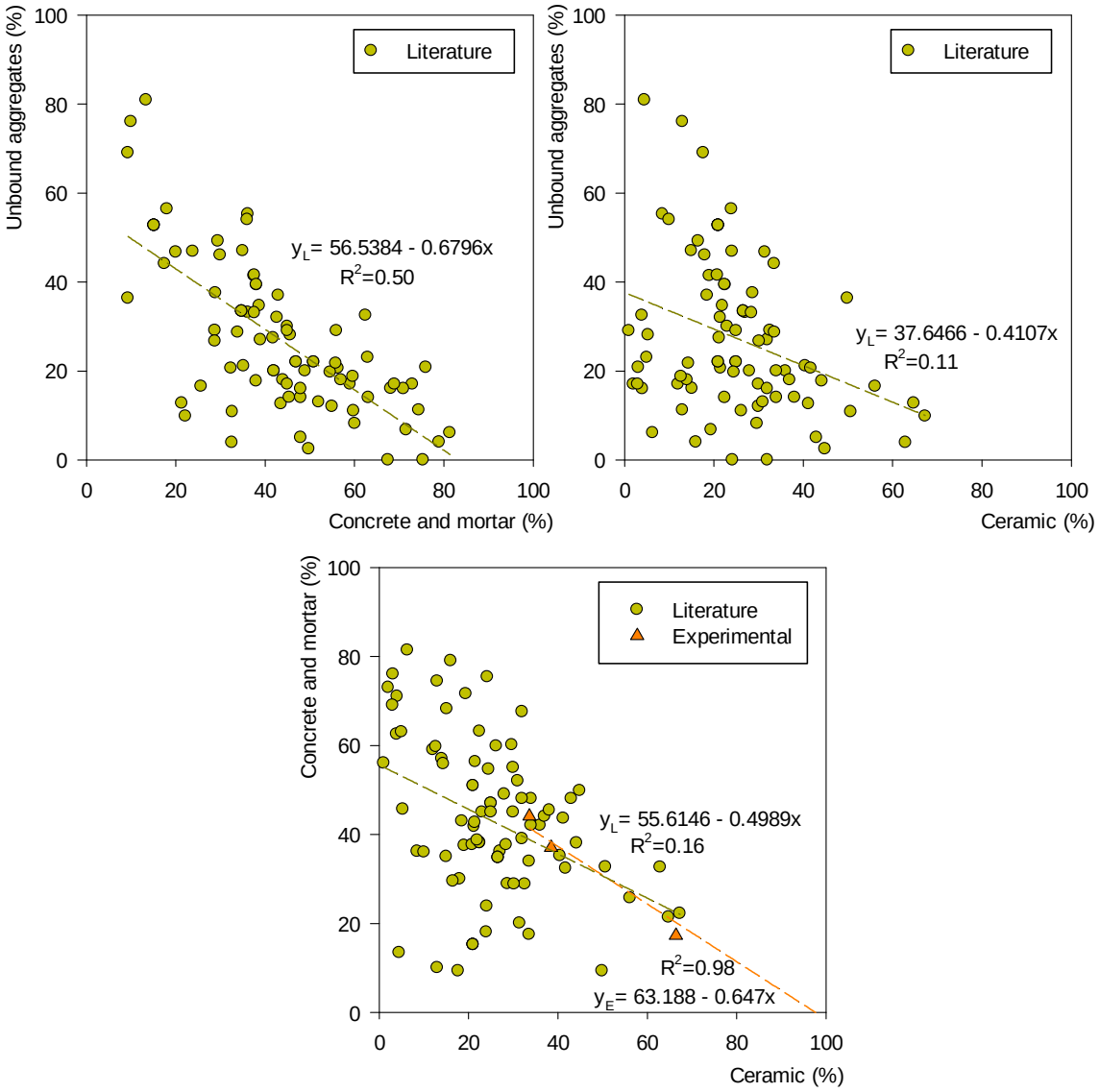

Figure 4.8: Linear regression analysis of the components of the recycled aggregates

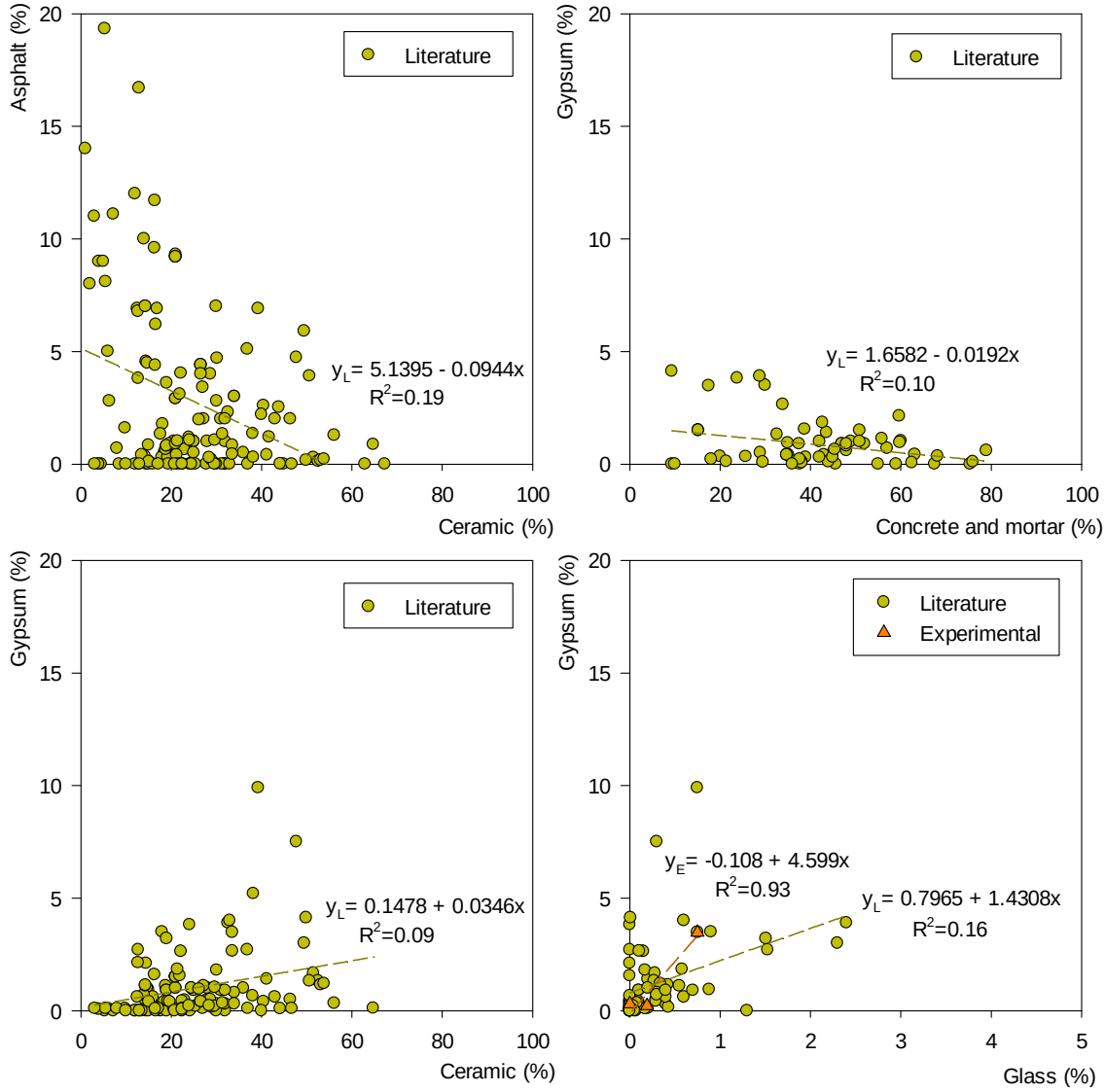

Figure 4.3: Linear regression analysis of the components of the recycled aggregates (continued)

3.1.2. PARTICLE SIZE DISTRIBUTION

The grading of the aggregates is a very important feature because it is directly related to the amount of cement and water to be used in the production of concrete; and as such, it is an essential parameter in the concrete mix design.

The EHE-08 (Permanent Commission on Concrete, 2008) defines the maximum size of an aggregate as the smallest sieve size that retains between 1% and 10% of the aggregate. Likewise, the minimum size is the higher sieve that retains between 85% and 100% of the aggregate. Table 4.8 shows the maximum (D) and minimum (d) size of aggregates, and also depicts the relationship between both sizes. For all the samples, the D/d ratio is greater than the limit stipulated of 1.40.

Table 4.8: Maximum (D) and minimum (d) particle size and D/d ratio

	D (mm)	d (mm)	D/d
Sand	4.00	0.00	-
Gravel-Phase I	16.00	4.00	4.00
Gravel-Phase II	8.00	2.00	4.00
Gravel-Phase II	16.00	8.00	2.00
RA-L(S)	16.00	6.30	2.54
RA-L(B)	20.00	4.00	5.00
RA-M(S)	20.00	6.30	3.17
RA-H(S)	20.00	4.00	5.00

The particle size distributions of the different fine and coarse fractions of natural aggregates used in the studies are displayed in Figure 4.9 and Figure 4.10 respectively, indicating the granulometric recommendations laid down in the Spanish EHE-08 (Permanent Commission on Concrete, 2008) by means of grey shading.

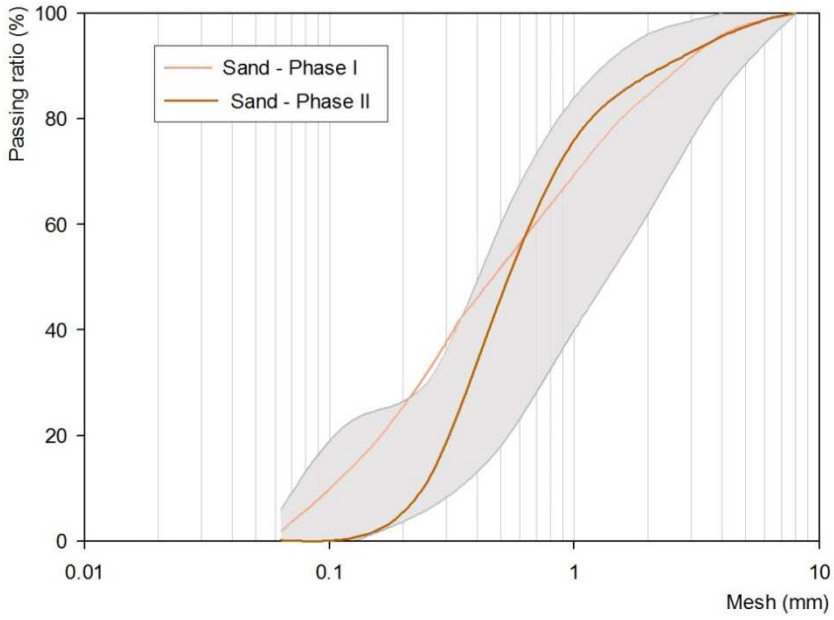

Figure 4.9: Particle size distribution of the fine natural aggregates (sand)

The grading of the four recycled aggregates, expressed as the percentage passing each sieve, is illustrated in Figure 4.11. All the particle size distribution curves show a similar continuous and non-uniform pattern, indicating that the recycled aggregates do not have deficiency or excess of any size. This grading allows a greater margin for interaction between the particles and produces a greater degree of compaction and mechanical strength in the concrete mixture. For recycled aggregates, the particle size distribution is highly dependent of the type of crushing and the sieving process in the CDW management plant, and to a lower extent on the composition and strength of the waste material (Güell-Ferré et al., 2012). Thus, it is reasonably easy to produce good quality coarse recycled aggregates by adjusting the treatment procedure (Hansen, 1992).

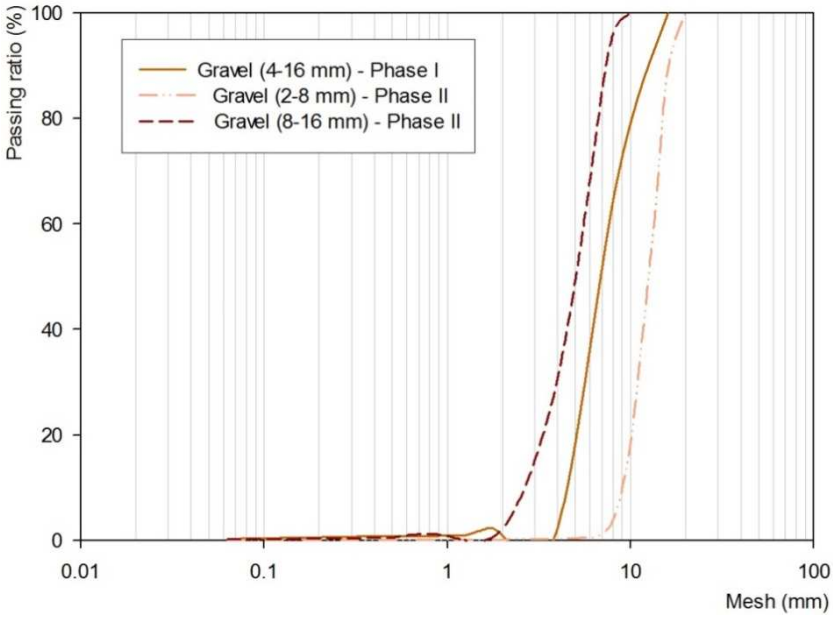

Figure 4.10: Particle size distribution of the coarse natural aggregates (gravel)

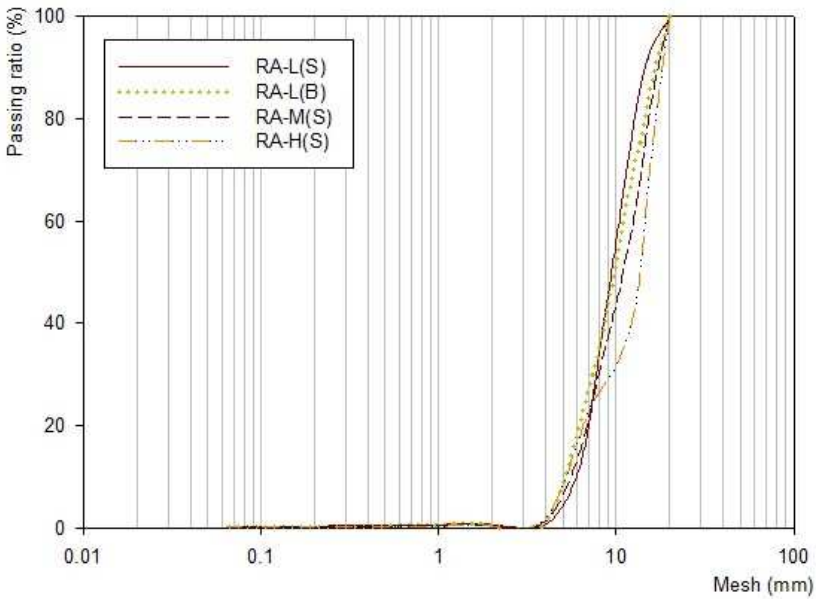

Figure 4.11: Particle size distribution of the recycled aggregates

The particle size distribution curves of the recycled aggregates were statistically processed. The results were first fitted to a two parameter Weibull cumulative distribution (4.1) as suggested in the works of Jiménez et al. (2011); however, higher R^2 values were found when a two parameter Log-logistic cumulative distribution (4.2) was employed (Table 4.9).

$$F(x) = 1 - \exp\left[-\left(\frac{x}{\lambda}\right)^{K}\right] \quad (4.1)$$

$$F(x) = \left[1 + \left(\frac{\lambda}{x}\right)^{K}\right]^{-1} \quad (4.2)$$

with *F(x)* the cumulative distribution function - Weibull in Equation (4.1) and Log-logistic in Equation (4.2) - [%], *x* the percentage of particles passing a specific sieve [%], *λ* the mean particle size [mm] and *K* the measure of particle size spread [-].

Table 4.9: Fitted curves of the particle size distribution of the recycled aggregates

	2 parameter Weibull			**2 parameter Log-Logistic**		
	λ	**K**	**R^2**	**λ**	**K**	**R^2**
RA-L(S)	15.697	4.0397	0.87	13.981	5.6574	0.96
RA-L(B)	15.649	3.8565	0.85	13.859	5.2974	0.95
RA-M(S)	15.927	3.9713	0.78	14.179	5.3877	0.91
RA-H(S)	16.226	3.9075	0.64	14.456	5.0967	0.78

3.1.3. GEOMETRY

The shape and texture of aggregates influence the workability, consistency and mechanical resistance of the concrete.

Recycled aggregates possess a rather different external morphology to that of natural aggregates. While the all the particles comprising the siliceous gravel were rounded and smooth, the shape and texture of the different recycled particles were dependent on the type of constituent forming the recycled aggregates (i.e. unbound aggregate, concrete or mortar, brick, asphalt, glass…). The cement based materials were characterised by a rough texture and irregular shape, the clay based materials produced round but mostly sharp and platy particles with rough texture and the impurities tended to present a great diversity of shapes and textures. In addition, the type of crushing procedure and the number of stages employed affect the geometry of the coarse recycled aggregates. According to Ferreira et al. (2011), recycled aggregates produced from a single crushing procedure (normally by means of a jaw crusher) tend to be more flat and sharp, whilst recycled aggregates arising from treatment plants with primary and secondary (normally a jaw crusher followed by a cone or impact crusher) crushing stages tend to have a spherical shape.

Although comparatively higher than the flakiness index of conventional coarse aggregates (Zega et al., 2010), all recycled aggregates (Table 4.10) comply with the 35% limit established in the EHE-08 (Permanent Commission on Concrete, 2008). The experimental obtained values for mixed recycled aggregates are in agreement with those found in the literature data (Table 4.11), and the flakiness index value (32.13%) of sample RA-H(S) is in good agreement with the results of Cachim (2009) on crushed bricks (30%).

Table 4.10: Flakiness index of the recycled aggregates

	Flakiness index (%)
Gravel	8.00
RA-L(S)	14.75
RA-L(B)	19.10
RA-M(S)	24.67
RA-H(S)	32.13

The literature review (Table 4.11) suggests that the shape of the aggregates is not a limiting factor for the suitability of the recycled aggregates in the concrete manufacture, since only two samples surpass the 35% limit. In addition, the different studies performed for 100% ceramic aggregates indicate that the type of clay based material (brick, sanitary waste, porcelain or mixed wastes) greatly influences the flakiness index of the recycled aggregate.

Table 4.11: Literature review on the flakiness index of recycled aggregates

	Flakiness index (%)
Mixed recycled aggregates	*16.71 (4.50-42.13)*
Ihobe and CEDEX (2011)	18.00 (6.00-30.00)
Vegas et al. (2011)	19.80 (9.00-32.00) 12.00 (9.00-17.00)
Agrela et al. (2012)	12.50 (11.00-14.00)
Barbudo et al. (2012a)	15.00 (8.00-29.00) 17.00 (10.00-22.00)
Martínez-Lage et al. (2012)	30.00
Geraldes (2013)	21.33 (20.00-23.00)
López-Gayarre et al. (2013)	15.00
Gómez-Meijide and Pérez (2014)	4.50
González-Corominas and Etxeberria (2014)	12.00
Rodríguez-Robles et al. (2014)	15.96 (4.64-42.13)
100% recycled ceramic aggregates	*23.67 (9.00-40.00)*
Dhir and Paine (2007) [a]	24.00
Cachim (2009) [a]	23.00 (16.00-30.00)
Vegas et al. (2011) [a]	40.00
Medina et al. (2013) [b]	23.00
Silvestre et al. (2013) [c]	9.00

[a] brick, [b] sanitary ware, [c] porcelain stoneware tiles

3.1.3.1. *Relationship between the flakiness index and the constituents*

The sample RA-H(S) possessed a higher flakiness index due to its composition, i.e. mainly bricks and tiles and their typical crushing morphology in elongated and platy form. This relationship between the presence of ceramic particles and an increased flakiness index of a sample was previously observed by several researchers (Table 4.12). However, the R^2 values of the proposed regressions are low, and the strength of the fit between the flakiness index and the ceramic content in the sample decreases when the study is extended to all the data collected from the literature review (Figure 4.12).

Table 4.12: Literature review on the correlations of the flakiness index (y) and the ceramic content (x)

	Proposed regression	R^2
Ihobe and CEDEX (2011)	y=0.3043x+7.7342	0.63
Güell-Ferré et al. (2012)	y=0.2054x+9.6491	0.24
Geraldes (2013)	y=0.3269x+9.1784	0.58

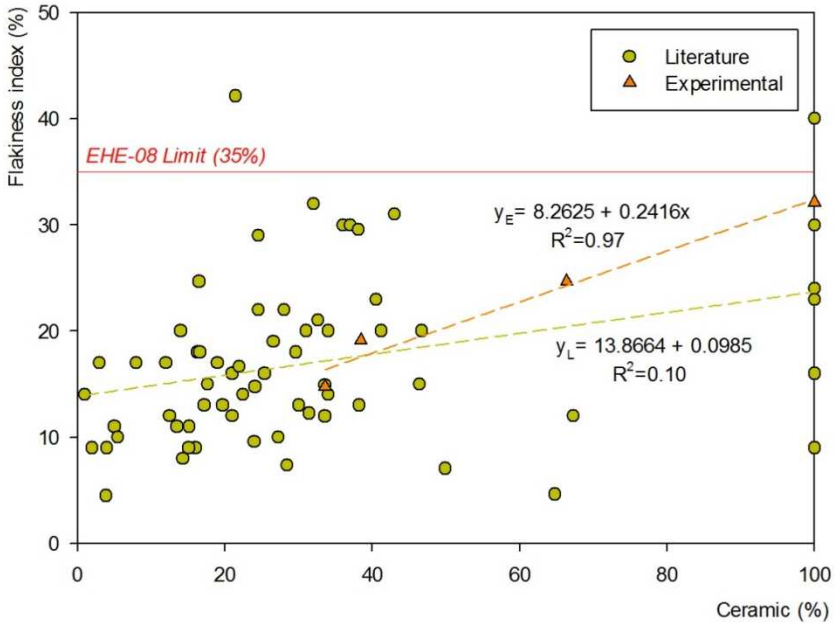

Figure 4.12: Relationship between the flakiness index and the ceramic content

Nonetheless, a Pearson product-moment correlation analysis was performed in order to assess the linear dependence between the composition parameters of the recycled aggregates from the literature review and their flakiness index values (Table 4.13). As expected, a significant correlation was found between the ceramic content and the flakiness index and in addition a relationship between the shape of the aggregates and the content of unbound aggregates and cement based materials has also became apparent (p-value<0.05). This second correlation is due to the existing substitution relationship between the ceramic and the unbound aggregates and cement based materials in the recycled aggregates as the three more abundant constituents, i.e. higher contents of ceramic materials translates in lower contents of unbound aggregates and cement based materials. In addition, only the ceramic and glass content presented a positive Pearson coefficient, as these materials usually have an elongated shape that would tend to increase the flakiness index.

Table 4.13: Pearson correlation analysis on the flakiness index of the mixed recycled aggregates in the literature review

	Rc	Ru	Rc+Ru	Rb	Ra	Rg	X_1	X_2
Flakiness index	-0.1280	-0.2520	-0.2920	0.2990	-0.1690	0.2170	-0.0059	-0.0180
	0.4120	0.1030	0.0173	0.0146	0.1750	0.0808	0.9630	0.8860

3.1.4. FINES ASSESSMENT

Although a certain amount of fines could improve the cohesiveness and avoid the bleeding of the fresh concrete, excessive quantities of fines are undesirable since they produce an increase of the water demand and hinder the cement paste bond, which could lead to the concrete failure (Hewlett, 2003).

The fines content of the recycled aggregates is dependent on their treatment procedure at the CDW management plant, and it is specifically related to the type of crusher and the number of crushing stages. According to Güell-Ferré et al. (2012), jaw crushers produce a lower quantity of fines than impact crushers. The screening process is also a limiting factor in the presence of fines in the recycled aggregate, although several screening stages could be implemented at the CDW management plant, usually the screening takes places after the secondary crushing.

The EHE-08 (Permanent Commission on Concrete, 2008) defines the fines as the percentage of the total weight of the sample passing through a 0.063 mm sieve. In terms of quantity, the limit for coarse aggregates is up to 1.50%. The results obtained, shown in Table 4.14, indicate that all recycled aggregates possess an amount of fines within the limit stipulated in the Spanish standard. However, a higher quantity of fines could be expected in the concrete than the one determined in the aggregate characterization, since recycled aggregates continue to generate dust and fines due to self-attrition of the particles during handling. To avoid any excessive production of fines due to the friability of the attached mortar and the ceramic materials, the mixing time was thoroughly controlled.

Table 4.14: Fines assessment

	Fines content (%)	Sand equivalent (%)
Gravel	0.09	-
RA-L(S)	0.06	38.10
RA-L(B)	0.03	-
RA-M(S)	0.05	27.30
RA-H(S)	0.08	11.50

As part of the fines assessment, their quality was tested by means of the sand equivalent test in order to evaluate the presence of clay-like fines, which should exceed 70% (I, IIa or IIb general classes of exposures) or 75% (the rest classes of exposure). Appendix A illustrates the equivalence between Spanish and European environmental exposures classes. However as a matter of fact, the method and requirements regarding the sand equivalent test are only compulsory for fine aggregates. Nonetheless, the method was performed on the 0/2 mm fraction retrieved from the sieving analysis of the coarse recycled aggregates to evaluate the fines content produced due to the friability of the attached mortar and the ceramic materials. The results (Table 4.14) indicate a questionable quality of the fines as none of the samples complied the requirements. Hence, the clay-like fines were further analysed by means of an X-ray diffraction test (section 3.2.2) and no expansive clays were detected that could negatively affect the recycled concrete performance or durability. Even so, it is worth mentioning that fines from CDW present pozzolanic activity (Medina et al., 2015).

From the literature review (Table 4.15) was made apparent that the fines content is not usually presented as a numeric figure and instead is evaluated from the particle size distribution curves presented in the research works. However, in most cases the representation scale used on the axis showing the passing or retained ratio prevent even a graphical determination of the amount of fines. In addition, as previously stated, this test is only compulsory to fine aggregates, which is the reason that only a limited amount of researchers (all of them Spanish) performed this test on coarse aggregates.

Table 4.15: Literature review on the fines assessment of the recycled aggregates

	Fines content (%)	**Sand equivalent (%)**
Mixed recycled aggregates	*6.33 (0.00-30.11)*	*43.14 (11.50-77.00)*
Corinaldesi and Moriconi (2011)	0.30	-
Ihobe and CEDEX (2011)	9.25 (0.50-18.00)	-
Jiménez et al. (2011)	6.08 (3.1-9.5)	44.00 (35.00-58.00)
Agrela et al. (2012)	-	66.50 (66.00-67.00)
Barbudo et al. (2012a)	7.30 (3.00-21.00)	-
	6.80 (0.00-14.00)	-
Jiménez et al. (2012a)	-	39.00
Jiménez et al. (2012b)	-	35.00
Geraldes (2013)	3.35 (2.20-5.30)	-
López-Gayarre et al. (2013)	20.00	20.00
Sheen et al. (2013)	22.56 (15.00-30.11)	-
Gómez-Meijide and Pérez (2014)	-	77.00
Rodríguez-Robles et al. (2014)	1.77 (0.04-7.09)	38.13 (11.50-65.90)
100% recycled ceramic aggregates	*0.54 (0.16-1.10)*	-
Medina et al. (2012) [a]	0.16	-
Halicka et al. (2013) [a]	0.37	-
Silvestre et al. (2013) [b]	1.10	-

[a] sanitary ware, [b] porcelain stoneware tiles

Regarding the fines content values retrieved from the literature review, it is possible to notice that roughly 18% of the mixed recycled aggregates complied with the 1.50% constraint. However, the EHE-08 (Permanent Commission on Concrete, 2008) also allows the use of aggregates with higher fines content if the total amount of fines in the concrete (from the coarse and fine aggregates and any limestone in the cement) does not exceed 175 kg/m^3. Provided this exception, an increment in the number of the mixed recycled aggregates suitable for the concrete manufacture is expected. Nonetheless, it is worth noting that the fines content requirement is considerably stricter when compared to other European standards (BS 8500-2, 2015) and recommendations (RILEM TC 121-DRG, 1994). For instance, according to the recommendations of Etxeberria Larrañaga et al. (2006) more than half of the mixed recycled aggregates could be used directly in the concrete manufacture, while the rest of them would require a screening treatment before their use.

In terms of quality, only the recycled aggregate studied by Gómez-Meijide and Pérez (2014) possess a sand equivalent value complying with the imposed thresholds, which suggests that the X-ray diffraction approach could be more efficient in the determination of possible problems associated to the presence of clays in the fines of recycled aggregates.

3.1.4.1. *Relationship between the fine content or the sand equivalent and the constituents*

In spite that no correlation has been previously proposed linking the fine content or the sand equivalent to any compositional parameter of the mixed recycled aggregates, a Pearson product-moment correlation analysis was performed on the data recovered from the literature review (Table 4.16). The results show a significant correlation (p-value<0.05) between the cement based materials and the fine content and the sand equivalent. Both relationships establish that a higher content of cement based materials increases the fine content due the friability of the attached mortar, and increases the sand equivalent since the fines arising from the cement materials do not have a clay-like nature.

Table 4.16: Pearson correlation analysis on the fines content and the sand equivalent of the mixed recycled aggregates in the literature review

	Rc	Ru	Rc+Ru	Rb	Ra	Rg	X_1	X_2
Fines content	0.4370	0.2450	0.0919	-0.0778	-0.0146	-0.1190	-0.1930	0.1120
	0.0420	0.2970	0.5480	0.6120	0.9240	0.4350	0.2030	0.4640
Sand equivalent	0.5020	-0.2120	0.4380	-0.3690	-0.1830	-0.2050	-0.2660	-0.0508
	0.0173	0.3440	0.0417	0.0910	0.4140	0.3610	0.2310	0.8220

Figure 4.13 and Figure 4.14 display the calculated linear regressions for the experimental and the literature results, both exhibiting low linear correlations for the data from the literature review due to the dispersion of the results.

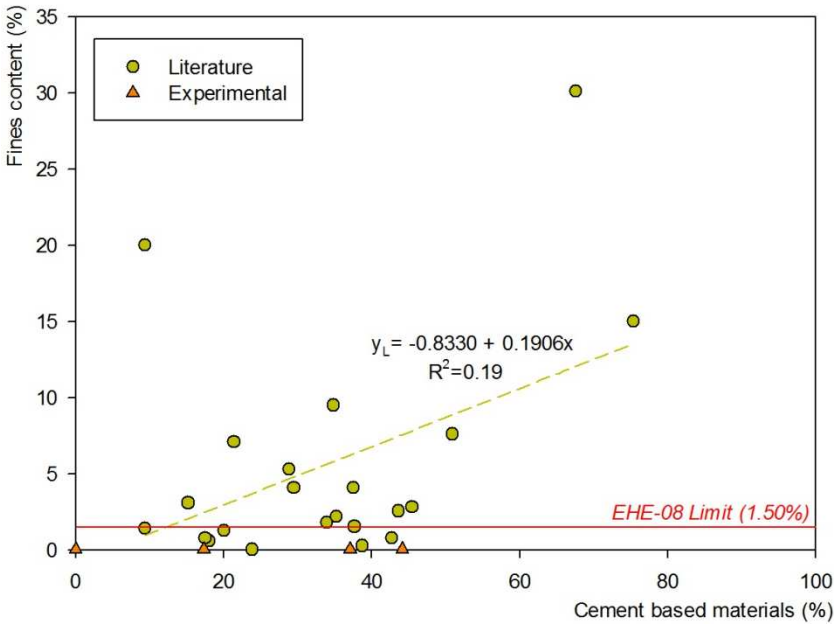

Figure 4.13: Relationship between the fines content and the cement based materials content

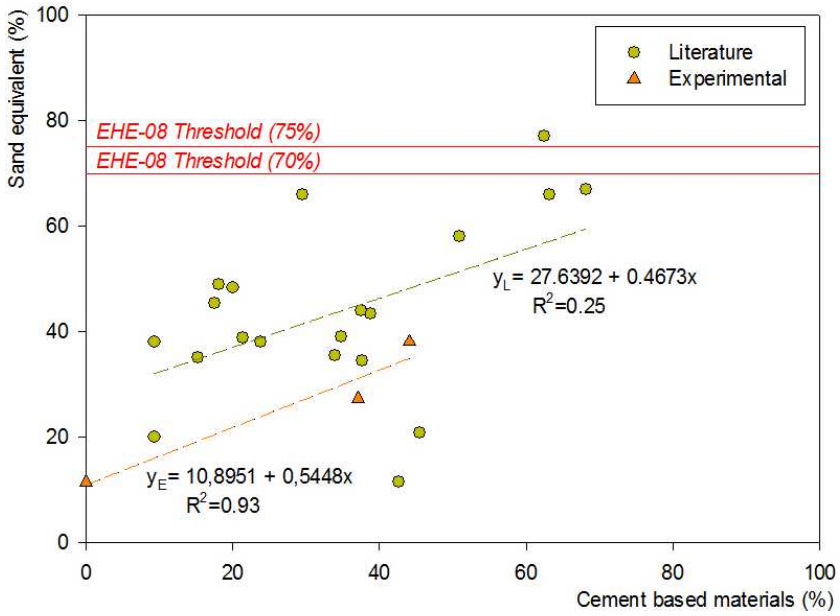

Figure 4.14: Relationship between the sand equivalent and the cement based materials content

3.1.5. DENSITY AND WATER ABSORPTION

The Spanish Code on structural concrete (Permanent Commission on Concrete, 2008) does not lay down any limitation for the density of the aggregates to be used in concrete; nevertheless, density is an essential physical property in the concrete mix design. On the contrary, several international standards use the density values as a classification parameter for the recycled aggregates and establish constraints in order to delimit their suitability for concrete applications (DIN 4226-100, 2002; NBR 15116, 2004; LNEC E-471, 2009). For instance, the RILEM recommendations (RILEM TC 121-DRG, 1994) suggest that dry particles coming from masonry rubble (Type I recycled aggregate) should have a minimum density of 1.50 Mg/m^3 in order to be suitable in the concrete manufacture.

As can be seen in Table 4.17, all the samples presented densities which varied within the same ranges as those obtained for other mixed recycled aggregates (1.80-2.50 Mg/m^3 on oven-dried basis) and ceramic materials (1.67-2.39 Mg/m^3 on oven-dried basis) by several researchers (Table 4.18). Interestingly, the density of all recycled aggregates was significantly lower (between 18% and 29% when oven dried densities are compared) than that of the natural aggregates, which ranged between 2.54-2.65 Mg/m^3.

These differences are explained by their elevated porosity due both to their ceramic nature and the presence of adhered mortar (Poon and Chan, 2006a; Debieb and Kenai, 2008). And as such, the differences are more severe as the general ceramic content increases (L, M and H) in the recycled aggregates. Nonetheless at a low level ceramic content, sample RA-L(S) (33.56% ceramic) has higher density values than sample RA-L(B) (38.44% ceramic) which could be explained by the different mechanical properties of the waste materials comprising the recycled aggregate.

Initially, it was believed that the compressive strength of the parent concrete does not affect the density of the recycled aggregates, provided a similar recycling procedure is applied (Hansen and Narud, 1983; Dhir et al., 1999); although more recently some studies (Nagataki et al., 2000; Gokce et al., 2011; Gonzalez and Etxeberria, 2014) have proven that the strength of the original concrete influences the density, i.e. a concrete material with high compressive strength will generate concrete recycled aggregates with higher density values. The same behaviour was reported for the compressive strength of the original bricks and the density of the resulting aggregates (Bazaz et al., 2006; Khalaf, 2006).

In contrast, water absorption is limited in the EHE-08 (Permanent Commission on Concrete, 2008) up to 7% for recycled concrete that contains no more than 20% recycled aggregate from crushed concrete and up to 5% for mixtures of gravel and more than 20% recycled concrete. As the EHE-08 does not contemplate the used of mixed recycled aggregates yet, Spanish researchers use the 7% limit to assess the absorption capacity of all types of recycled aggregates. Nonetheless, this limit is far inferior to those proposed in other international legislations. For example in Germany (DIN 4226-100, 2002), limits up to 10%, 15% and 20% are established for concrete waste, construction and demolition waste and masonry rubble respectively. As well, RILEM recommendations (RILEM TC 121-DRG, 1994) widen the Spanish water absorption constraint, and a 20% limit is set for Type I aggregates (originating from masonry rubble) and a 10% limit is established for Type II aggregates (originating from concrete rubble).

The water absorption of the gravel is in accordance with the values (1.00-3.50%) by Rao et al. (2007) and between 5 and 6.5 times lower than the recycled aggregates that are supposed to be used as its partial replacement. In view of the results obtained (Table 4.17), which are similar to those reported in the investigations consulted in the literature review (Table 4.18), the recycled aggregates do not comply with the specifications. If the recycled aggregates were judged according to the recommendations proposed by RILEM (RILEM TC 121-DRG, 1994), sample RA-H(S) would comply with the limit for masonry rubble, and the mixed aggregates (which could be considered as a mixture of Type I and Type II aggregates) would also comply, even with the most restrictive limitation of 10% water absorption.

A higher absorption coefficient was observed with the increase in the percentage of masonry, which agreed with the findings of Gomes and de Brito (2008) and de Brito et al. (2005). Similarly to the density values, the water absorption is related not only to the type of waste material but to their original compressive strength. While some studies registered a water absorption decrease as the compressive strength of the concrete increased (Poon et al., 2004a; Gonzalez and Etxeberria, 2014), the opposite comportment has also be observed (Katz, 2004); which indicates that no clear tendency exists between both properties. On the contrary, the mechanical resistance of the bricks has a strong influence of the water absorption of the recycled aggregate, with stronger bricks resulting in recycled aggregates with lower water absorption values (Khalaf and DeVenny, 2005).

Table 4.17: Density and water absorption values

	OD density (Mg/m^3)	SSD density (Mg/m^3)	Apparent density (Mg/m^3)	Water absorption (%)
Sand	2.63	2.64	2.65	0.13
Gravel	2.54	2.58	2.66	1.73
RA-L(S)	2.08	2.26	2.53	8.53
RA-L(B)	2.06	2.24	2.51	8.64
RA-M(S)	1.94	2.11	2.33	10.44
RA-H(S)	1.80	2.07	2.21	10.77

Density and water absorption are considered two decisive properties defining the quality of recycled aggregates, and as such both parameters have been the subject of a great number of investigations (Table 4.18). Generally, three types of density - oven dry (OD), saturated surface-dried (SSD) and apparent - could be distinguish; however, the literature review shows that the apparent density is not usually studied.

Table 4.18: Literature review on the density and water absorption of the recycled aggregates

	OD density (Mg/m^3)	SSD density (Mg/m^3)	Apparent density (Mg/m^3)	Water absorption (%)
Mixed recycled aggregates	*2.09 (1.80-2.50)*	*2.28 (2.00-2.60)*	*2.59 (2.49-2.68)*	*8.57 (2.00-16.45)*
Parra y Alfaro (2001)	2.02 (1.90-2.16)	2.25 (2.18-2.34)	-	11.47 (8.05-14.74)
Chen et al. (2003)	-	2.29 (2.28-2.29)	-	6.29 (5.04-7.54)
Sani et al. (2005)	-	-	-	7.40
Gomes and de Brito (2008)	2.16	2.30	-	16.30
Poon et al. (2009)	2.15 (2.13-2.16)	2.29 (2.26-2.32)	-	6.03 (5.81-6.25)
Thanaya (2009)	-	2.48	2.57	2.50
Agrela et al. (2011)	-	2.34 (2.22-2.58)	-	6.24 (2.1-8.8)
Corinaldesi and Moriconi (2011)	-	2.37	-	6.00
Ihobe and CEDEX (2011)	2.15 (1.80-2.50)	2.30 (2.00-2.60)	-	8.00 (2.00-14.00)
Agrela et al. (2012)	-	2.39 (2.32-2.46)	-	8.00 (6.80-9.20)
Barbudo et al. (2012a)	-	2.29 (2.15-2.46)	-	7.90 (5.10-10.10)
	-	2.23 (2.12-2.32)	-	9.90 (7.90-12.50)
Galvín et al. (2012)	-	2.17 (2.12-2.24)	-	7.85 (6.70-8.50)
Hoffmann et al. (2012)	2.27 (2.22-2.30)	-	1.51 (1.46-1.53)	5.13 (4.16-6.13)
Jiménez et al. (2012a)	-	-	-	8.30

Table 4.18: Literature review on the density and water absorption of the recycled aggregates (continued)

	OD density (Mg/m^3)	SSD density (Mg/m^3)	Apparent density (Mg/m^3)	Water absorption (%)
Jiménez et al. (2012b)	-	-	-	7.90
Martínez-Lage et al. (2012)	-	-	-	11.00
Mas et al. (2012a)	2.15 (2.12-2.21)	-	-	7.66 (7.22-7.96)
Mas et al. (2012b)	2.12 (2.04-2.19)	2.30 (2.24-2.36)	-	8.30 (7.35-9.59)
Galvín et al. (2013)	2.30 (2.23-2.34)	-	9.66 (9.16-9.95)	2.30 (2.23-2.34)
Geraldes (2013)	2.02 (1.98-2.04)	2.22 (2.18-2.24)	2.53 (2.49-2.55)	10.07 (9.70-10.40)
López-Gayarre et al. (2013)	2.16	-	-	4.15
Sheen et al. (2013)	-	2.37 (2.26-2.48)	-	6.29 (5.04-7.54)
Galvín et al. (2014)	-	2.12 (2.12-2.30)	-	8.33 (7.7-9.94)
Gómez-Meijide and Pérez (2014)	2.23	2.39	-	7.00
González-Corominas and Etxeberria (2014)	1.80	-	-	16.45
Rodríguez-Robles et al. (2014)	2.12 (1.91-2.32)	2.30 (2.17-2.44)	2.61 (2.56-2.68)	9.16 (5.21-13.46)
Sidorova et al. (2014)	1.89	-	2.53	13.30
Medina et al. (2015)	-	2.54	-	4.49
100% recycled ceramic aggregates	*1.95 (1.67-2.39)*	*2.12 (1.93-2.30)*	*2.17 (1.80-2.35)*	*11.52 (0.20-22.00)*
Akhtaruzzaman and Hasnat (1983)[a]	-	1.93	-	11.20
Khaloo (1995)[b]	1.69 (1.67-1.71)	1.95 (1.93-1.97)	-	15.25 (15.00-15.50)
Mansur et al. (1999)[b]	2.21	-	-	6.10
Parra y Alfaro (2001) [a]	1.85	2.16	-	16.66
Cachim (2009)[a]	1.81	-	-	15.81
	1.93	-	-	18.91
de Brito et al. (2005)[a]	2.03	2.27	-	12.00
Khalaf and DeVenny (2005)[a]	-	2.12 (1.94-2.25)	-	12.50 (7.40-19.80)
Senthamarai and Devadas Manoharan (2005)[c]	-	-	-	0.72
Correia et al. (2006)[a]	2.03	2.27	-	12.00
Poon and Chan (2006a)[a]	1.71	2.03	-	18.95
Debieb and Kenai (2008)[a]	-	-	-	11.50
Cabral et al. (2010)[a]	-	-	-	15.62
Liu et al. (2010)[a]	-	-	2.35	5.34

Table 4.18: Literature review on the density and water absorption of the recycled aggregates (continued)

	OD density (Mg/m^3)	SSD density (Mg/m^3)	Apparent density (Mg/m^3)	Water absorption (%)
Soutsos et al. (2011)[d]	2.11	2.26	-	8.83
Xiao et al. (2011)[a]	1.76	2.04	-	15.43
Xuan et al. (2011) [d]	-	-	2.35	8.68
Yang et al. (2011)[a]	2.04	2.24	-	10.20
Jankovic et al. (2012)[a]	-	-	-	20.65
Medina et al. (2012)[e]	2.39	-	-	0.55
Sadek (2012)[a]	-	-	-	12.35
Halicka et al. (2013)[e]	-	-	-	1.53
Katzer and Domski (2013) [d]	-	-	1.80	22.00
Sata et al. (2013) [a]	-	-	-	16.20
Silvestre et al. (2013)[f]	2.21	2.30	-	3.96
Alves et al. (2014)[a]	-	-	-	12.20
Alves et al. (2014)[e]	-	-	-	0.20
Hu et al. (2014)[a]	1.85	2.14	-	13.20
Sadek and El Nouhy (2014)[a]	-	-	-	8.00

[a] brick, [b] tile, [c] ceramic electric insulator, [d] masonry, [e] sanitary ware, [f] porcelain stoneware tiles

In terms of water absorption, the interest of the investigations goes beyond the knowledge of the water absorption value of the recycled aggregates and several researchers have also focused their studies on the speed with which the absorption of water takes place due to the fact that part of the water added during the mixing of the concrete will be absorbed for the recycled aggregates. For mixed recycled aggregates, Agrela et al. (2011) found that in a 10 minutes immersion 85% of the 24 hours water absorption is achieved. On the contrary according to Mas et al. (2012b), the 85% value was not even reached after more than 8 hours. García-González et al. (2014) indicated that a 5 minute period of immersion leads to the achievement of a 50% of the complete saturation of the mixed recycled aggregate but the complete saturation was not reached until 10 days. For ceramic recycled aggregates, DeVenny and Khalaf (1999) estimate that roughly 30 minutes are enough for the complete saturation. Cachim (2009) observed that bricks achieve at least the 75% of their water absorption in the two first minutes in soaking and that at 5 minutes 91% of the total water absorption was already reached. Alves et al. (2014) indicated that after 10 minutes the recycled brick aggregates absorbed more than 87% of their 24 hour potential absorption capacity and after 8 hours the complete saturation was achieved.

Since the high absorption capacity of mixed recycled aggregates and ceramic recycled aggregates could be detrimental to the workability of the concrete mixture (Rao et al., 2007), some techniques have been proposed. In order to compensate the mixing water absorbed by the recycled aggregates, some researchers have suggested the addition of extra water to the mixture in order to account for the predicable reduction of water (Tabsh and Abdelfatah, 2009; Ferreira et al., 2011; Mas et al., 2012a, 2012b; Matias et al., 2013; Beltrán et al., 2014; Soares et al., 2014).

For instance, Tabsh and Abdelfatah (2009) reported that the use of recycled aggregates would involve, on average, up to 10% more water than what is required in conventional concrete in order to achieve the same slump. Whilst other authors have recommended the use of recycled aggregates in a saturated state achieved through a stage of soaking in water before their use in the concrete manufacture (Khalaf and DeVenny, 2005; Debieb and Kenai, 2008; Agrela et al., 2011; García-González et al., 2014).

In spite of the beneficial effects that these methods have on the workability of the recycled concrete, some disadvantages of their use have also become apparent. In both cases, a profound knowledge of the water absorption value and its evolution with time is required to make the adjustments in the concrete mixture and control the effective water-cement ratio. On one hand, the mixing water compensation could lead to bleeding risks that alter the interfacial transition zone (ITZ) and influence the mechanical strength of the recycled concrete (Poon et al., 2004a, 2004b). On the other hand, the pre-saturation method requires a dry surface of the recycled aggregates in order to maintain the water-cement ratio of the mixture, which poses a problem at large scale that according to Etxeberria et al. (2007) could be solved by means of a system of sprinklers in the stockpile of the recycled aggregates. In addition, the pre-soaking procedures have resulted in reduction of the mechanical strength of the recycled concrete (Poon et al., 2004b; Ferreira et al., 2011; Mefteh et al., 2013; García-González et al., 2014) and the durability performance (Ferreira et al., 2011).

Furthermore, other techniques as the washing of the recycled aggregates have been offered as a method to reduce their water absorption due to the removal of fine particles; with this treatment Van Der Wegen and Haverkort (1998) reached water absorption reductions between 35% and 55%. Also, the use of superplasticizers (Barbudo et al., 2013; Matias et al., 2013) and admixtures (Kou et al., 2011a) have been contemplated to maintain a desired workability; for example, the studies of Kumar and Dhinakaran (2012) demonstrated that the use of superplasticizer in combination with 20% fly ash reduced by 12.50% the water demand in the recycled concrete.

Finally, Poon et al. (2004b) concluded that the workability and the compressive strength were similar to the conventional concrete when no more than 50% of recycled aggregates in air-dried state were used in the replacement and advised to use recycled aggregates in saturated surface-dried state in special situations only. Hence, in this research work none of the aforementioned techniques was employed. The concrete mix dosage was designed in such way that the mixing water was enough to achieve a proper workability of the fresh recycled concrete, which in addition did not hinder the mechanical properties and durability of the hardened recycled concrete.

3.1.5.1. *Relationship between the density and the particle size distribution*

As stated in several research works (Poon and Chan, 2006a, 2006b; Sánchez de Juan and Alaejos Gutiérrez, 2009; Tam and Tam, 2009; Gokce et al., 2011), a relationship between the particle size distribution and the density of the recycled aggregates was detected (Figure 4.15). It is worth mentioning that the linear regression analysis shows a high correlation for the OD density, closely followed by the apparent density.

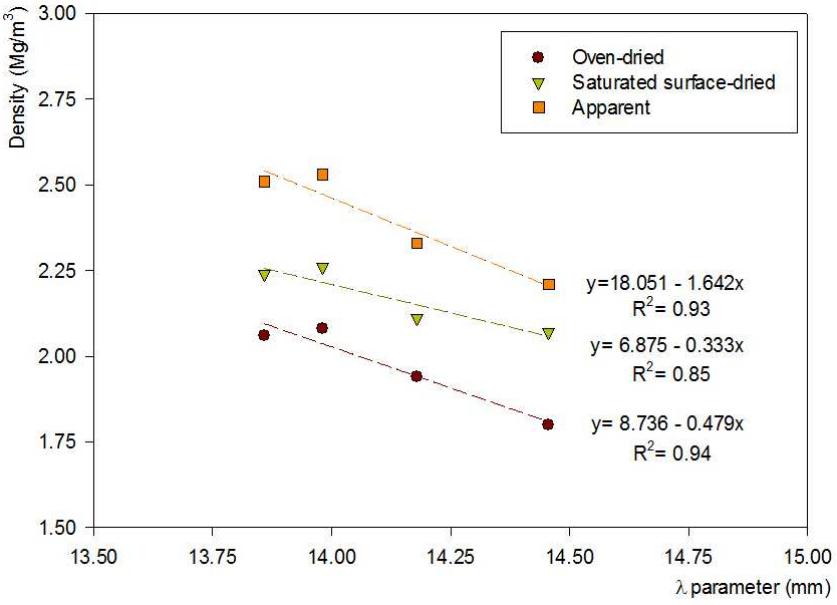

Figure 4.15: Relationship between the density and the mean particle size

3.1.5.2. *Relationship between the SSD density or the water absorption and the constituents*

According to Dhir et al. (2008), the particle density values of mixed recycled aggregates could be estimated in accordance with their composition ratios. Furthermore, the amount of ceramic materials in mixed recycled aggregates has been identified as a major influence in the density and water absorption of the recycled aggregates (Table 4.19 and Table 4.20). A linear regression analysis of the SSD density and the water absorption with the ceramic content was performed for the data from the literature review as well as for the results obtained in this research (Figure 4.16 and Figure 4.17).

Table 4.19: Literature review on the correlations of the SSD density (y) and the ceramic content (x)

	Proposed regression	**R^2**
Agrela et al. (2011)	y= -0.0064x+2.4437	0.65
Mas et al. (2012b)	y= -0.0064x+2.4437	0.65
Geraldes (2013)	y=-0.0031x+2.393	0.52

Table 4.20: Literature review on the correlations of the water absorption (y) and the ceramic content (x)

	Proposed regression	**R^2**
Ihobe and CEDEX (2011)	y=0.1874x+3.2975	0.74
Agrela et al. (2011)	y= 0.1797+3.5784	0.74
Barbudo et al. (2012a)	y= 0.149x+5.258	0.77
Mas et al. (2012b)	y=0.1797x+3.5784	0.74
Geraldes (2013)	y=0.0925x+5.4713	0.52

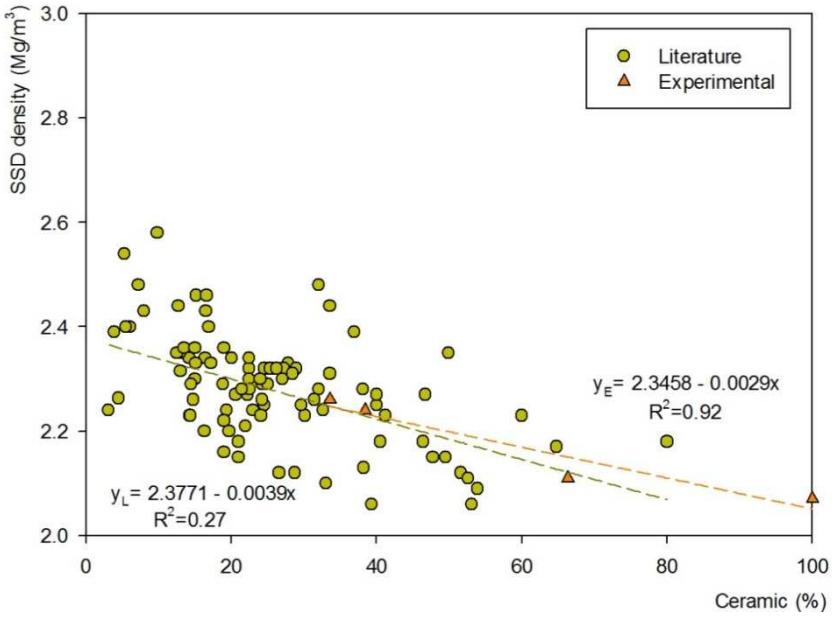

Figure 4.16: Relationship between the SSD density and the ceramic content

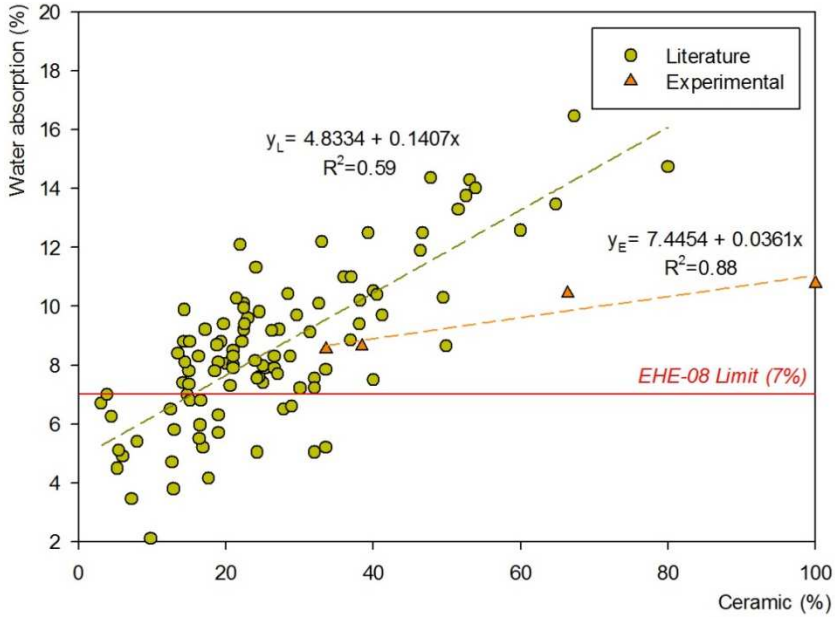

Figure 4.17: Relationship between the water absorption and the ceramic content

Given that the linear regression analysis performed showed weak R^2 values, a Pearson product-moment correlation evaluation was carried out in order to identify linear dependencies between the compositional variables and the SSD density or the water absorption (Table 4.21). Two strong significant linear correlations (p-value<0.05) were detected between the SSD density and the amount of unbound aggregates and cement based materials and between the SSD density and the ceramic content. While higher content of the former increased the SSD density, a decrease of the SSD density could be observed when the latter material increased.

For the water absorption property, significant linear dependencies (p-value<0.05) were identified for five constituents: unbound aggregates, unbound aggregates and cement based materials, ceramic, asphalt and gypsum. The porous nature of ceramic and gypsum is related with the increase of water absorption; meanwhile the rest of constituents have a negative Pearson correlation coefficient that translates in a lower water absorption with the increase of the quantity of such constituents (unbound aggregates and cement based materials and asphalt). It is worth mentioning that Barbudo et al. (2012a) proposed a linear regression between the water absorption (y) and the amount of unbound aggregates and cement based materials (x) (y=-0.127x+17.921; R^2=0.69).

Table 4.21: Pearson correlation analysis on the SSD density and the water absorption of the mixed recycled aggregates in the literature review

	Rc	**Ru**	**Rc+Ru**	**Rb**	**Ra**	**Rg**	**X_1**	**X_2**
SSD density	0.2930	0.0325	0.5460	-0.5220	0.1210	-0.1070	-0.3680	-0.0759
	0.0661	0.8440	0.0000	0.0000	0.2390	0.3000	0.0002	0.4630
Water absorption	-0.1790	-0.4820	-0.7360	0.7680	-0.3270	0.0452	0.3050	0.0115
	0.2200	0.0004	0.0000	0.0000	0.0006	0.6450	0.0015	0.9070

The Pearson correlation analysis has not detected a significant correlation (p-value>0.05) between the amount of cement based materials and neither the SSD density or the water absorption when all the data from the literature review were studied. However, Agrela et al. (2011) have found significant relationships within their data for these two properties proposing a linear regression between the SSD density (y) and the concrete content (x) (y= 0.006x+1.8671; R^2=0.65) and another one between the water absorption (y) and the quantity of concrete (x) (y= -0.1629x+19.384; R^2=0.70).

3.1.5.3. *Relationship between the water absorption and the density*

The literature review shows that strong linear relationships ($R^2 \geq 0.80$) have been established between water absorption and the density of recycled aggregates (Table 4.22 and Table 4.23). In this case, the study of the data from the literature review also displays adequate R^2 values (Figure 4.18 and Figure 4.19) in spite of the wider dispersion of the results found for other properties of the recycled aggregates.

Table 4.22: Literature review on the correlations of the water absorption (y) and the SSD density (x)

	Proposed regression	**R^2**
Ihobe and CEDEX (2011)	y=-17.286x+44.819	0.91
Agrela et al. (2011)	y=-24.086x+63.050	0.83
Mas et al. (2012b)	y=-24.086x+63.050	0.83

Table 4.23: Literature review on the correlations of the water absorption (y) and the OD density (x)

	Proposed regression	**R^2**
Ihobe and CEDEX (2011)	y=-24.224x+63.301	0.82
Silva et al. (2014)	$y= 1 \cdot 10^{-9}x^3+3 \cdot 10^{-6}x^2-0.0446x+78.745$	0.91

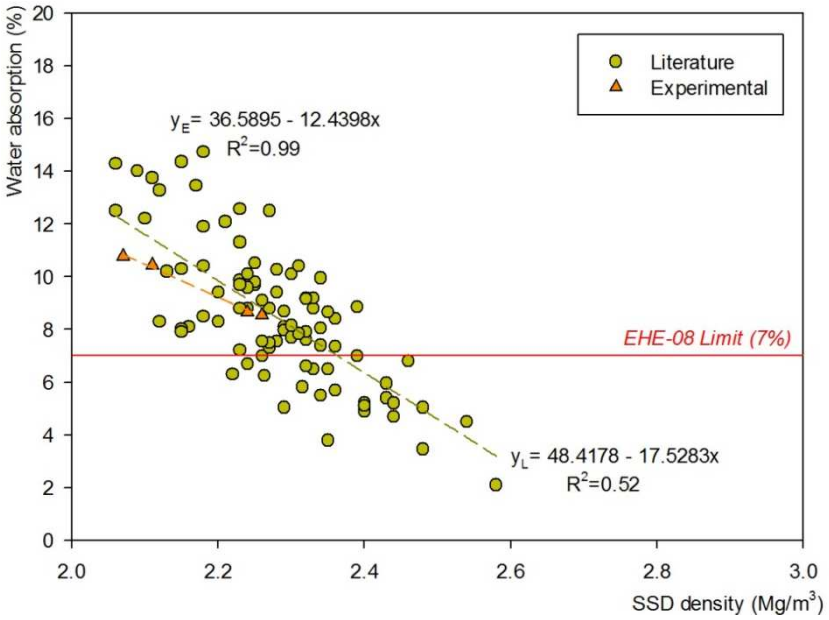

Figure 4.18: Relationship between the water absorption and the SSD density

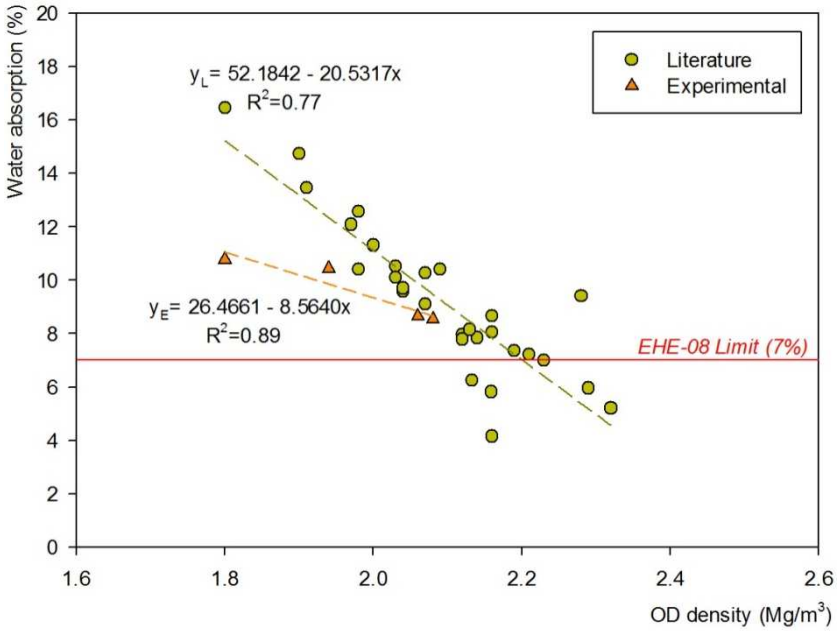

Figure 4.19: Relationship between the water absorption and the OD density

3.1.6. MECHANICAL RESISTANCE

Several test methods exist in order to evaluate the mechanical resistance of the aggregates, including aggregate crushing value, aggregate impact value, 10% fine value and Los Angeles abrasion value. The EHE-08 (Permanent Commission on Concrete, 2008) recommends the use of the Los Angeles test to assess resistance to erosion of coarse aggregates through abrasion, wear and impact, with higher values indicating a lower mechanical resistance of the aggregate.

Whilst a value of 40% is set as the general limit of this property, the Code on structural concrete (Permanent Commission on Concrete, 2008) also allows the use of aggregates with Los Angeles coefficient up to 50% in mass or reinforced concrete with target strength of 30 MPa provided that satisfactory experimental results exist supporting such use.

Table 4.24 displays the Los Angeles coefficient values for the recycled aggregates used in this research work, which are comparatively higher than the Los Angeles coefficient exhibited by the natural coarse aggregate. Although all of them could be deemed suitable under the EHE-08 (Permanent Commission on Concrete, 2008) restrictions, the sample RA-L(S) would only be apt for concrete with target strength up to 30 MPa. The obtained results are in good agreement with those found in the literature, as approximately 59% of the reviewed recycled aggregates have a Los Angeles coefficient between 33% and 41%.

Table 4.24: Los Angeles coefficient

	Los Angeles coefficient (%)
Gravel	18.00
RA-L(S)	40.99
RA-L(B)	39.00
RA-M(S)	33.23
RA-H(S)	40.00

Several authors have identified the mechanical resistance as a constraining property in the use of recycled aggregates from CDW because of the presence of weak components (attached mortar, ceramics and impurities) (Vegas et al., 2008; Jiménez et al., 2011). However from the research work performed by Silva et al. (2014), it is possible to conclude that the mechanical resistance of recycled aggregates comes in third as a limiting factor of the use of the recycled aggregates in the concrete manufacture after the oven-dry density and the water absorption. The analysis of the literature review (Table 4.25) shows that approximately 74% of the mixed recycled aggregates comply with the 40% limit stipulated, and nearly the remaining 25% of them are encompassed between the 40% and 50% limits, with just one sample exceeding the 50% limit. Nonetheless, a great dispersion of the result can be observed in the literature.

Table 4.25: Literature review on the Los Angeles coefficient of the recycled aggregates

	Los Angeles coefficient (%)
Mixed recycled aggregates	*38.09 (29.00-50.20)*
Parra y Alfaro (2001)	40.25 (36.00-43.00)
Dhir and Paine (2007)	32.33 (30.00-36.00)
Ihobe and CEDEX (2011)	40.00 (33.00-47.00)
Vegas et al. (2011)	39.20 (37.00-41.00) 30.60 (29.00-32.00)
Agrela et al. (2012)	38.40 (38.20-38.60)
Barbudo et al. (2012a)	38.00 (31.00-45.00) 38.00 (30.00-43.00)
Galvín et al. (2012)	35.25 (31.00-40.00)
Jiménez et al. (2012a)	36.00
Jiménez et al. (2012b)	31.00
Mas et al. (2012a)	43.33 (43.00-44.00)

Table 4.25: Literature review on the Los Angeles coefficient of the recycled aggregates (continued)

	Los Angeles coefficient (%)
Mas et al. (2012b)	41.00 (36.00-44.00)
Martínez-Lage et al. (2012)	49.00
Galvín et al. (2013)	34.26 (31.34-36.26)
Geraldes (2013)	42.33 (38.00-49.00)
López-Gayarre et al. (2013)	48.00
Galvín et al. (2014)	36.30 (31.00-43.00)
Gómez-Meijide and Pérez (2014)	38.00
Rodríguez-Robles et al. (2014)	38.91 (31.27-50.20)
100% recycled ceramic aggregates	*34.88 (20.00-60.00)*
Khaloo (1995) [a]	23.20 (22.80-23.60)
Parra y Alfaro (2001) [b]	36.00
Senthamarai and Devadas Manoharan (2005) [c]	28.00
Dhir and Paine (2007) [b]	53.00 (48.00-60.00)
Debieb and Kenai (2008) [b]	31.60
Vegas et al. (2011) [b]	34.00
Medina et al. (2013) [d]	20.00
Sata et al. (2013) [b]	42.50
Silvestre et al. (2013) [e]	21.00

[a] tiles, [b] brick, [c] ceramic electrical insulator, [d] sanitary ware, [e] porcelain stoneware tiles

3.1.6.1. *Relationship between the Los Angeles coefficient and the constituents*

In accordance with Vegas et al. (2011), the ceramic material is the fraction with the greatest influence in the mechanical resistance of the mixed recycled aggregates. As previously stated for the flakiness index of the mixed recycled aggregates, several researchers have proposed linear regressions correlating the Los Angeles coefficient and the ceramic content of the mixed recycled aggregates (Table 4.26).

Table 4.26: Literature review on the correlations of the Los Angeles coefficient (y) and the ceramic content (x)

	Proposed regression	R^2
Vegas et al. (2011)	y=0.2701x+31.13	0.80
Barbudo et al. (2012a)	y=0.2815x+32.95	0.79
Geraldes (2013)	y=-0.087x+39.115	0.23

According to the correlation proposed by Vegas et al. (2011), in order to comply with the 40% limit of the Los Angeles coefficient, the mixed recycled aggregate should contain less than 33% of ceramics. However, Figure 4.20 displaying the Los Angeles coefficient value of all the recovered investigations as a function of the ceramic content shows that recycled aggregates with a higher ceramic content are able to comply with the 40% limit. Both the linear regression calculated for the literature and experimental data show a low R^2 fitting as per the wide dispersion of the results.

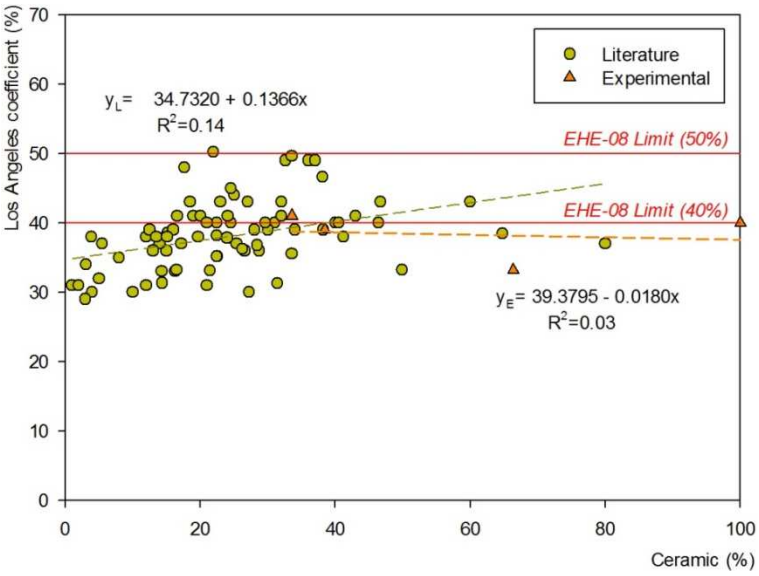

Figure 4.20: Relationship between the Los Angeles coefficient and the ceramic content

In spite of recycled concrete aggregates being more resistant to fragmentation than recycled ceramic aggregates, it has been found that the higher Los Angeles coefficient values of recycled concrete aggregates compared to natural coarse aggregates are due to the removal of the adhered mortar during Los Angeles test, which increments the mass loss in the recycled aggregates (Sánchez de Juan and Alaejos Gutiérrez, 2009). The results from the research works of Barbudo et al. (2012a) also indicated that the increasing content of unbound aggregates and cement based materials produced a decrease in the mass loss due to the Los Angeles abrasion test, proposing a linear correlation (y=-0.2369x+56.468; R^2=0.78) between the Los Angeles coefficient and the content of unbound aggregates and cement based materials in the mixed recycled aggregates. However, once again when the linear regression is extended to all the literature values (Figure 4.21), the strength of the correlation is extremely low due to the high dispersion of the retrieved values.

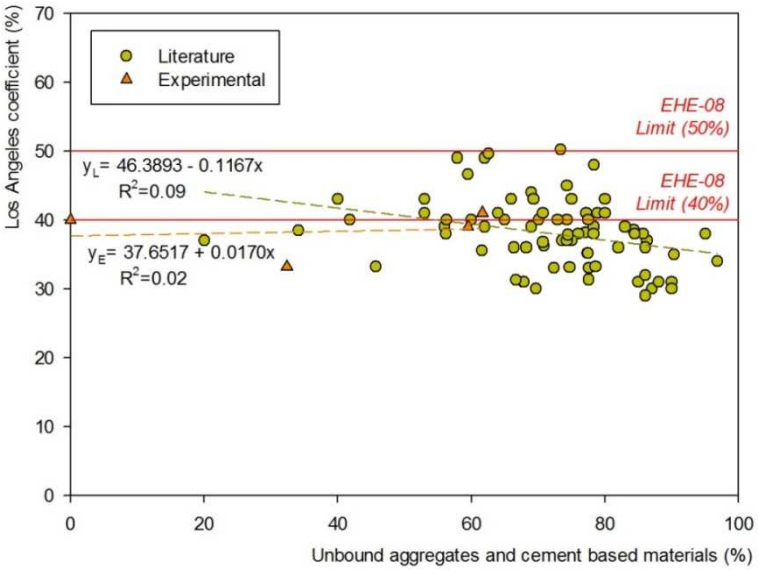

Figure 4.21: Relationship between the Los Angeles coefficient and the unbound aggregates and cement based materials content

Finally, in order to assess the possibility of more linear dependences between the composition parameters of the recycled aggregates from the literature review and their Los Angeles coefficient values, a Pearson product-moment correlation analysis was performed (Table 4.27). Four significant correlations were detected (p-value<005). Two of them were the expected linear dependencies between mechanical resistance and unbound and cement based materials (Barbudo et al., 2012a) and Los Angeles coefficient and ceramic content (Vegas et al., 2011; Barbudo et al., 2012a; Geraldes, 2013). In addition, a third correlation was identified linking the asphalt content and the Los Angeles coefficient, in such manner that an increase in the asphalt content produces a decrease in the Los Angeles coefficient. This relationship between the asphalt content and the resistance to fragmentation of the recycled aggregates has been also detected in the report signed by the Spanish institutions Ihobe and CEDEX (2011). Finally, the content of glass presented the lowest significant influence. Since the brittle nature of the glass, it is clear that higher amounts of this material would tend to lower the mechanical resistance of the recycled aggregate.

Table 4.27: Pearson correlation analysis on the Los Angeles coefficient of the mixed recycled aggregates in the literature review

	Rc	Ru	Rc+Ru	Rb	Ra	Rg	X1	X2
Los Angeles coefficient	-0.0493	-0.2040	-0.3060	0.3750	-0.4510	0.2180	0.1090	0.2650
	0.7060	0.1140	0.0044	0.0004	0.0000	0.0453	0.3210	0.0141

3.1.7. ADHERED MORTAR

The origin of the construction and demolition wastes and production procedure used at the CDW recycling plants are accountable for the composition of the recycled aggregates as a mixture of natural aggregates, concrete lumps, masonry particles and impurities but also for the amount of mortar attached to the aggregates. On one hand, the mortar content increases with the strength of the parent concrete due to a better bond mortar-aggregate (Padmini et al., 2009); on the other hand, the study of Nagataki et al. (2000) has illustrated how the crushing procedure influences the final mortar content of a sample and that when the RCA was subjected to a second step of jaw and impact crushing the mortar content could be reduced between 10% and 20%. In addition, the bond between the aggregate and the mortar is influenced by the shape, porosity and surface roughness of the aggregate.

Several researchers have found the presence of residual mortar attached to the surface of the particles comprising the recycled aggregates at fault for the worsening of the physical (porosity, density and water absorption) and mechanical performance of RCA due to the porous and weak nature of the layer of mortar covering the aggregates (Sánchez de Juan and Alaejos Gutiérrez, 2009; Ismail and Ramli, 2013; Pepe et al., 2014; Seo and Choi, 2014). Furthermore, given the evident relationship between the quality of the recycled aggregate and the performance of the new concrete, several investigations have been directed to assess the effect of the mortar attached to the RCA (Katz, 2003; Tam et al., 2007; Padmini et al., 2009; Quan et al., 2010; Ismail and Ramli, 2013; Pepe et al., 2014). However, an essential issue in these investigations has been the lack of a standardized method for assessing the amount of adhered mortar in recycled aggregates. Hence, different researchers have proposed and followed different approaches to quantify the mortar content of the recycled aggregates:

1. **Production of new concrete with coloured cement** (Hansen and Narud, 1983; Ravindrarajah and Tam, 1985). Since the new paste of the recycled concrete and the old mortar attached to the recycled aggregates present different colours, a quantification of the attached mortar as a volume percentage by means of a linear transverse method (similar to the air void determination) is simpler. More recently, Abbas et al. (Abbas et al., 2009) validated their method of soaking the recycled aggregate in a salt solution coupled with freeze-thaw cycles by assessing a polished slice of recycled concrete made with white cement by means of image analysis.

2. **Thermal shock**. This method is based on the detachment of the adhered mortar after subjecting a wet sample to a thermal shock, i.e. heating in a furnace (500ºC during 2 hours) and immediately submerging in cold water. According to Zoldners (1971), at temperatures higher than 400ºC the dehydration of the calcium hydroxide takes place. Then, any remaining mortar could be easily removed with a rubber hammer. The rapid evaporation of the water inside the mortar pores causes the disintegration of the mortar layer without damaging the aggregate, as the wetting time (2 hours) is not enough to saturate the aggregates pores. This technique has been predominantly employed by Spanish researchers (Barra Bizinotto, 1996; Sánchez de Juan, 2004; Sánchez de Juan and Alaejos Gutiérrez, 2009), although Pepe et al. (2014) also employed this method as a second step in their proposed method of autogenous cleaning. Butler et al. (2011) found this method to be the most effective with an almost complete mortar removal in the sample.

3. **Soaking in an acidic solution**. This has been the most employed method (Dhir et al., 1999; Limbachiya et al., 2000; Nagataki et al., 2000; Tam et al., 2007; Choi and Kang, 2008; Quan et al., 2010; Butler et al., 2011; Ismail and Ramli, 2013; Duan and Poon, 2014; Seo and Choi, 2014). The process consists of the immersion of the sample into an acid solution in order to remove the mortar and afterwards the recycled aggregates are washed to remove any acidic solvents. It has been proven that after the treatment, the recycled aggregates are not adversely affected in terms of chloride or sulphate contents (Tam et al., 2007). Currently, hydrochloric, sulphuric and phosphoric acid (Tam et al., 2007) and nitric acid (Butler et al., 2011) have been tested, although hydrochloric acid has been the most employed in the rest of the investigations. Concerning the concentration of the acid solution, Tam et al. (2007) suggested that a 0.10 M solution is enough to remove the mortar without compromising the aggregate quality and although Ismail and Ramli (2013) also concluded that lower concentrations (0.10 M and 0.50 M) could significantly reduce the mortar content, they preferred higher concentrations (0.8 M) due to the linear correlation between the effectiveness of the cleaning process and the molarity of the acid employed. Regarding the time needed for the treatment, differences exist among researchers, i.e. Tam et al. (2007) indicated 24 hours for the treatment, Ismail and Ramli (2013) suggested no more than 3 days and Seo and Choi (2014) recommended to repeat the 24 hours treatment as many times as necessary until no more changes in weight are detected.

The main disadvantage of this method is that it is not viable for limestone aggregates, since these would be attacked by the acid. Nonetheless, Nagataki et al. (2000) used this method for carbonate aggregates and applied a correction factor to account for the effect of the acid on the aggregate.

4. **Freeze-thaw cycles while soaking in a salt solution**. This method was proposed by Abbas et al. (2008) and consists of the immersion during 24 hours of the recycled aggregates in a salt solution (26 wt% sodium sulphate) before subjecting the sample to 5 cycles of freeze-thaw while submerged in the salt solution, where 16 hours of freezing (-17ºC) are followed by 8 hours of thawing (80ºC). In order to validate their method, Abbas et al. (Abbas et al., 2009) carried out a second experiment to determine the mortar attached by the image analysis of a concrete made with a binder of different colour. As part of their investigations comparing the effectiveness of three different methods, Butler et al. (2011) concluded that between a 80% and 90% rate of mortar removal is achieved with this method which is better than the acid soaking approach but worse than the thermal shock treatment.

5. **Mechanical abrasion and thermal shock**. The method is based on the fact that the processing (several crushing procedures) of the construction and demolition wastes produced a reduction in the content of mortar attached to the recycled aggregates. An autogenous cleaning method was proposed by Pepe et al. (2014). This method consists of the removal of the adhered mortar by the mechanical abrasion that the recycled aggregate particles generate when colliding ones against others in a rotating mill drum at 60 rpm during 30 minutes. However, after this procedure the authors followed the thermal method previously described.

6. **Microwave treatment**. The removal is based upon the differences in electromagnetic properties, water absorption and tensile strength of natural aggregates and mortar. The method consists of microwaving the saturated aggregates for 1 minute at 10 kW and immediately cooling them down in water at 25ºC, which is less aggressive than the conditions set up in the thermal shock or the acidic soaking method (Akbarnezhad et al., 2011).

Except the first approach, the actual quantification of the mortar content in all methods involves the same procedure. Before any measure is recorded the treated sample is washed, sieved in order to separate the disaggregated mortar and oven dried until a constant mass is reached. Then, the recorded weight is compared to the initial value registered for the sample and the mortar content is calculated as the percentage of the differential weight.

Table 4.28 and Figure 4.22 show the results obtained with the different methods found in the literature review. The wide dispersion of the results gives an idea about the different levels of effectiveness achieved with each technique.

Table 4.28: Literature review on the mortar content attached to recycled concrete aggregates (as percentage of the initial weight of aggregates with attached mortar)

Method	Reference	Mortar removed (%)
#1	Hansen and Narud (1983)	25.00-60.00
	Ravindrarajah and Tam (1985)	52.00- 54.00
	Abbas et al. (2009)	21.00-43.00
#2	Barra (1996)	51.70-52.90
	Sánchez de Juan and Alaejos Gutiérrez (2009)	23.00-55.00
	Butler et al. (2011)	46.00-56.00
	Pepe et al. (2014)	30.00
#3	Dhir et al. (1999)	5.50-7.20
	Limbachiya et al. (2000)	9.30-11.50
	Nagataki et al. (2000)	52.30- 55.70
	Quan et al. (2010)	8.00-68.40
	Butler et al. (2011)	20.00-32.00
	Ismail and Ramli (2013)	0.40-5.11
	Duan et Poon (2014)	14.30- 63.80
	Seo and Choi (2014)	4.50-6.60
#4	Abbas et al. (2008)	21.00-43.00
	Butler et al. (2011)	30.00-41.00
#5	Pepe et al. (2014)	15.00
#6	Akbarnezhad et al. (2011)	15.00-23.00

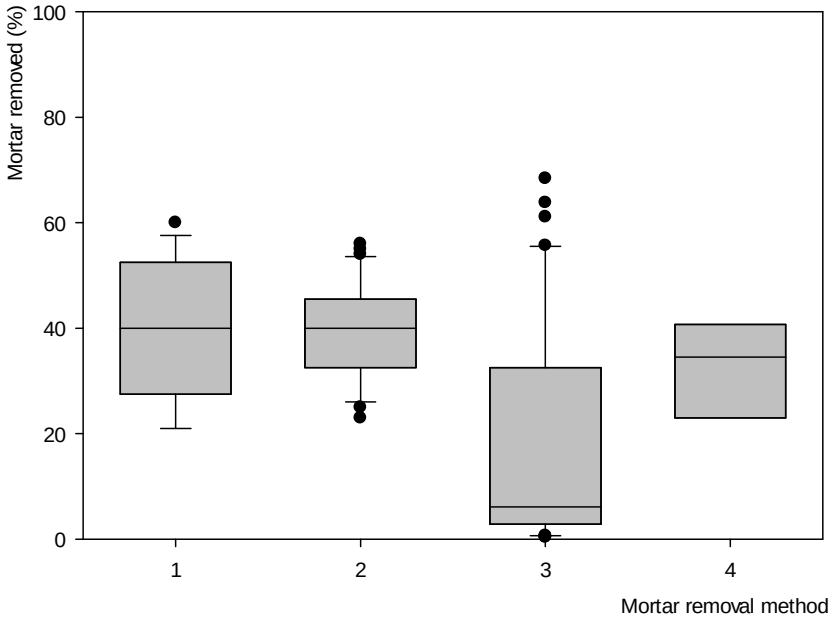

Figure 4.22: Literature review on the mortar content attached to recycled concrete aggregates

To date, all these methods have been employed on recycled concrete aggregates; and so, could be advisable to review their operating parameters for using them on other types of aggregates. For instance, the methods based on the thermal shock and the mechanical abrasion have the potential to damage the mixed and ceramic recycled aggregates as well as the mortar. In the first case, the highest and fastest water absorption capability of the ceramic components should be taken into account since a 2 hours period of soaking will lead to a high level of pore saturation in the interior of the aggregate and not only in the mortar attached. In section 3.1.5 of the present chapter, a detailed description of the evolution of water absorption with time can be consulted. In the second case, as proven with the results arising from the Los Angeles test, ceramic particles have been identified more susceptible to the abrasion, and thus the degradation produced with this method would not be limited to the outer layer of attached mortar covering the aggregates if applied to mixed or ceramic recycled aggregates.

In the end, the soaking in an acid environment and the freeze-thaw cycles while immersed in a salt solution were the approaches selected in this investigation as they were believed to be more suitable for mixed and ceramic recycled aggregates. Table 4.29 displays the results obtained for the different methods. After the treatment of the recycled aggregates with the 0.10 M hydrochloric acid solution, significant amounts of adhered mortar remained attached to the samples; hence in an attempt to remove the remaining cement paste a second treatment was performed. Although it was observed that the amount removed in this second stage was inferior, the recycled aggregates were not perfectly cleaned, which indicated that only the outer layer of mortar was removed in each soaking stage. According to the findings of Ismail and Ramli (2013), the increase of the molarity of the hydrochloric acid solution could be used to increase the rate of mortar removal. The results achieved with this adjustment in the method of soaking in acid are similar of those obtained with the frost damage approach, which is considered to have a higher rate of success in the cleaning of the recycled aggregates (Butler et al., 2011).

Table 4.29: Mortar content of recycled aggregates (as percentage of the initial weight of aggregates with attached mortar)

	Mortar loss (%)		
	RA-L(S)	**RA-L(B)**	**RA-H(S)**
0.10 M HCl-First treatment	1.97	1.77	1.10
0.10 M HCl-Second treatment	1.36	1.23	0.76
0.10 M HCl-Total	3.33	3.00	1.86
1.00 M HCl	33.38	27.51	8.00
26% Na_2SO_4	34.42	17.53	4.06

3.2. MICROSTRUCTURAL CHARACTERIZATION

3.2.1. X-RAY FLUORESCENCE

X-ray fluorescence (XRF) tests were employed to determine of the chemical composition of natural and recycled aggregates. The typical chemical - elemental composition, i.e. oxides, and the loss on ignition (LOI) - of the natural aggregates is that of a conventional siliceous sand and gravel respectively (Table 4.30).

Table 4.30: XRF analysis of the natural aggregates

	Siliceous sand	Siliceous gravel
SiO_2 (%)	95.90	98.090
Al_2O_3 (%)	2.340	1.170
Fe_2O_3 (%)	1.061	0.269
K_2O (%)	0.383	0.136
CaO (%)	0.161	0.054
TiO_2 (%)	0.167	-
MnO (%)	0.047	-
CuO (%)	0.027	-
ZrO_2 (%)	0.027	-
LOI (%)	0.57	0.25

The chemical composition, expressed as percentage by weight, of the three Spanish recycled aggregates is shown in Table 4.31.

Table 4.31: XRF analysis of the Spanish recycled aggregates

	RA-L(S)	RA-M(S)	RA-H(S)
SiO_2 (%)	48.49	53.25	59.63
Al_2O_3 (%)	10.26	10.68	18.51
CaO (%)	17.81	15.56	4.78
Fe_2O_3 (%)	2.45	3.36	5.92
K_2O (%)	3.21	2.38	3.59
MgO (%)	1.91	2.65	3.12
SO_3 (%)	2.62	0.4	0.42
Na_2O (%)	0.86	0.49	0.73
TiO_2 (%)	0.26	0.45	0.84
P_2O_5 (%)	0.13	0.1	0.15
MnO (%)	0.03	0.03	0.09
As (ppm)	3	15.5	16
Ba (ppm)	-	4.5	23
Cl (ppm)	232	200	215
Co (ppm)	12	34.5	34
Cr (ppm)	407	101.5	323
Cu (ppm)	-	126	6
Ni (ppm)	33	65	71
Pb (ppm)	26	41.5	233
Sb (ppm)	7	96.5	19
Sr (ppm)	146	21	95
Th (ppm)	75	49	192
V (ppm)	27	229.5	98
Zn (ppm)	17	70	125
Zr (ppm)	-	44	174
LOI (%)	11.93	10.65	2.15

The main oxides were silicon oxide (SiO_2) ranging between 48.49% and 59.63 %, aluminium oxide (Al_2O_3) which ranged from 10.26% to 18.51% and calcium oxide (CaO), followed by high loss on ignition (LOI) values (2.15-11.93 %). Note that both the amount of SiO_2 and Al_2O_3 increased as the aggregate presented a higher ceramic quantity and that the content of CaO and LOI decreased with the ceramic percentage in the sample (Figure 4.23).

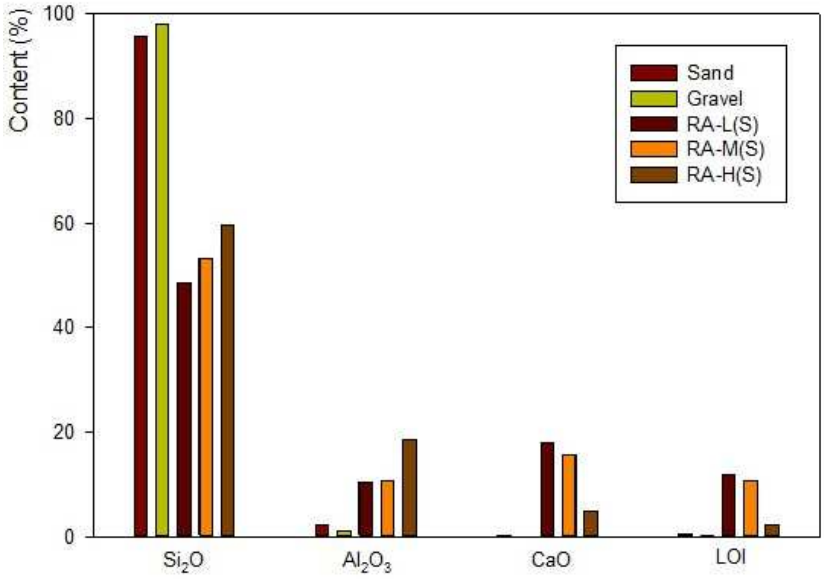

Figure 4.23: Comparison of main components in the aggregates

The great contents of Al_2O_3 and SiO_2 determined for all samples are indicative of the occurrence of clay minerals and quartz in the recycled aggregates. As both aluminium and silicon oxides are typical components of brick and tiles (Sánchez de Rojas et al., 2006), their content in the sample directly alludes to the ceramic content present in the recycled aggregate. Moreover, higher percentages of Al_2O_3 in the RA-H(S) sample are consistent with the origin of the recycled aggregate, i.e. red brick wastes (Angulo et al., 2009).

As CaO content principally originates from the binder (Angulo et al., 2009), the higher percentages in samples RA-L(S) and RA-M(S) are motivated by the presence of both adhered mortar and old concrete particles forming the mixed recycled aggregates, while the composition of the RA-H(S) sample, i.e. 100% ceramic recycled aggregates, contained lower CaO values partly resulting from some adhered mortar to the brick and tile waste.

The values of LOI indicate the mass loss due to carbon oxidation, decomposition of carbonates and water evaporation in the sample. The results obtained point out that the RA-H(S) sample presented fewer amounts of impurities, i.e. organic matter such as plastic, wood, cardboard and paper. However, the results of LOI should not be directly extrapolated to organic matter values due to the lack of selectiveness in the method (Vegas et al., 2011), as it was discussed in section 3.1.1 of this chapter.

Lastly, comparing the number and species of oxides detected, the analysis found 22 elements common to the three aggregates, while barium, cooper and zirconium were not detected in the RA-L(S) sample. For instance, the absence of zirconium in the recycled aggregate with lower ceramic content could suggest that no glazed materials formed part of the waste since this element is mainly associated to the enamel of certain ceramic materials (Medina Martínez, 2011).

Despite the importance of knowing the chemical composition of materials as heterogeneous as construction and demolition wastes, the studies conducted on the characterization of recycled aggregates is mostly based on the testing of physical and mechanical parameters. Currently, only a few research works (Dhir and Paine, 2007; Limbachiya et al., 2007; Angulo et al., 2009; Gedam et al., 2012; Leiva et al., 2013) determined the chemical composition of coarse recycled aggregates from CDW by means of XRF analysis (Figure 4.24 a and b).

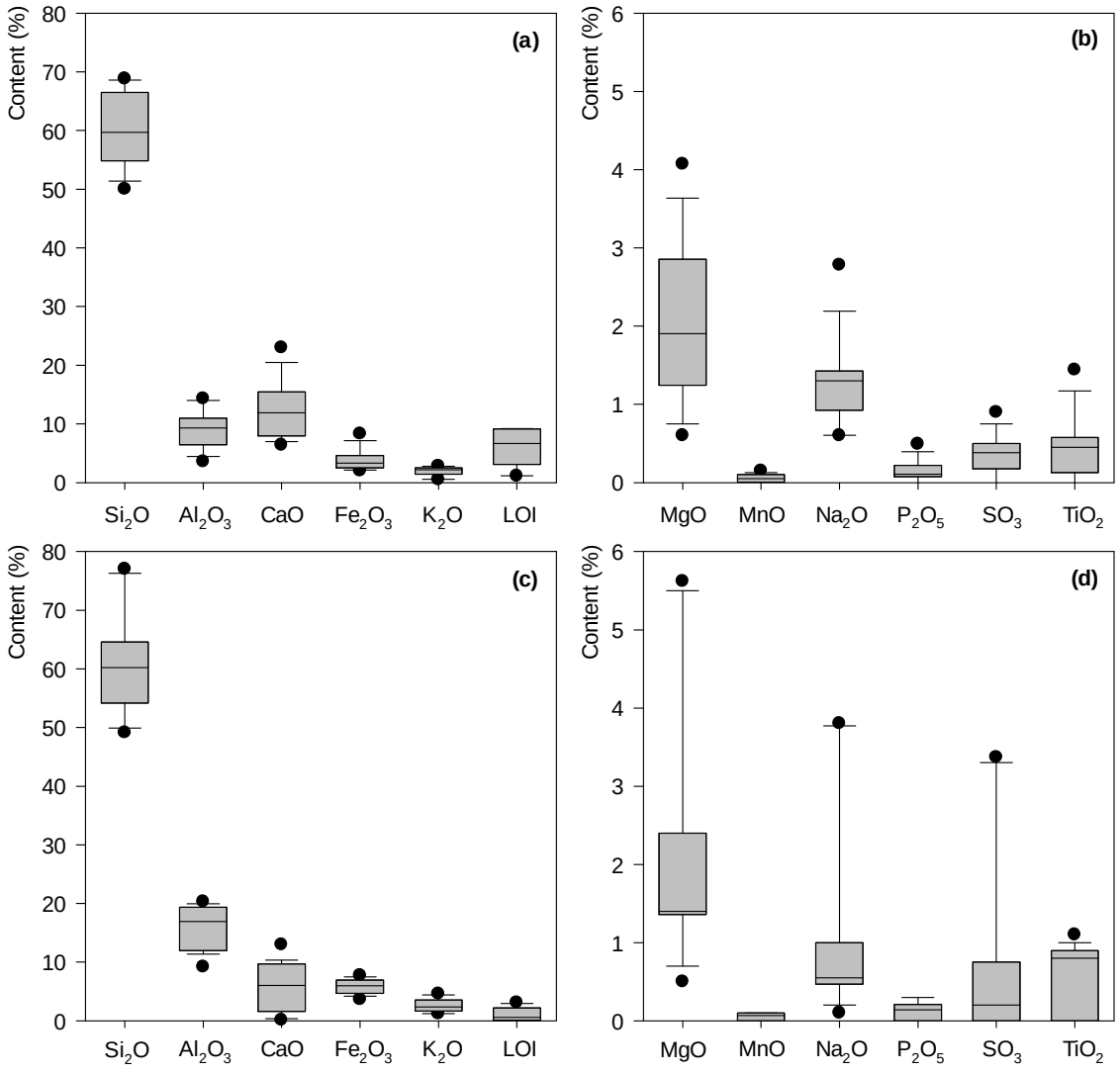

Figure 4.24: Main oxides of concrete and mixed CDW (a) and clay brick and tiles (c), and minor oxides of concrete and mixed CDW (b) and clay brick and tiles (d) found in the literature

Besides, the ceramic composition of the recycled aggregates, in particular that of the RA-H(S) sample, makes the review of XRF studies on clay bricks and tiles interesting (Sánchez de Rojas et al., 2006; Dhir and Paine, 2007; Sánchez De Rojas et al., 2007; Lavat et al., 2009; Molineux et al., 2009; Naceri and Hamina, 2009; Pacheco-Torgal and Jalali, 2010a; Reig et al., 2013a, 2013b) – the two more common ceramic components present - as well as the only work on masonry CDW (Müllller, 2004) in order to establish a point of comparison for the results obtained (Figure 4.24 c and d).

As shown in Figure 4.24, the literature review backs up the findings of SiO_2, Al_2O_3 and CaO as the major oxides, followed by LOI values in the CDW materials and Fe_2O_3 content in ceramic materials. The comparison of the results reviewed confirms that Al_2O_3 and Fe_2O_3 quantities are lower and the LOI values are higher for CDW without significant ceramic presence. In terms of minority components, the variability between works is higher indicating that the source of the waste as well as the conditions that these materials have been exposed to play an important role.

Finally, Figure 4.25 displays a common CaO-Al_2O_3-Si_2O ternary diagram where the different aggregates are plotted as function of the normalized content of the aforementioned oxides.

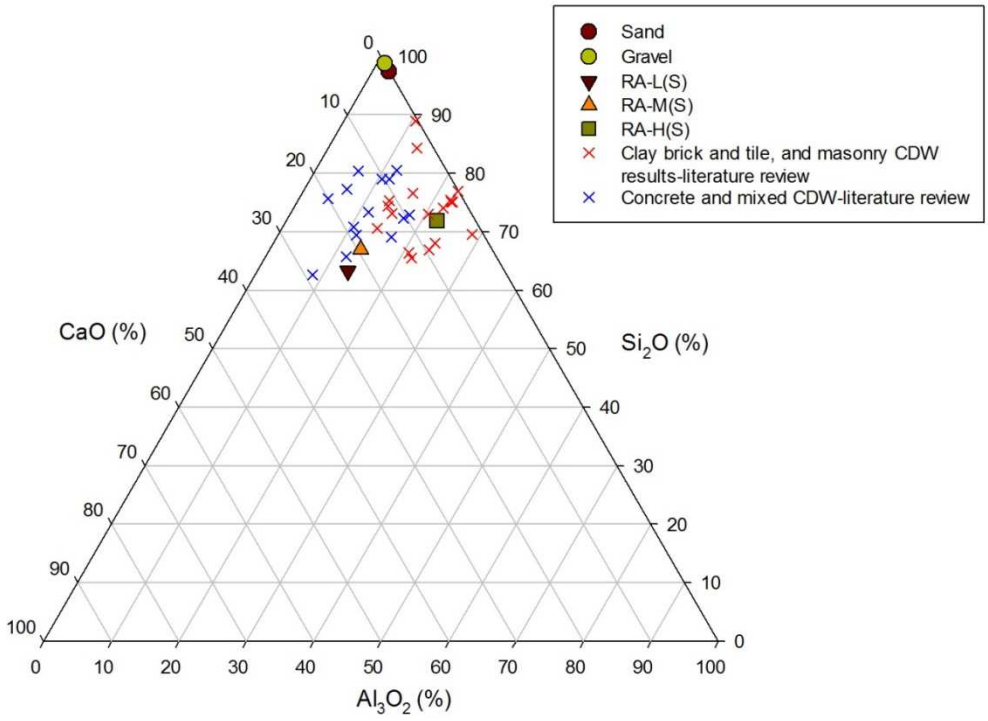

Figure 4.25: CaO-Al_2O_3-Si_2O ternary diagram

Natural sand and gravel are represented at the top of the triangle as they basically are composed of SiO_2 with minor quantities of CaO. The position occupied by the recycled aggregates in the plot suggests a composition typical of pozzolanic materials, but nonetheless the mixed and ceramic recycled aggregates are visibly separated in the diagram in two different groups integrated by the results collected from literature of XRF analysis on clay bricks and tiles, and masonry CDW (Müllller, 2004; Sánchez de Rojas et al., 2006; Dhir and Paine, 2007; Sánchez De Rojas et al., 2007; Lavat et

al., 2009; Molineux et al., 2009; Naceri and Hamina, 2009; Pacheco-Torgal and Jalali, 2010a; Reig et al., 2013a, 2013b) and concrete and mixed recycled aggregates from construction and demolition (Dhir and Paine, 2007; Limbachiya et al., 2007; Angulo et al., 2009; Gedam et al., 2012; Leiva et al., 2013).

3.2.1.1. *Alkali content and alkali reactive constituents*

The reaction between the cement alkalis and the reactive components of the aggregates, commonly known as alkali-aggregate reaction (AAR), is responsible for an expansion phenomenon causing the damage of the concrete. In addition, the presence of releasable alkalis when employing recycled aggregates should be assessed.

Although in conventional concrete the majority of alkalis come from the cement, recycled aggregates are susceptible to be a source of sodium and potassium oxides and contribute to the presence of these chemical species in recycled concrete if a release of alkalis takes place into the concrete pore solution. For example, aggregates containing feldspars tend to liberate significant amounts of alkalis with time (Bérubé et al., 2002), and a similar behaviour could be presumed for other alkali rich aggregates, which would enhance the possibility of a concrete expansion due to AAR. For the experimental data and the literature review, the alkali content was determined as a total equivalent sodium oxide (Na_2O_{eq}), calculated as the sodium oxide percentage plus 0.658 times the potassium oxide percentage (Table 4.32 and Table 4.33). The results show that the alkali content of the recycled aggregates is within the range of other CDW or ceramic materials, but 23-34 and 3-6 times higher than the gravel and the cement respectively. Hence, it is possible to conclude that the use of the recycled materials entails an additional risk.

Table 4.32: Alkali content of the materials used

	Na_2O_{eq} (%)
CEM III/A 42.5 N SR	0.53
CEM III/B 42.5 N SR LH LA	0.65
Siliceous sand	0.25
Siliceous gravel	0.09
RA-L(S)	2.97
RA-M(S)	2.06
RA-H(S)	3.09

Table 4.33: Alkali content of the literature data (calculated)

	Na_2O_{eq} (%)
Concrete and mixed CDW	2.52 (1.21-3.89)
Dhir and Paine (2007)	2.53 (1.85-3.01)
Limbachiya et al. (2007)	1.38 (1.21-1.59)
Angulo et al. (2009)	2.86 (2.48-3.08)
Gedam et al. (2012)	3.10 (2.91-3.44)
Leiva et al. (2013)	1.84
Medina et al. (2015)	3.89

Table 4.33: Alkali content of the literature data (calculated) (continued)

	Na_2O_{eq} (%)
Ceramic materials	2.89 (0.89-4.63)
Dhir and Paine (2007)	2.24 (0.89-3.74)
Molineaux et al. (2009)	2.50
Reig et al. (2013a, 2013b)	3.40
Naceri and Hamina (2009)	2.05
Sánchez de Rojas et al. (2006; 2007)	2.54
Lavat et al. (2009)	4.60 (4.59-4.63)
Pacheco-Torgal and Jalali (2010a)	3.20 (3.16-3.23)
Müller (2004)	3.20
Medina et al. (2015)	2.00

Regarding to the intrinsic reactivity of constituents of the recycled aggregates to the alkalis, the EHE-08 (Permanent Commission on Concrete, 2008) establishes that the recycled aggregates should be considered as potentially reactive and tested accordingly. Hence, further testing was performed in order to ascertain the possible deleterious effects that the alkalis present in the recycled aggregates pose to the durability performance of the recycled concrete (chapter 9).

3.2.1.2. *Sulphate content*

If compared the results arising from the XRF analysis (Table 4.31) with the 0.80% limit for sulphate content imposed by the EHE-08 (Permanent Commission on Concrete, 2008), only the sample RA-L(S) would be unsuitable for the concrete manufacture with a 2.62% sulphate content most likely due to the high gypsum content in the sample. Although some researchers consider that the limitation to the sulphate content would be more adequate if applied to the total sulphur content of the sample (Karlsen et al., 2002; Vincke et al., 2002), the requirement in the Spanish standard refers to water soluble sulphate. Thus, applying the formula ($y=0.301x+0.017$; $R^2=0.98$) proposed by Vegas et al. (2011) to transform the total sulphate content in water soluble sulphates values, the water soluble sulphate content of the sample RA-L(S) could be estimated at 0.81%, barely exceeding the Spanish limitation but complying with the recommendations imposed by RILEM TC 121-DRG (1994). In any case, to prevent a possible expansive problem that may be caused by the use of mixed recycled aggregates, sulphate-resistant cement should be used to ensure a good durability of the recycled concrete (Mas et al., 2012b).

The literature review (Table 4.34) shows that while some recycled aggregates do not have problems to comply the sulphates constraint others largely surpass the imposed limitation, which is mainly due to the proportions of the constituents in the sample.

Table 4.34: Literature review on the sulphate content of the mixed recycled aggregates

	Acid soluble sulphate (%)	Water soluble sulphate (%)
Dhir and Paine (2007)	0.50	-
	0.43 (0.00-1.90) [a]	-
Vegas et al. (2011)	-	0.34 (0.14-0.60)
	-	0.03 (0.02-0.04)
	-	0.03 [a]
Agrela et al. (2011)	0.56 (0.04-1.71)	-
	1.52 (0.56-4.45)	-
Agrela et al. (2012)	0.71 (0.69-0.72)	-
Barbudo et al. (2012a)	1.30 (0.32-4.56)	0.47 (0.01-1.56)
	1.80 (0.73-6.19)	0.87 (0.02-3.93)
Barbudo et al. (2012b)	-	0.89 (0.33-1.56)
Jiménez et al. (2012a)	-	0.70
Jiménez et al. (2012b)	-	1.60
Mas et al. (2012a)	3.54 (0.36-6.98)	-
Mas et al. (2012b)	4.76 (2.21-6.98)	-
Martínez-Lage et al. (2012)	0.32	0.12
Galvín et al. (2013)	-	1.07 (0.78-1.56)
Geraldes (2013)	1.75 (0.71-2.78)	0.45 (0.16-0.74)

[a] crushed brick

3.2.1.2.1. Relationship between the sulphate content and the constituents

The sulphate content in mixed recycled aggregates sources from the adhered mortar, the crushed clay bricks, the gypsum and even the natural aggregates, although comparatively this value is negligible. The sulphate originating from the concrete and mortar is due to the addition of gypsum to the clinker, in order to regulate, i.e. retard, the setting of the cement based materials. According to Sánchez de Juan et al. (2009), the maximum content of sulphates in an average concrete mixture is 0.50% since the UNE EN 197-1 (2011) limits to 4% the sulphate content in the cement. In terms of ceramic particles, the studies performed by Poon and Chan (2006a), Vegas et al. (2011), Agrela et al. (2012) and Barbudo et al. (2012b) indicate that the sulphate content of the recycled aggregates increases, to a limited extent, with the ceramic proportion on the sample. The gypsum is the main responsible for the sulphate content in mixed recycled aggregates due to its chemical composition and high solubility (Vegas et al., 2011); nonetheless, the findings obtained by Vegas et al. (2011) and Barbudo et al. (2012b) support the fact that other typical constituents (mortar and ceramic) contribute to the sulphate content of the mixed recycled aggregates, since this ionic species is still present even when no visible gypsum particles were detected according to UNE 933-11 (2009). Thus, several researchers have proposed formulas relating the sulphate content of a sample with its gypsum (Table 4.35) and ceramic (Table 4.36) content, in order to have a simpler way to assess the risk of using recycled aggregates. However, the R^2 values of the linear regressions when all the available data of sulphates content are linked with the amount of gypsum or ceramic of the recycled aggregates are extremely low due to the dispersion of the literature review data.

Table 4.35: Literature review on the relationship between the sulphate/sulphur (y) and gypsum content (x)

	Proposed regression	R^2
Acid soluble sulphate (%SO_3)		
Agrela et al. (2011)	$y=0.0265x^2+0.1232x+0.5247$	0.71
Barbudo et al. (2012a)	$y=1.1193x+0.624$	0.79
Barbudo et al. (2012b)	$y=0.3981x+0.6314$	0.84
Geraldes (2013)	$y=0.3479x+0.3181$	0.68
Water soluble sulphate (%SO_3)		
Barbudo et al. (2012a)	$y=0.6774x+0.1175$	0.78
Barbudo et al. (2012b)	$y=0.302x+0.401$	0.86
Total sulphur content (%SO_3)		
Vegas et al. (2011)	$y=1.2922x+0.243$	0.64

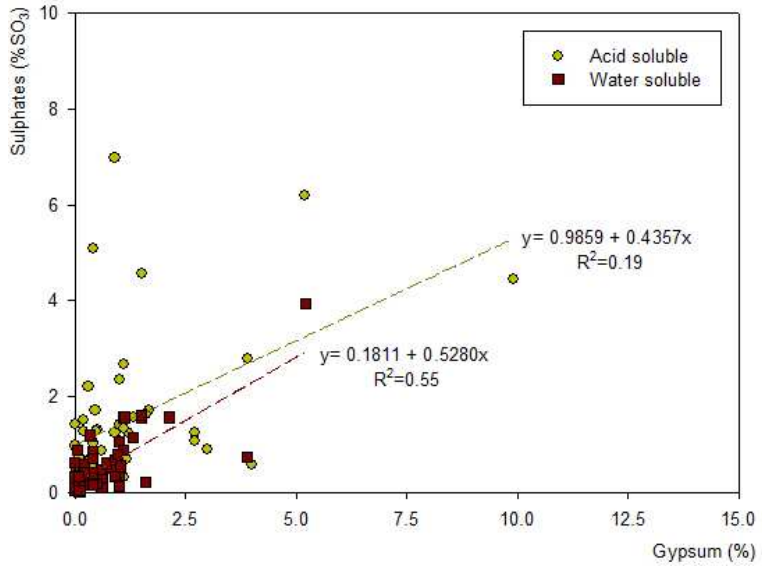

Figure 4.26: Literature review on the relationship between the sulphate and the gypsum content

Table 4.36: Literature review on the relationship between the sulphate/sulphur (y) and ceramic content (x)

	Proposed regression	R^2
Acid soluble sulphate (%SO_3)		
Geraldes (2013)	$y=0.0092x+0.5882$	0.12
Total sulphur content (%S)		
Mas et al. (2012a)	$y=0.0207x+0.0824$	0.62

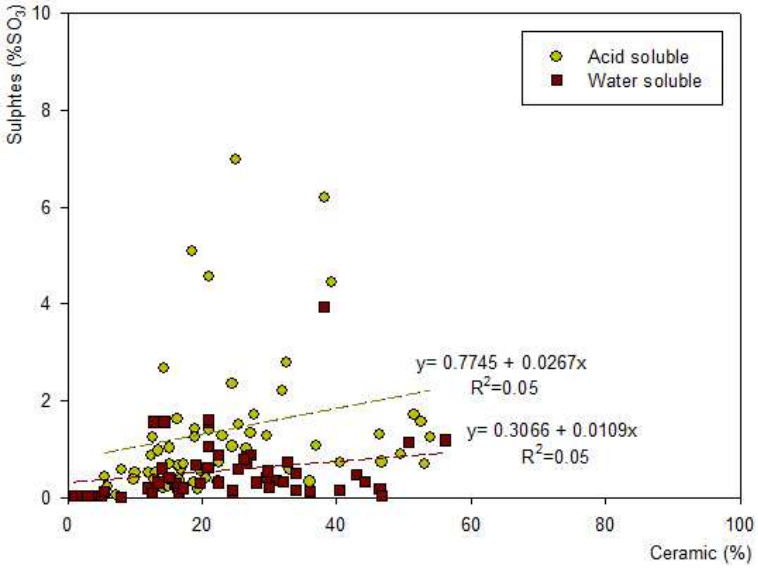

Figure 4.27: Literature review on the relationship between the sulphate and the ceramic content

3.2.1.2.2. Relationship between the sulphate content and the leaching of sulphates

At environmental level, some correlations (2012b) exists between the sulphate content of recycled aggregates and their leaching behaviour. Barbudo et al. (2012b) concluded that mixed recycled aggregates could be considered as non-hazardous according to the acceptance criteria (2000 mg/l) described in the EU Landfill Directive (European Council, 1999). Since the 1.73% limit for water soluble sulphates was not exceeded, the recycled aggregates employed in this thesis can also be considered as non-hazardous for the environment.

Table 4.37: Literature review on the relationship between the sulphate/sulphur (y) and ceramic content (x)

	Correlation parameters	Proposed regression	R^2
Barbudo et al. (2012b)	Water soluble sulphates- leached sulphates (mg SO_4/l)	y=0.0008x+0.132	0.76
	Water soluble sulphates- leached sulphates (%SO_3)	y=0.843x+0.132	0.76
Vegas et al. (2015)	Leached sulphates (%SO_3)-total sulphate content (%S)	y=0.439x-0.0737	0.93

3.2.1.3. *Chloride content*

Although a specific method for the determination of chloride ions exists (UNE EN 1744-1, 2010), other authors (Müller, 2004; Leiva et al., 2013) have previously used the results arising from an XRF analysis to justify the compliance with the chemical requirements imposed to the recycled aggregates. The EHE-08 (Permanent Commission on Concrete, 2008) establishes the chloride ion limit up to 0.05 % by mass of the aggregate, a value that was reached by none of the recycled aggregates (Table 4.31), with the obtained results situated in the lower range of those found in the literature (0.01-0.13%) (Mas et al., 2012a, 2012b; Sidorova et al., 2014).

Moreover, it is worth noting that according to Debieb et al. (2010) the chloride content of recycled aggregates should not mean their rejection since the immersion in water for 2 weeks is enough to avoid any risk of corrosion associated to their utilization.

3.2.1.4. *Other minority components*

For all samples, minor components were identified (Table 4.31), but in such small quantities that they should not represent a problem in the application of the recycled aggregates. The chemical composition exhibits low levels of heavy metals, the chromium being the most elevated due to the cement. These findings are in line with Vegas et al. (2015), who indicate that chromium, barium, lead and zinc are the metals with higher concentrations in the stony fraction of CDW. However, the environmental impact of these elements is determined by their likelihood to leach when in contact with water, and not by the amount of pollutant (Kosson et al., 2002). To date, the literature on this topic is limited (Sani et al., 2005; Barbudo et al., 2012b; Galvín et al., 2012, 2013, 2014; Medina et al., 2014a; Vegas et al., 2015); however, the investigation has shown that mixed recycled aggregates could be characterized as inert or non-hazardous to the environment under the limits of the EU Landfill Directive (European Council, 1999), as no specific limit values exist for waste-derived aggregates.

3.2.2. X-RAY POWDER DIFFRACTION

The natural and recycled aggregates were subjected to X-ray diffraction (XRD) to confirm and complement the results obtained by XRF since the atoms previously detected may be arranged in different geometries or crystal structures. Appendix B details all the Powder Diffraction Files (PDF) selected in the determination of the mineral compounds for natural and recycled aggregates.

As expected, the siliceous origin of the natural aggregates was ascertained by the sole occurrence of quartz peaks (Figure 4.28), while the heterogeneous nature of the recycled aggregates is manifested by the presence of intensity peaks corresponding to several mineralogical compounds.

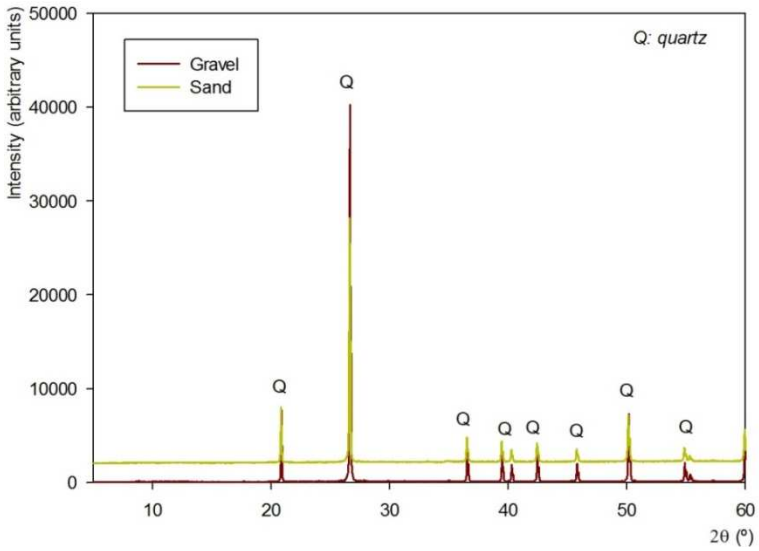

Figure 4.28: XRD pattern of the natural aggregates

Figure 4.29, Figure 4.30 and Figure 4.31 display the XRD patterns for all recycled aggregate samples. XRD plots are labelled in such way that the common mineral species for all samples are indicated by the placing of a letter on top of the peak in the line on the top. Note that in the case that other crystalline phases were detected just for some of the analysed samples, the indication of the compound is restricted to the corresponding peak of an isolated line.

Given that the XRD method performed was qualitative, the abundance of the different mineral species is inferred by the relative height of their X-ray diffraction peaks. Sharp peaks are associated to the major component while trace materials produce the smallest peaks that can be positively identified (although these compounds are not labelled in the figures).

Table 4.38: Inferred abundance of the mineralogical compounds in the recycled aggregates.

	High	**Medium**	**Traces**
RA-L(S) S1	Quartz, calcite	Anorthite, dolomite, feldspar potassian, hematite	Cristobalite, corundum
RA-L(S) S2	Quartz, calcite	Anorthite, dolomite, hematite, orthoclase	Muscovite, cristobalite, ferroan dolomite, gypsum
RA-L(S) S3	Quartz, calcite	Anorthite, orthoclase	Muscovite, cristobalite, ferroan dolomite
RA-L(S) S4	Quartz, calcite	Anorthite, orthoclase	Muscovite, cristobalite, ferroan dolomite
RA-M(S) S1	Quartz, calcite	Anorthite, orthoclase	Muscovite, cristobalite, ferroan dolomite, gypsum
RA-M(S) S2	Quartz, calcite	Dolomite, hematite, muscovite	Anorthite, orthoclase, corundum
RA-H(S)	Quartz	Anorthite, calcite, dolomite, hematite, illite, orthoclase	-

Due to the heterogeneous composition of mixed recycled aggregates (RA-L(S) and RA-M(S)), several samples were analysed. Nonetheless, the XRD results showed a good agreement with the composition of mixed recycled aggregates. For both recycled aggregates, quartz and calcite are the main minerals. The quartz content is correlated with the elevated SiO_2 values determined in the XRF analysis while the calcite occurrence is due both to the mortar adhered to the surface of the recycled particles (Dhir et al., 1999) and the presence of carbonate concrete aggregates (Limbachiya et al., 2007). The rest of components detected point to the relative ceramic content in the sample.

For all samples, feldspar phases were detected, which according to Limbachiya et al. (2007) is related to the ceramic content of the sample as these minerals are commonly used in the ceramic industry. While the identification of anorthite and orthoclase were widespread through all samples, a form of feldspar potassian ($K_{.5}Na_{.5}AlSi_3O_8$) was also isolated in sample RA-L(S) S1. Several authors (Limbachiya et al., 2007; Angulo et al., 2009; Vegas et al., 2011; Gedam et al., 2012) have also found feldspar diffraction peaks in CDW samples, in some occasions being able to identify specific feldspar minerals such as albite (Angulo et al., 2009) or microcline (Angulo et al., 2009; Vegas et al., 2011).

In the same manner, the presence of dolomite in some samples (RA-L(S) S1, S2 and RA-M(S) S2) is justified by the use of this mineral in the ceramic industry as a source of magnesia for refractory materials, and has been identified in clay brick previously (Bauluz et al., 2003; Cultrone et al., 2004).

Hematite is a mineral commonly found in ceramic materials since it is responsible for the characteristic red colour (Sánchez De Rojas et al., 2007; Lavat et al., 2009; Pacheco-Torgal and Jalali, 2010b), hence its presence in the characterization of the CDW suggests a ceramic component in the samples. Additionally, in those samples (RA-L(S) S1 and RA-L(S) S2) where hematite was identified, traces of corundum were detected as well, as they normally are associated together. For example, Pacheco-Torgal and Jalali (2010b) detected the association of both compounds in tiles wastes.

Traces of muscovite and cristobalite in the mixed recycled aggregates (RA-L(S) and RA-M(S)) also suggest a ceramic content in the samples, as both minerals could be found in bricks and tiles (Pacheco-Torgal and Jalali, 2010b). Also at trace level, gypsum was detected in samples RA-L(S) S2 and RA-M(S) S1, which indicates the presence of a contaminant potentially damaging for the performance and durability of recycled concrete. Further on, in the physical characterization of the recycled aggregates (section 3.1.1 of this chapter), the gypsum content is assessed by the results arising from the manual classification of the different components comprising the recycled aggregates. Nonetheless, Vegas et al. (2011), who also identified gypsum diffraction peaks in CDW samples, did not detect visible gypsum particles following the UNE EN 933-11 (2009) standard for all the contaminated samples.

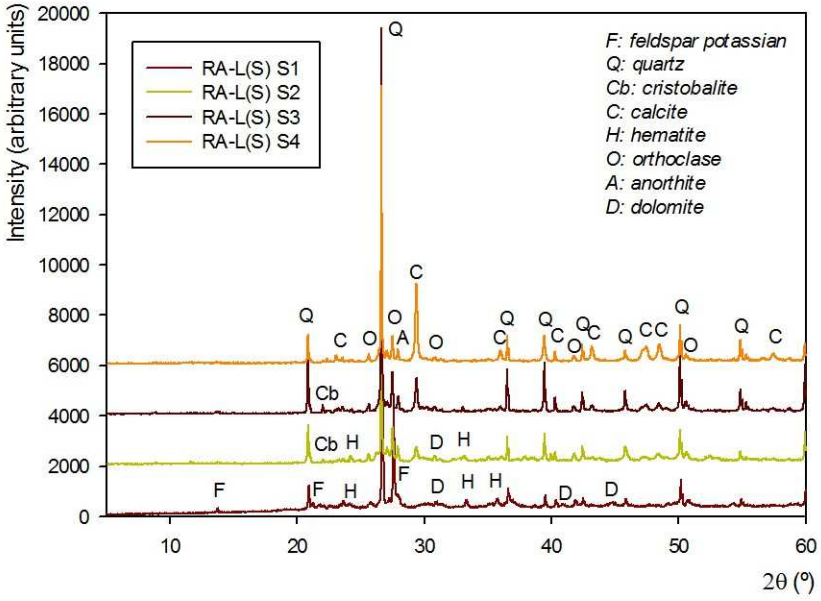

Figure 4.29: XRD pattern of RA-L(S) sample

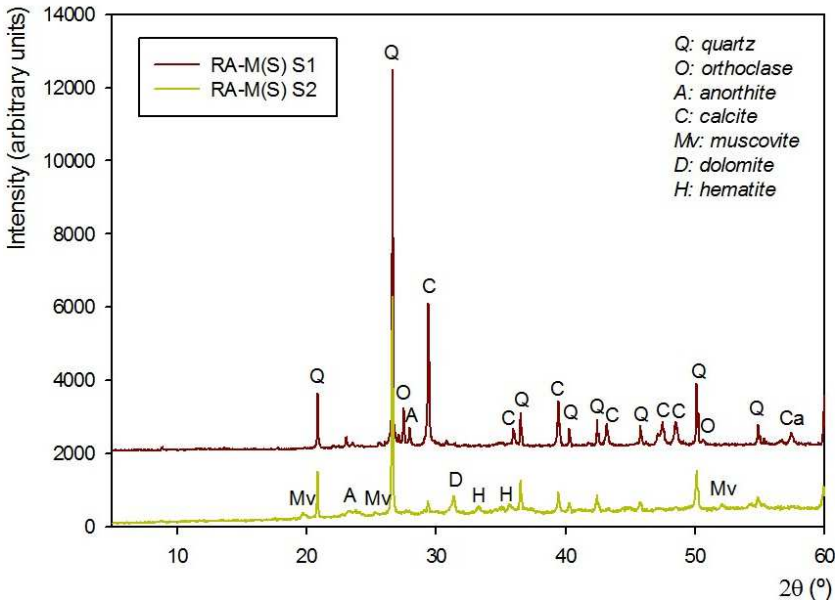

Figure 4.30: XRD pattern of RA-M(S) sample

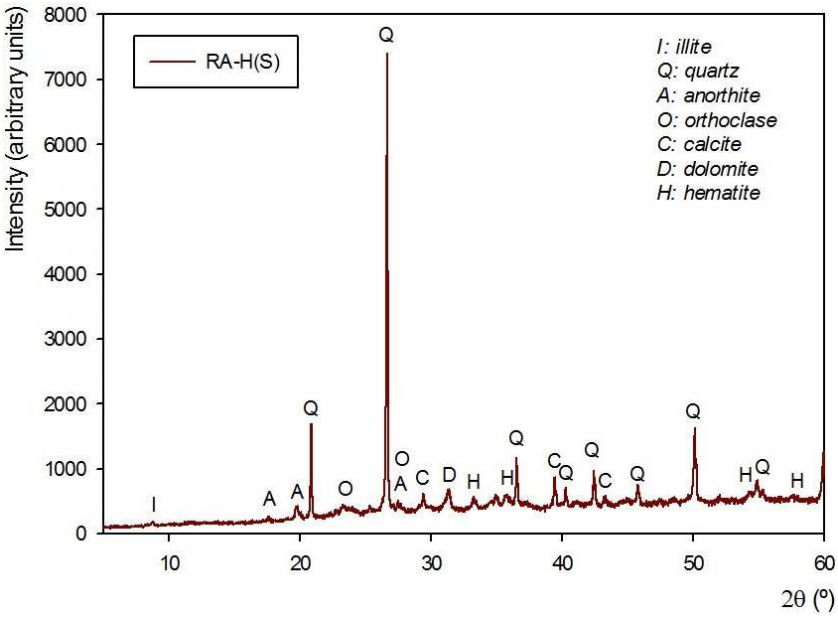

Figure 4.31: XRD pattern of RA-H(S) sample

Since the composition of RA-H(S) is the most homogenous, i.e. exclusively ceramic components, only one sample was analysed for this recycled aggregate. Similarly, quartz is the predominant mineralogical compound as expected from the chemical results. However, the quantity of calcite detected is lower than the amount detected in the mixed recycled aggregates. This finding is in accordance with the lower CaO identified in the XRF analysis and, as previously discussed, indicates a reduced presence of mortar adhered to the recycled particles (Dhir et al., 1999). The ceramic nature of this sample is clearly manifested by its mineralogical composition i.e. quartz, feldspar minerals (anorthite, orthoclase), illite, dolomite and hematite. Several authors have also identified these crystalline phases in ceramic wastes (Lavat et al., 2009; Pacheco-Torgal and Jalali, 2010b; Vegas et al., 2011).

Although this recycled aggregate is mainly comprised of brick and tiles wastes i.e. fired ceramic, mullite crystals were not detected. This same particularity was confronted by Lavat et al. (2009) in their investigation. According to Sujeong et al. (1999), the absence of high temperature products of dissociated clay minerals like mullite in the XRD diffraction patterns indicates that the original ceramic materials were produced at firing temperatures below 800ºC.

On the contrary, feldspar minerals used in the ceramic industry such as anorthite and orthoclase were easily identified in the sample. Both, anorthite and orthoclase, have been identified by other authors (Lavat et al., 2009; Pacheco-Torgal and Jalali, 2010b; Reig et al., 2013a, 2013b; Medina et al., 2015) in ceramic wastes. Moreover, within this mineral group, several researchers have also identified albite (Böke et al., 2006; Pacheco-Torgal and Jalali, 2010b; Reig et al., 2013a; Medina et al., 2015), anorthoclase (Pacheco-Torgal and Jalali, 2010b), microcline (Sánchez de Rojas et al., 2006; Sánchez De Rojas et al., 2007) and sanidine (Reig et al., 2013a) in XRD patterns of brick and tiles; however, none of this phases was detected in sample RA-H(S). Furthermore, other minerals commonly used in ceramic materials were detected, such as hematite (Böke et al., 2006; Sánchez De Rojas et al., 2007; Lavat et al., 2009; Pacheco-Torgal and Jalali, 2010b; Medina et al., 2015), dolomite (Bauluz et al., 2003; Cultrone et al., 2004) and illite (Limbachiya et al., 2007; Angulo et al., 2009; Lavat et al., 2009; Pacheco-Torgal and Jalali, 2010b). Note that, although the occurrence of clay minerals is limited to illite, this fact is rather usual in non-carbonated clay brick materials, i.e. with relatively high quartz content (>50%) (Bauluz et al., 2003).

3.2.3. SCANNING ELECTRON MICROSCOPY

From the visual analysis of the samples, the heterogeneity in morphology amongst the particles comprising the recycled aggregates is clearly noticeably. At x150 magnifications (Figure 4.33, Figure 4.34 and Figure 4.35), the different superficial texture of the most important constituents of the recycled aggregates (concrete and ceramic), makes clear the great difference in roughness when compared to the smooth superficial texture of the gravel (Figure 4.32b).

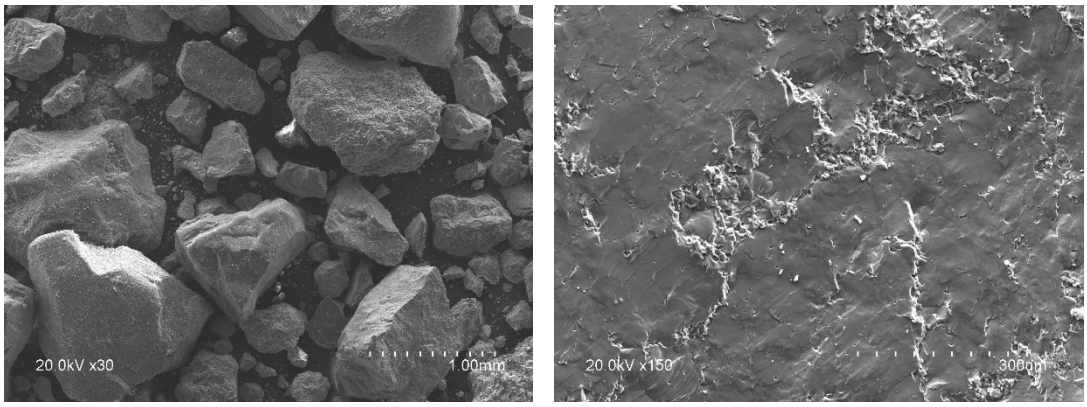

(a) **(b)**

Figure 4.32: Morphology of the natural aggregates: sand (a) and gravel (b)

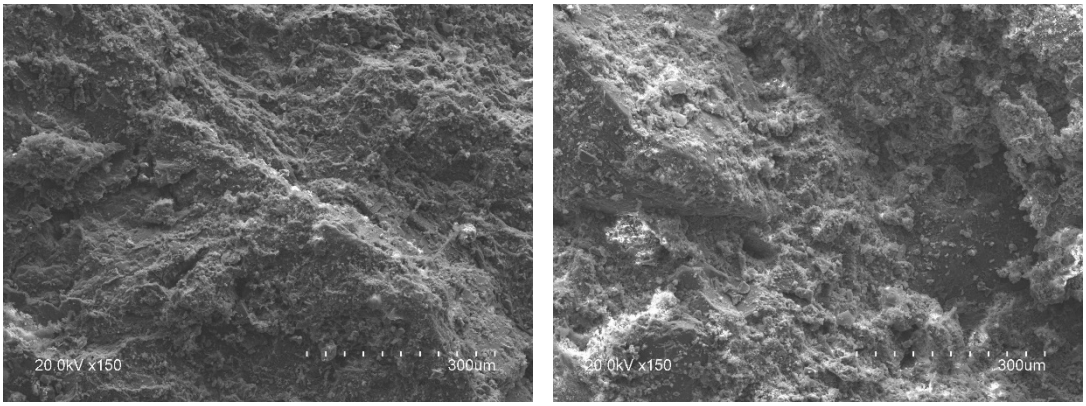

(a) **(b)**

Figure 4.33: Morphology of sample RA-L(S): ceramic (a) and concrete (b)

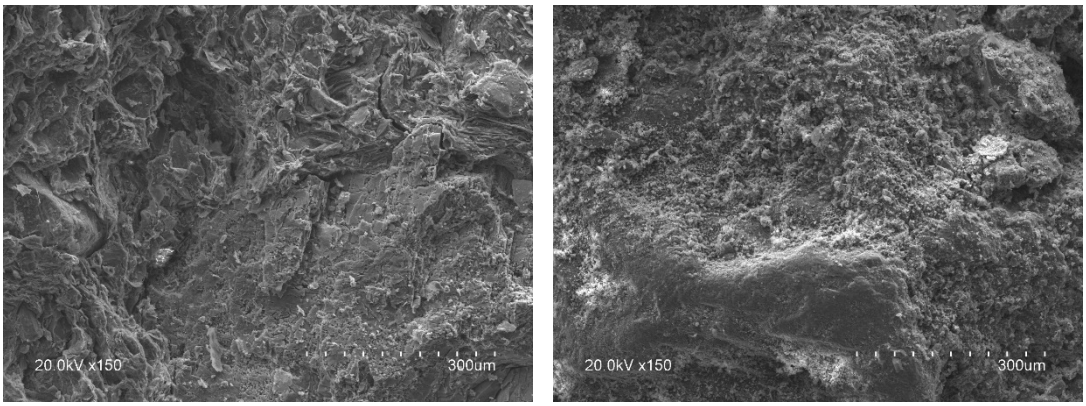

(a) **(b)**

Figure 4.34: Morphology of sample RA-M(S): ceramic (a) and concrete (b)

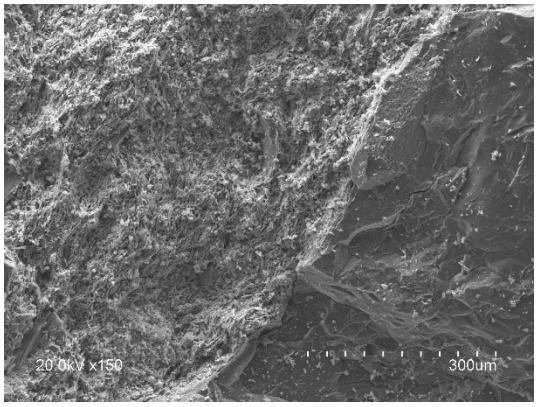

Figure 4.35: Morphology of sample RA-H(S)

Furthermore, the scanning electron microscopy analysis was performed in combination with an energy dispersive spectroscopy (EDS) in order to support the previous identification of the crystalline phases. As expected, the analysis on the sand (a) and gravel (b) illustrated in Figure 4.36 shows the siliceous nature of both samples in form of quartz crystals.

Figure 4.37a, Figurea and Figure 4.39 display the analysis of ceramic particles within the recycled aggregates, the peaks of silicon, aluminium and iron are the highest for the three samples due to the usual composition of ceramic materials with quartz as a space filler, clay minerals to provide plasticity and feldspar decreasing the melting point, while the rest of elements present (mainly potassium, magnesium and sodium) also forms part of their chemical structure. Regarding to the concrete constituent of the mixed recycled aggregates (RA-L(S) and RA-M(S) (Figure 4.37b and Figureb respectively), calcium and silicon are the principal peaks, which correspond to the C-S-H gel and C-H crystals in the hydrated concrete, and some trace amounts of aluminium, iron, sulphur, magnesium, potassium, sodium and titanium are present as impurities.

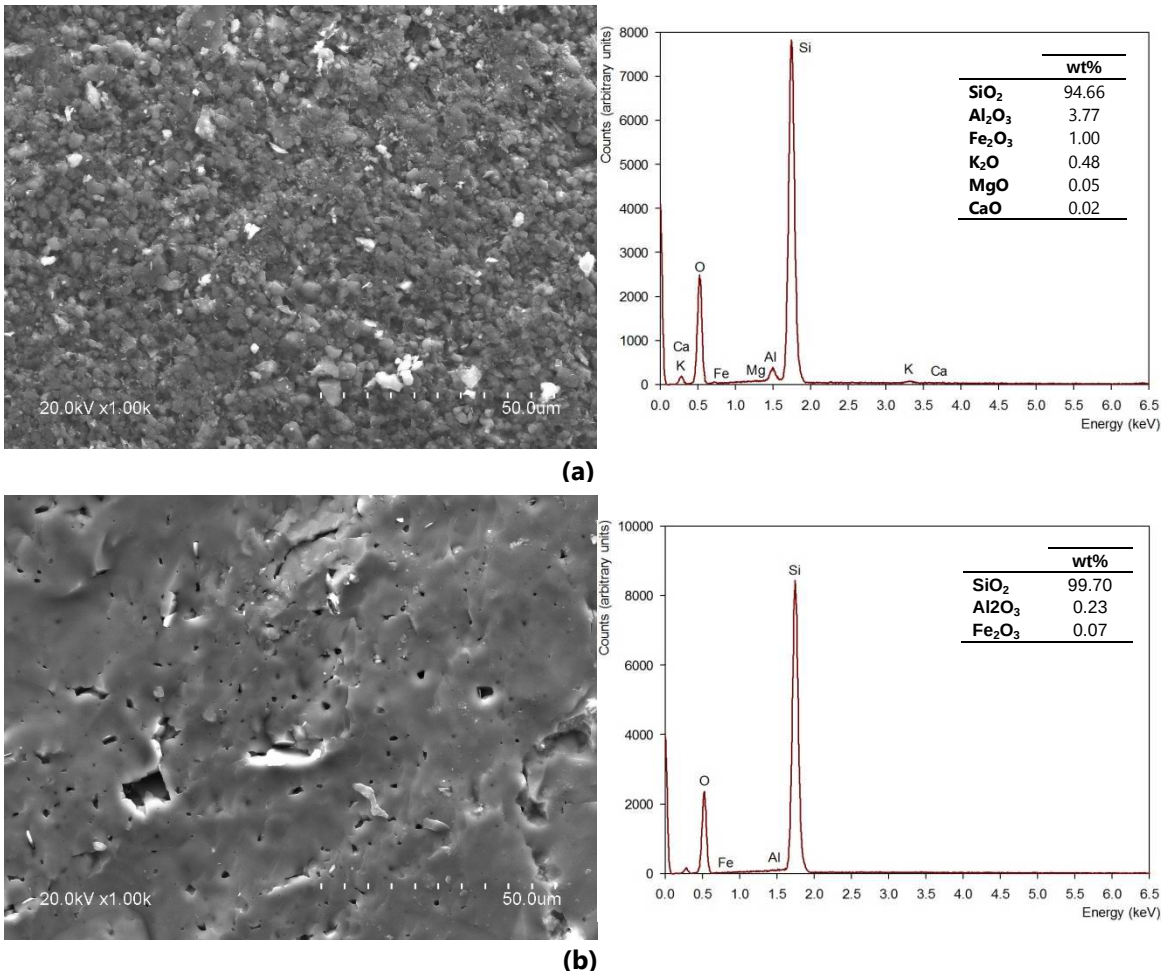

Figure 4.36: Micrographs of the natural aggregates: sand (a) and gravel (b)

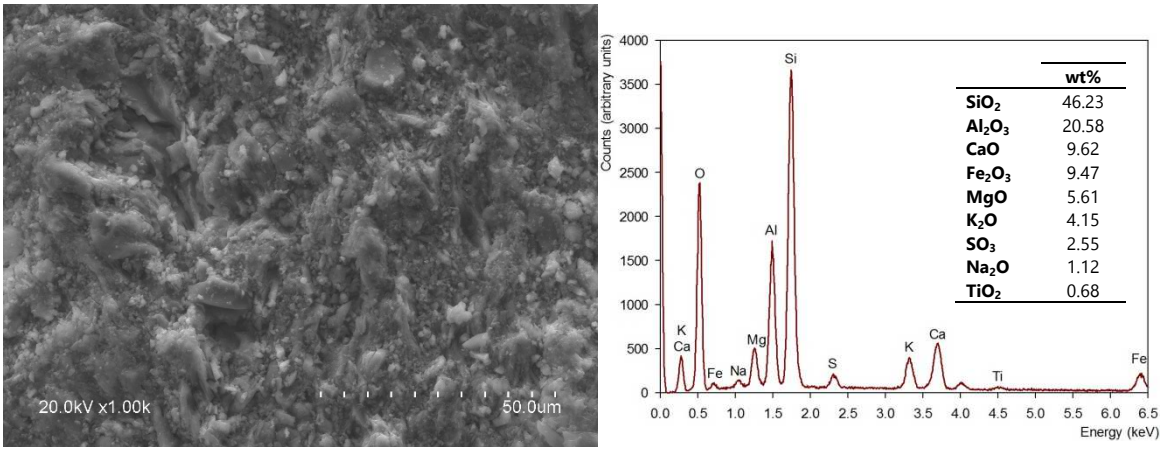

	wt%
SiO_2	46.23
Al_2O_3	20.58
CaO	9.62
Fe_2O_3	9.47
MgO	5.61
K_2O	4.15
SO_3	2.55
Na_2O	1.12
TiO_2	0.68

(a)

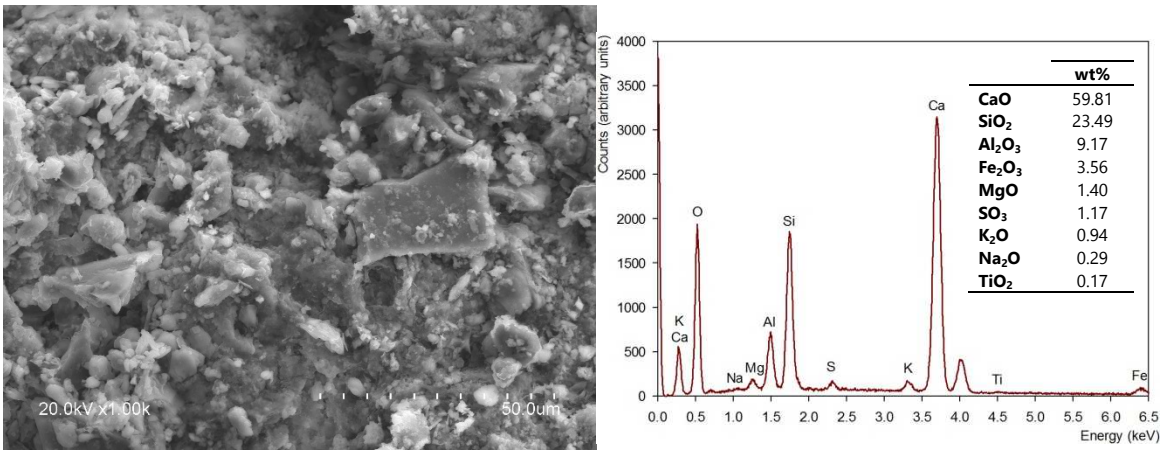

	wt%
CaO	59.81
SiO_2	23.49
Al_2O_3	9.17
Fe_2O_3	3.56
MgO	1.40
SO_3	1.17
K_2O	0.94
Na_2O	0.29
TiO_2	0.17

(b)

Figure 4.37: Micrographs of sample RA-L(S): ceramic (a) and concrete (b)

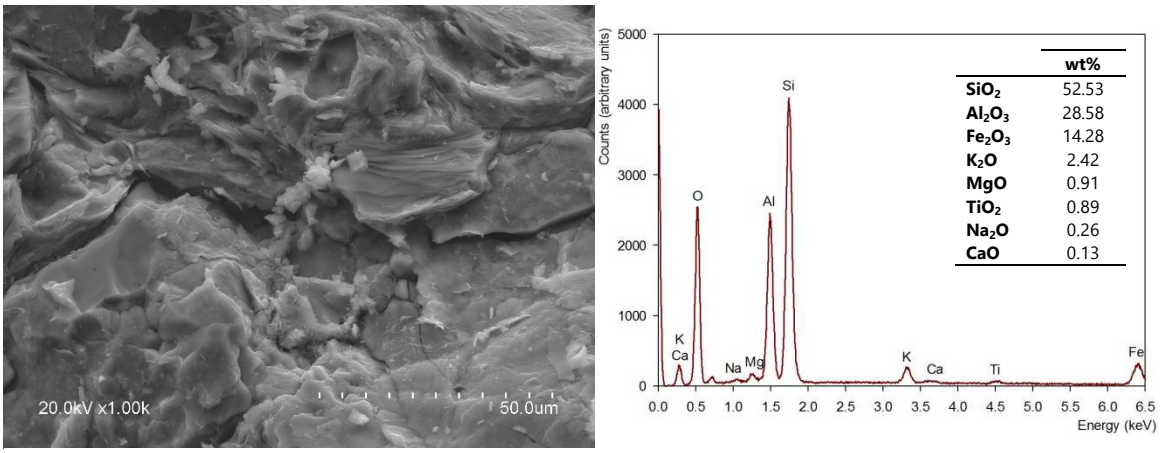

	wt%
SiO_2	52.53
Al_2O_3	28.58
Fe_2O_3	14.28
K_2O	2.42
MgO	0.91
TiO_2	0.89
Na_2O	0.26
CaO	0.13

(a)

Figure 4.38: Micrographs of sample RA-M(S): ceramic (a) and concrete (b)

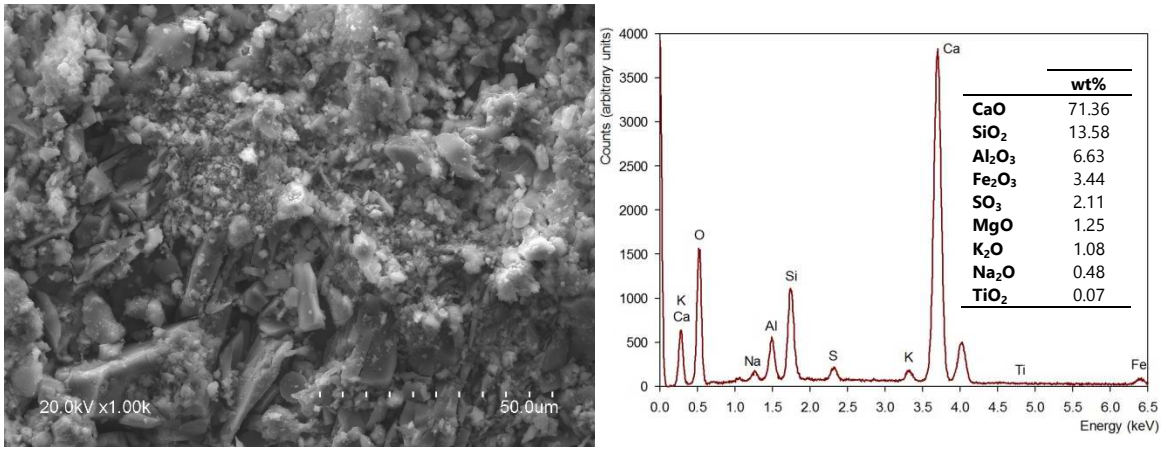

(b)

Figure 4.38: Micrographs of sample RA-M(S): ceramic (a) and concrete (b) (continued)

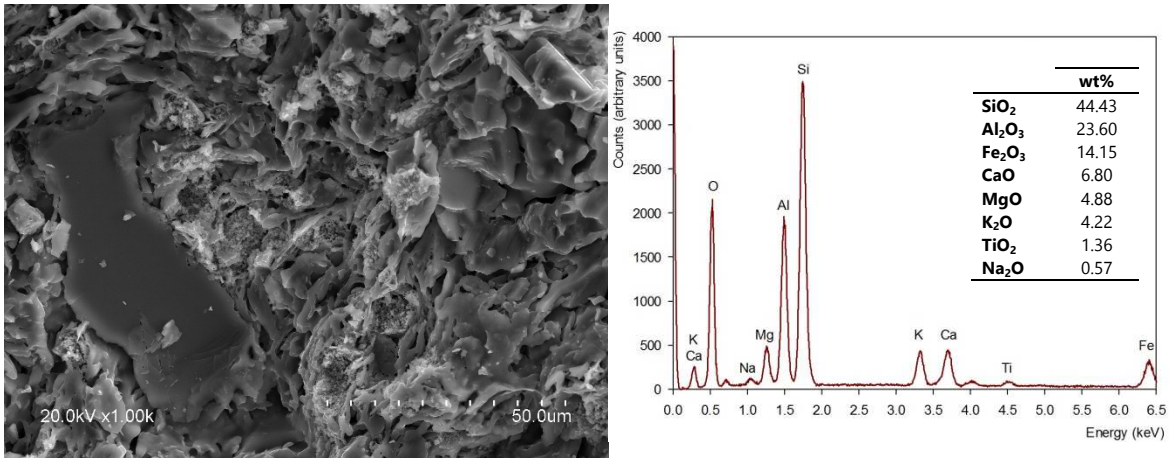

Figure 4.39: Micrograph of sample RA-H(S)

3.2.4. MERCURY INTRUSSION POROSIMETRY

Aggregates are porous solids, and as so the characteristics of their pore structure will greatly influence their own physical (density, water absorption, permeability…) and mechanical (strength, freeze-thaw resistance…) properties (Rübner and Hoffmann, 2006), and therefore their performance in applications such as the concrete manufacture. Nowadays, it is known that not only the total porosity, but the number, size, distribution and connectivity of the pores among other properties of the porous network of an aggregate affect the strength and specially the durability performance of a concrete mixture since the pores are the entry point for the aggressive agents -mainly of gas and liquid nature - that cause the deterioration. Therefore, a comprehensive characterization of the pore structure is necessary to assess the suitability of the coarse recycled aggregates as a total or partial replacement of the conventional gravel.

To evaluate the pore structure of the samples the common model of a cylindrical pore system accessible to the outer surface of the specimen was employed conjointly with Washburn's equation (3.3). The pore size distribution of the different samples is portrayed in Figure 4.40 by the plot of the cumulative mercury intrusion volume per oven-dried mass of the sample versus the pore size and in Figure 4.41 by the logarithmic values of the differential intrusion plotted against the pore diameters of the sample. Note that, although both intrusion and extrusion steps were carried out in the mercury intrusion tests (MIP), only the intrusion curves are represented in the figures. In addition, both figures are represented with the x axis decreasing toward the right side, in order to better represent the physical mechanism of intrusion, i.e. the larger pores are the firsts to be filled and with the subsequent increase of pressure smaller pores are intruded.

According to Rübner and Hoffman (2006), the appearance of the cumulative porosimetry curves (Figure 4.40) is distinctive of a type of material. The curve obtained for the RA-H(S) sample correlates in good agreement with the typical curves for bricks materials. Regarding the mixed recycled aggregates, the expected shape of their curves should be that of a mixture between the ceramic and concrete materials curves, which is partly satisfied for the RA-L(S) and RA-M(S) samples.

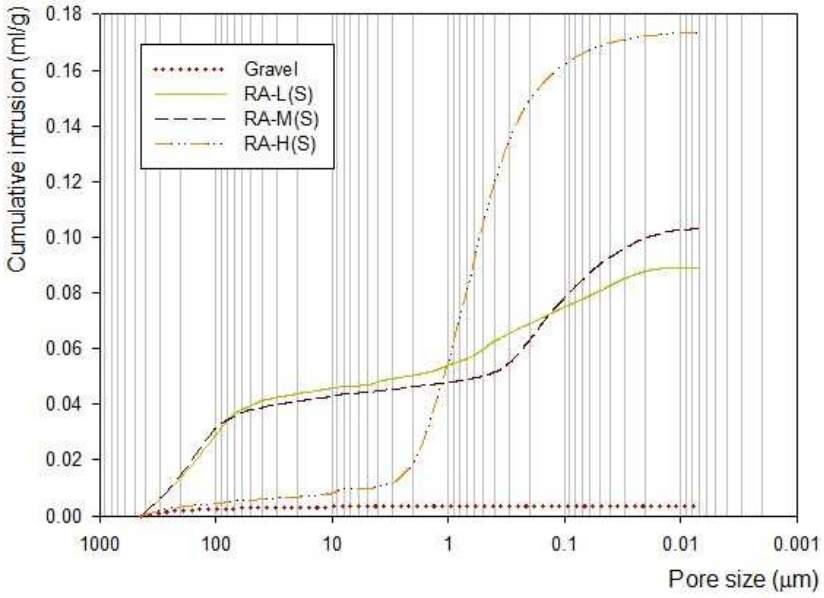

Figure 4.40: Pore size distribution

Moreover, interpreting Figure 4.40 at quantitative level, the total volume of pores intruded for the mixed recycled aggregates samples (RA-L(S) and RA-M(S)) is very similar, ranging between 89.20 to 102.90 mm^3/g of the dry sample, and the value is higher (173.40 mm^3/g) for the ceramic recycled aggregate (RA-H(S)). However, the data obtained for recycled aggregates is exponentially superior to the intrusion value for the natural coarse aggregate (3.6 mm^3/g), indicating the great differences of porosity between the two classes of aggregates. Furthermore, from the analysis of Figure 4.40 the average pore diameter of the samples could be determined as a function of four times the total volume intruded in the total pore area of the sample.

The values obtained show the same average pore diameter for the gravel and RA-L(S) sample (0.19 µm), while the average pore diameter was lower (0.12 µm) for RA-M(S) and higher (0.29 µm) for RA-H(S) sample, which impedes to establish any kind of tendency between the samples.

The main benefit of representing the MIP data as a logarithmical function of the differential mercury volume intruded (Figure 4.41) is the clear identification of the critical pore diameter of the sample. This parameter has been defined as the diameter above which no connected path could form throughout the sample (Cui and Cahyadi, 2001). The critical pore diameter corresponds to the steepest slope of the cumulative intrusion curve (Figure 4.40) and in the differential intrusion curve (Figure 4.41) is represented by the peaks of the line plot, which is easier to identify. Meanwhile the gravel and the RA-H(S) sample solely present one peak corresponding to the critical pore diameter, 439.19 µm and 0.67 µm respectively; for mixed recycled aggregates two peaks could be identified, 109.07 µm and 0.53 µm for RA-L(S) sample and 215.41 µm and 0.18 µm for RA-M(S) sample. This different behaviour for the mixed recycled aggregates could be caused by the adhered mortar and the concrete aggregates comprising the wastes originating the recycled aggregate, since the occurrence of several peaks - usually two - has been often observed for cement-based materials (Ye, 2003; Zhou et al., 2010).

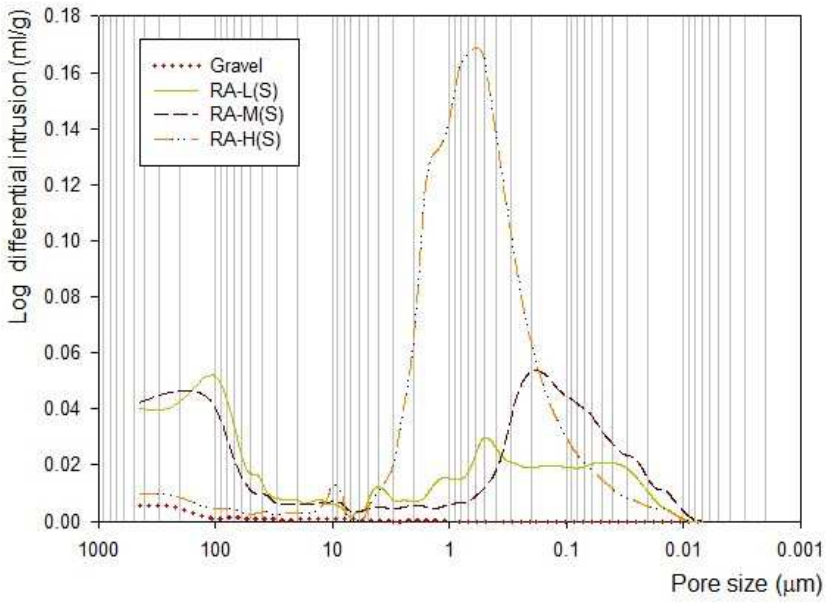

Figure 4.41: Differential pore size distribution

Regarding the higher critical pore diameters determined for the mixed recycled aggregates, the presence of natural aggregates forming part of the recycled aggregate could be an explanation. Finally, it is important to call the attention to the rounded shape of some of the peaks. Cook and Hover (1999) argued that rounded peaks could be the result of mercury forcing its intrusion due to higher pressures. As the more rounded peaks are predominantly distinguished for mixed recycled aggregates, the explanation of a breakage through the pores could correspond to the adhered mortar in the surface of the particles which could be held responsible for the relative roundness.

The total porosity of the samples was determined from the total volume intruded. Figure 4.42 clearly portrays the vast difference in porosity between natural (0.94%) and recycled aggregates (18.16%, 20.79% and 25.90% for RA-L(S), RA-M(S) and RA-H(S) samples respectively), which is an average of 23 times higher. Although the natural coarse aggregate studied in this research work presents a low porosity value similar to the one encountered for siliceous gravel by Medina et al. (2013), literature shows that natural gravel could have up to a 20% value of porosity (Heath, 1983), which is not that far from the calculated porosity of the recycled aggregates. However, the higher porosity of recycled aggregates is considered one of the main limitations of the use of recycled aggregates in the concrete manufacture.

Literature about recycled aggregates principally focuses on the determination of properties such as density and water absorption to characterize the pore structure. Hence, relatively few data on the porosity of recycled aggregates is available, and none of the works carried out a more thorough characterization than the determination of the porosity of the aggregate by means of mercury intrusion porosimetry. Moreover, the investigation of the porosity of construction and demolition wastes was centred on recycled concrete aggregates (RCA) and studies have not been performed for mixed recycled aggregates to date. Gómez-Soberón (2002) determined several parameters of the pore structure of RCA, in particular identified porosity values up to 14.86% for the 5/10 mm fraction and 13.42% for the 10/20 mm fraction. The porosity values determined by Poon et al. (Poon et al., 2004b) and Kou et al. (2011b) were lower, up to a 10.45% and 8.46%, respectively, for the 10/20 mm nominal size. Gonzalez-Fonteboa and Martínez-Abella (2008) also calculated the porosity of RCA for two different nominal sizes, with values up to 11.33% for the 4/12 mm fraction and 10.88% for the 10-25 mm fraction; these values were not obtained from MIP tests. Although the limited amount of results, the higher porosity associated to RCA has been attributed to the adhered mortar (Rao et al., 2007), which explains the variability amongst the research works.

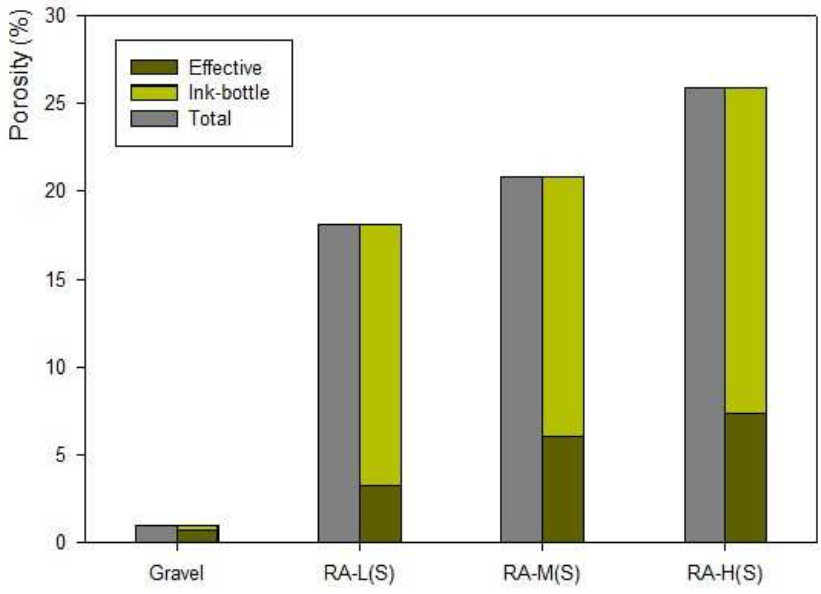

Figure 4.42: Porosity of natural and recycled aggregates

Due to the mixed and ceramic nature of the recycled aggregates, it is convenient compare the result obtained with other research works testing ceramic materials and wastes. Khalaf and DeVenny (2005) investigated ceramic materials and wastes encountering values of porosity ranging between 16.75% and 25.04% for bricks depending on their morphology and a porosity of 24.44% for the masonry waste. However, these results were calculated with a method developed by the authors (Khalaf and DeVenny, 2002). Later on, Koronthalyova (2011) examined two classes of bricks by means of a MIP test and obtained an average porosity of 28%. The results obtained for the RA-H(S) sample are slightly higher than those obtained by Khalaf and DeVenny (2005) for recycled masonry aggregate, but the difference between the data may be a result of the different test method employed.

In the absence of previous research on the porosity of mixed recycled aggregates, the values obtained are higher than of those expected for recycled concrete aggregates, which is in good agreement with the presence of ceramic components in the mixed recycled aggregates increasing the total porosity of the sample.

Further interpretation of the total porosity results require taking into account the hysteresis phenomena occurring between the intrusion and extrusion cycles of a MIP test. Whilst the total porosity was analysed under the assumption of a perfectly connected pore networks, which does not necessarily satisfy the real conditions. The amount of entrapped mercury suggest a porous structure based on large internal pores only accessible through narrow pores (Wardlaw and McKellar, 1981). This bias is known as ink-bottle porosity (Figure 4.42), which is a misrepresentation of the size of larger pores to which is assigned the size of the narrow pore that made them accessible to the mercury intrusion. While the ink-bottle porosity for the gravel (0.23%) is the minority component of the total porosity of the sample, for recycled aggregates the contrary phenomena occurs (14.92% for RA-L(S), 14.73% for RA-M(S) and 18.54% for RA-H(S). The higher values of ink-bottle porosity in the recycled aggregates are indicative of an elevated non-accessible porosity in the samples that translate in lower values of effective porosity, which according to Ye (2003) is accountable for the water permeability. At effective porosity level (Figure 4.42), the recycled aggregates have a porosity value 8 times higher than the gravel on average, which suggests that the performance gap between both types of aggregates is not as much obvious as initially considered. Furthermore, no clear trend could be found between the ceramic content of the sample and the effective porosity of the sample.

The influence that the different pore size fractions represent in the total porosity of the different aggregates is shown in Figure 4.43. As such, the relative porosity for six pore size intervals could be independently assessed since porous materials with similar total porosity but different pore size distribution could react in a different manner under the same conditions (Zdravkov et al., 2007).

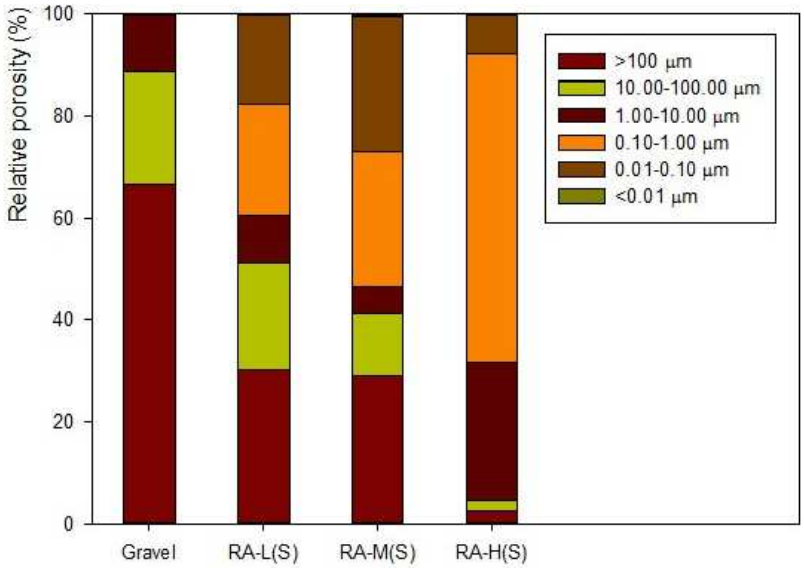

Figure 4.43: Relative porosity of natural and recycled aggregates

- < 0.01 µm: Except for RA-M(S) and RA-H(S) samples, pores inferior to 0.01 µm do not influence the total porosity values of the aggregates; and the influence in those samples is almost negligible (0.39% and 0.06% respectively).

- 0.01-0.10 µm: No clear tendency could be extrapolated for the variations among samples in this pore size interval. The relative porosity for RA-H(S) sample is the lower (7.55%), followed by RA-L(S) sample (17.49%) and RA-M(S) sample (26.43%), which initially does not point to a compositional factor.

- 0.10-1.00 µm: This pore size range is the main component in the total porosity of the ceramic recycled aggregate (60.84%). Koronthalyova (2011) indicated that 70% of the open porosity of bricks was created by pores from 0.30 µm to 1.8 µm. For this pore size interval, the RA-H(S) sample presents a relative porosity of 62.69%, which agrees with the previous findings of Koronthalyova (2011). However, for the mixed recycled aggregates this pore size range occupies a second place in importance, which could be related to the lower amount of ceramics in the samples. The fact that its influence on the RA-M(S) sample is higher (26.73%) than on the RA-L(S) sample (22.09%) supports the previous theory. Thus, the relative porosity between 0.10-1.00 µm for recycled aggregates containing ceramic particles will be higher as the ceramic content in the sample is increased.

- 1.00-10.00 µm: This is the lower interval influencing the total porosity of the gravel (11.11%). Meanwhile the relative porosity of the RA-H(S) sample (26.99%) is higher than that of the natural aggregate, which correlates good with the findings of Rübner and Hoffman (2006), that indicated that bricks are characterized by an increase of pore sizes in this interval. On the contrary, the mixed recycled aggregates present lower values than the gravel (9.30% and 5.05% for RA-L(S) and RA-M(S) respectively). Hence, no clear regression could be established between the obtained values and the ceramic content of the sample.

- 10-100.00 μm: The relative importance of this pore size range on the total porosity is indirectly interconnected with increase of the ceramic content in the sample, with values of 13.92% for RA-L(S), 6.15% for RA-M(S) and 2.13% for RA-H(S). In this size range, natural aggregates behave similarly (22.22%) to the mixed recycled aggregate with the lowest ceramic content (RA-L(S)). Nonetheless, a trend could be established for lower relative porosity as the ceramic content in the sample increases.

- >100.00 μm: The influence of this pore size range on the total porosity is higher for the natural aggregate (66.67%); within the recycled aggregates, the mixed samples present similar percentages (30.27% and 28.96% for RA-L(S) and RA-M(S) respectively) and the value for the ceramic aggregate is drastically inferior (2.42%). The results suggest that the ceramic composition is the factor responsible for the differences between the recycled aggregates.

Summarizing, the pore size range between 10 μm and 100.00 μm is accountable for the total porosity of the gravel; while all the pore size intervals contribute to the total porosity of the recycled aggregates, except for the RA-L(S) sample that does not present pores inferior to 0.01 μm influencing its porosity. Moreover, three clear tendencies were identified by the analysis of the figure; one showing an increase of relative porosity in the 0.10-1.00 μm pore size range correlated to the higher amount of ceramic in the sample and the two other trends leaning towards the reduction of the relative porosity in the 10.00-100.00 μm and >100 μm pore size intervals with increasing amounts of ceramic wastes.

From the study of the relative porosity it is possible to identify that recycled aggregates present a finer microstructure than the gravel. This affirmation is also supported by the critical pore diameter results, since according to Cui and Cahyadi (2001) smaller values of this parameter correspond to finer pore structures. Moreover, if the total pore area, as derived by Rootare and Prenzlow (1967), is employed to further differentiate the microporosity of the samples, the samples could be arranged as RA-H(S), RA-L(S), RA-M(S) from coarser to finer porosity, as it is generally accepted that higher values of total pore area are related to a finer pore structure.

Finally, the operating method followed in the mercury intrusion porosimetry also enabled the determination of the bulk and skeletal density of the samples, calculated when no pores are filled with mercury (lower pressure setting) and when all pores are filled (higher pressure setting) respectively (Giesche, 2002). The values obtained (Table 4.39) are in accordance with the results obtained by means of a pycnometer determination (section 3.1.5 of this chapter).

As a summary, all the different parameters that characterize the pore structure of the aggregates are compiled in Table 4.39.

Table 4.39: Parameters of the pore structure of the natural and recycled aggregates

	Gravel	RA-L(S)	RA-M(S)	RA-H(S)
Porosity (%)	0.94	18.16	20.79	25.90
Ink-bottle porosity (%)	0.23	14.92	14.73	18.54
Effective porosity (%)	0.71	3.24	6.06	7.36
Average pore diameter (μm)	0.19	0.19	0.12	0.29
Critical pore diameter (μm)	439.19	109.07 0.53	215.41 0.18	0.67
Total pore area (m^2/g)	0.001	1.915	3.370	2.395
Bulk density (kg/m^3)	2624.80	2036.10	2020.30	1493.90
Apparent density (kg/m^3)	2649.90	2488.30	2550.20	2016.00

3.2.4.1. *Relationship between the porosity and the constituents*

In order to validate the assumptions, first a Pearson product-moment correlation was employed to analyse the linear dependence between the compositional variable of the recycled aggregates and the relative porosity corresponding to the aforementioned pore size intervals. Table 4.40 shows the Pearson coefficient (top row) and the p-value (bottom row) for each pair of variables evaluated. For pairs with p-values lower than 0.05, which are displayed in grey coloured cells, there is a significant relationship between the two variables. The linear dependence identified statistically corresponds with the trend previously observed in Figure 4.43, the value of ceramic content tends to increase as the relative porosity of the pore size intervals >100.00 μm and 100.00-10.00 μm tends to decrease (negative correlation coefficients) and the values of ceramic content and relative porosity of the 1.00-0.10 μm pore size range tend to increase together (positive correlation coefficients).

Table 4.40: Pearson correlation (top row) and the p-value (bottom row) between the composition of the sample and the relative porosity of each pore size interval

	>100.00	100.00-10.00	10.00-1.00	1.00-0.10	0.10-0.01	<0.01
Ru	0.9440	0.6880	-0.2980	-0.8330	-0.6400	-0.3530
	0.0561	0.3120	0.7020	0.1670	0.3600	0.6470
Rc	-0.0812	0.4320	-0.5130	-0.1570	0.6080	-0.0108
	0.9190	0.5680	0.4870	0.8430	0.3920	0.9890
Rb	-0.9510	-0.9570	0.5860	0.9620	0.3520	0.3850
	0.0493	0.0425	0.4140	0.0382	0.6480	0.6150
Ra	-0.1080	0.2850	-0.7110	-0.1390	0.9050	0.4980
	0.8920	0.7150	0.2890	0.8610	0.0952	0.5020
Rg	-0.0694	0.4520	-0.4300	-0.1540	0.4920	-0.1560
	0.9310	0.5480	0.5700	0.8460	0.5080	0.8440
Xg	-0.0517	0.4640	-0.3060	-0.1450	0.3230	-0.3420
	0.9480	0.5360	0.6940	0.8550	0.6770	0.6580
X	-0.1020	0.0412	-0.7030	-0.0777	0.9400	0.8830
	0.8980	0.9590	0.2970	0.9220	0.0597	0.1170

Finally, in order to better describe the linear dependency between each pair of variables, a linear regression analysis was performed. Figure 4.44 displays the equations governing the observed tendencies, that as indicated by the high R^2 values (>0.90) are a good fit for the results obtained.

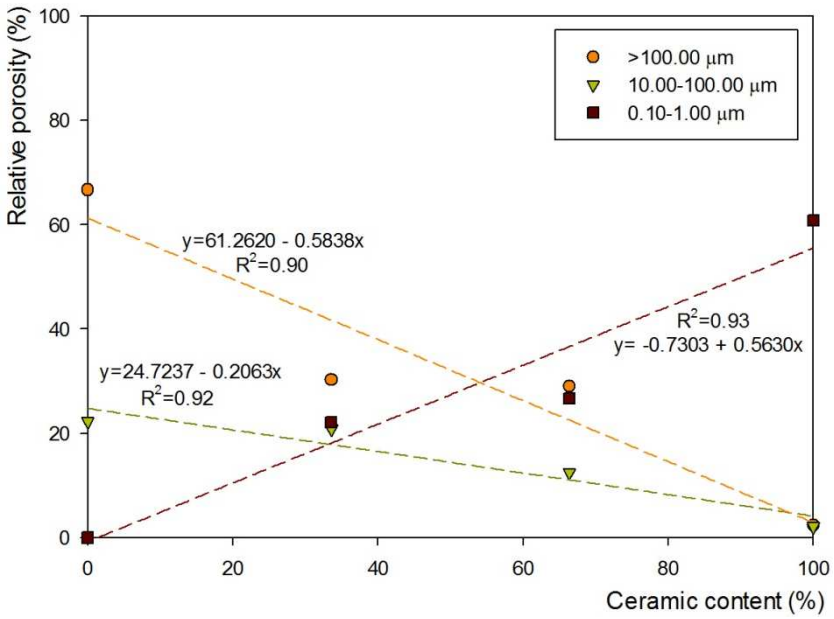

Figure 4.44: Relationships between relative porosity and ceramic content

Note that the correlations have been identified under the assumption of a homogenous behaviour from all the ceramic materials comprising the CDW. However, more underlying relationships related to the ceramic content of the sample are possible, as it is known that the pore structure parameters of the different ceramic materials are dependent of their mineralogical and chemical composition, the burning process and the incorporation of additives among other factors (Cultrone et al., 2004; Koronthalyova, 2011), facts that are unknown for the wastes collected.

3.2.4.2. *Relationship between the porosity and the density and water absorption*

Figure 4.45 shows the plot of water absorption values against the total and effective porosities of the gravel and the recycled aggregates. Strong quadratic relationships were detected between each pair of variables. As expected, the water absorption increases with the increment of the total and effective porosity of the recycled aggregates.

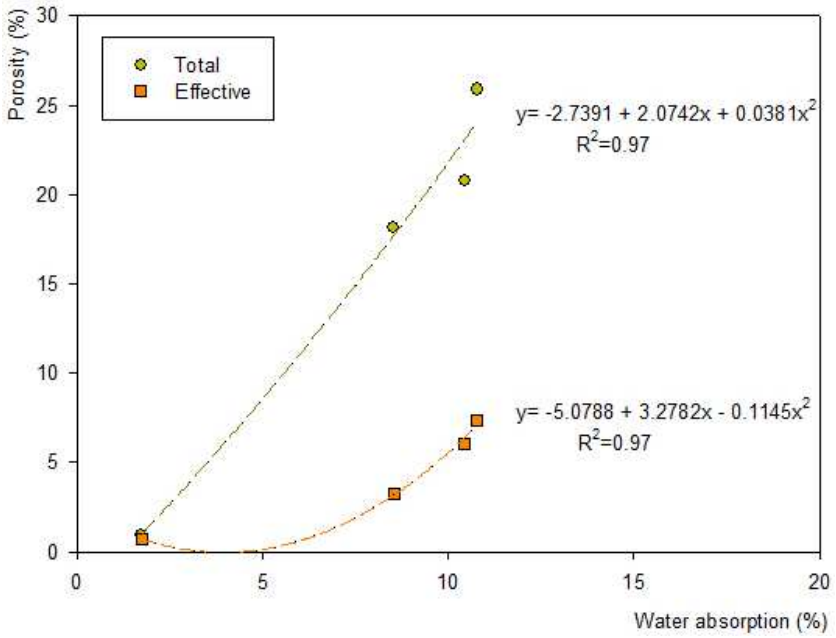

Figure 4.45: Relationship between the porosity and the water absorption of the recycled aggregates

3.2.4.3. *Relationship between the porosity and the frost resistance*

The structure of the pore system has a higher influence on the frost resistance of the recycled aggregates than their total pore volume, since the pore size distribution determines whether or not, and to what extent, a porous material can become critically saturated and susceptible of damage as a result of freeze and thaw cycles (Hewlett, 2003).

Kaneuji et al. (1980) proposed a relationship linking the results of the mercury intrusion porosimetry with the frost resistance of the aggregates. By means of equation (4.3), the expected durability factor (EDF) of an aggregate could be calculated and evaluated against a minimum acceptable EDF.

$$EDF = \frac{0.579}{PV} + 6.12 \times MD + 3.04 \quad (4.3)$$

with *EDF* the expected durability factor [-], *PV* the total intruded pore volume down to a diameter of 4.50 nm [ml/g] and *MD* the median diameter of intruded pores larger than 4.50 nm, based on pore volume [µm].

Table 4.41 displays the expected durability factor of the gravel and the recycled aggregates, which is compared against the minimum acceptable EDF proposed by Kaneuji et al. (1980) in Figure 4.46.

Table 4.41: Expected durability factor of the aggregates as proposed by Kaneuji et al. (1980)

	EDF
Gravel	1435.60
RA-L(S)	100.00
RA-M(S)	11.14
RA-H(S)	10.29

The results show that samples RA-M(S) and RA-H(S) could be susceptible to frost damage, while the gravel and the recycled aggregate with lower content of ceramic could be classified as durable aggregates in the case of exposure to freeze-thaw cycles. It is worth mentioning that the samples RA-M(S) and RA-H(S) possess an EDF nearly ten times lower than RA-L(S) and almost 140 times lower than the natural aggregate.

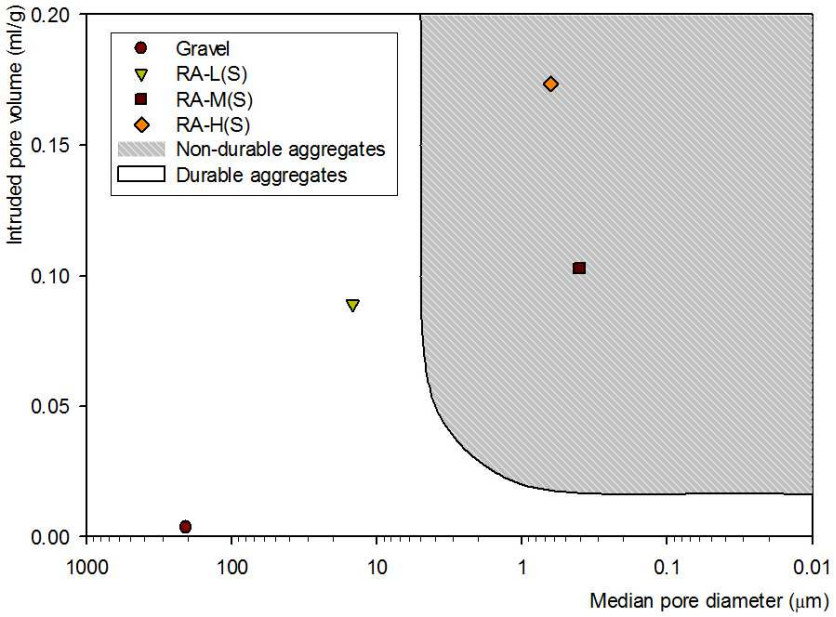

Figure 4.46: Classification of the aggregates using the expected durability factor proposed by Kaneuji et al. (1980)

3.3. OVERALL PERFORMANCE OF THE RECYCLED AGGREGATES

The laboratory tests normally used to characterize recycled aggregates as construction material are the same as those used for conventional aggregates, regardless of whether these are valid for the new materials. Consequently, establishing requirements for recycled aggregates on the basis of tests that may not be appropriate leaves these materials at a distinct disadvantage compared to conventional aggregates, and thus creates a barrier to their use. Nonetheless, provided an inferior quality, in a free market economy, the decision to purchase and use recycled aggregate will be based not only on the fulfilment of the technical requirements of the product but also on whether the cost or the environmental advantages are enough to compensate this fact.

Furthermore, based upon these methods, the traditional specifications on the use of recycled aggregates in the concrete manufacture confer the highest importance to their type, composition or origin. Hence, mixed recycled aggregates or ceramic recycled aggregates are normally relegated to low level applications, which limit the performance potential of these materials.

Silva et al. (2014) proposed a classification system based on the physical properties of the recycled (oven-dried density, water absorption and Los Angeles coefficient). Notwithstanding their composition, the recycled aggregates could be separated in four classes in accordance to their overall quality and their expected performance in the concrete manufacture.

Table 4.42: Classification system proposed by Silva et al. (2014)

Aggregate class		Minimum OD density (Mg/m^3)	Maximum water absorption (%)	Maximum Los Angeles coefficient (%)
	I	2.60	1.50	
A	**II**	2.50	2.50	40
	III	2.40	3.50	
	I	2.30	5.00	
B	**II**	2.20	6.50	45
	III	2.10	8.50	
	I	2.00	10.50	
C	**II**	1.90	13.00	50
	III	1.80	15.00	
D	**-**		No limits	

Predictably, all the recycled aggregates characterized belong to Class C (Table 4.43); and within this category, the recycled aggregates were separated in the three available types according to their general ceramic content (L, M and H). Therefore, according to Silva et al. (2014) recommendations, these aggregates should only be considered for use in low-grade applications (*i.e.*, non-structural concrete). However, it is worth mentioning that all samples were included in a lower category due to their minimum density values; meanwhile, the classification based on the maximum water absorption, i.e. the initially considered limiting factor, would render some of the samples in a higher category. In addition, this classification assesses the recycled aggregates and recommends applications based upon a 100% substitution of the natural coarse aggregate, while in most cases only the partial replacement is pursued. Consequently, the recycled aggregates obtained may be fit for use in higher-level applications when used in combination with natural coarse aggregates.

Table 4.43: Classification of the recycled aggregates according to their overall performance (Silva et al., 2014)

	Aggregate class
RA-L(S)	C-I
RA-L(B)	C-I
RA-M(S)	C-II
RA-H(S)	C-III

To broaden the performance-based analysis of the recycled aggregates, the results obtained for the different properties were transformed to index values. First, all the values were adjusted to the assumption that higher values of a determined property indicate a better performance, i.e. except for the sand equivalent and the expected durability index, the inverse value of each result was used for the construction of the different indexes. Then, the index was constructed as the ratio between the result for a recycled aggregate and the results of the gravel for each considered property. Thus, in this approach, the recycled aggregates are compared to the natural coarse aggregates that they are supposed to totally or partially substitute.

The radar plot of these indexes (Figure 4.47) reveals the extent of the lower performance of the recycled aggregates in comparison with the siliceous gravel normally used in conventional concrete mixtures. Nonetheless, it is worth mentioning that the recycled aggregate sample coming from Belgium presents a better performance regarding its fines content, which gives an idea of the efficiency in the treatment process at the CDW management plant. These results suggest that the recycled aggregate would be better suited as a partial substitution of the natural aggregate in order to reduce the influence that their differential qualities have on the fresh and hardened recycled concrete.

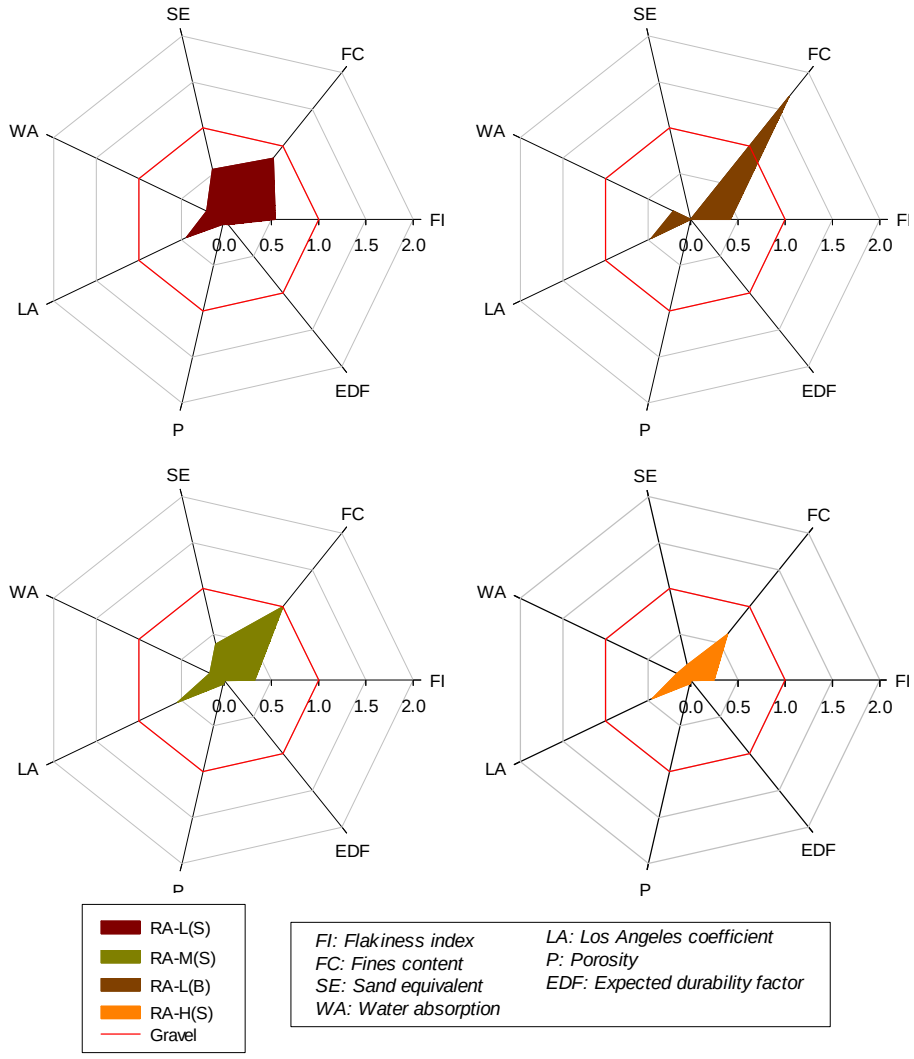

Figure 4.47: Performance indexes of the recycled aggregates

4. REFERENCES

Abbas, A., Fathifazl, G., Fournier, B., Isgor, O.B., Zavadil, R., Razaqpur, A.G., Foo, S., 2009. Quantification of the residual mortar content in recycled concrete aggregates by image analysis. *Materials Characterization* 60 (7): 716–728.

Abbas, A., Fathifazl, G., Isgor, O.B., Razaqpur, A., Fournier, B., Foo, S., 2008. Proposed method for determining the residual mortar content of recycled concrete aggregates. *Journal of ASTM International* 5 (1): 12.

ACI Committee 233, 2003. Slag Cement in Concrete and Mortar (No. 233R-03). American Concrete Institute.

Agrela, F., Barbudo, A., Ramírez, A., Ayuso, J., Carvajal, M.D., Jiménez, J.R., 2012. Construction of road sections using mixed recycled aggregates treated with cement in Malaga, Spain. *Resources, Conservation and Recycling* 58: 98–106.

Agrela, F., Sánchez de Juan, M., Ayuso, J., Geraldes, V.L., Jiménez, J.R., 2011. Limiting properties in the characterisation of mixed recycled aggregates for use in the manufacture of concrete. *Construction and Building Materials* 25 (10): 3950–3955.

Akbarnezhad, A., Ong, K.C.G., Zhang, M.H., Tam, C.T., Foo, T.W.J., 2011. Microwave-assisted beneficiation of recycled concrete aggregates. *Construction and Building Materials* 25 (8): 3469–3479.

Akhtaruzzaman, A.A., Hasnat, A., 1983. Properties of concrete using crushed brick as aggregate. *Concrete International* 5 (2): 58–63.

Alves, A.V., Vieira, T.F., de Brito, J., Correia, J.R., 2014. Mechanical properties of structural concrete with fine recycled ceramic aggregates. *Construction and Building Materials* 64: 103–113.

Angulo, S.C., Ulsen, C., John, V.M., Kahn, H., Cincotto, M.A., 2009. Chemical–mineralogical characterization of C&D waste recycled aggregates from São Paulo, Brazil. *Waste Management* 29 (2): 721–730.

Barbudo, A., Agrela, F., Ayuso, J., Jiménez, J.R., Poon, C.S., 2012a. Statistical analysis of recycled aggregates derived from different sources for sub-base applications. *Construction and Building Materials* 28 (1): 129–138.

Barbudo, A., de Brito, J., Evangelista, L., Bravo, M., Agrela, F., 2013. Influence of water-reducing admixtures on the mechanical performance of recycled concrete. *Journal of Cleaner Production* 59: 93–98.

Barbudo, A., Galvín, A.P., Agrela, F., Ayuso, J., Jiménez, J.R., 2012b. Correlation analysis between sulphate content and leaching of sulphates in recycled aggregates from construction and demolition wastes. *Waste Management* 32 (6): 1229–1235.

Barra Bizinotto, M., 1996. Study on recycled concrete durability for structural concrete [in Spanish]. Universitat Politècnica de Catalunya (UPV), Barcelona, Spain.

Bauluz, B., Mayayo, M.J., Fernández-Nieto, C., Cultrone, G., González López, J.M., 2003. Assessment of technological properties of calcareous and non-calcareous clays used for the brick-making industry of Zaragoza (Spain). *Applied Clay Science* 24 (1–2): 121–126.

Bazaz, J.B., Khayati, M., Akrami, N., 2006. Performance of concrete produced with crushed bricks as the coarse and fine aggregate, in: The Geological Society of London. 10.

Beltrán, M.G., Barbudo, A., Agrela, F., Galvín, A.P., Jiménez, J.R., 2014. Effect of cement addition on the properties of recycled concretes to reach control concretes strengths. *Journal of Cleaner Production* 79: 124–133.

Bérubé, M.-A., Duchesne, J., Dorion, J.F., Rivest, M., 2002. Laboratory assessment of alkali contribution by aggregates to concrete and application to concrete structures affected by alkali–silica reactivity. *Cement and Concrete Research* 32 (8): 1215–1227.

Böke, H., Akkurt, S., İpekoğlu, B., Uğurlu, E., 2006. Characteristics of brick used as aggregate in historic brick-lime mortars and plasters. *Cement and Concrete Research* 36 (6): 1115–1122.

BS 8500-2, 2015. Concrete. Complementary British standard to BS EN 206. Specification for constituent materials and concrete. BSI, London.

Butler, L., West, J.S., Tighe, S.L., 2011. The effect of recycled concrete aggregate properties on the bond strength between RCA concrete and steel reinforcement. *Cement and Concrete Research* 41 (10): 1037–1049.

Cabral, A.E.B., Schalch, V., Molin, D.C.C.D., Ribeiro, J.L.D., 2010. Mechanical properties modeling of recycled aggregate concrete. *Construction and Building Materials* 24 (4): 421–430.

Cachim, P.B., 2009. Mechanical properties of brick aggregate concrete. *Construction and Building Materials* 23 (3): 1292–1297.

Cao, H.T., Bucea, L., Ray, A., Yozghatlian, S., 1997. The effect of cement composition and pH of environment on sulfate resistance of Portland cements and blended cements. *Cement and Concrete Composites* 19 (2): 161–171.

CEN/TC 104/SC 1/TG 19, 2013. Draft for a new European Standard on use of aggregates in concrete. CEN, Brussels.

Chen, H.J., Yen, T., Chen, K.H., 2003. Use of building rubbles as recycled aggregates. *Cement and Concrete Research* 33 (1): 125–132.

Choi, H.B., Kang, K.I., 2008. Bond behaviour of deformed bars embedded in RAC. *Magazine of Concrete Research* 60 (6): 399–410.

Cook, R.A., Hover, K.C., 1999. Mercury porosimetry of hardened cement pastes. *Cement and Concrete Research* 29 (6): 933–943.

Corinaldesi, V., Moriconi, G., 2011. The role of industrial by-products in self-compacting concrete. *Construction and Building Materials* 25 (8): 3181–3186.

Correia, J.R., Brito, J. de, Pereira, A.S., 2006. Effects on concrete durability of using recycled ceramic aggregates. *Materials and Structures* 39 (2): 169–177.

Cui, L., Cahyadi, J.H., 2001. Permeability and pore structure of OPC paste. *Cement and Concrete Research* 31 (2): 277–282.

Cultrone, G., Sebastián, E., Elert, K., de la Torre, M.J., Cazalla, O., Rodriguez–Navarro, C., 2004. Influence of mineralogy and firing temperature on the porosity of bricks. *Journal of the European Ceramic Society* 24 (3): 547–564.

Debieb, F., Courard, L., Kenai, S., Degeimbre, R., 2010. Mechanical and durability properties of concrete using contaminated recycled aggregates. *Cement and Concrete Composites* 32 (6): 421–426.

Debieb, F., Kenai, S., 2008. The use of coarse and fine crushed bricks as aggregate in concrete. *Construction and Building Materials* 22 (5): 886–893.

de Brito, J., Pereira, A.S., Correia, J.R., 2005. Mechanical behaviour of non-structural concrete made with recycled ceramic aggregates. *Cement and Concrete Composites* 27 (4): 429–433.

Devenny, A., Khalaf, F., 1999. Use of crushed brick as coarse aggregate in concrete. *Masonry International* 12 (3): 81–84.

Dhir, R.K., 2008. Facilitating the wider use of coarse and fine recycled aggregates from washing plants (No. AGG 105-003). WRAP.

Dhir, R.K., El-Mohr, M.A.K., Dyer, T.D., 1996. Chloride binding in GGBS concrete. *Cement and Concrete Research* 26 (12): 1767–1773.

Dhir, R.K., Limbachiya, M.C., Leelawat, T., 1999. Suitability of recycled concrete aggregate for use in BS 5328 designated mixes. *Structures and Buildings* 134 (3): 257–274.

Dhir, R.K., Paine, K.A., 2007. Performance related approach to use of recycled aggregates (AGG0074). WRAP.

DIN 4226-100, 2002. Aggregates for mortar and concrete. Part 100: recycled aggregates. DIN, Berlin.

Duan, Z.H., Poon, C.S., 2014. Properties of recycled aggregate concrete made with recycled aggregates with different amounts of old adhered mortars. *Materials & Design* 58: 19–29.

Etxeberria Larrañaga, M., Barra Bizinotto, M., Vazquez Ramonich, E., 2006. Utilization of recycled aggregates in the structural concrete manufacture [in Spanish]. Asociación Científico-Técnica del Hormigón Estructural.

Etxeberria, M., Vázquez, E., Marí, A., Barra, M., 2007. Influence of amount of recycled coarse aggregates and production process on properties of recycled aggregate concrete. *Cement and Concrete Research* 37 (5): 735–742.

European Council, 1999. Directive 1999/31/EC, of 26 April, on the landfill of waste, Official Journal of the European Communities, L 182, 1-19.

Ferreira, L., de Brito, J., Barra, M., 2011. Influence of the pre-saturation of recycled coarse concrete aggregates on concrete properties. *Magazine of Concrete Research* 63 (8): 617–627.

Frearson, J.P.H., 1986. Sulfate resistance of combinations of Portland cement and ground granulated blast furnace slag. *ACI Special Publication* 91: 1495–1524.

Frigione, G., 1986. Manufacture and characteristics of Portland blast furnace slag cements, in: Blended Cements. ASTM International, 15–28.

Fulton, F.S., 1974. The properties of Portland cements containing milled granulated blast-furnace slag. Portland Cement Institute.

Galvín, A.P., Ayuso, J., Agrela, F., Barbudo, A., Jiménez, J.R., 2013. Analysis of leaching procedures for environmental risk assessment of recycled aggregate use in unpaved roads. *Construction and Building Materials* 40: 1207–1214.

Galvín, A.P., Ayuso, J., García, I., Jiménez, J.R., Gutiérrez, F., 2014. The effect of compaction on the leaching and pollutant emission time of recycled aggregates from construction and demolition waste. *Journal of Cleaner Production* 83: 294–304.

Galvín, A.P., Ayuso, J., Jiménez, J.R., Agrela, F., 2012. Comparison of batch leaching tests and influence of pH on the release of metals from construction and demolition wastes. *Waste Management* 32 (1): 88–95.

García-González, J., Rodríguez-Robles, D., Juan-Valdés, A., Morán-del Pozo, J.M., Guerra-Romero, M.I., 2014. Pre-saturation technique of the recycled aggregates: solution to the water absorption drawback in the recycled concrete manufacture. *Materials* 7 (9): 6224–6236.

Gedam, V.V., Jha, R., Labhasetwar, P., Engelsen, C.J., 2012. A comprehensive physico-chemical, mineralogical and morphological characterization of Indian mineral wastes. *Environmental Monitoring and Assessment* 185 (8): 6343–6352.

Geraldes, V.L., 2013. Study on non-structural recycled concretes with mixed recycled aggregate: Mechanical properties and expansion due to sulphates [in Spanish]. Universidad Politécnica de Madrid, Madrid, Spain.

Giesche, H., 2002. Mercury porosimetry, in: Schüth, F., Sing, K.S.W., Weitkamp, J. (Eds.), Handbook of Porous Solids. Wiley-VCH Verlag GmbH, 309–351.

Gokce, A., Nagataki, S., Saeki, T., Hisada, M., 2011. Identification of frost-susceptible recycled concrete aggregates for durability of concrete. *Construction and Building Materials* 25 (5): 2426–2431.

Gomes, M., Brito, J. de, 2008. Structural concrete with incorporation of coarse recycled concrete and ceramic aggregates: durability performance. *Materials and Structures* 42 (5): 663–675.

Gómez-Meijide, B., Pérez, I., 2014. Effects of the use of construction and demolition waste aggregates in cold asphalt mixtures. *Construction and Building Materials* 51: 267–277.

Gómez-Soberón, J.M.V., 2002. Porosity of recycled concrete with substitution of recycled concrete aggregate: An experimental study. *Cement and Concrete Research* 32 (8): 1301–1311.

Gonzalez, A., Etxeberria, M., 2014. Experimental analysis of properties of high performance recycled aggregate concrete. *Construction and Building Materials* 52: 227–235.

Gonzalez-Corominas, A., Etxeberria, M., 2014. Properties of high performance concrete made with recycled fine ceramic and coarse mixed aggregates. *Construction and Building Materials* 68: 618–626.

González-Fonteboa, B., Martínez-Abella, F., 2008. Concretes with aggregates from demolition waste and silica fume. Materials and mechanical properties. *Building and Environment* 43 (4): 429–437.

Güell-Ferré, A., Váquez-Ramonich, E., Varela-Pinto, E., Serna-Ros, P., Martínez-Abella, F., López-Gayarre, F., Barra-Bizinotto, M., Tirado-Alonso, A., Romero-Casado, A., Girbés-Clari, I., 2012. Spanish handbook on recycled aggregates from construction and demolition wastes (CDW) [in Spanish], Fueyo Editores. ed. Madrid, Spain.

Halicka, A., Ogrodnik, P., Zegardlo, B., 2013. Using ceramic sanitary ware waste as concrete aggregate. *Construction and Building Materials* 48: 295–305.

Hansen, T.C. (Ed.), 1992. Recycling of demolished concrete and masonry. E&FN Spon, London.

Hansen, T.C., Narud, H., 1983. Strength of recycled concrete made from crushed concrete coarse aggregate. *Concrete International* 5 (1): 79–83.

Heath, R.C., 1983. Development and validation of a geriatric depression screening scale: a preliminary report (No. 2200), U.S. Geological survey. USGS.

Hewlett, P. (Ed.), 2003. Lea's chemistry of cement and concrete. Butterworth-Heinemann.

Hoffmann, C., Schubert, S., Leemann, A., Motavalli, M., 2012. Recycled concrete and mixed rubble as aggregates: Influence of variations in composition on the concrete properties and their use as structural material. *Construction and Building Materials* 35: 701–709.

Hogan, F.J., Meusel, J.W., 1981. Evaluation for durability and strength development of a ground granulated blast furnace slag. *Cement, Concrete and Aggregates* 3 (1): 40–52.

Hu, L., Hao, J., Wang, L., 2014. Laboratory evaluation of cement treated aggregate containing crushed clay brick. *Journal of Traffic and Transportation Engineering (English Edition)* 1 (5): 371–382.

Ihobe, CEDEX, 2011. Uses of mixed recycled aggregates from construction and demolition wastes [in Spanish] (Pre-normative investigation). Ihobe.

Ismail, S., Ramli, M., 2013. Engineering properties of treated recycled concrete aggregate (RCA) for structural applications. *Construction and Building Materials* 44: 464–476.

Jankovic, K., Nikolic, D., Bojovic, D., 2012. Concrete paving blocks and flags made with crushed brick as aggregate. *Construction and Building Materials* 28 (1): 659–663.

Jiménez, J.R., Agrela, F., Ayuso, J., López, M., 2011. A comparative study of recycled aggregates from concrete and mixed debris as material for unbound road sub-base. *Materiales de Construcción* 61 (302): 289–302.

Jiménez, J.R., Ayuso, J., Agrela, F., López, M., Galvín, A.P., 2012. Utilisation of unbound recycled aggregates from selected CDW in unpaved rural roads. *Resources, Conservation and Recycling* 58: 88–97.

Jiménez, J.R., Ayuso, J., Galvín, A.P., López, M., Agrela, F., 2012. Use of mixed recycled aggregates with a low embodied energy from non-selected CDW in unpaved rural roads. *Construction and Building Materials* 34: 34–43.

Kaneuji, M., Winslow, D.N., Dolch, W.L., 1980. The relationship between an aggregate's pore size distribution and its freeze thaw durability in concrete. *Cement and Concrete Research* 10 (3): 433–441.

Karlsen, J., Petkovic, G., Lahus, O., 2002. A Norwegian certification scheme for recycled aggregates (RCA), in: Proceedings of the Third International Conference Sustainable Building. Oslo, Norway.

Katz, A., 2003. Properties of concrete made with recycled aggregate from partially hydrated old concrete. *Cement and Concrete Research* 33 (5): 703–711.

Katz, A., 2004. Treatments for the Improvement of Recycled Aggregate. *Journal of Materials in Civil Engineering* 16 (6): 597–603.

Katzer, J., Domski, J., 2013. Optimization of fibre reinforcement for waste aggregate cement composite. *Construction and Building Materials* 38: 790–795.

Khalaf, F.M., 2006. Using crushed clay brick as coarse aggregate in concrete. *Journal of materials in civil engineering* 18 (4): 518–526.

Khalaf, F.M., DeVenny, A.S., 2002. New tests for porosity and water absorption of fired clay bricks. *Journal of materials in civil engineering* 14 (4): 334–337.

Khalaf, F.M., DeVenny, A.S., 2005. Properties of new and recycled clay brick aggregates for use in concrete. *Journal of Materials in Civil Engineering* 17 (4): 456–464.

Khaloo, A.R., 1995. Crushed tile coarse aggregate concrete. *Cement, Concrete and Aggregates* 17 (2).

Koronthalyova, O., 2011. Moisture storage capacity and microstructure of ceramic brick and autoclaved aerated concrete. *Construction and Building Materials* 25 (2): 879–885.

Kosson, D.S., van der Sloot, H.A., Sanchez, F., Garrabrants, A.C., 2002. An integrated framework for evaluating leaching in waste management and utilization of secondary materials. *Environmental Engineering Science* 19 (3): 159–204.

Kou, S.C., Poon, C.S., Agrela, F., 2011a. Comparisons of natural and recycled aggregate concretes prepared with the addition of different mineral admixtures. *Cement and Concrete Composites* 33 (8): 788–795.

Kou, S.C., Poon, C.S., Etxeberria, M., 2011b. Influence of recycled aggregates on long term mechanical properties and pore size distribution of concrete. *Cement and Concrete Composites* 33 (2): 286–291.

Kumar, P.S., Dhinakaran, G., 2012. Effect of admixed recycled aggregate concrete on properties of fresh and hardened concrete. *Journal of Materials in Civil Engineering* 24 (4): 494–498.

Lavat, A.E., Trezza, M.A., Poggi, M., 2009. Characterization of ceramic roof tile wastes as pozzolanic admixture. *Waste Management* 29 (5): 1666–1674.

Lee, K.-M., Park, P.-J., 2005. Estimation of the environmental credit for the recycling of granulated blast furnace slag based on LCA. *Resources, Conservation and Recycling* 44 (2): 139–151.

Leite, F. da C., Motta, R. dos S., Vasconcelos, K.L., Bernucci, L., 2011. Laboratory evaluation of recycled construction and demolition waste for pavements. *Construction and Building Materials* 25 (6): 2972–2979.

Leiva, C., Solís-Guzmán, J., Marrero, M., García Arenas, C., 2013. Recycled blocks with improved sound and fire insulation containing construction and demolition waste. *Waste Management*, Special Thematic Issue: Urban Mining Urban Mining 33 (3): 663–671.

Limbachiya, M.C., Leelawat, T., Dhir, R.K., 2000. Use of recycled concrete aggregate in high-strength concrete. *Materials and Structures* 33 (9): 574–580.

Limbachiya, M.C., Marrocchino, E., Koulouris, A., 2007. Chemical–mineralogical characterisation of coarse recycled concrete aggregate. *Waste Management* 27 (2): 201–208.

Liu, J.L., Li, Y., Jiang, M., Zhou, H., 2010. Mechanical and frost-resistance properties of rural area building waste hollow bricks. *J. Wuhan Univ. Technol.-Mat. Sci. Edit.* 25 (6): 1017–1021.

LNEC E-471, 2009. Guide for the use of recycled coarse aggregates in concretes with hydraulic binder [in Portuguese]. LNEC, Lisbon.

López Gayarre, F., López-Colina, C., Serrano, M.A., López-Martínez, A., 2013. Manufacture of concrete kerbs and floor blocks with recycled aggregate from C&DW. *Construction and Building Materials* 40: 1193–1199.

Luo, R., Cai, Y., Wang, C., Huang, X., 2003. Study of chloride binding and diffusion in GGBS concrete. *Cement and Concrete Research* 33 (1): 1–7.

Mansur, M.A., Wee, T.H., Lee, S.C., 1999. Crushed bricks as coarse aggregate for concrete. *ACI Materials Journal* 96 (4): 478–484.

Martínez-Lage, I., Martínez-Abella, F., Vázquez-Herrero, C., Pérez-Ordóñez., J.L., 2012. Properties of plain concrete made with mixed recycled coarse aggregate. *Construction and Building Materials* 37: 171–176.

Mas, B., Cladera, A., Bestard, J., Muntaner, D., López, C.E., Piña, S., Prades, J., 2012a. Concrete with mixed recycled aggregates: Influence of the type of cement. *Construction and Building Materials* 34: 430–441.

Mas, B., Cladera, A., del Olmo, T., Pitarch, F., 2012b. Influence of the amount of mixed recycled aggregates on the properties of concrete for non-structural use. *Construction and Building Materials* 27 (1): 612–622.

Matias, D., de Brito, J., Rosa, A., Pedro, D., 2013. Mechanical properties of concrete produced with recycled coarse aggregates – Influence of the use of superplasticizers. *Construction and Building Materials* 44: 101–109.

Medina, C., Frías, M., Sánchez de Rojas, M.I., 2014a. Leaching in concretes containing recycled ceramic aggregate from the sanitary ware industry. *Journal of Cleaner Production* 66: 85–91.

Medina, C., Sánchez de Rojas, M.I., Frías, M., 2012. Reuse of sanitary ceramic wastes as coarse aggregate in eco-efficient concretes. *Cement and Concrete Composites* 34 (1): 48–54.

Medina, C., Sánchez de Rojas, M.I., Frías, M., 2013. Freeze-thaw durability of recycled concrete containing ceramic aggregate. *Journal of Cleaner Production* 40: 151–160.

Medina, C., Zhu, W., Howind, T., Frías, M., Sánchez de Rojas, M.I., 2015. Effect of the constituents (asphalt, clay materials, floating particles and fines) of construction and demolition waste on the properties of recycled concretes. *Construction and Building Materials* 79: 22–33.

Medina, C., Zhu, W., Howind, T., Sánchez de Rojas, M.I., Frías, M., 2014b. Influence of mixed recycled aggregate on the physical – mechanical properties of recycled concrete. *Journal of Cleaner Production* 68: 216–225.

Medina Martínez, C., 2011. Behaviour of recycled concrete with ceramic aggregate: Physical, mechanical, microstructural and durability study [in Spanish]. Universidad de León, León, Spain.

Mefteh, H., Kebaïli, O., Oucief, H., Berredjem, L., Arabi, N., 2013. Influence of moisture conditioning of recycled aggregates on the properties of fresh and hardened concrete. *Journal of Cleaner Production* 54: 282–288.

Meusel, J.W., Rose, J.H., 1983. Production of granulated blast furnace slag at sparrows point, and the workability and strength potential of concrete incorporating the slag. *ACI Special Publication* 79: 867–890.

Molineux, C.J., Fentiman, C.H., Gange, A.C., 2009. Characterising alternative recycled waste materials for use as green roof growing media in the U.K. *Ecological Engineering* 35 (10): 1507–1513.

Müllller, A., 2004. Lightweight aggregates from masonry rubble, in: Vazquez, E., Hendriks, C.F., Janssen, G.M.T. (Eds.), International RILEM Conference on the Use of Recycled Materials in Building and Structures. RILEM Publications SARL, 97–106.

Naceri, A., Hamina, M.C., 2009. Use of waste brick as a partial replacement of cement in mortar. *Waste Management* 29 (8): 2378–2384.

Nagataki, S., Gokce, A., Saeki, T., 2000. Effects of recycled aggregate characteristics on performance parameters of recycled aggregate concrete, in: Proceedings of the Fifth CANMET/ACI International Conference on Durability of Concrete. Barcelona, Spain, 51–71.

Nakamura, N., Saki, M., Swamy, R., 1992. Effect of slag fineness on the development of concrete strength and microstructure. *ACI Special Publication* 132: 1343–1366.

NBR 15116, 2004. Recycled aggregate of solid residue of building constructions. Requirements and methodologies [in Portuguese]. ABNT, Sao Paulo, Brazil.

Neville, A.M., 1995. Properties of concrete. Harlow, Essex: Longman.

Odler, I., Colán-Subauste, J., 1999. Investigations on cement expansion associated with ettringite formation. *Cement and Concrete Research* 29 (5): 731–735.

Olorunsogo, F.T., 1998. Particle size distribution of GGBS and bleeding characteristics of slag cement mortars. *Cement and Concrete Research* 28 (6): 907–919.

Osborne, G.J., 1999. Durability of Portland blast-furnace slag cement concrete. *Cement and Concrete Composites* 21 (1): 11–21.

Pacheco-Torgal, F., Jalali, S., 2010a. Compressive strength and durability properties of ceramic wastes based concrete. *Materials and Structures* 44 (1): 155–167.

Pacheco-Torgal, F., Jalali, S., 2010b. Reusing ceramic wastes in concrete. *Construction and Building Materials* 24 (5): 832–838.

Padmini, A.K., Ramamurthy, K., Mathews, M.S., 2009. Influence of parent concrete on the properties of recycled aggregate concrete. *Construction and Building Materials* 23 (2): 829–836.

Paine, K.A., Dhir, R.K., 2010. Recycled aggregates in concrete: a performance-related approach. *Magazine of Concrete Research* 62 (7): 519–530.

Panesar, D.K., Chidiac, S.E., 2007. Multi-variable statistical analysis for scaling resistance of concrete containing GGBFS. *Cement and Concrete Composites* 29 (1): 39–48.

Parra y Alfaro, J., 2001. Characterization of CDW in the Autonomous Community of Madrid as recycled aggregates in the concrete manufacture [in Spanish]. Universidad Politécnica de Madrid, Madrid, Spain.

Pepe, M., Toledo Filho, R.D., Koenders, E.A.B., Martinelli, E., 2014. Alternative processing procedures for recycled aggregates in structural concrete. *Construction and Building Materials* 69: 124–132.

Permanent Commission on Concrete, 2008. Code on structural concrete (EHE-08) [in Spanish]. Spanish Ministry of Public Works, Madrid.

Pigeon, M., Pleau, R., 1995. Durability of concrete in cold climates, Modern Concrete Technology. E&FN Spon.

Poon, C.S., Chan, D., 2006a. Feasible use of recycled concrete aggregates and crushed clay brick as unbound road sub-base. *Construction and Building Materials* 20 (8): 578–585.

Poon, C.S., Chan, D., 2006b. Paving blocks made with recycled concrete aggregate and crushed clay brick. *Construction and Building Materials* 20 (8): 569–577.

Poon, C.S., Kou, S.C., Wan, H.W., Etxeberria, M., 2009. Properties of concrete blocks prepared with low grade recycled aggregates. *Waste Management* 29 (8): 2369–2377.

Poon, C.S., Shui, Z.H., Lam, L., 2004a. Effect of microstructure of ITZ on compressive strength of concrete prepared with recycled aggregates. *Construction and Building Materials* 18 (6): 461–468.

Poon, C.S., Shui, Z.H., Lam, L., Fok, H., Kou, S.C., 2004b. Influence of moisture states of natural and recycled aggregates on the slump and compressive strength of concrete. *Cement and Concrete Research* 34 (1): 31–36.

Quan, H., Kasami, H., Tamai, T., 2010. Experimental study on effects of adhered mortar content on quality of recycled coarse aggregate and properties of concrete, in: Xiao, J.Z., Zhang, Y., Cheung, M.S., Chu, R.P.K. (Eds.), 2nd International Conference on Waste Engineering and Management - ICWEM 2010. RILEM Publications SARL, 491–500.

Rao, A., Jha, K.N., Misra, S., 2007. Use of aggregates from recycled construction and demolition waste in concrete. *Resources, Conservation and Recycling* 50 (1): 71–81.

Ravindrarajah, R.S., Tam, C., 1985. Properties of concrete made with crushed concrete as coarse aggregate. *Magazine of Concrete Research* 37 (130): 29–38.

Reig, L., Tashima, M.M., Borrachero, M.V., Monzó, J., Cheeseman, C.R., Payá, J., 2013a. Properties and microstructure of alkali-activated red clay brick waste. *Construction and Building Materials* 43: 98–106.

Reig, L., Tashima, M.M., Soriano, L., Borrachero, M.V., Monzó, J., Payá, J., 2013b. Alkaline activation of ceramic waste materials. *Waste Biomass Valor* 4 (4): 729–736.

RILEM TC 121-DRG, 1994. Specifications for concrete with recycled aggregates. *Materials and Structures* 27 (9): 557–559.

Rodríguez-Robles, D., García-González, J., Juan-Valdés, A., Morán-del Pozo, J.M., Guerra-Romero, M.I., 2014. Quality assessment of mixed and ceramic recycled aggregates from construction and demolition wastes in the concrete manufacture according to the Spanish standard. *Materials* 7 (8): 5843–5857.

Rootare, H.M., Prenzlow, C.F., 1967. Surface areas from mercury porosimeter measurements. *The Journal of physical chemistry* 71 (8): 2733–2736.

Rübner, K., Hoffmann, D., 2006. Characterization of mineral building materials by mercury intrusion porosimetry. *Particle & Particle Systems Characterization* 23 (1): 20–28.

Sadek, D.M., 2012. Physico-mechanical properties of solid cement bricks containing recycled aggregates. *Journal of Advanced Research* 3 (3): 253–260.

Sadek, D.M., Nouhy, H.A. El, 2014. Properties of paving units incorporating crushed ceramic. *HBRC Journal* 10 (2): 198–205.

Sánchez de Juan, M., 2004. Study on the use of recycled aggregate in structural concrete [in Spanish]. E.T.S.I. Caminos, Canales y Puertos (UPM), Madrid.

Sánchez de Juan, M., Alaejos Gutiérrez, M.P., 2009. Study on the influence of attached mortar content on the properties of recycled concrete aggregate. *Construction and Building Materials* 23 (2): 872–877.

Sánchez De Rojas, M.I., Marín, F.P., Frías, M., Rivera, J., 2007. Properties and performances of concrete tiles containing waste fired clay materials. *Journal of the American Ceramic Society* 90 (11): 3559–3565.

Sánchez de Rojas, M.I., Marín, F., Rivera, J., Frías, M., 2006. Morphology and properties in blended cements with ceramic wastes as a pozzolanic material. *Journal of the American Ceramic Society* 89 (12): 3701–3705.

Sani, D., Moriconi, G., Fava, G., Corinaldesi, V., 2005. Leaching and mechanical behaviour of concrete manufactured with recycled aggregates. *Waste Management* 25 (2): 177–182.

Sata, V., Wongsa, A., Chindaprasirt, P., 2013. Properties of pervious geopolymer concrete using recycled aggregates. *Construction and Building Materials* 42: 33–39.

Schouenborg, B., Aurstad, J., Hagnestal, L., Petursson, P., Winblad, J., 2004a. Test methods adapted for alternative and recycled, porous aggregates mnaterials. Part 3: Water absorption (NT Technical Report No. 550). Nordic Innovation Centre.

Schouenborg, B., Aurstad, J., Pétursson, P., 2004b. Test methods adapted to alternative aggregates, in: International RILEM Conference on the Use of Recycled Materials in Building and Structures, Barcelona, Spain.

Senthamarai, R., Devadas Manoharan, P., 2005. Concrete with ceramic waste aggregate. *Cement and Concrete Composites* 27 (9–10): 910–913.

Seo, D.S., Choi, H.B., 2014. Effects of the old cement mortar attached to the recycled aggregate surface on the bond characteristics between aggregate and cement mortar. *Construction and Building Materials* 59: 72–77.

Shayan, A., Xu, A., 2004. Value-added utilisation of waste glass in concrete. *Cement and Concrete Research* 34 (1): 81–89.

Sheen, Y.-N., Wang, H.-Y., Juang, Y.-P., Le, D.-H., 2013. Assessment on the engineering properties of ready-mixed concrete using recycled aggregates. *Construction and Building Materials* 45: 298–305.

Sherwood, P.., 1995. The use of waste and recycled materials in roads. *Proceedings of the ICE - Transport* 111 (2): 116–124.

Sidorova, A., Vazquez-Ramonich, E., Barra-Bizinotto, M., Roa-Rovira, J.J., Jimenez-Pique, E., 2014. Study of the recycled aggregates nature's influence on the aggregate–cement paste interface and ITZ. *Construction and Building Materials* 68: 677–684.

Silva, R.V., de Brito, J., Dhir, R.K., 2014. Properties and composition of recycled aggregates from construction and demolition waste suitable for concrete production. *Construction and Building Materials* 65: 201–217.

Silvestre, R., Medel, E., García, A., Navas, J., 2013. Using ceramic wastes from tile industry as a partial substitute of natural aggregates in hot mix asphalt binder courses. *Construction and Building Materials* 45: 115–122.

Sivasundaram, V., Malhotra, V.M., 1992. Properties of Concrete Incorporating Low Quantity of Cement and High Volumes of Ground Granulated Slag. *ACI Materials Journal* 89 (6): 554–563.

Smolczyk, H.G., 1980. Structure of slags and hydration of slag cements, in: Proceedings of the 7th International Cement Congress. 3–17.

Soares, D., de Brito, J., Ferreira, J., Pacheco, J., 2014. Use of coarse recycled aggregates from precast concrete rejects: Mechanical and durability performance. *Construction and Building Materials* 71: 263–272.

Soutsos, M.N., Tang, K., Millard, S.G., 2011. Concrete building blocks made with recycled demolition aggregate. *Construction and Building Materials* 25 (2): 726–735.

Sujeong, L., Kim, Y., Moon, H., 1999. Phase transformation sequence from kaolinite to mullite investigated by an energy-filtering transmission electron. *J Am Ceram Soc* 10: 2841–2848.

Tabsh, S.W., Abdelfatah, A.S., 2009. Influence of recycled concrete aggregates on strength properties of concrete. *Construction and Building Materials* 23 (2): 1163–1167.

Tamura, H., Arai, M., lmamoto, K., 2001. Innovative methods for water content control of recycled aggregate concrete: rapid absorption test for aggregate and continuous monitoring of freshly-mixed concrete at site. *ACI Special Publication* 200.

Tam, V.W.Y., Gao, X.F., Tam, C.M., Chan, C.H., 2008. New approach in measuring water absorption of recycled aggregates. *Construction and Building Materials* 22 (3): 364–369.

Tam, V.W.Y., Tam, C.M., 2009. Parameters for assessing recycled aggregate and their correlation. *Waste Management & Research* 27 (1): 52–58.

Tam, V.W.Y., Tam, C.M., Le, K.N., 2007. Removal of cement mortar remains from recycled aggregate using pre-soaking approaches. *Resources, Conservation and Recycling* 50 (1): 82–101.

Tazawa, E., Yonekura, A., Tanaka, S., 1989. Drying shrinkage and creep of concrete containing granulated blast furnace slag. *ACI Special Publication* 114: 1325–1344.

Thanaya, I.N.A., 2009. Asphalt-bound masonry block incorporating construction demolition waste. *Journal of Civil Engineering* 29 (1): pp–20.

Topçu, İ.B., Canbaz, M., 2004. Properties of concrete containing waste glass. *Cement and Concrete Research* 34 (2): 267–274.

UNE EN 197-1, 2011. Cement. Part 1: Composition, specifications and conformity criteria for common cements [in Spanish]. AENOR, Madrid.

UNE EN 932-1, 1997. Test for general properties of aggregates. Part 1: Methods for sampling [in Spanish]. AENOR, Madrid.

UNE EN 932-2, 1999. Tests for general properties of aggregates. Part 2: Methods for reducing laboratory samples [in Spanish]. AENOR, Madrid.

UNE EN 933-11, 2009. Tests for geometrical properties of aggregates. Part 11: Classification test for the constituents of coarse recycled aggregate [in Spanish]. AENOR, Madrid.

UNE EN 1367-1, 2008. Tests for thermal and weathering properties of aggregates. Part 1: Determination of resistance to freezing and thawing. AENOR, Madrid, Spain.

UNE EN 1367-2, 2010. Tests for thermal and weathering properties of aggregates. Part 2: Magnesium sulfate test. AENOR, Madrid, Spain.

UNE EN 1744-1, 2010. Tests for chemical properties of aggregates. Part 1: Chemical analysis. AENOR, Madrid.

UNE EN 1744-5, 2007. Tests for chemical properties of aggregates. Part 5: Determination of acid soluble chloride salts. AENOR, Madrid, Spain.

UNE EN 1744-6, 2007. Tests for chemical properties of aggregates. Part 6: Determination of the influence of recycled aggregate extract on the initial setting time of cement. AENOR, Madrid, Spain.

Van Der Wegen, G., Haverkort, R., 1998. Recycled construction and demolition wastes as a fine aggregate for concrete, in: Proceedings of the International Symposium on Sustainable Construction: Use of Recycled Concrete Aggregate. London, UK.

Vegas, I., Broos, K., Nielsen, P., Lambertz, O., Lisbona, A., 2015. Upgrading the quality of mixed recycled aggregates from construction and demolition waste by using near-infrared sorting technology. *Construction and Building Materials* 75: 121–128.

Vegas, I., Ibañez, J.A., Lisbona, A., Sáez de Cortazar, A., Frías, M., 2011. Pre-normative research on the use of mixed recycled aggregates in unbound road sections. *Construction and Building Materials* 25 (5): 2674–2682.

Vegas, I., Ibañez, J.A., San José, J.T., Urzelai, A., 2008. Construction demolition wastes, Waelz slag and MSWI bottom ash: a comparative technical analysis as material for road construction. *Waste Management (New York, N.Y.)* 28 (3): 565–574.

Vincke, E., Wanseele, E.V., Monteny, J., Beeldens, A., Belie, N.D., Taerwe, L., Gemert, D.V., Verstraete, W., 2002. Influence of polymer addition on biogenic sulfuric acid attack of concrete. *International Biodeterioration & Biodegradation* 49 (4): 283–292.

Virtanen, J., 1983. Freeze-thaw resistance of concrete containing blast-furnace slag, fly ash or condensed silica fume. *ACI Special Publication* 79: 923–942.

Vrancken, K.C., Laethem, B., 2000. Recycling options for gypsum from construction and demolition waste, in: G.R. Woolley, J.J.J.M.G. and P.J.W. (Ed.), Waste Management Series, Waste Materials in Construction Wascon 2000 Proceedings of the International Conference on the Science and Engineering of Recycling for Environmental Protection, Harrogate, England 31 May, 1–2 June 2000. Elsevier, 325–331.

Wainwright, P., Ait-Aider, H., 1995. The influence of cement source and slag additions on the bleeding of concrete. *Cement and Concrete Research* 25 (7): 1445–1456.

Wainwright, P.J., Rey, N., 2000. The influence of ground granulated blastfurnace slag (GGBS) additions and time delay on the bleeding of concrete. *Cement and Concrete Composites* 22 (4): 253–257.

Wan, H., Shui, Z., Lin, Z., 2004. Analysis of geometric characteristics of GGBS particles and their influences on cement properties. *Cement and Concrete Research* 34 (1): 133–137.

Wardlaw, N.C., McKellar, M., 1981. Mercury porosimetry and the interpretation of pore geometry in sedimentary rocks and artificial models. *Powder Technology* 29 (1): 127–143.

Xiao, Z., Ling, T.C., Kou, S.C., Wang, Q., Poon, C.S., 2011. Use of wastes derived from earthquakes for the production of concrete masonry partition wall blocks. *Waste Management* 31 (8): 1859–1866.

Xuan, D.X., Houben, L.J.M., Molenaar, A. a. A., Shui, Z.H., 2011. Mixture optimization of cement treated demolition waste with recycled masonry and concrete. *Materials and Structures* 45 (1-2): 143–151.

Yang, J., Du, Q., Bao, Y., 2011. Concrete with recycled concrete aggregate and crushed clay bricks. *Construction and Building Materials* 25 (4): 1935–1945.

Ye, G., 2003. Experimental study and numerical simulation of the development of the microstructure and permeability of cementitious materials. Delft University, Netherlands.

Zdravkov, B.D., Čermák, J.J., Šefara, M., Janků, J., 2007. Pore classification in the characterization of porous materials: A perspective. *Central European Journal of Chemistry* 5 (2): 385–395.

Zega, C.J., Villagrán-Zaccardi, Y.A., Maio, A.A.D., 2010. Effect of natural coarse aggregate type on the physical and mechanical properties of recycled coarse aggregates. *Materials and Structures* 43 (1-2): 195–202.

Zhang, M.-H., Bilodeau, A., Malhotra, V.M., Kim, K.S., Kim, J.-C., 1999. Concrete incorporating supplementary cementing materials: effect of curing on compressive strength and resistance to chloride-ion penetration. *ACI Materials Journal* 96 (2): 181–189.

Zhou, J., Ye, G., van Breugel, K., 2010. Characterization of pore structure in cement-based materials using pressurization–depressurization cycling mercury intrusion porosimetry (PDC-MIP). *Cement and Concrete Research* 40 (7): 1120–1128.

Zoldners, N.G., 1971. Thermal properties of concrete under sustained elevated temperatures. *ACI Special Publication* 25: 1–32.

Chapter 5

Concrete mixture design

1. INTRODUCTION

Besides the material selection, the quality of the concrete is controlled trough the mix proportioning of the concrete raw materials and the adequate handling of the fresh mixture (order in the addition of the concrete raw materials, mixing time, transport, casting, finishing and curing).

Provided that the replacement of the gravel by the recycled aggregates means the inclusion of a new constituent in the conventional concrete manufacture, a brief summary regarding the different manner in which this subject has been treated is provided in this chapter. Furthermore, the calculations for the different concrete mixes tested during the research are detailed as well as the procedures followed in the preparation of the test specimens and the storage conditions until their testing age.

2. THEORETICAL BACKGROUND

Concrete is a composite material composed of a binding medium (hard cement paste) formed by the reaction between cement and water, within which fine and coarse aggregates are embedded creating the granular skeleton of the mixture. The proportioning of these materials is known as the optimization or design of the concrete mixture, which involves the adaptation of the available resources in such a combination that the engineering technical criteria (workability of the fresh concrete, compressive strength and durability of the hardened concrete) are satisfied.

Currently, the proportioning of concrete mixtures could be calculated according to a plethora of methods. In essence, the different methods try to relate the amounts of the different constituents (water, cement and aggregates) to the future physical and mechanical properties of the fresh and hardened concrete. According to the initial predetermined parameter, two methods could be differentiated; one based upon a fixed amount of cement (e.g. Fuller and Bolomey) and the other focused on the target compressive strength of the hardened concrete (e.g. ACI and De la Peña).

Initially, these methods were only intended for the proportioning of conventional concrete mixtures. However, in the absence of specific methods for the design of recycled concrete mixtures, the common approach followed was to use these same methodologies while taking into account the differential properties between the natural and the recycled aggregates. Table 5.1 shows some investigations in which the traditional methods were adapted and employed for the design of recycled concrete mixtures.

Table 5.1: Examples on the adjustment of traditional proportioning methods for the design of recycled concrete mixtures

Proportioning method	References
Fuller (Fuller and Thompson, 1907)	Malesev et al. (2010) González-Corominas and Etxebarria (2014) González and Etxebarria (2014)
Bolomey (Bolomey, 1935)	López-Gayarre et al. (2009) Mas et al. (2012b) Beltran et al. (2014)
ACI (ACI Committee 211, 2002)	Kumar et al. (2009) Somna et al. (2012) Jiménez et al. (2013)
De la Peña (Jiménez Montoya et al., 2009)	del Río et al. (2004) Medina et al. (2012) Medina et al. (2015)

Usually, the recycled aggregates are only employed as a partial substitution of the natural coarse aggregate, which has led to the existence of two different replacement approaches: the direct weight replacement (DWR) and the direct volume replacement (DVR). In the DWR method (Dhir et al., 1999; Fathifazl et al., 2009), the amount of water, cement and total coarse aggregate (natural and recycled) is kept constant for any replacement ratio while the quantity of fines aggregates is slightly reduced since the recycled aggregates normally occupy a greater volume than natural aggregates. In the DVR approach, the corresponding percentage of natural coarse aggregate is replaced by given volume of recycled aggregate (Topçu and Şengel, 2004; Etxeberria et al., 2007; López-Gayarre et al., 2009).

Among the differences between the properties of the natural and recycled aggregates, the water absorption is the parameter that has the highest impact on the recycled concrete mix design, because its influence on the workability of the fresh concrete. As previously stated in chapter 4, the investigations regarding this parameter have been extensive, resulting in diverse techniques aimed to compensate the high water absorption of the recycled aggregates: addition of extra water (Tabsh and Abdelfatah, 2009; Ferreira et al., 2011; Mas et al., 2012a, 2012b; Matias et al., 2013; Beltrán et al., 2014; Soares et al., 2014), pre-soaking (Khalaf and DeVenny, 2005; Etxeberria

et al., 2007; Debieb and Kenai, 2008; Agrela et al., 2011; García-González et al., 2014), washing of the particles adhered to the recycled aggregates (Van Der Wegen and Haverkort, 1998; Rodrigues et al., 2013) and through the use of superplasticizers (Barbudo et al., 2013; Matias et al., 2013) and admixtures (Kou et al., 2011). On the contrary, Poon et al. (2004) concluded that when no more than 50% of recycled aggregates in air-dried state were used in the replacement the effect on the workability was not significant and advised to use recycled aggregates in saturated surface-dried state in special situations only.

Regarding the cement content, although the majority of the investigations maintained it constant for both conventional and recycled concrete mixes, some researchers (Etxeberria et al., 2007; Beltrán et al., 2014) have relied on the use of higher quantities of cement in order to achieve recycled concrete mixtures with similar mechanical strength than those of the conventional concrete. For instance, Etxeberria et al. (2007) registered the need of raising the cement content with approximately 20-30% in order to achieve similar compressive strength between the control concrete and a recycled concrete with a total substitution of the natural coarse aggregate. Nonetheless, the increase of the cement goes against the environmental principle of the reutilization of recycled aggregates in the concrete manufacture and results to be expensive as well; hence, this practice should not be encouraged.

In spite the adjustments made to the concrete mixture methods, the technology of recycled concrete production is bound to be different from the production procedure for concrete with natural aggregate. According to Poon et al. (2004), the differential properties of the recycled aggregates should also be taken into account for adjusting other technical parameters such as mixing or compacting time. In the literature, a plethora of mixing times and order of incorporation of the different components have been employed, which in some cases are totally opposites. For example, Exteberria et al. (2007) started the concrete mixture with the mixing of the cement and the water for a minute followed by the incorporation of the fine and coarse aggregates with a complete mixing time of 3 minutes, while Beltrán et al. (2014) mixed the fine and coarse aggregates for 1 minute before adding the cement and finally the water and extended the mixing time to 10 minutes.

Special mention deserves the two-stage mixing approach (TSMA) proposed by Tam et al. (2005). Opposed to the normal mixing approach in which all the dry components are placed in the mixer and then the water is added immediately before a pre-determined rotation period, the TSMA divides the mixing process in two parts. After the fine and coarse aggregates are mixed for 60 seconds, half of the required water is added and after another 60 seconds of mixing time the cement is added and 30 seconds later the remaining water is incorporated. The addition of the water at different timing leads to the formation of a thin layer of cement slurry on the surface of the recycled aggregates that permeates into the attached mortar filling up the old cracks and voids which finally translates in concretes with stronger interfacial transition zones (ITZ) and consequently higher compressive strength. To date, slight variations have been proposed by several researchers (Poon et al., 2007; Abd Elhakam et al., 2012; Mas et al., 2012b) based upon the two-stage mixing principle.

In line with the TSMA method, Kong et al. (2006) developed the triple method (TM) that involves the addition of pozzolanic admixtures (fly ash, slag or silica fume) besides a fragmented addition of the mixing water. Since the admixtures coat the surface of the recycled aggregates, the ITZ is improved by means of pozzolanic secondary reactions while some other properties of concrete, such as compressive and flexural strength, workability and packing density, are also improved (Li et al., 2009; Kong et al., 2010).

Recently, Fathifazl et al. (2009) proposed a specific proportioning method for recycled concrete mixtures containing recycled concrete aggregates (RCA) resulting in similar physical, mechanical and durability properties as the conventional concrete mixtures while using a lower quantity of cement. This method, termed EMV (Equivalent Mortar Volume), takes into account the fact that RCA is a two-phase material (virgin aggregate and attached mortar) and is based on the treatment of the residual mortar as part of the total mortar content in the recycled concrete, which should be equal to the mortar volume of a reference conventional concrete using the ACI method (ACI Committee 211, 2002). Hence, the replacement ratio of the natural aggregate depends upon the quantity of attached mortar in the RCA.

Since the research performed to date using the EMV method (Abbas et al., 2009; Razaqpur et al., 2010; Fathifazl et al., 2011) showed promising results, Jiménez et al. (2013) verified if the EMV method could be employed if another traditional proportioning method was used to design the reference conventional concrete. The results showed that the Bolomey method (Bolomey, 1935) could also be used when the principles of the EMV were employed in the optimization of recycled concrete mixtures. Later on, the investigations of Vázquez et al. (2014) and Jiménez et al. (2014) testing the durability properties of recycled concrete mixtures produced according to this method, served to further ascertain the validity of the adjustment.

3. CONCRETE MIXTURES DESIGN

The Spanish Code on structural concrete (Permanent Commission on Concrete, 2008) lays down some requirements regarding some parameters in the concrete dosage; however, the proportioning method is not prescribed in any form. In this research work, the De la Peña method (Jiménez Montoya et al., 2009) was selected for the proportioning of all concrete mixtures. Although this method is not too well known at international level, it is the most employed method in Spain since its development in 1955.

The aim of this investigation is to compare the fresh, microstructural, mechanical and durability properties of a reference conventional concrete mixture and those of recycled concrete mixtures made with recycled aggregates with different proportions of the ceramic materials, which would allow the assessment of the quality and performance of concrete produced by the partial substitution of the natural coarse aggregate with recycled aggregate derived from construction and demolition wastes (CDW). Hence, besides a reference concrete (CC), concrete mixes with a 50% replacement in weight of the natural coarse aggregate with recycled aggregates were manufactured (RC-L(S), RC-L(B), RC-M(S) and RC-H(S)) in each of the research phases (I and II). Figure 5.1 illustrates the cross-sectional area of the different concrete mixtures tested within the framework of this dissertation.

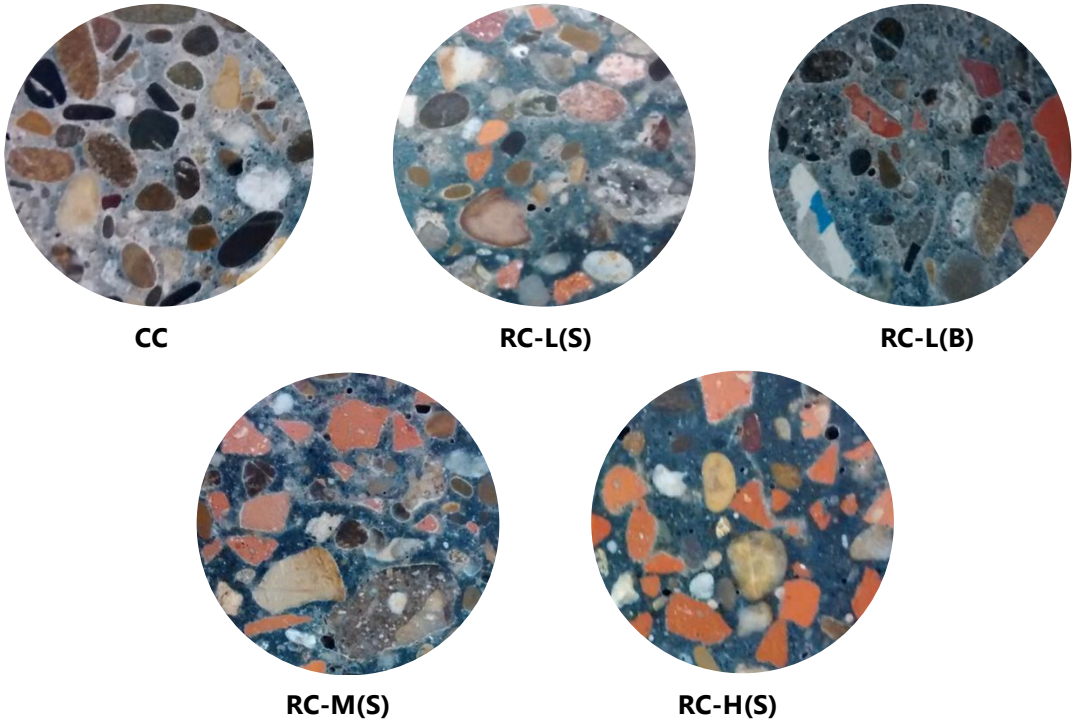

Figure 5.1: Cross-sectional area of the different concrete mixtures

Note that the roman number of the concrete mixture designation indicates the research phase in which the specific concrete dosage was employed. Since, the different mixtures were made from different recycled aggregates, i.e. not only different in origin but also with different ceramic content, the L, M and H letters in the nomenclature of the different concrete mixtures convey the idea of the ceramic percentage of the recycled aggregate employed in the substitution (low, medium or high) and the S and B letters indicate the spatial origin of the recycled aggregate (Spain or Belgium).

The experimental planning was based on establishing both the cement content and the total water/cement ratio as comparison parameters between conventional and recycled concrete mixtures in order to assess the influence of the recycled aggregate replacement, specifically the ceramic component included with the aggregate substitution, on the behaviour and performance of the concrete mixtures by means of a testing program focused on the fresh, microstructural, mechanical and durability properties of the concrete.

The proportioning method was based on the attainment of a target minimum 28 days compressive strength while observing other design parameters. Although the general practice points out that recycled concrete made with mixed recycled aggregate as a low quality product and therefore limited to not structural applications; the aim of this research work is to promote the use of this type of concrete in high end applications. As such, the concrete mixtures were designed having in mind a structural concrete, which translates in a minimum 25 MPa characteristic compressive strength at 28 days of testing.

Other design parameters adopted in the research works carried out were a maximum aggregate size of 20 mm and a S2 slump class as laid down in EHE-08 (Permanent Commission on Concrete, 2008), which is equivalent to a S3 slump in EN 206-1 (2005). In addition, with the purpose of achieving a durable concrete some limits, i.e. a maximum water/cement ratio of 0.55 and a minimum cement content of 300 kg/m^3, were followed as prescribed by EHE-08 (Permanent Commission on Concrete, 2008).

Taking into account all these predetermined parameters and requirements, the cement content was calculated by the selected minimum resistance target, the water content was set as a function of the desired slump class, the type of aggregates (round or crushed) and the maximum particle size. Normally, the proportioning of the fine and coarse aggregates is based upon tabulated values. However, as no available information exists for recycled aggregates, it was decided to employ the Fuller method (Fuller and Thompson, 1907) in this part of the calculations, as a means to give more importance to the differential characteristics of the natural and recycled aggregates, namely the particle size distribution and density.

4. CONCRETE MIXTURES CALCULATION

The calculations for the proportioning of both conventional and recycled concrete mixtures are here described in a detailed manner.

The first step of the method consisted of the calculation of the necessary water/cement ratio of the concrete mixture in order to attain the targeted compressive strength using equation (5.1). Given that the binders used were CEM III 42.5 N and the aggregates employed consisted of a mixture of natural (rounded) and recycled (crushed) origins, the K value was set to 0.0375. Thus, the maximum admissible water/cement ratio to achieve the desired 25 MPa strength was 0.60.

$$\frac{w}{c} = \frac{1}{Kb \cdot (1.2 \cdot f_{ck} + 1) + 0.5} \tag{5.1}$$

with *w/c* the water/cement ratio [wt%], *Kb* a positive integer varying as a function of the type of binder and aggregates [-] and f_{ck} the characteristic 28 days compressive strength measured on 150x300 mm cylindrical test specimens [MPa].

However, in order to achieve a durable concrete, the specifications laid down in the EHE-08 (Permanent Commission on Concrete, 2008) were followed. Hence, the minimum cement content and the maximum water/cement ratio were set accordingly to the limitation set up in the aforementioned standard as a function of the environmental exposure class to which the concrete element or structure is to be subjected. The typical design criterion for construction works in León of an environmental exposure class IIb was selected, which rendered a minimum cement content of 300 kg/m^3 and a maximum water/cement ratio of 0.55 as the operating limits for the concrete mixtures.

Once the water/cement ratio was fixed to 0.55, the second step focused on the determination of the water and cement contents. To establish the water content, the definition of the desired consistency of the fresh concrete is required. A S3 slump class as described in EHE-08 (Permanent Commission on Concrete, 2008), which is equivalent to a S2 slump in EN 206-1 (2005), was selected. Then, the water content was determined as a function of the type and maximum size of the aggregate against the targeted consistency, which amounted to 215 litres of water per cubic meter of concrete. And correspondingly the cement content was set as 390.91 kg/m^3.

Note that since this method was initially proposed for concrete exclusively made from natural aggregates, it was not expected that the planned consistency was achieved with the amount of water employed in the mixture in the recycled concrete slump test due to the well-known higher water absorption capabilities of the recycled aggregates and that no water correction was applied. Thus, the evaluation of the slump was only used as the control parameter to ensure the repetitiveness between concrete batches.

With the water and cement content fixed at this stage, the necessary volume of aggregates becomes a known value by means of a simple subtraction. Given that concrete properties are highly influenced by the aggregates employed in its manufacture, and as such taking into account some basic properties of the aggregates when designing the concrete mixture is necessary to ensure a satisfactory performance of the concrete. So, the third step of the method consisted of the calculation of the fine and coarse aggregates proportioning by adjusting the actual particle size curve of the different aggregates to Fuller's parabola calculated as per equation (5.2). However, the granulometic modulus method was chosen, which is based on the resolution of a first order polynomial equation that equals the Fuller's modulus to the sum of an unknown percentage of aggregate relating its granulometric modulus (Table 5.2).

$$y(x) = 100 \cdot \sqrt{\frac{d}{D}} \tag{5.2}$$

with *y(x)* the function describing the Fuller's parabola as the percentage accumulated at a certain sieve [wt%], *d* the size of the opening of each one of the sieves employed in the granulometric test [mm] and *D* the maximum size of the aggregate [mm].

Table 5.2: Granulometric moduli of the natural and recycled aggregates

	Phase I	**Phase II**
Sand	3.38	3.83
Gravel 4-16 mm	7.29	10.70
Gravel 2-8 mm	-	-
Gravel 8-16 mm	-	6.95
Recycled aggregate RA-L(S)	7.67	9.34
Recycled aggregate RA-L(B)	-	9.54
Recycled aggregate RA-M(S)	7.82	9.93
Recycled aggregate RA-H(S)	7.96	10.51

Figure 5.2 displays the particle size distribution of all the combined aggregates comprising each different concrete mixture compared with the Fuller's parabola. For both research phases, overall good adjustments were achieved to the adopted reference parabola that allows for the maximum compaction of granular elements. Nonetheless, the results obtained in phase II show a greater scattering, with the mixture of aggregates for the recycled concretes showing a better fit to the reference parabola than the mixture of aggregates for the conventional concrete.

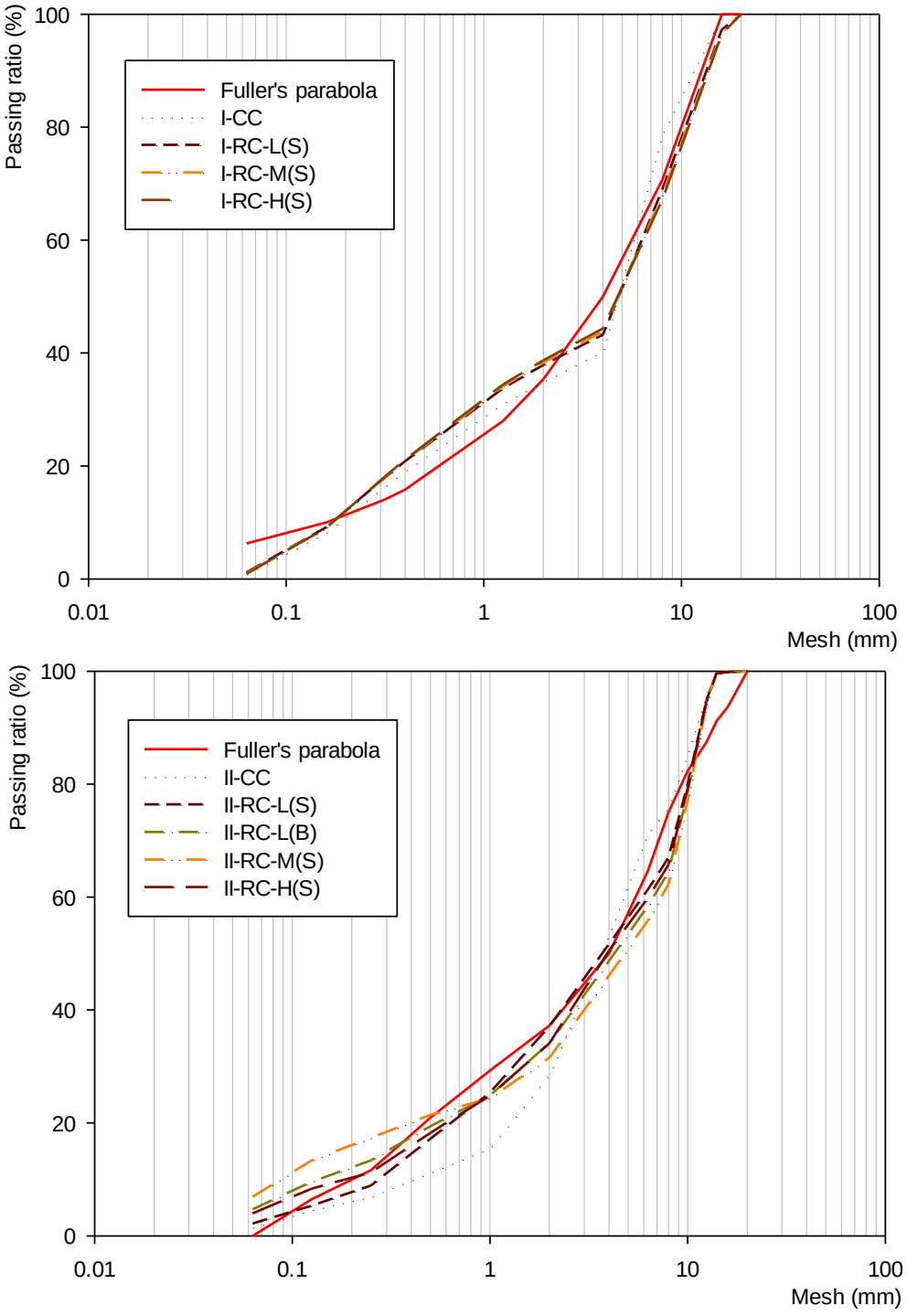

Figure 5.2: Adjustment of calculated concrete dosages to the Fuller's parabola

Lastly, in order to convert the volume percentages to weight percentages the density of each aggregate was employed in the conversions (Table 5.3).

	Density (Mg/m^3)
Sand	2.63
Gravel	2.54
RA-L(S)	2.08
RA-L(B)	2.06
RA-M(S)	1.94
RA-H(S)	1.80

Table 5.3: Density values

The final step of the method consisted of the correction of the amount of sand. The calculated fraction was reduced proportionally to the excess of cement calculated from the 300 kg/m^3 amount to which the method was originally developed. In addition, although it is not always included as a part of this method, the amount of sand was further decreased by discounting the air entrapped that was assumed up to 2%.

Table 5.4 and Table 5.5 display the concrete compositions calculated for concrete mixtures from phase I and phase II, respectively.

Table 5.4: Phase I concrete mixture proportions

	I-CC	**I-RC-L(S)**	**I- RC-M(S)**	**I- RC-H(S)**
Water (l/m^3)	215.00	215.00	215.00	215.00
Cement (kg/m^3)	390.91	390.91	390.91	390.91
Sand (kg/m^3)	650.49	715.89	734.20	751.88
Gravel 4-16 mm (kg/m^3)	1030.71	446.97	425.89	405.54
Recycled aggregate (kg/m^3)	0.00	446.97	425.89	405.54

Table 5.5: Phase II concrete mixture proportions

	II-CC	**II-RC-L(S)**	**II-RC-L(B)**	**II- RC-M(S)**	**II- RC-H(S)**
Water (l/m^3)	215.00	215.00	215.00	215.00	215.00
Cement (kg/m^3)	390.91	390.91	390.91	390.91	390.91
Sand (kg/m^3)	480.48	703.46	736.08	766.73	821.06
Gravel 2-8 mm (kg/m^3)	1000.30	368.32	356.90	335.93	307.79
Gravel 8-16 mm (kg/m^3)	250.07	92.08	89.23	83.98	76.95
Recycled aggregate (kg/m^3)	0.00	460.40	446.13	419.92	384.74

Figure 5.3 exposes a comparative analysis of the results achieved with the De la Peña method (Jiménez Montoya et al., 2009) for the different concrete dosages manufactured throughout the research works of this thesis. As stated previously, water and cement content remained constant during all the experiments, and a the content of both fine and coarse aggregates were adjusted in each research phase by means of the specific particle size distribution of the different aggregates.

Since the density value for the river gravel is higher than those of the recycled coarse aggregates, the recycled concrete mixtures contain higher amounts of sand. Thus, the amount of sand increased and the quantity of coarse aggregates (natural and recycled) decreased as the content of ceramic waste increased in the recycled aggregates, i.e. as the density of the recycled aggregates decreased. This trend was also observed by Medina-Martínez (2011) for recycled concrete mixtures incorporating 20% and 25% of sanitary ware aggregates using the De la Peña proportioning method (Jiménez Montoya et al., 2009).

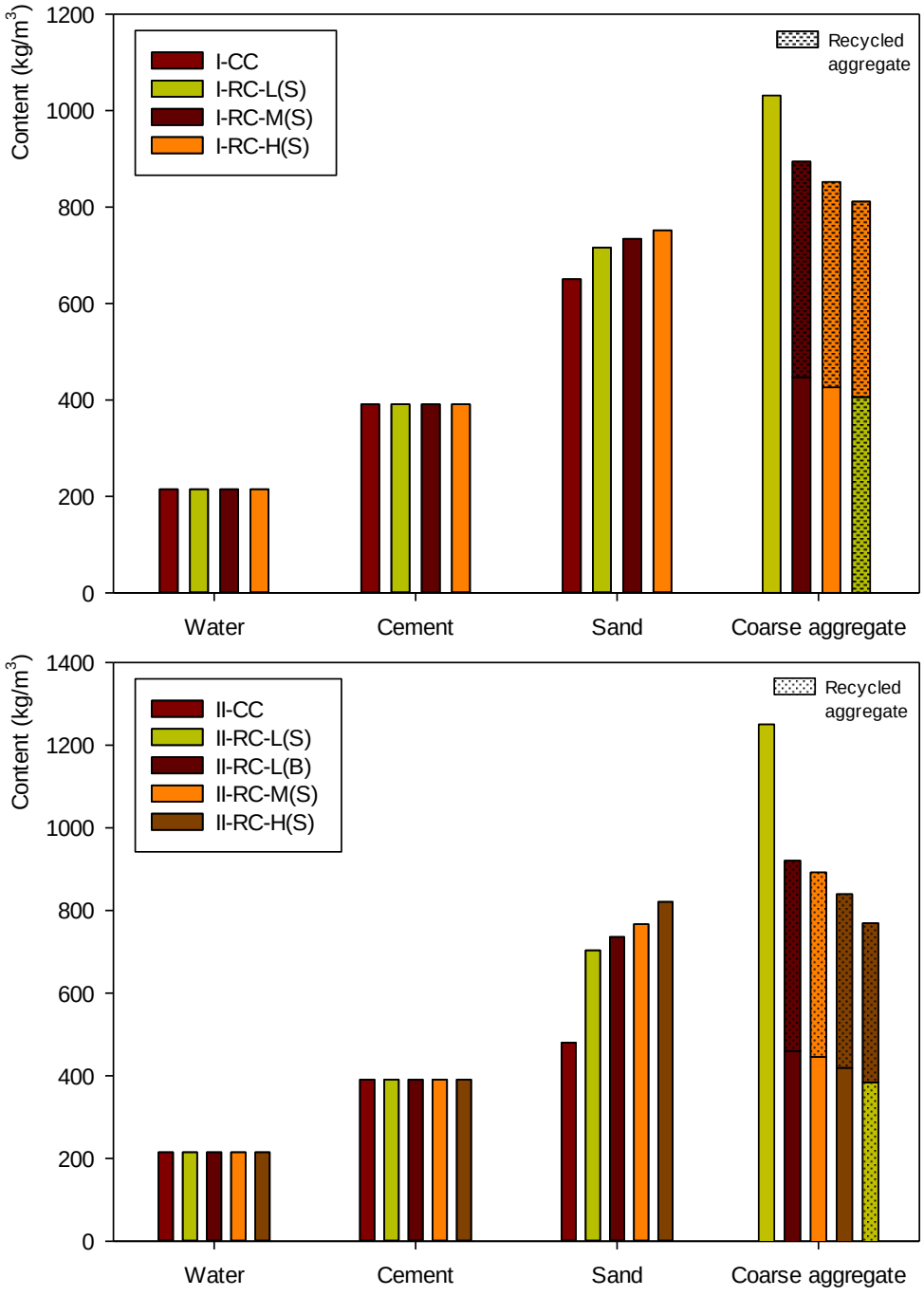

Figure 5.3: Comparison of the different constituents proportions of the concrete mixtures

Furthermore, despite the fact that all samples have been designed for a same total water/cement ratio (0.55), the higher water absorption of the recycled aggregates is responsible for the absorption of part of the water during the mixing period. According to Evangelista and de Brito (2007), during the mixing period the recycled aggregates are able to absorb up to a 50% of their maximum capacity due to the sealing effect that has the binder in the pores of the recycled aggregates which limits further water exchanges. Taking into account the quantity of recycled aggregates and half of their water absorption capacity, the effective water/cement ratio is 0.50 for all the recycled concrete mixtures.

5. TEST SPECIMENS MANUFACTURE

Throughout the thesis research, all aggregates employed (natural and recycled) were dry-sieved and air dried before their utilization in the concrete mixture to ensure a homogenous material for the different concrete batches. Note that no other pre-treatment of those described in the present chapter was followed.

After having all the components properly prepared, the dry components were placed in the mixer starting with the coarse aggregates (natural and recycled), the fine aggregates and finally the cement. The mixing procedure consisted of the dry-mixture of these materials aggregates for 2 minutes followed by the addition of the water while continuously mixing for 3 more minutes. All the mixtures were prepared following the described procedure with a drum mixer in phase I and a pan mixer was used in phase II. Note that the mixing time was carefully controlled in order to avoid the excessive generation of fines due to the known self-attrition presented by the recycled aggregates.

Test concrete specimens were manufactured following the instructions outlined in UNE EN 12390-1 (2013) and UNE EN 12390-2 (2009). The moulds were filled with three equal concrete layers compacted by means of a vibrating needle. After casting, all tests specimens were finished with steel trowel and were immediately covered with plastic film to avoid any water loss due to evaporation. After 24 hours, all the specimens were demoulded. Then, specimens were cured under water at 20±2ºC in phase I and in a fog room at 20±2ºC and 95 % relative humidity in phase II.

6. REFERENCES

Abbas, A., Fathifazl, G., Isgor, O.B., Razaqpur, A.G., Fournier, B., Foo, S., 2009. Durability of recycled aggregate concrete designed with equivalent mortar volume method. *Cement and Concrete Composites* 31 (8): 555–563.

Abd Elhakam, A., Mohamed, A.E., Awad, E., 2012. Influence of self-healing, mixing method and adding silica fume on mechanical properties of recycled aggregates concrete. *Construction and Building Materials* 35: 421–427.

ACI Committee 211, 2002. Standard practice for selecting proportions for normal, heavyweight, and mass concrete (ACI Manual of Concrete Practice). American Concrete Institute.

Agrela, F., Sánchez de Juan, M., Ayuso, J., Geraldes, V.L., Jiménez, J.R., 2011. Limiting properties in the characterisation of mixed recycled aggregates for use in the manufacture of concrete. *Construction and Building Materials* 25 (10): 3950–3955.

Barbudo, A., de Brito, J., Evangelista, L., Bravo, M., Agrela, F., 2013. Influence of water-reducing admixtures on the mechanical performance of recycled concrete. *Journal of Cleaner Production* 59: 93–98.

Beltrán, M.G., Barbudo, A., Agrela, F., Galvín, A.P., Jiménez, J.R., 2014. Effect of cement addition on the properties of recycled concretes to reach control concretes strengths. *Journal of Cleaner Production* 79: 124–133.

Bolomey, J., 1935. Particle size distribution and forecast of the predictable strength of concrete mixtures [in French]. *Travaux* 19 (30): 228–232.

Debieb, F., Kenai, S., 2008. The use of coarse and fine crushed bricks as aggregate in concrete. *Construction and Building Materials* 22 (5): 886–893.

del Río, L.M., Jiménez, A., López, F., Rosa, F.J., Rufo, M.M., Paniagua, J.M., 2004. Characterization and hardening of concrete with ultrasonic testing. *Ultrasonics* 42: 527–530.

Dhir, R.K., Limbachiya, M.C., Leelawat, T., 1999. Suitability of recycled concrete aggregate for use in BS 5328 designated mixes. *Structures and Buildings* 134 (3): 257–274.

EN 206-1, 2005. Concrete. Part 1: Specification, performance, production and conformity. CEN, Brussels.

Etxeberria, M., Vázquez, E., Marí, A., Barra, M., 2007. Influence of amount of recycled coarse aggregates and production process on properties of recycled aggregate concrete. *Cement and Concrete Research* 37 (5): 735–742.

Evangelista, L., de Brito, J., 2007. Mechanical behaviour of concrete made with fine recycled concrete aggregates. *Cement and Concrete Composites* 29 (5): 397–401.

Fathifazl, G., Abbas, A., Razaqpur, A.G., Isgor, O.B., Fournier, B., Foo, S., 2009. New mixture proportioning method for concrete made with coarse recycled Concrete aggregate. *Journal of Materials in Civil Engineering* 21 (10): 601–611.

Fathifazl, G., Ghani Razaqpur, A., Burkan Isgor, O., Abbas, A., Fournier, B., Foo, S., 2011. Creep and drying shrinkage characteristics of concrete produced with coarse recycled concrete aggregate. *Cement and Concrete Composites* 33 (10): 1026–1037.

Ferreira, L., de Brito, J., Barra, M., 2011. Influence of the pre-saturation of recycled coarse concrete aggregates on concrete properties. *Magazine of Concrete Research* 63 (8): 617–627.

Fuller, W.B., Thompson, S.E., 1907. The laws of proportioning concrete. *Transactions of the American Society of Civil Engineers* 59 (2): 67–143.

García-González, J., Rodríguez-Robles, D., Juan-Valdés, A., Morán-del Pozo, J.M., Guerra-Romero, M.I., 2014. Pre-saturation technique of the recycled aggregates: solution to the water absorption drawback in the recycled concrete manufacture. *Materials* 7 (9): 6224–6236.

Gonzalez, A., Etxeberria, M., 2014. Experimental analysis of properties of high performance recycled aggregate concrete. *Construction and Building Materials* 52: 227–235.

Gonzalez-Corominas, A., Etxeberria, M., 2014. Properties of high performance concrete made with recycled fine ceramic and coarse mixed aggregates. *Construction and Building Materials* 68: 618–626.

Jiménez, C., Aponte, D., Vázquez, E., Barra, M., Valls, S., 2013. Equivalent Mortar Volume (EMV) method for proportioning recycled aggregate concrete: validation under the Spanish

context and its adaptation to Bolomey methodology for concrete proportioning. *Materiales de Construcción* 63 (311): 341–360.

Jiménez, C., Barra, M., Valls, S., Aponte, D., Vázquez, E., 2014. Durability of recycled aggregate concrete designed with the Equivalent Mortar Volume (EMV) method: Validation under the Spanish context and its adaptation to Bolomey methodology. *Materiales de Construcción* 64 (313): e006.

Jiménez Montoya, P., Arroyo Portero, J.C., Morán Cabré, F., García Meseguer, Á., 2009. Structutal concrete. Based on the Spanish Code on structural concrete EHE-08 and adaptated to the Eurocode EC-2 [in Spanish]. Cartoné, Madrid.

Khalaf, F.M., DeVenny, A.S., 2005. Properties of new and recycled clay brick aggregates for use in concrete. *Journal of Materials in Civil Engineering* 17 (4): 456–464.

Kong, D., Lei, T., Zheng, J., Ma, C., Jiang, J., Jiang, J., 2010. Effect and mechanism of surface-coating pozzalanics materials around aggregate on properties and ITZ microstructure of recycled aggregate concrete. *Construction and Building Materials* 24 (5): 701–708.

Kong, D., Zheng, J., Zhou, X., 2006. Strengthening of the ITZ in recycled aggregate concrete, in: Proceedings of Architecture in Harmony. Presented at the Xi'an international conference on architecture and technology, Xian, PRC, 614–7.

Kou, S.C., Poon, C.S., Agrela, F., 2011. Comparisons of natural and recycled aggregate concretes prepared with the addition of different mineral admixtures. *Cement and Concrete Composites* 33 (8): 788–795.

Kumar, P.R., Heeralal, M., Rao, Y.V., Rakesh, B., 2009. Strength and performance aspects of recycled aggregate for use in rigid pavements. *Journal of Environmental Research And Developmen* 4 (2): 449–464.

Li, J., Xiao, H., Zhou, Y., 2009. Influence of coating recycled aggregate surface with pozzolanic powder on properties of recycled aggregate concrete. *Construction and Building Materials* 23 (3): 1287–1291.

López-Gayarre, F., Serna, P., Domingo-Cabo, A., Serrano-López, M.A., López-Colina, C., 2009. Influence of recycled aggregate quality and proportioning criteria on recycled concrete properties. *Waste Management* 29 (12): 3022–3028.

Malešev, M., Radonjanin, V., Marinković, S., 2010. Recycled concrete as aggregate for structural concrete production. *Sustainability* 2 (5): 1204–1225.

Mas, B., Cladera, A., Bestard, J., Muntaner, D., López, C.E., Piña, S., Prades, J., 2012a. Concrete with mixed recycled aggregates: Influence of the type of cement. *Construction and Building Materials* 34: 430–441.

Mas, B., Cladera, A., del Olmo, T., Pitarch, F., 2012b. Influence of the amount of mixed recycled aggregates on the properties of concrete for non-structural use. *Construction and Building Materials* 27 (1): 612–622.

Matias, D., de Brito, J., Rosa, A., Pedro, D., 2013. Mechanical properties of concrete produced with recycled coarse aggregates – Influence of the use of superplasticizers. *Construction and Building Materials* 44: 101–109.

Medina, C., Sánchez de Rojas, M.I., Frías, M., 2012. Reuse of sanitary ceramic wastes as coarse aggregate in eco-efficient concretes. *Cement and Concrete Composites* 34 (1): 48–54.

Medina, C., Zhu, W., Howind, T., Frías, M., Sánchez de Rojas, M.I., 2015. Effect of the constituents (asphalt, clay materials, floating particles and fines) of construction and demolition waste on the properties of recycled concretes. *Construction and Building Materials* 79: 22–33.

Medina Martínez, C., 2011. Behaviour of recycled concrete with ceramic aggregate: Physical, mechanical, microstructural and durability study [in Spanish]. Universidad de León, León, Spain.

Permanent Commission on Concrete, 2008. Code on Structural Concrete (EHE-08) [in Spanish]. Spanish Ministry of Public Works, Madrid.

Poon, C.S., Kou, S.C., Lam, L., 2007. Influence of recycled aggregate on slump and bleeding of fresh concrete. *Materials and Structures* 40 (9): 981–988.

Poon, C.S., Shui, Z.H., Lam, L., Fok, H., Kou, S.C., 2004. Influence of moisture states of natural and recycled aggregates on the slump and compressive strength of concrete. *Cement and Concrete Research* 34 (1): 31–36.

Razaqpur, A.G., Fathifazl, G., Isgor, B., Abbas, A., Foo, S., Fournier, B., 2010. How to produce high quality concrete mixes with recycled concrete aggregate, in: Proceedings of the 2nd International Conference on Waste Engineering and Management - ICWEM 2010. RILEM Publications SARL, Shanghai, 11–35.

Rodrigues, F., Carvalho, M.T., Evangelista, L., de Brito, J., 2013. Physical–chemical and mineralogical characterization of fine aggregates from construction and demolition waste recycling plants. *Journal of Cleaner Production* 52: 438–445.

Soares, D., de Brito, J., Ferreira, J., Pacheco, J., 2014. Use of coarse recycled aggregates from precast concrete rejects: Mechanical and durability performance. *Construction and Building Materials* 71: 263–272.

Somna, R., Jaturapitakkul, C., Chalee, W., Rattanachu, P., 2012. Effect of the water to binder ratio and ground fly ash on properties of recycled aggregate concrete. *Journal of Materials in Civil Engineering* 24 (1): 16–22.

Tabsh, S.W., Abdelfatah, A.S., 2009. Influence of recycled concrete aggregates on strength properties of concrete. *Construction and Building Materials* 23 (2): 1163–1167.

Tam, V.W.Y., Gao, X.F., Tam, C.M., 2005. Microstructural analysis of recycled aggregate concrete produced from two-stage mixing approach. *Cement and Concrete Research* 35 (6): 1195–1203.

Topçu, İ.B., Şengel, S., 2004. Properties of concretes produced with waste concrete aggregate. *Cement and Concrete Research* 34 (8): 1307–1312.

UNE EN 12390-1, 2013. Testing hardened concrete. Part 1: Shape, dimensions and other requirements for specimens and moulds [in Spanish]. AENOR, Madrid.

UNE EN 12390-2, 2009. Testing hardened concrete. Part 2: Making and curing specimens for strength tests [in Spanish]. AENOR, Madrid.

Van Der Wegen, G., Haverkort, R., 1998. Recycled construction and demolition wastes as a fine aggregate for concrete, in: Proceedings of the International Symposium on Sustainable Construction: Use of Recycled Concrete Aggregate. London, UK.

Vázquez, E., Barra, M., Aponte, D., Jiménez, C., Valls, S., 2014. Improvement of the durability of concrete with recycled aggregates in chloride exposed environment. *Construction and Building Materials* 67, Part A: 61–67.

Chapter 6

Properties of fresh concrete

1. INTRODUCTION

Once all the components comprising the concrete are mixed, the mixture acquires a rheological state characterized by its plasticity that plays an important role in the constructive practice (early age operations of transportation, placing, compaction and finishing) and could also affect the properties of the hardened concrete. Since the properties of the recycled aggregates from CDW are different from those of conventional aggregates, their use is expected to substantially modify the fresh properties of the recycled concrete.

In the first place, basic properties as the consistency, the air content and the density are studied in order to assess the fresh behaviour of recycled concrete mixes with varying ceramic waste replacement percentages in comparison with that of a conventional concrete. Afterwards, the mechanism of cement hydration in recycled concrete mixtures containing varying percentages of ceramic waste are compared to the control concrete by assessing both the heat of hydration and the setting time. Hence, semi-adiabatic calorimetric measurements and non-destructive ultrasonic measurements were employed to quantify the heat development and monitor the setting time respectively.

2. CONSISTENCY

The workability of fresh concrete is measured by its consistency that indicates the ability of freshly mixed concrete to flow, and as so, the ease with which the mixture could be manipulated (Powers, 1932). Among the factors controlling this property, aggregates exert a great influence in the consistency values, thus significant changes are to be expected when recycled aggregates are used in the manufacture of concrete.

Table 6.1 displays the slump values obtained for each concrete mixture and the slump reduction of the recycled concrete mixtures compared to the conventional concrete. Moreover, as previously stated in chapter 3, some differences exist regarding the slump classes according to the Spanish and European legislation, Table 6.1 also shows the slump category conforming to the respective standard.

Table 6.1: Slump values and classes

	CC	**RC-L(S)**	**RC-L(B)**	**RC-M(S)**	**RC-H(S)**
Phase I					
Slump (mm)	32	23	-	19	10
Slump reduction (%)	-	28.13	-	40.63	68.75
EHE-08 Slump class	S2	S2	-	S1	S1
EN 206-1 Slump class	S1	S1	-	S1	S1
Phase II					
Slump (mm)	162	115	130	40	15
Slump reduction (%)	-	29.01	19.75	75.31	90.74
EHE-08 Slump class	S5	S4	S4	S2	S1
EN 206-1 Slump class	S4	S3	S3	S1	S1

For both research phases, recycled concretes present lower workability values than the respective conventional concrete mixture (Figure 6.1), which responds to the higher water absorption presented by the recycled aggregates (oscillating between 4.93 and 6.22 times higher than the natural gravel for rising ceramic percentages). The conventional concrete reached a slump value of 32 mm in phase I, which is a fairly dry consistency and a slump of 162 mm in phase II, which represents a fluid consistency. Despite controlling most variables between research phases, the differences in slump of the conventional mixtures could be tracked back to the slight variances in grading as well as the different cement type, CEM III/A 42.5 N SR in phase I and CEM III/B 42.5 N SR LH in phase II. Thus, the best approach consists of the comparison of each phase separately. In the first phase, in a general more dry setting, the recycled concrete batches presented lower reductions of consistency, up to 28% for low ceramic content (I-RC-L(S)), around 41% for medium ceramic content (I-RC-M(S)) and roughly 69% for high ceramic content (I-RC-H(S)). In phase II, since the consistency of the conventional concrete is higher, the relative slump reductions are also higher, oscillating between 20% and 29% for the mixtures with low ceramic percentage (II-RC-L(S) and II-RC-L(B)), around 75% for medium ceramic content (II-RC-M(S)) and almost 91% for high ceramic content (II-RC-H(S)). These results are in line with those obtained by Jurič et al. (2006), who observed slump decreases between 43% and 86% for the incorporation of 9.1% and 23.1% of mixed recycled aggregates, respectively.

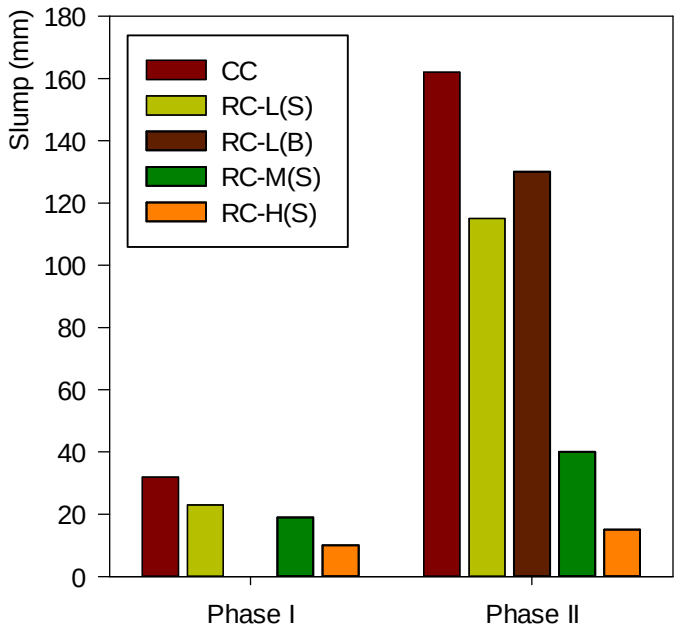

Figure 6.1: Consistency of the conventional and recycled concrete mixes

In spite of going against most of the research on recycled aggregates, some investigations have shown interest in the use of the recycled aggregates in an unsaturated moisture state. For example, Khalaf (2006) investigated the effect of using crushed brick recycled aggregates without pre-wetting and concluded that such use was feasible, although in this case the cement content was increased with respect to the reference concrete. In addition, Poon et al. (2004b) recommended the use of recycled aggregates in saturated surface-dried state for special situations only in order to avoid bleeding problems. The authors also concluded that the effect on the workability was not significant when no more than 50% of recycled concrete aggregates in air-dried state were used in the replacement. The findings of Ismail and Ramli (2014) indicated that the use of recycled concrete aggregates in oven-dried moisture state, which is not the case in the present research work, caused a total workability loss after 90 minutes of mixing, while their use in saturated surface-dried state prolonged the workability for 30 minutes. Mefteh et al. (2013), who also investigated the influence of the moisture conditioning of recycled concrete aggregates, noticed that oven-dry aggregates returned part of the absorbed water to the mortar after 30 minutes of mixing.

In this line of investigation, and as specified in chapter 5, the experimental program of this research work was based on establishing both the cement content and the total water/cement ratio as comparison parameters between conventional and recycled concrete mixtures in order to assess the unbiased influence of the recycled aggregate replacement, specifically the rising ceramic incorporation. Since no correction on the amount of water was carried out to the original proportioning method, which was designed for conventional mixtures, the reduction of slump resulting from the use of recycled aggregates was expected but acceptable workability levels were still reached.

For practical purposes, despite the lower consistency values, no problems in workability were detected when placing, compacting or casting the test specimens. As the true significance of this property relates to the future field application of the concrete mix, the type of construction, the placement method, the shape of the formworks and the structural design are the main aspects controlling the required workability (Khayat, 1999) and thus conditioning the use of recycled concrete mixtures without water correction. For instance, the guidelines of the ACI Committee 211 (2002) allow a minimum consistency of 20 mm for most types of constructions, a value that only would represent a problem for sample RC-H(S) under current proportioning conditions. Moreover, rather low consistency is preferred for road construction (Vahedifard et al., 2010) and precast elements (Xiao et al., 2011; Jankovic et al., 2012). In any case, possible workability problems arising at large-scale field applications should be preferably corrected by means of superplasticisers.

The effect of aggregates on the workability of concrete is due to the modification in the water demand to achieve the required level of consistency, which is mainly caused by their absorptivity properties, and as a result of rheological changes produced by their size, shape and grading. Figure 6.2 showcases the relationship between the slump and some controlling properties of the aggregates, namely water absorption of the total fraction of aggregates, flakiness index of the total coarse aggregate fraction and ceramic waste content incorporated.

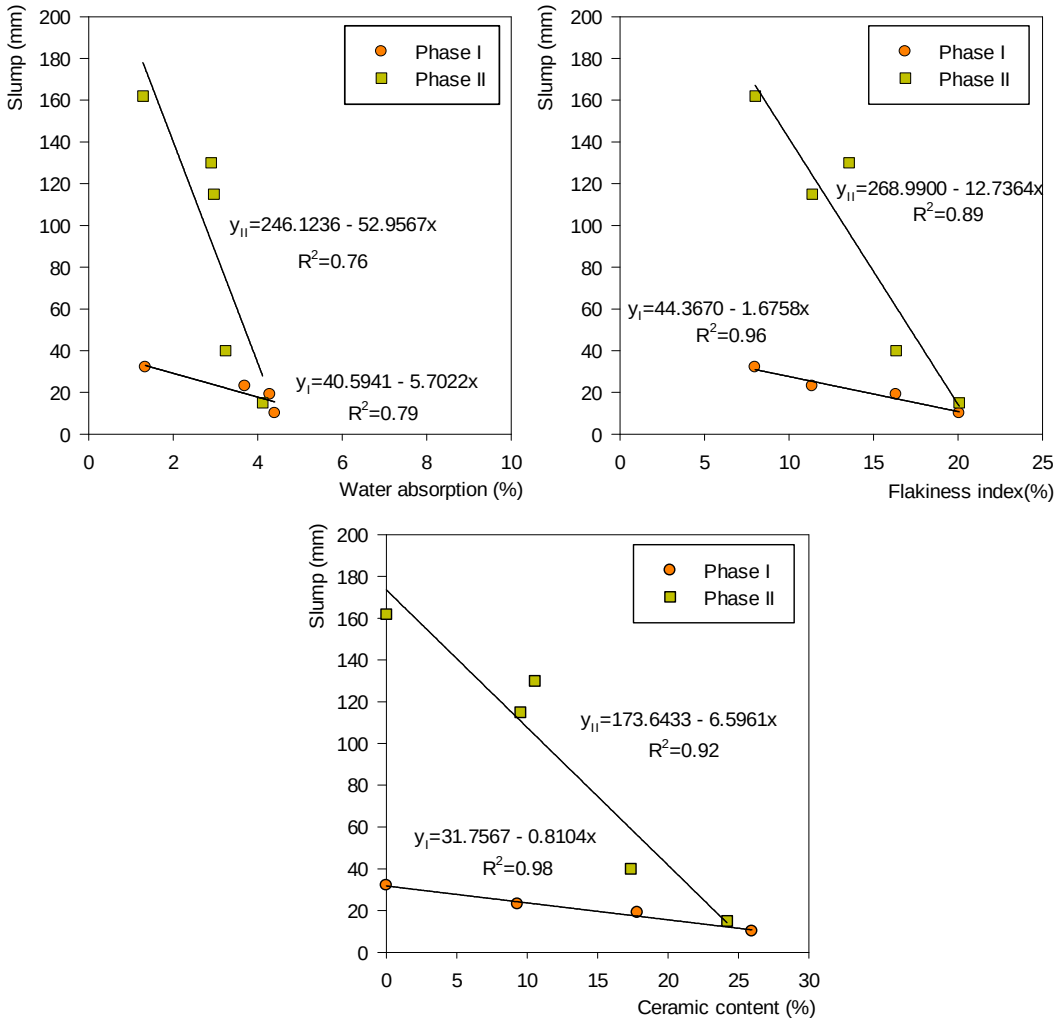

Figure 6.2: Properties of the aggregates controlling the slump

Regarding the first mechanism, despite the lack of consensus regarding the water absorption kinetics of the recycled aggregates from CDW (see section 3.1.5 of chapter 4), it is generally accepted that the incorporation of unsaturated recycled aggregates in a concrete mixture causes a reduction of the available mixing water by its absorption in the porous network of the aggregate, which in the end turns up as a decrease in the workability of the fresh concrete. Since the consistency highly depends on the availability of mixing water (Rao et al., 2007), the higher water absorption values of recycled aggregates from CDW play an important role on the differences of slump among conventional and recycled mixtures with the same total water/cement ratio, as it is the case in this dissertation. The left graph in Figure 6.2 shows the correlation between the water absorption of the aggregates employed in each concrete mixture, i.e. river sand and gravel in the conventional concrete mix and a 50% combination of the same river gravel with each recycled aggregate (RA-L(S), RA-L(B), RA-M(S) and RA-H(S)) mixed in the corresponding percentage with the river sand (see chapter 5) for the recycled concrete mixtures (RC-L(S), RC-L(B), RC-M(S) and RC-H(S) respectively), and the resulting slump of the fresh concrete. As expected, a reduction in the slump values could be observed for increasing water absorption values of the combination of aggregates in the concrete mix, which is in agreement with the results of Kim et al. (1993) and Yang and Kim (2005) who studied the relationship between the water absorption and the slump loss and reported the existence of an inverse relationship among both factors.

Contrary to the line of investigation followed in this dissertation, a common practice among research works consists of fixing the slump value at the expense of varying the total water/cement ratio necessary to achieve the desired consistency (Zaharieva et al., 2003; Debieb and Kenai, 2008; Tabsh and Abdelfatah, 2009; Sadek, 2012; Beltrán et al., 2014; Bravo et al., 2015). Consequently, the water/cement is modified by the addition of extra water (Ferreira et al., 2011; Mas et al., 2012a, 2012b; Matias et al., 2013; Zhang and Zong, 2014), the use of superplasticisers and the increase in the amount of mixing water (Hoffmann et al., 2012; Martínez-Lage et al., 2012; Mas et al., 2012a; Beltrán et al., 2014; Medina et al., 2014) or the pre-soaking of the recycled aggregates before their use (Khalaf and DeVenny, 2005; Khalaf, 2006; Debieb and Kenai, 2008; Bezerra-Cabral et al., 2010; Yang et al., 2011; García-González et al., 2014; Elçi, 2015; Miličević et al., 2015).

Notwithstanding the benefits that these techniques could have on the workability of the fresh mixes, the addition of extra water compromises the interfacial transition zone (ITZ) and the mechanical strength of the recycled concrete (Poon et al., 2004a, 2004b) and the pre-soaking causes decreases in the mechanical behaviour and durability performance of the recycled concrete mixtures (Poon et al., 2004b; Ferreira et al., 2011; Mefteh et al., 2013; García-González et al., 2014) as well as some concerns in the logistic of its industrial application. Although the use of superplasticiser does not endanger the recycled concrete performance, the increase in the final cost of the mixture could be considered a dissuading factor of such practice.

Besides, in some cases the water correction did not have the expected repercussions on the consistency. For instance, in terms of mixed recycled aggregates, Martínez-Lage et al. (2012) reported a 25% and 50% reduction in slump values for a 50% and 100% replacement ratio, respectively, despite adding extra water and superplasticiser. For 100% recycled concrete, Yang et al. (2011) reported slump decreases of 17% and 58% for mixed recycled aggregates containing 20% and 50% of ceramic waste respectively, despite the pre-soaking of the aggregates.

Concerning ceramic aggregates, Zhang and Zong (2014) reported slump decreases oscillating between 20% and 64% for replacement ratios between 30% and 50% despite the addition of extra water and Elçi (2015) registered reductions in the 48% to 52% range in recycled concrete made of 100% crushed tiles coarse and fine aggregates regardless of the pre-wetting procedure. The differences in the results could be explained by the high variability of procedures described to achieve the pre-saturation of the recycled aggregates, which results in the incorporation of the aggregates at different saturation percentages, or the miscalculations in the required additional water, since recycled aggregates presenting similar water absorption could result in different slump values due to different absorption kinetics (Belin et al., 2014).

Regarding the rheological modifications, the shape of the recycled aggregates also has a great influence on the differences between the slump of conventional and recycled mixtures (Buyle-Bodin and Hadjieva-Zaharieva, 2002; Matias et al., 2013; Bravo et al., 2015). The right graph in Figure 6.2 illustrates the nearly-linear correlation between the slump of the fresh concrete mixture and the flakiness index of the coarse aggregates employed, i.e. river gravel in the conventional concrete mix and a 50% combination of the same river gravel with each recycled aggregate (RA-L(S), RA-L(B), RA-M(S) and RA-H(S)) for the recycled concrete mixtures (RC-L(S), RC-L(B), RC-M(S) and RC-H(S) respectively). Hence, it was found that the increase of the flakiness index of the coarse aggregates employed, strongly associated to the ceramic content, was responsible for the workability loss since the higher angularity presented by the recycled aggregates implies a higher surface area to be wetted and more accessible voids to be filled with cement paste. These findings are in agreement with those from the investigations of Olorunsogo (1999), who reported that the higher angularity levels of the recycled concrete aggregates caused lower slump values. It is worth mentioning that the angularity of the recycled aggregates could be modified by the treatment at the CDW management plant since the type of crushing machine employed is responsible for the angularity of the final product. According to Marmash and Elliott (2000), the use of recycled aggregates produced in cone crushers is expected to cause the lowest reduction in slump values followed by the use of impact crushers and finally jaw crushers.

In addition, the superficial texture of the aggregates impacts on the workability (Sagoe-Crentsil and Brown, 1998; Mansur et al., 1999; Buyle-Bodin and Hadjieva-Zaharieva, 2002). The rough exterior of the recycled aggregates increases the surface area to be lubricated by the cement paste and the inter particle frictional resistance which have a worsening effect on the consistency of the fresh concrete. The particle size and grading of the aggregates are also recognised to affect consistency (Jiménez Montoya et al., 2009; Li, 2011). In particular, the presence of dust adhered to unwashed recycled aggregates has been pointed as a cause of the workability loss of recycled concretes (Chen et al., 2003; Sheen et al., 2013).

Furthermore, based on the acknowledged properties of certain wastes comprising the CDW, several researches have established inverse relationships between the amounts incorporated and the resulting slump value (Kumar et al., 2009; Yang et al., 2011; Martínez-Lage et al., 2012; Ismail and Ramli, 2013).

For example, the content of adhered mortar contributes to the decrease of the slump values in recycled concretes since it causes an overall increase of the aggregate water absorption and the modification of the particle size distribution of the concrete mix due to the generation of fines linked to the mortar detachment during the batching (Kumar et al., 2009; Yang et al., 2011; Pepe et al., 2014b). Medina et al. (2015) indicated that the content of asphalt also affected negatively the slump and proved that its removal could significantly improve the workability, especially in recycled mixtures with lower replacement ratios. Finally, the presence of crushed bricks within the recycled aggregates has also been identified as liable for harsher and less workable mixes (Khalaf and DeVenny, 2005; Bolouri Bazaz and Khayati, 2011; Sadek, 2012; Sheen et al., 2013; Medina et al., 2015) since, besides the high porosity of the ceramic materials, their relatively low roughness causes the generation of fines by attrition during blending (de Brito and Robles, 2010; Butler et al., 2011; Matias et al., 2013; Medina et al., 2015). According to the characteristics of this dissertation, the influence of the ceramic content of the slump was analysed. The bottom graph in Figure 6.2 illustrates the relationship found between the amount of ceramic waste incorporated with the total weight of aggregates and the resulting slump. In line with the previous comments, a very good correlation (R^2>0.90) was found for the detrimental effect of the incorporation of recycled aggregates containing ceramic wastes on the workability of the recycled concrete mixtures.

Finally, Knaack and Kurama (2013) also identified the proportioning method as a influencing aspect on the workability of recycled concrete mixtures. While the direct volume replacement method rendered similar slump values for conventional and recycled mixes, the direct weight replacement method resulted in lower slump for recycled concrete and even lower slump values were obtained for the equivalent mortar method since the mortar adhered to the recycled aggregates is computed within the total paste content of the mixture.

3. AIR CONTENT

In general, the occurrence of air bubbles in the fresh concrete stems from the presence of air in the mixing water and as a result of the energy produced during the mixing operations that is able to create a liquid/air interface (Powers, 1968). Without the addition of any air entrainment agent, the air bubbles are inherently unstable, which results in a dynamic air system during the fresh state of the concrete mixture (Du and Folliard, 2005). In the subsequent operations of placing and compaction, some of the air could migrate between the inter-particle spaces generated (Robeyst, 2009). Moreover, after casting, the entrapped air bubbles could dissolve in water if they have a small enough size or could increase in size by coalescence mechanisms which promotes their release to the surface due to the much lower density (Mielenz et al., 1958). Hence, air bubbles only remain trapped inside the concrete when adhered to cement or sand particles or surrounded by packed aggregates.

Table 6.2 shows the air content values obtained for each fresh concrete mixture in phase II of the research program, as well as the relative increase in entrapped air of the recycled concrete mixtures compared to the conventional concrete used as reference.

Table 6.2: Air content of concrete mixtures pertaining to phase II

	Air content (%)	Relative increase (%)
II-CC	1.50	-
II-RC-L(S)	2.10	40.00
II-RC-L(B)	2.70	80.00
II-RC-M(S)	2.70	80.00
II-RC-H(S)	2.70	80.00

Independently of the type of recycled aggregates employed (concrete, mixed or ceramic), recycled concrete generally possesses higher air content than conventional mixtures (Katz, 2003; Qasrawi and Marie, 2013; Schwerin et al., 2013; Elçi, 2015). Whilst a relationship between the increase of the replacement ratio and the upsurge of the air content has been stated (Debieb and Kenai, 2008; López-Gayarre et al., 2009; Qasrawi and Marie, 2013), Qasrawi and Marie (2013) indicated that up to 25% replacement of recycled concrete aggregates the effect was marginal and López-Gayarre et al. (2009) reported that at least 50% substitution of recycled concrete aggregate was needed in order to appreciate significant variations. In addition, Netinger et al. (2011) suggested that the presence of crushed bricks in the recycled aggregates has a higher impact on the growth of the air content than the occurrence of crushed tiles.

The results obtained show the same general trend towards higher air content in recycled concrete samples, with increases oscillating from 40% in RC-L(S) to 80% in RC-L(B), RC-M(S) and RC-H(S), as could be observed in Table 6.2. These results are in the upper part of the range of those reported in the literature. For recycled concrete made of recycled concrete aggregates, Qasrawi and Marie (2013) registered a 75% upsurge in air content with a 50% substitution, which is fairly similar to the results obtained for RC-L(B), RC-M(S) and RC-H(S), i.e. recycled concrete made of mixed and ceramic recycled aggregates.

The higher air content in recycled concrete mixtures is normally attributed to the presence of adhered mortar since its higher porosity favours the occlusion of air in its pores (Kobayashi and Kawano, 1988). In the same line, the higher porosity of ceramic aggregates also entails higher air content for concrete made of this type of aggregates. However, there are other factors relating to the use of recycled aggregates that also affect this property. For instance, shape and grading have also significant influence on the percentage of air entrapped in concrete. Crushed rocks generate more impact and shear during the mixing than river gravels, which promotes that smaller air bubbles are formed (Du and Folliard, 2005), which have a higher persistence in the concrete mix as their escape is prevented by buoyancy forces inferior to the yield stress of the cement paste. Moreover, the presence of higher amount of fine aggregates (see chapter 5) that create more space to hold the air bubbles also explains the higher air content in the recycled mixtures.

As previously stated, compositional differences, i.e. amount of aggregates with adhered mortar and ceramic particles, are usually listed as the main reason for air content variations among recycled mixtures. However, a significant air content discrepancy exists between RC-L(S) and RC-L(B) concrete batches, which present the more similar composition, while RC-L(B), RC-M(S) and RC-H(C), which present varying ceramic percentages from 38.44% to 100%, have the same air content value.

Quantitatively, RC-L(B) contains more ceramic (14.5%) than RC-L(S), which could be responsible for a marginal raise in air content, but also presents more unbound aggregates (28.3%) and less concrete and cement-based materials (16%) than RC-L(S), which could counteract the previous upsurge in air content. Since the recycled concrete made of Belgian recycled aggregate with low ceramic percentage (RC-L(S)) presents an increase in air content around 29% with respect to the recycled concrete made of Spanish recycled aggregate with low ceramic percentage, it is reasonable to state that the higher amount of sand (4.6%) and the better workability (13%) of RC-L(B) also play a part in this discrepancy. In addition, López-Gayarre et al. (2009) reported that recycled concrete mixtures with lower air content were a reflection of recycled aggregates of better quality.

According to the guidelines proposed for concrete mix design by the American Concrete Institute (ACI Committee 211, 2002), the expected air content for mixtures with 215 kg/m^3 of water and maximum aggregate size of 20 mm is around 2.00%. Despite this recommendation was made for conventional concretes, there is one of the recycled concrete mixtures (RC-L(S)) presenting a result close to the expected value, and the rest of the recycled concretes as well as the conventional mixture reflected significant deviations (Figure 6.3). On one hand, the differences registered for recycled mixtures vary from 5% to 35% increases and answer to the composition, shape and grading factors previously mentioned. On the other hand, the air content displayed for the conventional concrete mixture was 25% lower than expected. For slump values below 150 mm, an increase in workability causes an increase in the air content. Hence, since the slump value of the CC sample reached the 162 mm, low air content answers to the loss of stability of the larger air bubbles due to buoyancy forces (Du and Folliard, 2005).

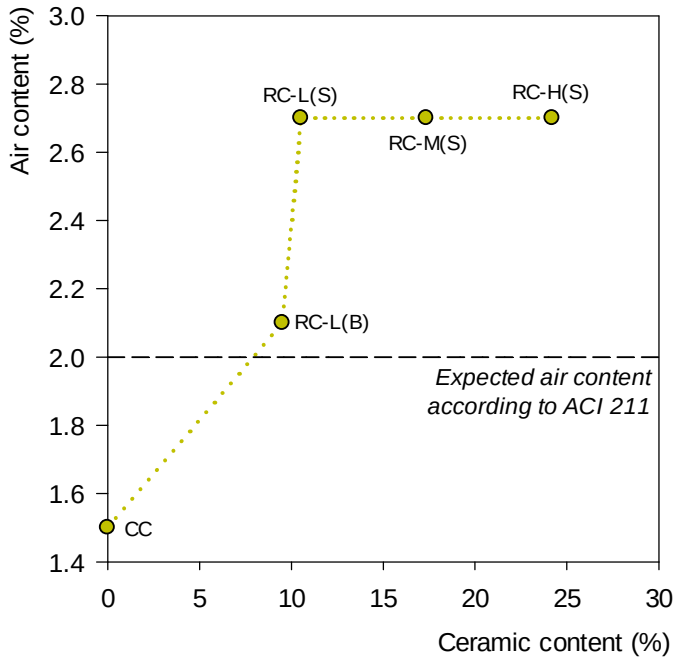

Figure 6.3: Relationship between the air content and the ceramic content incorporated in the total weight of aggregates for concrete batches in phase II

Finally, it is interesting to mention that the results displayed in Figure 6.3 illustrate a similar pattern to those represented for the relationship between the air content and the replacement ratio of recycled concrete aggregate reported by Qasrawi and Marie (2013). Moreover, the sigmoid-like function suggests the existence of a small effect for the incorporation of lower amounts of ceramic, a range of ceramic inclusion that highly accelerates the impact on the air content and a final part of slower growth until the climax is reached. Nonetheless, the effects of the incorporation of recycled aggregates containing a more comprehensive range of ceramic percentages should be tested to prove this assumption.

4. DENSITY

Fresh concrete density is the mass of fresh, normally compacted concrete, including its remaining voids per unit volume (de Brito and Saikia, 2013). Table 6.3 shows the fresh density values obtained for each concrete mixture in phase II of the research program, as well as the relative reduction in density of the recycled concrete mixtures compared to the conventional concrete used as reference.

Table 6.3: Fresh density values of concrete mixtures pertaining to phase II

	Density (kg/m^3)	Relative reduction (%)
II-CC	2312.50	-
II-RC-L(S)	2275.00	1.62
II-RC-L(B)	2237.50	3.24
II-RC-M(S)	2243.75	2.97
II-RC-H(S)	2187.50	5.41

Since the density of the mixed and ceramic recycled aggregates is lower than that of the natural aggregates, the fresh density of recycled concrete mixes is also lower than the conventional concrete. The fresh density values obtained (2187.50-2275.00 kg/m^3) are within the density range of 2130 kg/m^3 to 2400 kg/m^3 reported by other researchers for recycled concrete mixtures (González-Fonteboa, 2002; Sánchez de Juan, 2004; Working group 2/5, 2006; Rao et al., 2007).

Several researches have reported a nearly linear correlation between the reduction of fresh density of recycled concrete mixtures and the increasing percentage of natural aggregates replaced by recycled aggregates (Topçu and Canbaz, 2004; de Brito et al., 2005; Cachim, 2007; Martínez-Lage et al., 2012; Bravo et al., 2015). This reduction answers to the lower density values of recycled aggregates and the cumulative reduction effect associated to increasing replacement ratios. Despite that the replacement ratio was fixed at 50% for all concrete batches, a trend towards the reduction of the fresh density values associated to the increase in the ceramic content incorporated in the total weight of aggregates for each recycled concrete mix was observed in this research work (Figure 6.4). This tendency is based on the same premise, since the ceramic fraction is characterized by a lower density than other wastes comprising the recycled aggregates, such as concrete rubble and unbound aggregates, which are the main fractions for the mixed recycled aggregates employed in this research work.

Thus, an increasing percentage of ceramic within the aggregate total volume is responsible for the reduction in density among the four recycled concrete mixtures. The modest correlation value (R^2=0.89) suggests the existence of another explanatory variable. Since the fresh density measure also includes the mass of the remaining air voids, and as previously stated this factor varies among the conventional and recycled concrete mixtures, a multiple linear regression was performed to model the fresh density values by the relationship with the ceramic content incorporated in the total weight of aggregates (CerC) and the resulting air content of each mixture (AC), which resulted in a good correlation (R^2=0.92) for the equation fresh density=2353.571 - (3.594 x CerC) - (24.808 x AC).

Regarding the values of the relative decrease (Table 6.3), the 50% substitution of the river gravel by recycled aggregates with varying percentages of ceramic waste from CDW caused decreases oscillating between 1% and 6%. These results are in line with those reported by Sánchez de Juan (2004) for a 50% recycled concrete aggregate replacement ratio (1-5%) and the slight difference observed is due to the effect that the lower density of ceramic rubble compared to concrete rubble has on the substitution. Similarly, Sánchez de Juan (2004) indicated that a decrease between 4% and 15% was common for a total recycled concrete aggregates substitution, while Debieb and Kenai (2008) registered reductions up to 17% for a 100% replacement ratio of natural aggregates by crushed bricks recycled aggregates.

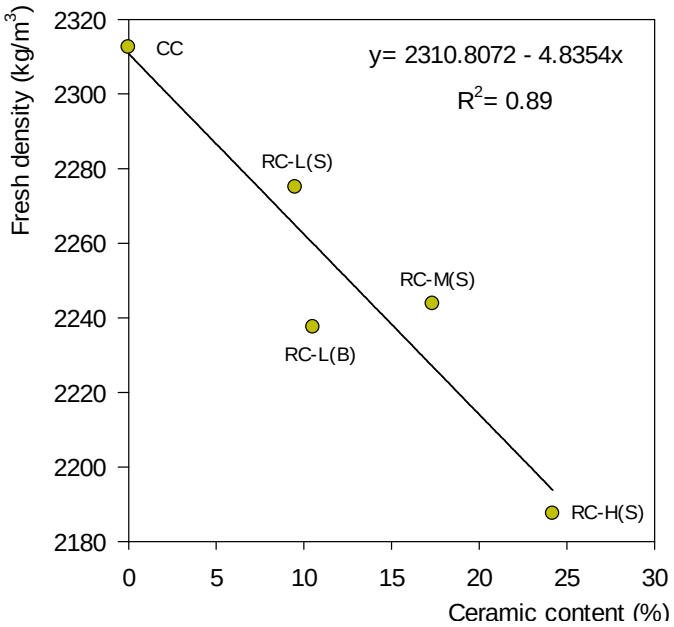

Figure 6.4: Relationship between the fresh density and the ceramic content incorporated in the total weight of aggregates in phase II

5. HYDRATION HEAT

Once the water is added to the mixture, the wetted cement begins to hydrate in a set of exothermic chemical reactions responsible for the concrete hardening. Hence, the study of the heat development during the cement hydration points indirectly to the chemical reactions occurring.

In Portland cement, alite (C_3S) and aluminate (C_3A) are the phases responsible for most of the heat liberation (Table 6.4). Thus, their hydration is used to stablish different stages in the typical heat curve representing the cement hydration process.

Table 6.4: Hydration characteristics of cement compounds (Wang et al., 2006)

Compound	Reaction rate	Amount of heat released	Contribution to cement heat release
C_3S	Moderate	Moderate	High
C_2S	Slow	Low	Low
$C_3A+C\bar{S}H_2$	Fast	Very high	Very high
$C_4AF+ C\bar{S}H_2$	Moderate	Moderate	Moderate

Figure 6.5 illustrates the isothermal heat release in the early hydration process of Portland cement which is generally described by five stages:

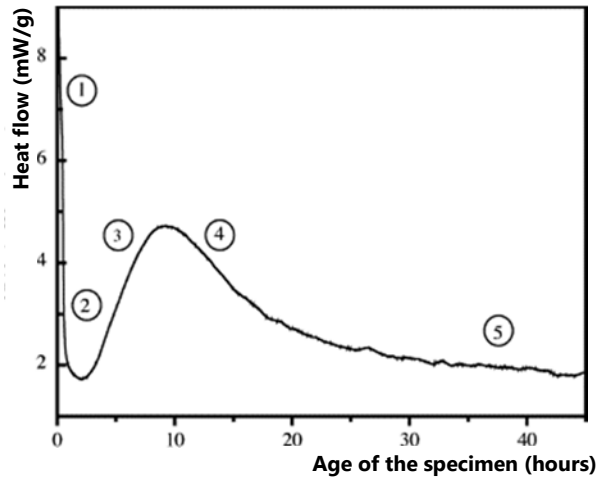

Figure 6.5: Isothermal heat release (Mostafa and Brown, 2005)

1. Initial period: Within the two first minutes, a rapid heat release occurs due to the initial wetting of the cement and the hydration of the aluminate (C_3A), the gypsum hemihydrate ($CaSO_4 \cdot 0.5H_2O$) and the free lime (CaO) (Mostafa and Brown, 2005).

2. Induction period: Lasting for about 2.5 hours depending on the temperature, fineness and chemical composition of the cement, this period is associated to the necessary time to increase the permeability or destruct the layer formed around the particles of alite (C_3S) (Brown et al., 1985; Grutzeck and Ramachandran, 1987). As the reaction is relatively slow, the concrete remains plastic and workable. The end of the dormant period is generally related to the initial setting (Ye, 2003).

3. Acceleration period: In this stage, the final setting of concrete takes places as the alite (C_3S) hydrates rapidly resulting in the second peak of the graph (Mostafa and Brown, 2005). Bullard et al. (2011) presume that the rate of hydration in this stage is linked to the content of C-S-H. Normally, this phase lasts for 3 to 12 hours after mixing (Hewlett, 2003).

4. Deceleration period: Once the smaller particles have been depleted by the hydration process, the heat release becomes slower. The lack of space or water have also been pointed as liable for this period (Bullard et al., 2011). Some investigations have reported the presence of two peaks along this period. The first one, occurring shortly after the start of the deceleration stage, has been attributed to the transformation of ettringite in monosulphate (Baert, 2009), the new formation of ettringite (Taylor, 1997; Hewlett, 2003) or the point of exhaustion of solid gypsum (Bullard et al., 2011). A second diffuse peak is sometimes observed at the end of this phase corresponding to the ferrite hydration (Taylor, 1997) or to the conversion of ettringite in monosulphate (Taylor, 1997; Hewlett, 2003; Bullard et al., 2011).

5. Slow continued reaction period: Despite most of the heat liberation occurs during the first days, the hydration process continues for a long time and it is responsible for the reduction of the porosity and the subsequent strength gain.

When Portland cement is blended with blast furnace slag (BFS), the typical curve showing the heat development (Figure 6.6) displays a completely separated peak or a shoulder in the graph resulting from the blast furnace slag hydration (De Schutter and Taerwe, 1995; Escalante-Garcia and Sharp, 2004; Bougara et al., 2010). Nonetheless, there is no consensus about other resulting modifications of the use of blast furnace slag. According to Bougara et al. (2010), the peak corresponding to the Portland cement hydration occurs at the same moment in blended cements; but controversially the findings of others authors point out to an acceleration (Escalante-García and Sharp, 1998) or deceleration (Singh et al., 1995) of the Portland cement hydration. On the contrary, it is generally recognised that the use of secondary cementitious materials delays the maximum temperature rise (Douglas et al., 1990; Schindler and Folliard, 2003).

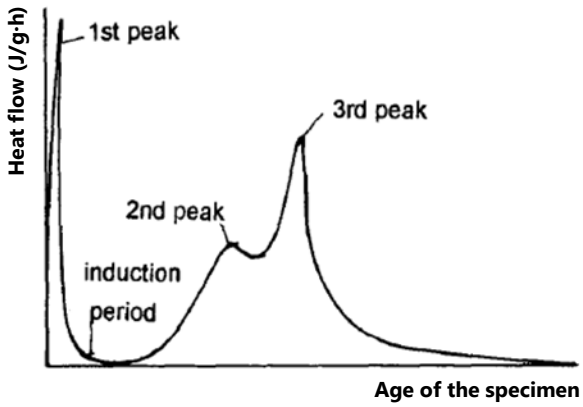

Figure 6.6: Isothermal heat release of blast furnace cement at 20 ºC (De Schutter and Taerwe, 1995)

Investigations regarding the heat of hydration of sustainable concretes mainly refer to the use of secondary cementitious materials such as fly ash and blast furnace slag. Currently, it is recognised that the use of untreated coarse recycled aggregates from CDW alters the microstructural behaviour of recycled concrete mixes (see chapter 7) since the higher porosity reduces the effective water available for the cement hydration.

However, few studies exist examining the influence of the replacement on the heat liberation during the cement hydration. Koenders et al. (2014) and Pepe et al. (2014a) studied the influence of the incorporation of recycled concrete aggregates, both in dry and saturated moisture condition, on the evolution of the heat of hydration of recycled concrete mixtures with a 30% and 100% replacement ratio of the natural coarse aggregates, respectively. In addition, a model to simulate the hydration evolution and a relationship between the hydration process and the compressive strength is offered for recycled concrete mixtures

5.1. SEMI-ADIABATIC CALORIMETER

As previously stated, the cement hydration produces a temperature rise inside of the mixture that induces thermal stresses which could result in the early age formation of cracks in mass concrete elements, and thus reduce their life span. In order to assess this problem, the use of a semi-adiabatic calorimeter is preferable since those conditions are a good simulation of those occurring in mass concrete (pavements or smaller elements) or at the centre of a large pour of concrete (RILEM TC 119-TCE, 1997).

Despite the exothermic nature of the cement hydration plays a key role in the risk of early age crack formation, the thermal conductivity of concrete and the temperature of the surroundings (the atmosphere or other surfaces at lower temperature) are essential in the generation of the temperature gradients leading to the development of tensile stresses responsible for the superficial cracking if the tensile strength of the specimen is not enough to bear those forces (Weiss et al., 2000). Moreover, the cooling phase could also originate cracks in the interior of the concrete if the thermal contraction in the interior of the concrete is hindered by the already stiffened exterior (Waller et al., 2004). Hence, to avoid the risk of thermal cracking the temperature difference between the interior and exterior surface of the concrete should be lower than 20ºC (Kosmatka et al., 2002) and the cooling rate should be slower than 3ºC/h (Nawy, 2008).

Figure 6.7 displays the temperature evolution in the semi-adiabatic calorimeter and Table 6.5 shows the quantitative parameters of the temperature development. Although the hydration proceeds for longer periods, the heat release was monitored only for 72 hours, since most of the heat liberations take place in the first days after mixing.

The different temperature curves reveal the actual influence of the use of recycled aggregates containing varying percentages of ceramic waste on the cement hydration. Regarding the key temperature points, all recycled concrete mixtures presented lower initial temperature values at the start of the experiment (after no longer than 12 minutes after mixing) ranging from -9% (II-RC-L(S)) to -17% (II-RC-M(S)) despite all ingredients presented the same ambient temperature at the start of mixing, and registered higher temperature values at the end of the experiment oscillating from 1% (II-RC-L(S)) to 4% (II-RC-H(S)). The recycled concretes presented an unequal behaviour with respect to the peak temperature: while II-RC-L(S), II-RC-L(B) and II-RC-H(S) samples showed higher temperature values (0.5% to 3.8%), the II-RC-M(S) sample displayed a peak temperature 1.8% lower than the conventional concrete. However, all recycled concrete samples took longer (9%-18%) to reach the peak temperature.

In terms of rate of the hydration reaction, the temperature rate in the ascending branch is higher for the recycled concrete mixtures oscillating between 15% and 29% with respect to the conventional concrete, while no clear tendency exists with respect to the cooling rate among all the studied samples.

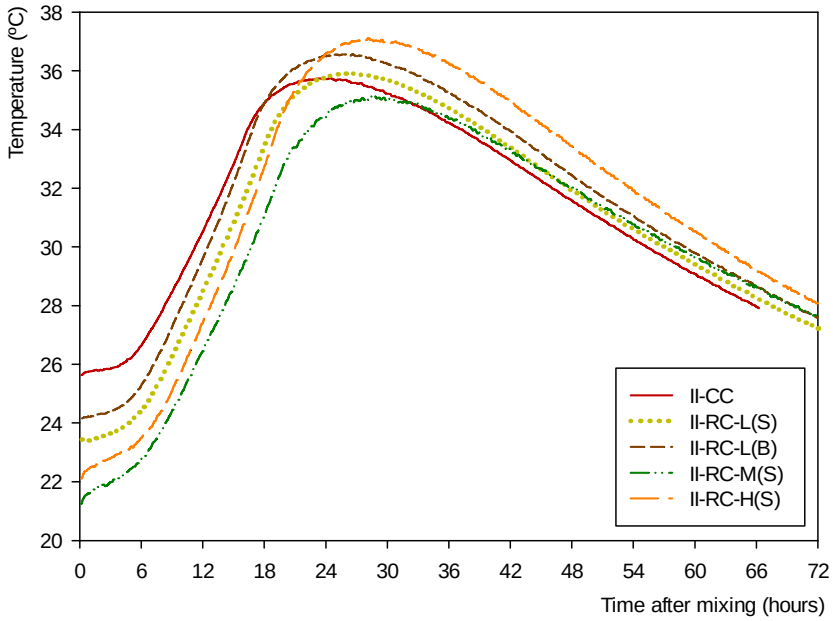

Figure 6.7: Temperature rising during the hydration process

Table 6.5: Parameters of the temperature development during the hydration process

	Temperature range (ºC)		Temperature variation (ºC)	Elapsed time (h)	Temperature rate (ºC/h)
Heating phase					
II-CC	25.63	35.76	10.13	24.42	0.41
II-RC-L(S)	23.44	35.93	12.49	26.53	0.47
II-RC-L(B)	24.17	36.57	12.4	26.64	0.47
II-RC-M(S)	21.24	35.13	13.89	28.80	0.48
II-RC-H(S)	22.11	37.12	15.01	28.15	0.53
Cooling phase [a]					
II-CC	35.76	27.91	-7.85	41.84	-0.19
II-RC-L(S)	35.93	28.21	-7.72	39.75	-0.19
II-RC-L(B)	36.57	28.60	-7.97	39.67	-0.20
II-RC-M(S)	35.13	28.57	-6.56	37.42	-0.18
II-RC-H(S)	37.12	29.15	-7.97	38.08	-0.21

[a] *The calculations were performed assuming the end of the measurements at 66 hours after mixing in order to have experimental data for all concrete mixtures*

In order to assess the relationship between the semi-adiabatic temperature parameters of each concrete mixture and the ceramic content incorporated in the total weight of aggregates, a simple linear regression analysis was carried out, which is shown in Figure 6.8.

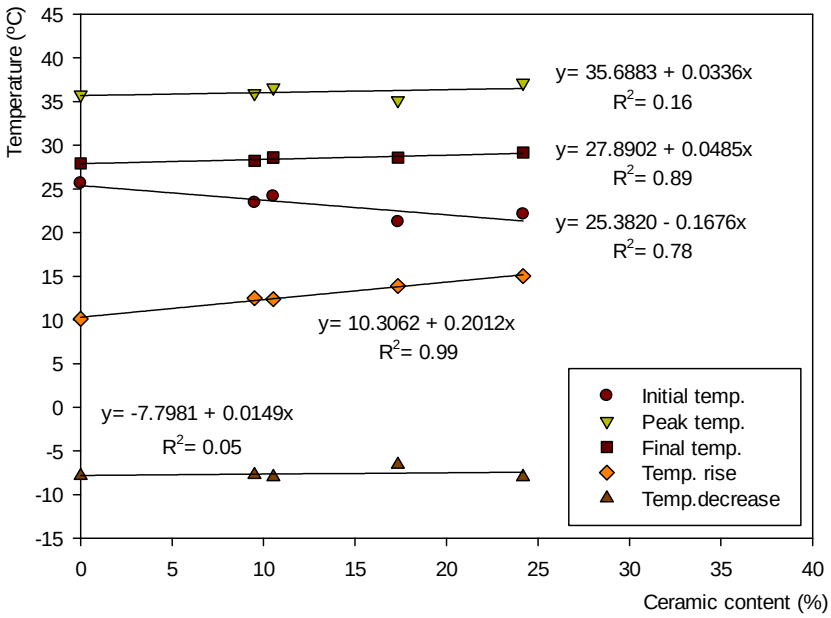

Figure 6.8: Relationship between the semi-adiabatic temperature parameters and the ceramic content incorporated in the total weight of aggregates

While a clear lack of correlation could be observed between the ceramic content and, respectively, the peak temperature and the temperature decrease in the descending branch of the semi-adiabatic curve as shown by the lower R^2 values; some significant relationships exist between the rising content of ceramic in the concrete and the calorimetric behaviour of the mixture. For instance, a nearly perfect (R^2=0.99) linear correlation exists among the increasing incorporation of ceramic waste as recycled aggregate and the temperature rise in the ascending branch of the semi-adiabatic curve. The initial and final temperature of the concrete batch is also significantly correlated (R^2=0.78 and R^2=0.89) with the amount of ceramic waste incorporated in the total fraction of aggregates. All of these relationships suggest that the use of rising amounts of ceramic recycled aggregates increases the heat of hydration of the recycled concrete mixtures.

As previously stated, the semi-adiabatic temperature rise of the concrete is not the sole factor affecting the early thermal crack formation. For instance, the coefficient of thermal expansion (CTE) of the aggregates has a great influence in the phenomenon. The CTE provides an indication of how the material will expand or contract when exposed to temperature changes. While siliceous gravel and sand exhibit CTE between $10x10^{-6}$ mm/mm/ºC to $13x10^{-6}$ mm/mm/ºC (Mukhopadhyay et al., 2007); ceramic materials present CTE ranging from $4x10^{-6}$ mm/mm/ºC to $8x10^{-6}$ mm/mm/ºC (IPC, 2011). Since the choice of aggregates with low CTE is beneficial to reduce the restrained strain due to thermal stresses (Choktaweekarn and Tangtermsirikul, 2010), it is expected that the use of recycled aggregates containing significant percentages of ceramic waste will reduce the probability of early-age cracking. Nevertheless, in order to avoid any complications in this regard when using recycled aggregates, the selection of low heat of hydration cements is preferable.

Besides the temperature evolution during the cement hydration, the semi-adiabatic measurements allowed the calculation of the cumulative heat production according to equation (3.14) in chapter 3 and the heat production rate was determined as the derivative of the cumulative heat production. Figure 6.9 illustrates the cumulative heat production and the heat production curves obtained for each concrete mixture studied in phase II and Table 6.6 shows the maximum values reached for both parameters in each of the concrete batches.

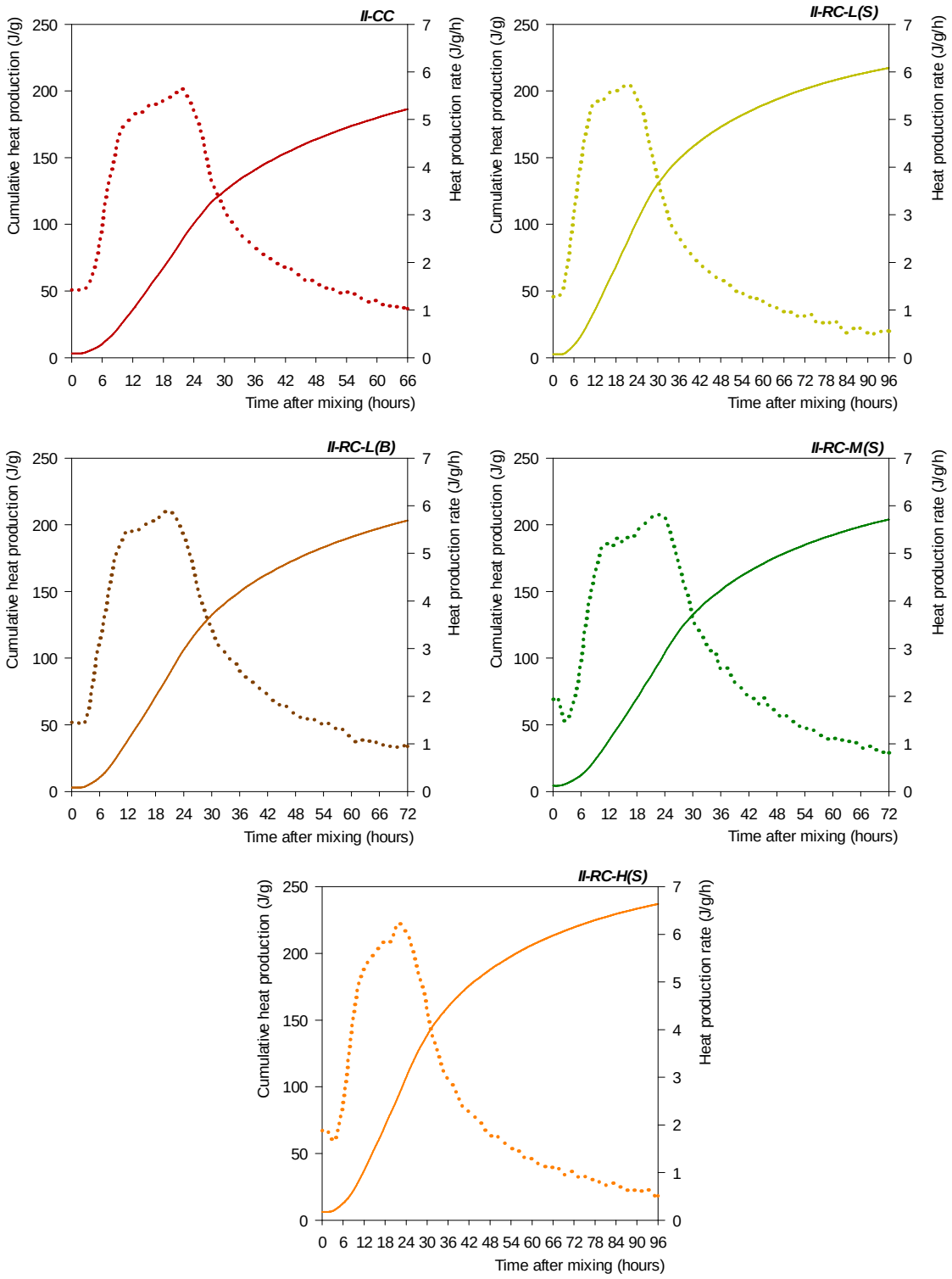

Figure 6.9: Cumulative heat production (solid line) and heat production rate (dotted line) under semi-adiabatic conditions for each concrete batch studied in phase II

Table 6.6: Total heat release and maximum heat production rate for each concrete batch studied in phase II

	Total heat released (J/g)	Maximum heat production rate (J/g/h)
II-CC	192.21	5.65 (21.40 h)
II-RC-L(S)	201.81	5.71 (21.13 h)
II-RC-L(B)	203.79	5.86 (20.76 h)
II-RC-M(S)	204.82	5.81 (23.16 h)
II-RC-H(S)	220.37	6.24 (21.68 h)

The heat of hydration is the quantity of heat produced by both the exothermic chemical reactions, and the heat of adsorption of water in the gel layers of the calcium silicate hydrate (C-S-H) matrix, the latter of which accounts for approximately one quarter of the total heat of hydration (Neville, 1995). In order to facilitate the comparison among the conventional and recycled concrete mixtures, Figure 6.10 illustrates the cumulative heat release of all samples. The recycled concretes showed higher total heat release than the conventional concrete (Table 6.6), which supports the idea that the use of recycled aggregates multiplies the risk of early age thermal crack formation. Nonetheless, the heat production growth, ranging between 5% and 15%, entailed a strong relationship (R^2=0.91) between the total heat released and the ceramic content incorporated in the total weight of aggregates (Figure 6.12).

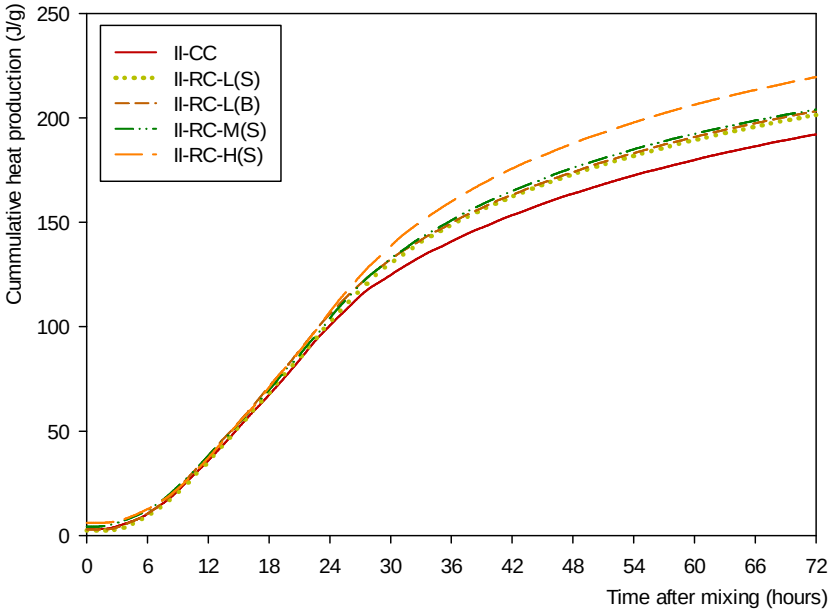

Figure 6.10: Cumulative heat production under semi-adiabatic conditions

Besides the heat liberation, the evolution of the heat production rate is also important. Thus, similarly, Figure 6.11 illustrates the heat production rate of all samples in the same graph in order to facilitate the comparison between the conventional and recycled concrete mixtures. Since the mixing was performed outside the calorimeter the first peak resulting from the initial wetting of the cement was not recorded. In addition, contrarily to the depiction of the typical hydration curve of blast furnace cement exemplified in Figure 6.6, the second and third peaks that characterize this type of cement hydration do not appear as separated peaks but unified showing a shoulder,

which is also a common occurrence (De Schutter and Taerwe, 1995; Escalante-Garcia and Sharp, 2004; Bougara et al., 2010). In order to achieve a more precise comparison among concrete mixtures, solely the absolute magnitude and time of occurrence data regarding the highest peak was studied (Table 6.6). While the peak value followed an acceptable pattern with regard to the ceramic content in the concrete (R^2=0.75) with increases ranging from 1.06% to 10.44% respect to the conventional concrete (Figure 6.12), the peak occurrence barely showed a correlation (R^2=0.17) with the ceramic content incorporated within the aggregate fraction of concrete (Figure 6.12). Hence, the incorporation of ceramic aggregates produced both a maximum expedition of 3% and a maximum delay of 8% in the peak occurrence when compared to the peak manifestation in the conventional mixture.

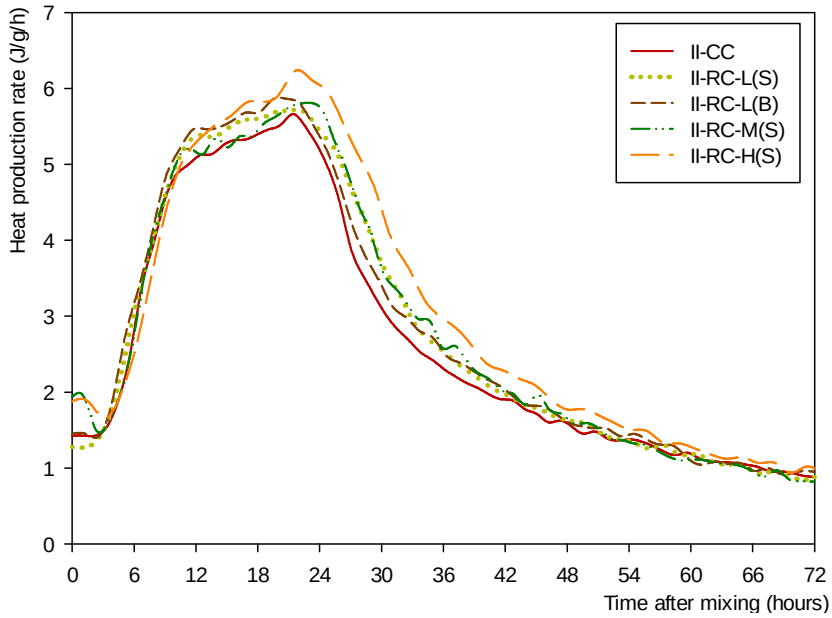

Figure 6.11: Heat production rate under semi-adiabatic conditions

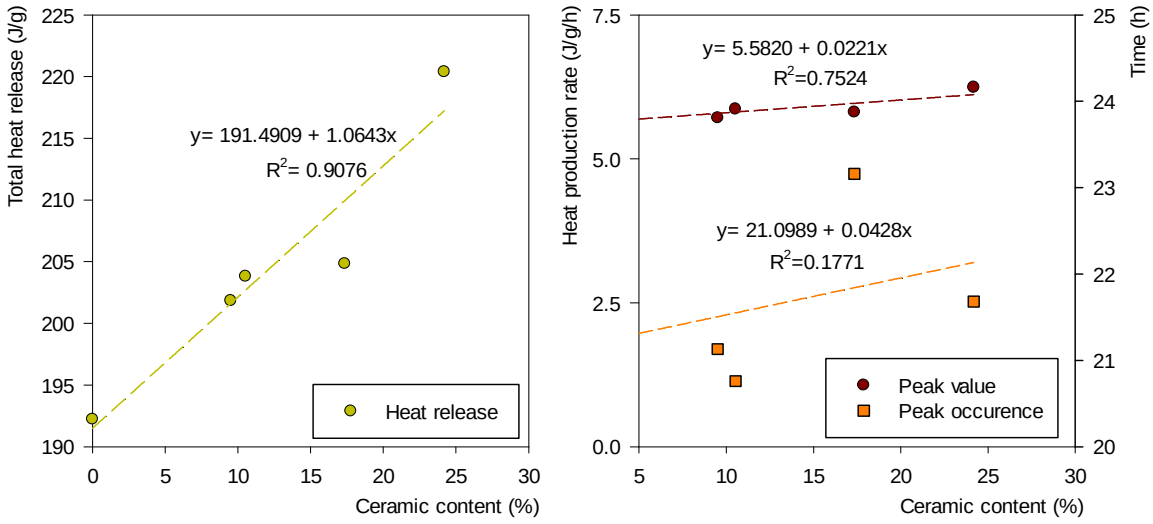

Figure 6.12: Relationship between the heat release or the peak data (value and occurrence) and the ceramic content incorporated in the total weight of aggregates

6. SETTING TIME

Soon after the mixing of cement and water, the cement paste enters in a dormant period characterized by a slow reaction process that allows the concrete batch to retain its plasticity and workability, but the paste becomes stiffer as the hydration process continues. The particularities of the recycled aggregates from CDW, in particular their porosity and water absorption, are expected to modify the setting behaviour of the concrete mixture.

A schematic diagram of the development of the concrete structure during the hydration process is represented in Figure 6.13. While the black dots symbolize the cement grains, the growing grey area around them denotes the precipitation of the hydration products as the hydration moves forward. As the available space, i.e. the capillary porosity, decreases, the paste becomes unworkable due to the increase of inter-particle frictional resistance pointing to the initial setting. The continuous increase of the thickness of the layer turns in a bond between cement grains that creates a continuity (percolation path) leading to a gain in stiffness that signals the final setting. In the hardening stage, the hydration products continue to expand and the bonds between cement grains gain in rigidity which leads to the ultimate strength development.

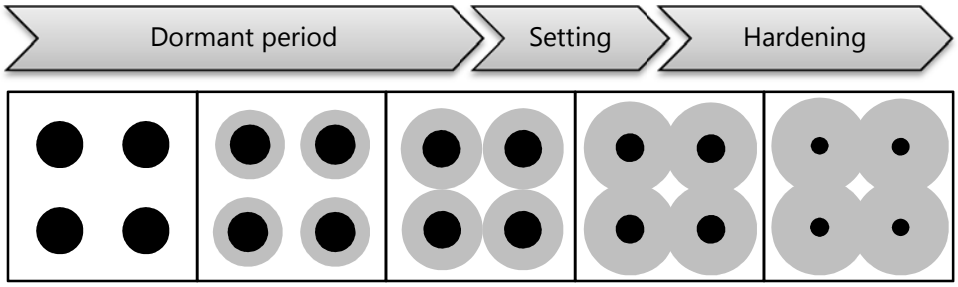

Figure 6.13: Representation of the structure growth in a cement paste. After Soroka (2003)

According to Neville (1995), the initial and final setting are arbitrarily defined times in the transition of a concrete batch from fluid to solid state. However, it is fully recognized that the determination of the initial setting is characterized by the loss of plasticity and the final setting is defined by an increasing gain in stiffness. Hence, the traditional tests, such as ASTM C403M-08 (2008) and UNE EN 196-3 (2009), are based upon the change in penetration resistance of a needle in the cement paste. A major disadvantage of these methods is the impossibility to be directly used on concrete specimens because the hamper that the coarse aggregates would represent to the needle penetration.

Some researchers have proposed the determination of the setting times by means of calorimetric measurements, since the heat released during hydration is correlated to the microstructural development of the concrete and thus the setting phenomena (Sandberg and Liberman, 2007; Struble et al., 2010; Weakley, 2010; Rupnow et al., 2011). Nonetheless, more recently, non-destructive techniques have been accepted for examining the development of early-age concrete properties (RILEM TC 185-ATC, 2005).

One of these techniques, the wave transmission method, is based upon the measure of the travelling time of an ultrasonic wave through the tested material. These type of waves are of acoustical nature but undetectable for the human hearing (20 kHz) and originate perpendicular (longitudinal, compression or p-wave) and parallel (transverse, shear or s-wave) to the propagation point. Several researchers have employed this method in order to evaluate the setting time of cement based materials (Ye, 2003; Lee et al., 2004; Reinhardt and Grosse, 2004; De Belie et al., 2005, 2008; Voigt et al., 2005; Robeyst et al., 2008; Robeyst, 2009; Trtnik and Gams, 2014). A detailed analysis of the different set-ups implemented to date can be found in Robeyst (2009) and Trtnik and Gams (2014).

6.1. CALORIMETRIC MEASUREMENTS

Sandberg and Liberman (2007) proposed two methods for the determination of the initial and final setting times based on the temperature rise profile of the concrete mixture. On one hand, the fraction method defines the initial setting time as the point in which the 21% of the maximum heat release is reached. Analogously, the final setting is determined as the time when 42% of the total semi-adiabatic temperature rise is obtained. On the other hand, the derivatives method determines the final setting as the maximum slope of the hydration peak (maximum in the first derivative) and the initial setting as the maximum curvature of the semi-adiabatic profile (i.e. maximum in the second derivative).

For all concrete mixtures of phase II, Table 6.7 registers the initial and final setting times calculated through the derivatives and fraction methods. Additionally, Figure 6.14 displays the temperature development of the concrete specimen during the semi-adiabatic test, as well as the first and second derivatives of the recorded temperature rise as per calculation requirements in the derivatives method.

Table 6.7: Setting times according to the calorimetric measurements

	Derivatives method		**Fraction method**	
	Initial setting (h)	**Final setting (h)**	**Initial setting (h)**	**Final setting (h)**
II-CC	6.69	13.46	7.95	11.10
II-RC-L(S)	9.65	13.74	8.66	12.21
II-RC-L(B)	8.66	13.34	8.37	11.73
II-RC-M(S)	9.44	16.68	8.64	12.80
II-RC-H(S)	10.63	15.5	9.18	13.26

In general, the assessment of the initial and final setting times by means of the two calorimetric methods suggests that the use of recycled aggregates from CDW in the concrete manufacture delays the setting. Regarding to the initial setting time, the derivatives method found differences ranging from 29.45% to 58.89%, while in the fraction method the delay in the initial setting time oscillated between 5.28% and 15.47%. Contrarily, both methods encounter similar retardation in the final setting times with variations up to 23% when compared to the conventional mix. The delay in the setting times could be attributed to the presence of organic substances identified in the recycled aggregates derived from CDW (see section 3.1.1 in chapter 4).

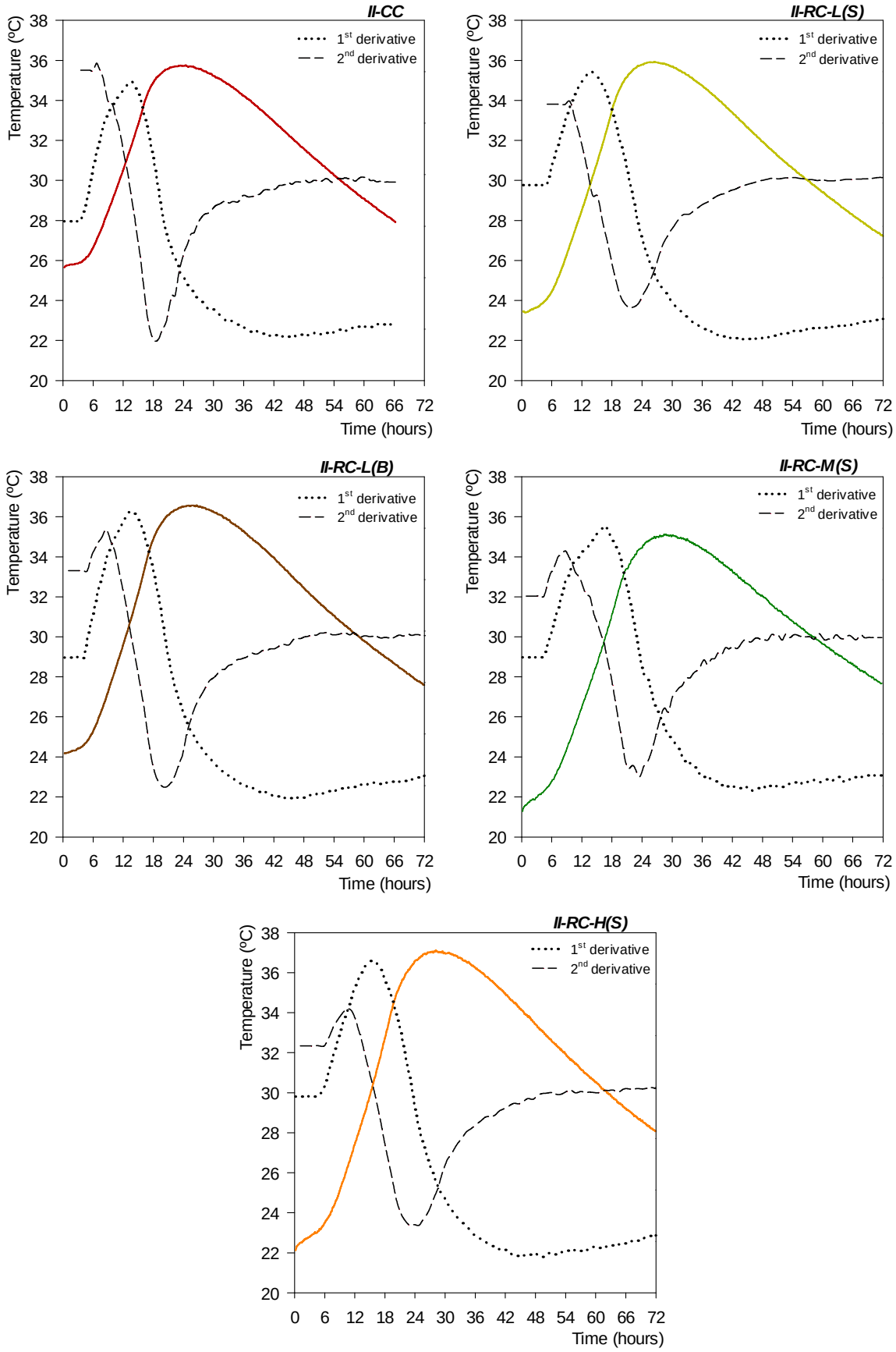

Figure 6.14: First and second derivatives of the temperature rise

Since the increase in the final setting time is less than 2 hours, as calculated per both methods, the recycled aggregates comply with the limit set in the Spanish Code on structural concrete (Permanent Commission on Concrete, 2008) for the presence of organic matter in the aggregates used in the production of concrete. Moreover, clear relationships exist between the delay in the setting time determined by the fractions method and the ceramic content in the concrete mixture as showed by the high correlation factors identified in Figure 6.15. It is worth mentioning that commonly the fraction method is considered more robust than the derivatives method (Wang et al., 2008; Weakley, 2010). Nevertheless, all these initial and final setting values should be considered as a first approximation to the influence of the recycled aggregates in the concrete manufacture and be contrasted with the results arising from the methods developed in subsequent sections of this chapter.

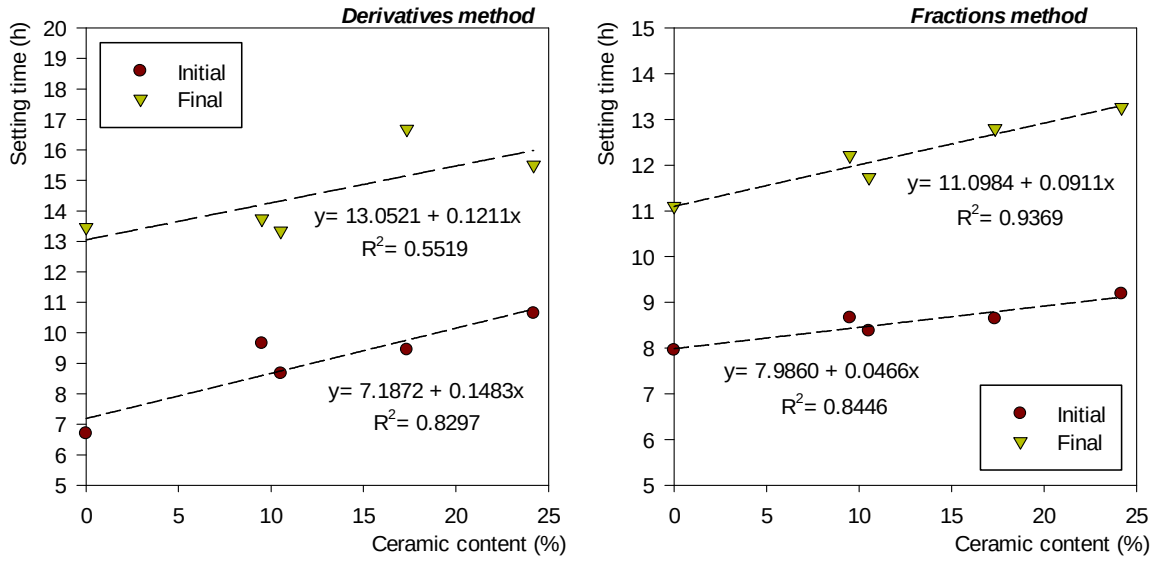

Figure 6.15: Relationship between the initial and final setting times determined by the calorimetric measurements and the ceramic content incorporated in the total weight fraction of aggregates

6.2. ULTRASONIC VELOCITY

According to Ye (2003), the typical representation of the ultrasonic p-wave velocity through concrete at early-ages can be divided in three sections. The first part corresponds to the dormant period and is characterized by a constant low velocity, which is mainly dominated by the presence of air bubbles that reduce the wave transmission. Afterwards, the second section coincides with the acceleration stage, where the velocity increases rapidly due to the creation of percolation paths that increase the connectivity of the solid phase and thus the wave propagation. Finally, in the third region, the ultrasonic velocity increases slowly until it reaches an asymptotic value that reflects the deceleration stage.

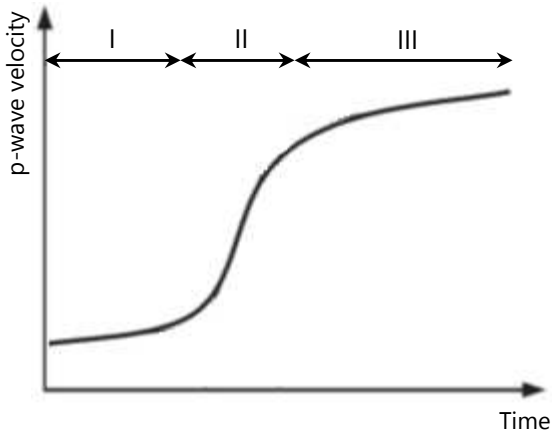

Figure 6.16: Representation of a typical ultrasonic p-wave velocity curve

It is generally accepted that the changes in the p-wave velocity have a direct correspondence with the cement hydration and the stiffening process (Ye, 2003; Lee et al., 2004; Reinhardt and Grosse, 2004; De Belie et al., 2005, 2008; Voigt et al., 2005; Robeyst et al., 2008; Robeyst, 2009; Trtnik and Gams, 2014). While the early increase in the p-wave velocity has been associated to the consolidation of the heavier particles which favours the wave transmission (Voigt et al., 2005), the migration of the air bubbles to the surface due to bleeding (Ye, 2003) or the formation of ettringite in the early age concrete (Kamada et al., 2005; Voigt et al., 2005), the maximum velocity increase of the ultrasonic wave is generally related to the concrete setting since it corresponds to the percolation of the hydration products during cement hydration (Ye et al., 2004).

Despite the use of recycled aggregates with varying percentages of ceramic waste in the production of the recycled concrete mixtures, the same stages in the p-wave velocity curve can be recognized for in the conventional and recycled mixtures evaluated in this investigation (Figure 6.17).

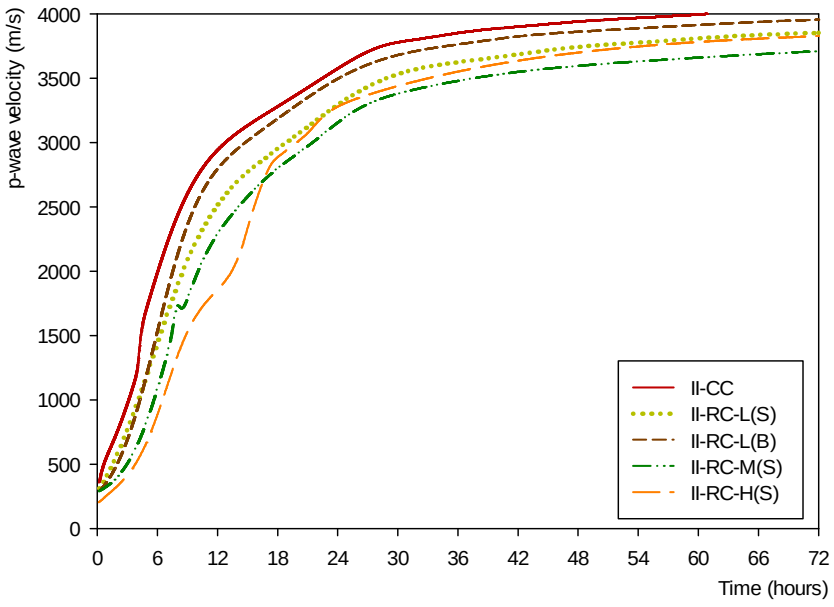

Figure 6.17: Ultrasonic wave velocity

At first glance, it could be observed that the initial ultrasonic velocity is below 500 m/s. This fact has also been observed for other researches (Hwang and Shen, 1991; Lee et al., 2004; Ye et al., 2004; Trtnik et al., 2008), who attributed p-wave velocity values lower than 600 m/s to the presence of air. In addition, Sukontasukkul et al. (2012) found that the fine/coarse aggregate ratio affected the velocity curves after 6 hours, resulting in higher velocity values for decreasing fine/coarse aggregate ratio after 24 hours. Similar performance could be observed in this research work for samples with rising ceramic content, which present a higher fine/coarse aggregate ratio and thus displayed a lower ultrasonic wave velocity.

Several criteria have been constructed around the determination of the initial setting of concrete based on the values of the wave velocity: 1000-1500 m/s (Van der Winden, 1990), 2300-2700 m/s (Herb, 2003) and 1100-2000 m/s (Lee et al., 2004). In the same manner, ranging p-wave velocity values have also been proposed for the determination of the final setting time: 3000 m/s (Van der Winden, 1990), 2790-3180 m/s (Herb, 2003) and 2000-3000 m/s (Lee et al., 2004). In order to further improve the accuracy posed by this approach, the inflection point of the velocity curve could be considered as the initial setting time (Reinhardt and Grosse, 2004; Voigt et al., 2005; Robeyst et al., 2008; Trtnik et al., 2008, 2009) and the point at which the derivative of the velocity curve decreased to 20% of its maximum value could be used to determine the final setting time (Robeyst, 2009) which coincides with the start of the flattening in the p-wave velocity curve.

Table 6.8 shows the initial and final setting times determined for the conventional and recycled mixtures according to the criteria established by Robeyst (2009) and Lee et al. (2004), respectively.

Table 6.8: Initial and final setting times

	Robeyst (2009)		**Lee et al. (2004)**	
	Initial setting (h) [$(dv/dt)_{max}$]	**Final setting (h) [0.2x$(dv/dt)_{max}$]**	**Initial setting (h) [1100-2000 m/s]**	**Final setting (h) [2000-3000 m/s]**
II-CC	4.26	8.92	3.59-6.01	6.01-12.76
II-RC-L(S)	5.62	25.62	4.53-8.53	8.53-18.87
II-RC-L(B)	5.89	14.64	4.56-7.56	7.56-14.72
II-RC-M(S)	7.63	13.30	5.97-10.5	10.5-21.47
II-RC-H(S)	7.79	24.95	6.96-13.52	13.52-20.21

Regarding the initial setting times, it could be observed that all the determined values through the criteria established by Robeyst (2009) are within the range proposed by Lee et al. (2004). Hence, the results confirm one another and point towards the delay of the initial setting times between 31.92% and 38.26% for the recycled mixtures with lower ceramic content (II-RC-L(S) and II-RC-L(B)), 79.11% for the II-RC-M(S) mixture and 82.86% for the II-RC-H(S). Compared to the previous methods, the II-RC-L(S) and II-RC-L(B)) mixtures exhibited comparable delays to those obtained by the derivative method. However, in the rest of the cases, the delays determined through p-wave measurements are well above those registered by any of the previous methods. Nonetheless, similarly to the relationship identified between the initial setting time by means of the fraction method and the ceramic content, a strong tendency (R^2=0.94) can be observed between the initial setting time through ultrasonic measurements and the ceramic content in Figure 6.18.

In terms of the final setting time, some discrepancies can be observed as not all the values obtained according the criteria established by Robeyst (2009) fitted within the interval proposed by Lee et al. (2004). Since the lack of coincidence is due to extreme values (final setting times higher than 1 day) and no problems were identified in the demoulding of specimens after 24 hours, some concerns appeared about the accuracy of the criteria proposed by Robeyst (2009) when dealing with recycled mixtures. In any case, if these values are assumed correct, the recycled mixtures suffered delays in the final setting between 0.57 and 2.87 times higher, which exceeds the limit established in the EHE-08 (Permanent Commission on Concrete, 2008).

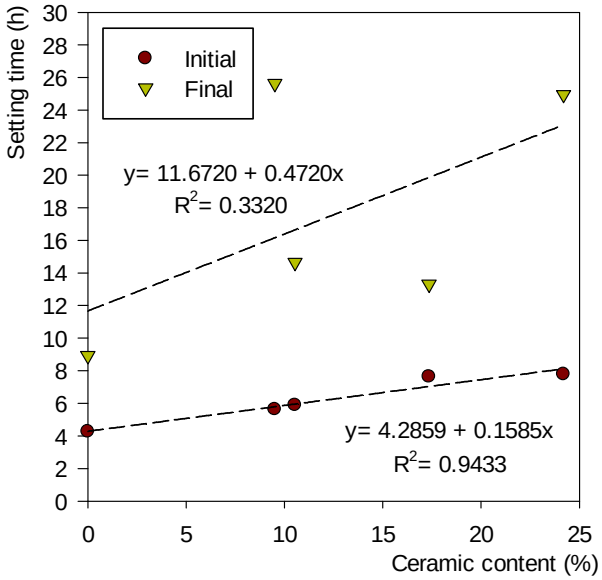

Figure 6.18: Relationship between the setting times and the ceramic content

6.2.1. RELATIONSHIP BETWEEN THE ULTRASONIC VELOCITY AND THE HYDRATION HEAT

According to Nonat and Mutin (1992) hydration and setting are closely related, which makes a comparison between ultrasonic and calorimetric measurements relevant. Nonetheless, since the two tests were performed at different temperatures, a previous adjustment of the time-temperature relationship by means of the maturity method (Freiesleben Hansen and Pedersen, 1977) was carried out. In order to apply this maturity method the activation energy should be taken into account. Whilst the theoretical hydration heat of Portland cement could be determined using the Bogue's formulas (Bogue, 1947), the heat of hydration of blended slag cements should be experimentally determined and it is expected to be higher (Kishi and Maekawa, 1995; Hewlett, 2003). Due the difficulties separating the heat release from the Portland cement and the blast furnace slag in semi-adiabatic conditions, the activation energy of the blended cement was set as 33.50 kJ/mol according to guidelines proposed by Robeyst (2009). Furthermore, it has been assumed that the activation energy remains constant, which according to D'Aloia (2003) is viable at early ages as the evolution of the activation energy shows an initial plateau. Figure 6.19 compares the p-wave velocity and the heat production rate expressed by mass of total binder and plotted against the equivalent age at 20°C.

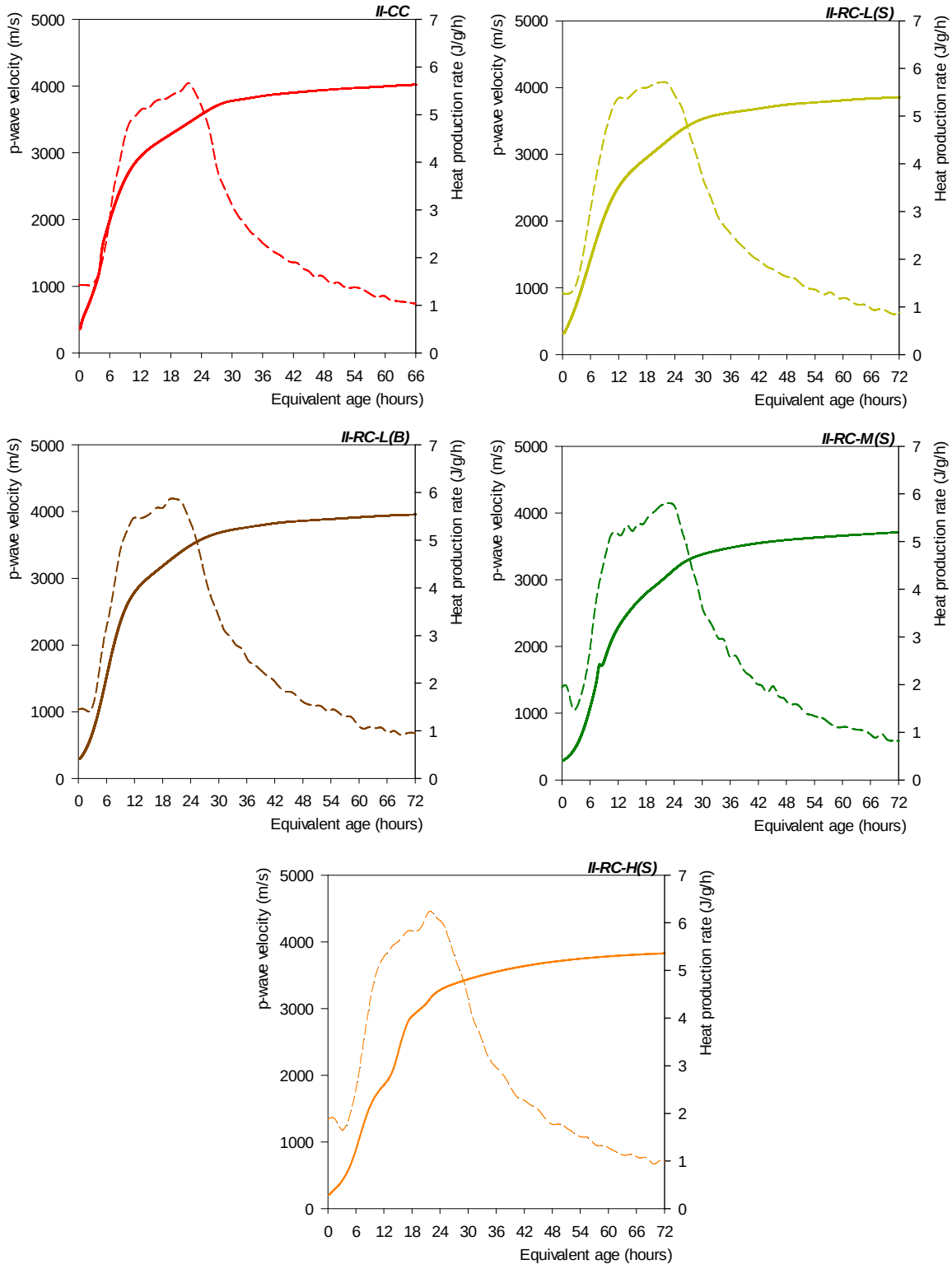

Figure 6.19: Comparison between the ultrasonic velocity (solid line) and the hydration heat (dotted line) as a function of the equivalent age at 20ºC

At first glance, a good agreement exists between the resulting peak, which combines the heat release caused by the hydration of the Portland cement and the blast furnace slag, and the point at which the increase of the velocity eases off. Kim and Yoon (1988) and Zhang et al. (2012) also demonstrated that the p-wave velocity curve presents a good correlation with the heat evolution curve. For all mixtures, the setting time occurred at least after 18 hours. As expected, the use of recycled aggregates delayed the setting but just around 1%, which does not pose any problem to the limitations established in the EHE-08 (Permanent Commission on Concrete, 2008) for the use of this type of aggregates.

6.3. FREQUENCY SPECTRA

Parallel to the wave velocity monitoring, the FreshCon system provides information about the frequency spectra that can be used to deduce the microstructure development of a concrete sample and thus confirm the accuracy of the ultrasonic measurements. Although it is recognized that the analysis of the complete signal spectrum could provide details of the stiffening of concrete, few research has focused on this aspect of the ultrasonic measurements (Robeyst, 2009; Robeyst et al., 2009; Trtnik and Gams, 2013).

The frequency spectra could be explained by the transition of the concrete from fluid to solid state. At early ages, the propagation of the ultrasonic waves is hindered due to the water-like viscous nature of the concrete at that time. As the hydration moves forwards, the concrete becomes a water-saturated porous solid which favours the wave propagation of low-frequency components first and the high-frequency components later when the solid structure is established (Lee et al., 2004).

To study the frequency spectra, the Fast Fourier Transformation (FFT) has been employed to identify the dominant components in the frequency bandwidth (Grosse and Reinhardt, 2000; Robeyst et al., 2009; Trtnik and Gams, 2013). In order to reduce the registered frequency measurements, only the values corresponding to a frequency lower than 100 kHz were selected. In addition, the time values were reduced to 15 minutes steps completing the first 24 hours of measured evolution. Figure 6.20 displays the frequency spectra of the conventional and recycled mixtures. It can be observed that the frequency spectrum of the concrete at early ages is dominated by two frequency ranges (lower and higher than 30 kHz). In general terms, no distinctive frequencies were observed at very early age, and the lower components of frequencies did not appear until minimum 6 hours of testing. The dominance of the low frequency range lasted for at least 8 hours until the higher components of the frequencies became apparent. Albeit differences exist regarding the dominant frequency ranges, this behaviour agrees with the findings of other researchers (De Belie et al., 2005; Trtnik and Gams, 2013).

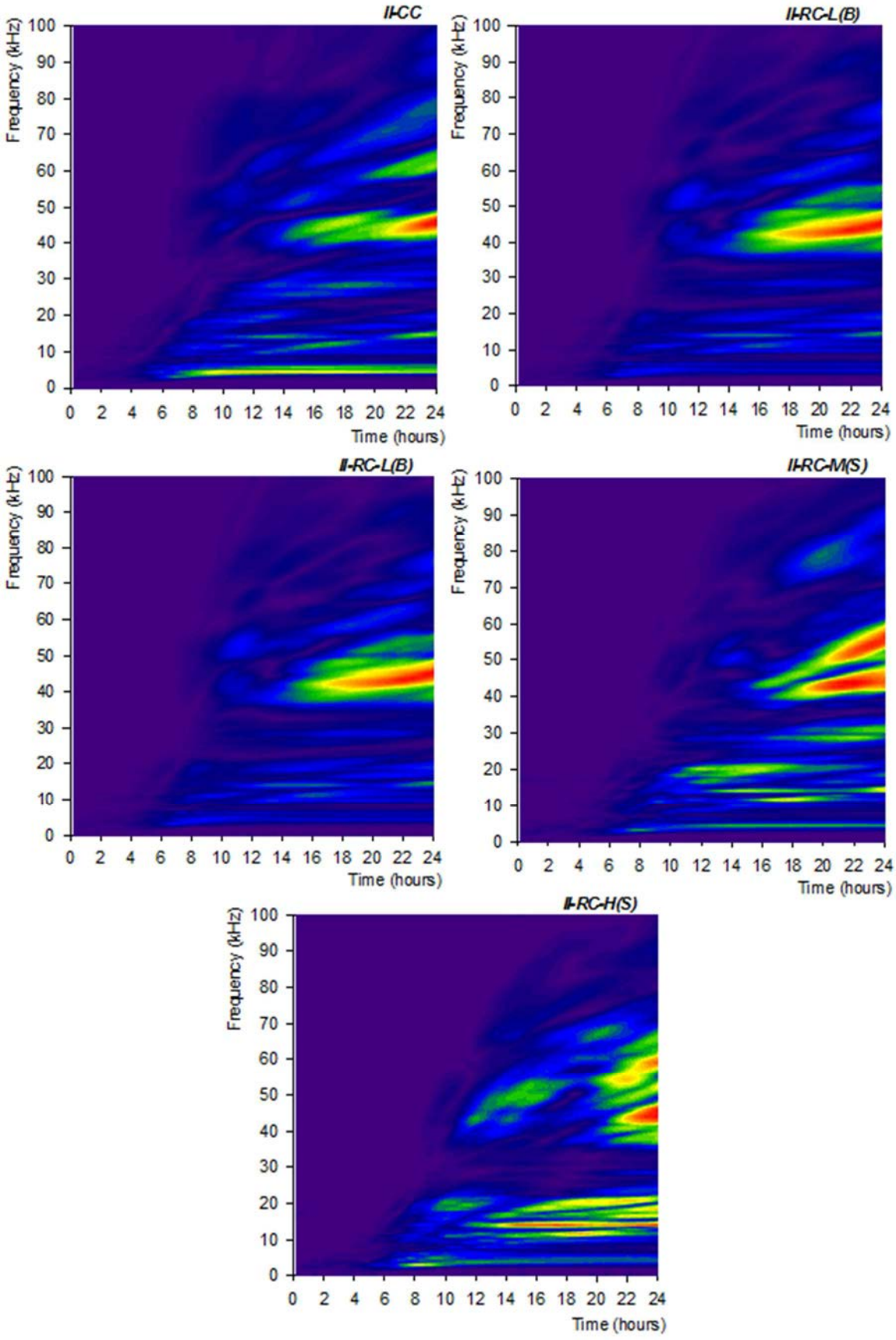

Figure 6.20: Frequency spectra of the conventional and recycled concrete mixtures

Since higher frequencies only transmit when the concrete begins to set (Gams and Trtnik, 2013; Trtnik and Gams, 2013), De Belie et al. (2005) stated that the point at which the frequency spectra shifts corresponds with the deceleration phase of the hydration and the reduction in the increase of the p-wave velocity. Hence, it can be assumed that a similar change in frequencies can be expected among the concrete mixtures studied, but the shift would occur at different times depending on the type of recycled aggregates used in the replacement.

Despite the general development of the frequency spectrum was presented in Figure 6.20, the shift between low and high frequencies could be evaluated in more detail through the study of the evolution of the TG parameter defined in equation (3.17) and initially proposed by Trtnik and Gams (2013). According to the formula, the TG parameter ranges from -1 to 1. Negative values represent predominance of lower frequencies, while positive values indicate proliferation of high frequencies in the spectra. The typical evolution of the TG parameter is illustrated in Figure 6.21. In the first stage, the TG parameter decreases almost to -1 due to the lack of transmission of high frequency waves. The second stage is characterized by a stabilization of the TG parameter around values of -1. After a certain time, the TG begins to increase as the dampening of the high frequencies diminishes along the hydration process occurring in stage 3. The final stage initiates when the curve displays positive values for the first time.

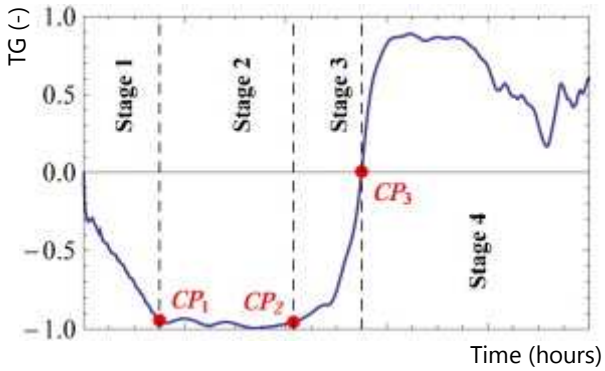

Figure 6.21: General evolution of the TG curve (Trtnik and Gams, 2013)

Figure 6.22 illustrates the evolution of the TG parameter with time for all concrete mixtures studied and Table 6.9 displays the three points characterizing each of the TG curves. Since the FreshCon measurement started in the first 15 minutes after mixing, CP_1 could not be determined. The CP_2 value was determined at the point in which the curve stops to oscillate around -0.90 and begins to increase monotonously and CP_3 reflects the time at which the curve reached a nil value.

Table 6.9: Characteristic points in the TG curve

	CP_2 (h)	**CP_3 (h)**
II-CC	4.79	19.31
II-RC-L(S)	5.01	18.47
II-RC-L(B)	4.06	14.04
II-RC-M(S)	5.15	18.05
II-RC-H(S)	4.93	24.03

The beginning of the setting can be linked to the CP_2 point of the TG curve. In general, the recycled samples presented a delayed initial setting time with respect to the conventional concrete with a maximum of 7.52%. Nonetheless, the II-RC-M(S) mixtures showed the opposite behaviour displaying gains of stiffness before the reference concrete. Since no evidence of an accelerated setting behaviour has been observed through the previous analysis, more research is necessary about the accuracy of the use of the frequency spectra to analyse setting by means of the TG parameter for recycled mixtures.

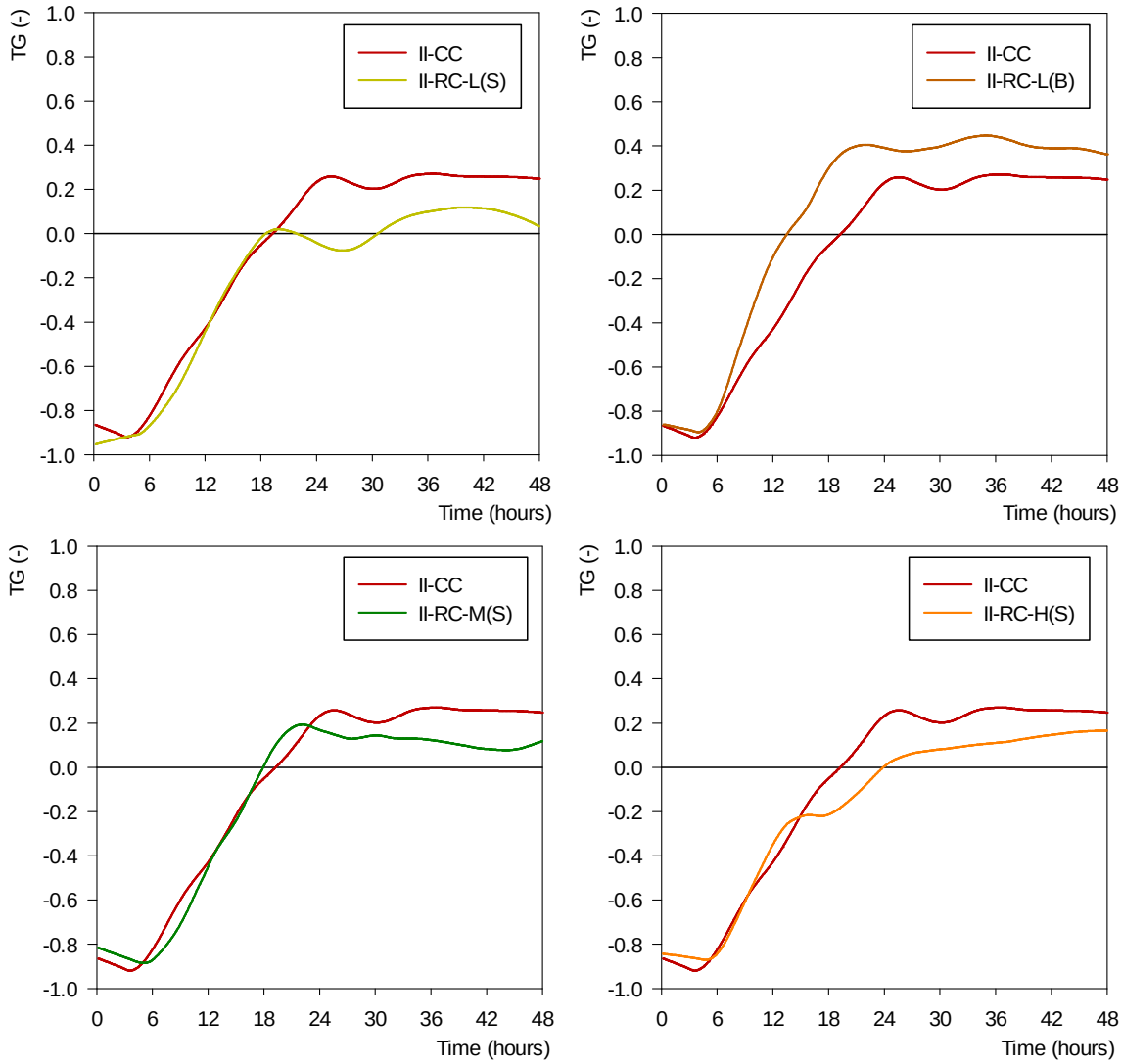

Figure 6.22: TG parameter of the concrete mixtures

Similarly, the CP_3 point of the TG curve can be considered the end of the setting. In this case, the general tendency points to a reduction oscillating between 4.35% and 27.29% in the time necessary to reach the aforementioned point for most of the recycled mixtures. Once again, none of the previous methods pointed to this pattern. However, the values obtained around 18 hours after mixing are in line with those obtained by the compassion between the p-wave curves and the heat production rate as function of the equivalent age at 20ºC (Figure 6.19).

It is worth mentioning that the II-RC-H(S) mixture manifested the opposite performance and a 24.44% delay was registered compared to the conventional mixture. By this estimation, the setting did not occur after more than one day, which agrees with the prediction carried out following the criteria established by Robeyst (2009) but stands against the physical evidence. Anyhow, a great variability among recycled aggregates concrete types is clear which highlights the importance of a proper selection in order to produce the minimum disturbances in the setting behaviour of recycled concretes. Due to the lack of investigations regarding the continuous setting monitoring of recycled mixtures, is yet undecided if the TG parameter proposed by Trtnik and Gams (2013) conveys a correct representation of the frequency spectra.

6.3.1. RELATIONSHIP BETWEEN THE FREQUENCY SPECTRA AND THE CALORIMETRIC MEASUREMENTS

The relationship between the TG parameter and the temperature is shown in Figure 6.23, where the TG parameter is represented as a solid line and the temperature is displayed by means of a dotted line. Analogously to the results of Trtnik and Gams (2013), the changes in the temperature are limited until the end of the second stage in the evolution of the TG parameter. During the third stage, a rapid increase in the temperature as well as the TG parameter could be observed for all concrete mixtures. According to Trtnik and Gams (2013), this behaviour validates the assumption that the TG parameter is related to stiffness gain of the material, and thus its applicability for recycled mixtures.

6.3.2. RELATIONSHIP BETWEEN THE FREQUENCY SPECTRA AND THE ULTRASONIC VELOCITY

According to Trtnik and Gams (2013), the development of the TG parameter in time is proof of the existing relationship between the frequency and the hydration process. Hence, similarities between this parameter and the p-wave velocity should be observed (Figure 6.24). For example, the CP_2 point in the TG curve reflects the beginning of the development of the higher frequencies, which at microstructural level signifies the sudden stiffness of the material and the beginning of the setting. As previously stated, the initial setting time can be identified from the p-wave velocity curve as its inflection point. A good correspondence between those two characteristics points can be observed for all concrete mixtures. Analogously, there is also a good correspondence between the CP_3 point in the TG curve and the moment at which the ultrasonic velocity curve starts to level off, which is commonly accepted as the end of the concrete setting.

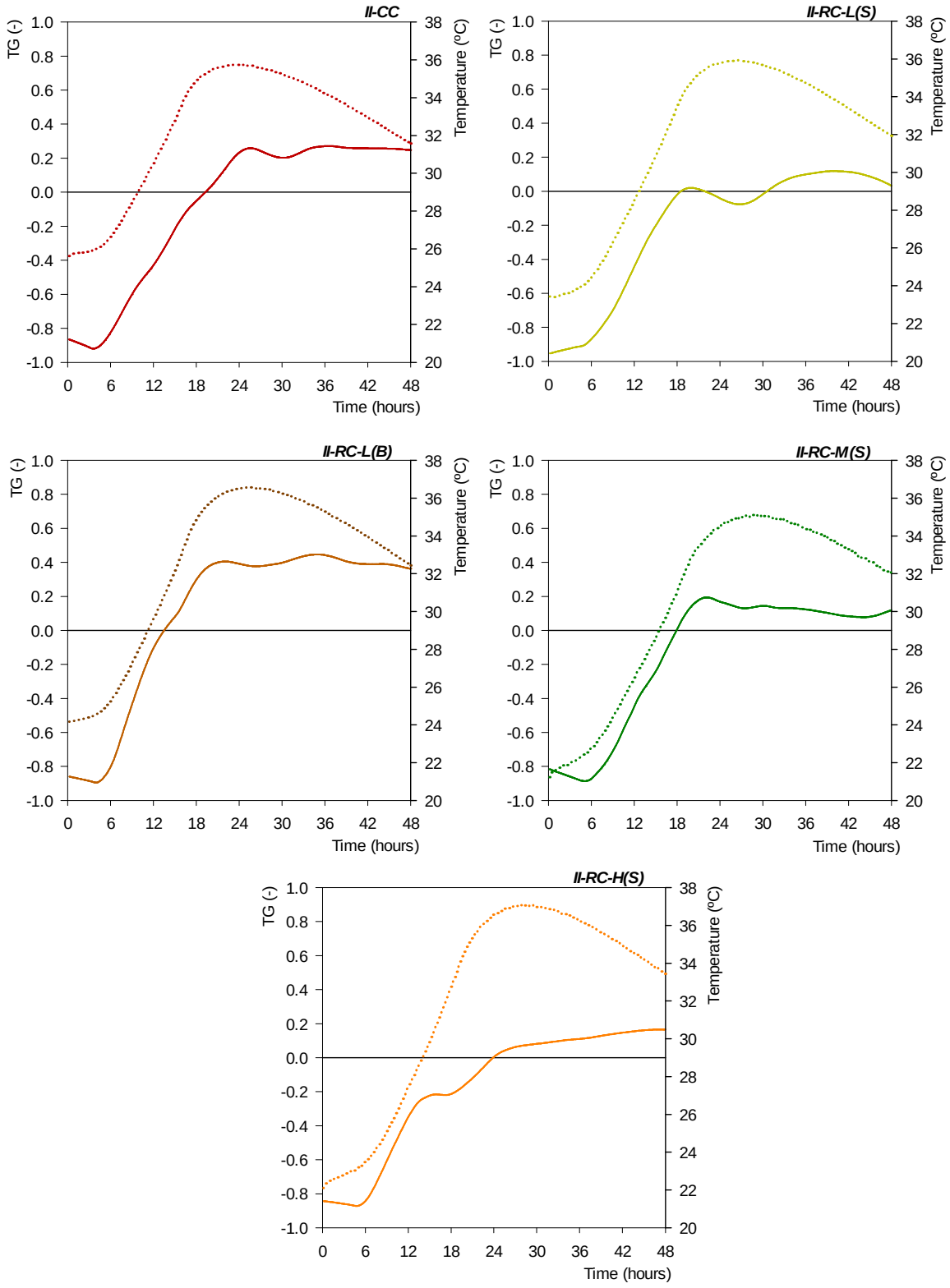

Figure 6.23: Relationship between the TG parameter (solid line) and the temperature rise (dotted line)

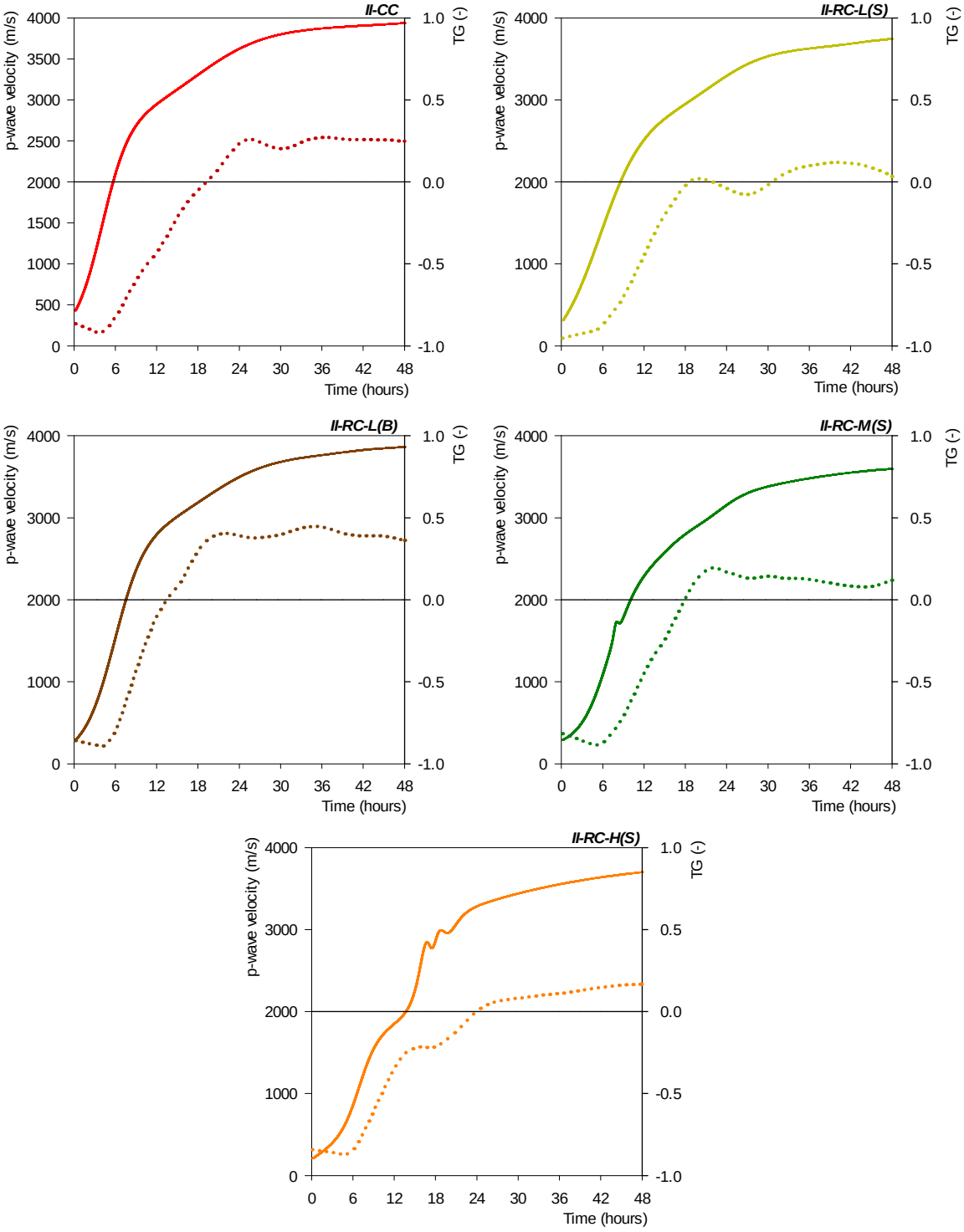

Figure 6.24: Relationship between the TG parameter (solid line) and the ultrasonic wave velocity (dotted line)

7. REFERENCES

ACI Committee 211, 2002. Standard practice for selecting proportions for normal, heavyweight, and mass concrete (ACI Manual of Concrete Practice). American Concrete Institute.

ASTM C403M-08, 2008. Test method for time of setting of concrete mixtures by penetration resistance. ASTM International, Pennsylvania.

Baert, G., 2009. Physico-Chemical Interactions in Portland Cement - (HighVolume) Fly Ash Binders. (dissertation). Ghent University.

Belin, P., Habert, G., Thiery, M., Roussel, N., 2014. Cement paste content and water absorption of recycled concrete coarse aggregates. *Mater Struct* 47 (9): 1451–1465.

Beltrán, M.G., Barbudo, A., Agrela, F., Galvín, A.P., Jiménez, J.R., 2014. Effect of cement addition on the properties of recycled concretes to reach control concretes strengths. *Journal of Cleaner Production* 79: 124–133.

Bezerra-Cabral, A.E., Schalch, V., Carpena Coitinho Dal Molin, D., Duarte Ribeiro, J.L., 2010. Mechanical properties modeling of recycled aggregate concrete. *Construction and Building Materials* 24 (4): 421–430.

Bogue, R.H., 1947. The chemistry of Portland cement. Reinhold publishing corporation, New York, USA.

Bolouri Bazaz, J., Khayati, M., 2011. Properties and performance of concrete made with recycled low-quality crushed brick. *Journal of Materials in Civil Engineering* 24 (4): 330–338.

Bougara, A., Lynsdale, C., Milestone, N.B., 2010. Reactivity and performance of blastfurnace slags of differing origin. *Cement and Concrete Composites* 32 (4): 319–324.

Bravo, M., de Brito, J., Pontes, J., Evangelista, L., 2015. Mechanical performance of concrete made with aggregates from construction and demolition waste recycling plants. *Journal of Cleaner Production*.

Brown, P.W., Pommersheim, J., Frohnsdorff, G., 1985. A kinetic model for the hydration of tricalcium silicate. *Cement and Concrete Research* 15 (1): 35–41.

Bullard, J.W., Jennings, H.M., Livingston, R.A., Nonat, A., Scherer, G.W., Schweitzer, J.S., Scrivener, K.L., Thomas, J.J., 2011. Mechanisms of cement hydration. *Cement and Concrete Research*, Conferences Special: Cement Hydration Kinetics and Modeling, Quebec City, 2009 & CONMOD10, Lausanne, 2010 41 (12): 1208–1223.

Butler, L., West, J.S., Tighe, S.L., 2011. The effect of recycled concrete aggregate properties on the bond strength between RCA concrete and steel reinforcement. *Cement and Concrete Research* 41 (10): 1037–1049.

Buyle-Bodin, F., Hadjieva-Zaharieva, R., 2002. Influence of industrially produced recycled aggregates on flow properties of concrete. *Mat. Struct.* 35 (8): 504–509.

Cachim, P.., 2007. Concrete produced using crushed bricks as aggregate, in: Portugal Sb07-Sustainable Construction, Materials and Practices: Challenge of the Industry for the New Millennium. Lisbon, Portugal, 950–956.

Chen, H.J., Yen, T., Chen, K.H., 2003. Use of building rubbles as recycled aggregates. *Cement and Concrete Research* 33 (1): 125–132.

Choktaweekarn, P., Tangtermsirikul, S., 2010. Effect of aggregate type, casting, thickness and curing condition on restrained strain of mass concrete. *Sonklanakarin Journal of Science and Technology* 32 (4): 391.

D'Aloia, A., 2003. Early age kinetics: Activation energy, maturity and equivalent age, in: Early Age Cracking in Cementitious Systems - Report of RILEM Technical Committee 181-EAS - Early Age Shrinkage Induced Stresses and Cracking in Cementitious Systems. RILEM Publications SARL, 127–148.

De Belie, N., Grosse, C., Baert, G., 2008. Ultrasonic transmission to monitor setting and hardening of fly ash concrete. *ACI Materials Journal* 105 (3): 221–226.

De Belie, N., Grosse, C.U., Kurz, J., Reinhardt, H.-W., 2005. Ultrasound monitoring of the influence of different accelerating admixtures and cement types for shotcrete on setting and hardening behaviour. *Cement and Concrete Research* 35 (11): 2087–2094.

Debieb, F., Kenai, S., 2008. The use of coarse and fine crushed bricks as aggregate in concrete. *Construction and Building Materials* 22 (5): 886–893.

de Brito, J., Pereira, A.S., Correia, J.R., 2005. Mechanical behaviour of non-structural concrete made with recycled ceramic aggregates. *Cement and Concrete Composites* 27 (4): 429–433.

de Brito, J., Robles, R., 2010. Recycled aggregate concrete (RAC) methodology for estimating its long-term properties. *Indian Journal of Engineering & Materials Sciences* 17 (6): 449–462.

de Brito, J., Saikia, N., 2013. Recycled aggregate in concrete, Green Energy and Technology. Springer London, London.

De Schutter, G., Taerwe, L., 1995. General hydration model for portland cement and blast furnace slag cement. *Cement and Concrete Research* 25 (3): 593–604.

Douglas, E., Elola, A., Malhotra, V., 1990. Characterization of ground granulated blast-furnace slags and fly ashes and their hydration in Portland cement blends. *Cement, concrete and aggregates* 12 (1): 38–46.

Du, L., Folliard, K.J., 2005. Mechanisms of air entrainment in concrete. *Cement and Concrete Research* 35 (8): 1463–1471.

Elçi, H., 2015. Utilisation of crushed floor and wall tile wastes as aggregate in concrete production. *Journal of Cleaner Production* (In press): 10.1016/j.jclepro.2015.07.003.

Escalante-Garcia, J.-I., Sharp, J.H., 2004. The chemical composition and microstructure of hydration products in blended cements. *Cement and Concrete Composites*, Scanning electron microscopy of cements and concretes 26 (8): 967–976.

Escalante-García, J.I., Sharp, J.H., 1998. Effect of temperature on the hydration of the main clinker phases in portland cements: part ii, blended cements. *Cement and Concrete Research* 28 (9): 1259–1274.

Ferreira, L., de Brito, J., Barra, M., 2011. Influence of the pre-saturation of recycled coarse concrete aggregates on concrete properties. *Magazine of Concrete Research* 63 (8): 617–627.

Freiesleben Hansen, P., Pedersen, J., 1977. Maturity computer for controlled curing and hardening of concrete. *Nordisk Betong* 1: 19–34.

Gams, M., Trtnik, G., 2013. A new US procedure to determine setting period of cement pastes, mortars, and concretes. *Cement and Concrete Research* 53: 9–17.

García-González, J., Rodríguez-Robles, D., Juan-Valdés, A., Morán-del Pozo, J.M., Guerra-Romero, M.I., 2014. Pre-saturation technique of the recycled aggregates: solution to the water absorption drawback in the recycled concrete manufacture. *Materials* 7 (9): 6224–6236.

González-Fonteboa, B., 2002. Concrete with recycled aggregates from demolition works: Dosage, mechanical behaviour and shear performance [in Spanish]. Universidade da Coruña, A Coruña, Spain.

Grosse, C.U., Reinhardt, H.W., 2000. Ultrasound technique for quality control of cementitious materials. Presented at the Proceedings of the 15th Conference on Nondestructive Testing.

Grutzeck, M.W., Ramachandran, A.R., 1987. An integration of tricalcium silicate hydration models in light of recent data. *Cement and Concrete Research* 17 (1): 164–170.

Herb, A.T., 2003. Indirect monitoring of the setting and hardening of cement, mortar and concrete by acoustic wave propagation [in Dutch]. University of Stuttgart, Stuttgart, Germany.

Hewlett, P. (Ed.), 2003. Lea's chemistry of cement and concrete. Butterworth-Heinemann.

Hoffmann, C., Schubert, S., Leemann, A., Motavalli, M., 2012. Recycled concrete and mixed rubble as aggregates: Influence of variations in composition on the concrete properties and their use as structural material. *Construction and Building Materials* 35: 701–709.

Hwang, C.-L., Shen, D.-H., 1991. The effects of blast-furnace slag and fly ash on the hydration of portland cement. *Cement and Concrete Research* 21 (4): 410–425.

IPC, 2011. Physico-chemical characteristics: Linear thermal expansion. Spanish Institute for the promotion of ceramic materials (www.ipc.org.es), Valencia, Spain.

Ismail, S., Ramli, M., 2013. Engineering properties of treated recycled concrete aggregate (RCA) for structural applications. *Construction and Building Materials* 44: 464–476.

Ismail, S., Ramli, M., 2014. Effect of different moisture states of surface-treated recycled concrete aggregate on properties of fresh and hardened concrete. *International Journal of Civil, Architectural, Structural and Construction Engineering* 8: 65–71.

Jankovic, K., Nikolic, D., Bojovic, D., 2012. Concrete paving blocks and flags made with crushed brick as aggregate. *Construction and Building Materials* 28 (1): 659–663.

Jiménez Montoya, P., Arroyo Portero, J.C., Morán Cabré, F., García Meseguer, Á., 2009. Structutal concrete. Based on the Spanish Code on structural concrete EHE-08 and adaptated to the Eurocode EC-2 [in Spanish]. Cartoné, Madrid.

Jurič, B., Hanžič, L., Ilić, R., Samec, N., 2006. Utilization of municipal solid waste bottom ash and recycled aggregate in concrete. *Waste Management* 26 (12): 1436–1442.

Kamada, T., Uchida, S., Rokugo, K., 2005. Nondestructive Evaluation of Setting and Hardening of Cement Paste Based on Ultrasonic Propagation Characteristics. *Journal of Advanced Concrete Technology* 3 (3): 343–353.

Katz, A., 2003. Properties of concrete made with recycled aggregate from partially hydrated old concrete. *Cement and Concrete Research* 33 (5): 703–711.

Khalaf, F.M., 2006. Using crushed clay brick as coarse aggregate in concrete. *Journal of materials in civil engineering* 18 (4): 518–526.

Khalaf, F.M., DeVenny, A.S., 2005. Properties of new and recycled clay brick aggregates for use in concrete. *Journal of Materials in Civil Engineering* 17 (4): 456–464.

Khayat, K., 1999. Workability, testing, and performance of self-consolidating concrete. *ACI Materials Journal* 96 (3).

Kim, H.C., Yoon, S.S., 1988. Ultrasonic measurements during early-stage hydration of ordinary Portland cement. *J Mater Sci* 23 (2): 611–616.

Kim, M., Nam, S., Kim, J., 1993. An experimental study on the workability and engineering properties of recycled aggregate concrete according to the combination condition of recycled aggregate. *Journal of the Archichectural Institute of Korea* 9 (11): 109–120.

Kishi, T., Maekawa, K., 1995. Thermal and mechanical modelling of young concrete based on hydration process of multi-component cement minerals, in: RILEM PROCEEDINGS. CHAPMAN & HALL, 11–11.

Knaack, A.M., Kurama, Y.C., 2013. Design of concrete mixtures with recycled concrete aggregates. *ACI Materials Journal* 110 (5).

Kobayashi, S., Kawano, H., 1988. Properties and usage of recycled aggregate concrete, in: Proceedings of the Second International RILEM Symposium on Demolition and Reuse of Concrete and Masonry. Japan, 547–556.

Koenders, E.A.B., Pepe, M., Martinelli, E., 2014. Compressive strength and hydration processes of concrete with recycled aggregates. *Cement and Concrete Research* 56: 203–212.

Kosmatka, S.H., Panarese, W.C., Kerkhoff, B., 2002. Design and control of concrete mixtures. Portland Cement Association.

Kumar, P.R., Heeralal, M., Rao, Y.V., Rakesh, B., 2009. Strength and performance aspects of recycled aggregate for use in rigid pavements. *Journal of Environmental Research And Developmen* 4 (2): 449–464.

Lee, H.K., Lee, K.M., Kim, Y.H., Yim, H., Bae, D.B., 2004. Ultrasonic in-situ monitoring of setting process of high-performance concrete. *Cement and Concrete Research* 34 (4): 631–640.

Li, Z., 2011. Fresh Concrete, in: Advanced Concrete Technology. John Wiley & Sons, Inc., 94–139.

López-Gayarre, F., Serna, P., Domingo-Cabo, A., Serrano-López, M.A., López-Colina, C., 2009. Influence of recycled aggregate quality and proportioning criteria on recycled concrete properties. *Waste Management* 29 (12): 3022–3028.

Mansur, M.A., Wee, T.H., Lee, S.C., 1999. Crushed bricks as coarse aggregate for concrete. *ACI Materials Journal* 96 (4): 478–484.

Marmash, B., Elliott, K., 2000. The properties of recycled precast concrete hollow core slabs for use as replacement aggregate in concrete, in: G.R. Woolley, J.J.J.M.G. and P.J.W. (Ed.), Waste Management Series, Waste Materials in Construction Wascon 2000Proceedings of the International Conference on the Science and Engineering of Recycling for Environmental Protection, Harrogate, England 31 May, 1–2 June 2000. Elsevier, 769–781.

Martínez-Lage, I., Martínez-Abella, F., Vázquez-Herrero, C., Pérez-Ordóñez., J.L., 2012. Properties of plain concrete made with mixed recycled coarse aggregate. *Construction and Building Materials* 37: 171–176.

Mas, B., Cladera, A., Bestard, J., Muntaner, D., López, C.E., Piña, S., Prades, J., 2012a. Concrete with mixed recycled aggregates: Influence of the type of cement. *Construction and Building Materials* 34: 430–441.

Mas, B., Cladera, A., Olmo, T. del, Pitarch, F., 2012b. Influence of the amount of mixed recycled aggregates on the properties of concrete for non-structural use. *Construction and Building Materials* 27 (1): 612–622.

Matias, D., de Brito, J., Rosa, A., Pedro, D., 2013. Mechanical properties of concrete produced with recycled coarse aggregates – Influence of the use of superplasticizers. *Construction and Building Materials* 44: 101–109.

Medina, C., Zhu, W., Howind, T., Frías, M., Sánchez de Rojas, M.I., 2015. Effect of the constituents (asphalt, clay materials, floating particles and fines) of construction and demolition waste on the properties of recycled concretes. *Construction and Building Materials* 79: 22–33.

Medina, C., Zhu, W., Howind, T., Sánchez de Rojas, M.I., Frías, M., 2014. Influence of mixed recycled aggregate on the physical – mechanical properties of recycled concrete. *Journal of Cleaner Production* 68: 216–225.

Mefteh, H., Kebaïli, O., Oucief, H., Berredjem, L., Arabi, N., 2013. Influence of moisture conditioning of recycled aggregates on the properties of fresh and hardened concrete. *Journal of Cleaner Production* 54: 282–288.

Mielenz, R.C., Wolkodoff, V.E., Backstrom, J.E., Flack, H.L., 1958. Orgin, Evolution, and Effects of the Air Void System in Concrete. Part 1-Etrained Air in Unhardend Concrete. *ACI Journal Proceedings* 55 (7): 95–121.

Miličević, I., Bjegović, D., Siddique, R., 2015. Experimental research of concrete floor blocks with crushed bricks and tiles aggregate. *Construction and Building Materials* 94: 775–783.

Mostafa, N.Y., Brown, P.W., 2005. Heat of hydration of high reactive pozzolans in blended cements: Isothermal conduction calorimetry. *Thermochimica Acta* 435 (2): 162–167.

Mukhopadhyay, A.K., Neekhra, S., Zollinger, D.G., 2007. Preliminary characterization of aggregate coefficient of thermal expansion and gradation for paving concrete (Project 0-1700). Texas Transportation Institute, Texas, USA.

Nawy, E.G. (Ed.), 2008. Concrete construction engineering handbook. CRC press.

Netinger, I., Kesegic, I., Guljas, I., 2011. The effect of high temperatures on the mechanical properties of concrete made with different types of aggregates. *Fire Safety Journal* 46 (7): 425–430.

Neville, A.M., 1995. Properties of concrete. Harlow, Essex: Longman.

Nonat, A., Mutin, J.., 1992. From hydration to setting, in: Proceedings of the 2nd International RILEM Symposium on Hydration and Setting.

Olorunsogo, F.T., 1999. Early age properties of recycled aggregate concrete, in: Dhir, R.K. (Ed.), Exploiting Wastes in Concrete. Thomas Telford, 163–170.

Pepe, M., Koenders, E.A.B., Faella, C., Martinelli, E., 2014a. Structural concrete made with recycled aggregates: Hydration process and compressive strength models. *Mechanics Research Communications* 58: 139–145.

Pepe, M., Toledo Filho, R.D., Koenders, E.A.B., Martinelli, E., 2014b. Alternative processing procedures for recycled aggregates in structural concrete. *Construction and Building Materials* 69: 124–132.

Permanent Commission on Concrete, 2008. Code on structural concrete (EHE-08) [in Spanish]. Spanish Ministry of Public Works, Madrid.

Poon, C.S., Shui, Z.H., Lam, L., 2004a. Effect of microstructure of ITZ on compressive strength of concrete prepared with recycled aggregates. *Construction and Building Materials* 18 (6): 461–468.

Poon, C.S., Shui, Z.H., Lam, L., Fok, H., Kou, S.C., 2004b. Influence of moisture states of natural and recycled aggregates on the slump and compressive strength of concrete. *Cement and Concrete Research* 34 (1): 31–36.

Powers, T., 1932. Studies of workability of concrete, in: ACI Journal Proceedings. ACI, 419–448.

Powers, T.C., 1968. The properties of fresh concrete. John Wiley & Sons, New York, USA.

Qasrawi, H., Marie, I., 2013. Towards better understanding of concrete containing recycled concrete aggregate, towards better understanding of concrete containing recycled concrete aggregate. *Advances in Materials Science and Engineering, Advances in Materials Science and Engineering* 2013, 2013: e636034.

Rao, A., Jha, K.N., Misra, S., 2007. Use of aggregates from recycled construction and demolition waste in concrete. *Resources, Conservation and Recycling* 50 (1): 71–81.

Reinhardt, H.W., Grosse, C.U., 2004. Continuous monitoring of setting and hardening of mortar and concrete. *Construction and Building Materials* 18 (3): 145–154.

RILEM TC 119-TCE, 1997. TCE1: Adiabatic and semi-adiabatic calorimetry to determine the temperature increase in concrete due to hydration heat of the cement. *Mat. Struct.* 30 (8): 451–464.

RILEM TC 185-ATC, 2005. Advanced Testing of Cement-Based Materials during Setting and Hardening. RILEM Publications.

Robeyst, N., 2009. Monitoring setting and microstructure development in fresh concrete with the ultrasonic through-transmission method. Ghent University, Ghent, Belgium.

Robeyst, N., Grosse, C.U., De Belie, N., 2009. Monitoring fresh concrete by ultrasonic transmission measurements: Exploratory multi-way analysis of the spectral information. *Chemometrics and Intelligent Laboratory Systems* 95 (1): 64–73.

Robeyst, N., Gruyaert, E., Grosse, C.U., De Belie, N., 2008. Monitoring the setting of concrete containing blast-furnace slag by measuring the ultrasonic p-wave velocity. *Cement and Concrete Research* 38 (10): 1169–1176.

Rupnow, T.D., Wang, K., Schaefer, V.R., Tikalsky, P., 2011. A simple method for characterizing and predicting temperature behavior of ternary cementitious systems. *Construction and Building Materials* 25 (5): 2290–2297.

Sadek, D.M., 2012. Physico-mechanical properties of solid cement bricks containing recycled aggregates. *Journal of Advanced Research* 3 (3): 253–260.

Sagoe-Crentsil, K., Brown, T., 1998. Guide for specification of recycled concrete aggregates (RCA) for concrete production. EcoRecycled Victoria, CSIRO, Building Construction and Engineering, Victoria, Australia.

Sánchez de Juan, M., 2004. Study on the use of recycled aggregate in structural concrete [in Spanish]. E.T.S.I. Caminos, Canales y Puertos (UPM), Madrid, Spain.

Sandberg, J., Liberman, S., 2007. Monitoring and evaluation of cement hydration by semi-adiabatic field calorimetry. *ACI Special Publication* 241: 13–24.

Schindler, A.K., Folliard, K.J., 2003. Influence of supplementary cementing materials on the heat of hydration of concrete, in: Advances in Cement and Concrete IX Conference, Copper Mountain Conference Resort in Colorado.

Schwerin, D.E., Cavalline, T.L., Weggel, D.C., 2013. Use of recycled brick masonry aggregate and recycled brick masonry aggregate concrete in sustainable construction. *Journal of Construction Engineering and Project Management* 3 (1): 28–34.

Sheen, Y.-N., Wang, H.-Y., Juang, Y.-P., Le, D.-H., 2013. Assessment on the engineering properties of ready-mixed concrete using recycled aggregates. *Construction and Building Materials* 45: 298–305.

Singh, N.B., Bhattacharjee, K.N., Shukla, A.K., 1995. Hydration of portland blended cements. *Cement and Concrete Research* 25 (5): 1023–1030.

Soroka, I., 2003. Concrete in hot environments. CRC Press.

Struble, L.J., Chung, C.W., Suraneni, P., Popovics, J.S., Shah, S., Chen, C.T., Zhang, H., 2010. Characterization of setting, in: 7th International Symposium on Cement & Concrete, The Chinese Ceramic Society, St. Louis.

Sukontasukkul, P., Sanpetch, B., Songpiriyakit, S., 2012. Use of Ultrasonic Pulse to Monitor Setting Process in Concrete: Effect of Aggregate Size and Content. *The Journal of KMUTNB* 22 (1): 491–497.

Tabsh, S.W., Abdelfatah, A.S., 2009. Influence of recycled concrete aggregates on strength properties of concrete. *Construction and Building Materials* 23 (2): 1163–1167.

Taylor, H.F., 1997. Cement chemistry. Thomas Telford.

Topçu, İ.B., Canbaz, M., 2004. Properties of concrete containing waste glass. *Cement and Concrete Research* 34 (2): 267–274.

Trtnik, G., Gams, M., 2013. The use of frequency spectrum of ultrasonic P-waves to monitor the setting process of cement pastes. *Cement and Concrete Research* 43: 1–11.

Trtnik, G., Gams, M., 2014. Recent advances of ultrasonic testing of cement based materials at early ages. *Ultrasonics* 54 (1): 66–75.

Trtnik, G., Kavcic, F., Turk, G., 2009. Prediction of concrete strength using ultrasonic pulse velocity and artificial neural networks. *Ultrasonics* 49 (1): 53–60.

Trtnik, G., Turk, G., Kavčič, F., Bosiljkov, V.B., 2008. Possibilities of using the ultrasonic wave transmission method to estimate initial setting time of cement paste. *Cement and Concrete Research* 38 (11): 1336–1342.

UNE EN 196-3, 2009. Methods of testing cement. Part 3: Determination of setting times and soundness. AENOR, Madrid, Spain.

Vahedifard, F., Nili, M., Meehan, C.L., 2010. Assessing the effects of supplementary cementitious materials on the performance of low-cement roller compacted concrete pavement. *Construction and Building Materials* 24 (12): 2528–2535.

Van der Winden, N.G.B., 1990. Ultrasonic measurement for setting control of concrete, in: Proceeding of the International Workshop on Testing during Concrete Construction. Mainz, Germany, 122–137.

Voigt, T., Grosse, C.U., Sun, Z., Shah, S.P., Reinhardt, H.-W., 2005. Comparison of ultrasonic wave transmission and reflection measurements with P- and S-waves on early age mortar and concrete. *Mat. Struct.* 38 (8): 729–738.

Waller, V., D'Aloia, L., Cussigh, F., Lecrux, S., 2004. Using the maturity method in concrete cracking control at early ages. *Cement and Concrete Composites* 26 (5): 589–599.

Wang, K., Ge, Z., Grove, J., Ruiz, J.M., Rasmussen, R.O., 2006. Developing a simple and rapid test for monitoring the heat evolution of concrete mixtures for both laboratory and field applications. Federal Highway Administration and Iowa State University, Iowa, USA.

Wang, K., Ruiz, J.M., Hu, J., Ge, Z., Xu, Q., Grove, J., Rasmussen, R., 2008. Developing a simple and rapid test for monitoring the heat evolution of concrete mixtures for both laboratory and field applications-phase III (FHWA DTFH-61-06-H-00011). National Concrete Pavement Technology Center Iowa State University.

Weakley, R., 2010. Evaluation of Semi-Adiabatic Calorimetry to Quantify Concrete Setting (thesis).

Weiss, W., Yang, W., Shah, S., 2000. Factors influencing durability and early-age cracking in high-strength concrete structures. *ACI Special Publication* 189: 387–410.

Working group 2/5, 2006. Use of recycled aggregates in the manufacture of structural concrete [in Spanish] (No. M-11). ACHE, Madrid, Spain.

Xiao, Z., Ling, T.C., Kou, S.C., Wang, Q., Poon, C.S., 2011. Use of wastes derived from earthquakes for the production of concrete masonry partition wall blocks. *Waste Management* 31 (8): 1859–1866.

Yang, J., Du, Q., Bao, Y., 2011. Concrete with recycled concrete aggregate and crushed clay bricks. *Construction and Building Materials* 25 (4): 1935–1945.

Yang, K., Kim, Y., 2005. An evaluation of slump loss for elapsed time and mechanical behavior of the recycled aggregate concrete mixed with blast furnace slag. *Journal of the Archichectural Institute of Korea* 21 (4): 117–124.

Ye, G., 2003. Experimental study and numerical simulation of the development of the microstructure and permeability of cementitious materials. Delft University, Netherlands.

Ye, G., Lura, P., van Breugel, K., Fraaij, A.L.A., 2004. Study on the development of the microstructure in cement-based materials by means of numerical simulation and ultrasonic pulse velocity measurement. *Cement and Concrete Composites* 26 (5): 491–497.

Zaharieva, R., Buyle-Bodin, F., Skoczylas, F., Wirquin, E., 2003. Assessment of the surface permeation properties of recycled aggregate concrete. *Cement and Concrete Composites* 25 (2): 223–232.

Zhang, S., Zong, L., 2014. Properties of concrete made with recycled coarse aggregate from waste brick. *Environ. Prog. Sustainable Energy* 33 (4): 1283–1289.

Zhang, W., Zhang, Y., Liu, L., Zhang, G., Liu, Z., 2012. Investigation of the influence of curing temperature and silica fume content on setting and hardening process of the blended cement paste by an improved ultrasonic apparatus. *Construction and Building Materials* 33: 32–40.

Chapter 7

Microstructure

1. INTRODUCTION

The structure of concrete is defined by the type, amount, size, shape and distribution of its different phases. Figure 7.1 illustrates the multiscale nature of the structure of concrete. At macrostructural level, concrete is composed of a binding medium (mortar) within which coarse aggregates are embedded. Nonetheless, a more detailed definition of the concrete structure is possible whenever magnified under an optical microscope. Finally by means of SEM analysis, the microstructure of concrete becomes apparent and hydration products, unhydrated cement and a porous network can be identified within the cement paste.

Nowadays it is widely recognised that the properties of a material emanate from its internal structure. Thus, the knowledge of the microstructure of concrete is essential to better understand the mechanical and durability behaviour of an engineering material, and especially important for a concrete mixture since its structure does not remain stable but evolves with time due to the hydration process and the exposure to environmental agents.

Hence, in this chapter the analysis of the microstructure of the conventional and recycled mixtures will be discussed. The influence of the replacement of the natural coarse aggregates with recycled aggregates derived from CDW with variable percentages of ceramic wastes on the interfacial transition zone (ITZ) and the porous network of the concrete microstructure will be the main focus of the research.

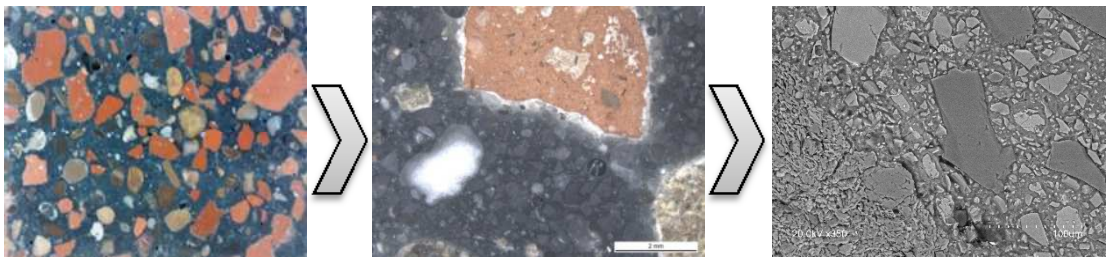

Naked eye
Concrete=coarse aggregates
+ mortar

Optical microscope
Concrete=coarse aggregates +
sand + cement paste

Scanning electron microscope
Concrete=coarse aggregates
+ sand + products of hydration
+ voids

Figure 7.1: Structure of concrete at different levels

2. MICROSTRUCTURE: SOLID PHASES

Although the development of the microstructure of concrete varies with the chemistry and fineness of the cement, the water/cement ratio, the use of admixtures, the mixing procedures, the curing temperature and variations in the hydration conditions (Diamond, 2004), a general model for the hydration process of cement particles could be assumed.

According to Nonat and Mutin (1992), after mixing, the anhydrous cement grains are dispersed in the water resulting in a partial solution of the cement minerals. Initially, the coagulation is hindered by electrostatic repulsion, but this phenomenon is progressively reduced with the progressing of the chemical reactions comprising the hydration process which eventually leads to the coagulation of the cement grains. Afterwards, the precipitation of hydration products in the space originally occupied by the aqueous phase around the coagulated cement grains, binds them together forming a denser and more rigid structure as the hydration process progresses. At macro scale, this phenomenon is observed by the development of the strength, hardness, stiffness and permeability of the concrete mixture (Van Breugel, 1991).

Figure 7.2 illustrates the schematic representation of the sequence of microstructure formation as proposed by Locher et al. (1976). While alite (C_3S) does not start to react after the dormant stage, aluminate (C_3A) is the most active phase during the first stage of hydration. Figure 7.2a represents the formation of ettringite (small needles) and portlandite (hexagonal crystals) respectively at the surface and in the surroundings of the cement grain at early ages. As the time passes, the ettringite needles continue to grow and bridge the interparticle spaces (Figure 7.2b) until a basic skeleton is established after 7-28 days of curing (Figure 7.2c). The hydration continues to evolve (Figure 7.2d) and new solid products are formed in the spatial network originally built up by the ettringite needles.

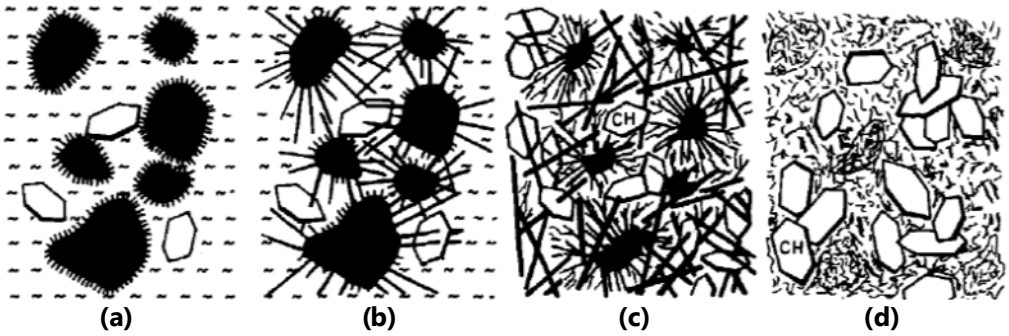

Figure 7.2: Formation of the concrete structure. Plastic phase (a), setting stage (b), basic skeleton (c) and stable skeleton (d) (Locher et al., 1976)

It is worth mentioning that an area exists within the hardened cement paste in the vicinity of the aggregates in which the hydration process presents some singularities, which is known as interfacial transition zone (ITZ). The origin of the ITZ lies within the denominated wall effect (Scrivener et al., 2004), since in the mixing process the random placing of the aggregates disrupts the normal packing of the cement grains resulting in a zone closer to the aggregates with higher porosity and small cement particles, which in turn create an adjacent zone depleted of small grains (Figure 7.3).

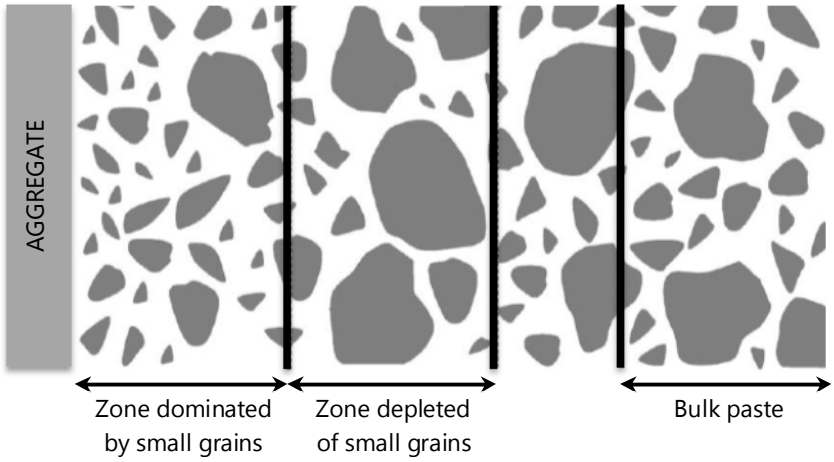

Figure 7.3: The wall effect and the grading of cement grains in the ITZ. After Scrivener et al. (2004)

In addition, the formation of a water film around the coarse aggregates leads to a higher water/cement ratio in the zone, which in combination with the presence of the smaller cement grains leads to a faster hydration process and lower amount of unreacted cement grains (Scrivener et al., 2004; Li, 2011). Hence, the mineralogical development is more propitious towards the aggregates (Carles-Gibergues et al., 1993) that act as a nucleation site for the C-S-H gel, which directly precipitates at the interface in early ages of the hydration process (Scrivener and Pratt, 1984), and a higher proliferation of CH crystals is seen (Scrivener et al., 2004). Moreover, the portlandite appears orientated in perpendicular layers to the surface of the aggregates due to the presence of water films (Ollivier et al., 1995; Prokopski and Halbiniak, 2000; Li, 2011). Finally, the mobility of ions through the zone is also accountable for the different microstructure of the ITZ.

For instance, the high mobility of ions forming ettringite enables the increasing amount of the AFt phase in the ITZ (Monteiro and Mehta, 1985; Scrivener and Nemati, 1996; Scrivener et al., 2004). And lately, the inert nature of the aggregates has been questioned due to the capability of aggregates to leach ions that modify the microstructure of the ITZ (Tasong et al., 1998, 1999).

Despite the schematic representation shown in Figure 7.3, there is no discrete boundary separating the ITZ and the bulk cement paste, although values ranging between 20 μm and 50 μm are generally accepted to describe the ITZ thickness (Langton et al., 1980; Scrivener et al., 2004). As the described mineralogical growth is intrinsically associated to the development of the porous structure, ITZ present an excess in porosity as well as a particular structure (composition, density and morphology) that influence the mechanical and durability properties of the concrete at macro scale (Maso, 1980; Mindess et al., 1986; Scrivener et al., 2004).

Since the ITZ is the bridge between the cement paste and the aggregates comprising the concrete, its properties are affected by factors relating to both constituents such as the water/cement ratio, the hydration age, the fineness of cement, the aggregate size and type (RILEM TC 108-ICC, 1996; Tasong et al., 1999; Elsharief et al., 2003). In terms of the effect of the cementitious materials, a higher water/cement ratio increases the porosity (Maso, 1980; Gao et al., 2014), the ITZ thickness decreases with the hydration age (Maso, 1980) and the use of finer particles like silica fume reduces the porosity as well as the thickness of the ITZ (Katz, 2004; Xiao et al., 2013).

Regarding to the aggregate, it has been reported that the particle size does not have a definitive impact on the ITZ thickness (Ping et al., 1991; Elsharief et al., 2003), while the increase of the amount of aggregate reduces the ITZ transport properties by enhancement of its structure (Delagrave et al., 1997; Gao et al., 2013, 2014) and the type of aggregate influences the bond with the cement paste since the surface roughness, the rock structure and strength determine the characteristics of the ITZ (Tasong et al., 1999) and some types react affecting the ITZ (Tasong et al., 1998, 1999). However, special attention should be paid when using recycled aggregates, because their high porosity values and the presence of the old ITZ produce weaker ITZ in recycled concretes. On one hand, the higher porosity of the recycled aggregate is accountable for a high ITZ porosity in recycled concrete (Poon et al., 2004; Etxeberria et al., 2006). On the other hand, part of the new ITZ would be formed between the old adhered mortar and the new cement paste. The last investigations comparing both ITZ have shown that the new ITZ is slightly wider and has a modulus of elasticity around 10% higher (Xiao et al., 2013), mainly because the stiffness of the old ITZ was compromised during the recycling procedure (Nagataki et al., 2004; Lee and Choi, 2013). Furthermore, by comparing the new ITZ formed in recycled concretes and that of conventional concretes, a different crystallization becomes apparent. The new ITZ around particles with adhered mortar results in higher CH content in the pores and the surface of the recycled aggregate (Kong et al., 2010) accompanied by a high content of sulphoaluminate crystals (Sidorova et al. 2014), while the interface around ceramic particles will also present a C-S-H nucleus (Sidorova et al. 2014).

Finally, the concrete production also influences the ITZ properties. Hence, some researchers (Diamond and Huang, 2001; Diamond, 2004) argue that if bleeding is eliminated by means of a proper mixing, hardly any microstructural changes could be detected throughout the bulk paste, and thus they oppose the ITZ concept. Nonetheless, provided the existence of a transition zone, the compaction and the mixing approach have been mentioned as factors controlling the ITZ. Leeman et al. (2006) concluded that when concrete was vibrated higher values of both porosity and width were determined in the ITZ when compared to self-compacting concrete. The burgeoning use of recycled aggregates in the concrete manufacture has promoted the investigation about the impact that the mixing approach has on the ITZ. Results show that varying the order of mixing could partly control the absorption capacity of the recycled aggregates (Etxeberria et al., 2006). The two-stage mixing approach (TSMA) and the triple mixing method (TM) prevail among these investigations. According to Tam et al. (2005), the use of half of the required water in the first stage of the TMSA creates a slurry around the recycled aggregates able to permeate in the attached mortar of the recycled aggregates filling their cracks and pores and thus enhancing the ITZ. Later on, Kong et al. (2006) proposed the TM that in addition of the fraction addition of the mixing water also involves the coating of the recycled aggregates with admixtures (fly ash, slag and silica fume) in order to achieve a filler effect and a pozzolanic reaction to strengthen the microstructure of the ITZ.

2.1. CHEMICAL REACTIONS

Mixing cement with water triggers a number of complex chemical and physical reactions as part of the hydration process. When blast furnace cements are employed, the hydration process is even more complex as the two constituents, i.e. blast furnace slag and Portland cement, hydrate simultaneously but at different rates depending on the water/cement ratio, the temperature, the fineness and the reactivity of slag (Chen, 2006).

Portland cement is comprised of alite (C_3S), belite (C_2S), aluminate (C_3A) and ferrite (C_4AF). The hydration of the tricalcium and dicalcium silicates results in an exothermic reaction that produces calcium silicate hydrate ($C_3S_2H_3$) and calcium hydroxide (CH), also known as portlandite as per Eq. (7.1) and (7.2) (Robeyst, 2009). Since the calcium silicate hydrates do not have a well-defined composition, it is usually referred to as C-S-H and normally characterized by its C/S ratio.

$$2{\cdot}C_3S+6{\cdot}H\rightarrow C_3S_2H_3+3{\cdot}CH \quad (7.1)$$

$$2{\cdot}C_2S+4{\cdot}H\rightarrow C_3S_2H_3+CH \quad (7.2)$$

To avoid the violent reaction of the tricalcium aluminate (C_3A) with water, gypsum ($C\bar{S}H_2$) is added as setting regulator (Neville, 1995). Thus, the aluminate reacts in the presence of water with the gypsum to produce ettringite ($C_6A\bar{S}_3H_{32}$ or AFt) (Eq. (7.3)). Once all the gypsum is consumed, the ettringite reacts with the remaining aluminate to form crystals of monosulfate aluminate hydrate ($C_4A\bar{S}H_{12}$ or AFm) (Ye, 2003) as indicated in Eq. (7.4). Since the monosulphate is about 2.50 times smaller (Jons and Osbaeck, 1982), the conversion is associated to volume changes impacting on the strength of the paste. In addition, the presence of CH produced during the alite and belite hydration influences the reactions of the aluminate with water producing tetracalcium aluminate hydrate (C_4AH_{13}) (Brouwers, 2005), as shown in Eq. (7.5).

$$C_3A+3C\bar{S}H_2+26\cdot H\rightarrow C_6A\bar{S}_3H_{32} \quad (7.3)$$
$$2\cdot C_3A+C_6A\bar{S}_3H_{32}+4\cdot H\rightarrow 3\cdot C_4A\bar{S}H_{12} \quad (7.4)$$
$$C_3A+CH+12\cdot H\rightarrow C_4AH_{13} \quad (7.5)$$

Finally, the ferrite (C_4AF) reacts with the alite (C_3S) and belite (C_2S), producing hydrogarnet ($C_6AFS_2H_8$), as indicated in Eq. (7.6) and (7.7) (Brouwers, 2005).

$$C_4AF+2\cdot C_3S+12\cdot H\rightarrow C_6AFS_2H_8+4\cdot CH \quad (7.6)$$
$$C_4AF+2\cdot C_2S+10\cdot H\rightarrow C_6AFS_2H_8+2\cdot CH \quad (7.7)$$

Regarding to the slag hydration, it is worth mentioning that the reaction depends on the reactivity of the slag, usually being faster at early ages (Chen, 2006). The main hydration products are CS(A)H, hydrotalcite (M_5AH_{13} according to Chen and Brouwers (2007)) and ettringite ($C_6A\bar{S}_3H_{32}$). In minor amounts, iron-containing hydrogarnet ($C_6AFS_2H_8$), tetracalcium aluminate hydrate (C_4AH_{13}) and strätlingite (C_2ASH_8) could also be detected (Chen and Brouwers, 2007; Meinhard and Lackner, 2008). A general expression for the reaction is given in Eq. (7.8) (Gruyaert, 2011).

$$C,S,A,M,\bar{S},F+H\rightarrow CS(A)H+M_5AH_{13}+C_6AFS_2H_8+C_6A\bar{S}_3H_{32}+C_2ASH_8+C_4AH_{13} \quad (7.8)$$

Furthermore, both hydration processes are influenced by each other, as the alkalis and CH produced in the hydration of the Portland cement act as a activators for the slag hydration (Neville, 1995; Hewlett, 2003) and the CH is consumed during the slag hydration since it also acts as a reactant in the formation of secondary C-S-H gel (Chen, 2006) due to its pozzolanic characteristics (reaction with lime) (Taylor, 1997; Escalante-García and Sharp, 1998). Therefore, the hydration products from both hydration reactions are formed, being C-S-H the most abundant product, although with a lower C/S ratio due to the CH consumption (Richardson and Groves, 1992; Chen and Brouwers, 2007) and higher A/S ratio (Richardson and Groves, 1992). In summary, the main hydration products of blast furnace cements are C-S-H, CS(A)H, CH, hydrotalcite (M_5AH_{13}), ettringite ($C_6A\bar{S}_3H_{32}$) and tetracalcium aluminate hydrate (C_4AH_{13}).

2.2. MORPHOLOGY

The study of the microstructure of concrete has led to the morphological identification of the different hydration products by means of scanning or transmission electron microscope (SEM and TEM respectively). Several factors such as the chemical composition of the cement, the presence of gypsum and additives, the degree of hydration, the water/cement ratio, the curing temperature and the external pressure are liable for their shape and size (Van Breugel, 1991).

Although, in general terms, the morphology of the different hydration products is similar in both Portland cement and Portland slag cement pastes, some differences have been identified regarding the C-S-H gel morphology. Generally, the C-S-H gel is the main product and appears around unhydrated cement cores. For Portland cement pastes, a plethora of morphologies have been used to describe the morphology of C-S-H gels, a fact that could be partly explained by the findings of Diamond (1986) who observed morphological changes along the development of the hydration. Thus, four different C-S-H formations were identified: elongated fibres corresponding

to early ages (type I), subsequently honeycombs or reticular networks presenting branches (type II), tightly packed equi-dimensional grains in older pastes (type III), and finally massive and featureless inner products (type IV). The main morphological difference between Portland cement and Portland slag blended cements pastes is that the C-S-H gel is more foil-like instead of fibrillary with increasing slag content, being the limitation of space the responsible for a finer or coarse hydration product (Richardson and Groves, 1992; Chen, 2006). It has been suggested that this fibrillar disposition is liable for the improvement of the slag on the diffusion rates of concrete mixtures (Page et al., 1981).

Despite that a low presence of CH phase is observed due to its role as a reactant in the slag hydration, the portlandite appears as hexagonal plate crystals and tends to form in large voids around big unhydrated cement cores (Ye, 2003). According to Diamond (1986), these crystals become larger than CSH particles when in the vicinity of the surface of aggregates. Nonetheless for recycled aggregates (concrete or ceramic), the findings of Sidorova et al. (2014) suggest that the portlandite will appear as badly-formed crystals in thin layers.

Ettringite crystallizes as slender needles without branches. According to Richardson and Groves (1992), the formation of both aluminate hydrates (AFt and AFm) in cement pastes with slag is identical of that in pure Portland cement pastes, although some compositional changes could be detected on the AFm phase. Similarly, hydrogarnet particles detected in Portland cement and Portland slag cement pastes present a small, almost round, poorly crystalline morphology with a rich iron and aluminium chemical composition (Richardson and Groves, 1992). Furthermore, when recycled aggregates are used the sulphoaluminate crystals develop a whisker-like (Poon et al., 2004) or acicular (Sidorova et al. 2014) morphology.

Finally, except when the concrete is subjected to a long period of extensive leaching, amorphous residual unhydrated cement particles are to be identified in the SEM observations, being easily identified as brighter areas (practically fully white) in back-scattered mode (Diamond, 2004).

2.3. SCANNING ELECTRON MICROSCOPY

The morphology of the microstructure has typically been investigated by means of a scanning electron microscope, because the direct observation of the back-scatter images allows the identification of the different phases based on their relative value on the grey-scale as well as the ITZ surrounding the aggregates. Although the ITZ constitutes a narrow zone around the aggregates (20 μm to 50 μm), it has been estimated that it accounts for 20% to 40% of the total volume of the cement paste (Mindess et al., 2002). Therefore, in this research work, the SEM examinations were focused on the effects that the replacement of natural coarse aggregates with recycled aggregates from CDW with varying percentages of ceramic wastes has on the matrix-coarse aggregate interfacial regions.

Figure 7.4 presents the general evolution of the microstructure of the concrete mixtures studied in phase I at 28, 56 and 90 days of curing.

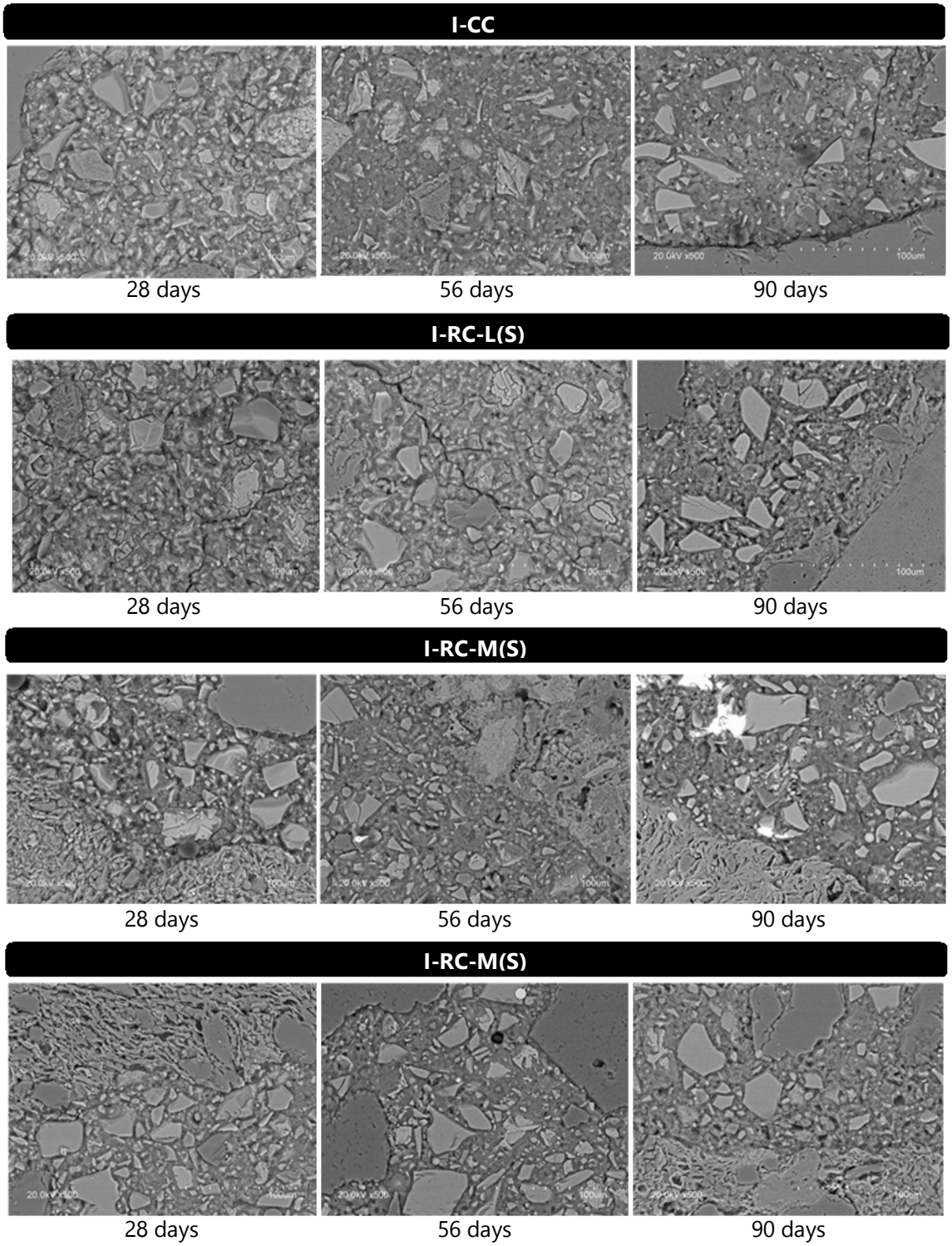

Figure 7.4: Evolution of microstructure of the concrete mixtures in phase I

At first glance, a large number of unreacted slag particles can be observed for all mixtures after 90 days of curing. Nonetheless, this behaviour is in agreement with the slow hydration process commonly identified in slag blended concretes (Tanaka et al., 1983). Contrarily, it is also possible to observe darker rims around some of the slag particles, which are mostly comprised of MgO, as a result of their hydration.

Despite the presence of some micro-cracks in both the conventional and recycled concrete mixtures, the fracture zones remain empty which suggests the lack of any alkali-silica reaction due to the incorporation of recycled aggregates. Nevertheless, a more detailed study in this regard could be consulted in chapter 9.

Similarly to the results obtained in the investigations of Etxeberria et al. (2006) and Medina et al. (2015), the interfaces observed between concrete and ceramic recycled aggregates with the cement matrix were fairly dense and continuous comparable to those observed for the natural aggregate (Figure 7.11, Figure 7.13, Figure 7.15, Figure 7.17, Figure 7.19, Figure 7.21, Figure 7.23, Figure 7.25 and Figure 7.27). The good quality of ITZ is also due to the lower effective water/cement ratio, the internal curing effect produced as the recycled aggregates return part of the water absorbed to the cement matrix, the use of a blended slag cement and the additional pozzolanic activity of the recycled aggregates, especially in its superficial zone due to the presence of CDW fines (Medina et al., 2015), which resulted in hydration products filling the interfacial bond between the aggregates and the cement. This improvement effect of the recycled aggregates in the ITZ was also observed by other researchers (Poon et al., 2004; Corinaldesi and Moriconi, 2009; Li et al., 2009; Li and Zhang, 2013).

Researchers also found that the surface textures of the aggregates have great influences on ITZ properties (Tasong et al., 1999). Compared to the river gravel, recycled aggregates present a more porous and rough surface that can account for a stronger and thinner ITZ. Senthamarai et al. (2011) also appreciated this beneficial effect due to the incorporation of ceramic aggregates derived from electrical insulators. In addition, according to Bentur and Alexander (2000), the improvement of the ITZ is also due to the sharper outlines of the recycled aggregates. Therefore, the incorporation of recycled aggregates from CDW with varying ceramic contents was not detrimental to the microstructural morphology of the recycled concretes.

2.3.1. CONCRETE MIXTURE I-CC

A more detailed inspection of the microstructure of the conventional concrete mixture can be observed in Figure 7.5, Figure 7.7 and Figure 7.9 that include the micrographs obtained by the EDS analysis of the natural coarse aggregates (NA) and the cement paste (P) at 28, 56 and 90 days of curing. In addition, Figure 7.6, Figure 7.8 and Figure 7.9 illustrate the distribution density of the chemical elements in the aforementioned areas by means of a mapping scan.

In the first place, the results obtained for the analysis of the natural aggregate show a pure siliceous aggregate, which is in consonance with the previous analysis performed on the aggregate (see chapter 4). As this pattern was unaltered for all natural coarse aggregates evaluated, both in the conventional and recycled mixtures, no more micrographs were included in this regard.

In terms of the cement paste, calcium and silicon are the major elements but, since the cement incorporated blast furnace slag, significant amounts of elements such as magnesium and aluminium were also identified. In addition, the presence of sulphur originated from the retardant compound used in the cement. The Ca/Si ratio ranged between 1.74 and 2.22, which lies within the interval for conventional mixtures proposed by other researchers (Taylor, 1997; Hewlett, 2003). In general, the higher values corresponded to cement paste in the surroundings of portlandite or anhydrous C_3S particles.

Regarding to the distribution of the elements, silicon can be observed both in the aggregate and the cement paste, whereas the presence of calcium was limited to the cement paste. As previously mentioned, the magnesium and aluminium are good markers for the presence of slag.

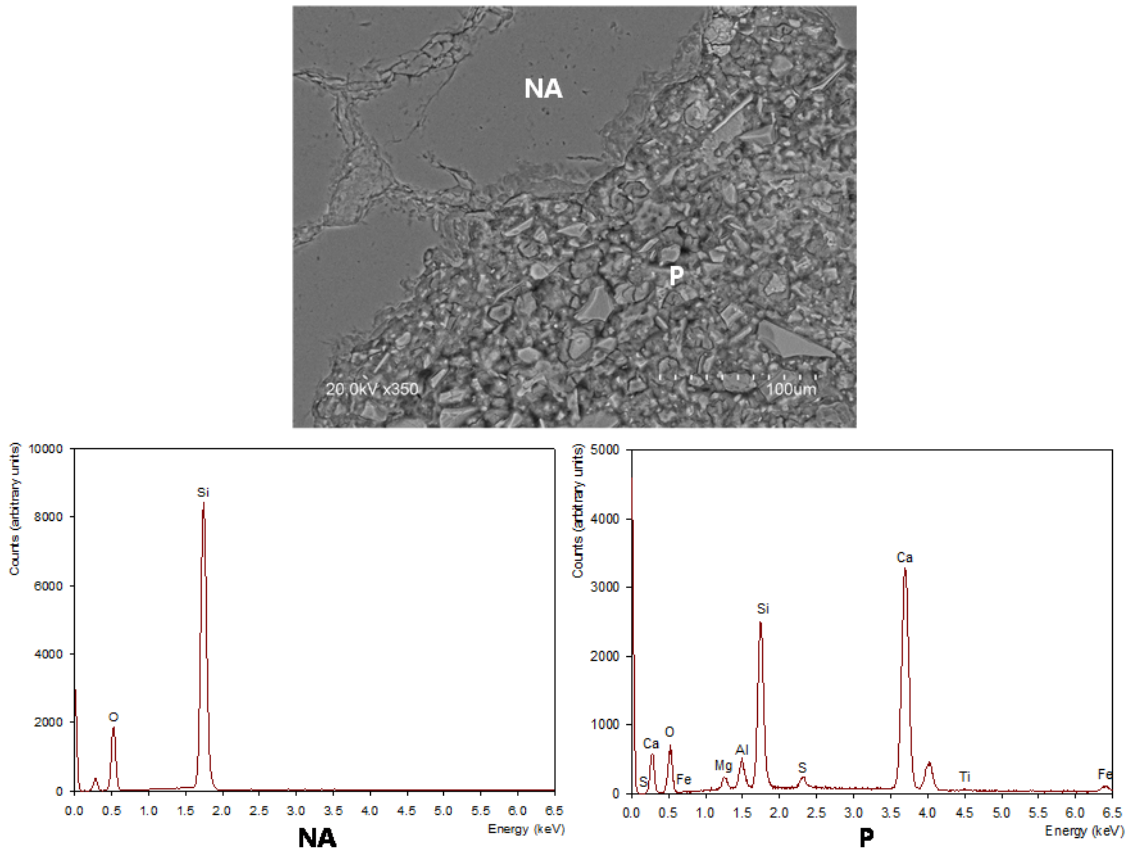

Figure 7.5: Micrograph of the ITZ of I-CC at 28 days

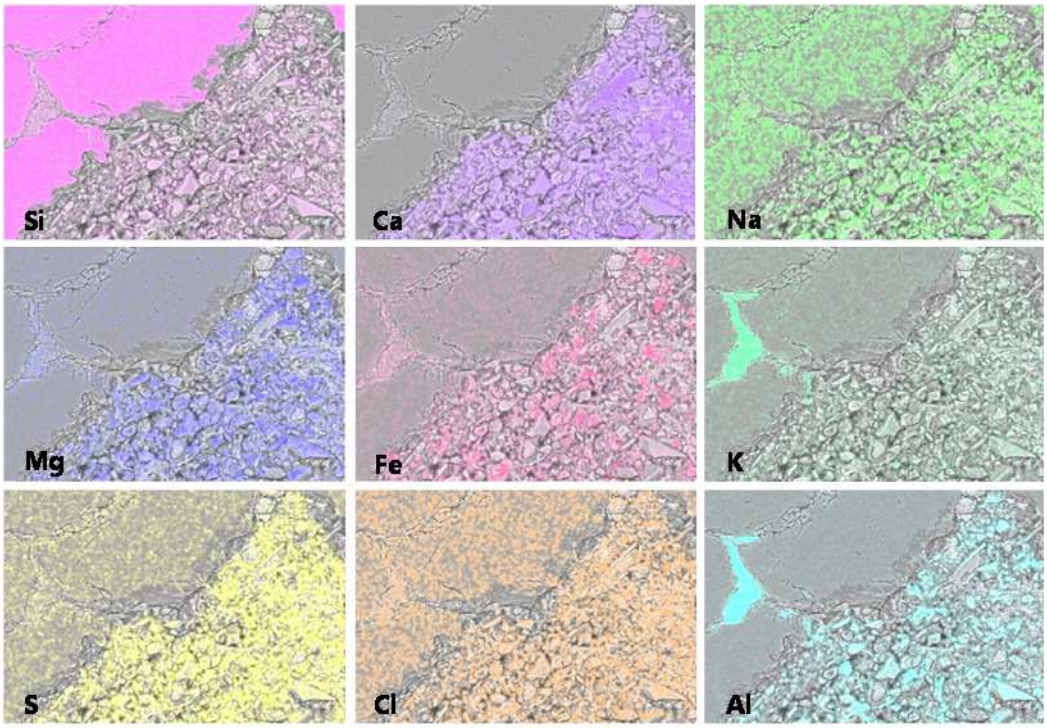

Figure 7.6: Mapping of the ITZ of I-CC at 28 days

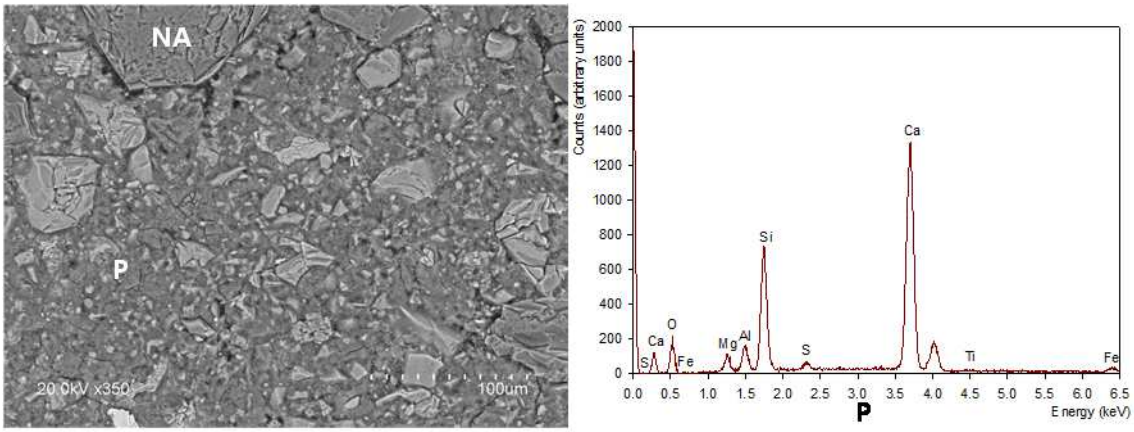

Figure 7.7: Micrograph of the ITZ of I-CC at 56 days

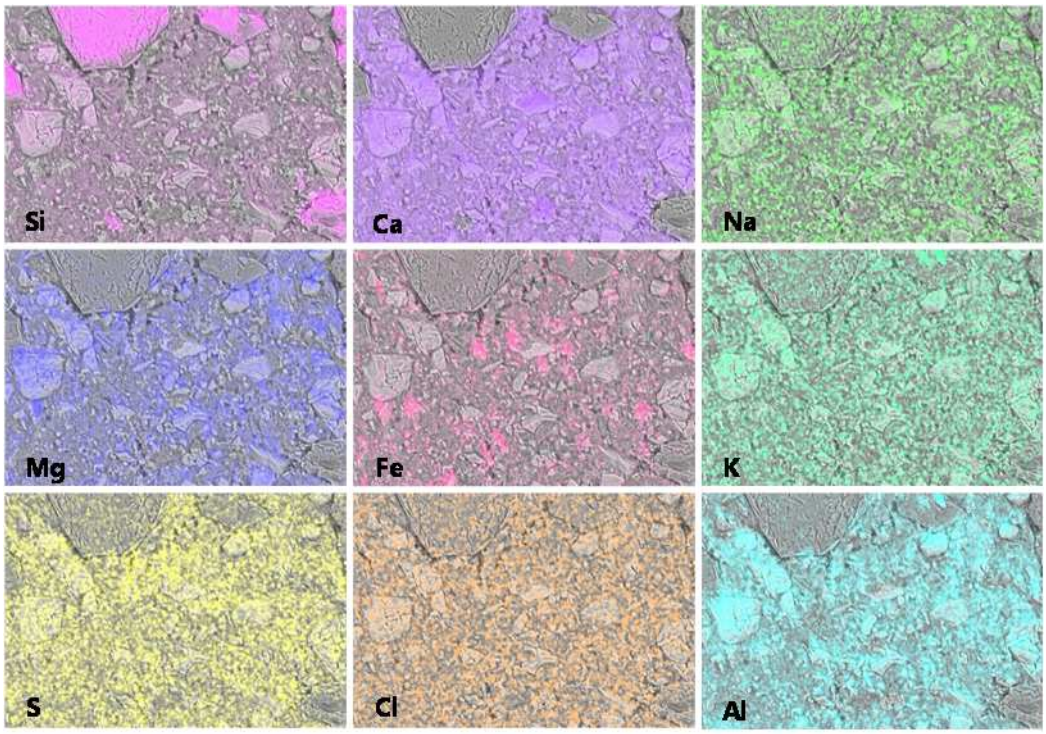

Figure 7.8: Mapping of the ITZ of I-CC at 56 days

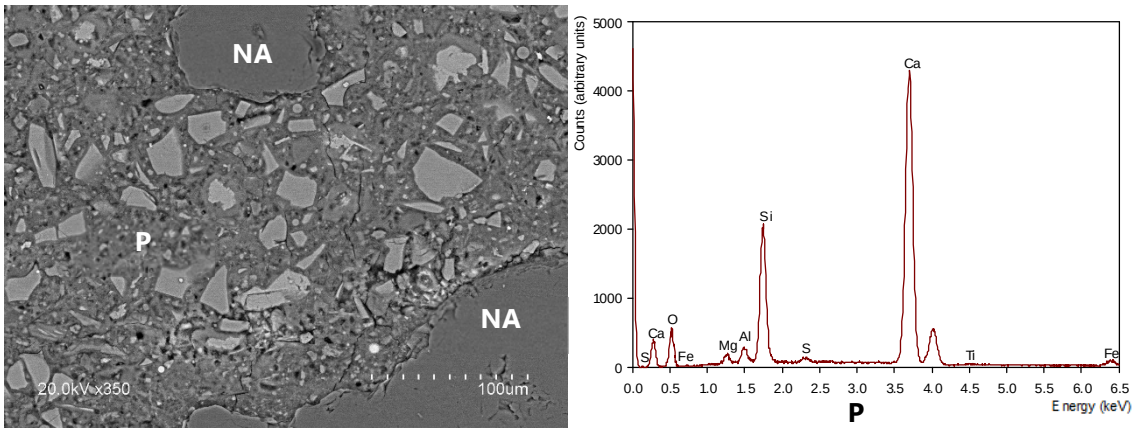

Figure 7.9: Micrograph of the ITZ of I-CC at 90 days

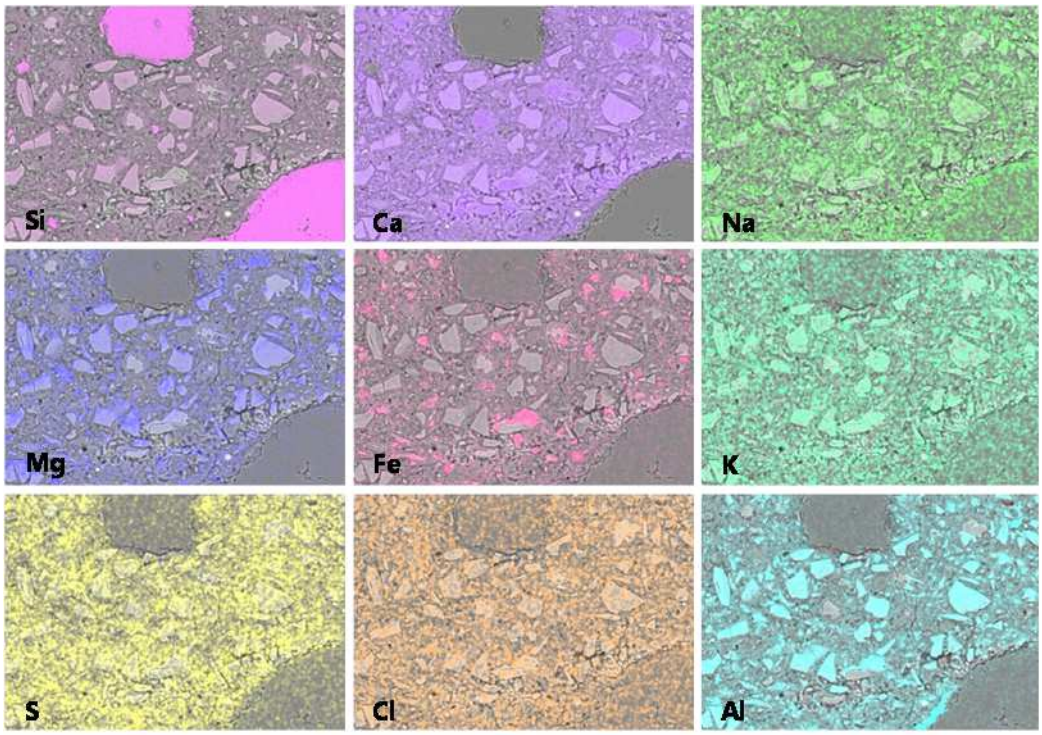

Figure 7.10: Mapping of the ITZ of I-CC at 90 days

2.3.2. CONCRETE MIXTURE I-RC-L(S)

Analogously to the previous analysis, Figure 7.11, Figure 7.13 and Figure 7.15 illustrate the microstructure of the concrete mixture with low ceramic content by the EDS analysis micrographs of the recycled aggregates (RA) and the cement paste (P) at 28, 56 and 90 days of curing and Figure 7.12, Figure 7.14 and Figure 7.16 display the mapping results of the corresponding areas.

It is widely recognized that the microstructure of recycled concretes is more complicated than that in normal concrete. As part of the mortar remains attached to the recycled aggregates, two different interfacial zones can be identified under the SEM examination. Figure 7.11 is an example of this situation. In this particular case, the old ITZ seems to have a better quality as the boundary between RA-M (adhered mortar with a high concentration of iron) and RA-N (natural aggregate) comprising the recycled aggregate is less clear than that with the new cement paste. Nonetheless, the ITZ between the recycled aggregates (RA-C) in Figure 7.13 and Figure 7.15, which were identified as ceramic by their aluminium-silicate nature, and the cement paste presented a good bond as an be observed by the sharp delimitation between the calcium-silicon elements in the mapping analyses.

Despite the incorporation of this type of aggregates, the composition of the cement paste was similar to the one found for the conventional mixture, i.e. calcium and silicon as major elements, magnesium and aluminium as consequence of the slag particles and sulphur coming from the hydration retardant agent in the cement. The Ca/Si ratio was around 1.51-1.67, which is in the range for normal concretes (Taylor, 1997; Hewlett, 2003) and similar to the 1.60 value found by Medina et al. (2012) for recycled concretes made with ceramic sanitary ware.

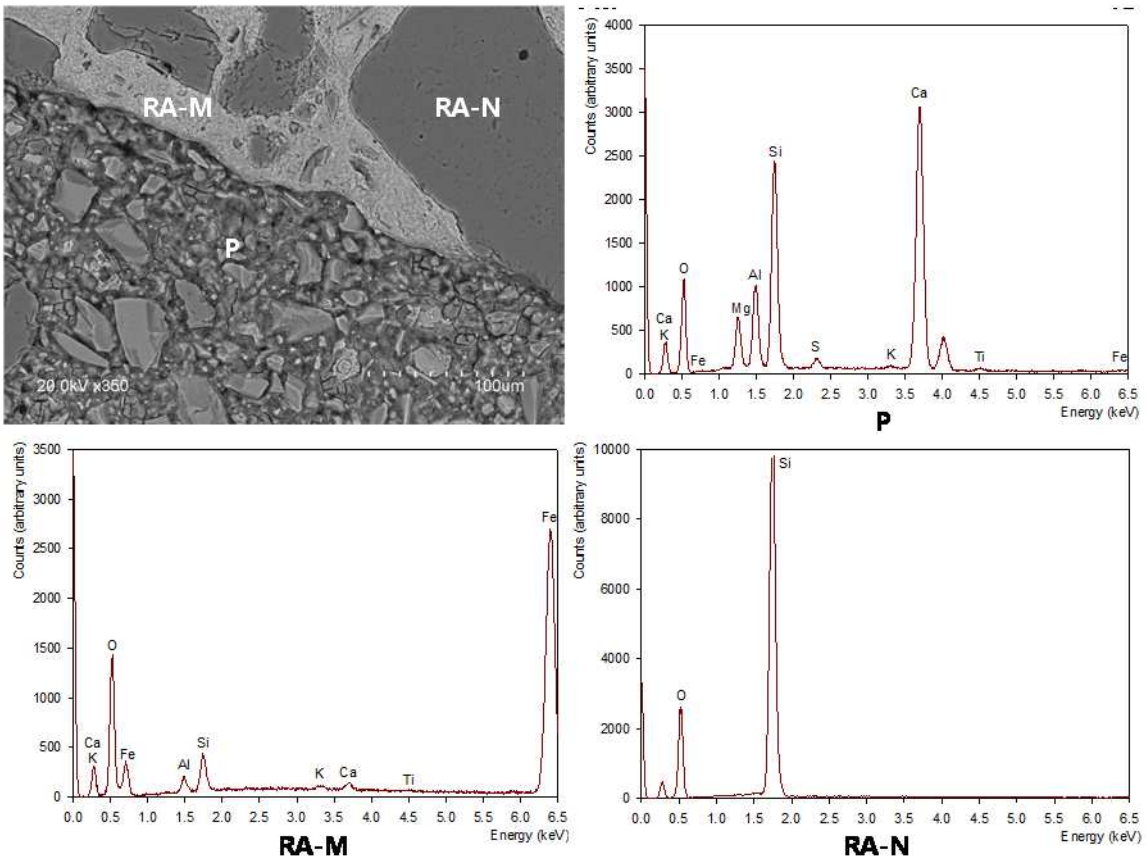

Figure 7.11: Micrograph of the ITZ of I-RC-L(S) at 28 days

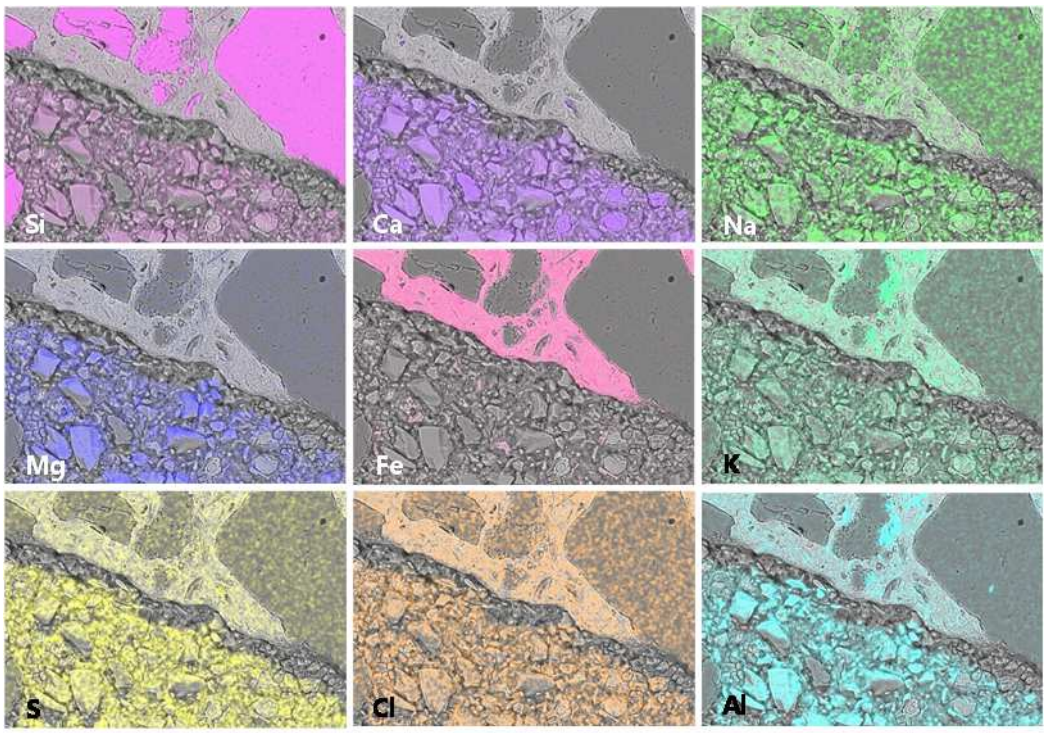

Figure 7.12: Mapping of the ITZ of I-RC-L(S) at 28 days

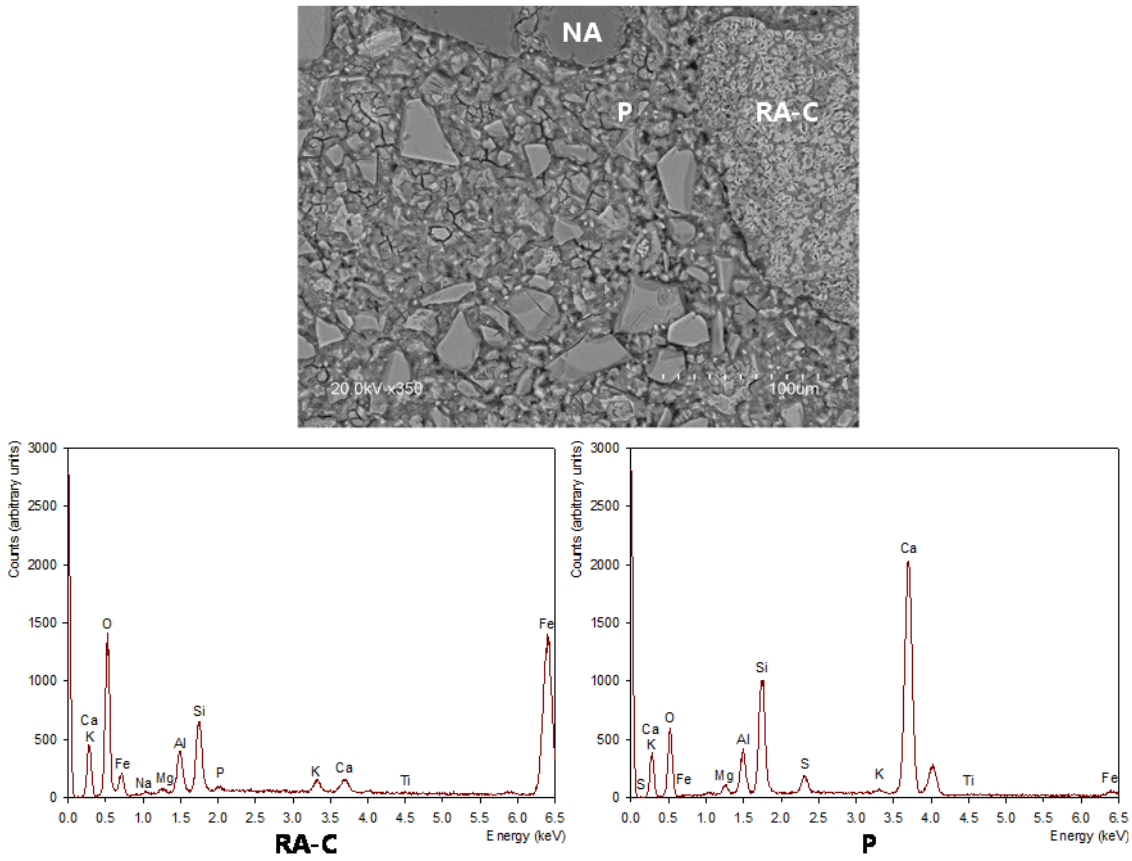

Figure 7.13: Micrograph of the ITZ of I-RC-L(S) at 56 days

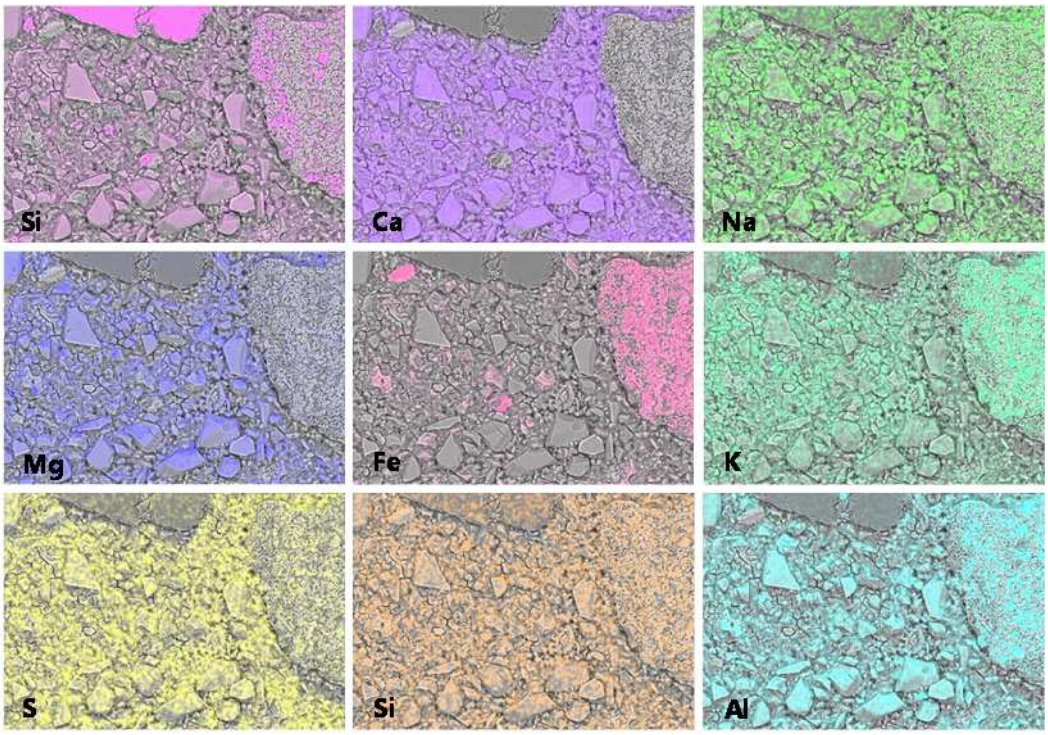

Figure 7.14: Mapping of the ITZ of I-RC-L(S) at 56 days

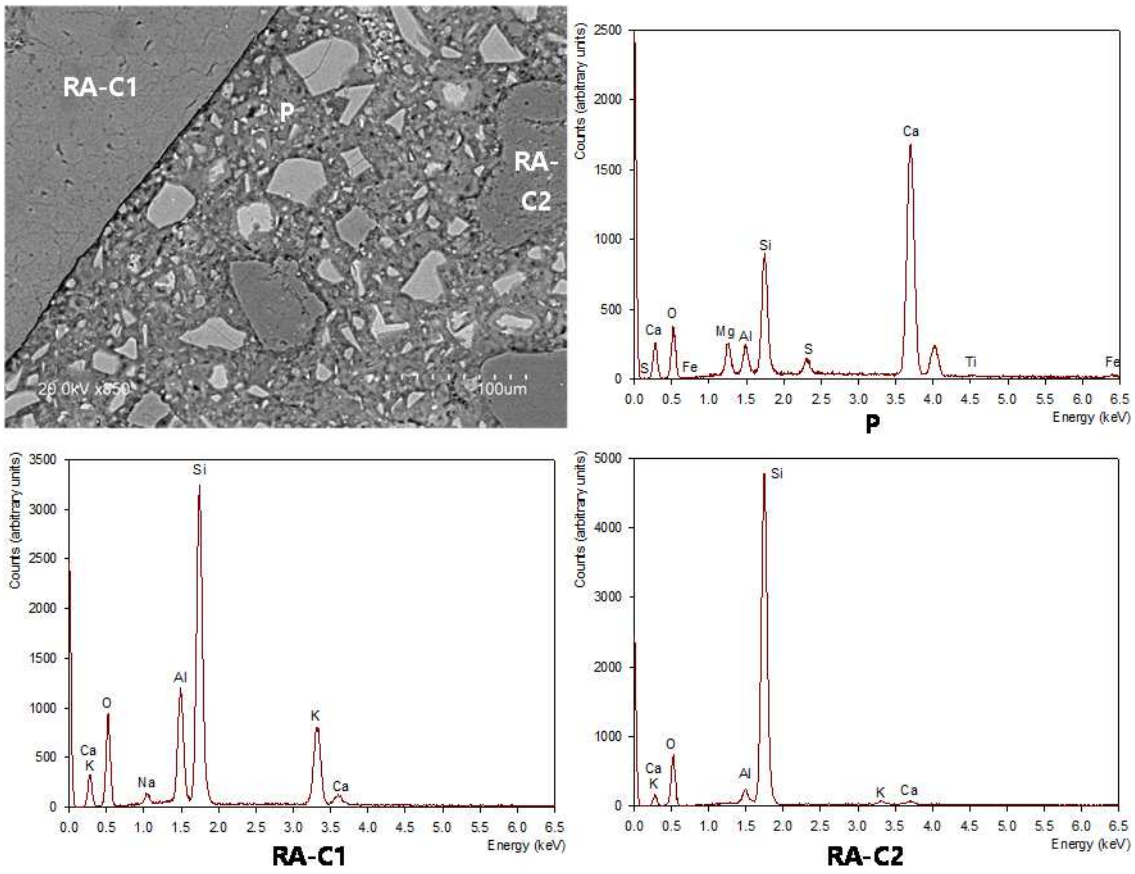

Figure 7.15: Micrograph of the ITZ of I-RC-L(S) at 90 days

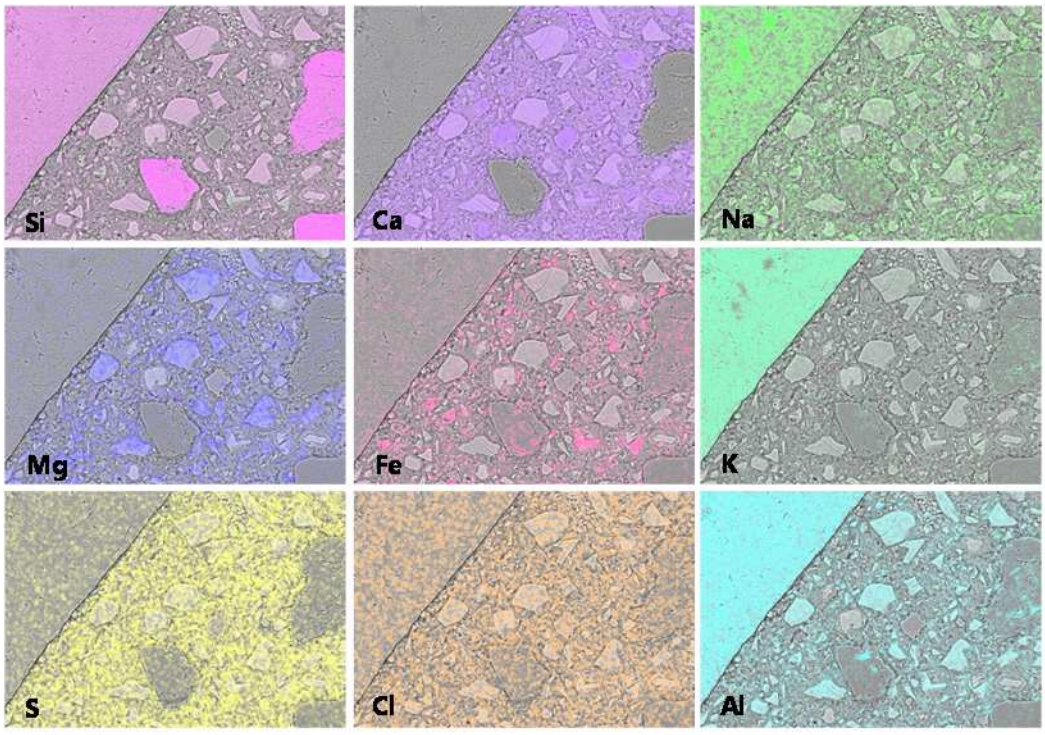

Figure 7.16: Mapping of the ITZ of I-RC-L(S) at 90 days

2.3.3. CONCRETE MIXTURE I-RC-M(S)

For the concrete mixture containing a medium amount of ceramic waste materials, the EDS micrographs corresponding to the recycled aggregates (RA) and the cement paste (P) are presented in Figure 7.17, Figure 7.19 and Figure 7.21; while Figure 7.18, Figure 7.20 and Figure 7.22 display the mapping analysis at 28, 56 and 90 days of curing.

Similarly to the analysis carried out for mixture I-RC-L(S), the ITZ between strictly ceramic recycled aggregates (Figure 7.17 and Figure 7.21) and the cement paste resulted to be stronger than that of ceramic recycled aggregates (RA-C) with adhered mortar (RA-M) as shown by the looser bond presented in Figure 7.19 and Figure 7.20.

Once again, the cement paste identified presented both the same elements (calcium, silicon, magnesium, aluminium and sulphur), and typical distribution than that of a conventional mixture, Regarding the Ca/Si ratio, values oscillating from 1.36 to 2.02 were observed and thus are within the thresholds found for normal concretes by other authors (Taylor, 1997; Hewlett, 2003).

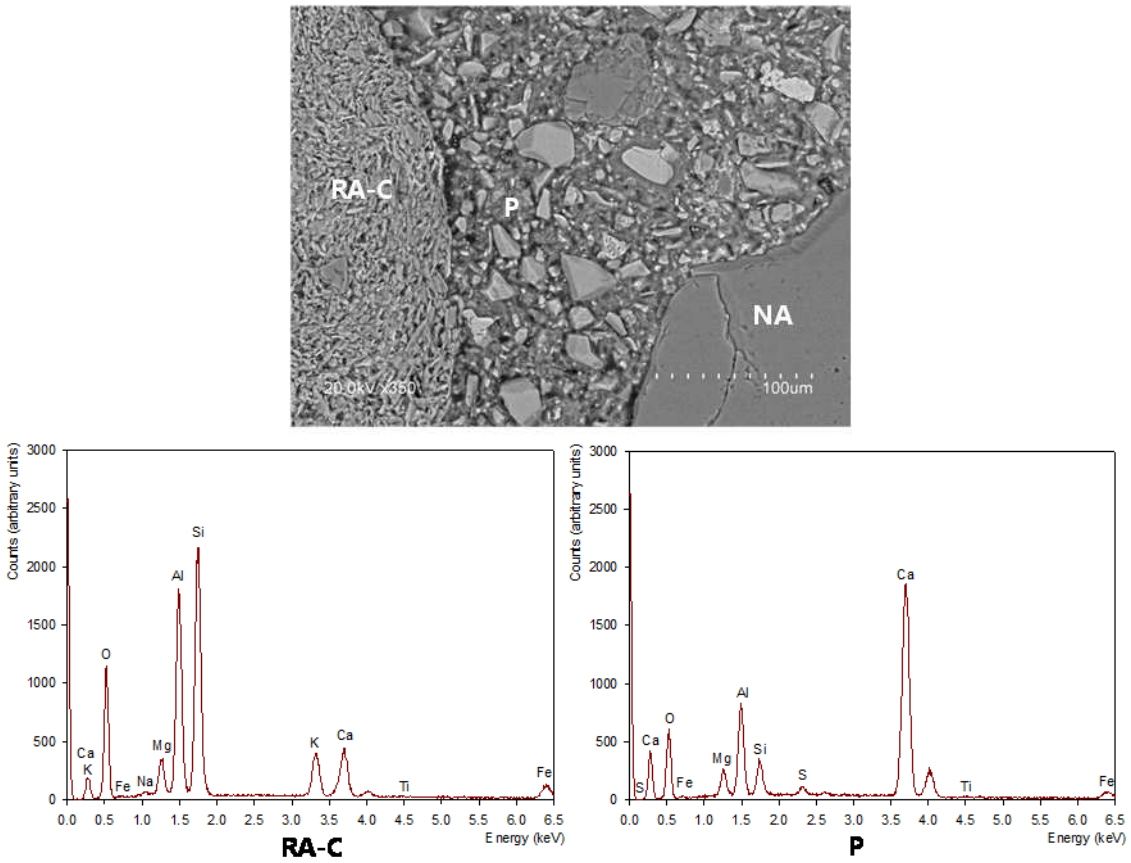

Figure 7.17: Micrograph of the ITZ of I-RC-M(S) at 28 days

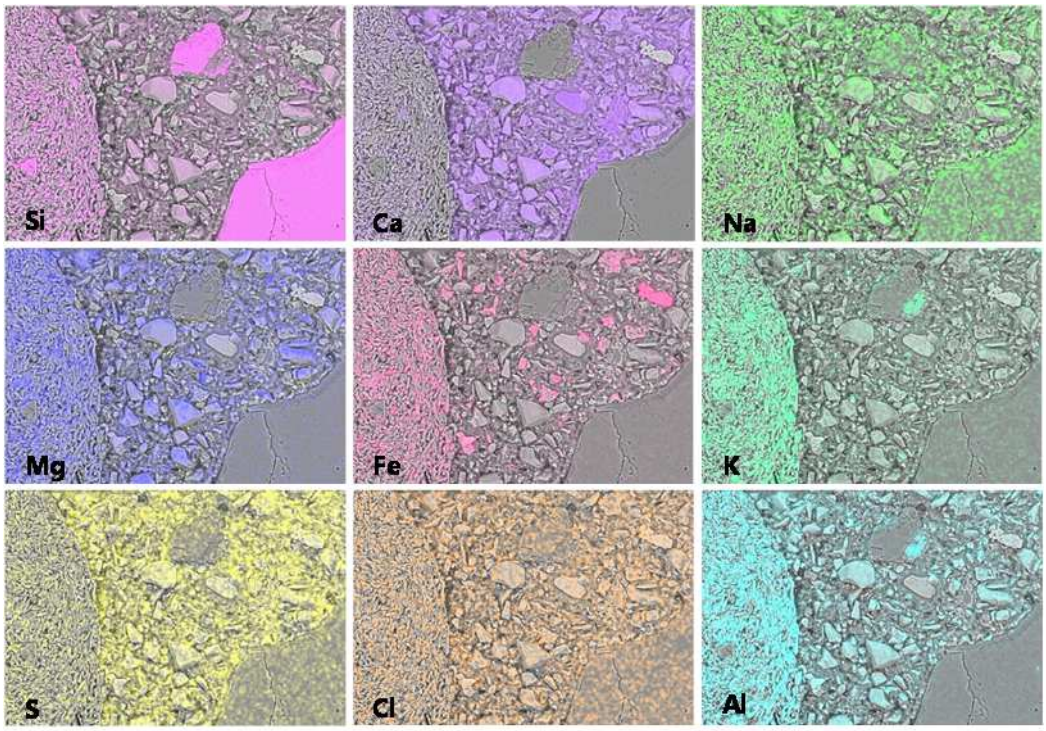

Figure 7.18: Mapping of the ITZ of I-RC-M(S) at 28 days

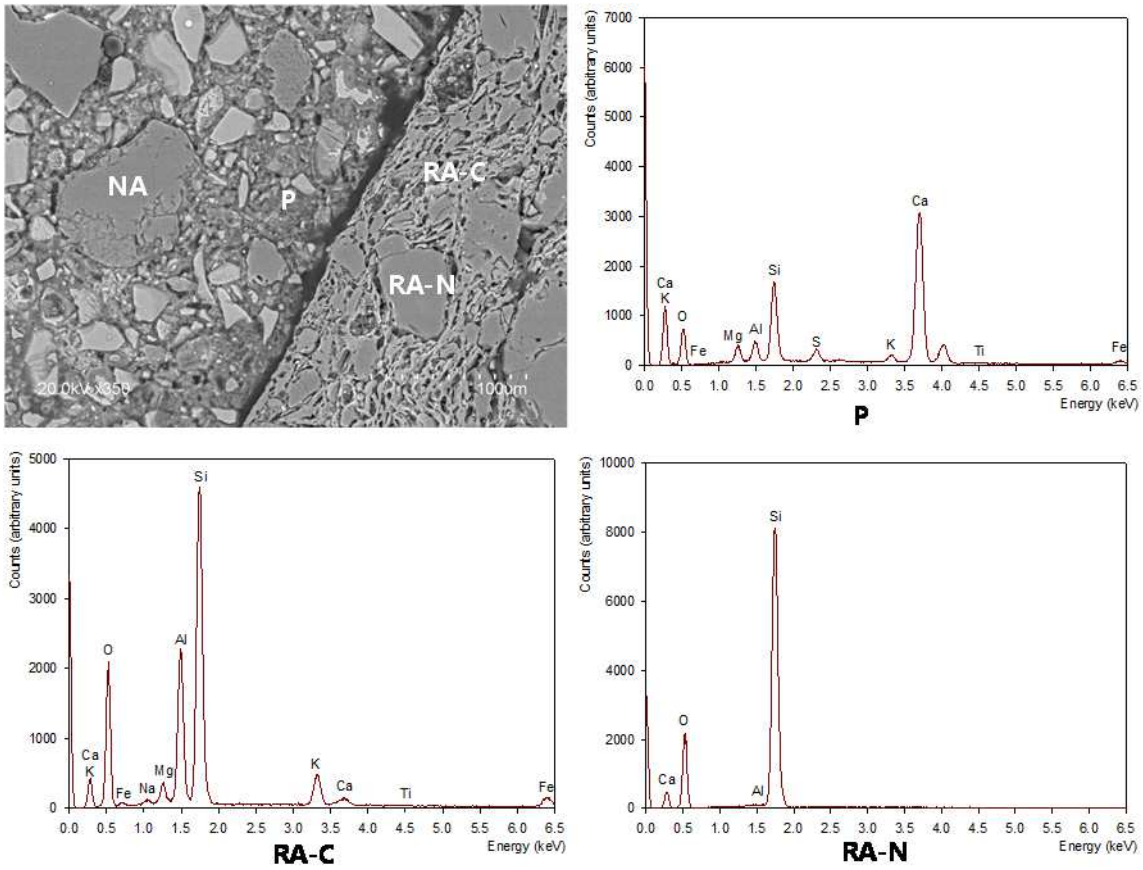

Figure 7.19: Micrograph of the ITZ of I-RC-M(S) at 56 days

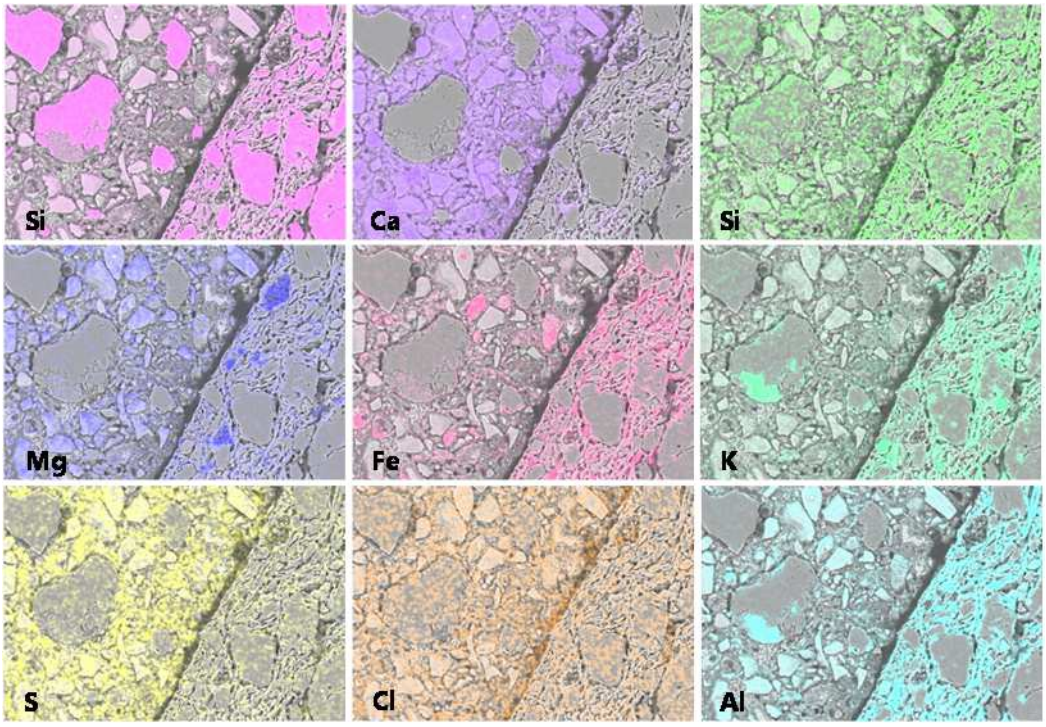

Figure 7.20: Mapping of the ITZ of I-RC-M(S) at 56 days

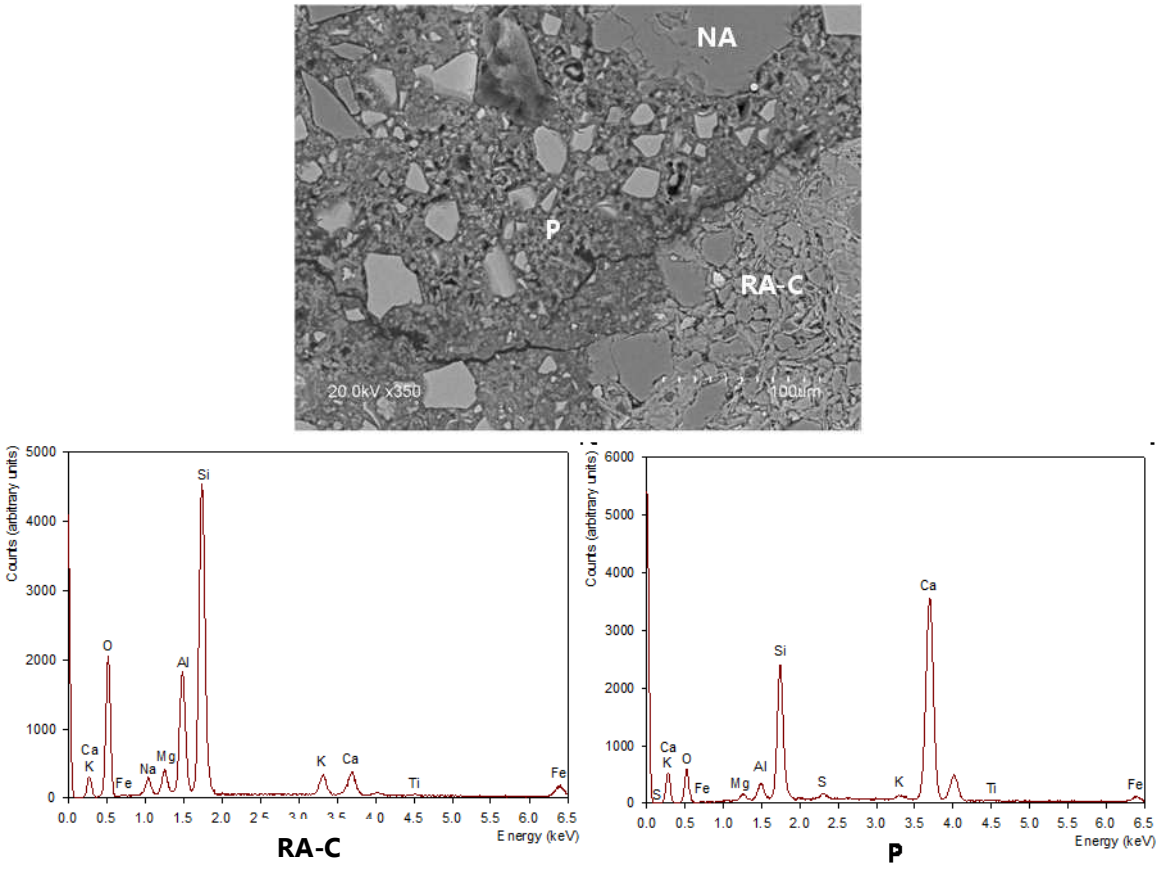

Figure 7.21: Micrograph of the ITZ of I-RC-M(S) at 90 days

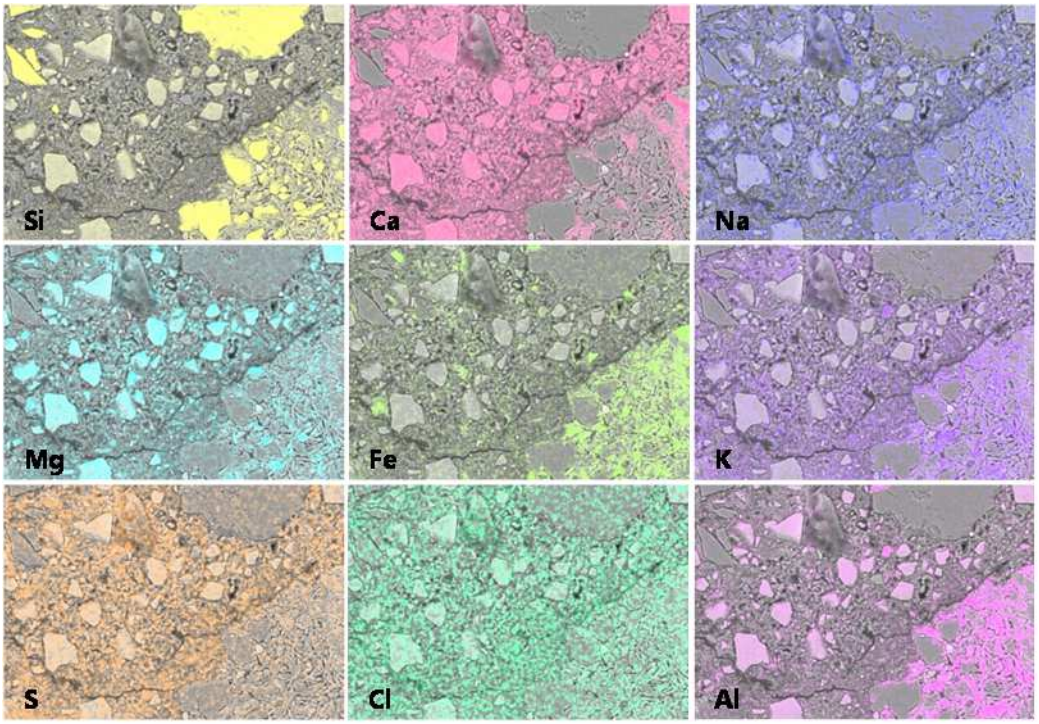

Figure 7.22: Mapping of the ITZ of I-RC-M(S) at 90 days

2.3.4. CONCRETE MIXTURE I-RC-H(S)

In Figure 7.23, Figure 7.25 and Figure 7.27 the EDS micrographs for the recycled aggregates (RA) and the cement paste (P) of the concrete mixture containing the higher amount of ceramic recycled aggregates are displayed at 28, 56 and 90 days of curing. Similarly, Figure 7.24, Figure 7.26 and Figure 7.28 illustrate the mapping analysis of the corresponding areas.

The previous trend regarding the better bond of the ceramic aggregates than other recycled aggregates to the cement paste is also confirmed for mixture I-RC-H(S). Hence, Figure 7.23 and Figure 7.25, which presented ceramic aggregates without adhered mortar, exhibited a denser ITZ than the bond observed for the combination of ceramic aggregate (RA-C) and ceramic-mortar aggregate (RA-M) shown in Figure 7.27.

For all curing ages, the cement paste displayed a similar composition and distribution than that of the conventional and the other recycled mixtures, and presented a Ca/Si ratio between 1.58 and 1.79, which confirms that the use of recycled aggregates does not chemically alter the cement matrix in a significant manner.

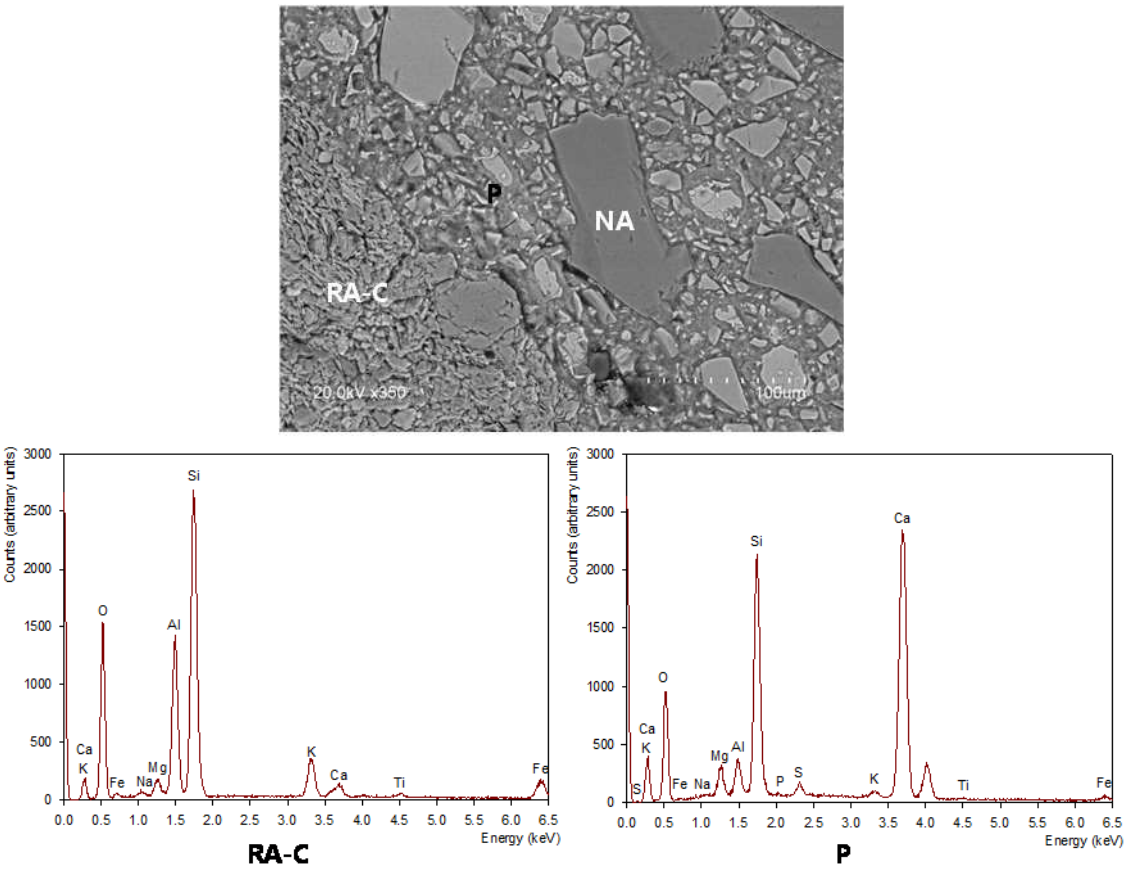

Figure 7.23: Micrograph of the ITZ of I-RC-H(S) at 28 days

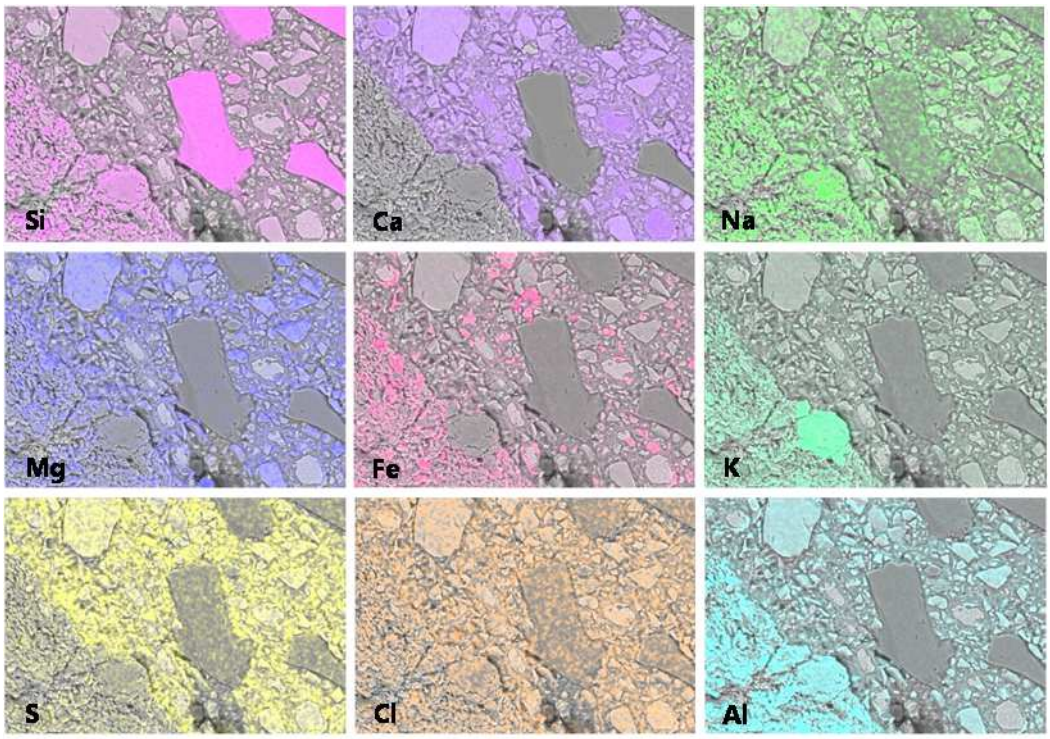

Figure 7.24: Mapping of the ITZ of I-RC-H(S) at 28 days

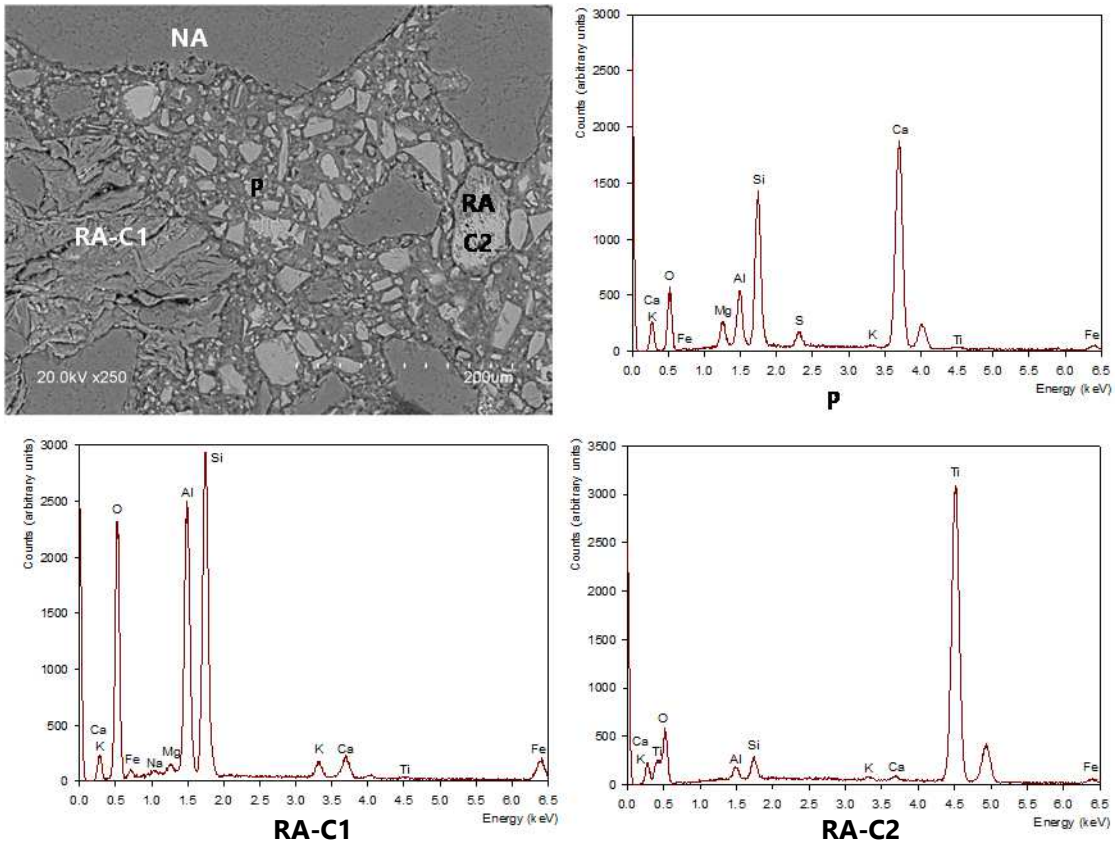

Figure 7.25: Micrograph of the ITZ of I-RC-H(S) at 56 days

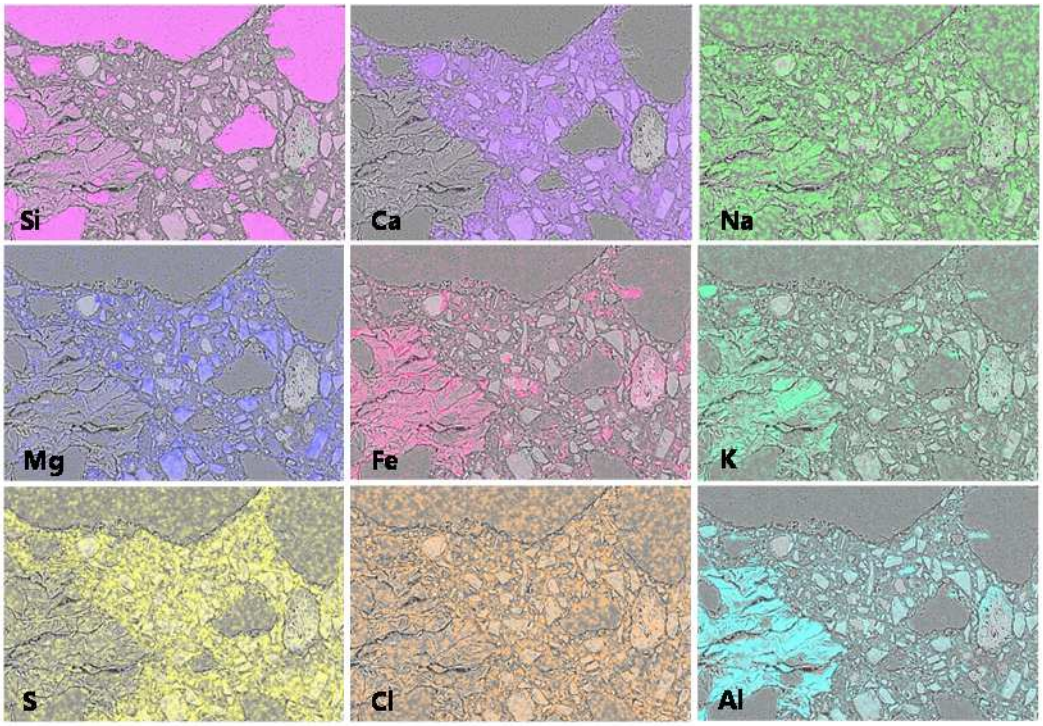

Figure 7.26: Mapping of the ITZ of I-RC-H(S) at 56 days

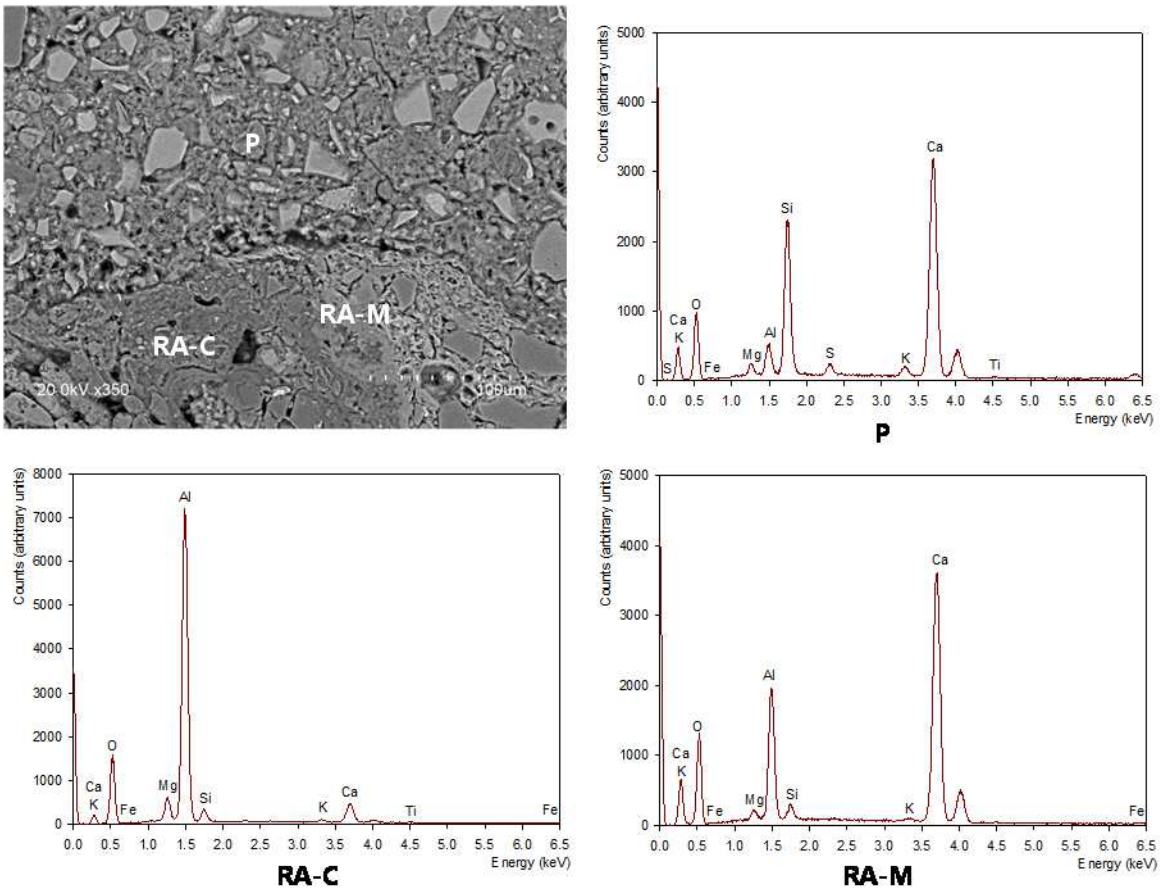

Figure 7.27: Micrograph of the ITZ of I-RC-H(S) at 90 days

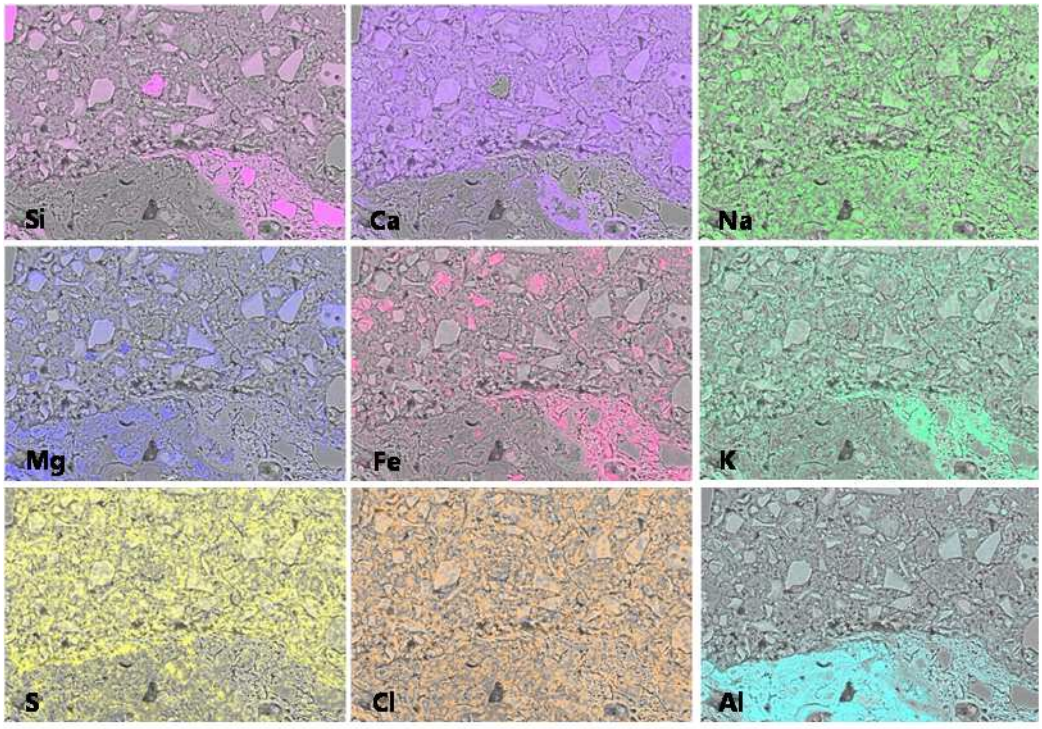

Figure 7.28: Mapping of the ITZ of I-RC-H(S) at 90 days

3. MICROSTRUCTURE: POROUS NETWORK

The porosity of the recycled concrete is comprised by that of the aggregates and the cement paste matrix. On one hand, the recycled aggregates possess higher porosity values than natural aggregates (see section 3.2.4 in chapter 4) and as such should be taken into account. On the other hand, the pore structure of the cement paste largely depends on the hydration process. Cement reacts with water resulting in the creation of hydration products that leads to a decrease in volume, known as chemical shrinkage, since the volume of the hydration products is lower than the initial volume of the reacting cement and water. Finally, the space not filled by the hydration products or the unhydrated cement particles comprises the porous network (Figure 7.29).

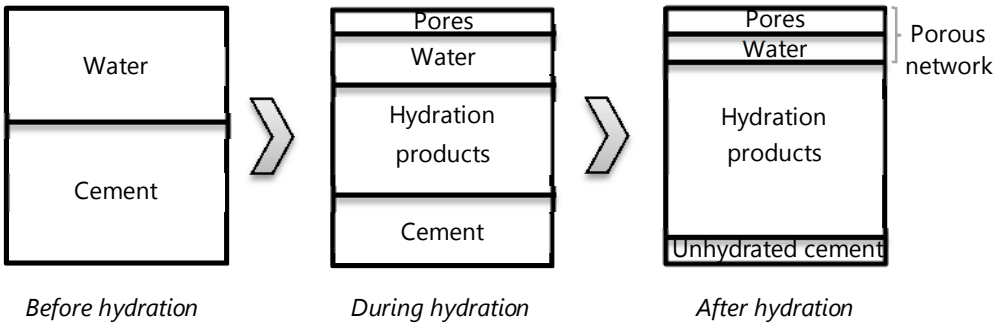

Figure 7.29: Volumetric changes associated to cement hydration

In the beginning of cement hydration, the pores are part of a continuous network. However, the pore structure gets disconnected due to the increasing volume of the solid phase (hydration products and unhydrated cement) forming the microstructure of the concrete (Powers, 1958). Generally, the volume of large pores decreases and that of small pores increases with the hydration process which impacts on the pore size distribution (Shi-Ping and Grandet, 1989).

Furthermore, the water/cement ratio also influences the pore network. According to Odler et al. (1972), higher water/cement ratio results in increases the amount of all pore sizes barely affecting the pore size distribution. Contrarily, other researchers have concluded that an increase of the water/cement ratio would preferably result in an increase of the capillary porosity (larger pores) and the mean pore size (Kroone and Crook, 1961; Shi-Ping and Grandet, 1989; Ye, 2003).

It is widely recognised that a better understanding of the pore structure of concrete could be used to model other properties of the hardened concrete such as the mechanical resistance and the transport mechanism impacting the durability (Rübner and Hoffmann, 2006). A normal characterization of the porous structure is based upon the determination of the volume, surface and distribution by size of the pores. Although these parameters may be useful to link porosity and strength, the knowledge about the topological properties of the pore structure such as connectivity and tortuosity are more decisive when the porosity is related to the permeability of concrete (Jennings et al., 2008). However, no single technique can adequately characterize all the components of the pore system due to their great size variability (from nanometres to

millimetres). Thus, in this research several techniques have been employed jointly to overcome the problem.

3.1. CLASSIFICATION SYSTEMS

The pore size distribution of concrete mixtures comprises pores ranging from 1 nm to 1 mm, 6 orders of magnitude (Neville, 1995). In order to differentiate the pores, several researchers have proposed different classifications systems (Everett, 1972; Locher, 1976; Bazant and Wittmann, 1982; Oberholster, 1986; Espinosa and Franke, 2006). In spite of all the investigations, the precise definition of different pore types is still lacking (Jennings et al., 2008).

Initially, the classification was based upon the pore size. For instance, the International Union of Pure and Applied Chemistry (IUPAC) distinguishes three types of pores in cement-based materials: micropores (<2 nm), mesopores (2-50 nm) and macropores (>50 nm) (Everett, 1972). Lately, the classification system combined the pore size with the origin of the pore space which ended with the subdivision in gel pores, capillary pores and air voids. Although in this research work the IUPAC classification system was employed, the notions of gel and capillarity porosity have also been taken into account.

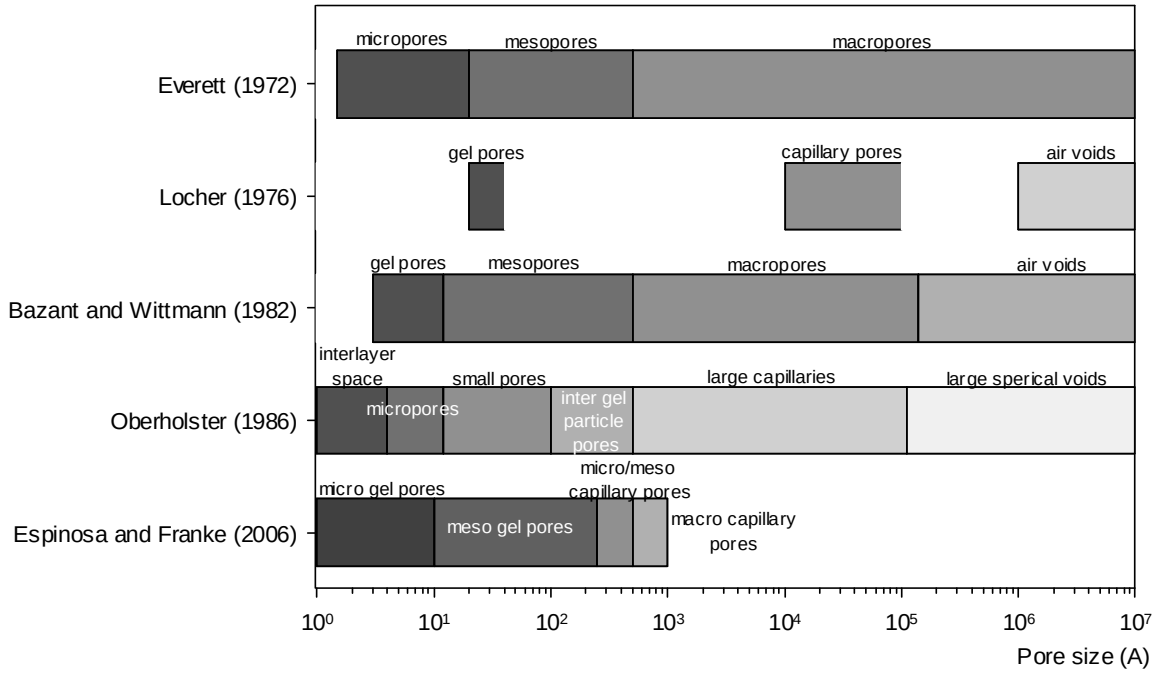

Figure 7.30: Pore sizes classification systems

- Gel pores are an intrinsic part of the C-S-H gel phase, contain adsorbed water molecules and are central to several important properties such as shrinkage and creep (Jennings et al., 2008).

- Capillary pores appear as a direct result of the hydration of cement and are linked to the excess of water employed during the mixing stage. These pores influence the mechanical resistance and transport properties (permeability and ion migration) of the concrete (Jennings et al., 2008).

- Air voids are generally classified in two groups, entrapped if created unintentionally during the mixing and placing stage or entrained if a specific admixture is employed. Whilst entrapped air voids are irregularly shaped and distributed through the concrete specimen, the entrained air voids are generally smaller, spherical and evenly distributed. These pores do not influence the transport mechanisms due to lack of connectivity, but impact the mechanical and freeze-thaw resistance of the concrete (Neville, 1995).

3.2. GEL AND CAPILLARY POROSITY: MERCURY INTRUSION POROSIMETRY

Mercury intrusion porosimetry (MIP) has been extensively used for the characterization of the porous network of concrete despite presenting certain limitations (Diamond, 1971, 2000; Cook and Hover, 1993; Lange et al., 1994; Abell et al., 1999; Gallé, 2001; Kumar and Bhattacharjee, 2003). Nonetheless, the MIP characterization is generally accepted as a reasonable estimate for cement-based materials (Bermejo et al., 2010).

The first limitation is due to the necessity to assume a pore shape model to convert the mercury intrusion data into a pore size distribution. While the application of the Washburn equation for cylindrical pores entirely accessible from the outer surface to the mercury intrusion is the most employed method; the real pore geometry is not cylindrical but presents a high degree of convolution and a significantly elongated shape (Wang and Diamond, 1994; Diamond, 2000) and the pressure increase necessary for the further infiltration of the mercury is liable to break the pore walls to ease their path along a non-continuous pore system which turns is a coarsening of the real porous structure (Feldman, 1984; Olson et al., 1997; Diamond, 2000).

Another important weakness of the MIP analysis lay down in the so-called "ink-bottle" effect. This is also due to a geometry aspect, as the irregular shape of connected pores with successive narrow and wide passages leads to the need of higher pressures to fill wider pores connected to the surface of the sample through smaller throats, which in the end overestimates the volume of finer pores.

Finally, and as most characterization techniques, MIP requires a pre-conditioning of the sample in order to remove the water within the pores. Several studies have detected changes in the microstructure of the sample subjected to different drying procedures (Winslow and Diamond, 1970; Konecny and Naqvi, 1993; Gallé, 2001, 2003; Rübner et al., 2002; Diamond, 2003; Kumar and Bhattacharjee, 2003). Bearing in mind that oven-drying can result in considerable changes to the concrete microstructure due to capillary stresses, desiccation of the hydration products and micro-cracks formation (Snoeck et al., 2014), a temperature of 40ºC was selected in order to avoid the dehydration of the calcium silicate hydrates which befalls at 105ºC (Moukwa and Aïtcin, 1988), the decomposition of the monosulfoaluminate and ettringite phases that temperatures higher than 60ºC generate (Zhang and Glasser, 2000) and the polymerization of silicate anion chains occurring at 50ºC (Aono et al., 2007).

Despite porosity is recognized as one of the most troublesome properties of the recycled aggregates, the investigation of the porosity of recycled concrete mixtures has received little attention to date. While some research works have included porosity values for recycled concrete, few investigations have assessed the porous network in further detail and reported information regarding the pore size or distribution (Gómez-Soberón, 2002; Manzi et al., 2013).

Due to the porous characteristics of the recycled aggregate, recycled concrete possesses a higher porosity than conventional mixtures. For recycled concretes made of recycled concrete aggregates, the reported porosity values at 28 days of curing range from 10.79% to 22.60% (Barra Bizinotto, 1996; Buyle-Bodin and Hadjieva-Zaharieva, 2002; Gómez-Soberón, 2002; Zaharieva et al., 2003; Nagataki et al., 2004; Kou et al., 2011; Ulloa Mayorga, 2012), which is between 1.12 and 3 times higher than the values obtained for the respective reference concrete mixtures.

In Figure 7.31, the porosity results for the conventional and recycled concrete mixtures studied in phase I are plotted for 28 and 56 days of curing.

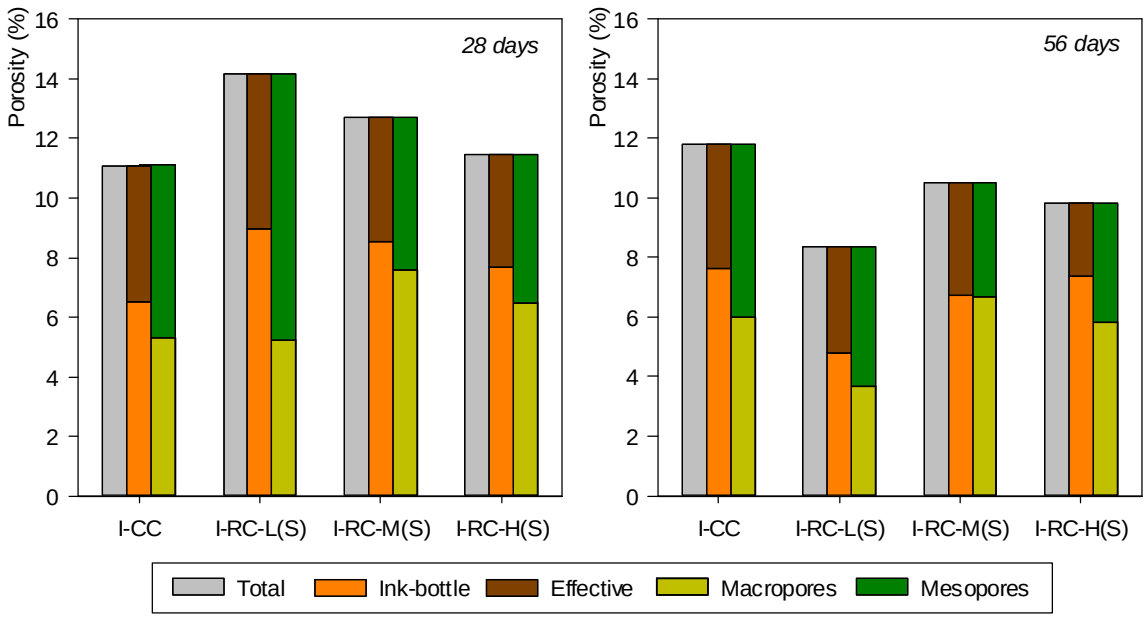

Figure 7.31: Porosity of the concrete mixtures of phase I at 28 and 56 days

Similar to the findings of the literature previously mentioned, the recycled concretes presented a higher total porosity than the conventional concrete at 28 days. In particular, higher differences were found for lower ceramic incorporations, ranging from 27.7 % higher porosity versus the reference for low ceramic recycled concrete (I-RC-L(S)) and 14.6% for medium ceramic recycled concrete (I-RC-M(S)) to 3.3% for high ceramic recycled concretes, which suggest an inverse relationship between the total porosity of the recycled concretes and the percentage of ceramic waste included as aggregate. However, the situation is reversed after 56 days of curing and recycled mixtures presented a lower porosity than that of the conventional concrete, around 29% for I-RC-L(S), 11% for I-RC-M(S) and 17% for I-RC-H(S).

Therefore, the recycled concretes acquired a significant decrease in porosity, up to a 41% for I-RC-L(S), 26% for I-RC-M(S) and 31% for I-RC-H(S). This reduction is due to the evolution in the hydration process since hydration products gradually fill in the available space in cement paste. Other researchers have also noticed that the reduction in porosity of the recycled concretes made of recycled concrete aggregates is higher than that experienced for conventional concretes (Gómez-Soberón, 2002; Kou et al., 2011; Ulloa Mayorga, 2012). Notwithstanding the variation with time, both the conventional and recycled concrete mixture presented a good quality in terms of porosity according to the guidelines proposed by the CEB (1998) since the registered values were lower than 15%.

Besides total porosity, Figure 7.31 also illustrates the accessibility and size components of the porous network of the studied concretes. On one hand, the porosity is denoted as a function of the mercury accessibility during the processes of intrusion and extrusion as effective and ink-bottle porosity, the latter representing the volume of mercury that remains in the specimen after the MIP test. The ink-bottle porosity is higher than the effective porosity for all samples oscillating from 59% to 67% at 28 days of curing and between 58% and 75% at 56 days of curing.

This fact indicates that most of the pores intruded by mercury required the exertion of a force superior to their actual size since they were accessed through narrow throats or smaller pores. In addition, for the conventional concrete and the high ceramic recycled concrete (I-RC-H(S)) a trend towards the increase in the ink-bottle porosity could be observed (around 10% and 13% respectively). This could be explained by the refinement of the porous network due to the evolution of the hydration process. For practical reasons, the presence of high ink-bottle pores is beneficial as it means a higher resistance of the concrete to the penetration of aggressive external agents.

On the other hand, porosity is represented in function of the contribution of mesopores (2-50 nm) and macropores (>50 nm). At 28 days, mesopores slightly dominate the performance for the conventional concrete (52%) and the low ceramic recycled mixture (I-RC-L(S)) (63%); while in samples I-RC-M(S) and I-RC-H(S), the macropores have a higher influence (60% and 57% respectively). However, after 56 days of curing, the macropores govern the porosity performance of all samples presenting values of 51% for I-CC, 44% for I-RC-L(S), 64% for I-RC-M(S) and 59% for I-RC-H(S). While the general increase is about 4% to 6%, the low ceramic recycled concrete (I-RC-L(S)) displayed an upsurge around 18.5%. Despite these variations seem contrary to the expected refinement of the porosity, the percentages are relative to the total porosity and thus the absolute macroporosity decreased with the hydration time since the hydration products fill the large pores at first and later on the smaller ones (Jennings et al., 2008). Moreover, as the cement used in phase I of this investigation contains blast furnace slag (36-65%), the hydration process was slowed down in comparison with ordinary Portland cement (Fulton, 1974; Hogan and Meusel, 1981; Wainwright and Ait-Aider, 1995). Thus, it is possible that after 56 days of curing the definitive porosity shift did not take place yet.

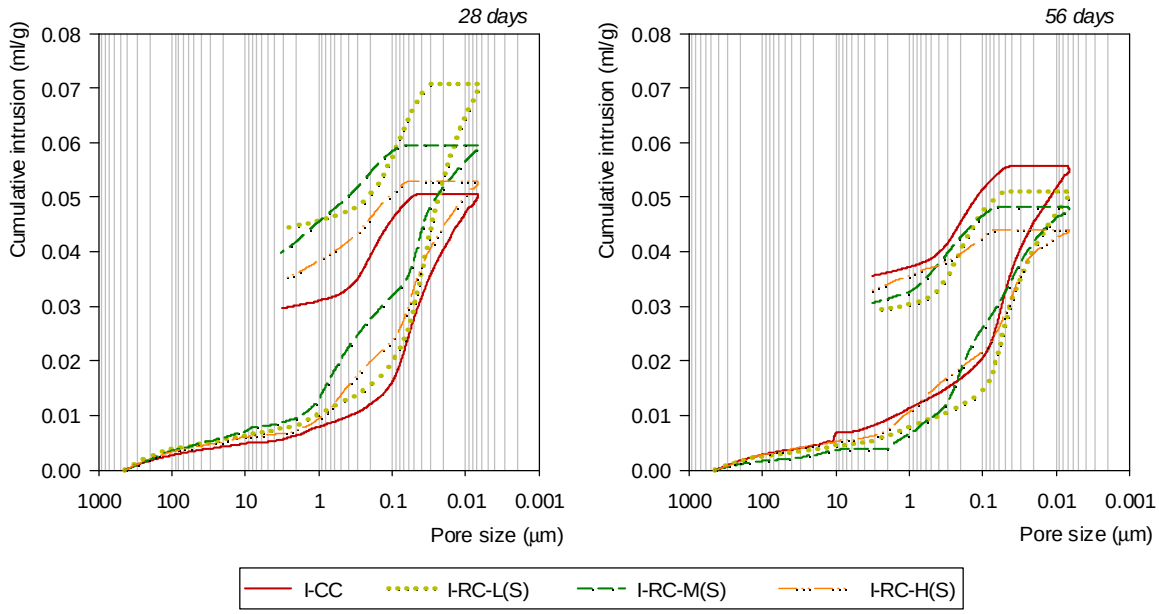

Figure 7.32: Cumulative pore intrusion of the concrete mixtures in phase I at 28 and 56 days

Figure 7.32 shows the plot of the cumulative mercury intrusion volume per oven-dried mass of the sample versus the pore size. Note that, both graphs are represented with the x-axis decreasing toward the right side in order to better represent the physical mechanism of intrusion, i.e. the larger pores are the firsts to be filled and with the subsequent increase of pressure smaller pores are intruded. Moreover, Figure 7.33 portrays a simplified pore size distribution of the concrete mixtures studied in phase I at 28 and 56 days of curing in order to facilitate the comparison among concrete mixtures and curing ages.

At 28 days of curing, the cumulative intruded volume curves show that recycled concrete presents higher porosity than the conventional concrete, in particular for the 0.001-1 µm range. For instance, Sagoe-Crentsil et al. (2001) reported that the increase of the porosity of recycled concretes made of recycled concrete aggregates compared to a conventional mixture was centred around pore sizes lower than 0.06-0.07 µm, Sánchez de Juan (2004) registered similar results since recycled concretes presented greater number of pores inferior to 0.05 µm, which was attributed to the porosity of the cement paste adhered to the aggregates. In addition, the higher content in pores in the 0.5-10 µm range presented by the recycled aggregates could be explained by the micro-cracks produced during the crushing procedure (Mueller and Winkler, 1998). However, after 56 days of curing, the conventional concrete presented higher intrusion values for most pore sizes, except in the 0.1-1 µm interval for the recycled mixtures containing medium and high percentages of ceramic wastes, which is the main component (60.84%) in the pore size range of the ceramic material comprising the recycled aggregates used, as explained in section 3.2.4 in chapter 4.

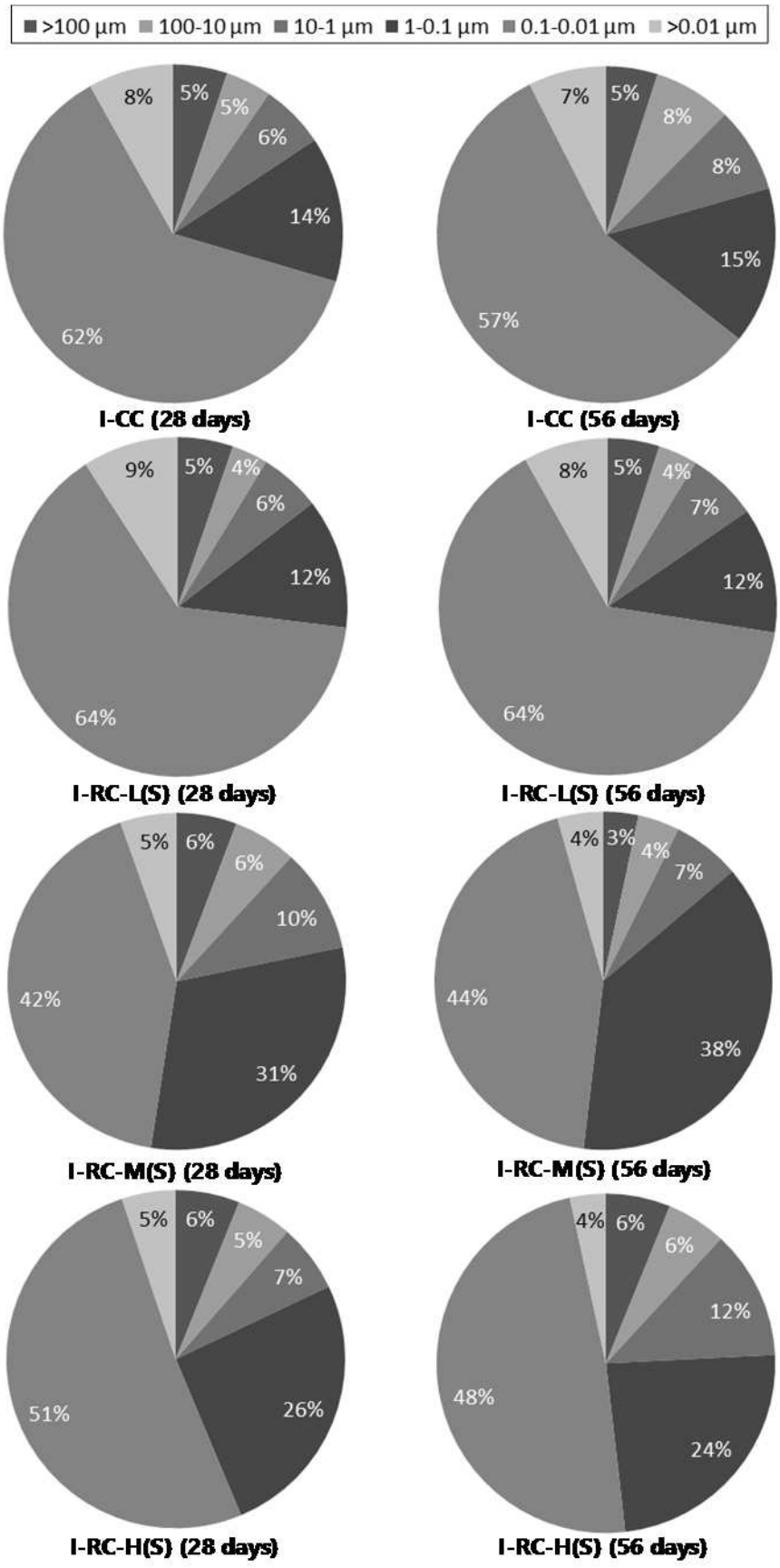

Figure 7.33: Pore size distribution of the concrete mixtures in phase I at 28 and 56 days

Based on the intrusion curves, the total pore area as well as the average and median diameters could be assessed for all samples (Table 7.1). First, the total pore area is calculated as the surface underneath the intrusion curve. Hence, the values of this parameter decrease with time, less than 1% for I-CC but ranging from 20% to 36% for the recycled concrete mixtures. While no significant relationship was uncovered among total pore area and the rising ceramic content in the concrete mixture at 28 days of curing, a good correlation (R^2= 0.81) was obtained for the same variables at 56 days of curing (Figure 7.34). Furthermore, the average pore diameter of the samples could be determined as a function of four times the total volume intruded in the total pore surface of the sample (Table 7.1). The values obtained show that the rising ceramic content in the recycled concrete entails an increase in the average pore diameter for both 28 and 56 days of curing, despite the weakness of the correlations (R^2=0.52 and R^2=0.71 for 28 and 56 days respectively) (Figure 7.34).

Similarly, Gómez-Soberón (2002) reported that the average pore diameter increased for higher replacement ratios of recycled concrete aggregates, which could be assimilated to the situation encountered in this research work since the inclusion of higher amounts of the component responsible for the modifications in the porosity of concrete results in an growth of the average pore size. However, contrary to the results reported by Gómez-Soberón (2002) and Kou et al. (2011), the average pore diameter also increases with time, which is a reflection of the evolution of the pore size distribution shown in Figure 7.33. Finally, the median pore diameter was determined as the diameter at which the 50% of the total volume of mercury is intruded, i.e. median pore diameter by volume, or the diameter at which the 50% of the total pore area is intruded, i.e. median pore diameter by area. The MIP procedure and subsequent calculations cause that the median pore diameter by volume is weighed to larger pores and the median pore diameter by area is weighed to smaller pores. This effect is obvious for the different values obtained for each parameter (Table 7.1). For both cases the values increase with time and with the ceramic content in the concrete. However, only the median pore diameter by area presented a significant correlation (R^2=0.83 and R^2=0.81 at 28 and 56 days respectively) with the rising of the percentage of ceramic waste incorporated as aggregate (Figure 7.34).

Furthermore, the results obtained from the MIP tests at 28 and 56 days of curing are represented as a logarithmical function of the differential mercury volume intruded plotted against the pore diameter in Figure 7.35. Analogously with the cumulative representation, both graphs are represented with the x-axis decreasing toward the right side. The main benefit of this type of representation is the clear identification of the critical pore diameter of the sample as the peak in the curve since this diameter corresponds to the steepest slope of the cumulative intrusion curves (Figure 7.32). The physical meaning underneath this parameter is the small pore size that completes the first interconnected pore pathway in the porous network (Ye, 2003).

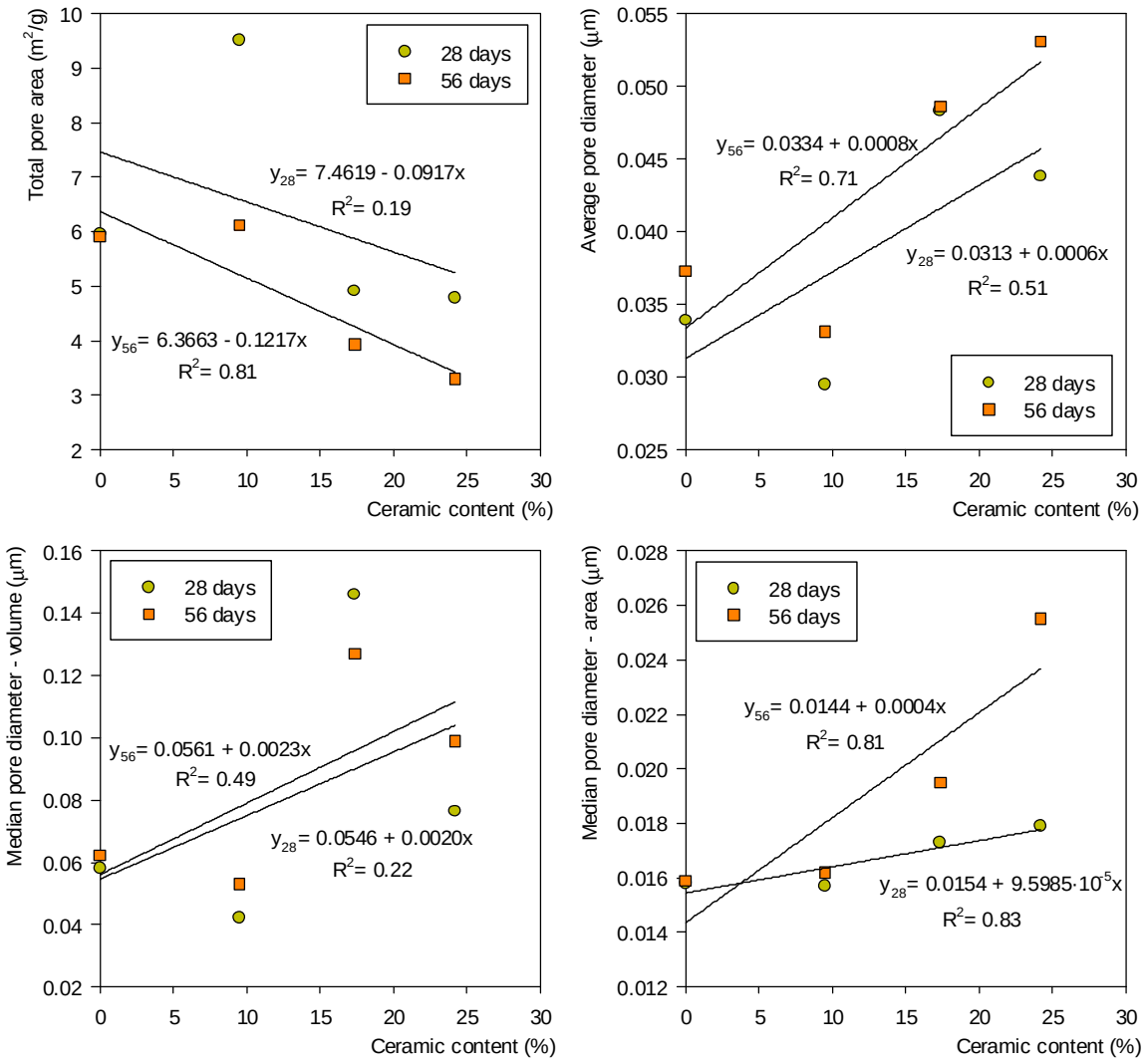

Figure 7.34: Relationship between the porous network and the ceramic content

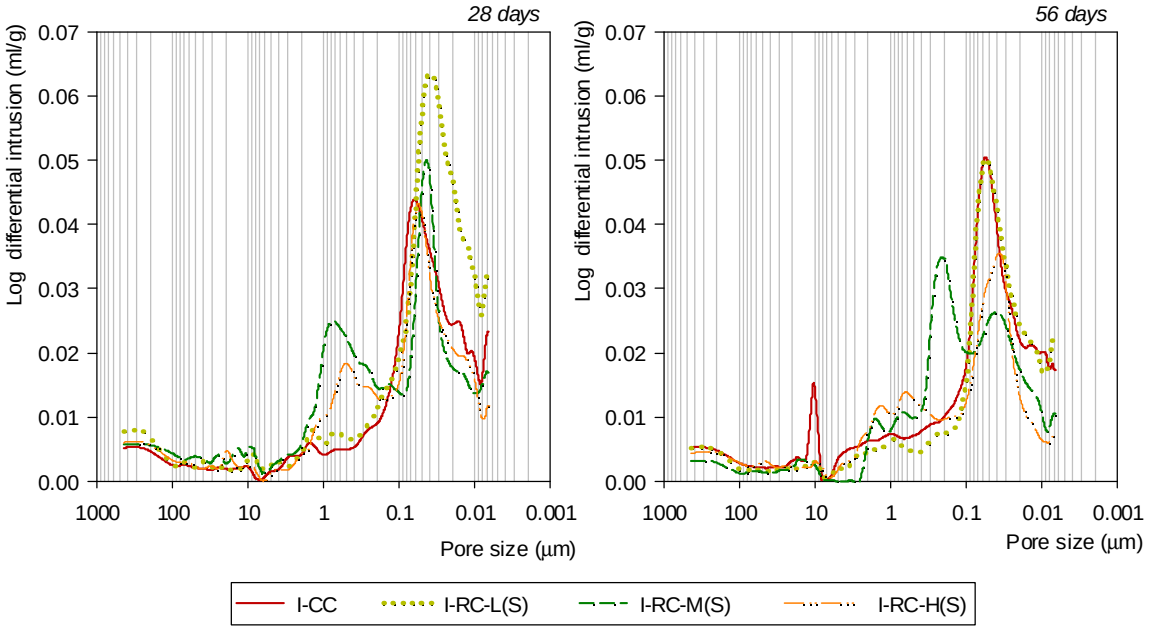

Figure 7.35: Differential intrusion of the concrete mixtures in phase I at 28 and 56 days

At 28 days of age, the conventional concrete and the low ceramic recycled concrete (I-RC-L(S)) presented a unimodal peak distribution while the medium and high ceramic recycled concrete mixtures (I-RC-M(S) and I-RC-H(S)) displayed a mostly bimodal peak distribution. Moreover, after 56 days of curing, the recycled concrete mixtures showed the same peak distribution meanwhile the conventional concrete shifted towards a bimodal peak distribution. Although it is worth mentioning these differences, the appearance of several peaks in the differential intrusion curve is a common occurrence for concrete materials (Cook and Hover, 1999; Ye, 2003; Zhou et al., 2010).

The conventional concrete presented a critical pore diameter of 0.0612 µm at 28 and 56 days of curing as well as another peak at 10 µm at 56 days of age. For I-RC-L(S), the peak occurs for a pore diameter of 0.0393 µm at 28 days and 0.0612 µm at 56 days. In the recycled concrete incorporating a medium content of ceramic aggregates (I-RC-M(S)), the two peaks correspond to a pore diameter of 0.049 µm and 0.8230 µm at 28 days, and 0.0393 µm and 0.2222 µm at 56 days. Finally, the recycled concrete made with a 50% replacement of completely ceramic recycled aggregates (I-RC-H(S)) also presented two peaks located at pore sizes values of 0.0612 µm and 0.5260 µm at 28 days, and 0.0393 µm and 0.6718 µm at 56 days.

In general, recycled aggregates presented lower critical pore sizes than the respective conventional mixture which is indicative of finer pore structures (Hu, 2004). At 28 days, the reduction oscillated between 20% and 36% and after 56 days of curing, the difference was around 36%. In terms of the evolution of the critical pore size with time, lower values were found for increasing curing ages, except for sample I-RC-L(S). Once again, the explanation falls back on the evolution of the hydration process since the filling of the larger pores with the hydration products forces the connecting pathway through smaller pores (Cook and Hover, 1999; Ye, 2003; Hu, 2004).

As a summary, all the different parameters that characterize the pore structure of the concrete mixtures pertaining to phase I are compiled in Table 7.1.

Table 7.1: Characterization parameters of the porosity of the recycled concretes in phase I

	I-CC	**I-RC-L(S)**	**I-RC-M(S)**	**I-RC-H(S)**
28 days				
Porosity (%)	11.09	14.17	12.71	11.45
Porosity-mesopores (%)	5.33	5.25	7.61	6.49
Porosity-macropores (%)	5.77	8.91	5.10	4.96
Ink-bottle porosity (%)	6.51	8.95	8.55	7.67
Effective porosity (%)	4.58	5.21	4.16	3.78
Total pore area (m^2/g)	5.958	9.515	4.912	4.781
Average pore diameter (µm)	0.0339	0.0295	0.0483	0.0438
Median pore diameter –volume (µm)	0.0581	0.0422	0.1459	0.0764
Median pore diameter-area (µm)	0.0158	0.0157	0.0173	0.0179
Critical pore diameter (µm)	0.0612	0.0393	0.049	0.0612
	-	-	0.8230	0.5260

Table 7.1: Characterization parameters of the porosity of the recycled concretes in phase I (continued)

	I-CC	I-RC-L(S)	I-RC-M(S)	I-RC-H(S)
56 days				
Porosity (%)	11.80	8.36	10.51	9.83
Porosity-mesopores (%)	5.99	3.67	6.68	5.81
Porosity-macropores (%)	5.82	4.69	3.83	4.02
Ink-bottle porosity (%)	7.64	4.81	6.73	7.38
Effective porosity (%)	4.16	3.55	3.78	2.45
Total pore area (m^2/g)	5.908	6.113	3.934	3.296
Average pore diameter (μm)	0.0373	0.0331	0.0486	0.0531
Median pore diameter –volume (μm)	0.0623	0.0531	0.127	0.099
Median pore diameter-area (μm)	0.0159	0.0162	0.0195	0.0255
Critical pore diameter (μm)	0.0612	0.0612	0.0393	0.0393
	10	-	0.2222	0.6718

3.3. AIR VOIDS: LINEAR TRAVERSE METHOD

Despite that the total air void content is routinely measured in fresh state, the characterization of the air void system in hardened concrete is not so common, and to date few investigations exists reporting air void parameters for recycled concrete in hardened state (Hansen and Hedegkd, 1984; Limbachiya et al., 1998; Salem et al., 2003; Gokce et al., 2004, 2011; Etxeberria et al., 2006).

While the total air content is commonly the only parameter specified for fresh concrete, the analysis of the air void system on hardened concrete also includes information about the air void size and distribution, which are considered more influential factors on other properties of the material such as the frost resistance since the air void system could act as an instrument to protect concrete against freeze-thaw actions relieving some of the increasing hydraulic pressure generated upon the freezing of water in the pore space of concrete. Nonetheless, further discussion on the frost resistance of the recycled concrete mixtures will be presented in chapter 9.

In the assessment of the air void system of the hardened concrete mixtures, the paste content in the tested surface should be a known parameter as per requirement of the method proposed by Powers (1949). Since the calculation of this parameter does not fall under the capabilities of the RapidAir test machine, the cement paste content was manually determined and supplied for the automatic estimations performed by the RapidAir software. For all concrete mixtures, the cement paste content was fairly similar ranging from 32.89% for the recycled concrete with the high ceramic content (II-RC-H(S)) to 33.80% for the conventional concrete (II-CC). In addition, the use of this type of equipment requires that the samples present a black and white contrast between the air voids (white), and the cement paste and aggregates (black), thus the samples were pre-treated as explained in chapter 3 (see section 3.5). Figure 7.36 shows the final appearance of one sample of each concrete batch after being coloured black and filled white $BaSO_4$ powder. At first glance, the images allow an easy identification of the air voids as well as their size, amount and spacing in the different concrete mixtures.

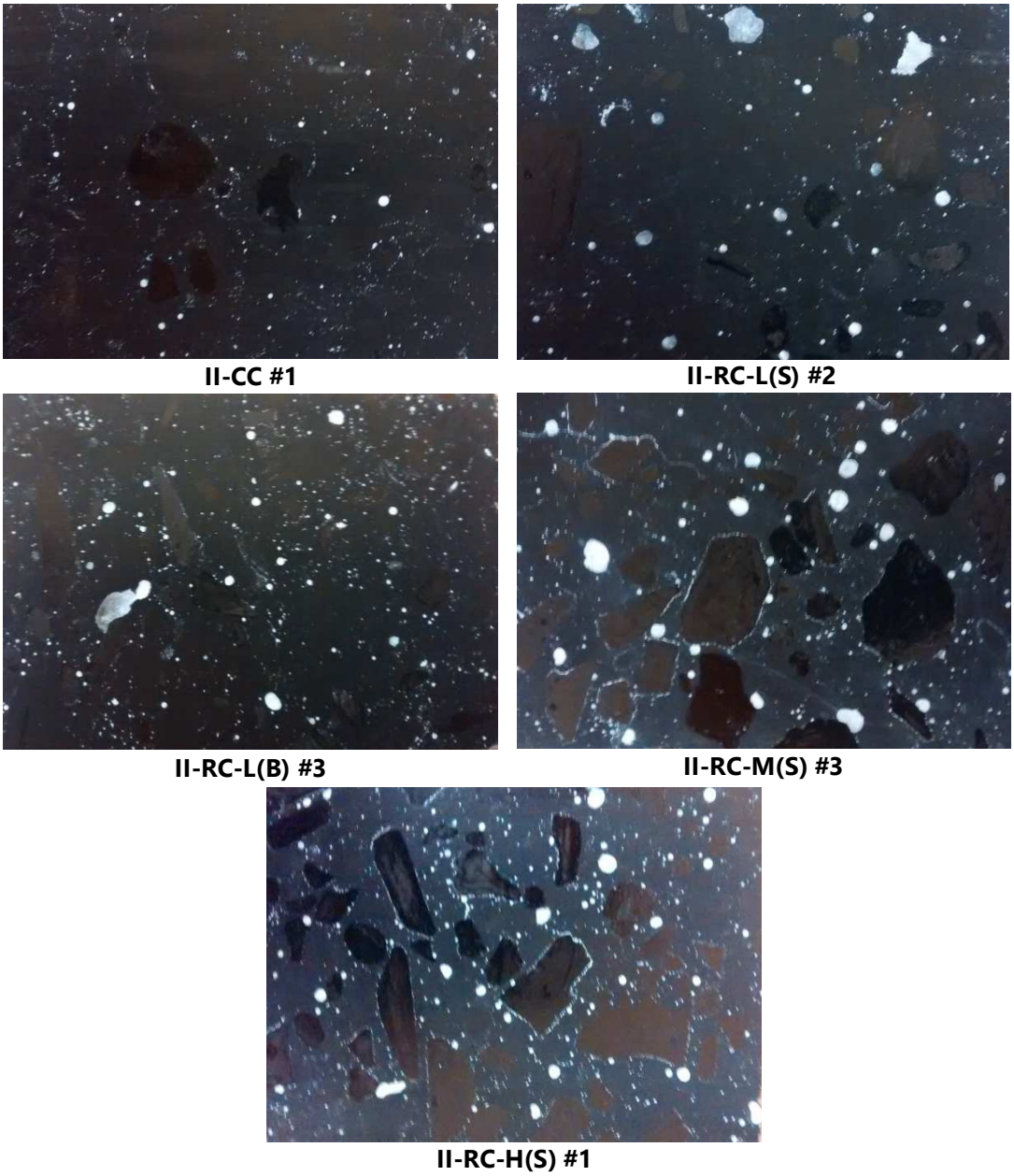

Figure 7.36: Appearance of some samples after being coloured black and filled white $BaSO_4$ powder

Table 7.2 shows the parameters used to fully characterize the air void system, i.e. the air content, the specific surface, the spacing factor and the average chord length, which were automatically calculated by the RapidAir software.

Table 7.2: Characterization parameters air void system of the concrete mixtures in phase II

	Air content (%)	Specific surface (mm^{-1})	Spacing factor (mm)	Average chord length (mm)
II-CC	0.96	36.03	0.33	0.12
II-RC-L(S)	1.57	22.43	0.45	0.20
II-RC-L(B)	2.55	18.56	0.40	0.22
II-RC-M(S)	2.72	18.00	0.44	0.25
II-RC-H(S)	2.40	16.53	0.46	0.25

The total air content is the percentage by volume of the air voids in the total volume of concrete. Analogously to the results of air content for the fresh mixtures (see Table 6.2 in chapter 6), all recycled concrete mixtures presented higher air content values than the conventional concrete. Except for mixture II-RC-M(S) that presented the same air content value in both states, the air content in hardened state is lower than that in the fresh state of the same concrete batch.

Figure 7.37 displays the relationship among both air content values in a nearly perfect linear correlation (R^2=0.96). Although for concretes made of natural aggregates, Li et al. (2013) also found a good correlation (y=1.1566x-1.2429; R^2=0.78) among the air content in hardened concrete measured by a similar technique to the linear transverse method employed in this dissertation and the air content in fresh concrete calculated by the pressure method. As stated in chapter 6 (see section 3), air bubbles are created during the concrete mixing but are highly unstable in the absence of an air entrainment agent. Hence, the handling operations (casting, compaction and finishing) result in a reduction of the air content as the air content evolves after the fresh measurements have been carried out (Van den Heede, 2014). Therefore, the fact that the air content in the fresh state evolves with time explains the mismatch between the values registered in fresh and hardened concrete.

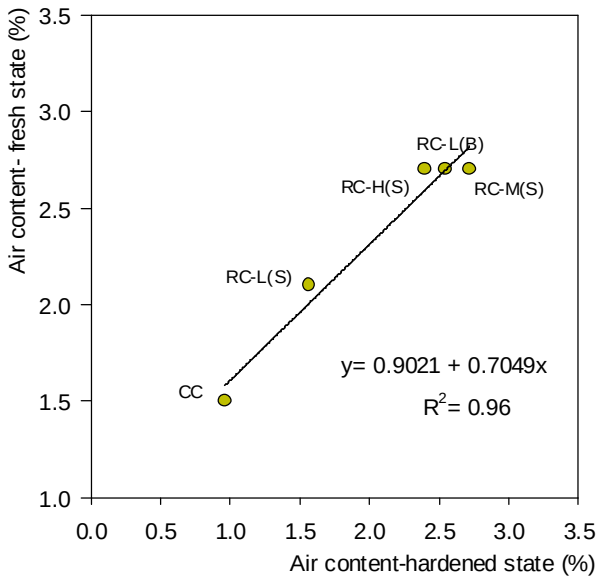

Figure 7.37: Relationship between the air content in fresh and hardened state

Generally, air content values ranging from 5% to 8% are considered necessary to ensure the frost resistance of concrete (Chatterji, 2003). Since no air entrainment agent was employed in the design of the mixtures, the air content values for all the studied batches in phase II fall below those figures. The minimum air content was presented by the conventional concrete (0.96%) and higher values, oscillating between 1.6 and 2.5 times greater, were registered for the recycled concrete mixtures as expected from the visual examination of the pre-treated samples (Figure 7.36).

Other researchers have also noticed that recycled concrete mixtures possess greater air content values than the reference concretes (Limbachiya et al., 1998; Salem et al., 2003; Etxeberria et al., 2006). In particular, Exteberria et al. (2006) reported that the air content values are higher for increasing replacement levels of recycled aggregates. A similar pattern was found in this research work (Figure 7.38), as for rising percentages of ceramic waste incorporated within the total aggregate faction the air content of the concrete tended to increase (R^2=0.62). According to Bektas et al. (2009), the crushed bricks from CDW could provide a similar behaviour than an air-entrainment agent due to their higher porosity values. However, the concentration of the air voids within the brick aggregates instead of a well distribution throughout the sample is expected to hinder the beneficial behaviour.

In addition to sufficient air content, the size and distribution of the air bubbles is of great importance. The specific surface represents the total surface of all voids divided by their total volume, which indirectly expresses the average size of the air void system (Pinto and Hover, 2001; Kosmatka et al., 2002). Thus, higher specific surface values are preferable since they indicate a larger number of small air voids since smaller bubbles possess a larger surface area-to-volume ratio. The results (Table 7.2) show that the use of recycled aggregates with varying percentages of ceramic decreases the specific surface values, i.e. the conventional concrete presented finer air void pores than the recycled concrete mixtures. Moreover, a modest correlation (R^2=0.76) was found among the reduction of the specific surface (oscillating between 37% and 54%) and the increasing amounts of ceramic aggregates incorporated in the recycled concrete mixtures (Figure 7.38).

According to Pigeon and Pleu (1995), specific surface values in the range of 25 mm^{-1} to 45 mm^{-1} are considered acceptable for freeze/thaw resistance of the concrete. However, only the conventional concrete mostly complies with the recommendation without using an air entrainment agent.

Regarding to the adequate distribution of the air bubbles, Powers and Willis (1949) proposed the spacing factor parameter to directly relate the air void system to the susceptibility of a concrete mixture to frost damage. The spacing factor represents the path length that water should travel before entering an air void; thus, smaller values are required for a higher reduction in pressure. Once again, recycled concrete mixtures displayed a worse performance compared to the conventional concrete with a decrease in the spacing factors ranging from 21% to 39%.

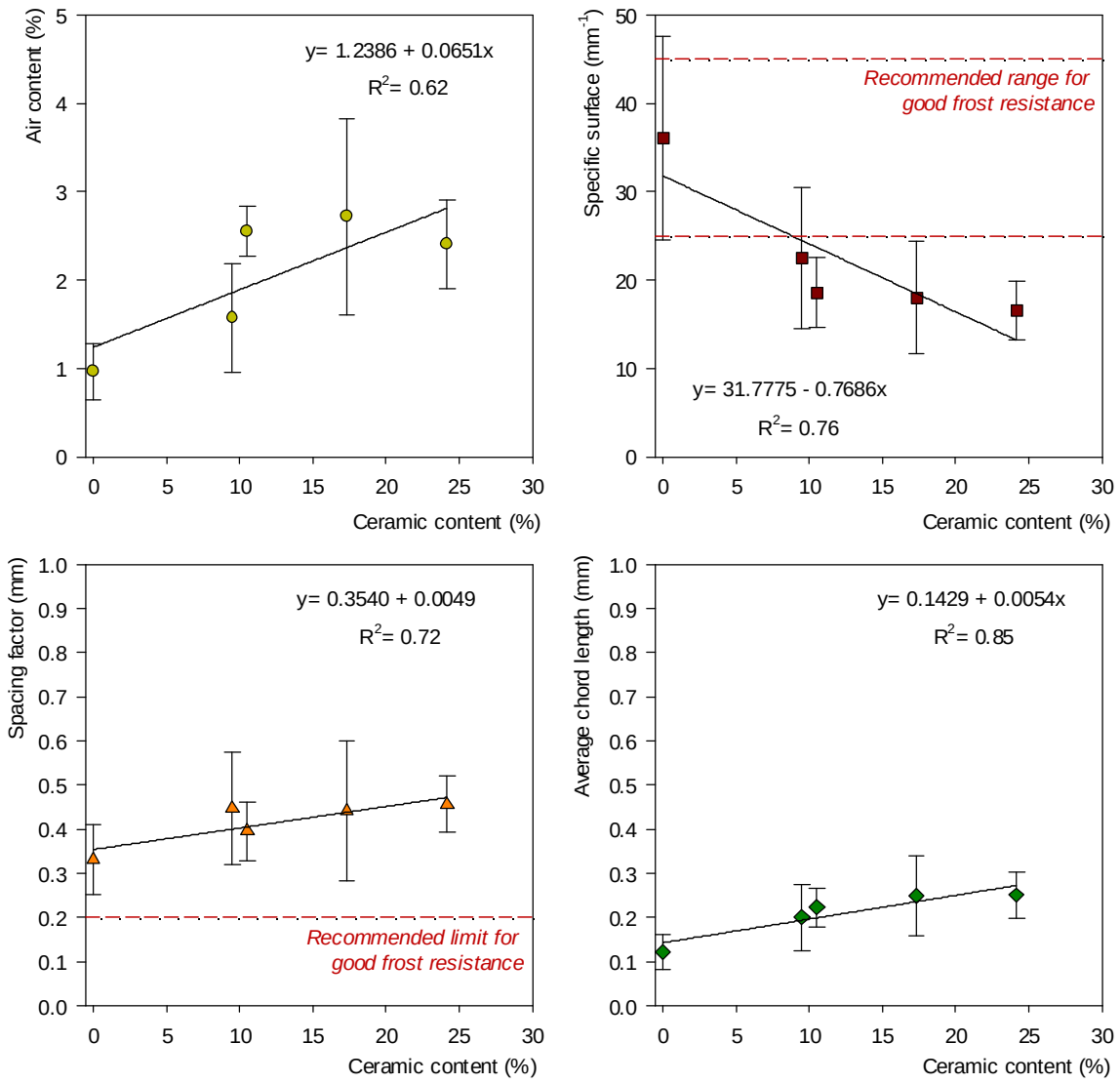

Figure 7.38: Relationship between the characterization parameters of the air void system (air content, specific surface, spacing factor and average chord length) and the ceramic content incorporated in the total weight of aggregates

Figure 7.38 suggests that also a modest correlation (R^2=0.72) could be established between the spacing factor and the percentage of ceramic waste incorporated in the recycled concrete as part of the total weight of aggregates. In general, a maximum spacing factor up to 0.20 mm is recommended for ordinary concretes in order to guarantee a good frost resistance (Powers, 1975). However, all concrete mixes studied exceed this value.

Notwithstanding the fact that none of the recycled concrete mixtures comply with the recommendations in air content, specific surface or spacing factor, some researchers have suggested that the inherent porosity of the CDW may provide a greater air void system that could aid in the control of the freeze/thaw damage in the recycled concrete (Richardson et al., 2011). Thus, further discussions regarding this topic can be found in chapter 9.

Finally, the average chord length of the recycled concrete mixtures is between 1.7 and 2 times higher than that of the conventional concrete, which is in agreement with the decreasing results for specific surface exhibited by the use of recycled aggregates. Both facts indicate the presence of finer pores in conventional concrete as could be observed in Figure 7.36. In addition, Figure 7.38 shows a direct relationship between the coarsening of the air void system and the rising incorporation of ceramic recycled aggregates in the total weight of aggregates (R^2=0.85) due to the higher porosity of this material.

In order to assess the air void size distribution in a more detailed manner, Figure 7.39 shows the chord length frequency of all chords traversed during the analysis and the air content included in the respective chord size interval. Since small air voids play a key role guaranteeing the frost resistance of concrete, the percentage of chord length equal or inferior to 500 μm from the total air void system has been assessed for all concrete samples. As expected, the conventional concrete showed the higher proportion (69%), followed by one of the recycled mixtures with low ceramic (II-RC-L(S)) with a percentage up to 51%. Both, the other recycled mixture with low ceramic (II-RC-L(B)) and the recycled mixture with high ceramic (II-RC-H(S)) presented similar percentages, 45% and 42%, respectively. Finally, the recycled mixture with medium ceramic (II-RC-M(S)) displayed the lower proportion (37%). All these results continue to suggest a worse performance against freeze-thaw cycles, since the proportion of smaller air voids in the recycled concrete mixtures is lower.

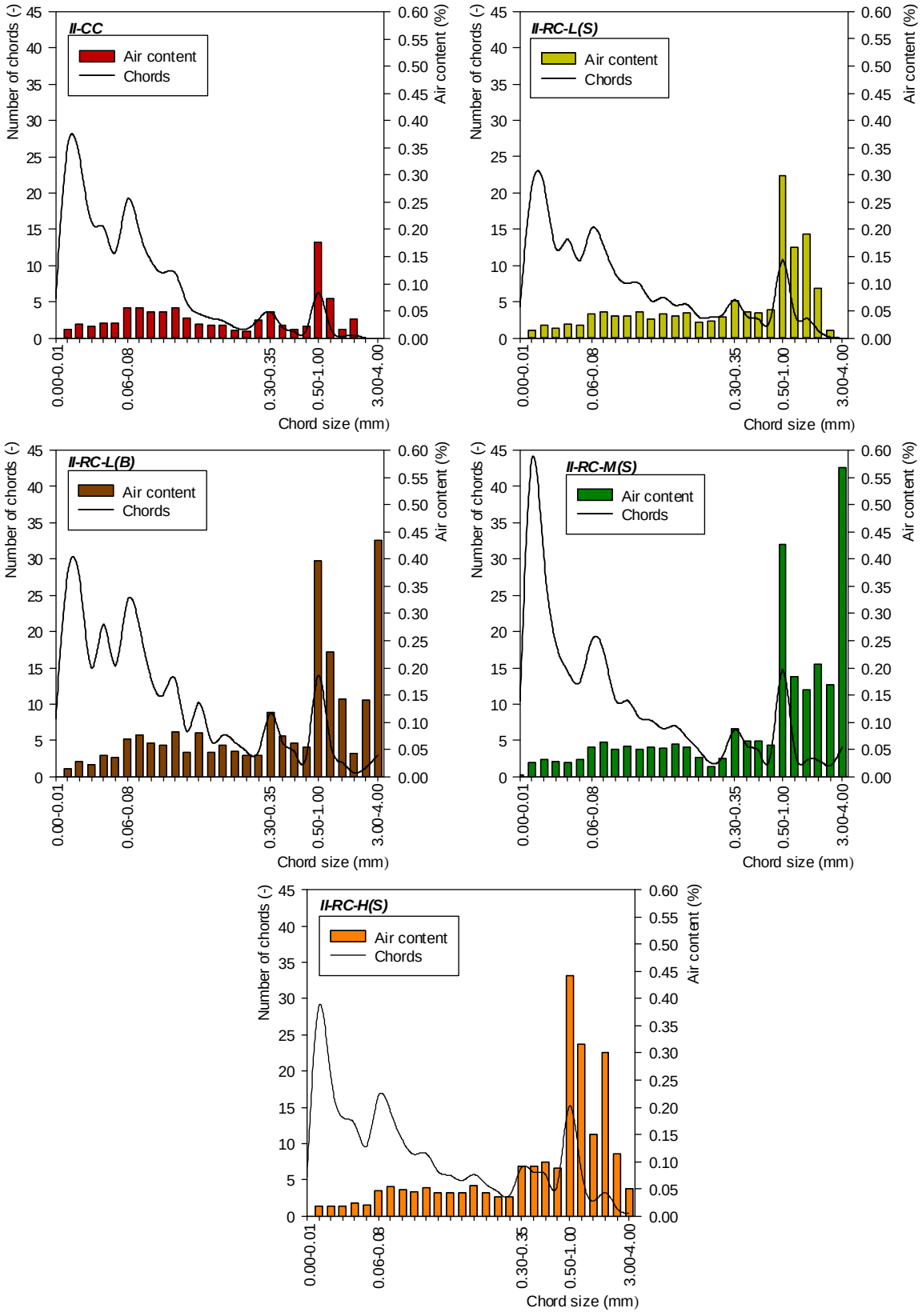

Figure 7.39: Chord length distribution and air content

4. REFERENCES

Abell, A.B., Willis, K.L., Lange, D.A., 1999. Mercury intrusion porosimetry and image analysis of cement-based materials. *Journal of Colloid and Interface Science* 211 (1): 39–44.

Aono, Y., Matsushita, F., Shibata, S., Hama, Y., 2007. Nano-structural changes of C-S-H in hardened cement paste during drying at 50°C. *Journal of Advanced Concrete Technology* 5 (3): 313–323.

Barra Bizinotto, M., 1996. Study on recycled concrete durability for structural concrete [in Spanish]. Universitat Politècnica de Catalunya (UPV), Barcelona, Spain.

Bazant, Z.P., Wittmann, F.H. (Eds.), 1982. Creep and shrinkage in concrete structures. Wiley Chichester.

Bektas, F., Wang, K., Ceylan, H., 2009. Effects of crushed clay brick aggregate on mortar durability. *Construction and Building Materials*, Compatibility of Plasters and Renders on Salt Loaded Substrates 23 (5): 1909–1914.

Bentur, A., Alexander, M.G., 2000. A review of the work of the RILEM TC 159-ETC: Engineering of the interfacial transition zone in cementitious composites. *Materials and structures* 33 (2): 82–87.

Bermejo, E.B., Moragues, A., Gálvez, J.C., Fernández Cánovas, M., 2010. Permeability and pore size distribution in medium strength self-compacting concrete. *Materiales de Construcción* 60 (299): 37–51.

Brouwers, H.J.H., 2005. The work of Powers and Brownyard revisited: Part 2. *Cement and Concrete Research* 35 (10): 1922–1936.

Buyle-Bodin, F., Hadjieva-Zaharieva, R., 2002. Influence of industrially produced recycled aggregates on flow properties of concrete. *Mat. Struct.* 35 (8): 504–509.

Carles-Gibergues, A., Saucier, F., Grandet, J., Pigeon, M., 1993. New-to-old concrete bonding: Influence of sulfates type of new concrete on interface microstructure. *Cement and Concrete Research* 23 (2): 431–441.

CEB, 1998. Strategies for testing and assessment of concrete structures affected by reinforcement corrosion (CEB Bulletin 243). CEB, Switzerland.

Chatterji, S., 2003. Freezing of air-entrained cement-based materials and specific actions of air-entraining agents. *Cement and Concrete Composites* 25 (7): 759–765.

Chen, W., 2006. Hydration of slag cement: theory, modeling and application. University of Twente, Netherlands.

Chen, W., Brouwers, H.J.H., 2007. The hydration of slag. Part 2: reaction models for blended cement. *J Mater Sci* 42 (2): 444–464.

Cook, R.A., Hover, K.C., 1993. Mercury porosimetry of cement-based materials and associated correction factors. *Construction and Building Materials* 7 (4): 231–240.

Cook, R.A., Hover, K.C., 1999. Mercury porosimetry of hardened cement pastes. *Cement and Concrete Research* 29 (6): 933–943.

Corinaldesi, V., Moriconi, G., 2009. Influence of mineral additions on the performance of 100% recycled aggregate concrete. *Construction and Building Materials* 23 (8): 2869–2876.

Delagrave, A., Bigas, J.P., Ollivier, J.P., Marchand, J., Pigeon, M., 1997. Influence of the interfacial zone on the chloride diffusivity of mortars. *Advanced Cement Based Materials* 5 (3–4): 86–92.

Diamond, S., 1971. A critical comparison of mercury porosimetry and capillary condensation pore size distributions of portland cement pastes. *Cement and Concrete Research* 1 (5): 531–545.

Diamond, S., 1986. The microstructure of cement paste in concrete, in: Proceedings of the 8th International Congress on the Chemistry of Cement. Rio de Janeiro, Brazil, 122–147.

Diamond, S., 2000. Mercury porosimetry: An inappropriate method for the measurement of pore size distributions in cement-based materials. *Cement and Concrete Research* 30 (10): 1517–1525.

Diamond, S., 2003. A discussion of the paper "Effect of drying on cement-based materials pore structure as identified by mercury porosimetry: a comparative study between oven, vacuum, and freeze-drying" by C. Gallé. *Cement and Concrete Research* 33 (1): 169–170.

Diamond, S., 2004. The microstructure of cement paste and concrete—a visual primer. *Cement and Concrete Composites* 26 (8): 919–933.

Diamond, S., Huang, J., 2001. The ITZ in concrete – a different view based on image analysis and SEM observations. *Cement and Concrete Composites*, Special Theme Issue on Image Analysis 23 (2–3): 179–188.

Elsharief, A., Cohen, M.D., Olek, J., 2003. Influence of aggregate size, water cement ratio and age on the microstructure of the interfacial transition zone. *Cement and Concrete Research* 33 (11): 1837–1849.

Escalante-García, J.I., Sharp, J.H., 1998. Effect of temperature on the hydration of the main clinker phases in portland cements: part ii, blended cements. *Cement and Concrete Research* 28 (9): 1259–1274.

Espinosa, R.M., Franke, L., 2006. Influence of the age and drying process on pore structure and sorption isotherms of hardened cement paste. *Cement and Concrete Research* 36 (10): 1969–1984.

Etxeberria, M., Vázquez, E., Mari, A., 2006. Microstructure analysis of hardened recycled aggregate concrete. *Magazine of Concrete Research* 58 (10): 683–690.

Everett, D.H., 1972. Manual of symbols and terminology for physicochemical quantities and units. Appendix II: Definitions, terminology and symbols in colloid and surface chemistry. *Pure and Applied Chemistry* 31 (4): 577–638.

Feldman, R.F., 1984. Pore structure damage in blended cements caused by mercury intrusion. *Journal of the American Ceramic Society* 67 (1): 30–33.

Fulton, F.S., 1974. The properties of Portland cements containing milled granulated blast-furnace slag. Portland Cement Institute.

Gallé, C., 2001. Effect of drying on cement-based materials pore structure as identified by mercury intrusion porosimetry: A comparative study between oven, vacuum, and freeze-drying. *Cement and Concrete Research* 31 (10): 1467–1477.

Gallé, C., 2003. Reply to the discussion by S. Diamond of the paper "Effect of drying on cement-based materials pore structure as identified by mercury intrusion porosimetry: a comparative study between oven, vacuum and freeze-drying." *Cement and Concrete Research* 33 (1): 171–172.

Gao, Y., De Schutter, G., Ye, G., Huang, H., Tan, Z., Wu, K., 2013. Porosity characterization of ITZ in cementitious composites: Concentric expansion and overflow criterion. *Construction and Building Materials* 38: 1051–1057.

Gao, Y., De Schutter, G., Ye, G., Tan, Z., Wu, K., 2014. The ITZ microstructure, thickness and porosity in blended cementitious composite: Effects of curing age, water to binder ratio and aggregate content. *Composites Part B: Engineering* 60: 1–13.

Gokce, A., Nagataki, S., Saeki, T., Hisada, M., 2004. Freezing and thawing resistance of air-entrained concrete incorporating recycled coarse aggregate: The role of air content in demolished concrete. *Cement and Concrete Research* 34 (5): 799–806.

Gokce, A., Nagataki, S., Saeki, T., Hisada, M., 2011. Identification of frost-susceptible recycled concrete aggregates for durability of concrete. *Construction and Building Materials* 25 (5): 2426–2431.

Gómez-Soberón, J.M.V., 2002. Porosity of recycled concrete with substitution of recycled concrete aggregate: An experimental study. *Cement and Concrete Research* 32 (8): 1301–1311.

Gruyaert, E., 2011. Effect of blast-furnace slag as cement replacement on hydration, microstructure, strength and durability of concrete. Ghent University, Ghent, Belgium.

Hansen, T.C., Hedegkd, S.E., 1984. Properties of recycled aggregate concretes as affected by admixtures in original concretes. *ACI Journal Proceedings* 81 (1).

Hewlett, P. (Ed.), 2003. Lea's chemistry of cement and concrete. Butterworth-Heinemann.

Hogan, F.J., Meusel, J.W., 1981. Evaluation for durability and strength development of a ground granulated blast furnace slag. *Cement, Concrete and Aggregates* 3 (1): 40–52.

Hu, J., 2004. Porosity of concrete. Morphological study of model concrete. Delft University, Netherlands.

Jennings, H.M., Bullard, J.W., Thomas, J.J., Andrade, J.E., Chen, J.J., Scherer, G.W., 2008. Characterization and modeling of pores and surfaces in cement paste: correlations to processing and properties. *Journal of Advanced Concrete Technology* 6 (1): 5–29.

Jons, E.S., Osbaeck, B., 1982. The effect of cement composition on strength described by a strength-porosity model. *Cement and Concrete Research* 12 (2): 167–178.

Katz, A., 2004. Treatments for the Improvement of Recycled Aggregate. *Journal of Materials in Civil Engineering* 16 (6): 597–603.

Konecny, L., Naqvi, S.J., 1993. The effect of different drying techniques on the pore size distribution of blended cement mortars. *Cement and Concrete Research* 23 (5): 1223–1228.

Kong, D., Lei, T., Zheng, J., Ma, C., Jiang, J., Jiang, J., 2010. Effect and mechanism of surface-coating pozzalanics materials around aggregate on properties and ITZ microstructure of recycled aggregate concrete. *Construction and Building Materials* 24 (5): 701–708.

Kong, D., Zheng, J., Zhou, X., 2006. Strengthening of the ITZ in recycled aggregate concrete, in: Proceedings of Architecture in Harmony. Presented at the Xi'an international conference on architecture and technology, Xian, PRC, 614–7.

Kosmatka, S.H., Panarese, W.C., Kerkhoff, B., 2002. Design and control of concrete mixtures. Portland Cement Association.

Kou, S.C., Poon, C.S., Etxeberria, M., 2011. Influence of recycled aggregates on long term mechanical properties and pore size distribution of concrete. *Cement and Concrete Composites* 33 (2): 286–291.

Kroone, B., Crook, D.N., 1961. Studies of pore size distribution in mortars. *Magazine of Concrete Research* 13 (39): 127–132.

Kumar, R., Bhattacharjee, B., 2003. Study on some factors affecting the results in the use of MIP method in concrete research. *Cement and Concrete Research* 33 (3): 417–424.

Lange, D.A., Jennings, H.M., Shah, S.P., 1994. Image analysis techniques for characterization of pore structure of cement-based materials. *Cement and Concrete Research* 24 (5): 841–853.

Langton, C.A., Grutzeck, M.W., Roy, D.M., 1980. Chemical and physical properties of the interfacial region formed between unreactive aggregate and hydrothermally cured cement. *Cement and Concrete Research* 10 (3): 449–454.

Lee, G.C., Choi, H.B., 2013. Study on interfacial transition zone properties of recycled aggregate by micro-hardness test. *Construction and Building Materials* 40: 455–460.

Leemann, A., Münch, B., Gasser, P., Holzer, L., 2006. Influence of compaction on the interfacial transition zone and the permeability of concrete. *Cement and Concrete Research* 36 (8): 1425–1433.

Li, H., Xie, Y., Yang, L., 2013. Air-void parameters measurement of fresh concrete and hardened concrete. *Journal of Central South University* 20 (4): 1103–1108.

Li, J., Xiao, H., Zhou, Y., 2009. Influence of coating recycled aggregate surface with pozzolanic powder on properties of recycled aggregate concrete. *Construction and Building Materials* 23 (3): 1287–1291.

Limbachiya, M., Leelawat, T., Dhir, R., 1998. RCA concrete: a study of properties in the fresh state, strength development and durability, in: Proceedings of the International Symposium on Sustainable Construction: Use of Recycled Concrete Aggregate. London, UK.

Li, W., Zhang, H.Y., 2013. Analysis of Microstructure of Interfacial Transition Zone (ITZ) in Recycled Aggregate Concrete. *Advanced Materials Research* 811: 249–253.

Li, Z., 2011. Structure of Concrete, in: Advanced Concrete Technology. John Wiley & Sons, Inc., 140–163.

Locher, F., Richartz, W., Sprung, S., 1976. Solidification of cement [in German]. *Zement-Kalk-Gips* 29 (10): 435–442.

Locher, F.W., 1976. Strength of cement [in German]. *Beton* 26 (8): 283–286.

Manzi, S., Mazzotti, C., Bignozzi, M.C., 2013. Short and long-term behavior of structural concrete with recycled concrete aggregate. *Cement and Concrete Composites* 37: 312–318.

Maso, J., 1980. The bond between aggregates and hydrated cement pastes, in: Proceedings of the 7th International Cement Congress. 3–15.

Medina, C., Frías, M., Sánchez de Rojas, M.I., 2012. Microstructure and properties of recycled concretes using ceramic sanitary ware industry waste as coarse aggregate. *Construction and Building Materials* 31: 112–118.

Medina, C., Zhu, W., Howind, T., Frías, M., Sánchez de Rojas, M.I., 2015. Effect of the constituents (asphalt, clay materials, floating particles and fines) of construction and demolition waste on the properties of recycled concretes. *Construction and Building Materials* 79: 22–33.

Meinhard, K., Lackner, R., 2008. Multi-phase hydration model for prediction of hydration-heat release of blended cements. *Cement and Concrete Research* 38 (6): 794–802.

Mindess, S., Odler, I., Skalny, J., 1986. Significance to concrete performance of interfaces and bond: challenges of the future, in: Proceedings of the 8th International Congress on the Chemistry of Cement. Rio de Janeiro, Brazil, 151–157.

Mindess, S., Young, J.F., Darwin, D., 2002. Concrete, 2 edition. ed. Prentice Hall, Upper Saddle River, NJ.

Monteiro, J.J.M., Mehta, P.K., 1985. Ettringite formation on the aggregate — cement paste interface. *Cement and Concrete Research* 15 (2): 378–380.

Moukwa, M., Aïtcin, P.-C., 1988. The effect of drying on cement pastes pore structure as determined by mercury porosimetry. *Cement and Concrete Research* 18 (5): 745–752.

Mueller, A., Winkler, A., 1998. Characteristics of processed concrete rubble, in: Uses of Recycled Concrete Aggregate. Sustainable Construction. Tomas Telford, London, UK, 1109–1119.

Nagataki, S., Gokce, A., Saeki, T., Hisada, M., 2004. Assessment of recycling process induced damage sensitivity of recycled concrete aggregates. *Cement and Concrete Research* 34 (6): 965–971.

Neville, A.M., 1995. Properties of concrete. Harlow, Essex : Longman.

Nonat, A., Mutin, J.., 1992. From hydration to setting, in: Proceedings of the 2nd International RILEM Symposium on Hydration and Setting.

Oberholster, R., 1986. Pore structure, permeability and diffusivity of hardened cement paste and concrete in relation to durability: status and prospects, in: Proceedings of the 8th International Congress on Chemistry of Cement. Rio de Janeiro, Brazil, 323–335.

Odler, I., Hagymassy Jr., J., Bodor, E.E., Yudenfreund, M., Brunauer, S., 1972. Hardened portland cement pastes of low porosity IV. Surface area and pore structure. *Cement and Concrete Research* 2 (5): 577–589.

Ollivier, J.P., Maso, J.C., Bourdette, B., 1995. Interfacial transition zone in concrete. *Advanced Cement Based Materials* 2 (1): 30–38.

Olson, R.A., Neubauer, C.M., Jennings, H.M., 1997. Damage to the pore structure of hardened Portland cement paste by mercury intrusion. *Journal of the American Ceramic Society* 80 (9): 2454–2458.

Page, C.L., Short, N.R., El Tarras, A., 1981. Diffusion of chloride ions in hardened cement pastes. *Cement and Concrete Research* 11 (3): 395–406.

Pigeon, M., Pleau, R., 1995. Durability of concrete in cold climates, Modern Concrete Technology. E&FN Spon.

Ping, X., Beaudoin, J.J., Brousseau, R., 1991. Effect of aggregate size on transition zone properties at the portland cement paste interface. *Cement and Concrete Research* 21 (6): 999–1005.

Pinto, R.C.A., Hover, K.C., 2001. Frost and scaling resistance of high-strength concrete (No. RD122), Research & Development Bulletin. Portland Cement Association.

Poon, C.S., Shui, Z.H., Lam, L., 2004. Effect of microstructure of ITZ on compressive strength of concrete prepared with recycled aggregates. *Construction and Building Materials* 18 (6): 461–468.

Powers, T., 1975. Freezing effects in concrete. *ACI Special Publication* 47: 1–12.

Powers, T.C., 1958. Structure and Physical Properties of Hardened Portland Cement Paste. *Journal of the American Ceramic Society* 41 (1): 1–6.

Powers, T.C., Willis, T.F., 1949. The air requirement of forest resistance concrete. *Highway Research Board Proceedings* 29: 184–211.

Prokopski, G., Halbiniak, J., 2000. Interfacial transition zone in cementitious materials. *Cement and Concrete Research* 30 (4): 579–583.

Richardson, A., Coventry, K., Bacon, J., 2011. Freeze/thaw durability of concrete with recycled demolition aggregate compared to virgin aggregate concrete. *Journal of Cleaner Production* 19 (2–3): 272–277.

Richardson, I.G., Groves, G.W., 1992. Microstructure and microanalysis of hardened cement pastes involving ground granulated blast-furnace slag. *Journal of Materials Science* 27 (22): 6204–6212.

RILEM TC 108-ICC, 1996. Interfacial transition zone in concrete. CRC Press.

Robeyst, N., 2009. Monitoring setting and microstructure development in fresh concrete with the ultrasonic through-transmission method. Ghent University, Ghent, Belgium.

Rübner, K., Fritz, T., Jacobs, F., 2002. Precision of porosity measurements on cementitious mortars, in: F. Rodriguez-Reinoso, B.M. J. Rouquerol and K. Unger (Ed.), Studies in Surface Science and Catalysis, Characterization of Porous Solids VI Proceedings of the 6th International Symposium on the Characterization of Porous Solids (COPS-VI). Elsevier, 459–466.

Rübner, K., Hoffmann, D., 2006. Characterization of mineral building materials by mercury intrusion porosimetry. *Particle & Particle Systems Characterization* 23 (1): 20–28.

Sagoe-Crentsil, K.K., Brown, T., Taylor, A.H., 2001. Performance of concrete made with commercially produced coarse recycled concrete aggregate. *Cement and Concrete Research* 31 (5): 707–712.

Salem, R.M., Burdette, E.G., Jackson, N.M., 2003. Resistance to freezing and thawing of recycled aggregate concrete. *ACI Materials Journal* 100 (3): 216–221.

Sánchez de Juan, M., 2004. Study on the use of recycled aggregate in structural concrete [in Spanish]. E.T.S.I. Caminos, Canales y Puertos (UPM), Madrid, Spain.

Scrivener, K.L., Crumbie, A.K., Laugesen, P., 2004. The Interfacial transition zone (ITZ) between cement paste and aggregate in concrete. *Interface Science* 12 (4): 411–421.

Scrivener, K.L., Nemati, K.M., 1996. The percolation of pore space in the cement paste/aggregate interfacial zone of concrete. *Cement and Concrete Research* 26 (1): 35–40.

Scrivener, K.L., Pratt, P.L., 1984. Backscattered electron images of polished cement sections in the scanning electron microscope, in: Proceedings of the International Conference on Cement Microscopy. New Mexico, U.S.A, 145–155.

Senthamarai, R., Manoharan, P.D., Gobinath, D., 2011. Concrete made from ceramic industry waste: Durability properties. *Construction and Building Materials* 25 (5): 2413–2419.

Shi-Ping, J., Grandet, J., 1989. Compared evolution of a slag cement mortar with Portland cement mortars [in French]. *Cement and Concrete Research* 19 (3): 487–496.

Sidorova, A., Vazquez-Ramonich, E., Barra-Bizinotto, M., Roa-Rovira, J.J., Jimenez-Pique, E., 2014. Study of the recycled aggregates nature's influence on the aggregate–cement paste interface and ITZ. *Construction and Building Materials* 68: 677–684.

Snoeck, D., Velasco, L.F., Mignon, A., Van Vlierberghe, S., Dubruel, P., Lodewyckx, P., De Belie, N., 2014. The influence of different drying techniques on the water sorption properties of cement-based materials. *Cement and Concrete Research* 64: 54–62.

Tam, V.W.Y., Gao, X.F., Tam, C.M., 2005. Microstructural analysis of recycled aggregate concrete produced from two-stage mixing approach. *Cement and Concrete Research* 35 (6): 1195–1203.

Tanaka, H., Totani, Y., Saito, Y., 1983. Structure of hydrated glassy blast furnace slag contents. *SP* 79: 963–978.

Tasong, W.A., Cripps, J.C., Lynsdale, C.J., 1998. Aggregate-cement chemical interactions. *Cement and Concrete Research* 28 (7): 1037–1048.

Tasong, W.A., Lynsdale, C.J., Cripps, J.C., 1999. Aggregate-cement paste interface: Part I. Influence of aggregate geochemistry. *Cement and Concrete Research* 29 (7): 1019–1025.

Taylor, H.F., 1997. Cement chemistry. Thomas Telford.

Ulloa Mayorga, V.A., 2012. Durability of reinforced recycled concrete: assessment of the chloride corrosion on a marine environment [in Spanish]. Universitat Politècnica de València, Valencia, Spain.

Van Breugel, K., 1991. Simulation of hydration and formation of structure in hardening cement-based materials. Delft University, Netherlands.

Van den Heede, P., 2014. Durability and sustainability of concrete with high volumes of fly ash. Ghent University, Ghent, Belgium.

Wainwright, P., Ait-Aider, H., 1995. The influence of cement source and slag additions on the bleeding of concrete. *Cement and Concrete Research* 25 (7): 1445–1456.

Wang, Y., Diamond, S., 1994. An approach to quantitative image analysis for cement pastes, in: Proceedings of Material Research Society. Presented at the Symposia Va/Vb – Microstructure of Cement-Based Systems/Bonding and Interfaces in Cement..., Pittsburgh, U.S.A.

Winslow, D.N., Diamond, S., 1970. A mercury porosimetry study of the porosity in Portland cement. *Journal of Materials (ASTM)* 5 (3): 564–585.

Xiao, J., Li, W., Sun, Z., Lange, D.A., Shah, S.P., 2013. Properties of interfacial transition zones in recycled aggregate concrete tested by nanoindentation. *Cement and Concrete Composites* 37: 276–292.

Ye, G., 2003. Experimental study and numerical simulation of the development of the microstructure and permeability of cementitious materials. Delft University, Netherlands.

Zaharieva, R., Buyle-Bodin, F., Skoczylas, F., Wirquin, E., 2003. Assessment of the surface permeation properties of recycled aggregate concrete. *Cement and Concrete Composites* 25 (2): 223–232.

Zhang, L., Glasser, F.P., 2000. Critical examination of drying damage to cement pastes. *Advances in Cement Research* 12 (2): 79–88.

Zhou, J., Ye, G., van Breugel, K., 2010. Characterization of pore structure in cement-based materials using pressurization–depressurization cycling mercury intrusion porosimetry (PDC-MIP). *Cement and Concrete Research* 40 (7): 1120–1128.

Chapter 8

Mechanical behaviour

1. INTRODUCTION

Numerous are the investigations reporting conclusions regarding the effect that a partial or total substitution of the coarse aggregate fraction by recycled aggregates have on the mechanical performance of recycled mixtures when compared to a reference concrete. It is widely recognised that quality of recycled aggregates influence the concrete strength. Nonetheless, there are a predominance of studies focusing on recycled concrete aggregates as this type of aggregates are more homogenous and only differ from natural aggregates in the adhered mortar. This chapter aims to study the mechanical behaviour of recycled concrete made with recycled aggregates from CDW with varying percentages of ceramic waste.

2. DENSITY

It is widely recognized that the density of concrete is mainly influenced by the density of the aggregates employed in its manufacture (Matias et al., 2013). Hence, the hardened density of recycled concretes is lower than that of conventional mixtures due to the lower density of the recycled aggregates as consequence of the presence of adhered mortar, clay-based particles and floating materials (González-Fonteboa and Martínez-Abella, 2008; Medina et al., 2014).

Beltrán et al. (2014b) observed that the use of additional amounts of cement did not mitigate the density loss of the recycled mixtures with respect to the conventional concrete. For 20%, 50% and 100% substitution levels, a maximum 2.51%, 4.18% and 6.28% reduction was reported, respectively. For the same replacement ratios, González-Corominas and Etxeberria (2014)

registered declines of 3.19%, 6.37% and 12.75% in the dry hardened density of recycled concrete compared to a conventional control mixture. For a 50% substitution, Medina et al. (2014, 2015) estimated a decline of 2.11% in the hardened density of recycled concrete. The authors also observed that the removal of the floating particles present in the mixed recycled aggregates reduced the density loss of the recycled concrete by 29.86%. Rodríguez-Robles et al. (2015) observed saturated density values 2.10% and 3.36% lower for recycled mixtures with a 50% replacement ratio of mixed recycled aggregates containing 34% and 68% of ceramic wastes. The regression estimates of Martínez-Lage et al. (2012) pointed to decreases of 3.91% and 7.76% for replacement ratios of 50% and 100%. For a full substitution, Sheen et al. (2013) registered declines between 3.14% and 6.49% in the unit weight of recycled concrete with mixed recycled aggregates containing ceramic wastes up to 67%. The authors explained the density loss through the higher porosity of the recycled aggregates, and the higher air content of the recycled concrete compared to the reference mixture. When replacing all natural aggregates by mixed recycled aggregates, density losses around 10% were observed by Beltrán et al. (2014a) and Dilbas et al. (2014) for total replacements, whereas López-Gayarre et al. (2015) reported an average decrease of 11.56%. The authors also observed that the density values of recycled concrete diminished for increasing water/cement ratios, which is in agreement with the results of Thomas et al. (2013b) for recycled concrete aggregates.

Regarding the use of ceramic aggregates, Khalaf (2006) registered average declines of 10.96% and 12.28% for recycled brick concretes with normal and high strength compared to conventional mixtures, respectively. For 100% crushed tile coarse aggregates, Topçu and Canbaz (2007) observed a 5.90% reduction in the unit weight of the hardened concrete compared to the conventional mixture. For full replacement with crushed bricks, Afify and Soliman (2014) observed an average density loss of 14.10% compared to that of the concrete made with dolomite aggregates without admixtures or silica fume. Zhang and Zong (2014) observed an approximately decline of 6.80% when 40% crushed bricks were used as recycled coarse aggregates. For a 50% substitution level with crushed bricks, Zong et al. (2014) noticed a decline in the hardened density up to 12.43%. Finally, Adamson et al. (2015) observed decreases between 3.75% and 5.42% for replacements of the natural aggregates by crushed clay bricks ranging from 25% to 50%.

The saturated surface-dried density results of the hardened concrete are given in Table 8.1. As expected, the conventional concrete presented the highest density value and the recycled mixtures oscillated between 2200 kg/m^{3}and 2330 kg/m^3, which represents reductions ranging from 2.06% to 7.52%. The differences among the recycled mixes are directly related to the composition of the aggregates (Figure 8.1).

Table 8.1: Density of the hardened concrete mixtures

	Phase II (kg/m^3)	**Variation (%)**
CC	2379	-
RC-L(S)	2330	-2.06
RC-L(B)	2232	-6.18
RC-M(S)	2220	-6.68
RC-H(S)	2200	-7.52

Several researchers have reported that the hardened density of the concrete decreased as the natural aggregate replacement with mixed recycled aggregates increased (Martínez-Lage et al., 2012; Mas et al., 2012a, 2012b; Beltrán et al., 2014b; Gonzalez-Corominas and Etxeberria, 2014; Medina et al., 2014, 2015). In addition, increasing percentages of ceramic aggregates have also been linked to proportional decreases of the concrete density (Sheen et al., 2013; Zhang and Zong, 2014; Zong et al., 2014; Adamson et al., 2015). Thus, the relationship observed between the hardened density and the ceramic content incorporated in the concrete mixture (R^2=0.80) agrees with the tendency observed in the literature review (Figure 8.1).

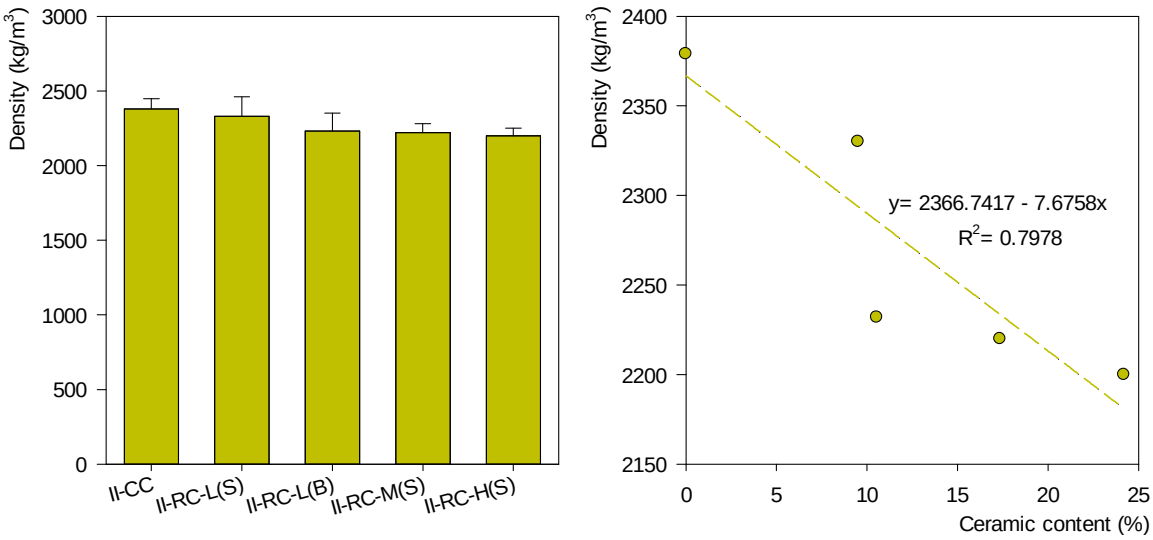

Figure 8.1: Density of the hardened concrete mixtures and its relationship with the ceramic content incorporated in the total weight of aggregates

3. COMPRESSIVE STRENGTH

The characteristic compressive strength is often the only engineering property of concrete that is consistently specified since it constitutes the basis for the estimation of most of the other mechanical properties. Hence, the influence of the use of recycled aggregates on this property has been thoroughly investigated. Despite the agreement regarding the decrease in compressive strength for increasing replacement ratios (Dhir et al., 1999; Xiao et al., 2005; Etxeberria et al., 2007; Yang et al., 2008), there is no consensus in the magnitude of the resistance loss. Besides, the differences are more pronounced at lower water/cement ratios (Dhir et al., 1999; Chen et al., 2003a; Otsuki et al., 2003; Rao et al., 2007; Gonzalez and Etxeberria, 2014). Initially, marginal declines are to be expected for substitution levels below 30% (Dhir and Paine, 2004; Rao et al., 2011; Yang et al., 2011). However, recycled mixtures with a 100% replacement ratio of recycled concrete aggregates can exhibit a compressive strength between 20% and 30% lower than that of a conventional concrete (Hansen, 1992; Dhir et al., 1999; Poon et al., 2004b; Topçu and Şengel, 2004; González-Fonteboa and Martinez-Abella, 2005; Etxeberria et al., 2007; Butler et al., 2011). Nonetheless, Domingo-Cabo et al. (2009b), who did not perform a water compensation upon addition of the recycled aggregates, observed a growth in the strength of the recycled mixtures as consequence of a lower effective water/cement ratio.

Generally, the quality of the parent concrete is considered an important factor in the resistance of the recycled mixtures (Dhir et al., 1999; Poon et al., 2004a; Dhir and Paine, 2007; Eguchi et al., 2007; López-Gayarre et al., 2009). Hence, the use of mixed and ceramic recycled aggregates is expected to have a higher effect on the compressive strength because of their relatively low quality compared to recycled concrete aggregates. However, Amorim-Carneiro et al. (2014) reported a 9% increase in the compressive strength of concrete made with 23% mixed recycled aggregates. The authors attributed the enhancement to the rough surface of the recycled aggregates and the penetration of cement in their pores and cracks, as well as the use of superplasticizers. According to Mas et al. (2012a), the use of slag blended cement is responsible for the improvement of the results as the slag particles penetrate the pores and micro-cracks in the recycled aggregates resulting in a better ITZ. In particular, the use of CEM V in recycled mixtures with 50% and 75% replacement ratios of mixed recycled aggregates resulted in strength increases of 11.70% and 13.20% at 7 days, 26.60% and 14.40% at 28 days and 7.50% and 7.40% at 90 days. Moreover, De Pauw et al. (1998), who manufactured two concretes containing two types of mixed recycled aggregates, stated that comparable strength can be achieved between the recycled mixtures and the concrete made with natural aggregates due to improvement of the ITZ by the internal curing as well as the rough and porous surface of the recycled aggregates. Nonetheless, Beltrán et al. (2014b) stated that a 12% increase of the cement content in recycled mixtures with a 100% replacement of the natural coarse aggregates led to comparable compressive strength to that of a conventional concrete. In any case, the increase of the cement goes against the environmental principle of the reutilization of recycled aggregates in the concrete manufacture and thus this practice should not be encouraged.

In terms of reduced performance, Dhir and Paine (2007) stated the compressive strength was declined by 2.50%, 3.20%, 5.40% and 21% for 20%, 30%, 40% and 100% substitutions of the natural coarse aggregates with recycled aggregates containing around 10% of ceramic particles, whereas the decreases ranged from 4%-8% and 27%-33% for 20% and 100% replacement ratios of mixed recycled aggregates with a ceramic content of 30% and 70%, respectively. Bezerra-Cabral (2010) reported declines of 17% and 34% for 50% and 100% substitution levels with coarse recycled aggregates of brick ceramic with respect to the reference concrete. The authors attributed the behaviour to the angular shape of the affricates due to inefficiency in the packing that led to large amounts of voids (Agamuthu, 2008). Compared to the control concrete, Yang et al. (2011) observed reductions of 5.33% and 15.33% in the compressive strength of recycled concrete made with mixed aggregates containing 20% and 50% of ceramic aggregates. Martínez-Lage et al. (2012) reported reductions of 11.50% and 23.00% when using 50% and 100% mixed recycled aggregates in the concrete manufacture. Mas et al. (2012a) reported maximum decreases in the compressive strength of 25.40% and 21.60% if CEM II or III were employed in recycled mixtures containing 30% mixed recycled aggregates. Besides, Mas et al. (2012b) registered the highest reduction in compressive strength (32%) at 90 days for a 40% substitution of mixed recycled aggregates. Schubert et al. (2012) observed an average reduction of 13.10% and 27.76% for mixtures with replacement ratios of 50% and 100% mixed recycled aggregates. Sheen et al. (2013) registered decreases between 14.36% and 24.73% in the 28-days compressive strength of recycled mixtures with ceramic content ranging from 0% and 67%.

For 20%, 50% and 100% replacement ratios, González-Corominas and Etxeberria (2014) observed declines of 0.48%, 14.76% and 29.20% in cubic specimens and 12.23%, 26.79% and 41.53% in cylindrical specimens of the 28-days compressive strength. For mixed recycled aggregates with 28.60% of masonry-clay materials, Bravo et al. (2015) observed that the 28-days compressive strength declined on average 5.10%, 13.35%, 15.55% and 30.05% in cubic specimens and 7.00%, 11.25%, 12.3% and 26.55% in cylindrical specimens for replacement ratios of 10%, 25%, 50% and 100%, respectively. Medina et al. (2014, 2015) found that compressive strength for recycled concrete with 25% and 50% replacement ratios was 8.70%-15.94% and 15.07%-18.44% lower than for reference concrete at 7 and 28 days of curing respectively, and that the removal of the contaminants such as the floating particles or the asphalt diminished the strength differences between recycled and reference concrete because of the weaker interface created between those impurities and the cement matrix. For a 50% substitution with mixed recycled aggregates containing 34% and 68% of ceramic wastes, Rodríguez-Robles et al. (2015) reported an average decline in the compressive strength of 17.81% and 19.03% at 7 days and 6.34% and 7.31% at 28 days. The report of Ihobe and Cedex (2011) indicated decreases of 10.91% and 24.63% for 50% and 100% substitution levels. For a complete substitution, Chen et al. (2003a) registered decreases between 15% and 25% as the brick and tile content in the sample increased from 0% to 67%. Based on these results, the authors concluded that an inclusion up to 67% of ceramic particles in the total aggregate fraction was acceptable. The studies of Hoffman et al. (2012) and López-Gayarre et al. (2015) showed reductions in the 28-days compressive strength of concrete with 100% mixed recycled aggregates of 26.63% and 5.09%-15.52%, respectively. For mixed recycled aggregates containing 14% of ceramic particles, Beltrán et al. (2014a) reported decreases of 23.15%, 27.77% and 32.58% in 100% recycled concrete at 7, 28 and 90 days of curing. Moreover, Dilbas et al. (2014) observed a reduction of 4.70% when using 100% mixed recycled aggregates with 11% ceramic content. The authors found that using silica fume improved the compressive strength of recycled mixtures due to the penetration in the pores and cracks of the recycled aggregate that allowed a stronger bond with the cement paste.

A lack of agreement with respect to the effect of ceramic recycled aggregates on the compressive strength of recycled mixtures is also manifest among researchers. Khaloo (1994, 1995) reported that the compressive strength of recycled concrete was a 7% lower for crushed clinker (hard burnt) brick aggregates and 2% higher or crushed tile aggregates, respectively. Mansur et al. (1999) observed that recycled concrete using crushed bricks as coarse aggregates displayed comparable compressive strength to the reference mixture. For a complete replacement, Zakaria (1999) registered a 4% decrease of the compressive strength. For normal-strength concrete, Khalaf (2006) stated that this type of recycled aggregates can be used in the production of high quality concrete since the maximum compressive strength loss experienced was lower than 18% at 28 days, while an increase around 2.20% was achieved if high quality crushed bricks were used. Similarly, the maximum decrease reached 20% when high-strength concretes were manufactured with crushed bricks as recycled aggregates. When the ceramic aggregates are derived from electrical insulators, Senthamarai and Devadas Manoharan (2005) registered marginal declines (2.15%) in the compressive strength. De Brito et al. (2005) and Correia et al. (2006) observed declines of 21.89%, 24.03% and 44.21% when one, two and three thirds of the natural coarse aggregate were replaced by crushed brick aggregates, respectively.

For 20%, 40% and 100% replacement ratios, Dhir and Paine (2007) registered decreases of 7%, 12% and 41% compared to the reference concrete. Topçu and Canbaz (2007) recorded declines of 43% for concrete made with crushed tile aggregates as a consequence of their higher porosity and lower resistance than natural aggregates. For substitution levels ranging from 25 to 100%, Debieb and Kenai (2008) registered decreases between 10% and 35% when using coarse crushed brick aggregates with respect to the conventional mixture. For a replacement ratio of 30%, Cachim (2009) reported average declines of 15% compared to the conventional concrete. The author also observed that 15% substitution of the natural aggregates by ceramic aggregates caused marginal losses (around 7.5% on average) or slight growths (6%) in the compressive strength. For sanitary ceramic ware, Medina et al. (2012b) reported increases in the 28-days compressive strength between 3.82% and 11.04% for substitutions levels ranging from 15% to 25% because of the pozzolanic activity of the waste and the better integration of the recycled aggregates in the cement matrix. Afify and Soliman (2014) observed decreases in the compressive strength of recycled brick concrete up to 14.00% and 12.32% at 7 and 28 days. Nonetheless, the authors reported that the use of admixtures and silica fume led to increases in the compressive resistance up to 61.60%. The use of crushed brick aggregates in replacement ratios of 30%, 40% and 50% caused declines in the compressive strength of 5.60%, 12.32% and 25.37% (Zhang and Zong, 2014) and 16%, 27% and 44% (Zong et al., 2014). Finally, for 25% and 50% crushed brick replacements, Adamson et al. (2015) observed a higher compressive strength than that of a conventional concrete due to the relatively low strength of the natural aggregates measured in the Los Angeles test.

Table 8.2 and Figure 8.2 show the results of compressive strength of the mixtures pertaining to the two research phases of this dissertation. At first glance, it could be observed that the conventional and recycled mixtures exhibited compressive strengths over 25 MPa like targeted in the mixture dosage and the strength values would be expected to continue to rise with age due to cement hydration. In addition, since the reduction in the compression strength at 28 days is less than 20%, it is possible to conclude that the use of recycled aggregates with presence of organic matter does not have a significant influence in this property. Thus, albeit the observed declines in resistance in most of the mixtures, the use of recycled aggregates from CDW does not pose a problem in the mechanical performance of concrete.

Table 8.2: Compressive strength

	CC	**RC-L(S)**	**RC-L(B)**	**RC-M(S)**	**RC-H(S)**
Phase I-150x300 mm cylinders (MPa)					
7 days	23.70	19.48	-	20.23	24.23
Variation (%)	-	-17.81	-	-14.64	2.24
28 days	38.46	36.02	-	34.19	40.53
Variation (%)	-	-6.34	-	-11.10	5.38
Phase II-150 mm cubes (MPa)					
7 days	31.52	24.72	29.29	29.06	32.72
Variation (%)	-	-21.57	-7.07	-7.80	3.81
28 days	40.90	40.18	38.58	37.03	43.71
Variation (%)	-	-1.76	-5.67	-9.46	6.87
91 days	41.97	43.12	42.63	39.62	49.52
Variation (%)	-	2.74	1.57	-5.60	17.99

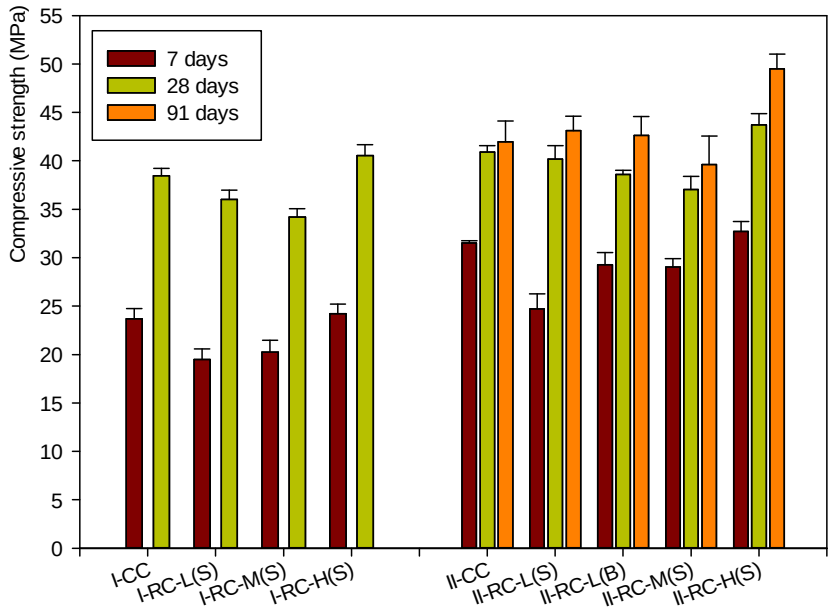

Figure 8.2: Compressive strength

The presence of adhered mortar, ceramic materials, as well as some other impurities such as wood, plastic, gypsum…, in the mixed recycled aggregates is often regarded as responsible for the poorer performance of recycled concretes which results in higher porosities and weaker bond between the recycled aggregate and the cement paste. Nevertheless, it is worth mentioning that the results obtained for the recycled concrete mixture containing the higher ceramic content (RC-H(S)) in the two research phases indicate a positive influence of the recycled aggregates on this property, which has been also previously observed in the literature review (Medina et al., 2012b; Adamson et al., 2015). These results suggest that the presence of ceramic particles has a smaller influence on the strength loss than the presence of adhered mortar or other impurities. Similar conclusions were drawn by Medina et al. (2014, 2015). The rest of the concrete mixtures presented decreases in the compressive strength at 7 and 28 days of curing. However, the reductions are in the lower range of the results in the literature review, with a maximum of 21.57% for I-RC-L(S) at 7 days and 11.10% for I-RC-M(S) at 28 days.

Behind the good performance of the recycled mixtures regarding some of the results observed by other researchers in the previous literature review are several factors. Firstly, the aggregate/cement ratio of the mixtures decreases with rising ceramic ratio, which can be a factor in the improvement of the compressive strength (Poon and Chan, 2007). Secondly, Poon et al. (2004b) stated that the use of recycled aggregates in air-dried condition causes lower compressive strength decreases in the recycled concrete than their use in a saturated surface-dried state. In addition, it is of common knowledge that the compressive resistance increases for lower water/cement ratios that, in this case, are caused by the lack of compensation of the water absorption of the recycled aggregates. Thirdly, according to Hansen (1992), the mixture procedure chosen in this investigation, i.e. the mixing of the aggregates before adding the cement and water, can lead to a gain in compressive strength between 10% and 35% due to the detaching of the adhered mortar, the modification of the particle shape and the acceleration in the cement hydration due to the particles of mortar released.

At the fourth place, the use of a slag blended cement allows the filling of part of the pores and micro-cracks in the recycled aggregates which results in a better ITZ (Mas et al., 2012a). Moreover, the pozzolanic activity of the CDW, particularly that of the ceramic particles, also plays a role in the compressive strength of the recycled mixtures (Medina et al., 2014, 2015). Finally, the superficial roughness of the recycled aggregates and their ability to return of the water absorbed during the mixing to produce an internal curing effect enhance the bond between the recycled aggregates and the cement matrix and thus the overall resistance (De Pauw et al., 1998; Hoffmann et al., 2012).

Figure 8.3 illustrates the evolution of the compressive strength with time. In both phases, a similar evolution of this property can be observed for all concrete mixtures. It is noteworthy that the loss of compressive strength is more pronounced at 7 days in both research phases and it is progressively reduced the older the concrete becomes. Therefore, the recycled mixtures display a higher strength development ratio than the conventional concrete. This finding is in agreement with those of Pacheco-Torgal and Jalali (2010), who found that the differences between conventional and recycled mixtures with ceramic recycled aggregates were lower at longer ages. Mas et al. (2012a) observed that the reduction in compressive strength between conventional and recycled mixtures was lower at 90 days than after 28 days of curing. The effect was explained by the presence of unhydrated cement particles in the recycled aggregates that contributed to the resistance gain. González-Corominas and Etxeberria (2014) also noticed that the strength development for 28 to 180 days was higher for recycled concretes with mixed coarse aggregates than for conventional concretes. According to Khatib (2005), the presence of ceramic fines, which are expected to generate by self-attrition during the mixing, are also responsible for an increase in the rate of strength development of the recycled mixtures. Contrarily, Sheen et al. (2013) noticed higher strength differences at 28 days than at 7 days for mixtures containing mixed recycled aggregate, but they did not observed the same tendency for increasing curing ages. Bravo et al. (2015) also noticed higher decreases in the compressive strength for rising curing ages, which suggested that recycled mixtures present a lower strength development with age.

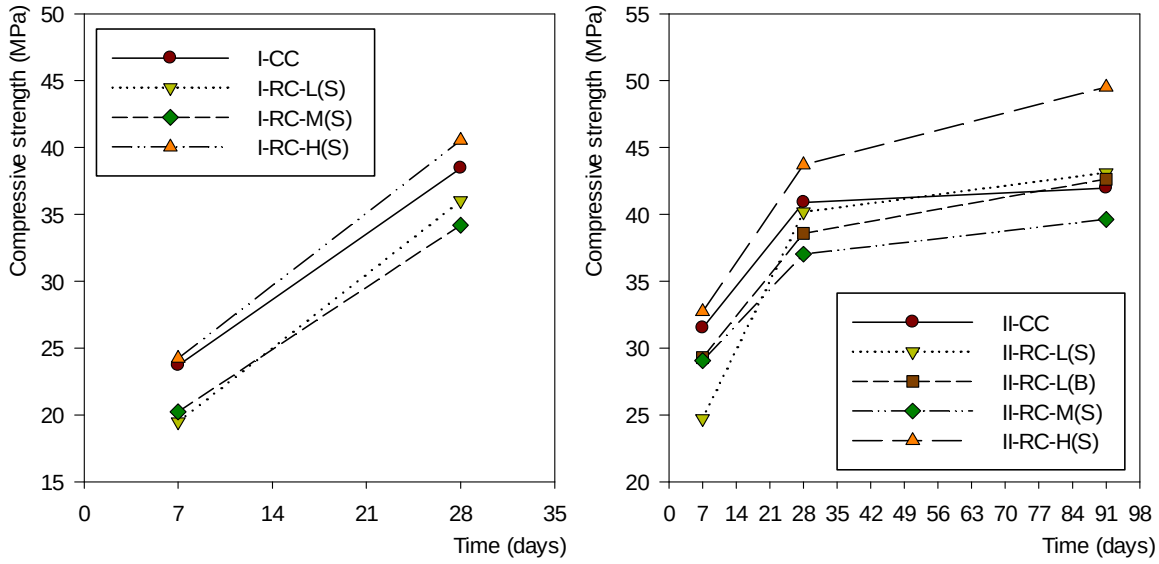

Figure 8.3: Evolution of the compressive strength with time

3.1. COMPRESSIVE STRENGTH INDEXES

The contribution of the recycled aggregates to the compressive strength is shown in Figure 8.4. The calculation of the strength indexes was based on (8.1) (Cachim, 2009; Medina et al., 2015)

$$R_n = \frac{fc}{q_{nat}}; \quad R_r = R_n\,(q=x) - R_n(q=100); \quad Ks = \frac{R_n\,(q=x)}{R_n\,(q=100)}; \quad Ps = \frac{R_r}{R_n} x100 \tag{8.1}$$

With R_n the contribution to strength of the natural aggregates [MPa], *fc* the compressive strength [MPa], q_{nat} the percentage of natural aggregates [%], R_r the contribution to strength of the recycled aggregates [-], *Ks* the specific strength ratio [-], P the strength contribution in percentage [%]. A Ks value higher than 1 indicates a strength reduction smaller than the percentage of natural aggregate replaced. Moreover, a Ps value higher than the replacement ratio indicates a positive contribution to the overall strength of the concrete mixture.

Table 8.3: Strength indexes

	fc	q	Rn	Rr	Ks	Ps
Phase I-7 days						
CC	23.70	100.00	0.24	0.00	1.00	0.00
RC-L(S)	19.48	50.00	0.39	0.15	1.64	39.17
RC-M(S)	20.23	50.00	0.40	0.17	1.71	41.42
RC-H(S)	24.23	50.00	0.48	0.25	2.04	51.09
Phase I-7 days						
CC	38.46	100.00	0.38	0.00	1.00	0.00
RC-L(S)	36.02	50.00	0.72	0.34	1.87	46.61
RC-M(S)	34.19	50.00	0.68	0.30	1.78	43.76
RC-H(S)	40.53	50.00	0.81	0.43	2.11	52.55
Phase II-7 days						
CC	31.52	100.00	0.32	0.00	1.00	0.00
RC-L(S)	24.72	50.00	0.49	0.18	1.57	36.25
RC-L(B)	29.29	50.00	0.59	0.27	1.86	46.19
RC-M(S)	29.06	50.00	0.58	0.27	1.84	45.77
RC-H(S)	32.72	50.00	0.65	0.34	2.08	51.83
Phase II-28 days						
CC	40.9	100.00	0.41	0.00	1.00	0.00
RC-L(S)	40.18	50.00	0.80	0.39	1.96	49.10
RC-L(B)	38.58	50.00	0.77	0.36	1.89	46.99
RC-M(S)	37.03	50.00	0.74	0.33	1.81	44.77
RC-H(S)	43.71	50.00	0.87	0.47	2.14	53.21
Phase II-91 days						
CC	41.97	100.00	0.42	0.00	1.00	1.00
RC-L(S)	43.12	50.00	0.86	0.44	2.05	51.33
RC-L(B)	42.63	50.00	0.85	0.43	2.03	50.77
RC-M(S)	39.62	50.00	0.79	0.37	1.89	47.03
RC-H(S)	49.52	50.00	0.99	0.57	2.36	57.62

Figure 8.4 displays the percentage of contribution of the recycled aggregates, as well as the threshold of strength contribution associated to the 50% replacement ratio carried out in all recycled mixtures. Further to the aforementioned definition, the replacement of natural by recycled aggregates has a favourable effect in mixture RC-H(S) at all curing ages and both research phases and in the specimens of II-RC-L(S) and II-RC-L(B) at 90 days of curing. Consequently, the adverse effect of the substitution is confirmed for the rest of the concrete mixtures as the contribution to strength is somewhat smaller than the amount of natural coarse aggregate replaced. While Medina et al. (2015) reported a general negative effect of a 25% and 50% substitution with mixed recycled aggregates at 7 and 28 days, the findings of Cachim (2009) showed adverse effect at 28 days but mostly positive outcomes for the contribution of crushed bricks replacements after 90 days of curing.

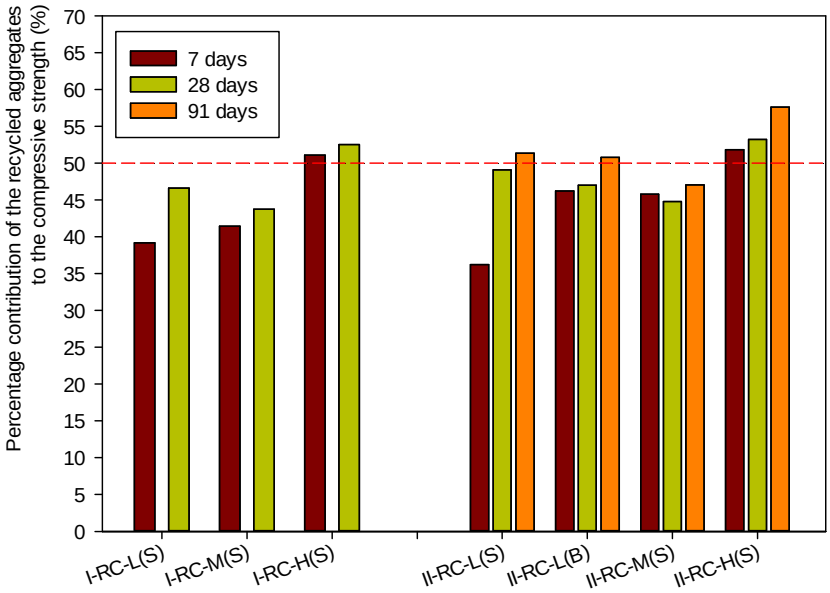

Figure 8.4: Compressive strength ratios

4. FLEXURAL STRENGTH

The study of the flexural strength of concrete is not too common, certainly not for concrete made with recycled concrete aggregates. While several authors have reported a marginal influence of the use of recycled concrete aggregates on the flexural strength of recycled concretes, even when full substitutions are carried out (Ravindrarajah and Tam, 1985; Razaqpur et al., 2010; Rao et al., 2011), the decreases are generally correlated with rising replacement ratios (Topçu and Şengel, 2004). Some researchers have reported decreases up to 10% (Hansen, 1992; Yang et al., 2008; Malešev et al., 2010), whereas other scientists have registered declines between 10% and 17% (Katz, 2003; Wang et al., 2013; Beltrán et al., 2014a). In particular, Yamato et al. (1998) observed decreases of 20%, 30% and 45% for coarse aggregate replacement of 30%, 50% and 100%, respectively.

In terms of the use of mixed recycled aggregates in the concrete manufacture, Chen et al (2003) reported decreases in flexural strength between 9% and 22% for 100% substitution with ceramic contents up to 67%. Dhir and Paine (2007) found that substitution levels up to 40% of mixed recycled aggregates have little effect on the flexural strength due to the higher angularity of these aggregates. However, a total substitution produced a maximum decrease of 23%. Ihobe and Cedex (2011) reported a decline of 20% and 31% for 50% and 100% replacement ratios. Contrarily, for 100% recycled concrete, Yang et al. (2011) observed a slightly greater (0.40%) or comparable (5.90%) 28-days flexural behaviour of concrete made with mixed recycled aggregates containing 20% and 50% of brick particles, respectively. Hoffman et al. (2012) observed a maximum reduction up to 45.45% in the flexural strength of recycled concrete incorporating mixed recycled aggregates with a percentage of ceramic waste ranging between 10% and 25% compared to a reference mixture. Mas et al. (2012a) observed declines of 7.90%, 16.30% and 20.30% for 25%, 50% and 75% replacement ratios. When 20% and 40% mixed recycled aggregates were added, Mas et al. (2012b) detected an average reduction of 3.50% and 21.50% in tensile strength. For a full substitution of the coarse natural aggregates, Schubert et al. (2012) noticed a decrease up to 14.58% regardless if the masonry content in the mixed recycled aggregates was around 10% or 25%, whereas 50% replacements led to comparable or slightly greater tensile strength. For a 100% substitution, López-Gayarre et al. (2013) registered a 33.56% decrease in the flexural strength when using mixed recycled aggregates with a 17.67% masonry content. Sheen et al. (2013) reported that concrete prepared with 100% mixed recycled aggregates has a 10–23% lower flexural strength than the control concrete, presenting better performance for rising brick and tile contents. By using a 20% replacement with mixed recycled aggregates containing a 25% brick content, Amorim-Carneiro et al. (2014) registered a 7.73% decline in the flexural strength compared to the reference concrete. Beltrán et al. (2014a) also reported declines of 25.42% for a complete substitution. González-Corominas and Etxeberria (2014) registered variations of 7.26%, -14.99%, -18.86% in the 7-days flexural strength for a 20%, 50% and 100% replacement ratio with mixed recycled aggregates compared to the control concrete. For a 50% replacement of the natural coarse aggregates, Rodríguez-Robles et al. (2015) observed a decrease between 7.96% and 8.94% in the flexural tensile values for recycled aggregates containing 34% and 68% of ceramic wastes.

Regarding the use of ceramic recycled aggregates, their typical angular-shape and superficial roughness are expected to have beneficial influence on the flexural strength of recycled mixtures (Neville and Brooks, 2010). In this regard, Hansen (1992) reported a strength increase up to 10% and Khaloo (1994, 1995) registered higher values in recycled concrete made with crushed bricks (15%) or crushed tiles (29%), respectively. For a full replacement, Zakaria (1999) stated that recycled brick concrete experienced a 10% growth of the flexural strength. However, other researchers have registered both positive and negative effects when using this type of aggregates. For instance, Kibriya and Speare (1996) noticed that conventional bricks led to decreases of the flexural strength, on average 9.25% for a 100% substitution; while the use of calcareous bricks resulted in both increases around 14% or decreases about 8%. Moreover, compared to a conventional concrete, Zhang and Zong (2014) observed variations of 3.24%, -6.48% and -9.94% in the 28-days flexural strength for replacement ratios of 30%, 40% and 50% of crushed brick aggregates.

Since the quality of the recycled aggregates, in particular regarding water absorption and oven-dried density, strongly affects the flexural tensile strength of the recycled mixtures (Yang et al., 2008), it is normal that a great majority of the investigations indicate an adverse influence of the use of ceramic aggregates in the concrete manufacture. Concrete with crushed brick as recycled aggregates exhibited a flexural strength between 8% and 15% lower than conventional concrete (Khalaf and DeVenny, 2004; Khalaf, 2006). De Brito et al. (2005) observed decreases of 8.57%, 15.71% and 25.71% in the flexural tensile strength of small slabs made with 33%, 66% and 100% ceramic coarse aggregate, respectively. By using ceramic aggregates derived from electrical insulators, Senthamarai and Devadas Manoharan (2005) registered a decline of 4.14%. Dhir and Paine (2007) found that substitutions levels up to 40% of ceramic recycled aggregates have little effect on the flexural strength. However, a total substitution produced a maximum decrease of 29%. For crushed bricks coarse aggregates, Debieb and Kenai (2008) reported reductions of 19.73%, 32.11%, 27.09% and 33.11% for 25%, 50%, 75% and 100% replacement ratios, which suggest that the ceramic content is not directly correlated with the strength loss. Under similar water/cement ratios and lack of admixtures, the flexural strength of recycled brick concretes has been found to be around 11.83% lower than that of a conventional mixture; whereas the use of admixtures or silica fume and admixtures can improve the flexural strength of recycled mixtures around 8.81% or 46.07% (Afify and Soliman, 2014). In the study of Zong et al. (2014), the flexural strength decreased by 16%, 22% and 33% when the content of bricks was 30%, 40% and 50%, respectively.

Table 8.4 shows the results of flexural tensile strength, as well as the variations with respect to the conventional concrete. It is worth mentioning that the differences in magnitude observed between research phases partially respond to the use of different methodologies (four-point and three-point bending tests in phase I and II, respectively) (Spooner and Helmrath, 1997).

Table 8.4: Flexural strength

	Phase I (MPa)	Variation (%)	Phase II (MPa)	Variation (%)
CC	7.16	-	5.21	-
RC-L(S)	6.59	-7.96	4.21	-19.19
RC-L(B)	-	-	4.20	-19.39
RC-M(S)	7.76	8.38	4.08	-21.69
RC-H(S)	7.23	0.98	4.53	-13.05

In phase I, only the I-RC-L(S) mixture suffered a decrease in the flexural strength. The value, around 8%, was well below those reported by Ihobe and Cedex (2011) and Mas et al. (2012a) for recycled concretes incorporating 50% of mixed recycled aggregates, which indicates a marginal adverse effect. Contrarily, the results for I-RC-M(S) and I-RC-H(S) mixtures showed an increase in flexural strength with a maximum around 8%. These values agree with the findings of Schubert et al. (2012), who noticed comparable or slightly greater tensile strength with 50% replacements of mixed recycled aggregates. This change in behaviour can be attributed to the increased ceramic content with respect to the I-RC-L(S) mixture. In fact, several researchers have stated the beneficial effect of the incorporation of crushed bricks on this property (Hansen, 1992; Khaloo, 1994, 1995; Zakaria, 1999).

Nevertheless, the positive pattern was not maintained by the specimens tested in phase II, which exhibited decreases in flexural strength independently of the ceramic content of the mixture. The lack of agreement between research phases suggests that, besides the percentage of ceramic wastes, the quality of the recycled aggregates has a strong influence on the outcome of this property. This assumption has been confirmed by Kibriya and Speare (1996), who stated that the nature of the bricks, i.e. conventional or calcareous, greatly influenced the flexural behaviour of concrete mixtures incorporating the same amount of ceramic materials. For the results in this research, Figure 8.5 illustrates the relationship between the flexural strength and the ceramic content. The weak correlation (R^2<0.30) between both variables serves as proof for the existence of a supplementary variable controlling the effect of the incorporation of recycled aggregates from CDW on the flexural strength of concrete. Moreover, the correlation factors for linear regression were still weak (R^2=0.33 for phase I and R^2=0.44 for phase II) when the values for the recycled mixtures were the only ones assessed. The findings of Debieb and Kenai (2008) also suggested that the ceramic content is not directly correlated with the strength loss.

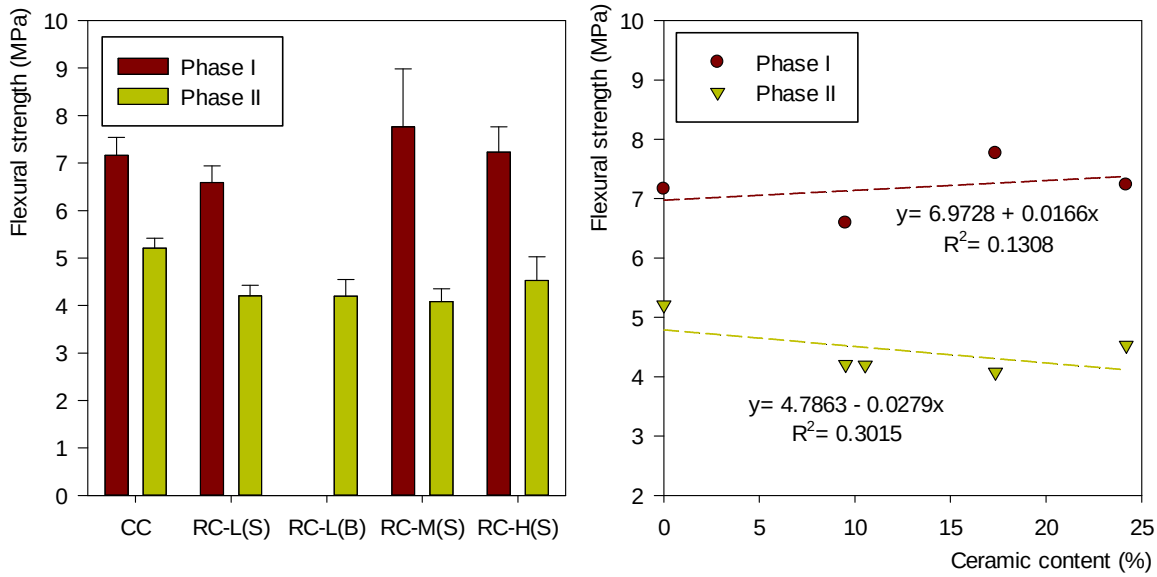

Figure 8.5: Flexural strength and its relationship with the ceramic content incorporated in the total weight of aggregates

Regarding the decreases observed in phase II, those corresponding to II-RC-L(S), II-RC-L(B) and II-RC-M(S) are in the 20% range reported by Ihobe and Cedex (2011) and Mas et al. (2012a) for concretes made with 50% mixed recycled aggregates. The 13% decline experimented by II-RC-H(S) is lower than the losses registered by Debieb and Kenai (2008) and Zong et al. (2014), but in line with those reported by Khalaf (2006) and Afify and Soliman (2014) for the same replacement ratio with crushed brick aggregates.

4.1. RELATIONSHIP BETWEEN THE FLEXURAL STRENGTH AND THE COMPRESSIVE STRENGTH

The flexural tensile strength of concrete is a common manner to experimentally determine the direct tensile strength of the mixture. Since the tensile strength fluctuates proportionally to the compressive strength, the Eurocode-2 proposes equation (8.2) to correlate both variables and consequently the flexural strength with both of them in conventional concretes. Correspondingly, the ACI Committee 318 (2014) also provides equation (8.3) as a model to predict the flexural strength through the compressive strength of concrete.

$$f_{ct} = \frac{f_{cf}}{1.6 - \frac{d_1}{1000}} = 0.30 \times f_{ck}^{\frac{2}{3}} \tag{8.2}$$

$$f_{cf} = 0.62 \times f_{ck}^{0.50} \tag{8.3}$$

With f_{ct} the direct tensile strength [MPa], f_{cf} the flexural strength [MPa], d_1 the lateral dimension of the specimen [mm] and f_{ck} the 28-days characteristic compressive strength in cylindrical specimens [MPa].

According to Beltrán et al. (2014a), the high correlation between the flexural and compressive strength of recycled mixtures ensures the reliability of the determination of one property through the values of the other. Figure 8.6 displays the equations proposed in both international codes, as well as the experimental results, in order to assess the accuracy of such prediction models for recycled concrete mixtures. Note that the compressive strength results arising from cubic samples in phase II were conveniently transformed to the equivalent resistance in cylindrical specimens. While the results arising from phase II display a good fitting to the Eurocode-2 curve (UNE EN 1992 1-1, 2013), the values obtained in phase I are well above the prediction in the standard. The methodology differences between the two phases suggest that the prediction model established in equation (8.2) could be acceptable for flexural strength values obtained by means of centre-point bending tests. Regarding to the equation proposed by the ACI Committee 318 (2014), a clear inadequacy to predict the experimental values can be observed. Similarly, Xiao et al. (2006) stated that the use of the ACI equation (8.3)led to underestimations for recycled mixtures.

In addition, the lack of significant differences in the relationship between the compressive strength and flexural strength of the recycled concretes in comparison with the control concrete show that the bond between paste and aggregate in the recycled concrete mixes was comparable to the one in the control concrete as confirmed by Kheder and Al-Windaw (2005) and Hoffman et al. (2012).

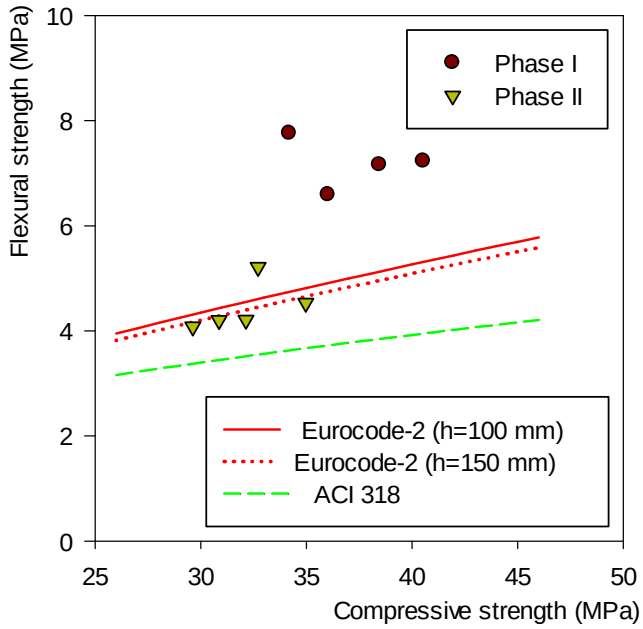

Figure 8.6: Comparison between the model equations proposed in international codes and the experimental results

5. SPLITTING TENSILE STRENGTH

Like flexural resistance, the splitting tensile strength is not often experimentally determined but estimated through the compressive strength. It is widely accepted that the use of recycled aggregates in the concrete manufacture causes declines in the splitting tensile strength of the mixture (Kou et al., 2007; Kou and Poon, 2009; Akbarnezhad et al., 2011; Fonseca et al., 2011; González-Fonteboa et al., 2011b; Kwan et al., 2012; Kim et al., 2013; Manzi et al., 2013; Matias et al., 2013; Thomas et al., 2013a; Wang et al., 2013; Duan and Poon, 2014; Folino and Xargay, 2014; Gonzalez and Etxeberria, 2014; Gonzalez-Corominas and Etxeberria, 2014; Pedro et al., 2014a, 2014b; Çakır, 2014). In few cases, recycled mixtures containing recycled concrete aggregates exhibited similar or even slightly greater tensile strength (Ravindrarajah and Tam, 1985; Sagoe-Crentsil et al., 2001; Poon et al., 2004b; González-Fonteboa and Martinez-Abella, 2005; Etxeberria et al., 2007; Yang et al., 2008; Kong et al., 2010; Butler et al., 2011) due to the improved bond between the rough surface of the recycled aggregate as consequence of the adhered mortar and the cement paste.

Regarding recycled mixtures incorporating mixed recycled aggregates, Poon and Chan (2006) reported decreases in splitting tensile strength for increasing replacement with crushed bricks. Ihobe and Cedex (2011) registered decreases up to 16% for total substitutions of mixed recycled aggregates. Compared to the control concrete, Yang et al. (2011) reported declines up to 30.80% and 33.90% in 100% recycled concrete with 20% and 50% percentages ceramic content, respectively. Martínez-Lage et al. (2012) reported reductions up to 24% for a 100% replacement level, whereas a 50% replacement ratio led to a similar tensile strength than that of a conventional concrete.

Mas et al. (2012a) observed declines of 14.20%, 6.20% and 20.40% for 25%, 50% and 75% replacement ratios; while, when 20% and 40% mixed recycled aggregates were added, Mas et al. (2012b) detected an average reduction of 7.00% and 22.00% in tensile strength. By using a 20% replacement with mixed recycled aggregates containing a 25% brick content, Amorim-Carneiro et al. (2014) registered a decline lower than 2% in the tensile splitting strength compared to the reference concrete. For 11% ceramic waste in the mixed recycled aggregates, Dilbas et al. (2014) stated that the tensile splitting strength of specimens was 7.11% greater than that of the control concrete. Recycled mixtures containing 50% mixed recycled aggregates exhibited reduction of 20.1% in tensile strength (Gomes et al., 2014). González-Corominas and Etxeberria (2014) reported decreases up to 10.14%, 12.28% and 17.54% for 20%, 50% and 100% substitution level when compared to the conventional concrete. Medina et al. (2014) found that the splitting-tensile strength decreased with up to 16.5% in recycled concrete incorporating 50% mixed recycled aggregates, but this negative effect was reduced to a 2.90% decline if the floating particles were removed. For a 50% substitution with mixed recycled aggregates containing 34% and 68% of ceramic wastes, Rodríguez-Robles et al. (2015) observed a decrease between 8.85% and 13.37% in the splitting tensile values. Bravo et al. (2015) reported a 24.30% lower tensile strength for a 100% substitution with recycled aggregates with 28.60% ceramic particles.

In terms of the influence of using of ceramic recycled aggregates on the splitting tensile strength, no consensus exists among researchers. The findings of Khaloo (1995) indicated that 70% increase of the tensile strength can be registered for recycled concrete with 100% crushed tile as coarse aggregates. Mansur et al. (1999) observed that recycled concrete using crushed bricks as coarse aggregates displayed greater tensile strength than the reference mixture. Zakaria (1999) registered an increase of 21% when using a full substitution of the coarse aggregates by ceramic recycled aggregates. For sanitary ceramic ware, Medina et al. (2012a) noticed that the splitting tensile strength increased up to 10.78%, 19.70% and 25.65% for replacements of 15%, 20% and 25%, respectively. Cachim (2009) observed an average 0.99% increase and 6.00% decline in the splitting tensile strength of 17.50% and 35% recycled brick concrete mixtures. Despite using higher cement quantities than in the conventional concrete, Kibriya and Speare (1996) observed average declines of 18.00% and 17.75% for 100% substitution of the natural coarse aggregate with conventional and calcareous bricks respectively. For ceramic aggregates derived from electrical insulators, Senthamarai and Devadas-Manoharan (2005) registered an average decrease of 16.42%. Correia et al. (2006) registered decreases up to 8.57%, 15.71% and 25.71% for replacements ratios of 33%, 66% and 100% crushed bricks aggregates. Under similar water/cement ratios and without admixtures, the splitting tensile strength of recycled brick concrete has been found to be around 11.75% lower than that of a conventional mixture; whereas the use of admixtures, or silica fume and admixtures, can improve the splitting tensile strength of recycled mixtures around 8.89% or 46.19% (Afify and Soliman, 2014).

The results of the tensile splitting strength and the variations with respect to the conventional concrete are presented in Table 8.5. It is interesting mentioning that part of the differences between research phases answer to the diverse shape of the test specimens (cylinders and prisms in phase I and II, respectively) (Spooner and Helmrath, 1997).

Table 8.5: Splitting tensile strength

	Phase I (MPa)	Variation (%)	Phase II (MPa)	Variation (%)
CC	2.94	-	3.61	-
RC-L(S)	2.68	-8.84	3.13	-13.30
RC-L(B)	-	-	3.18	-11.91
RC-M(S)	2.79	-5.10	3.3	-8.59
RC-H(S)	2.92	-0.68	3.52	-2.49

These results are in agreement with the conclusion of De Brito and Robles (2010), who stated that the use of recycled concrete aggregates had a lesser negative effect on the splitting tensile strength than the compressive strength. The declines obtained for the RC-H(S) mixture in both research phases are far below any result found in the literature and can be considered as negligible. Despite that Martínez-Lage et al. (2012) reported that 50% replacement ratio with mixed recycled aggregates lead to a similar tensile strength than that of a conventional concrete. The results in this investigation point to reductions between 5% and 13%. Mas et al. (2012a), González-Corominas and Etxeberria (2014) and Medina et al. (2014) have also registered declines within that range for 50% replacements, whereas the findings of Gomes et al. (2014) indicated decreases up to 20%. As stated by Medina et al. (2014, 2015), the cleanliness of the recycled aggregates resulted in the reduction of the strength loss due to a lesser extent of weaker ITZ. Hence, the lack of any contaminants in the ceramic recycled aggregates also influenced the overall performance of RC-H(S) mixture. In any case, the results obtained provide further evidence of the good bonding between the ceramic particles and the cement paste as consequence of the internal curing phenomenon caused by the return of the water absorbed during mixing.

Similarly to the explanation of the good compressive strength outcomes, there are others factors behind the good results of splitting tensile strength. Once again, the proportioning method consisting in the mix of the recycled aggregates prior to the water and cement addition can be held responsible for an increase between 10% and 35% due to the detaching of the adhered mortar, the modification of the particle shape and the acceleration in the cement hydration due to the particles of mortar released (Hansen, 1992), Moreover, the presence of pozzolanic activity within the fines of the recycled aggregates (Medina et al., 2014, 2015), as well as its incorporation in the slag blended cement, has also been proven as an effective method to avoid the strength losses caused by the use of recycled aggregates (Kong et al., 2010). Finally, the lack of any water compensation technique led to a decrease in the effective water/cement ratio in the recycled mixtures that works towards higher mechanical performances. Nonetheless, similar tensile strength has been achieved in recycled mixtures by adding extra water to the mixture (Poon et al., 2004b; Kong et al., 2010). Contrarily, the pre-saturation technique has been evidenced to cause higher performance losses (Ferreira et al., 2011).

As the quality of the recycled aggregates, in particular regarding water absorption and oven-dried density, strongly affects the splitting tensile strength of the recycled mixtures (Yang et al., 2008), the reductions experimented by all recycled concrete mixtures answer principally to the overall physical characteristics of the recycled aggregates rather than the ceramic content in the mixture. Figure 8.7, illustrates the relationship between the splitting tensile strength and the ceramic content. While no tendency whatsoever was identified when the values of the conventional concrete were also considered in the linear regression (R^2<0.01 for both phases), the correlation between the two variables for the results of the recycled mixtures is strong (R^2>0.98). This fact is indicative of an underlying relationship between the physical property of the recycled aggregates and the percentage of ceramic components as explained in chapter 4.

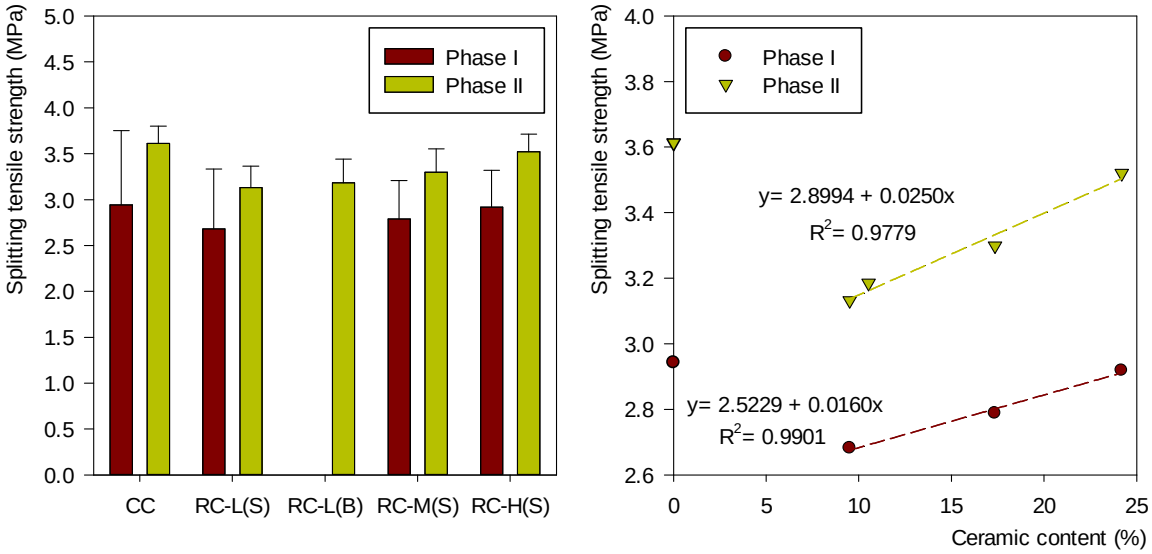

Figure 8.7: Splitting tensile strength and its relationship with the ceramic content incorporated in the total weight of aggregates

The analysis of the fracture zone of specimens subjected to splitting tensile strength testing is presented in Figure 8.8. The primary fracture mode in the conventional specimen was through the aggregate/paste interface, i.e. stone pull-out. Besides the failure mode between the natural aggregates and the cement matrix, the recycled concretes exhibited fracture surfaces through the adhered mortar and the ceramic particles, which agree with the general consideration of these materials as the weakest links in the mechanical performance of recycled mixtures due to their lower strength and stiffness. According to Amorim-Carneiro et al. (2014), the stronger ITZ in recycled concretes can also be a factor affecting this different cracking pattern. Nevertheless, some ceramic pull-outs can also be observed in Figure 8.8.

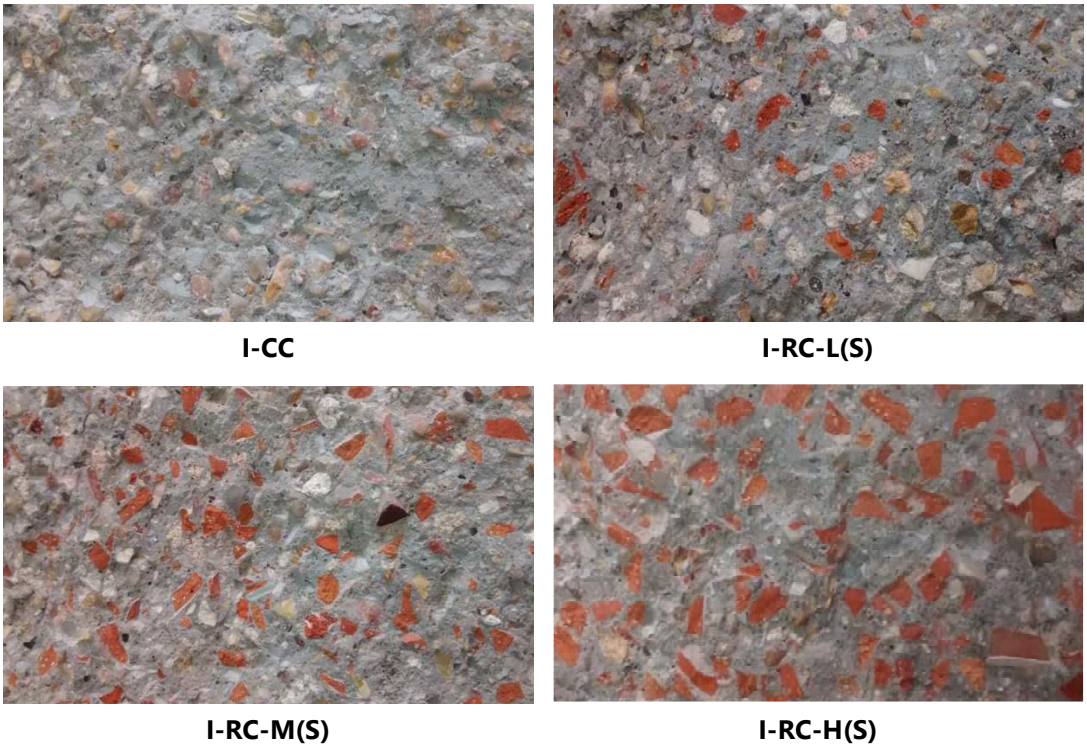

Figure 8.8: Fracture mode of the conventional and recycled concrete mixtures in phase I

5.1. RELATIONSHIP BETWEEN THE SPLITING-TENSILE STRENGTH AND THE COMPRESSIVE STRENGTH

Similarly to the flexural strength, the splitting tensile strength of concrete is often used to experimentally determine the direct tensile strength of the mixture. Since the tensile strength varies with the compressive strength, the Eurocode-2 proposes equation (8.4) to correlate both variables and, consequently, the splitting tensile strength with both of them, in conventional concretes. Correspondingly, the ACI Committee 318 (2014) also provides equation (8.5) as a model to predict the splitting tensile strength through the compressive strength of concrete.

$$f_{ct}=0.90\times f_{cst}=0.30\times f_{ck}^{\frac{2}{3}} \tag{8.4}$$

$$f_{cst}=0.56\times f_{ck}^{0.50} \tag{8.5}$$

With f_{ct} the direct tensile strength [MPa], f_{cst} the splitting tensile strength [MPa], and f_{ck} the 28-days characteristic compressive strength in cylindrical specimens [MPa],

According to Xiao et al. (2006), the tendency showing increasing splitting tensile strength with rising compressive strength can still be recognized in recycled mixtures. Figure 8.9 presents the relationship between the tensile strength and compressive strength set in both international codes and the experimental results obtained in each research phase. Note that the compressive strength results arising from cubic samples in phase II were conveniently transformed to the equivalent resistance in cylindrical specimens.

In this case, both equations result in overestimations of the results arising from phase I. Xiao et al. (2006) also noticed that the use of the ACI equation (8.5) results in a significant overestimation of the splitting tensile strength of the recycled concrete. However, the model proposed in the Eurocode-2 (UNE EN 1992 1-1, 2013) seems a good fit for the experimental results of splitting tensile strength on cubic specimens. Similarly, the findings of Cachim (2009), Paine et al. (2009) and Silva et al. (2015a) indicate that the existing relationship between compressive and splitting tensile strength for conventional concretes Eurocode-2 (UNE EN 1992 1-1, 2013) is also acceptable for recycled concrete mixtures.

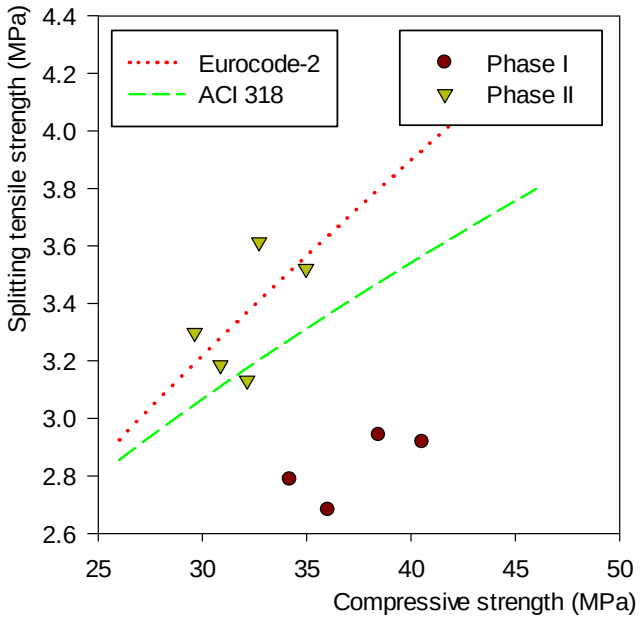

Figure 8.9: Comparison between the model equations proposed in international codes and the experimental results

6. MODULUS OF ELASTICITY

For structural concrete, the modulus of elasticity is an important mechanical parameter reflecting the ability of the concrete to deform elastically. The modulus of elasticity of the concrete is a function of the modulus of elasticity of the aggregates and the cement matrix and their relative proportions (Yang, 1998). Since the density is the major controlling factor of the stiffness of aggregates (Zhou et al., 1995), when mixed or ceramic recycled aggregates are used in the concrete manufacture a decrease in the values of this property is expected as the modulus of elasticity of recycled aggregates is lower than coarse natural aggregates. Moreover, the findings of Xiao et al. (2013) indicated that the old ITZ is between 20% and 30% weaker than the new ITZ.

The effect that the use of recycled concrete aggregates has on the reduction of the modulus of elasticity of recycled mixtures has been thoroughly investigated (Bezerra-Cabral et al., 2010; Lovato et al., 2012; Qasrawi and Marie, 2013; Safiuddin et al., 2013; Thomas et al., 2013b; Duan and Poon, 2014; Pepe et al., 2014; Yehia et al., 2015).

Although the quality of the parent concrete strongly affects the modulus of recycled concrete (Padmini et al., 2009; Gonzalez and Etxeberria, 2014; Pedro et al., 2014b), the great majority of studies are focused on the consequences that several replacement ratios of aggregates with unknown characteristics have on the mechanical performance of the resulting recycled concrete. According to several researchers (Etxeberria et al., 2006; López-Gayarre et al., 2009, 2011; Malešev et al., 2010), replacement ratios lower than 50% of recycled concrete aggregates led to unremarkable variations, not higher than 9% compared to the reference concrete. Moreover, Rahal et al. (2007) reported that the modulus of elasticity of concrete incorporating a total substitution of recycled concrete aggregates was only 3% lower than the conventional concrete in the strength range of 25 MPa to 30 MPa. However, for 100% replacements with recycled concrete aggregates, the elastic moduli has been commonly reported to decrease up to 25% (Etxeberria et al., 2006; López-Gayarre et al., 2009, 2011; Malešev et al., 2010; González-Fonteboa et al., 2011a; Gonzalez and Etxeberria, 2014; Pedro et al., 2014b; Soares et al., 2014) or 45% (Xiao et al., 2005; Yang et al., 2008; Rao et al., 2011; Kwan et al., 2012; Surya et al., 2013) below the one of conventional concrete. In any case, the research works suggest that the modulus of elasticity decreases with rising contents of recycled concrete aggregates (Eguchi et al., 2007; Etxeberria et al., 2007; Padmini et al., 2009; Zega et al., 2010; Rao et al., 2011; Qasrawi and Marie, 2013; Surya et al., 2013; Soares et al., 2014).

According to Gomes and de Brito (2009) and Gomes et al. (2014), the modulus of elasticity is slightly affected by the incorporation of 25% mixed recycled aggregates (15.80% loss). For a total replacement of the coarse natural aggregates, Chen et al. (2003b) reported decreases between 22% and 29% for mixed recycled aggregates containing ceramic wastes up to 67%. Martínez-Lage et al. (2012) registered a 34.00% reduction in the modulus of elasticity for a 100% substitution. Hoffman et al. (2012) observed reductions between 11.70% and 21.90% in the modulus of elasticity of recycled concrete incorporating mixed recycled aggregates with a percentage of ceramic waste ranging between 10% and 25% compared to a reference mixture. Schubert et al. (2012) registered decreases up to 31% and 51% for substitution levels of 50% and 100% regardless the masonry content in the mixed recycled aggregates was around 10% or 25%. Sheen et al. (2013) reported an average 25.81% reduction with respect to the original concrete when using 100% mixed coarse recycled aggregates containing ceramic wastes percentages between 0% and 67%. Amorim-Carneiro et al. (2014) registered a comparable elastic modulus for a 20% substitution of mixed recycled aggregates containing 25% brick wastes. Recurring to additional amounts of cement for rising mixed recycled aggregates contents, Beltrán et al. (2014b) mitigated the reductions of the elastic modulus, which reached declines up to 4.00%, 5.50% and 8.10% for 20%, 50% and 100% substitutions levels. Nonetheless, if the cement content was raised equally in conventional and recycled mixtures, similar declines were reported, which suggested that the modulus of elasticity is more strongly affected by the amount of recycled aggregates than the quantity of cement. For 11% ceramic waste in the mixed recycled aggregates, Dilbas et al. (2014) stated that the tensile splitting strength of specimens was 10.42% lower than that of the control concrete. González-Corominas and Etxeberria (2014) reported decreases up to 12.86%, 23.89% and 35.77% for 20%, 50% and 100% substitution level when compared to the conventional concrete. Rodríguez-Robles et al. (2015) registered declines up to 0.23% and 7.53% when using mixed recycled aggregates with ceramic contents of 34% and 68% in a 50% substitution of the natural coarse aggregates.

By using 100% mixed recycled coarse aggregates (50% concrete waste and 50% brick rubble), López-Gayarre et al. (2015) observed average reductions of 52.52% in the elastic modulus compared to conventional concrete, with more noticeable differences for rising water/cement ratios. For mixed recycled aggregates containing around 28% of masonry aggregates (samples sourced from Valnor and Retria), Bravo et al. (2015) reported decreases up to 5.20%, 13.40%, 25.10% and 41.50% for 10%, 25%, 50% and 100% substitutions respectively, which suggests a linear relationship between the performance decline and the amount of recycled aggregates incorporated in the recycled concrete. In addition, Gomes et al. (2014) found that the variation of the elastic modulus was linearly correlated with the relative ceramic content of the mixed recycled aggregates.

When ceramic recycled aggregates are used in the replacement of the natural coarse aggregates, the elastic modulus of the resulting recycled concrete is inferior to that of conventional concretes. Nonetheless, substitutions below 20-30% do not lead to significant reductions according to Dhir and Paine (2007). Several researchers have reported that full substitutions with crushed brick aggregates are responsible for drops about 30-40% in the modulus of elasticity compared to the respective reference concrete (Akhtaruzzaman and Hasnat, 1983; Hansen, 1992; Zakaria, 1999; Correia et al., 2006; Debieb and Kenai, 2008). However, reductions up to 55% have also been described for 70% replacement ratios of crushed bricks compared to conventional mixtures with a similar compressive strength (RILEM TC 121-DRG, 1994). Topçu and Canbaz (2007) registered declines up to 25% when crushed tiles are used to totally replace the natural aggregates. For ceramic aggregates derived from electric insulators, Senthamarai and Devadas Manoharan (2005) observed reductions ranging from 11.47% to 2.42% for water/cement ratios oscillating from 0.35 to 0.60. Similarly to the other types of recycled aggregates, increasing amounts of ceramic aggregates are correlated with higher declines of the elastic modulus in the recycled concrete (Dhir and Paine, 2007; Topçu and Canbaz, 2007).

Table 8.6 shows the elastic modulus of the concrete mixtures. Generally, normal-density concrete with a 28-days compressive strength of 25 MPa presents elastic moduli around 31 GPa (UNE EN 1992 1-1, 2013). Albeit the slightly lower values obtained for the conventional mixes, the test registered a maximum 8.00% decline compared to the respective reference concrete. Therefore, a comparable performance between the conventional and recycled mixtures can be assumed for 50% substitution of recycled aggregates from CDW regardless the percentage of ceramic waste. Nevertheless, a correlation between the decrease in elastic modulus and the ceramic content of the recycled aggregates was identified in both phases of the investigation (Figure 8.10), albeit the relationship was stronger for the mixtures tested in the phase I (R^2=0.86).

Table 8.6: Modulus of elasticity

	CC	**RC-L(S)**	**RC-L(B)**	**RC-M(S)**	**RC-H(S)**
Phase I					
Modulus of elasticity (GPa)	25.49	25.43	-	24.58	23.57
Reduction (%)	-	0.24	-	3.57	7.53
Phase II					
Modulus of elasticity (GPa)	29.90	28.10	28.50	29.5	27.4
Reduction (%)	-	6.02	4.68	1.34	8.36

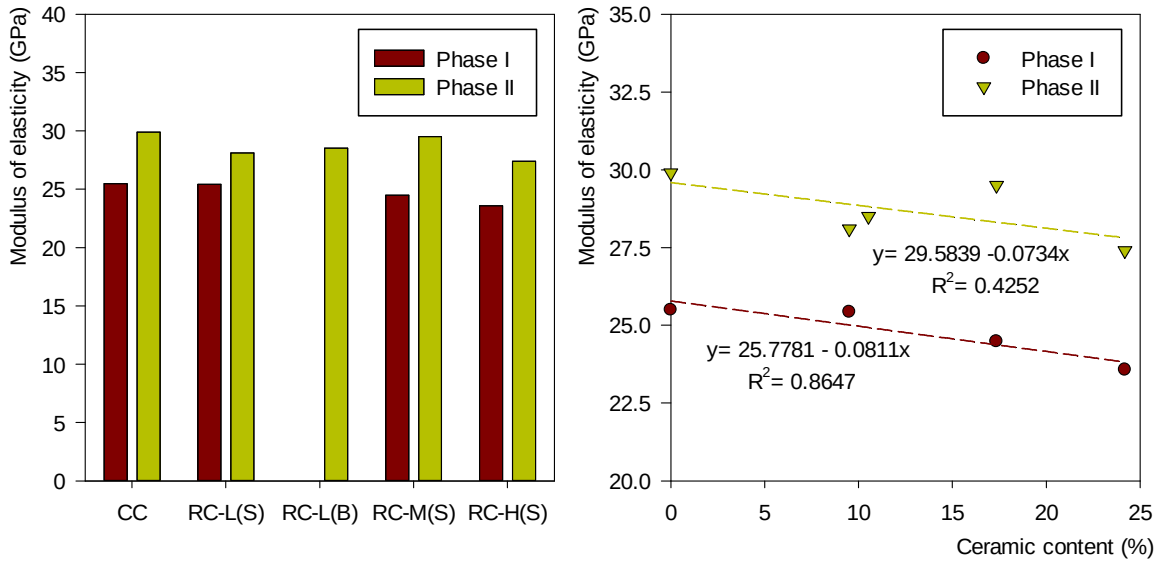

Figure 8.10: Modulus of elasticity and its relationship with the ceramic content incorporated in the total weight of aggregates

Several researchers have reported that the use of recycled aggregates has a higher negative impact on the modulus of elasticity than the compressive strength (Sánchez de Juan, 2004; Rao et al., 2011; Thomas et al., 2013b; Behera et al., 2014). However, that is not the case in this research. As mentioned in section 2.3 of chapter 7, the recycled concretes presented a good quality ITZ, in part due to the internal curing effect produced as the recycled aggregates return part of the water absorbed to the cement matrix, the use of a blended slag cement and the additional pozzolanic activity of the recycled aggregates which resulted in hydration products filling the interfacial bond between the aggregates and the cement. This improvement effect of the recycled aggregates in the ITZ was also observed by other researchers (Poon et al., 2004a; Corinaldesi and Moriconi, 2009; Li et al., 2009). The results obtained in this research are also explained by the lower effective water/cement ratio of the recycled mixtures resulting from the lack of water compensation as lower water/cement ratio led to more stiff cement paste. Finally, the proportioning method can also be behind the good results. According to Hansen (1992), when the recycled aggregates are blended before adding the cement and water the elastic modulus can grow with up to 8% due to the detaching of the adhered mortar, the modification of the particle shape and the acceleration in the cement hydration due to the particles of mortar released.

Hence, despite the registered falls in the elastic modulus, the results obtained for this property indicate that the recycled concretes are still satisfactory for structural purposes. Besides, this fact point to a relatively small difference between the modulus of elasticity of the hardened cement and the modulus of elasticity of the aggregate, and a better response to bond stresses, which could turn into less sensibility to cracking (Bremner and Holm, 1986; Neville, 1997; Berndt, 2009).

6.1. RELATIONSHIP BETWEEN THE MODULUS OF ELASTICITY AND THE DENSITY OF THE AGGREGATES

According to Zhou et al. (1995), the density of the coarse aggregates play a fundamental role in their elastic modulus and consequently in the modulus of elasticity of the concrete. Figure 8.11 illustrates the relationship between the elastic modulus of the concrete mixes and the oven dry density of the coarse aggregates employed in their manufacture, i.e. gravel for the conventional concrete and a mix of 50% gravel and 50% the respective recycled aggregate for the recycled concrete mixtures. Although correlations were identified in the two research phases, the interrelation was stronger for phase I (R^2=0.66). Dhir and Paine (2010) also observed a linear regression between both variables with correlation factors ranging from 0.64 to 0.72 depending on the water/cement ratio of the concrete mix. And Gomes et al. (2014) explained the reduction of the modulus of elasticity of recycled brick concrete through the lower density of the ceramic aggregates employed in its manufacture.

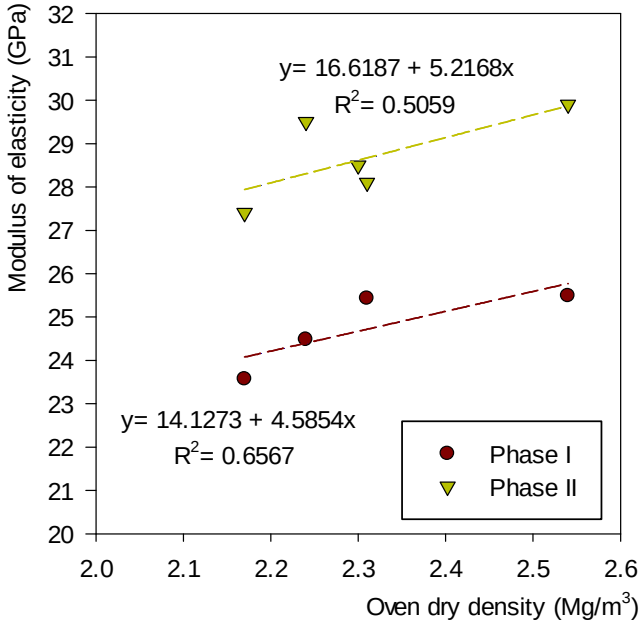

Figure 8.11: Relationship between the modulus of elasticity and the density of the aggregates

6.2. RELATIONSHIP BETWEEN THE MODULUS OF ELASTICITY AND THE COMPRESSIVE STRENGTH

To date, the current codes on structural concrete only provide empirical formulas to link the elastic modulus and the compressive strength of conventional concretes. Some examples can be found in equation (8.6) set forth in the Eurocode-2 (UNE EN 1992 1-1, 2013) or equation (8.7) proposed by the ACI Committee 318 (2014).

$$E_s = 22000 \times \left(\frac{f_{cm}}{10}\right)^{0.3} \quad (8.6)$$

$$E_s = 0.043 \times \rho^{1.5} \times \sqrt{f_{cm}} \quad (8.7)$$

with E_s the modulus of elasticity [MPa], ρ the density of concrete [kg/m^3], and f_{cm} the 28-days mean compressive strength on cylindrical specimens [MPa].

To ascertain the accuracy of these formulas in the determination of elastic moduli of recycled concretes, the experimental results were compared to the calculated values (Figure 8.12). Note that the compressive strength results from phase II were correspondingly transformed to their equivalent values for cylindrical specimens to allow a joint assessment. The comparison shows that the elastic modulus of most concrete types is overestimated by the equations based on compressive strength, especially in phase I. Thus, the current models for the prediction of this property are not acceptable when recycled aggregates are used to replace the natural coarse aggregates. Nonetheless, the formula proposed by the ACI 318-14 could lead to better approximations due to the incorporation of the density parameter.

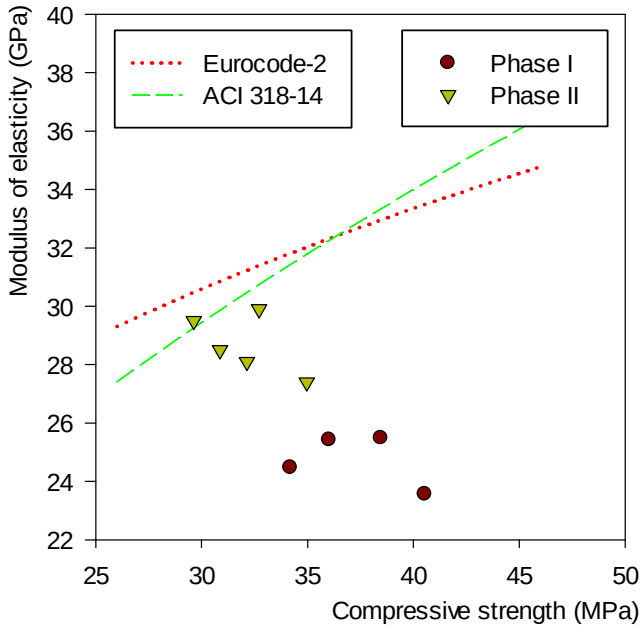

Figure 8.12: Comparison between the model equations proposed in international codes and the experimental results

For the same type of comparison, Rahal et al. (2007) observed a considerable scatter when using recycled concrete aggregates and thus concluded that the ACI equation overestimated the modulus of elasticity of 100% recycled concretes. Qasrawii and Marie (2013) did not find a good correlation between the ACI Committee 318 (2014) formula and their experimental results either. Cachim (2009) reported that the Eurocode-2 formula agreed relatively well for recycled brick concrete mixtures.

Nevertheless, González-Fonteboa et al. (2011a) also observed that the equation established in the Eurocode-2 led to an overestimation of the elastic moduli in recycled concretes. Thus, the authors introduced a correction factor to take into account the reduction effect exerted by the incorporation of a known amount of recycled concrete aggregates on the modulus of elasticity of recycled mixtures. López-Gayarre (2015) also showed that the elastic modulus of recycled concrete containing mixed recycled aggregates was lower (40%) than the one predicted by the Eurocode-2 formula.

Numerous researchers have proposed their own equations correlating the modulus of elasticity and the compressive strength of recycled mixtures. Some examples can be found in the works of Ravindrarajah and Tam (1985), Kakizaki et al. (1988), Dillmann (1998), Dhir et al. (1999), Mellmann (1999), Zilch and Roos (2001), Xiao et al. (2006), Corinaldesi (2010) and Qasrawi and Marie (2013) for recycled concrete aggregates substitutions, whereas the formula proposed by López-Gayarre et al. (2015) deals with mixed recycled aggregates. It is worth mentioning that the equations suggested by Kakizaki et al. (1988) and Zilch and Roos (2001) also take into consideration the density of the aggregates and the formula offered by Qasrawi and Marie (2013) includes the recycled aggregate to normal aggregate ratio. Nevertheless, all those equations share the same limitation, as they are tailor-made for the experimental results of a specific research work. Thus, a great variability can be observed among them and their applicability outside the investigation from which were derived from.

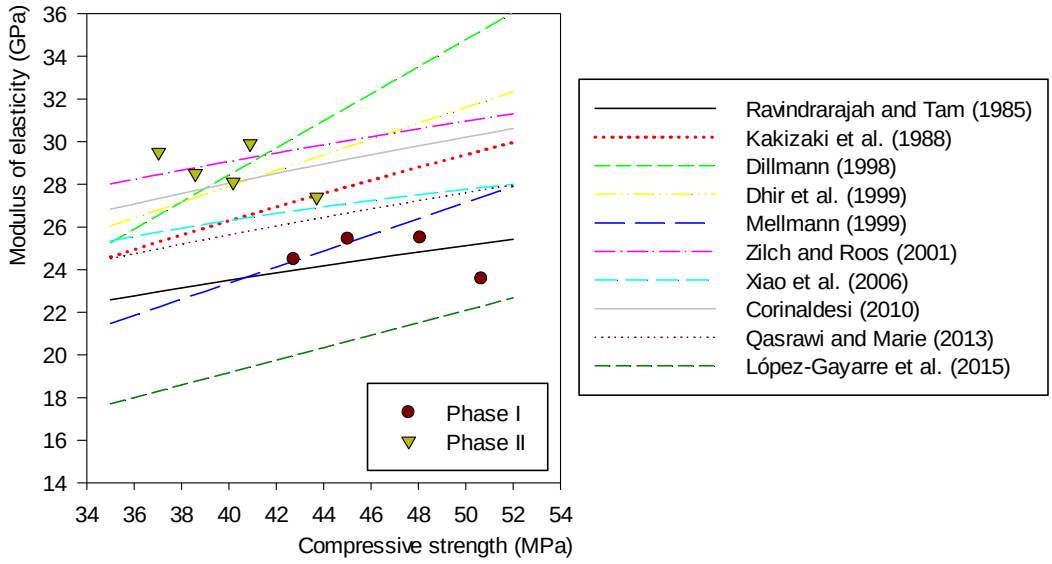

Figure 8.13: Comparison between the model equations for the determination of the elastic modulus proposed by several authors and the experimental results

Figure 8.13 showcases the fitting of the experimental results of this research work to the equations collected from the literature review. Note that, in this case, the compressive strength results from phase I were correspondingly transformed to their equivalent values for cubic specimens to allow a combined assessment. Besides, to facilitate a better fit, the mean density of the concretes was used in the equations proposed by Kakizaki et al. (1988) and Zilch and Roos (2001) and a 0.50 ratio of natural and recycled aggregate was employed in the formula suggested by Qasrawi and

Marie (2013). However, none of the equations provide a good enough fit for all the values pertaining to each research phase. Nevertheless, it is interesting to mention that the equation proposed by López-Gayarre et al. (2015), i.e. the only formula for mixed recycled aggregates, result in the worst estimation as all experimental results displayed higher values. Hence, the use of recycled aggregates form CDW with varying ceramic contents can show a similar performance than recycled coarse aggregates when no pre-saturation or water compensation treatment is employed in the manufacture of the recycled mixtures.

7. STRESS-STRAIN CURVES

The analysis of the stress-strain curves of a concrete mixture conveys information regarding the toughness performance of the material. However, to date, the studies on the stress-strain behaviour of recycled concretes are still few and mainly focused on mixtures made with variable replacement ratios of recycled concrete aggregates. Currently, there are two studies on the stress-strain behaviour of concrete mixtures incorporating mixed recycled aggregates (Martínez-Lage et al., 2012; Rodríguez-Robles et al., 2015) and one research about the load-deflection curves of concretes incorporating ceramic recycled aggregates (Cachim, 2009).

When using recycled concrete aggregates, several authors have reported that recycled mixtures with a 100% coarse replacement produced peak strain values around 20% larger than those of conventional concretes (Xiao et al., 2005; González-Fonteboa et al., 2011a). Nonetheless, lower figures have also been reported. For instance, Rahal et al. (2007) observed an average increase of 5.50%, Liu et al. (2011) registered differences up to 11% larger for recycled mixtures and Wang et al. (2013) reported rises of 6.10%, 9.30%, 6.30%, 5.00% and 4.80% for recycled concretes of 45 MPa, 50 MPa, 55 MPa, 60 MPa and 70 MPa target strength versus the respective control concretes. Moreover, Tsujino et al. (2007) found marginal differences between the stress-strain behaviour of a conventional concrete and a mixture made with untreated recycled concrete aggregates, and Folino and Xargay (2014) also detected minor differences in the deformation corresponding to the peak stress of conventional and recycled mixtures. For mixed recycled aggregates, Martínez-Lage et al. (2012) observed that the ultimate strain, i.e. the deformation at which failure is defined, increased up to 9.52% and 19.05% for concrete mixtures with 50% and 100% substitutions levels, respectively. Finally, Cachim (2009) studied the effect of two types of brick on the stress-strain curves of 17.50% and 35% recycled brick concrete and concluded that their elastic behaviour was similar to that of a conventional concrete, whereas higher deformations were observed in the descending branch of the recycled mixtures. Generally, all these variations are explained by the presence of adhered mortar, concrete wastes and ceramic rubble, which exhibit a lower stiffness than the natural coarse aggregates and consequently increase the deformations (González-Fonteboa et al., 2011a).

Figure 8.14 illustrates the stress-strain behaviour of the conventional and recycled mixtures assessed in both research phases. Note that the deformation values are not plotted against the absolute stress values, but against the relative stress, i.e. the ratio between the applied load and the 28 days compressive strength of each concrete mixture.

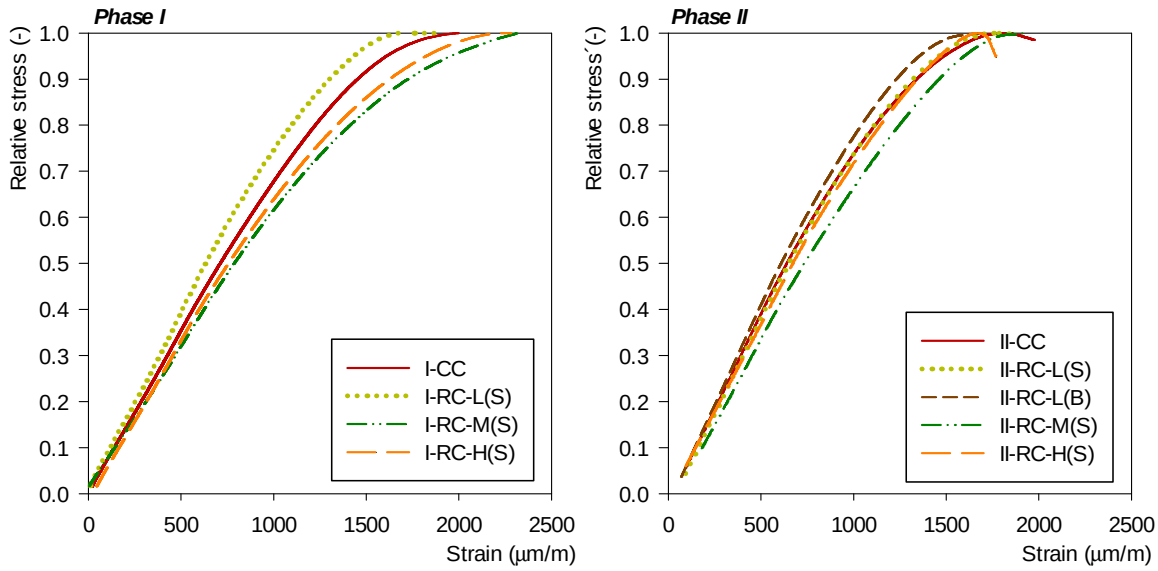

Figure 8.14: Stress-strain curves

Regarding the shape of the ascending branch, it could be observed that both conventional and recycled mixtures displayed a similar behaviour in the first part of the curve regardless of the ceramic content incorporated as a partial substitution of the river gravel. For all concrete mixes, an analogous linear performance is displayed up to a relative stress of 0.40. Notwithstanding the differential state of pores and internal micro-cracks whiten the aggregates or the cement paste before the test, no propagation of micro-cracks occurs at relative low loads (Amorim-Carneiro et al., 2014), which explains the similarities among all concrete mixtures in this first stage. From that point onwards, the curve became parabolic and differences among mixtures are noticeable, since the existing micro-cracks start to develop. For the same relative stress units, the recycled mixtures with low ceramic content (I-RC-L(S), II-RC-L(S) and II-RC-L(B)) exhibit lower deformations than the conventional concrete, whereas the recycled mixtures with medium and high ceramic contents (I-RC-M(S), II-RC-M(S), I-RC-H(S) and II-RC-H(S)) displayed higher deformations than their respective reference mixtures. Albeit the former tendency has been rarely reported in the literature, the improvement observed in this research is explained by the good quality of the ITZ due to the internal curing effect, the use of blended slag cement and the additional pozzolanic activity of the recycled aggregates. While these characteristics are common to all recycled mixtures, it seems that the beneficial effect is dampened for higher amounts of ceramic wastes. Regarding to the latter trend, the shift towards greater deformations for the recycled mixtures than the reference concrete has been observed by several researchers for all types of recycled aggregates substitutions (Xiao et al., 2005; Cachim, 2009; González-Fonteboa et al., 2011a; Rao et al., 2011; Martínez-Lage et al., 2012). The increases respond to the fact that crack propagation in recycled mixtures can take place through the cement but also through the recycled aggregate due to the lower strength and stiffness of some constituents such as adhered mortar or ceramic particles.

Despite the limited extension of the descending branches of the stress-strain curves, a parallel profile can be identified between the conventional and the recycled mixtures with the exception of the II-RC-H(S) mixture. According to Amorim-Carneiro et al. (2014), the negative tangential stiffness of the softening curve conveys the brittleness of the material. Hence, the abrupt negative

slope occurs as consequence of the lack of ductility of the fire-clay brick aggregates that constitute half of the coarse aggregates of the aforementioned mixture. Once again, González-Fonteboa (2011a) registered a shift towards greater deformations in the descending branch of recycled concretes. Nevertheless, Xiao et al. (2005) indicated that recycled mixtures have a more brittle behaviour than that of conventional concrete, and thus the descending branches shifted towards smaller deformations with the amount of recycled concrete aggregate incorporated.

Similarly to Martínez-Lage et al. (2012), all the curves were best fitted ($R^2 \geq 0.99$) to third order polynomials, which are shown in Table 8.7. In addition, the experimental data were compared to model equation (8.8) for the stress–strain curve of conventional concrete proposed in the Eurocode-2 (UNE EN 1992 1-1, 2013) in order to ascertain its accuracy for recycled concrete mixtures (Figure 8.15 and Figure 8.16).

$$\frac{\sigma_c}{f_{cm}} = \frac{k\eta - \eta^2}{1+(k-2)\eta} \qquad \text{where:} \quad k = 1.05 \times E_s \times \frac{|\varepsilon_{c1}|}{fcm}, \quad \eta = \frac{\varepsilon_c}{\varepsilon_{c1}} \tag{8.8}$$

with σ_c/f_{cm} the relative stress [-], E_s the modulus of elasticity [GPa], f_{cm} the mean compressive strength [MPa], ε_c the strain caused at a certain load [‰] and ε_{c1} the peak strain [‰].

Table 8.7: Best fitted stress-strain curves

	Phase I	**Phase II**
CC	$y = -7.96x10^{-11}x^3 + 5.83x10^{-8}x^2 + 0.0007x$	$y = -1.10\ x10^{-10}x^3 + 7.69\ x10^{-8}x^2 + 0.0008x$
RC-L(S)	$y = -1.05x10^{-10}x^3 + 6.03\ x10^{-8}x^2 + 0.0008x$	$y = -1.43x10^{-10}x^3 + 1.75\ x10^{-7}x^2 + 0.0007x$
RC-L(B)	-	$y = -1.73x10^{-10}x^3 + 1.92x10^{-7}x^2 + 0.0008x$
RC-M(S)	$y = -3.54x10^{-11}x^3 - 2.59x10^{-8}x^2 + 0.0007x$	$y = -1.10x10^{-10}x^3 + 1.65x10^{-7}x^2 + 0.0006x$
RC-H(S)	$y = -5.61x10^{-11}x^3 + 2.32x10^{-8}x^2 + 0.0007x$	$y = -1.50x10^{-10}x^3 + 2.03x10^{-7}x^2 + 0.0007x$

In general, the prediction model proposed by the Eurocode-2 (UNE EN 1992 1-1, 2013) resulted in underestimations of the deformations experimented along the ascending branch of all concrete mixtures. Nonetheless, the differences between the experimental and the calculated data are higher for the recycled mixtures with medium and high ceramic contents and greater for the results in phase I than in phase II. González-Fonteboa et al. (2011a), who also compared their results with the Eurocode-2 (UNE EN 1992 1-1, 2013) prediction model, observed the same tendency for the ascending branch but was disregarded as acceptable. The authors also noticed a worse fitting for the descending branch of the stress-strain curve. In spite of proposing some correction factors to take into account the effects caused by the increasing amounts of recycled aggregates, the resulting curves still showed some degree of inaccuracy, in particular in the descending branch.

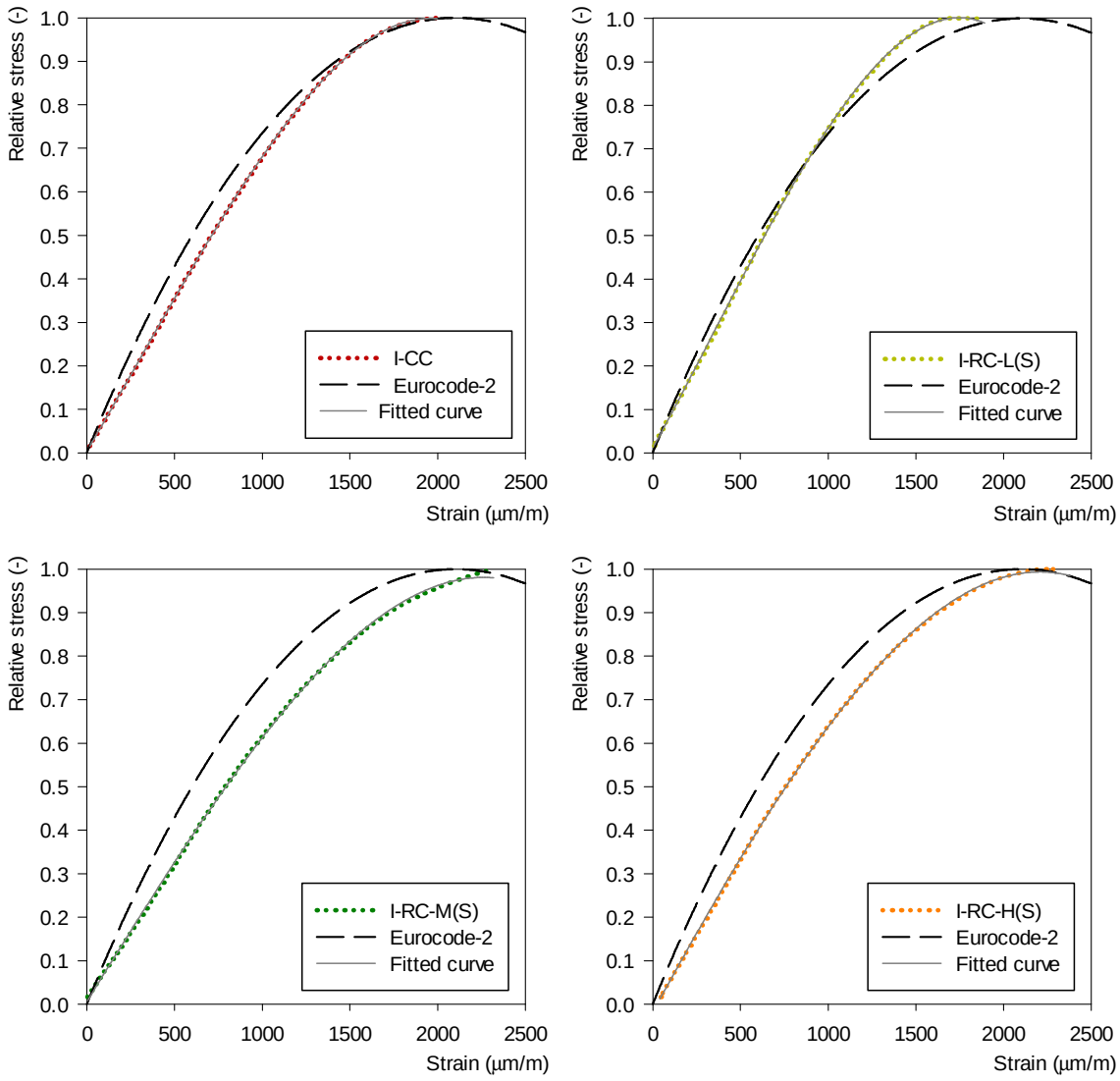

Figure 8.15: Comparison of the experimental results in phase I with the Eurocode-2 prediction and the proposed fitted curve

Table 8.8 shows the experimental values of the peak strain, i.e. the deformation value at the maximum stress, for the conventional and recycled concrete mixtures pertaining to each research phase and their comparison to the respective reference mixture. In addition, the predicted peak strain values according to the formula (8.9) proposed in the Eurocode-2 (UNE EN 1992 1-1, 2013) and the error of such estimation are included as well.

$$\varepsilon_{c1} = 0.7 \times f_{cm}^{\ 0.31} \tag{8.9}$$

with ε_{c1} the peak strain [‰] and f_{cm} the mean compressive strength [MPa].

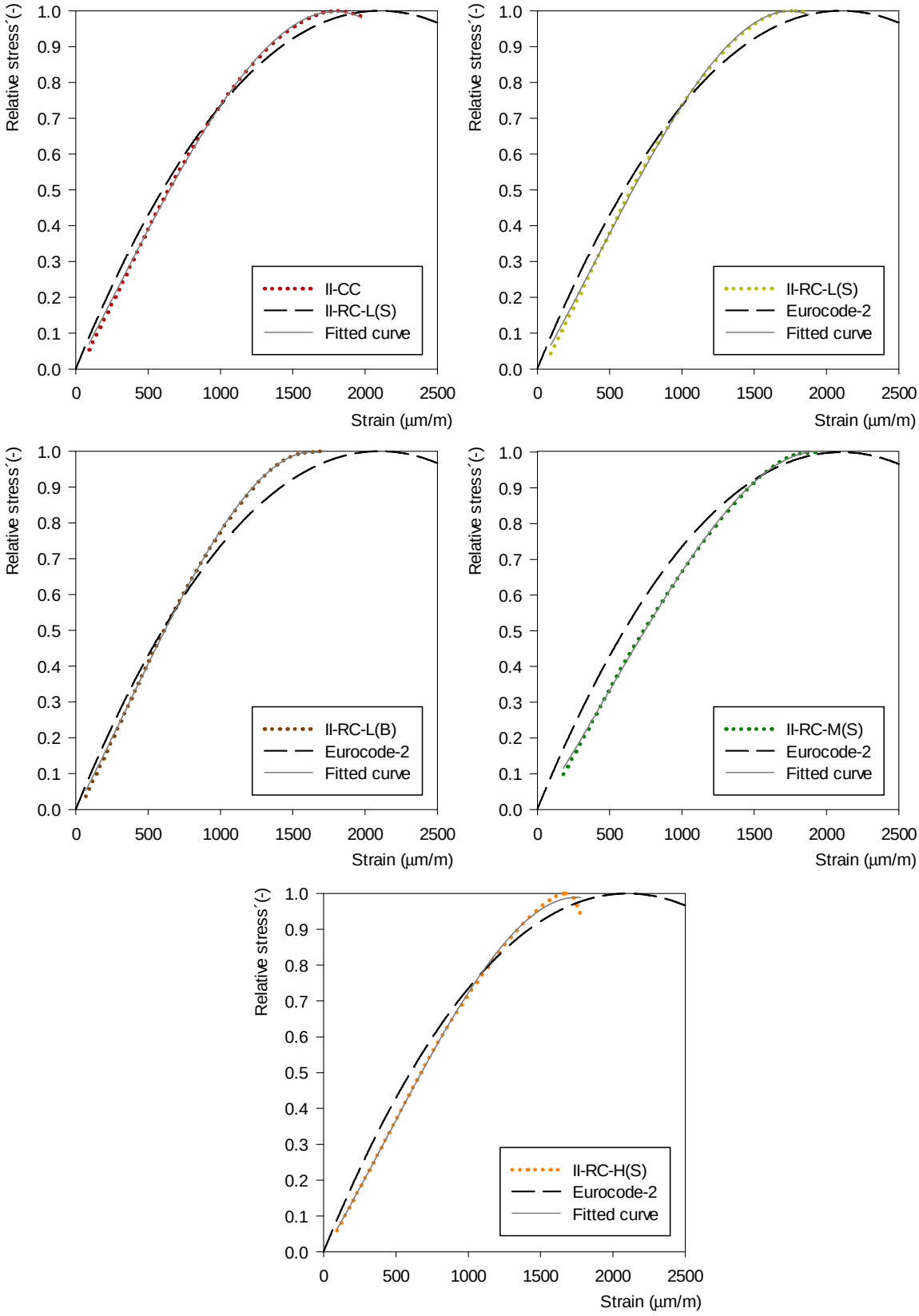

Figure 8.16: Comparison of the experimental results in phase II with the Eurocode-2 prediction and the proposed fitted curve

Table 8.8: Defining parameters of the stress-strain curves

	CC	RC-L(S)	RC-L(B)	RC-M(S)	RC-H(S)
Phase I					
Peak strain (‰)	2.00	1.94	-	2.32	2.38
Variation (%)	-	-3.00	-	16.00	19.00
Predicted peak strain (‰)	2.14	2.09	-	2.20	2.09
Error (%)	7.00	7.73	-	-5.17	-12.18
Phase II					
Peak strain (‰)	1.81	1.77	1.69	1.94	1.68
Variation (%)	-	-2.21	-6.63	7.18	-7.18
Predicted peak strain (‰)	2.14	2.09	2.07	2.19	2.12
Error (%)	18.23	18.08	22.49	12.89	26.19

The peak strain results show that the conventional concrete mixtures are close to the generally accepted 2.1‰ for normal concretes of 25 MPa (UNE EN 1992 1-1, 2013), while the values for the recycled mixtures are both above and below that value (Figure 8.17). On average, the recycled mixtures with low ceramic contents (I-RC-L(S), II-RC-L(S) and II-RC-L(B)) presented a deformation 3.95% lower than the reference concrete. Contrarily, the recycled mixtures with medium ceramic contents (I-RC-M(S), II-RC-M(S)) showed an increase up to 11.59% and the recycled mixtures with high ceramic contents (I-RC-H(S) and II-RC-H(S)) exhibited a mean rise of 5.91%. Nonetheless, the differences between conventional and recycled concretes are marginal, which is in agreement with the findings of Tsujino et al. (2007) and Folino and Xargay (2014). Therefore, no significant negative implications should befall from the use of recycled aggregates from CDW with varying amounts of ceramic wastes on this mechanical property.

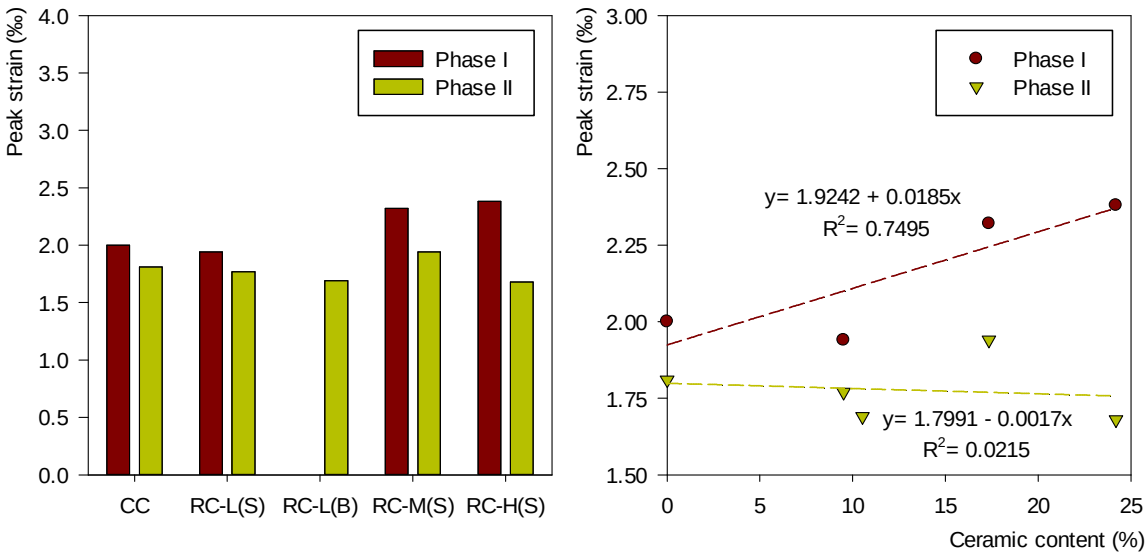

Figure 8.17: Peak strain and its relationship with the ceramic content incorporated in the total weight of aggregates

Several researchers have reported the increase of the peak strain for rising amounts of recycled concrete aggregates (Topçu and Günçan, 1995; Xiao et al., 2005; González-Fonteboa et al., 2011a; Martínez-Lage et al., 2012). A similar relationship between the peak strain and the ceramic content has been identified in this research work for the results arising from phase I (R^2=0.75).

Regarding the comparison between the experimental and the predicted values of the peak strain, the observed scatter is indicative that the current model (8.9) does not render a good fit when applied to recycled mixtures with a 50% replacement ratio of recycled aggregates from CDW with varying ceramic contents. González-Fonteboa et al. (2011a) reached the same conclusion for mixtures made with several replacement ratios of recycled concrete aggregates. Nevertheless, the results in this research work point generally to an overestimation by means of the mathematical determination, whereas González-Fonteboa et al. (2011a) identified the opposite problem.

8. SHRINKAGE

The moment the hardening process initiates, the concrete begins to shrink as a consequence of water loss, which leads to the formation of micro-cracks that can affect other mechanical and durability properties of concrete. There are two main mechanisms controlling the desiccation phenomenon, the consumption of water in the cement hydration (autogenous shrinkage) and the evaporation of the capillary water caused by exposition to low relative humidity environment (drying shrinkage) (Jiménez Montoya et al., 2009).

Since the aggregates play an important role in the restraining of the cement paste during the contractions caused by the shrinkage phenomenon, the substitution of the natural coarse aggregate by recycled aggregates strongly affects the concrete behaviour with respect to this property.

As usual, the studies focusing on the influence of the use of recycled concrete aggregates from CDW are more numerous. Generally, the use of these aggregates led to greater shrinkage than that of a concrete made with natural aggregates (Dillmann, 1998; Limbachiya et al., 1998, 2000; Sagoe-Crentsil et al., 2001; Buyle-Bodin and Hadjieva-Zaharieva, 2002; Gomez-Soberon, 2002; Poon et al., 2002, 2009; Katz, 2003; Eguchi et al., 2007; Kou et al., 2007, 2011; Rao et al., 2007; Tsujino et al., 2007; Domingo-Cabo et al., 2009a, 2009b; Malešev et al., 2010; Ferreira et al., 2011; Henry et al., 2011; Amorim et al., 2012; Kwan et al., 2012; Manzi et al., 2013; Wang et al., 2013; Duan and Poon, 2014). For 100% substitutions, increases up to 60% for 90 days, 70% for 180 days and 80% for 1 year have been reported by Amorim et al. (2012), Domingo-Cabo et al. (2009b) and Buyle-Bodin and Hadjieva-Zaharieva (2002), respectively. Nonetheless, Corinaldesi (2010) stated that replacement ratios of recycled concrete aggregates below 30% barely generated differences with respect to the shrinkage performance of a control concrete.

Despite the findings of Fraaij et al. (2002), Meddah and Sato (2010) and Hoffmann et al. (2012), who stated that recycled concretes incorporating mixed recycled aggregates exhibited lower shrinkages (total and autogenous, respectively) than mixtures using natural aggregates, the general results show that the use of these types of recycled aggregates increases the shrinkage strains.

Dhir and Paine (2007), who studied the influence of several replacement ratios of mixed recycled aggregates containing around 12% of brick particles, stated that substitution levels below 30% had little effect on the shrinkage. Nonetheless, for a total substitution of the coarse aggregates the strains were, on average, 33.33% higher than that of the reference mixture. Beltrán et al. (2014a) reported that the shrinkage of concrete with 100% mixed recycled coarse aggregates containing 14% of ceramic particles was two times higher than that of a concrete mixture made with natural gravel. By employing additional amounts of cement to achieve a similar mechanical performance among conventional and recycled mixes, Beltrán et al. (2014b) observed average increases of 30.19%, 45.24% and 74.78% for replacement rates of 20%, 50% and 100% compared to the reference concrete. The findings of Gomes et al. (2014) suggest that mixtures containing less than 12.50% mixed recycled aggregates display lower shrinkage strains than conventional concretes. In addition, for 12.50% and 50% replacement ratios this tendency was also observed in the first 35 days, although later on the situation was reversed. The authors explained this behaviour through the release of free water contained in the recycled aggregates which mitigated the autogenous shrinkage. De Pauw et al. (1998), Corinaldesi and Moricone (2010) and Kenai and Debieb (2010) also perceived this effect.

Regarding the use of ceramic recycled aggregates, a similar tendency could be observed within the literature. While Mansur et al. (1999) reported that recycled concretes using crushed bricks as the coarse aggregate presented lower drying shrinkage, the rest of the research works point to the worsening effect of the crushed brick aggregates on the shrinkage. For a 20% replacement of crushed brick aggregates, Dhir and Paine (2007) reported a 80% increase of the shrinkage compared to a conventional concrete. Debieb and Kenai (2008) observed a lower shrinkage behaviour for mixtures with several amounts of crushed bricks as coarse aggregates with respect to the conventional concrete during the first 28 days of testing. Later on, the situation was reversed and an abrupt increase up to 80% was observed at 90 days of age when the replacement reached the 100%. It is worth noting that the lack of consensus shown by the findings of some authors could be explained by the differences between types of ceramic aggregates since Kibriya and Speare (1996) noticed that the nature of the crushed bricks strongly affected the degree of shrinkage. For instance, calcareous bricks caused, on average, deformations 2 times greater than conventional bricks.

Figure 8.18 illustrates the shrinkage deformations suffered by the specimens pertaining to the concrete mixtures of phase II, which are a good reflection of the conclusions extracted from the literature review. In general, the use of recycled aggregates produces an increase of the shrinkage strains compared to that of the conventional concrete regardless the type of recycled aggregate employed. The differences in performance seen in the experiments are caused by their variations in elastic modulus and porosity of the mixed and ceramic aggregates. Nonetheless, one of the concrete mixtures (II-RC-L(B)) exhibited a behaviour comparable to the concrete made with river gravel, which can be explained by the lower content of attached mortar and ceramic particles, and even the nature of the latter as stated by Kibriya and Speare (1996) since the other mixture presenting a low ceramic content (II-RC-L(S)) resulted in the greater deformations. These results are similar to those reported by Hoffmann et al. (2012), who observed that concrete mixtures made with 100% mixed recycled coarse aggregates displayed slightly lower and equivalent 91-days shrinkage values than the respective reference concrete.

Regarding the influence of the ceramic content incorporated, the results do not follow the expected pattern of increase in shrinkage with rising percentages of ceramic wastes as stated by Dhir and Paine (2007). The better performance displayed by the concrete mixtures with medium and high ceramic contents (II-RC-M(S) and II-RC-H(S)) can be explained by their higher water absorption capabilities that can foster an improvement in the internal curing (Silva et al., 2015b) and the fact that the content of attached mortar of the II-RC-L(S) mixture had a higher detrimental effect.

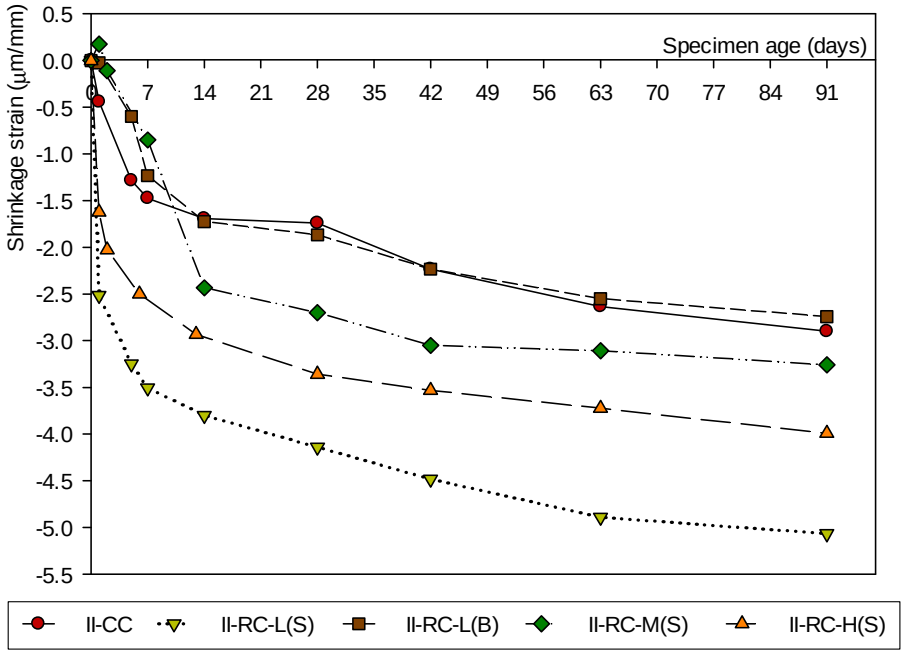

Figure 8.18: Total shrinkage strain

In terms the evolution of shrinkage with time, both the conventional and recycled mixtures presented parallel behaviours as hyperbolic curves that tend to an asymptotic value. In addition, the II-RC-M(S) concrete mixture displayed a lower shrinkage strain during the 10 first days of testing and exhibited greater deformations from that point onwards, which is in agreement with the results of De Pauw et al. (1998), Kenai and Debieb (2010) and Gomes et al. (2014). Quantitatively (Table 8.9), at the end of the test, the results for the recycled mixtures with lower ceramic content (II-RC-L(S) and II-RC-L(B)) show the opposite effect and provide results near the other limit of the range of shrinkage strains observed in the literature review. Albeit not that evident, the deformations obtained for the sample containing the medium and high percentage of ceramic waste are in the lower range of the results reported in the literature. This fact can be explained by the lack of water compensation in the proportioning of the mixtures. On one hand, Ferrerira et al. (2011) demonstrated that the use of pre-saturated recycled aggregates resulted in almost a 30% greater shrinkage than that of mixtures compensating the water absorption by the addition of extra water; on the other hand it is widely accepted that concretes with lower water/cement ratio experiment less shrinkage due to a lower availability of evaporable water (Neville, 1995).

Table 8.9: 91-days total shrinkage

	Shrinkage (µm/mm)	Variation (%)
II-CC	-2.90	-
II-RC-L(S)	-5.07	74.71
II-RC-L(B)	-2.74	-5.46
II-RC-M(S)	-3.26	12.36
II-RC-H(S)	-3.99	37.64

Therefore, it is possible to conclude that the recycled aggregates from CDW, both mixed and ceramic, presented a lower restraining capacity of the cement paste compared to the river gravel. Based on the findings of Sagoe-Crentsil et al. (2001), if Portland cement is used instead of slag cement, an improvement in the total shrinkage up to 25% can be expected. Moreover, the use of fly ash as a partial substitution of the cements has also been proven beneficial due to its dilution effect (Kou et al., 2007; Henry et al., 2011).

8.1. RELATIONSHIP BETWEEN THE SHRINKAGE AND THE POROSITY

Several researchers have related the shrinkage degree of concrete with its amount of pores smaller than 50 nm, i.e. mesopores (Bazant and Wittmann, 1982; Mehta and Monteiro, 2006). The results obtained from the comparison of both variables (Figure 8.19) confirm that a similar relationship exists for recycled concrete mixtures (R^2=0.71).

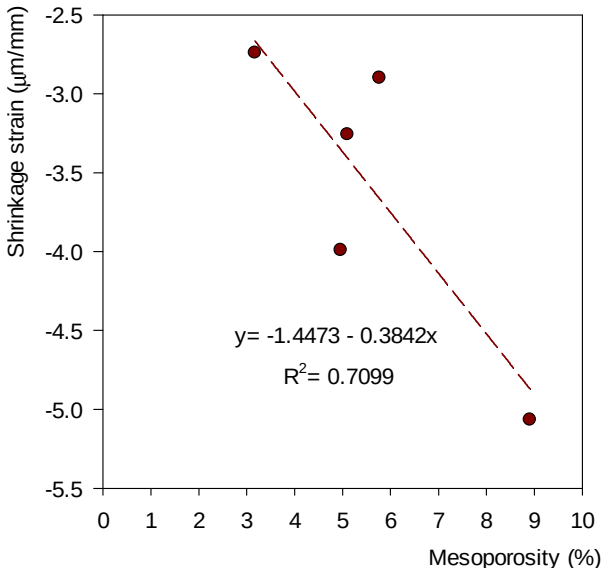

Figure 8.19: Relationship between the shrinkage and the mesoporosity

8.2. RELATIONSHIP BETWEEN THE SHRINKAGE AND THE MODULUS OF ELASTICITY

By using a large compilation of shrinkage results of recycled concrete mixtures, Silva et al. (2015b) observed the existence of a linear relationship (R^2=0.77) between the shrinkage increase as consequence of the recycled aggregate replacement and the elastic modulus of the recycled aggregates employed.

Figure 8.20 illustrates the relationship between both variables for the results of the present investigation, which shows a weaker relationship (R^2= 0.36) than the one found by Silva et al. (2015b).

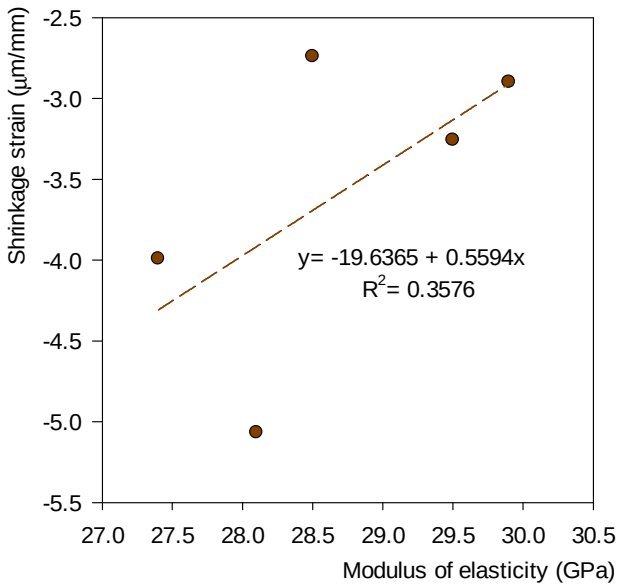

Figure 8.20: Relationship between the shrinkage and the modulus of elasticity

9. CREEP

Analogously to shrinkage, creep is a time-dependent deformation of concrete occurring when the cement matrix is subjected to a sustained stress. Although creep mechanisms are still not completely understood, it is widely accepted that the occurrence of creep strains can be explained by the loss of absorbed water in the C-S-H gel of the cement paste. Thus, it is recognised that the amount and properties of the aggregates constituting the concrete play an important role restraining the cement paste during the applied loads. Consequently, the lower elastic moduli and higher porosity of recycled aggregates are responsible for the worse creep performance when natural aggregates are replaced. However, the creep behaviour of recycled concrete is an issue less studied than the shrinkage.

Several researchers have found the creep strain of concrete incorporating recycled concrete aggregates to be greater than that of the conventional concrete (Limbachiya et al., 2000; Gómez Soberón, 2002; Lamond et al., 2002; Poon et al., 2004a; Kou et al., 2007; Tam and Tam, 2007; Tsujino et al., 2007; Waleed and Canisius, 2007; Anderson et al., 2009; Domingo-Cabo et al., 2009a, 2009b; Paine et al., 2009; Butler et al., 2011; Manzi et al., 2013).

For replacement ratios up to 30%, Limbachiya et al. (2000) reported that recycled mixtures exhibited similar creep coefficients than conventional concrete but increased deformations occurred from that substitution level onwards. Depending on the quality of the recycled aggregates employed, a range of 30–60% in creep increase can be observed according to Lamond et al. (2002).

Anderson et al. (2009) further delimited the variation between 20% and 40% compared to conventional concrete. Domingo-Cabo et al. (2009a, 2009b) registered creep increases between 35% and 51% for replacement ratios from 20% to 100%. Besides the lower moduli and higher porosity, the negative effect is also attributed to the fact that recycled concrete aggregates contribute to increase the cement paste volume of the recycled mixture as a consequence of the old mortar attached (Behera et al., 2014). For instance, by using the EMV proportioning method, i.e. taking into account the adhered mortar to avoid any increase of the paste content in the recycled mixtures, Fathifazl et al. (2011) observed comparable or even lower creep values in recycled mixtures than in the respective conventional concrete.

For the use of mixed recycled aggregates in the concrete manufacture, Fraaij et al. (2002) showed that recycled concretes showed greater creep deformations than mixtures using natural aggregates. De Pauw et al. (1998) studied the creep of concretes containing either mixed recycled aggregates or recycled concrete aggregates and observed increases in the creep strain around 14% and 36% respectively. Hoffmann et al. (2012) reported that concrete mixtures made with 100% mixed recycled coarse aggregates displayed 91-days creep values ranging from 2.28 to 3.97 times higher than the respective reference concrete.

To date, only two research works have studied the effect on creep of the use of crushed bricks as replacement of the conventional coarse aggregate in the concrete manufacture. While, Mansur et al. (1999) indicated that recycled concretes using that type of aggregates presented almost similar specific creep than the conventional concrete, Kibriya and Speare (1996) noticed greater creep values that strongly depended on the nature of the crushed bricks employed. For instance, calcareous bricks caused, on average, deformations 2.54 times greater than conventional bricks (Kibriya and Speare, 1996).

Figure 8.21 illustrates the evolution of the creep data with time undergone by the conventional and recycled mixtures. The basic creep was determined from the measurements in sealed samples and the total creep through the results of unsealed samples. In addition, the difference between both results corresponds to the drying creep of the specimens.

The creep curves in Figure 8.21 shows a parallel behaviour for the conventional and recycled mixtures as a hyperbolic curve that tends to an asymptotic value. Whereas the basic creep seems to have reached the plateau stage at the end of the research period (approximately 80 days), the slope of the drying creep continues to increase. Some authors have identified the stabilization of the creep deformations of recycled mixtures at 90 days (Kou et al., 2007; Waleed and Canisius, 2007; Paine et al., 2009). Nonetheless, there is also precedent of recycled mixtures containing recycled concrete aggregates that only reached the equilibrium after 300 days (Tsujino et al., 2007; Fathifazl et al., 2011) or even continued experiencing creep deformations beyond 1 year of testing (Manzi et al., 2013).

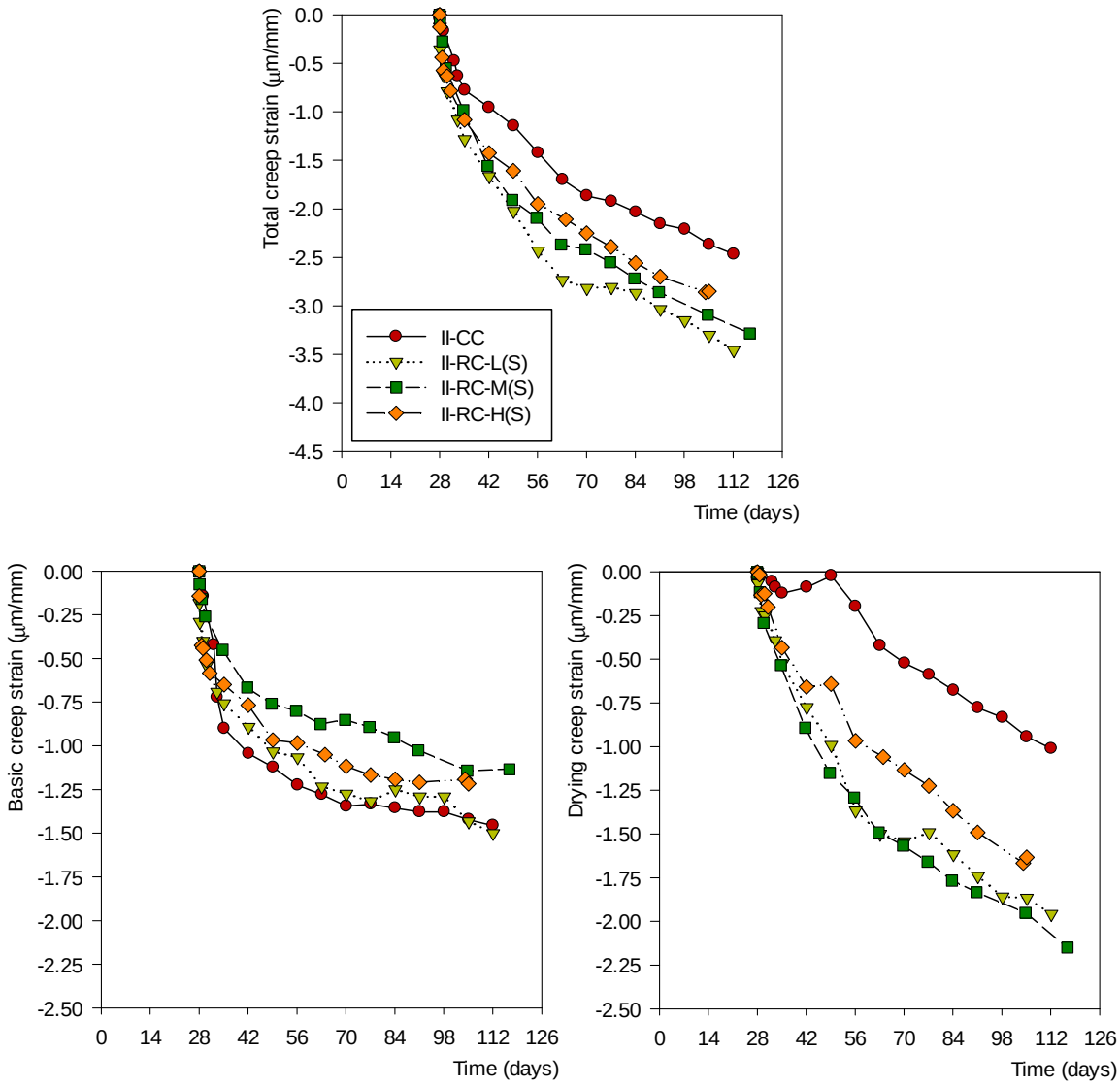

Figure 8.21: Creep strains

In terms of basic creep, recycled concretes presented a better behaviour than the conventional concrete. After 77 days of loading, the creep strains reached values 0.75% lower for the recycled concrete with low ceramic continent (II-RC-L(S)), 33.08 lower for the recycled concrete with medium ceramic content (II-RC-LM(S)) and 12.03% lower recycled concrete with high ceramic content (II-RC-H(S)). By means of a linear regression analysis between the results at the 77-days mark of the test and the ceramic content incorporated to the mixtures, it was possible to identify a low correlation (R^2= 0.35) between the two variables, which suggests that the decrease in the basic creep is not associated to rising amounts of ceramic wastes (Figure 8.22).

Regarding the drying creep performance, a shift is clear between the behaviour of concrete containing recycled aggregates and all recycled mixtures acted worse than the conventional concrete and exhibited higher values throughout all the experiment. However, in this case, the increase in the drying creep was up to 152.54%, 181.36% and 42.07% for low (II-RC-L(S)), medium (II-RC-M(S)) and high (II-RC-H(S)) contents, respectively (Table 8.10). Nevertheless, the relationship between the creep strain and the ceramic content incorporated (Figure 8.22) resulted in a non-significant correlation factor (R^2=0.40).

Finally, the total creep deformations reflect the previous two behaviours, as the recycled mixtures continue to exhibit greater creep strains that the conventional concrete, reaching increases between 24.48% and 46.35% at the 77-days mark (Table 8.10), but their relative performance is influenced by the degree of basic creep experimented by the mixture. Hence, the relationship between the total creep and the ceramic content is weaker (R^2=0.21) than in any other the case (Figure 8.22).

Table 8.10: 77-days creep deformations

	Total (µm/mm)	Variation (%)	Basic (µm/mm)	Variation (%)	Drying (µm/mm)	Variation (%)
II-CC	-1.92	-	-1.33	-	-0.59	-
II-RC-L(S)	-2.81	46.35	-1.32	-0.75	-1.49	152.54
II-RC-M(S)	-2.55	32.81	-0.89	-33.08	-1.66	181.36
II-RC-H(S)	-2.39	24.48	-1.17	-12.03	-1.23	108.47

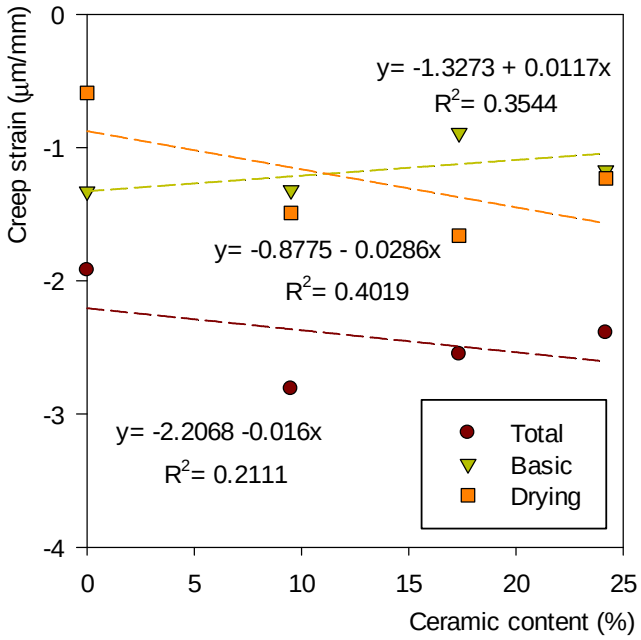

Figure 8.22: Relationship between the 77-days creep strain and the ceramic content incorporated with the total weight of aggregates

Analogously to the shrinkage deformations, it is possible to conclude that the recycled aggregates from CDW, both mixed and ceramic, generally presented a lower restraining capacity of the cement paste compared to the river gravel regarding the effects of creep which led to higher total deformations. Based on the findings of Tam and Tam (2007), changing the normal mixing procedure to a two-stage mixing approach (TSMA) can improve the creep behaviour of recycled mixtures up to a 23%. In addition, the use of fly ash has been proven to enhance the creep behaviour of recycled mixtures (Kou et al., 2007). Contrarily, it is expected that the pre-saturation or compensation for the water absorption of the recycled aggregates can lead to higher deformations, since there is more free water (not required for the cement hydration) that can be lost during the loading of the specimens, in particular under unsealed conditions.

10. REFERENCES

ACI Committee 318, 2014. Building code requirements for structural concrete and commentary (ACI 318-14). American Concrete Institute.

Adamson, M., Razmjoo, A., Poursaee, A., 2015. Durability of concrete incorporating crushed brick as coarse aggregate. *Construction and Building Materials* 94: 426–432.

Afify, M.R., Soliman, N.M., 2014. Improvement Properties of Recycle Concrete using Clay Brick as a Coarse Aggregate. *International Journal of Current Engineering and Technology. 4 (1), 119* 127: 100.

Agamuthu, P., 2008. Challenges in sustainable management of construction and demolition waste. *Waste Management & Research* 26 (6): 491–492.

Akbarnezhad, A., Ong, K.C.G., Zhang, M.H., Tam, C.T., Foo, T.W.J., 2011. Microwave-assisted beneficiation of recycled concrete aggregates. *Construction and Building Materials* 25 (8): 3469–3479.

Akhtaruzzaman, A.A., Hasnat, A., 1983. Properties of concrete using crushed brick as aggregate. *Concrete International* 5 (2): 58–63.

Amorim-Carneiro, J., Lopes-Lima, P.R., Batista-Leite, M., Dias-Toledo-Filho, R., 2014. Compressive stress–strain behavior of steel fiber reinforced-recycled aggregate concrete. *Cement and Concrete Composites* 46: 65–72.

Amorim, P., De Brito, J., Evangelista, L., 2012. Concrete made with coarse concrete aggregate: influence of curing on durability. *ACI Materials Journal* 109 (2): 195–204.

Anderson, K.W., Uhlmeyer, J.S., Russell, M.A., 2009. Use of recycled concrete aggregate in PCCP: literature search. Washington State Department of Transportation, Washington DC, USA.

Bazant, Z.P., Wittmann, F.H. (Eds.), 1982. Creep and shrinkage in concrete structures. Wiley Chichester.

Behera, M., Bhattacharyya, S.K., Minocha, A.K., Deoliya, R., Maiti, S., 2014. Recycled aggregate from C&D waste & its use in concrete – A breakthrough towards sustainability in construction sector: A review. *Construction and Building Materials* 68: 501–516.

Beltrán, M.G., Agrela, F., Barbudo, A., Ayuso, J., Ramírez, A., 2014a. Mechanical and durability properties of concretes manufactured with biomass bottom ash and recycled coarse aggregates. *Construction and Building Materials* 72: 231–238.

Beltrán, M.G., Barbudo, A., Agrela, F., Galvín, A.P., Jiménez, J.R., 2014b. Effect of cement addition on the properties of recycled concretes to reach control concretes strengths. *Journal of Cleaner Production* 79: 124–133.

Berndt, M.L., 2009. Properties of sustainable concrete containing fly ash, slag and recycled concrete aggregate. *Construction and Building Materials* 23 (7): 2606–2613.

Bezerra-Cabral, A.E., Schalch, V., Carpena Coitinho Dal Molin, D., Duarte Ribeiro, J.L., 2010. Mechanical properties modeling of recycled aggregate concrete. *Construction and Building Materials* 24 (4): 421–430.

Bravo, M., de Brito, J., Pontes, J., Evangelista, L., 2015. Mechanical performance of concrete made with aggregates from construction and demolition waste recycling plants. *Journal of Cleaner Production*.

Bremner, T.W., Holm, T.A., 1986. Elastic compatibility and the behavior of concrete. *ACI Journal Proceedings* 83 (2): 244–250.

Butler, L., West, J.S., Tighe, S.L., 2011. The effect of recycled concrete aggregate properties on the bond strength between RCA concrete and steel reinforcement. *Cement and Concrete Research* 41 (10): 1037–1049.

Buyle-Bodin, F., Hadjieva-Zaharieva, R., 2002. Influence of industrially produced recycled aggregates on flow properties of concrete. *Mat. Struct.* 35 (8): 504–509.

Cachim, P.B., 2009. Mechanical properties of brick aggregate concrete. *Construction and Building Materials* 23 (3): 1292–1297.

Çakır, Ö., 2014. Experimental analysis of properties of recycled coarse aggregate (RCA) concrete with mineral additives. *Construction and Building Materials* 68: 17–25.

Chen, H.J., Yen, T., Chen, K.H., 2003a. Use of building rubbles as recycled aggregates. *Cement and Concrete Research* 33 (1): 125–132.

Chen, H.J., Yen, T., Chen, K.H., 2003b. The use of building rubbles in concrete and mortar. *Journal of the Chinese Institute of Engineers* 26 (2): 227–236.

Corinaldesi, V., 2010. Mechanical and elastic behaviour of concretes made of recycled-concrete coarse aggregates. *Construction and Building Materials* 24 (9): 1616–1620.

Corinaldesi, V., Moriconi, G., 2009. Influence of mineral additions on the performance of 100% recycled aggregate concrete. *Construction and Building Materials* 23 (8): 2869–2876.

Corinaldesi, V., Moriconi, G., 2010. Recycling of rubble from building demolition for low-shrinkage concretes. *Waste Management* 30 (4): 655–659.

Correia, J.R., Brito, J. de, Pereira, A.S., 2006. Effects on concrete durability of using recycled ceramic aggregates. *Materials and Structures* 39 (2): 169–177.

Debieb, F., Kenai, S., 2008. The use of coarse and fine crushed bricks as aggregate in concrete. *Construction and Building Materials* 22 (5): 886–893.

de Brito, J., Pereira, A.S., Correia, J.R., 2005. Mechanical behaviour of non-structural concrete made with recycled ceramic aggregates. *Cement and Concrete Composites* 27 (4): 429–433.

de Brito, J., Robles, R., 2010. Recycled aggregate concrete (RAC) methodology for estimating its long-term properties. *Indian Journal of Engineering & Materials Sciences* 17 (6): 449–462.

De Pauw, P., Thomas, P., Vyncke, J., Desmyter, J., 1998. Shrinkage and creep of concrete with recycled materials as coarse aggregates, in: Sustainable Construction: Use of Recycled Concrete Aggregate. Thomas Telford Publishing, 213–225.

Dhir, R.K., Limbachiya, M.C., Leelawat, T., 1999. Suitability of recycled concrete aggregate for use in BS 5328 designated mixes. *Structures and Buildings* 134 (3): 257–274.

Dhir, R.K., Paine, K., 2004. Suitability and practicality of using coarse RCA in normal and high-strength concrete, in: 1st International Conference on Sustainable Construction: Waste Management. Singapore, 108–123.

Dhir, R.K., Paine, K.A., 2007. Performance related approach to use of recycled aggregates (AGG0074). WRAP.

Dilbas, H., Şimşek, M., Çakır, Ö., 2014. An investigation on mechanical and physical properties of recycled aggregate concrete (RAC) with and without silica fume. *Construction and Building Materials* 61: 50–59.

Dillmann, R., 1998. Concrete with recycled concrete aggregate. Presented at the Proceedings of International Symposium on Sustainable Construction: Use of Recycled Concrete Aggregate, Dundee, UK, 239–253.

Domingo-Cabo, A., Lázaro, C., López Gayarre, F., Serrano-López, M.A., López-Colina, C., 2009a. Long term deformations by creep and shrinkage in recycled aggregate concrete. *Mater Struct* 43 (8): 1147–1160.

Domingo-Cabo, A., Lázaro, C., López-Gayarre, F., Serrano-López, M.A., Serna, P., Castaño-Tabares, J.O., 2009b. Creep and shrinkage of recycled aggregate concrete. *Construction and Building Materials* 23 (7): 2545–2553.

Duan, Z.H., Poon, C.S., 2014. Properties of recycled aggregate concrete made with recycled aggregates with different amounts of old adhered mortars. *Materials & Design* 58: 19–29.

Eguchi, K., Teranishi, K., Nakagome, A., Kishimoto, H., Shinozaki, K., Narikawa, M., 2007. Application of recycled coarse aggregate by mixture to concrete construction. *Construction and Building Materials* 21 (7): 1542–1551.

Etxeberria, M., Vázquez, E., Mari, A., 2006. Microstructure analysis of hardened recycled aggregate concrete. *Magazine of Concrete Research* 58 (10): 683–690.

Etxeberria, M., Vázquez, E., Marí, A., Barra, M., 2007. Influence of amount of recycled coarse aggregates and production process on properties of recycled aggregate concrete. *Cement and Concrete Research* 37 (5): 735–742.

Fathifazl, G., Ghani Razaqpur, A., Burkan Isgor, O., Abbas, A., Fournier, B., Foo, S., 2011. Creep and drying shrinkage characteristics of concrete produced with coarse recycled concrete aggregate. *Cement and Concrete Composites* 33 (10): 1026–1037.

Ferreira, L., de Brito, J., Barra, M., 2011. Influence of the pre-saturation of recycled coarse concrete aggregates on concrete properties. *Magazine of Concrete Research* 63 (8): 617–627.

Folino, P., Xargay, H., 2014. Recycled aggregate concrete – Mechanical behavior under uniaxial and triaxial compression. *Construction and Building Materials* 56: 21–31.

Fonseca, N., de Brito, J., Evangelista, L., 2011. The influence of curing conditions on the mechanical performance of concrete made with recycled concrete waste. *Cement and Concrete Composites* 33 (6): 637–643.

Fraaij, A.L., Pietersen, H.S., De Vries, J., 2002. Performance of concrete with recycled aggregates, in: International Conference: Sustainable Concrete Construction. Dundee, UK, 187–198.

Gomes, M., Brito, J. de, 2009. Structural concrete with incorporation of coarse recycled concrete and ceramic aggregates: durability performance. *Materials and Structures* 42 (5): 663–675.

Gomes, M., de Brito, J., Bravo, M., 2014. Mechanical Performance of Structural Concrete with the Incorporation of Coarse Recycled Concrete and Ceramic Aggregates. *Journal of Materials in Civil Engineering* 26 (10): 04014076.

Gomez-Soberon, J.M., 2002. Shrinkage of concrete with replacement of aggregate with recycled concrete aggregate. *ACI Special Publication* 209: 475–496.

Gómez Soberón, J.M.V., 2002. Creep of concrete with substitution of normal aggregate by recycled concrete aggregate. *ACI Special Publication* 209: 461–474.

Gonzalez, A., Etxeberria, M., 2014. Experimental analysis of properties of high performance recycled aggregate concrete. *Construction and Building Materials* 52: 227–235.

Gonzalez-Corominas, A., Etxeberria, M., 2014. Properties of high performance concrete made with recycled fine ceramic and coarse mixed aggregates. *Construction and Building Materials* 68: 618–626.

González-Fonteboa, B., Martinez-Abella, F., 2005. Recycled aggregates concrete: aggregate and mix properties. *Materiales de Construcción* 55 (279): 53–66.

González-Fonteboa, B., Martínez-Abella, F., 2008. Concretes with aggregates from demolition waste and silica fume. Materials and mechanical properties. *Building and Environment* 43 (4): 429–437.

González-Fonteboa, B., Martínez-Abella, F., Carro-López, D., Seara-Paz, S., 2011a. Stress–strain relationship in axial compression for concrete using recycled saturated coarse aggregate. *Construction and Building Materials* 25 (5): 2335–2342.

González-Fonteboa, B., Martínez-Abella, F., Eiras-López, J., Seara-Paz, S., 2011b. Effect of recycled coarse aggregate on damage of recycled concrete. *Mater Struct* 44 (10): 1759–1771.

Hansen, T.C. (Ed.), 1992. Recycling of demolished concrete and masonry. E&FN Spon, London.

Henry, M., Pardo, G., Nishimura, T., Kato, Y., 2011. Balancing durability and environmental impact in concrete combining low-grade recycled aggregates and mineral admixtures. *Resources, Conservation and Recycling* 55 (11): 1060–1069.

Hoffmann, C., Schubert, S., Leemann, A., Motavalli, M., 2012. Recycled concrete and mixed rubble as aggregates: Influence of variations in composition on the concrete properties and their use as structural material. *Construction and Building Materials* 35: 701–709.

Ihobe, CEDEX, 2011. Uses of mixed recycled aggregates from construction and demolition wastes [in Spanish] (Pre-normative investigation). Ihobe.

Jiménez Montoya, P., Arroyo Portero, J.C., Morán Cabré, F., García Meseguer, Á., 2009. Structutal concrete. Based on the Spanish Code on structural concrete EHE-08 and adaptated to the Eurocode EC-2 [in Spanish]. Cartoné, Madrid.

Kakizaki, M., Harada, M., Soshiroda, T., Kubota, S., Ikeda, T., Kasai, Y., 1988. Strength and elastic modulus of recycled aggregate concrete, in: Proceedings of the Second International RILEM Symposium on Demolition and Reuse of Concrete and Masonry. Tokyo, Japan, 565–574.

Katz, A., 2003. Properties of concrete made with recycled aggregate from partially hydrated old concrete. *Cement and Concrete Research* 33 (5): 703–711.

Kenai, S., Debieb, F., 2010. Caractérisation de la durabilité des bétons recyclés à base de gros et fins granulats de briques et de béton concassés. *Mater Struct* 44 (4): 815–824.

Khalaf, F.M., 2006. Using crushed clay brick as coarse aggregate in concrete. *Journal of materials in civil engineering* 18 (4): 518–526.

Khalaf, F.M., DeVenny, A.S., 2004. Recycling of demolished masonry rubble as coarse aggregate in concrete: review. *Journal of materials in civil engineering* 16 (4): 331–340.

Khaloo, A.R., 1994. Properties of concrete using crushed clinker brick as coarse aggregate. *ACI Materials Journal* 91 (4): 401–407.

Khaloo, A.R., 1995. Crushed tile coarse aggregate concrete. *Cement, Concrete and Aggregates* 17 (2): 119–125.

Khatib, J.M., 2005. Properties of concrete incorporating fine recycled aggregate. *Cement and Concrete Research* 35 (4): 763–769.

Kheder, G.F., Al-Windawi, S.A., 2005. Variation in mechanical properties of natural and recycled aggregate concrete as related to the strength of their binding mortar. *Mat. Struct.* 38 (7): 701–709.

Kibriya, T., Speare, P.R.S., 1996. The use of crushed brick coarse aggregate in concrete, in: International Congress on "Concrete in the Service of Mankind." Dundee, UK, 495–503.

Kim, K., Shin, M., Cha, S., 2013. Combined effects of recycled aggregate and fly ash towards concrete sustainability. *Construction and Building Materials* 48: 499–507.

Kong, D., Lei, T., Zheng, J., Ma, C., Jiang, J., Jiang, J., 2010. Effect and mechanism of surface-coating pozzalanics materials around aggregate on properties and ITZ microstructure of recycled aggregate concrete. *Construction and Building Materials* 24 (5): 701–708.

Kou, S.C., Poon, C.S., 2009. Properties of self-compacting concrete prepared with coarse and fine recycled concrete aggregates. *Cement and Concrete Composites* 31 (9): 622–627.

Kou, S.C., Poon, C.S., Agrela, F., 2011. Comparisons of natural and recycled aggregate concretes prepared with the addition of different mineral admixtures. *Cement and Concrete Composites* 33 (8): 788–795.

Kou, S.C., Poon, C.S., Chan, D., 2007. Influence of fly ash as cement replacement on the properties of recycled aggregate concrete. *Journal of Materials in Civil Engineering* 19 (9): 709–717.

Kwan, W.H., Ramli, M., Kam, K.J., Sulieman, M.Z., 2012. Influence of the amount of recycled coarse aggregate in concrete design and durability properties. *Construction and Building Materials* 26 (1): 565–573.

Lamond, J.F., Campbell, R.L., Giraldi, A., Jenkins, N.J.T., Campbell, T.R., Halczak, W., Miller, R., Cazares, J.A., Hale, H.C., Seabrook, P.T., 2002. Removal and reuse of hardened concrete. *ACI Materials Journal* 99 (3): 300–325.

Li, J., Xiao, H., Zhou, Y., 2009. Influence of coating recycled aggregate surface with pozzolanic powder on properties of recycled aggregate concrete. *Construction and Building Materials* 23 (3): 1287–1291.

Limbachiya, M.C., Leelawat, T., Dhir, R.K., 2000. Use of recycled concrete aggregate in high-strength concrete. *Materials and Structures* 33 (9): 574–580.

Limbachiya, M., Leelawat, T., Dhir, R., 1998. RCA concrete: a study of properties in the fresh state, strength development and durability, in: Proceedings of the International Symposium on Sustainable Construction: Use of Recycled Concrete Aggregate. London, UK.

Liu, Q., Xiao, J., Sun, Z., 2011. Experimental study on the failure mechanism of recycled concrete. *Cement and Concrete Research* 41 (10): 1050–1057.

López-Gayarre, F., Blanco Viñuela, R., Serrano-López, M.A., López-Colina, C., 2015. Influence of the water variation on the mechanical properties of concrete manufactured with recycled mixed aggregates for pre-stressed components. *Construction and Building Materials* 94: 844–850.

López-Gayarre, F., López-Colina, C., Serrano-López, M.A., García Taengua, E., López Martínez, A., 2011. Assessment of properties of recycled concrete by means of a highly fractioned factorial design of experiment. *Construction and Building Materials* 25 (10): 3802–3809.

López Gayarre, F., López-Colina, C., Serrano, M.A., López-Martínez, A., 2013. Manufacture of concrete kerbs and floor blocks with recycled aggregate from C&DW. *Construction and Building Materials* 40: 1193–1199.

López-Gayarre, F., Serna, P., Domingo-Cabo, A., Serrano-López, M.A., López-Colina, C., 2009. Influence of recycled aggregate quality and proportioning criteria on recycled concrete properties. *Waste Management* 29 (12): 3022–3028.

Lovato, P.S., Possan, E., Molin, D.C.C.D., Masuero, Â.B., Ribeiro, J.L.D., 2012. Modeling of mechanical properties and durability of recycled aggregate concretes. *Construction and Building Materials* 26 (1): 437–447.

Malešev, M., Radonjanin, V., Marinković, S., 2010. Recycled concrete as aggregate for structural concrete production. *Sustainability* 2 (5): 1204–1225.

Mansur, M.A., Wee, T.H., Lee, S.C., 1999. Crushed bricks as coarse aggregate for concrete. *ACI Materials Journal* 96 (4): 478–484.

Manzi, S., Mazzotti, C., Bignozzi, M.C., 2013. Short and long-term behavior of structural concrete with recycled concrete aggregate. *Cement and Concrete Composites* 37: 312–318.

Martínez-Lage, I., Martínez-Abella, F., Vázquez-Herrero, C., Pérez-Ordóñez., J.L., 2012. Properties of plain concrete made with mixed recycled coarse aggregate. *Construction and Building Materials* 37: 171–176.

Mas, B., Cladera, A., Bestard, J., Muntaner, D., López, C.E., Piña, S., Prades, J., 2012a. Concrete with mixed recycled aggregates: Influence of the type of cement. *Construction and Building Materials* 34: 430–441.

Mas, B., Cladera, A., Olmo, T. del, Pitarch, F., 2012b. Influence of the amount of mixed recycled aggregates on the properties of concrete for non-structural use. *Construction and Building Materials* 27 (1): 612–622.

Matias, D., de Brito, J., Rosa, A., Pedro, D., 2013. Mechanical properties of concrete produced with recycled coarse aggregates – Influence of the use of superplasticizers. *Construction and Building Materials* 44: 101–109.

Meddah, M.S., Sato, R., 2010. Effect of Curing Methods on Autogenous Shrinkage and Self-Induced Stress of High-Performance Concrete. *MJ* 107 (1): 65–74.

Medina, C., Frías, M., Sánchez de Rojas, M.I., 2012a. Microstructure and properties of recycled concretes using ceramic sanitary ware industry waste as coarse aggregate. *Construction and Building Materials* 31: 112–118.

Medina, C., Sánchez de Rojas, M.I., Frías, M., 2012b. Reuse of sanitary ceramic wastes as coarse aggregate in eco-efficient concretes. *Cement and Concrete Composites* 34 (1): 48–54.

Medina, C., Zhu, W., Howind, T., Frías, M., Sánchez de Rojas, M.I., 2015. Effect of the constituents (asphalt, clay materials, floating particles and fines) of construction and demolition waste on the properties of recycled concretes. *Construction and Building Materials* 79: 22–33.

Medina, C., Zhu, W., Howind, T., Sánchez de Rojas, M.I., Frías, M., 2014. Influence of mixed recycled aggregate on the physical – mechanical properties of recycled concrete. *Journal of Cleaner Production* 68: 216–225.

Mehta, P.K., Monteiro, P.J., 2006. Concrete: microstructure, properties, and materials. McGraw-Hill New York.

Mellmann, G., Meinhold, U., Maultzsch, M., 1999. Processed concrete rubble for the reuse as aggregate, in: Proceeding of the International Seminar on Exploiting Waste in Concrete. Dundee, UK, 171–178.

Neville, A.M., 1995. Properties of concrete. Harlow, Essex: Longman.

Neville, A.M., 1997. Aggregate bond and modulus of elasticity of concrete. *ACI Materials Journal* 94 (1): 71–74.

Neville, A.M., Brooks, J.J., 2010. Concrete technology. Pearson, London, UK.

Otsuki, N., Miyazato, S., Yodsudjai, W., 2003. Influence of recycled aggregate on interfacial transition zone, strength, chloride penetration and carbonation of concrete. *Journal of materials in civil engineering*.

Pacheco-Torgal, F., Jalali, S., 2010. Reusing ceramic wastes in concrete. *Construction and Building Materials* 24 (5): 832–838.

Padmini, A.K., Ramamurthy, K., Mathews, M.S., 2009. Influence of parent concrete on the properties of recycled aggregate concrete. *Construction and Building Materials* 23 (2): 829–836.

Paine, K.A., Collery, D.J., Dhir, R.K., 2009. Strength and deformation characteristics of concrete containing coarse recycled and manufactured aggregates, in: Proceedings of the 11th International Conference on Non-Conventional Materials and Technologies (NOCMAT 2009). Bath, UK, 1–9.

Paine, K.A., Dhir, R.K., 2010. Recycled aggregates in concrete: a performance-related approach. *Magazine of Concrete Research* 62 (7): 519–530.

Pedro, D., Brito, J. de, Evangelista, L., 2014a. Performance of concrete made with aggregates recycled from precasting industry waste: influence of the crushing process. *Mater Struct* : 1–14.

Pedro, D., de Brito, J., Evangelista, L., 2014b. Influence of the use of recycled concrete aggregates from different sources on structural concrete. *Construction and Building Materials* 71: 141–151.

Pepe, M., Toledo Filho, R.D., Koenders, E.A.B., Martinelli, E., 2014. Alternative processing procedures for recycled aggregates in structural concrete. *Construction and Building Materials* 69: 124–132.

Poon, C.S., Chan, D., 2006. Paving blocks made with recycled concrete aggregate and crushed clay brick. *Construction and Building Materials* 20 (8): 569–577.

Poon, C.-S., Chan, D., 2007. Effects of contaminants on the properties of concrete paving blocks prepared with recycled concrete aggregates. *Construction and Building Materials* 21 (1): 164–175.

Poon, C.S., Kou, S.C., Lam, L., 2002. Use of recycled aggregates in molded concrete bricks and blocks. *Construction and Building Materials* 16 (5): 281–289.

Poon, C.S., Kou, S.C., Wan, H.W., Etxeberria, M., 2009. Properties of concrete blocks prepared with low grade recycled aggregates. *Waste Management* 29 (8): 2369–2377.

Poon, C.S., Shui, Z.H., Lam, L., 2004a. Effect of microstructure of ITZ on compressive strength of concrete prepared with recycled aggregates. *Construction and Building Materials* 18 (6): 461–468.

Poon, C.S., Shui, Z.H., Lam, L., Fok, H., Kou, S.C., 2004b. Influence of moisture states of natural and recycled aggregates on the slump and compressive strength of concrete. *Cement and Concrete Research* 34 (1): 31–36.

Qasrawi, H., Marie, I., 2013. Towards better understanding of concrete containing recycled concrete aggregate, towards better understanding of concrete containing recycled concrete aggregate. *Advances in Materials Science and Engineering, Advances in Materials Science and Engineering* 2013, 2013: e636034.

Rahal, K., 2007. Mechanical properties of concrete with recycled coarse aggregate. *Building and Environment* 42 (1): 407–415.

Rao, A., Jha, K.N., Misra, S., 2007. Use of aggregates from recycled construction and demolition waste in concrete. *Resources, Conservation and Recycling* 50 (1): 71–81.

Rao, M.C., Bhattacharyya, S.K., Barai, S.V., 2011. Influence of field recycled coarse aggregate on properties of concrete. *Materials and Structures* 44 (1): 205–220.

Ravindrarajah, R.S., Tam, C., 1985. Properties of concrete made with crushed concrete as coarse aggregate. *Magazine of Concrete Research* 37 (130): 29–38.

Razaqpur, A.G., Fathifazl, G., Isgor, B., Abbas, A., Foo, S., Fournier, B., 2010. How to produce high quality concrete mixes with recycled concrete aggregate, in: Proceedings of the 2nd International Conference on Waste Engineering and Management - ICWEM 2010. RILEM Publications SARL, Shanghai, 11–35.

RILEM TC 121-DRG, 1994. Specifications for concrete with recycled aggregates. *Materials and Structures* 27 (9): 557–559.

Rodríguez-Robles, D., García-González, J., Juan-Valdés, A., Morán-del Pozo, J.M., Guerra-Romero, M.I., 2015. Effect of mixed recycled aggregates on mechanical properties of recycled concrete. *Magazine of Concrete Research* 67 (5): 247–256.

Safiuddin, M., Alengaram, U.J., Rahman, M.M., Salam, M.A., Jumaat, M.Z., 2013. Use of recycled concrete aggregate in concrete: a review. *Journal of Civil Engineering and Management* 19 (6): 796–810.

Sagoe-Crentsil, K.K., Brown, T., Taylor, A.H., 2001. Performance of concrete made with commercially produced coarse recycled concrete aggregate. *Cement and Concrete Research* 31 (5): 707–712.

Sánchez de Juan, M., 2004. Study on the use of recycled aggregate in structural concrete [in Spanish]. E.T.S.I. Caminos, Canales y Puertos (UPM), Madrid, Spain.

Schubert, S., Hoffmann, C., Leemann, A., Moser, K., Motavalli, M., 2012. Recycled aggregate concrete: Experimental shear resistance of slabs without shear reinforcement. *Engineering Structures* 41: 490–497.

Senthamarai, R., Devadas Manoharan, P., 2005. Concrete with ceramic waste aggregate. *Cement and Concrete Composites* 27 (9–10): 910–913.

Sheen, Y.-N., Wang, H.-Y., Juang, Y.-P., Le, D.-H., 2013. Assessment on the engineering properties of ready-mixed concrete using recycled aggregates. *Construction and Building Materials* 45: 298–305.

Silva, R.V., de Brito, J., Dhir, R.K., 2015a. Tensile strength behaviour of recycled aggregate concrete. *Construction and Building Materials* 83: 108–118.

Silva, R.V., de Brito, J., Dhir, R.K., 2015b. Prediction of the shrinkage behavior of recycled aggregate concrete: A review. *Construction and Building Materials* 77: 327–339.

Soares, D., de Brito, J., Ferreira, J., Pacheco, J., 2014. Use of coarse recycled aggregates from precast concrete rejects: Mechanical and durability performance. *Construction and Building Materials* 71: 263–272.

Spooner, D.C., Helmrath, C., 1997. Inter-laboratory comparison to support revision to CEN/ISO standards called up in EN 206, concrete (Contract No. MAT1-CT94-0043), Measurements and Testing. European Commision, Brussels.

Surya, M., Vvl, K.R., Lakshmy, P., 2013. Recycled aggregate concrete for transportation infrastructure. *Procedia - Social and Behavioral Sciences* 104: 1158–1167.

Tam, V.W.Y., Tam, C.M., 2007. Assessment of durability of recycled aggregate concrete produced by two-stage mixing approach. *J Mater Sci* 42 (10): 3592–3602.

Thomas, C., Cimentada, A., Polanco, J.A., Setién, J., Méndez, D., Rico, J., 2013a. Influence of recycled aggregates containing sulphur on properties of recycled aggregate mortar and concrete. *Composites Part B: Engineering* 45 (1): 474–485.

Thomas, C., Setién, J., Polanco, J.A., Alaejos, P., Sánchez de Juan, M., 2013b. Durability of recycled aggregate concrete. *Construction and Building Materials* 40: 1054–1065.

Topçu, İ.B., Şengel, S., 2004. Properties of concretes produced with waste concrete aggregate. *Cement and Concrete Research* 34 (8): 1307–1312.

Topçu, I., Canbaz, M., 2007. Utilization of crushed tile as aggregate in concrete. *Iranian Journal of Science and Technology* 31 (B5): 561.

Topçu, ilker B., Günçan, N.F., 1995. Using waste concrete as aggregate. *Cement and Concrete Research* 25 (7): 1385–1390.

Tsujino, M., Noguchi, T., Tamura, M., Kanematsu, M., Maruyama, I., 2007. Application of conventionally recycled coarse aggregate to concrete structure by surface modification treatment. *Journal of Advanced Concrete Technology* 5 (1): 13–25.

UNE EN 1992 1-1, 2013. Eurocode 2: Design of concrete structures. Part 1-1: General rules and rules for buildings. AENOR, Madrid, Spain.

Waleed, N., Canisius, T.D.G., 2007. Engineering properties of concrete containing recycled aggregates. WRAP.

Wang, W., Kou, S., Xing, F., 2013. Deformation properties and direct shear of medium strength concrete prepared with 100% recycled coarse aggregates. *Construction and Building Materials* 48: 187–193.

Xiao, J., Li, J., Zhang, C., 2005. Mechanical properties of recycled aggregate concrete under uniaxial loading. *Cement and Concrete Research* 35 (6): 1187–1194.

Xiao, J., Li, W., Sun, Z., Lange, D.A., Shah, S.P., 2013. Properties of interfacial transition zones in recycled aggregate concrete tested by nanoindentation. *Cement and Concrete Composites* 37: 276–292.

Xiao, J.-Z., Li, J.-B., Zhang, C., 2006. On relationships between the mechanical properties of recycled aggregate concrete: An overview. *Mater Struct* 39 (6): 655–664.

Yamato, T., Emoto, Y., Soeda, M., 1998. Mechanical properties, drying shrinkage and resistance to freezing and thawing of concrete using recycled aggregate. *ACI Special Publication* 179: 105–122.

Yang, C.C., 1998. Effect of the Transition Zone on the Elastic Moduli of Mortar. *Cement and Concrete Research* 28 (5): 727–736.

Yang, J., Du, Q., Bao, Y., 2011. Concrete with recycled concrete aggregate and crushed clay bricks. *Construction and Building Materials* 25 (4): 1935–1945.

Yang, K.-H., Chung, H.-S., Ashour, A.F., 2008. Influence of type and replacement level of recycled aggregates on concrete properties. *MJ* 105 (3): 289–296.

Yehia, S., Helal, K., Abusharkh, A., Zaher, A., Istaitiyeh, H., 2015. Strength and Durability Evaluation of Recycled Aggregate Concrete. *International Journal of Concrete Structures and Materials* 9 (2): 219–239.

Zakaria, M., 1999. Strength and elasticity of bricks and artificial aggregate concrete, in: Exploiting Wastes in Concrete: Proceedings of the International Seminar. University of Dundee. Dundee, UK, 179–188.

Zega, C.J., Villagrán-Zaccardi, Y.A., Maio, A.A.D., 2010. Effect of natural coarse aggregate type on the physical and mechanical properties of recycled coarse aggregates. *Materials and Structures* 43 (1-2): 195–202.

Zhang, S., Zong, L., 2014. Properties of concrete made with recycled coarse aggregate from waste brick. *Environ. Prog. Sustainable Energy* 33 (4): 1283–1289.

Zhou, F.P., Lydon, F.D., Barr, B.I.G., 1995. Effect of coarse aggregate on elastic modulus and compressive strength of high performance concrete. *Cement and Concrete Research* 25 (1): 177–186.

Zilch, K., Roos, F., 2001. An equation to estimate the modulus of elasticity of concrete with recycled aggregates [in German]. *Bauingenieur* 76 (4): 187–190.

Zong, L., Fei, Z., Zhang, S., 2014. Permeability of recycled aggregate concrete containing fly ash and clay brick waste. *Journal of Cleaner Production* 70: 175–182.

Chapter 9

Durability performance

1. INTRODUCTION

Generally, concrete is specified on the basis of its compressive strength after 28 days of curing and in its design sufficient high security factors are employed. Thus, concrete elements are expected to exhibit, at least, their minimum required performance after having completed the construction. However, it should be also anticipated that the continuous contact with the external aggressive agents will result in a loss of durability that will reduce the safety of concrete structure to a certain extent. Sommerville (1984) described graphically this gradual deterioration as a function of time. In Figure 9.1, curve 1 represents the unlikely situation of minimal deterioration, curve 2 illustrates the most common situation of loss of durability and its subsequent gain due to maintenance works and curve 3 shows a catastrophic loss of durability.

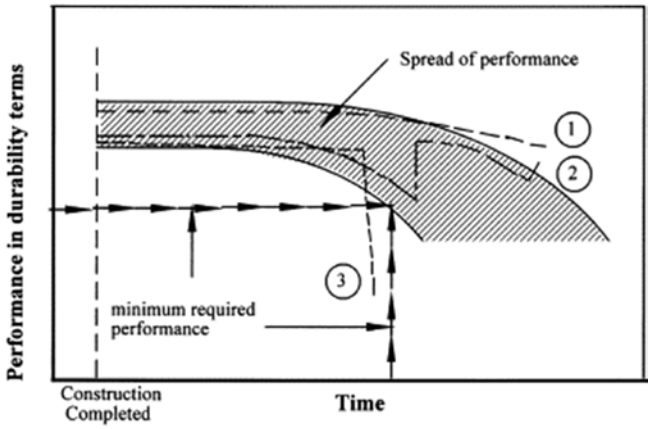

Figure 9.1: Deterioration of concrete with time (Sommerville, 1984)

Hence, the capacity to withstand, for the duration of its designed service life, the physical and chemical conditions to which it is exposed, and which could cause deterioration as a result of effects other than the loads and stresses considered in its structural analysis is known as the durability of concrete (Permanent Commission on Concrete, 2008).

As previously stated in chapter 6, concrete is characterised by a complex porous network that allows the transport of the aggressive agents of the environment such as liquids, gases and ions within the structure. Thus, the resistance that concrete opposes to the penetration of external agents could be used to assess its durability (Hilsdorf and Kropp, 2004). The main transport mechanisms within a concrete structure are permeability due to flow under a differential pressure, sorption that represents the absorption of liquid due to the surface tension within the capillary porous network, diffusivity which is the ease with which dissolved solids and ions are transported through a saturated or partially saturated porous material due to a concentration gradient, and migration that characterizes the movement of ions in a solution under an electrical field.

Figure 9.2 illustrates some of the principal causes of deterioration due to the aggressiveness of the environment to which the concrete is exposed during its service life. Particularly for physical and mechanical mechanisms, the porous network of concrete is a central factor behind the durability loss and the consequent decrease in the strength properties which would result in a circular relationship between the crack formation and the exacerbation of the durability problem due to an increase in the access to the external agents that caused the damage in the first place.

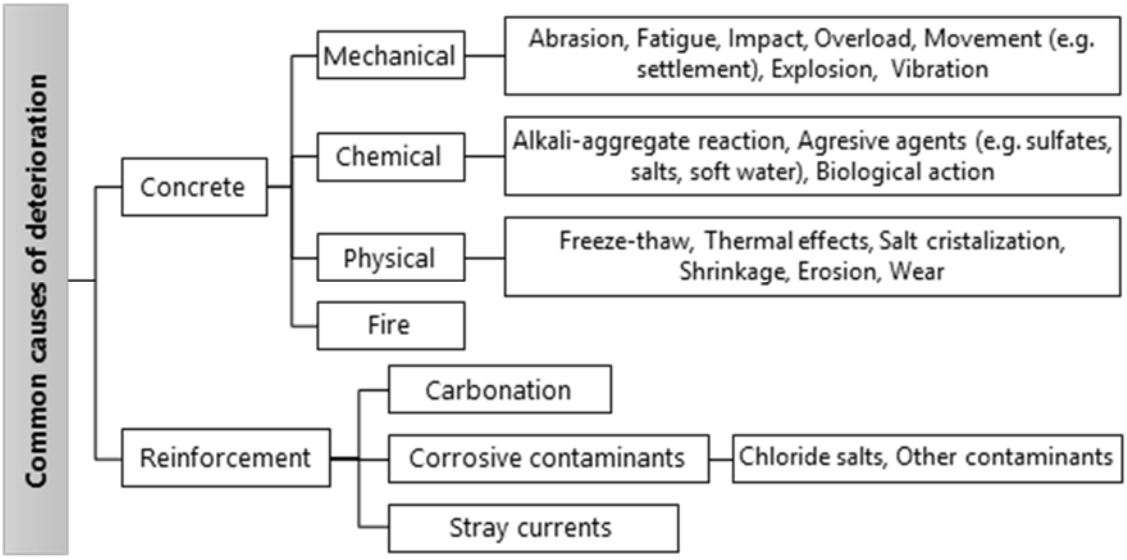

Figure 9.2: Common causes of concrete deterioration

Since the adequate selection of the raw materials as an essential factor to ensure the durability performance of a concrete mixture (Permanent Commission on Concrete, 2008), several research works have focused on the study of the influence of the use of recycled aggregates on the durability performance of recycled concrete. However, to date, there is no definite consensus regarding the effect of the use of recycled aggregates from construction and demolition wastes (CDW) on the durability performance of recycled concrete. Investigations regarding water

permeability, freeze-thaw, carbonation and chloride ingress resistance of recycled concrete mixtures have shown both worse durability results (Sagoe-Crentsil et al., 2001; Buyle-Bodin and Hadjieva-Zaharieva, 2002; Otsuki et al., 2003; Topçu and Şengel, 2004; Kou et al., 2007; Ann et al., 2008; Yang et al., 2008; Gokce et al., 2011; Rao et al., 2011; Sim and Park, 2011) and similar, or even improved, durability performance results (Dhir et al., 1999; Limbachiya et al., 2000; Olorunsogo and Padayachee, 2002; Otsuki et al., 2003; Levy and Helene, 2004; Zaharieva et al., 2004; Tu et al., 2006; Eguchi et al., 2007; Abbas et al., 2009; Debieb et al., 2010; Kong et al., 2010; Kou et al., 2011b; Richardson et al., 2011) when compared to conventional concrete mixtures. While, the aggregate porosity and the micro-cracks originated during their processing are held responsible for the decrease in durability performance (Olorunsogo and Padayachee, 2002), the improvement in the interfacial transition zone (ITZ) and the drastic reduction in porosity with time exhibited by the recycled concrete mixtures (Kou et al., 2011b) have been also used to justify the durability increase. Nonetheless, the variability points to the selection of recycled aggregates with a good quality as a decisive factor on the durability of recycled concretes.

In this chapter, several durability properties (gas permeability, carbonation, water absorption by capillarity, under vacuum and under pressure, frost resistance, chloride penetration, electrical resistivity, alkali-silica reaction and resistance to organic acids) are assessed in order to better understand the effect of the replacement of natural coarse aggregates by recycled aggregates from CDW with varying percentages of ceramic waste.

2. GAS PERMEABILITY

The gas permeability coefficient characterizes the ease with which a gas passes through the concrete specimen due to the action of a differential pressure. Although gas permeability mainly depends on the permeability of the cement matrix, its curing history and the type and amount of coarse aggregates can be expected to influence this property (Lydon and Broadley, 1994). Since recycled aggregates from CDW are characterized by a high porosity and the presence of micro-cracks due to the crushing stage during their processing, their use in the concrete manufacture could result in an increase of the concrete permeability.

2.1. NATURE OF THE GAS FLOW

In order to assess this property, the nature of the gas flow must be verified. Hence, the flow rate values were plotted against the pressure gradient between each test pressure and the atmospheric pressure resulting in quasi-linear relationships between both variables, which confirmed that the gas flow was mostly laminar (Figure 9.3 and Figure 9.4). Consequently, the apparent permeability coefficient was calculated according to Darcy's law and the Hagen-Poiseuille equation (3.27) for laminar flow of a compressible fluid through a porous media with small capillaries under steady-state conditions.

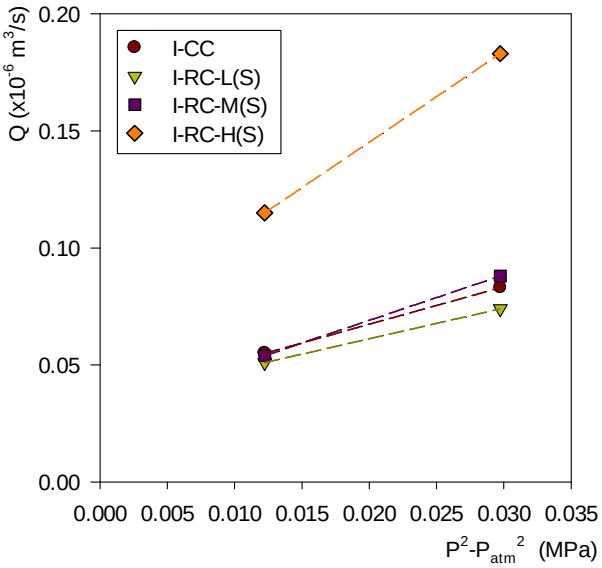

Figure 9.3: Flow rate in function of the pressure gradient in phase I

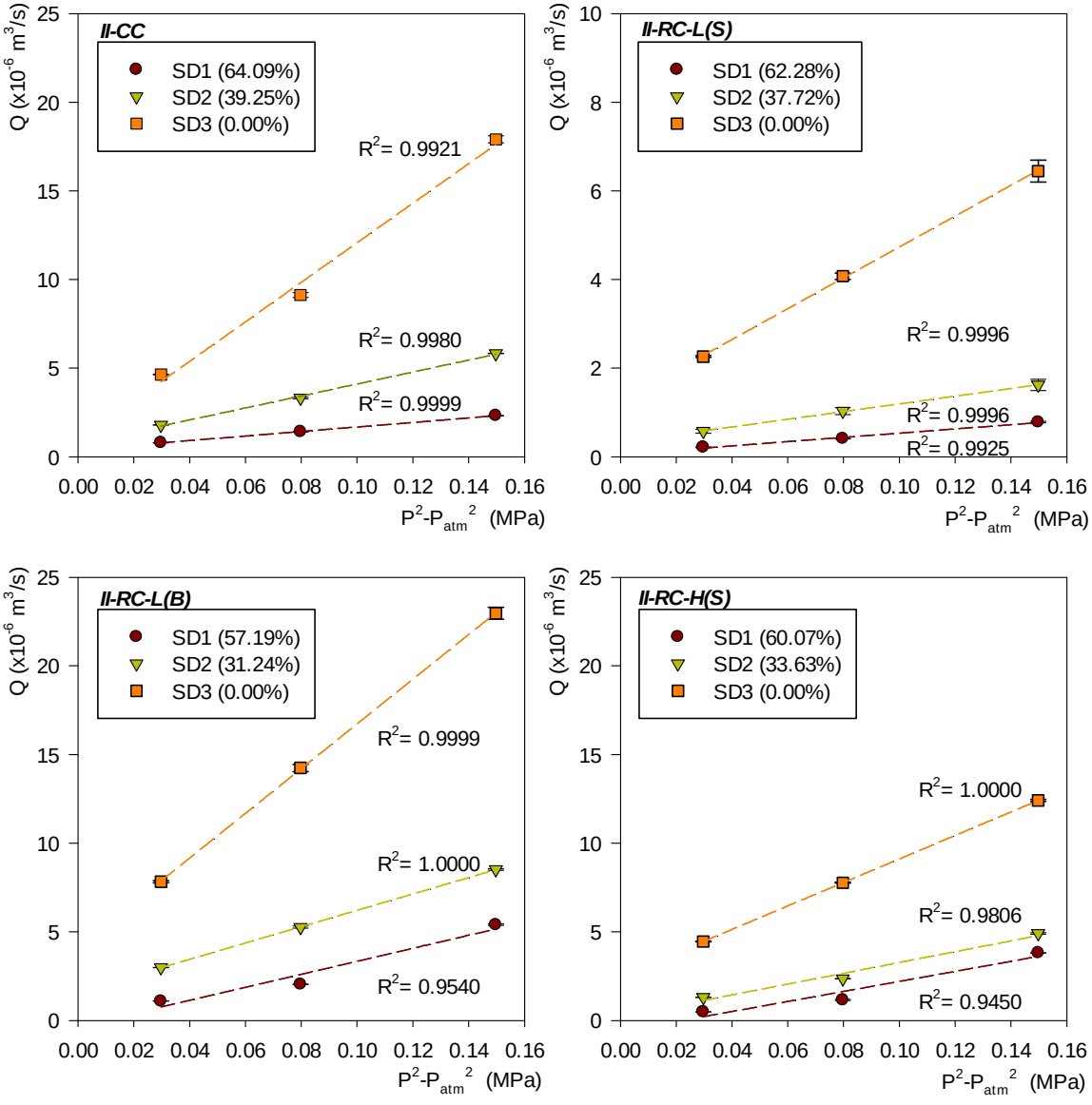

Figure 9.4: Flow rate in function of the pressure gradient in phase II

2.2. APPARENT GAS PERMEABILITY COEFFICIENT

Several researchers (Yanagi et al., 1988; Wainwright et al., 1993; Limbachiya et al., 2000; Olorunsogo and Padayachee, 2002; Zaharieva et al., 2003; Li, 2008; Henry et al., 2011; Hoffmann et al., 2012; Kwan et al., 2012; Thomas et al., 2013) have registered higher air permeability coefficients for concrete mixtures made of recycled concrete aggregates as replacing the natural coarse aggregates. In addition, it has been observed that the increase of the replacement ratio is linked to the durability loss of recycled mixtures (Limbachiya et al., 2000; Olorunsogo and Padayachee, 2002; Li, 2008; Henry et al., 2011; Kwan et al., 2012; Thomas et al., 2013). The main reasons explaining this tendency toward increased air permeability results are the higher porosity and micro-cracks of the recycled aggregates, and the weaker cement matrix and ITZ of recycled concretes (Otsuki et al., 2003; Poon et al., 2004; Xiao et al., 2014).

Despite that Pacheco-Torgal and Jalali (2010) reported that recycled concrete with a total replacement of the coarse granite aggregates by ceramic coarse aggregate resulted in a decrease in the oxygen permeability coefficient, other researchers have identified a tendency towards the increase of the gas permeability similar to the one found for recycled concretes made of recycled concrete aggregates (Medina et al., 2012; Zong et al., 2014). Hence, the results suggest that the type of ceramic aggregates affects the permeability change. While the use of ceramic sanitary ware caused an upsurge between 1.42% and 2.55% (Medina et al., 2012), the replacement with mixed recycled aggregates containing crushed clay bricks generated a three-fold increase in gas permeability with respect to the control concrete. However, in both cases, the replacement ratio had a limited contribution to the increase of the gas permeability (Medina et al., 2012; Zong et al., 2014).

It is also worth noting that the influence of the use of recycled aggregates on the gas permeability of recycled concrete mixtures is smaller for increasing ages of curing (Henry et al., 2011; Kwan et al., 2012). For instance, Kwan et al. (2012) registered larger permeability reductions in concretes containing recycled concrete aggregates (16.3%) than those experienced by the reference mixtures (7.4%). This unequal decline is related to the different pore refinement behaviour of conventional and recycled mixtures. As explained section 3.2 of chapter 7, the decrease of porosity is higher for recycled concretes than conventional concretes (Gómez-Soberón, 2002; Kou et al., 2011b; Ulloa Mayorga, 2012), which turns into larger permeability decline at long term.

Table 9.1 shows the results obtained for the apparent gas permeability coefficient in both phases of the research despite the use of a different methodology in each stage. Note that the results for phase I correspond to a saturation degree (SD) around 65-75%, while the results for phase II are linked to three saturation degrees at the moment of testing since the sequential conditioning method proposed by Carcasses et al. (2002) was followed to achieve a broader understanding of the phenomenon.

Table 9.1: Apparent gas permeability coefficients (m^2) for different pressures and saturation degrees (SD)

	CC	RC-L(S)	RC-L(B)	RC-M(S)	RC-H(S)
Phase I					
0.15 MPa	0.530 x10^{-16}	0.459 x10^{-16}	-	0.514 x10^{-16}	1.044 x10^{-16}
0.20 MPa	0.525 x10^{-16}	0.437 x10^{-16}	-	0.549 x10^{-16}	1.091 x10^{-16}
Phase II-SD1	*64.09%*	*62.28%*	*57.19%*		*60.07%*
0.20 MPa	3.044 x10^{-16}	0.843 x10^{-16}	4.240 x10^{-16}	-	1.891 x10^{-16}
0.30 MPa	2.011 x10^{-16}	0.595 x10^{-16}	2.965 x10^{-16}	-	1.665 x10^{-16}
0.40 MPa	1.760 x10^{-16}	0.609 x10^{-16}	4.180 x10^{-16}	-	3.771 x10^{-16}
Phase II-SD2	*39.25%*	*37.72%*	*31.24%*		*33.63%*
0.20 MPa	6.921 x10^{-16}	2.272 x10^{-16}	11.609 x10^{-16}	-	5.037 x10^{-16}
0.30 MPa	4.729 x10^{-16}	1.506 x10^{-16}	7.660 x10^{-16}	-	3.398 x10^{-16}
0.40 MPa	4.428 x10^{-16}	1.261 x10^{-16}	6.596 x10^{-16}	-	2.925 x10^{-16}
Phase II-SD3	*0.00%*	*0.00%*	*0.00%*		*0.00%*
0.20 MPa	17.891 x10^{-16}	8.929 x10^{-16}	30.532 x10^{-16}	-	17.224 x10^{-16}
0.30 MPa	13.021 x10^{-16}	5.961 x10^{-16}	20.722 x10^{-16}	-	11.210 x10^{-16}
0.40 MPa	13.608 x10^{-16}	5.022 x10^{-16}	17.798 x10^{-16}	-	9.531 x10^{-16}

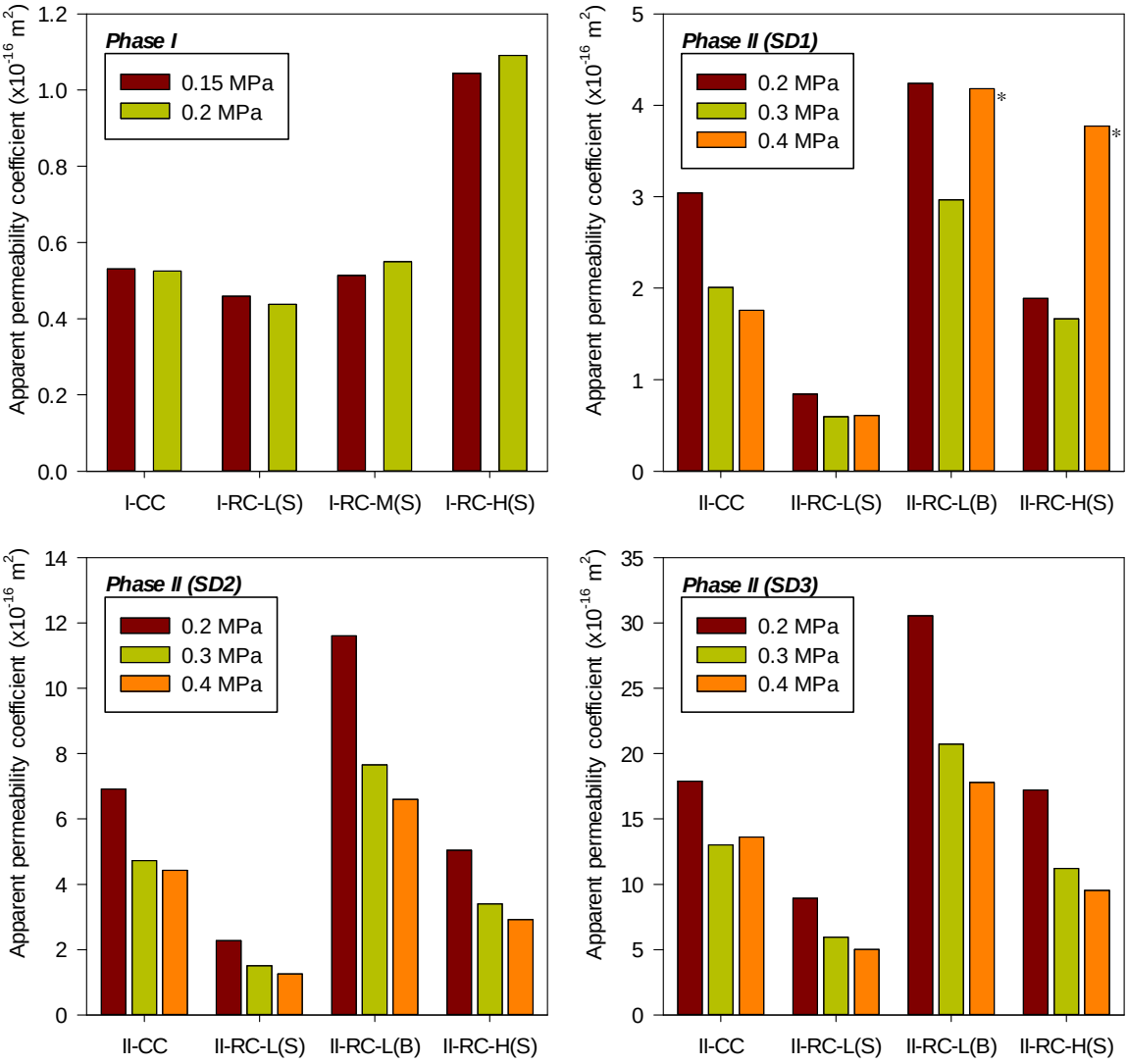

Figure 9.5: Apparent gas permeability coefficient at different pressures and saturation degrees

Figure 9.5 illustrates the apparent gas permeability coefficients of the conventional and recycled concrete specimens as a function of the inlet pressure and the saturation degree. Firstly, it could be observed that the gas permeability coefficient decreases for increasing pressure due to the effect of gas slippage. Nonetheless, note that the apparent gas permeability coefficient determined for samples II-RC-L(B) and II-RC-H(S) at 0.40 MPa, which are marked in Figure 9.5 with an asterisk, does not follow the explained behaviour which reveals a possible leakage of the experimental set up (Abbas et al., 1999; Carcasses et al., 2002). Hence, these values were disregarded for any further analysis.

To perform an overall assessment among mixtures, the permeability results obtained were transformed to oxygen permeability index (OPI) values (Figure 9.6), which implies their expression as the negative logarithm of the apparent gas permeability coefficient. According to the performance ranges proposed by Alexander et al. (1999), all mixtures presented an excellent durability class since the OPI values exceed 10 logarithmic units. Thus, although the variation of the gas permeability between the conventional and recycled concretes is clear, the differences resulting from the use of recycled aggregates with varying percentages of ceramic waste in the concrete manufacture are not expected to cause a significant durability loss.

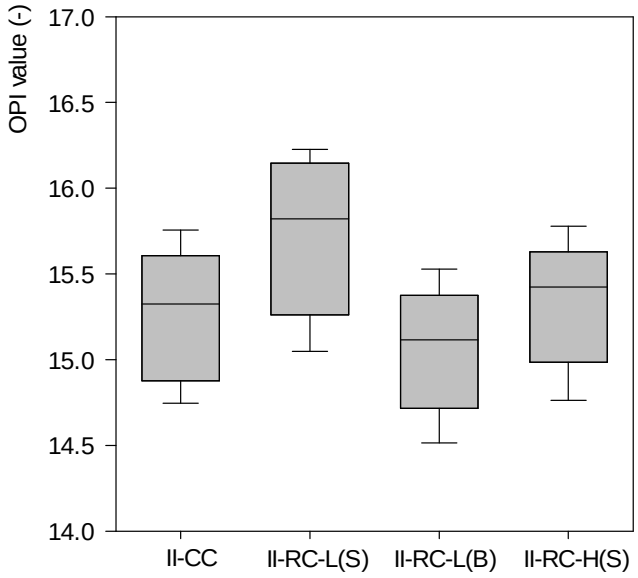

Figure 9.6: OPI values of the apparent gas permeability coefficients

In general terms, the results obtained in phase I suggest higher gas permeability for increasing ceramic content in the recycled mixture. While the apparent permeability coefficient in the mixture with the low ceramic content (I-RC-L(S)) was 15.10% lower than the conventional concrete, the concrete containing a 50% replacement of ceramic aggregates (I-RC-H(S)) displayed a permeability coefficient two times higher than the conventional mixture. However, the opposite behaviour was observed in phase II since the two samples with the similar ceramic composition (II-RC-L(S) and II-RC-L(B)) presented opposed tendencies in comparison with the reference conventional concrete. While the II-RC-L(S) mixture presented a lower gas permeability than the conventional concrete, the results of the apparent gas permeability coefficient of II-RC-L(B) are higher than those of the II-CC for all inlet pressures and saturation degrees. In addition, in phase

II, the concrete mixture with the higher ceramic content (II-RC-H(S)) displays an intermediate performance with respect to the two other recycled concrete mixtures. Thus, the effect of the amount of ceramic incorporated in the recycled concrete as recycled coarse aggregate could not be considered as a direct indicator of the gas permeability alterations between conventional and recycled mixtures. Nevertheless, the variation in composition has been identified as a source for the porosity changes that are responsible, in the end, for the gas permeability variations among mixtures (see section 2.3 of the present chapter).

The differences observed among the research phases could be traced back to the different methodologies employed (see section 6.1 of chapter 3). In particular, the disagreement in terms of the magnitude of the results obtained from each method could respond to the different saturation degree of the samples at the moment of testing (Abbas et al., 1999; RILEM TC 116-PCD, 1999). According to Parrot (1994), the gas transport is highly inhibited at saturation degrees greater than 60%, and since the preconditioning method used in phase I (UNE-83981, 2008) aimed to attain a saturation degree between 65% and 75%, the lower results obtained are confirmation of the high moisture content of the samples.

To further study the influence of the saturation degree on the gas permeability of recycled concretes, the preconditioning proposed by Carcasses et al. (2002) was followed to test the concrete specimens at three saturation degrees covering the 0-70% moisture range. Although the same methodology was followed in the treatment of all concrete mixtures, the actual saturation degrees were different for all batches while ranging around the same figures at a particular preconditioning stage (Table 9.1). Similarly to the variation of the apparent gas permeability coefficient, the changes among mixtures are not directly linked to the ceramic content in the recycled concrete (linear R^2 ranging between 0.27 and 0.37) but to the porosity of the concrete mixtures that influenced the drying behaviour of the specimen. Regarding the variation of the gas transport with the saturation degree, the apparent gas permeability coefficient increases as the saturation degree declines for each inlet pressure. Note that the gas permeability growth is larger for the recycled mixtures than the conventional concrete for a specific inlet pressure.

Since, in real circumstances, concrete would have a certain saturation degree as consequence of the mix design and the environmental conditions, the influence of the saturation degree should be assessed. In Figure 9.7, the gas permeability of the samples is presented by the relative gas permeability coefficient (9.1), which is defined as the ratio between the permeability measured at a given saturation degree and the permeability measured in dry state (Verdier and Carcasses, 2004). Moreover, the obtained values were modelled by the formula (9.2) proposed by Van Genuchten (1980), which has been found a good fit for concrete mixtures (Boel et al., 2007).

$$K_r = \frac{K_{app}(SD=i)}{K_{app}(SD=0)} \tag{9.1}$$

$$K_r = \sqrt{1\text{-}SD_i} \times \left(1\text{-}SD^b\right)^{\frac{2}{b}} \tag{9.2}$$

with K_r the relative gas permeability coefficient [-], K_{app} the apparent gas permeability coefficient [m^2], *SD* the saturation degree during each permeability test [%] and *b* the Van Genuchten parameter [-].

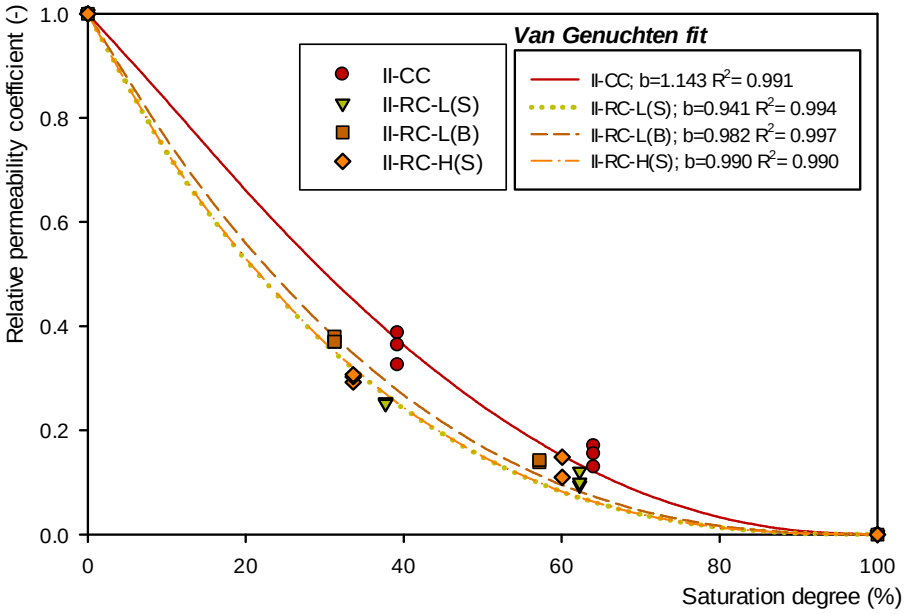

Figure 9.7: Relative permeability coefficient as a function of the saturation degree

Despite that no clear tendency could be established between the factor b in the Van Genuchten formula (9.2) and the content of ceramic waste incorporated with the recycled aggregates (linear R^2 of 0.60), the parameter was lower for recycled concretes when compared to the conventional mixture. Consequently, the relative gas permeability of recycled concrete mixtures is lower than that of conventional concrete for a specific saturation degree.

2.3. RELATIONSHIP BETWEEN THE GAS PERMEABILITY AND THE POROSITY BY MIP

Although there is no defined relationship between porosity and permeability, it is widely recognized that the permeability of a concrete specimen is influenced by the pore system (volume, distribution and connectivity). As recommended by Van den Heede et al. (2010), the apparent gas permeability coefficient at the lowest pressure and full dry state were used for the comparison among samples. Figure 9.8 shows the relationships between gas permeability and the total porosity and macro-porosity, respectively.

According to Neville (1995), discontinuous pores, pores containing adsorbed water and those with a narrow entrance do not contribute to the permeability of concrete. Hence, since not all pores present in a material take part in the gas permeation transport mechanism, the relationship existing between the apparent gas permeability coefficient and the total porosity of the concrete mixture measured by MIP displayed a modest correlation factor (R^2=0.55). In line with the results presented by Medina et al. (2012), the gas permeability increased with the total porosity of the concrete mixture and thus the resistance to oxygen permeation declined with rising porosity.

Since it is widely accepted that pores with a diameter larger than 50 nm are responsible for the concrete permeability (Mehta and Monteiro, 2006), the differences in the macropores or capillary pore network of the different concrete mixtures should be expected to play a major role in the gas permeability of each concrete. Consequently, the linear regression between the apparent gas permeability coefficient and the macro-porosity resulted in a higher level correlation (R^2=0.82). Specific parameters describing the pore size of a concrete mixture render similar correlations with the gas permeability. For instance, the linear regression between permeability and average pore diameter presented a R^2=0.86 and the linear relationship between permeability and median pore diameter by volume displayed a R^2=0.81.

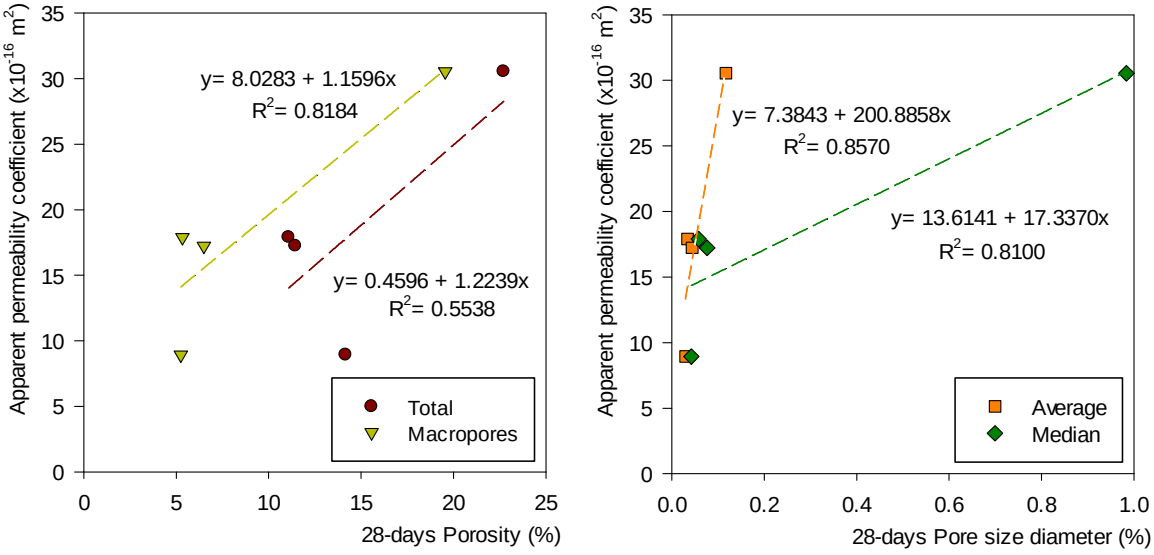

Figure 9.8: Relationship between the apparent permeability coefficient and the porosity

3. CARBONATION

Corrosion is one of the most damaging degradation phenomena for reinforced concrete and is usually induced by carbonation or chloride penetration. Since two thirds of concrete structures are exposed to environmental conditions favouring carbonation (Parrott, 1996), the study of the carbonation-induced corrosion is highly relevant despite that chloride penetration is considered to have worse effects on the rebar corrosion.

Carbon dioxide, which primarily penetrates concrete through diffusion mechanism, fosters a reduction in the pH that enables the destruction of the passivation layer protecting the steel bars. Moreover, otherwise bound chlorides may be liberated causing a combined carbonation and chloride-induced corrosion (Bertolini et al., 2013).

The CO_2 in the air combines with the free water in the concrete porous network to produce carbonic acid that reacts with portlandite to create calcium carbonate (Heiyantuduwa et al., 2006). This type of carbonation itself does not deteriorates concrete, in fact the concrete may experience a reduced permeability and a slightly higher strength as a result of the precipitation of the $CaCO_3$ (Neville and Brooks, 2010). Although initially slowly, CO_2 also combines with the C-S-H gel producing calcium carbonate, silica gel and hydrated aluminium and iron oxides, which leads to some level of shrinkage due to the removal of the calcium in the C-S-H gel interlayers (Thiery et al., 2007; Borges et al., 2010).

It is widely accepted that, since the porosity of the recycled aggregates is greater than that of the natural aggregates, the resistance against the carbonation of recycled concrete is reduced with respect to a conventional mixture (Sagoe-Crentsil et al., 2001; Buyle-Bodin and Hadjieva-Zaharieva, 2002; Ryu, 2002; Otsuki et al., 2003; Zaharieva et al., 2003; Amorim et al., 2012; Kou and Poon, 2013; Thomas et al., 2013). For instance, Pedro et al. (2014b) observed better performance of recycled mixtures incorporating recycled concrete aggregates subjected to both primary and secondary crushing procedures due to the reduction of the adhered mortar content and the production of more spherical aggregates which allow a better packing of concrete. Nonetheless, the authors noticed increases in the carbonation depth with the replacement ratio and the decrease of the target strength. For full substitution, the carbonation depth was reported to increase approximately 15%. However, Ryu et al. (2002) observed increases up to 20% in the carbonation depth and concluded that varying amounts of adhered mortar and the quality of the parent concrete had little effect on the resistance to the CO_2 penetration. Similar results were reported by Eguchi et al. (2007). In addition, when supplementary cementing materials were used in concretes made with recycled concrete aggregates, the carbonation depth of recycled concretes continued to be higher than that of the reference concrete due to the lower amount portlandite content capable of becoming carbonated as consequence of its consumption as part of the pozzolanic reaction (Shayan and Xu, 2003; Abbas et al., 2009; Limbachiya et al., 2012; Kou and Poon, 2013). In general terms, the literature review carried out by Silva et al. (2015) suggested that concrete made with 100% recycled concrete aggregates showed carbonation depths 2.15 greater than those of mixtures incorporating natural coarse aggregates.

Nonetheless, several investigations have also reported comparable penetration depth between conventional and recycled mixtures (Shayan and Xu, 2003; Soares et al., 2014). For example, Limbachiya et al. (2012) reported that recycled concrete presented similar carbonation depth than that of a conventional mixture for target strength of 20 MPa regardless the replacement ratio. However, the resistance against the carbonation decreased with the substitution levels for 30 MPa and 35 MPa concrete classes. However, the adjustment of the water/cement ratio (Limbachiya et al., 1998, 2000; Dhir et al., 1999; Paine et al., 2009) or the use of the EMV proportioning method (Razaqpur et al., 2010) is behind these results. In this line, Ridzuan et al. (2005), who employed the recycled concrete aggregates in air-dried state, observed lesser carbonation depths as consequence of the decrease of the total water/cement ratio by the absorption of part of the mixing water.

Comparatively, the number of research works focused on the effect of mixed recycled aggregates on the carbonation of recycled concrete is very limited. Dhir and Paine (2007) observed 11.11% and 44.44% decreases in the carbonation depth of concrete made with 20% and 100% mixed recycled aggregates. Gomes and de Brito (2009), who used mixed recycled aggregates containing 70% concrete rubble and 30% ceramic wastes, observed carbonation depths up to 8.38% and 28.07% higher than the conventional mixture when 25% and 37.5% replacement ratios were employed. Contrarily, Corinaldesi and Moriconi (2009), who used fly ash in recycled mixtures incorporating a total substitution of fine and coarse aggregates by mixed recycled aggregates, reported lower penetration depths as consequence of the lower effective water/cement ratio.

When recycled masonry aggregates were used, Levy and Helene (2004) observed that recycled concretes displayed better carbonation performance than the reference mixture. Declines in the penetration depth between 27.08%-37.14%, 20.83%-88.57% and 55.21%-100% were reported for 20%, 50% and 100% replacement ratios of mixtures with target strength ranging from 20 MPa to 40 MPa. Dhir and Paine (2007) registered declines in the carbonation depth of around 28% for 100% substitutions with crushed bricks aggregates. Medina et al. (2012) observed decreases in the penetration depth for increasing ceramic contents. Thus, performance improvements up to 2.89% and 3% were observed for 20% and 25% replacement ratios of ceramic sanitary ware. For concrete mixtures without admixtures, Zhang and Zong (2014) observed comparable carbonation values for 30% substitution level but approximately increases of 20% and 14% for a 40% replacement ratio at 28 and 56 days. The use of 10% and 15% of fly ash caused bigger differences between the conventional and recycled mixtures. For 30%, 40% and 50% replacement ratios, Zong et al. (2014) registered a 17.98%, 53.93% and 62.92% higher carbonation penetration depth in recycled mixtures than concretes made with natural aggregates. For CDW sourced from Valnor and Retria, Bravo et al. (2015) registered average increases in the 28-days carbonation depth up to 3.35%, 23.15%, 24.05% and 76.90% for 10%, 25%, 50% and 100% replacement ratios with mixed recycled aggregates. The higher amount of cement used in the recycled mixtures was behind this improved performance as the alkaline reserve of the mixtures had a beneficial effect on the resistance against the carbonation.

Figure 9.9 illustrates some examples of the carbonation profile of concrete specimens in phase I. The carbonation front was determined after spraying phenolphthalein solution on a freshly broken surface. The purple-red colouration indicates the alkalinity of the concrete and corresponds to the non-carbonated part of the specimen, while in the carbonated part, the original grey concrete colour is observed. At first glance, it can be noticed that the incorporation of recycled aggregates, which are more porous than the natural gravel, contributed to a greater carbonation depth as consequence of a higher diffusion of CO_2 through concrete. Hence, for the recycled mixtures, the carbonation front was very irregular and presented carbonation peaks were identified corresponding with the more porous recycled aggregates, i.e. ceramic materials.

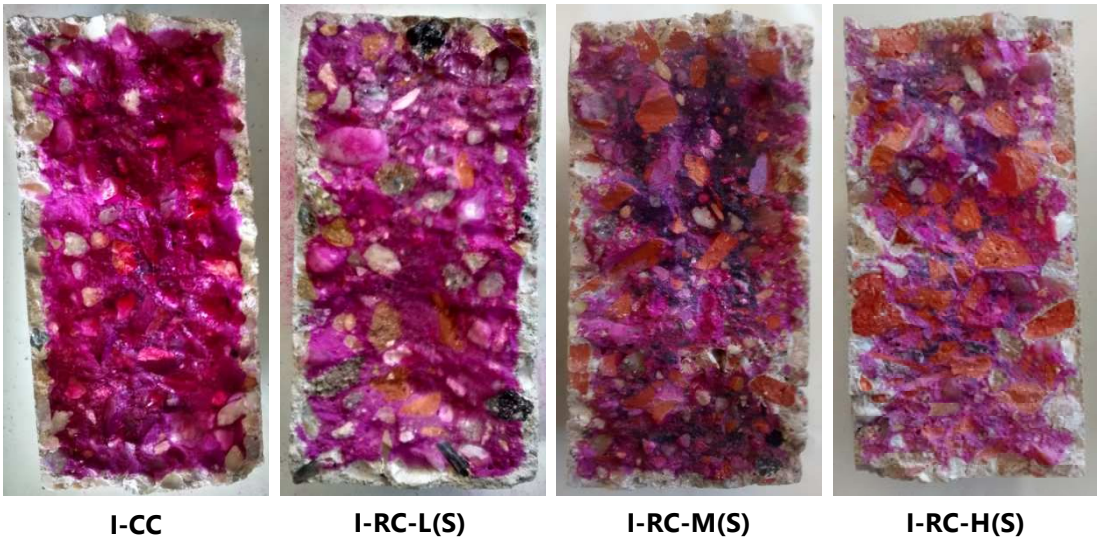

Figure 9.9: Examples of the carbonation profile of concrete mixtures in phase I

Table 9.2 displays the natural carbonation coefficients for concrete mixtures in phase I. While mixture I-RC-L(S) presented a slightly lower (6.75%) carbonation diffusion than the conventional concrete, the recycled concretes tended to present carbonation coefficients between 70% and 75% higher after 1 year of exposure to the outdoor CO_2 environment due to the higher porosity of the recycled concretes (R^2=0.81), particularly for pore sizes higher than 0.067 µm (Medina et al., 2012). These results obtained showed also a good correlation (R^2=0.72) between the carbonation coefficient and the ceramic content incorporated into the concrete mixture (Figure 9.10).

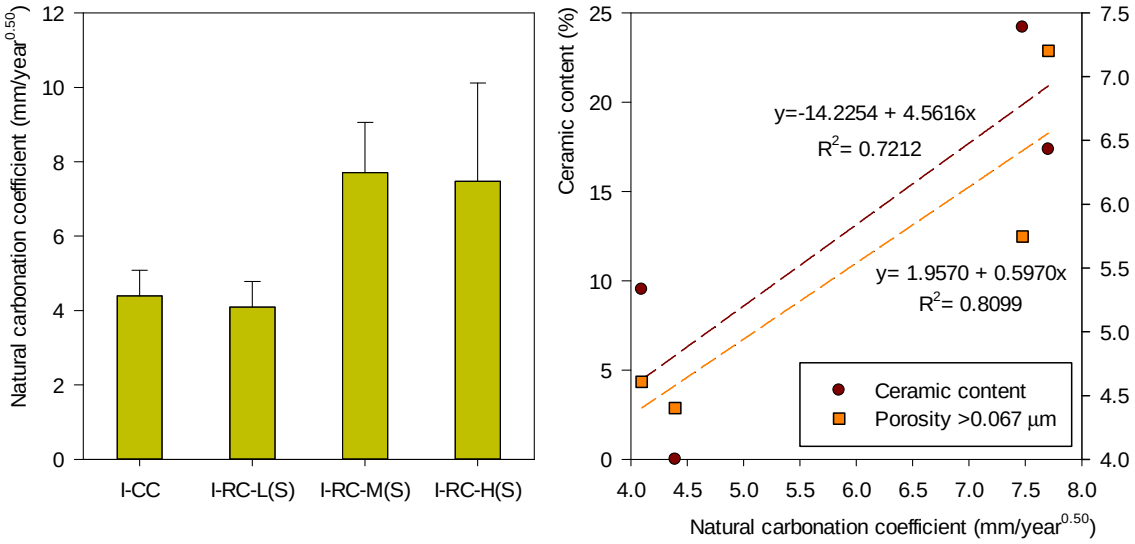

Figure 9.10: Natural carbonation coefficients for concrete mixtures in phase I and their relationship with the ceramic content in the total weight of aggregates and the porosity.

Table 9.2: Natural carbonation coefficients after 1 year of exposure for concretes in phase I

	Natural carbonation coefficient (mm/year$^{0.50}$)	Variation (%)
I-CC	4.39	-
I-RC-L(S)	4.10	-6.75
I-RC-M(S)	7.70	75.42
I-RC-H(S)	7.48	70.23

In Figure 9.11, the evolution of the carbonation depth in function of time is presented for conventional and recycled concrete specimens in phase II exposed to 10% CO_2 environment in an accelerated test. A nearly linear relationship can be observed between the carbonation depth and the square-root of exposure time ($R^2 \geq 0.95$). Despite that after one month of exposure, the recycled mixtures II-RC-L(S) and II-RC-L(B) presented 33.14% and 27.05% lower penetration depth than the conventional concrete, these differences were smaller after two months of exposure (18.71% and 1.72%) to finally reach slightly higher values than the conventional mixture (1.18% and 4.87%). Since the recycled mixtures presented a lower effective water/cement ratio and the ceramic materials present a higher alkaline reserve (Corinaldesi and Moriconi, 2009), the carbonation diffusion was initially hindered an thus recycled concrete presented a better performance. However, as the exposure time progressed, the higher porosity of recycled aggregates and the pozzolanic activity overpowers the alkaline protection against the carbonation mechanism leading to increased penetration depths compared to the conventional mixture after three months of exposure. The final results of this evolution are in agreement with the findings of the recycled mixture with low ceramic content identified in the natural carbonation test carried out in the phase I of this research work.

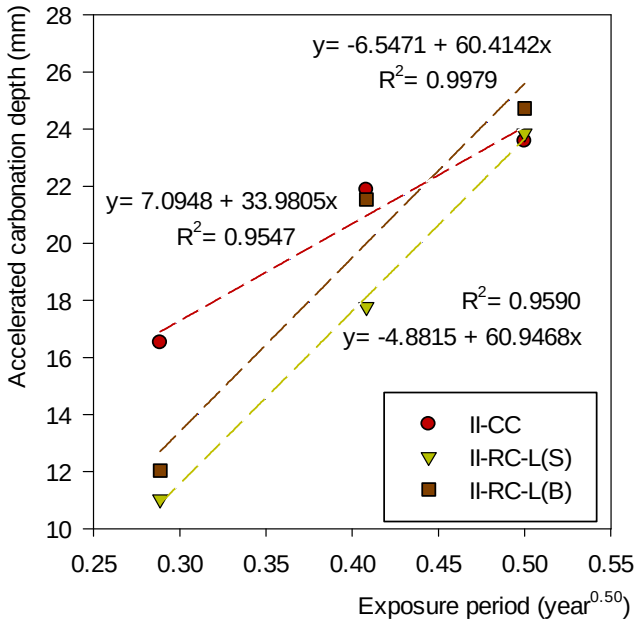

Figure 9.11: Evolution of the carbonation depth of concrete mixtures in phase II

Based on the penetration values, the carbonation coefficients were determined for the concrete mixtures in phase II. Table 9.3 shows both the accelerated and the corrected carbonation coefficients transformed by means of equation (3.30) assuming a 0.06% CO_2 concentration in natural conditions.

Table 9.3: Accelerated and corrected carbonation coefficients for concrete mixtures in phase II

	Accelerated carbonation coefficient (mm/year$^{0.50}$)	**Variation (%)**	**Corrected carbonation coefficient (mm/year$^{0.50}$)**
1 month of exposure			
II-CC	57.20	-	4.43
II-RC-L(S)	38.24	-33.14	2.96
II-RC-L(B)	41.73	-27.05	3.23
2 months of exposure			
II-CC	53.57	-	4.15
II-RC-L(S)	43.55	-18.71	3.37
II-RC-L(B)	52.75	-1.52	4.09
3 months of exposure			
II-CC	47.15	-	3.65
II-RC-L(S)	47.70	1.18	3.70
II-RC-L(B)	49.44	4.87	3.83

Figure 9.12 illustrates the variation in the accelerated carbonation coefficients as a function of the period of exposure of the concrete mixtures in phase II. Analogously to the penetration depths, a worsening in the performance of the recycled mixtures against the carbonation diffusion can be observed for increasing exposure times.

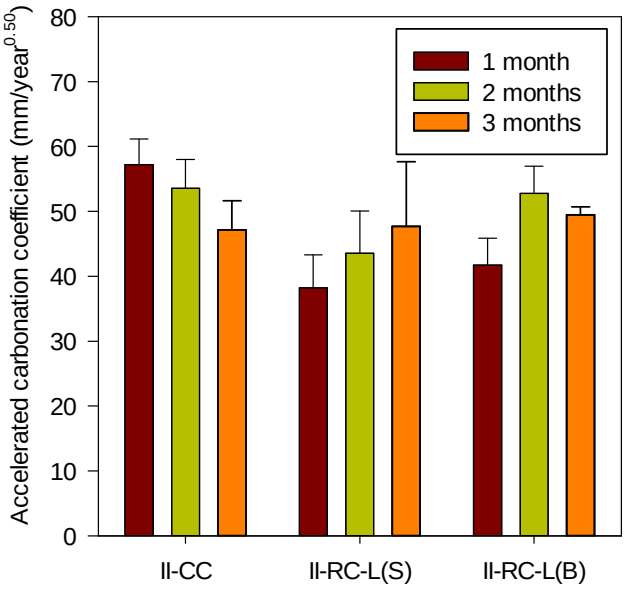

Figure 9.12: Accelerated carbonation coefficients for concrete mixtures in phase II

4. WATER ABSORPTION BY CAPILLARITY

When a non-saturated concrete element is in contact with water at one of its surfaces and also exposed to evaporation, the difference of pressure between the free water front and the water inside the concrete capillaries generates a hydraulic potential responsible for the absorption of water by capillarity within the structure. Although the aggregate absorptivity does not usually affect the overall permeability of concrete (Hewlett, 2003), the use of recycled aggregates, which are characterized by higher porosity, is expected to influence the resistance that recycled concrete presents against the capillary water sorption. Thus, the measure of this property provides data on the water accessible porosity of concrete and thus could be used as a durability indicator (Alexander et al., 1999).

Numerous studies have shown the adverse effect of the use of recycled aggregates on the water absorption by capillarity. Amorim et al. (2012) stated that this tendency is independent of the curing conditions, but it is especially relevant for dry settings. In replacements with recycled concrete aggregates, Olorunsogo and Padayachee (2002) observed rises up to 13% and 27% in water sorptivity of recycled concrete made with 50% and 100% replacement ratios. The authors also noticed that the differences between conventional and recycled mixtures were reduced for increasing curing times due to the faster pore refinement experimented by recycled concretes. For a complete substitution with recycled concrete aggregates, Gomes and de Brito (2009) registered that the capillary coefficient after 72 hours of testing increased by less than 10%. Kanellopoulos et al. (2014) also observed increments up to 28% and 66% in the sorptivity of recycled mixtures with replacements of recycled concrete aggregates between 30% and 100% of the natural coarse aggregates. Soares et al. (2014) observed growths in the capillary absorption ranging from 10.90% to 41.70% for replacement ratios between 25% and 100%. Contrarily, González and Etxeberria (2014) registered similar sorptivity values for conventional and recycled concretes with replacement ratios oscillating between 20% and 100% of recycled concrete aggregates obtained from parent concrete with 40 MPa, 60 MPa and 100 MPa characteristic strength, which was attributed to the lower water/cement ratio of all mixtures.

For mixtures containing mixed recycled aggregates, Gomes and de Brito (2009) reported an increase up to 33% of the capillary coefficient after 72 hours of testing when a mix of recycled concrete aggregates (25%) and recycled brick aggregates (50%) were employed. González-Corominas and Etxeberria (2014), who employed mixed recycled aggregates containing a 67% of ceramic waste, observed that recycled concretes with replacement ratios from 20% to 100% presented sorptivity values between 1.5 and 2.6 times higher for 28 days of curing. The authors also found an average rise of 64% in those differences for curing times of 180 days. Zong et al. (2014) registered increases between 5.10% and 14.50% depending on the replacement level (30%-50%). While Medina et al. (2014, 2015) registered higher sorptivity values (15%-46%) in recycled concrete mixtures when employing a 50% replacement ratio of mixed recycled aggregates, if the substitution level was fixed at 25%, the capillary sorption was lower (2%-5%) than that of concrete using conventional coarse aggregates. The authors attributed the reduction to the presence of CDW fines with pozzolanic activity that causes a refinement of the pore structure hindering the water accessibility. Finally, Bravo et al. (2015) indicated that natural coarse aggregates substitutions below 10% did not deteriorate the sorptivity of recycled concretes.

Regarding replacements with ceramic recycled aggregates, Correia et al. (2006) registered increments of sorptivity between 25.60% and 70.30% for replacement ratios ranging between 33% and 100%. Topçu and Canbaz (2007) observed increased capillarity coefficients for recycled concretes containing crushed tile coarse aggregates. The authors also detected that the effect was more evident when higher percentages of recycled aggregates in the 4-16 mm size range were employed in the mixtures. The findings of Debieb and Kenai (2008) disputed the assumption proposed by Correia et al. (2006) of increases in the sorptivity with rising replacement ratios as the mixture with a 75% replacement exhibited the minimum water absorption in the 25% to 100% range of substitution. Similar results were found by Gomes and de Brito (2009), who identified the 12.50% replacement ratio as the one responsible for the higher increase in the capillary coefficient (120% at 72 hours) despite testing recycled concretes containing greater amounts of ceramic aggregates. For 100% ceramic electrical insulator waste coarse aggregate concrete, Senthamarai et al. (2011) observed higher capillary sorption values (8%-63%) than in conventional concretes independently of the water/cement ratio. When using sanitary ceramic ware in the replacement, Medina et al. (2013) reported growths in water sorptivity between 10.59% and 37.91% for substitutions levels of 20% and 25% respectively. Contrary to the tendency shown by the previously reviewed literature, Pacheco-Torgal and Jalali (2010) who soaked the aggregates during 24 hours and then air-dried them to a saturated surface dry moisture state, registered that the water sorptivity of 100% recycled concrete was 55.80% lower than that of the control concrete.

Commonly, the increase in water absorption by capillarity is justified by the greater porosity of the recycled aggregates (Topçu and Canbaz, 2007; Pedro et al., 2014a). Nonetheless, the increase in capillary sorption is also due to the additional water used to compensate the water absorption capabilities of the recycled aggregates (Soares et al., 2014). In the research on lightweight aggregates, some researchers had already pointed out that the use of dry coarse aggregates could be advantageous from a durability standpoint of view due to the avoidance of increases in the porosity of the ITZ due to the pre-wetting of the aggregates, which in the end will improve the capillarity sorption behaviour of concrete (Punkki and Gjbrv, 1995; Punkki et al., 1996; Elsharief et al., 2005). This theory was also confirmed by Pereira de Olivera et al. (2014), who obtained higher water sorptivity when recycled concrete aggregates were pre-saturated for the manufacture of self-compacting recycled concrete. Specifically, the research of Ferreira et al. (2011) indicated that if the recycled aggregates were pre-saturated the water absorption by capillarity was higher than if additional water was employed in the mix design. For the recycled concrete aggregates without pre-conditioning, Pereira de Olivera et al. (2014) obtained decreases in the capillary sorption between 4.90% and 13.29% for replacement ratios ranging from 20% and 100%. Also for self-compacting concrete with replacement ratios of recycled concrete aggregates between 20% and 60%, Tuyan et al. (2014) observed lower primary (0.40%-37%) and secondary (54%-73%) sorptivity rates than for the corresponding control concrete.

Figure 9.13 shows the capillary water absorption per unit area as a function of square root of time for all concrete mixtures. All the sorptivity curves present a parallel behaviour, which indicates that the water absorption process is similar for conventional and recycled concretes. The first part of the curve corresponds to the water absorption due to the filling of capillary pores while the second part displays the continued filling of the pores via diffusion and dissolution of air (Fagerlund, 1982).

The progressive decline in the absorption rate of the first part of the curve is due to the hydration and rehydration phenomena of the unreacted and dehydrated components of the cement paste that modify the pore connectivity (Hall et al., 1995; Taylor et al., 1999). In addition, the intersection point between the first and second part of the curve matches the moment when the water reaches the upper surface of the sample, i.e. the attainment of saturation which can be confirmed by reaching constant mass (UNE 83982, 2008).

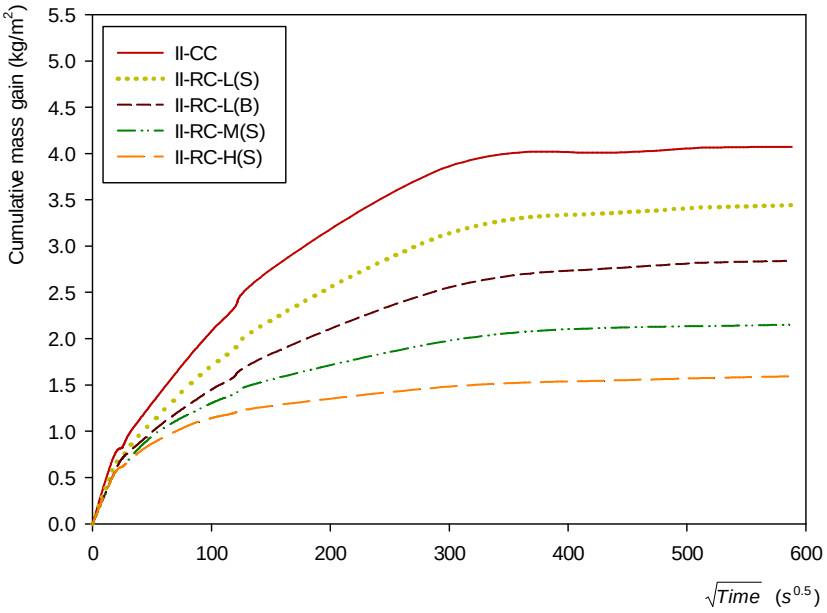

Figure 9.13: Kinetics of the water absorption by capillarity of conventional and recycled concretes

Recycled concrete displayed a lower capillary water absorption than the conventional concrete during the complete testing procedure, particularly after the first hour. These results fall in line with the findings of Gonçalves et al. (2004) and Etxeberria and Vegas (2015), who reported that the quality of the cement matrix has a more strong effect on the sorptivity than the presence of recycled aggregates. Therefore, the improvement shown by the recycled concretes can be explained by the mix design followed in this research work. Since the same amount of water was proportioned to all concrete mixtures, i.e. no pre-soaking technique was used or extra water was added to the mix, the effective water/cement ratio of the recycled concretes was lower than that of the conventional concrete, which entails an increase in the quality of the cement paste and thus an improved durability as determined through capillary absorption. Nevertheless, at a fixed water/cement ratio, the type of coarse aggregate should be considered as the factor affecting the water sorptivity (Güneyisi et al., 2013). Bravo et al. (2015), who experimented with recycled aggregates from different CDW management plants, found that the composition is a key factor on the variability of this property. Hence, the comparison among the recycled mixtures shows a reduction in the water absorption for increasing content of ceramic wastes incorporated in the recycled aggregates.

Table 9.4 shows the initial water absorption, which represents the quantity of water absorbed by unit surface area during the first hour of testing, and the amount of water absorbed until the saturation of the specimen, which coincides with the saturation point in Figure 9.13. Rabehi et al. (2013) concluded that the initial water absorption is an increasing function of the water/cement ratio, which is in agreement with the results obtained in this research work. The water uptake in the first hour of testing is between 16.15% and 36.19% lower in the recycled concretes due to the lower effective water/cement ratio of these mixtures. Moreover, the differences among recycled mixtures can be explained by the increasing amounts of ceramic content, which are the main contributors of fines with pozzolanic activity responsible for the refinement of the porous network (Medina et al., 2015). Figure 9.14 illustrates the strong correlation (R^2=0.92) between both variables. A similar good relationship (R^2=0.96) was also identified between the water absorbed at the intersection point and the ceramic content incorporated in the concrete mixtures. In this regard, the decreases ranged between 15.91% and 62.04% for rising ceramic contents.

Table 9.4: Water uptake in the first hour and at the saturation point

	First hour (kg/m²)	Variation (%)	Saturation point (kg/m²)	Variation (%)
II-CC	1.47	-	4.06	-
II-RC-L(S)	1.23	-16.15	3.42	-15.91
II-RC-L(B)	1.10	-25.24	2.74	-32.49
II-RC-M(S)	1.04	-29.30	2.14	-47.43
II-RC-H(S)	0.94	-36.19	1.54	-62.04

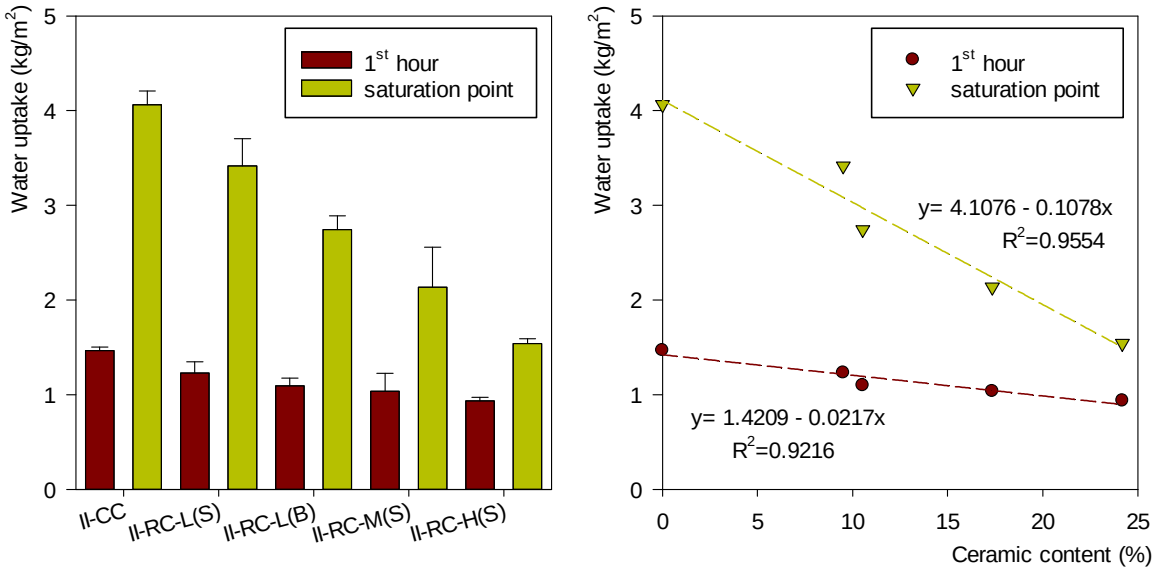

Figure 9.14: Water uptake in the first hour and at the saturation point

In addition, the capillary water absorption coefficients were calculated according the equations established in the Spanish standard UNE 83982 (2008). Figure 9.15 shows the average capillary water absorption coefficients of four concrete specimens of each concrete mixture plotted against the time elapsed since the beginning of the test.

Similarly to Soares et al. (2014), the evolution of the capillary absorption is best fitted through logarithmic regression ($R^2 \geq 0.96$) since the coefficient decreases rapidly during the first hours and the reductions becomes slower after 10 hours of contact of the concrete specimen with water, which is in accordance with the physical phenomenon, i.e. the water is absorbed faster at the beginning of the test tending to stabilize with time. The similarity between the equations describing the fitted curves confirms the matching behaviour of conventional and recycled mixtures regarding capillary sorption, which was also indicated by the findings of other researchers (Debieb and Kenai, 2008; Soares et al., 2014).

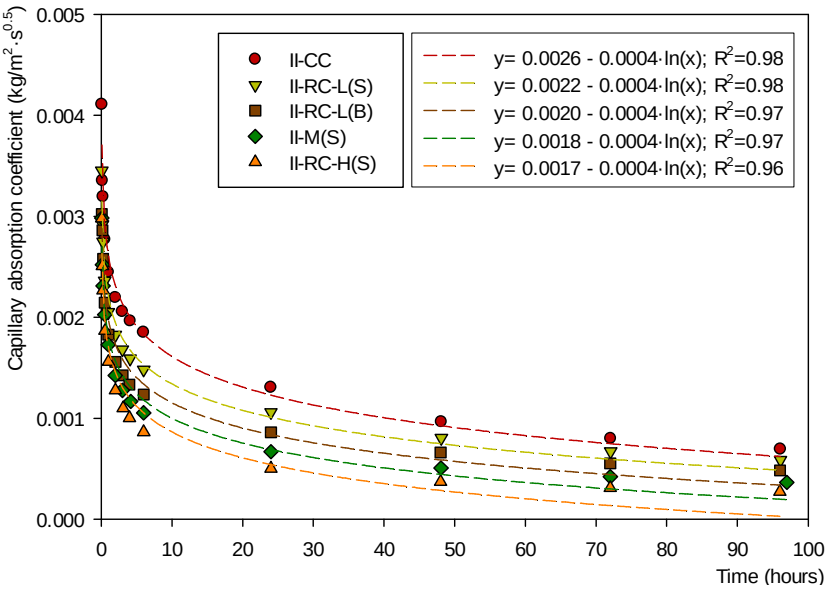

Figure 9.15: Evolution of capillary absorption coefficients over time

In order to quantitatively compare the capillary water coefficients among concrete mixtures, the results at the saturation moment, i.e. the intersection point between the two parts of the water absorption curve, were selected (Figure 9.16). The recycled mixtures exhibited a decline in capillary absorption coefficient at saturation between 15.91% and 53.51%, which was again strongly correlated with the proportion of ceramic aggregates incorporated in the recycled concrete mixture (R^2=0.93). A similar linear correlation was also found by Correia et al. (2006) between the water sorptivity and the ceramic content incorporated in the recycled concretes. However, in his research, the relationship was inversely proportional due to the water compensation performed to compensate the higher porosity of the crushed bricks aggregates.

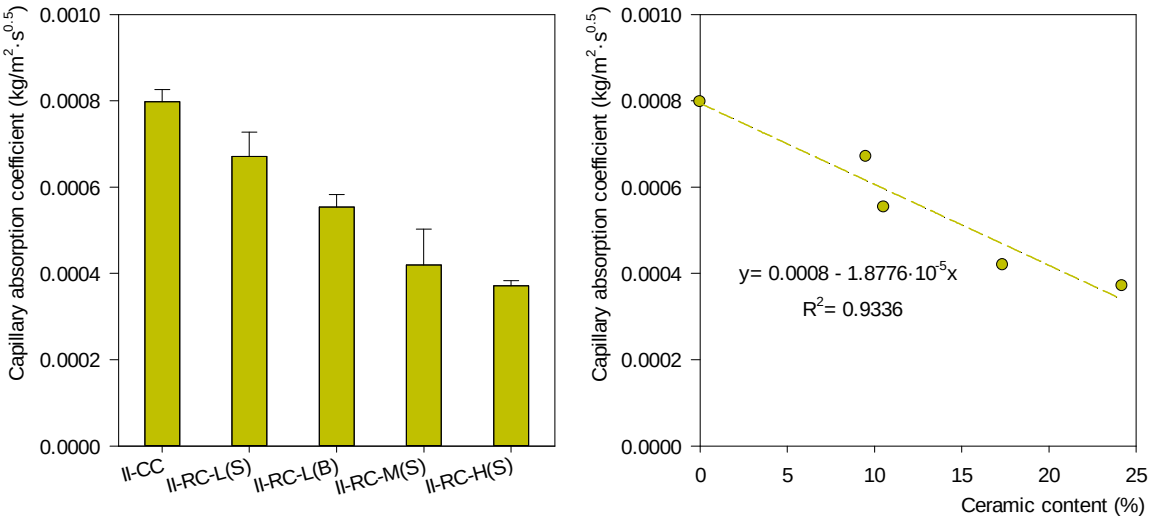

Figure 9.16: Capillary absorption coefficient at complete saturation and its relationship with the ceramic content by weight incorporated in the total fraction of aggregates

The primary sorptivity was determined as the slope of the curve during the first 6 hours of testing, while secondary sorptivity was determined using the data points from 1 day of testing to the end of the measurements. As could be observed in Figure 9.17, very good correlation factors ($R^2 \geq 0.90$) were found between the test results and the correspondent regression lines in all concrete mixes.

Table 9.5 shows the sorptivity values obtained for the conventional and recycled concrete. Thus, the decline in the sorptivity coefficients could be indicative of capillary suction in smaller pores or due to effects of moisture diffusion (Martys and Ferraris, 1997). The primary sorptivity gives information on the continuity of the pore system in the surface layer of concrete (Basheer et al., 2001). Hence, poorly interconnected porous networks can be assumed in the recycled mixtures, which agrees well with the effect of the pozzolanic nature of the CDW on the refinement of the pore structure and thus hindering the water accessibility (Medina et al., 2015). In addition, a strong relationship was identified between the decreases in primary sorptivity and the percentage of ceramic aggregate incorporated in the recycled mixture (Figure 9.18).

Table 9.5: Primary and secondary sorptivity rates

	Primary sorptivity ($kg/m^2 \cdot s^{0.5}$)	Variation (%)	Secondary sorptivity ($kg/m^2 \cdot s^{0.5}$)	Variation (%)
II-CC	0.0156	-	0.0008	-
II-RC-L(S)	0.0122	-21.79	0.0011	37.50
II-RC-L(B)	0.0095	-39.10	0.0011	37.50
II-RC-M(S)	0.0079	-49.36	0.0006	-25.00
II-RC-H(S)	0.0058	-62.82	0.0004	-50.00

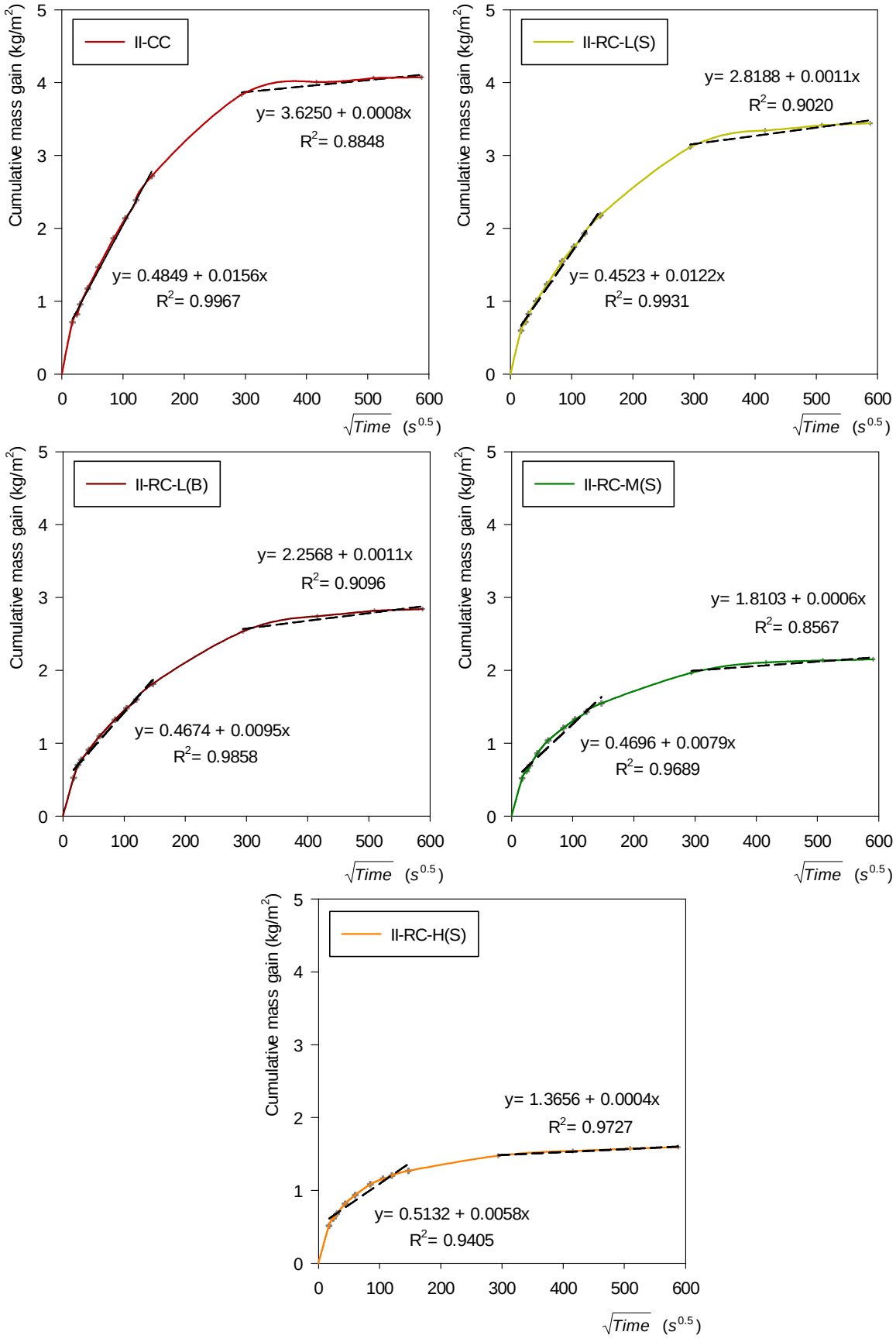

Figure 9.17: Primary and secondary sorptivity curve fit

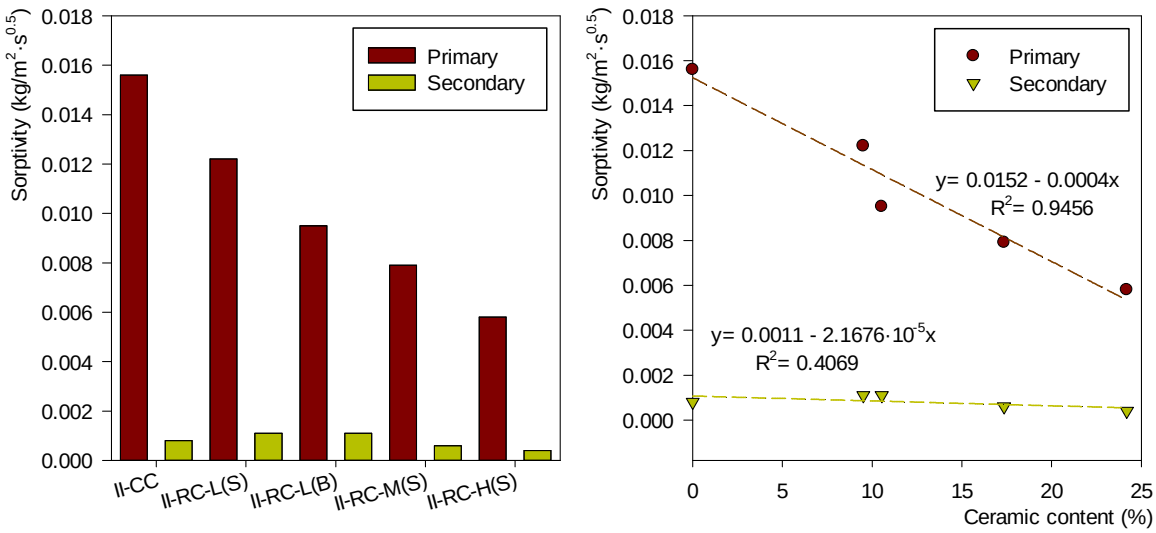

Figure 9.18: Primary and secondary sorptivity rates and its relationship with the ceramic content incorporated in the total weight of aggregates

According to the performance ranges proposed by Alexander et al. (1999), all mixtures presented an excellent durability class since the sorptivity values for all samples were below 0.10 kg/m^2·s$^{0.5}$. Even considering the recommendations of lowering that limit to 0.05 kg/m^2·s$^{0.5}$ (Menendez et al., 2007), all concrete mixtures continue to be exceptionally durable. Therefore, all the mixtures present excellent resistance to the penetration of water or other aggressive environmental agents dissolved in water, such as deleterious salts or chloride and sulphate ions, and the use of recycled aggregates containing ceramic wastes constitutes an improvement of durability if no extra water is used in the design of the recycled mixtures.

4.1. RELATIONSHIP BETWEEN THE WATER ABSORPTION BY CAPILLARITY AND THE POROSITY BY MIP

The water absorption by capillarity allows an indirect study of the capillary porosity of a concrete mixture through the differentiation of large and fine capillaries. Figure 9.19 illustrates the relationship between this property and the porosity results of the concrete mixtures determined by MIP. As the effective porosity increases leading to higher interconnected porous network, the concrete presents higher sorptivity rates. Nonetheless, the relationship between both variables was higher for the secondary sorptivity than the primary sorptivity.

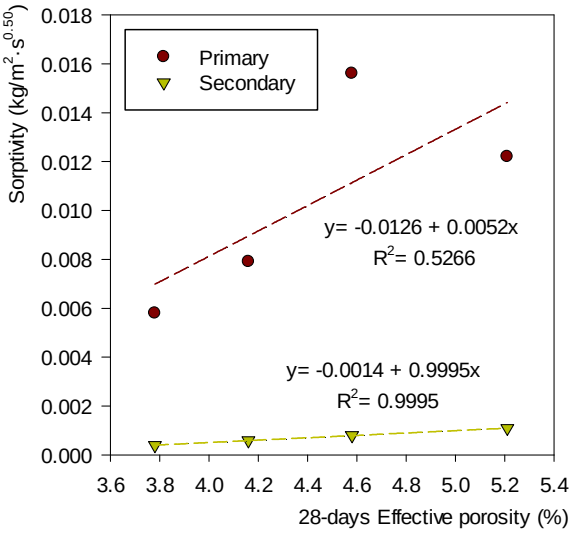

Figure 9.19: Relationship between the sorptivity and the porosity

5. WATER ABSORPTION UNDER VACUUM

The potentially aggressive substances form the environment can penetrate concrete dissolved in water. The determination of the open porosity, which is the porosity accessible from the concrete surface, can also serve as a durability indicator of concrete (Audenaert and De Schutter, 2007).

The literature review showed a direct relationship between the use of recycled aggregates and the upsurge of the open porosity, which is justified by the higher porosity of the recycled aggregates, in particular due to the presence of mortar adhered or ceramic particles. Thomas et al. (2013) found that the open porosity of concrete made with recycled concrete aggregates increases with the water/cement ratio and the replacement ratio. The rise of the water absorption under vacuum with the substitution levels was also observed by Beltrán et al. (2014b), who increased the cement content in order to avoid the strength drawbacks associated with the use of recycled aggregates. The authors registered increases in the water absorption under vacuum between 7% and 41% compared to the reference mixture when using recycled concrete aggregates in the concrete manufacture. For self-compacting concrete made with recycled concrete aggregates, Kanellopoulus et al. (2014) observed increases up to 11%, 19% and 29% when 100% of the natural aggregates were replaced by 4/10 mm, 8/20 mm and 4/20 mm, respectively.

To date, the research focused on recycled concrete made with mixed or ceramic recycled aggregates is very limited. In his PhD, Geraldes (2013) obtained average upsurges of 21% and 50% in the open porosity of recycled concretes with replacement ratios of 50% and 100% of mixed recycled aggregates respectively. Pacheco-Torgal and Jalili (2010) registered differences in open porosity up to 20% between conventional and recycled concretes made of 100% ceramic coarse aggregates.

The results of water accessible porosity under vacuum for the concrete mixtures of this investigation are presented in Table 9.6 and Figure 9.20. Since the test was carried out after two different drying temperatures, the results allow the assessment of different types of open porosity. According to Audenaert and De Schutter (2007) and Lothenbach (2008), capillary porosity can be related to the results arising from the test specimens dried at low temperatures, such as 40ºC; while the values obtained after drying at elevated temperatures, such as 105ºC, correspond to the total open porosity. Hence, the difference between both test results can be associated to the gel porosity accessible to water.

Table 9.6: Water accessible porosity under vacuum

	Capillary (%) ($\varphi_{40ºC}$)	**Variation (%)**	**Gel (%) ($\varphi_{105ºC-40ºC}$)**	**Variation (%)**	**Total (%) ($\varphi_{105ºC}$)**	**Variation (%)**
II-CC	11.68	-	6.30	-	17.98	-
II-RC-L(S)	12.79	9.50	7.50	19.05	20.29	12.85
II-RC-L(B)	14.7	25.86	5.55	-11.90	20.25	12.63
II-RC-M(S)	16.38	40.24	4.41	-30.00	20.79	15.63
II-RC-H(S)	16.13	38.10	4.95	-21.43	21.08	17.24

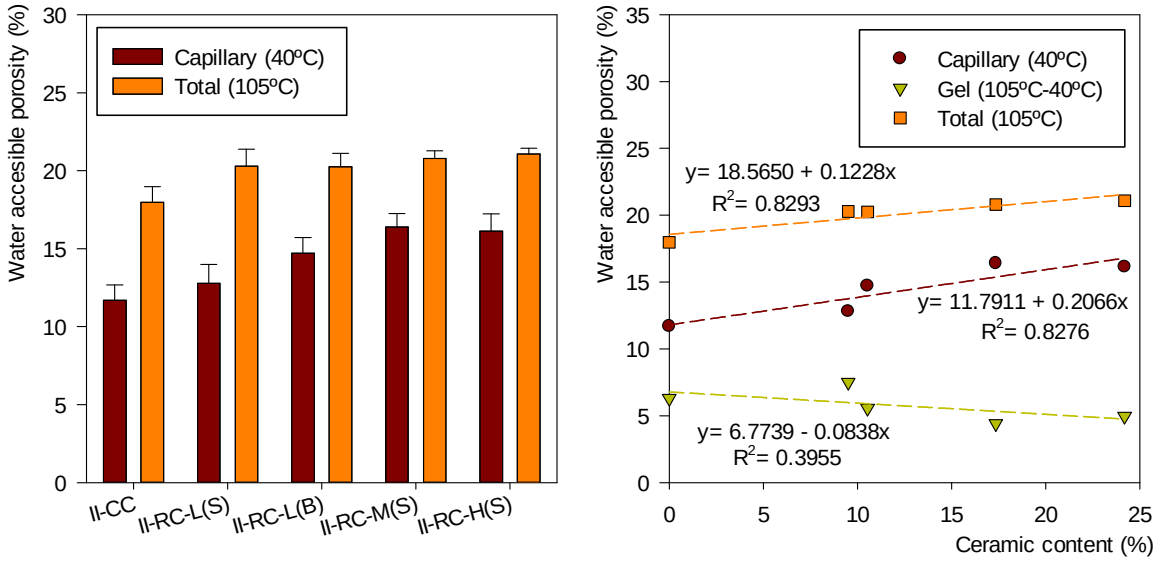

Figure 9.20: Water accessible porosity under vacuum

The results indicate that the capillary open porosity was greater for recycled concretes. The upsurge, which ranged from 9.50% to 40.25%, was strongly affected (R^2=0.83) by the ceramic content in the mixture (Figure 9.20). However, this tendency was reversed in the assessment of the gel open porosity and a decrease between 11.90% and 30% was observed for three of the mixtures. Nonetheless, one of the mixtures incorporating the lower ceramic content (II-RC-L(S)) showed a 19.05% higher gel open porosity than the conventional mixture. The great difference in the behaviour between II-RC-L(S) and II-RC-L(B) indicates that the percentage of ceramic is not the only factor controlling this property, which is proven by the weak relationship (R^2=0.40) identified between both variables (Figure 9.20).

In fact, the recycled aggregates employed in the II-RC-L(S) mixture presented a 16% higher amount of adhered mortar, which is also responsible for the porosity differences between concretes. In any case, the total open porosity was increased between 12.85% and 17.24% as a function (R^2=0.83) of the ceramic wastes present in the recycled aggregates used in the replacement (Figure 9.20). Therefore, the incorporation of recycled aggregates from CDW with varying ceramic content causes a decrease in the concrete durability since it leads to a rise in the water open porosity.

5.1. RELATIONSHIP BETWEEN THE WATER ABSORPTION UNDER VACUUM AND THE POROSITY BY MIP

To date, there is no consensus to which extent the water absorption under vacuum after drying at 40ºC gives an adequate estimation of the capillary open porosity (Gruyaert, 2011). Thus, the conformity between the capillary porosity accessible to water after drying at 40ºC and the macro-porosity obtained by MIP at 28 days of curing was assessed in Table 9.7. The comparison resulted in an average 2.32 times higher estimation of the capillary pores determined through water absorption under vacuum. The relationship between both variables (Figure 9.21) rendered an acceptable linear correlation factor (R^2=0.82), which suggests that the results arising from this measuring technique should be cautiously related to the capillary porosity of a concrete mixture. A similar conclusion was reached from the experiments carried out by Gruyaert (2011). The difference between results can be related to the wetting nature of water compared to mercury and the fact that the water absorption test was carried out without air in the pores. Nonetheless, the values obtained could be used to compare the behaviour among concrete mixtures.

Moreover, the drying stage at 105ºC has also been subjected to criticism since such temperatures can produce the modification of the microstructure of concrete (Jennings, 2000; Safiuddin and Hearn, 2005). However, in this regard, it is accepted that results from absorption under vacuum after drying at 105ºC corresponds with the total (gel and capillary) open porosity (Kearsley and Wainwright, 2001; Cnudde et al., 2009). However, since the gel open porosity is calculated as the difference between the total and capillary values, the same concerns about the accuracy of the method still apply. In Table 9.7, the gel porosity accessible to water and the meso-porosity obtained by MIP at 28 days of curing were compared and a similar correspondence (R^2=0.82) between the results was found (Figure 9.21).

Table 9.7: Comparison between the capillary porosity accessible to water and the macro and meso-porosity obtained by MIP at 28 days of curing

	Capillary porosity		**Gel porosity**	
	$\varphi_{40ºC}$ (%)	**$MIP_{macropores}$ (%)**	**$\varphi_{105ºC-40ºC}$ (%)**	**$MIP_{mesopores}$ (%)**
II-CC	11.68	5.33	6.30	5.77
II-RC-L(S)	12.79	5.25	7.50	8.91
II-RC-L(B)	14.70	-	5.55	-
II-RC-M(S)	16.38	7.61	4.41	5.10
II-RC-H(S)	16.13	6.49	4.95	4.96

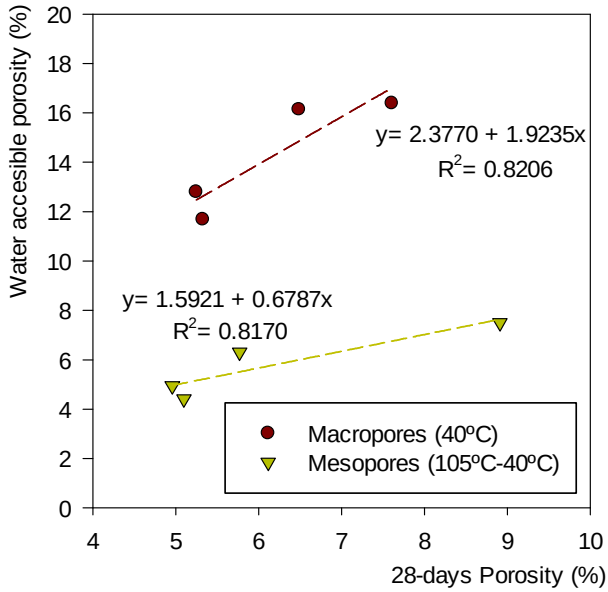

Figure 9.21: Relationship between the capillary porosity accessible to water and the macro and meso-porosity obtained by MIP at 28 days of curing

5.2. RELATIONSHIP BETWEEN THE WATER ABSORPTION UNDER VACUUM AND THE WATER ABSORPTION BY CAPILLARITY

Kanellopoulus et al. (2014), who studied self-compacting concrete incorporating recycled concrete aggregates, detected a linear relationship between sorptivity and open porosity measured at 105ºC (R^2=0.98 for 4/10 mm recycled aggregates and R^2=0.77 for 8/20 mm recycled aggregates). Figure 9.22 illustrates the relationships between the water absorption under vacuum and the sorptivity of the concretes in this research work.

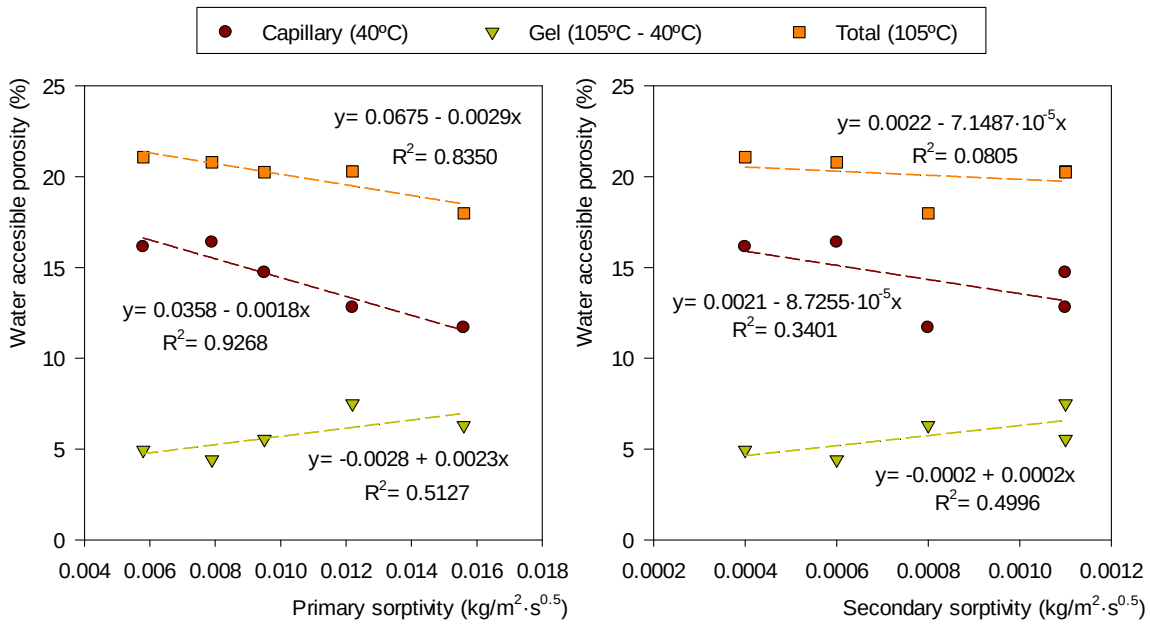

Figure 9.22: Relationship between water accessible porosity and the water absorption by capillarity results, i.e. sorptivity rate and capillary absorption coefficient at saturation

While a similar relationship was identified between the total porosity and the primary sorptivity (R^2=0.84), no correlation exists with the secondary sorptivity. In general, a lack of relationships between the secondary sorptivity and the different types of open porosity can be assumed. Contrarily, the results of the primary sorptivity presented better correlations with the water absorption under vacuum, in particular with the capillary open porosity (R^2=0.93), which is indicative of similarities in both mechanisms of water absorption.

6. WATER PENETRATION UNDER PRESSURE

The water penetration under pressure, also known as water permeability, measures the ease with which a fluid passes through the concrete specimen due to the action of a differential pressure. The maximum depth of water penetration reflects the open permeability of the concrete mixtures.

There is considerable discrepancy in the literature on the effect that recycled aggregates have on the water permeability of concrete. Since, according to Hoseini et al. (2009), this property is more strongly influenced by the inherent permeability of the concrete constituents than that of the ITZ in the cement matrix, the differences in the results can be explained by the variable quality of the recycled aggregates employed.

For replacements with recycled concrete aggregates, Zega and Di Maio (2011) observed that the average depth of water penetration was similar for a conventional mixture and three recycled concretes made with 25%, 50% and 75% substitution levels of recycled concrete aggregate, while the maximum depth values were lower for recycled mixtures, on average a 34%. The authors attributed the differences to the use of the recycled aggregates in air-dry condition, which resulted in a denser ITZ between the cement paste and the recycled aggregate and lower effective water/cement ratio for the recycled mixtures. In spite of the high variability in their results, López-Gayarre et al. (2011) also reported a decrease of 16.11% and 48.89% in the water permeability of recycled concrete mixtures incorporating 20% and 100% recycled concrete aggregates, respectively. Pereira de Oliveira et al. (2014) indicated that self-compacting concrete made with recycled concrete aggregates presented lower depth of water penetration values than a conventional self-compacting mixture for replacement ratios greater than 40%. For instance, the authors reported declines up to 30% and 25% for replacement ratios of 40% and 100%, respectively; while they observed a 21% increase in the water permeability when only 20% of the natural coarse aggregates were substituted. In this line, Zaharieva et al. (2003) reported that the water permeability coefficients of the recycled mixtures were two times higher than that of the control concrete. Berndt et al. (2009), who compared the water permeability coefficient of conventional and recycled concrete mixtures designed with different cement types, observed that the increase of the permeability was independent of the type of binder but the differences were lower when 50% and 70% of blast furnace slag was blended with the Portland cement. Thomas et al. (2013) reported that the increase in the depth of penetration suffered by the recycled concrete mixtures was higher for rising substitution levels and water/cement ratios. Nonetheless, these differences were reduced for increasing curing ages. The authors observed that the fitted curves tended to converge at water penetration values of around 30 mm for a water/cement ratio less than 0.45.

Despite increasing the cement content with rising replacement ratios, Beltrán et al. (2014b) observed that recycled mixtures made with 20%, 50% and 100% recycled concrete aggregates experienced average increases of 12.94%, 34.26% and 43.00%, respectively. Similarly to Thomas et al. (2013), the authors also noticed that the increments were higher for increasing replacement ratios and water/cement ratios. Finally, Jiménez et al. (2014) concluded that the application of the equivalent mortar volume (EMV) to the Bolomey proportioning method mitigated the 3.35 times higher depth of water penetration caused by a 20% replacement of recycled concrete aggregates in a recycled concrete mixture with a water/cement ratio of 0.45. Nevertheless, the authors did not achieve the same effect when recycled concretes with a water/cement ratio of 0.60 were tested.

The same lack of consensus exists when mixed recycled aggregates are used in the production of concrete. Martínez-Lage et al. (2012) reported that, in most cases, the water penetration was lower for rising replacement ratios of mixed recycled aggregates, which was attributed to the incomplete saturation of the recycled aggregate that led to further water absorption or the fact that the water/cement ratio was greater for rising replacement ratios due to water compensation of the recycled aggregate. For example, a total substitution of the natural course aggregate led to a decline of the average penetration depth up to 26%. Contrarily, Mas et al. (2012a, 2012b) indicated that the upsurge in depth of water penetration was directly proportional to the amount of mixed recycled aggregates employed in the substitution, but less significant when CEM III and CEM V were used, which agrees with the findings of Berndt et al. (2009). Beltrán el at. (2014a) reported depths of water penetration up to 94.77% higher when using mixed recycled aggregates.

When recycled brick aggregates are used, Debieb and Kenai (2008) registered a depth of water penetration 2.33 times higher than that of the conventional concrete. For a 100% replacement with ceramic coarse aggregates, Pacheco-Torgal and Jalali (2010) observed, approximately, an increase up to 33% in the water permeability of recycled concrete with respect to the control concrete. Medina et al. (2013) registered a similar maximum depth of water penetration regardless the amount of sanitary ceramic employed in the recycled concrete. However, the average depth of water penetration increased with the replacement ratio, on average, 11% and 20% for 20 and 25% substitution levels respectively. The findings were attributed to the particularities regarding the porosity, since higher porosity levels displayed by the recycled concretes were compensated by lower mean pore size and volume of macropores (Bermejo et al., 2010; Medina et al., 2013).

Figure 9.23 illustrates the water penetration zone in specimens pertaining to concrete mixtures of phase I. The resulting water penetration depth in both research phases are presented in Table 9.8. At first glance, it can be observed that the recycled mixtures generally exhibited a better performance than the conventional concrete, which has also been observed in some of the literature. Regarding the maximum penetration depth, reductions between 2.12% and 32.25% were observed for decreasing ceramic contents for phase I and declines ranging from 0.62% to 55.62% were registered in specimens pertaining to phase II. In terms of average depth, mixtures I-RC-L(S) and I-RC-M(S) displayed a 35.77% and 62.31% lower permeability than the conventional concrete; while the I-RC-H(S) mixture showed a 17.44% higher water penetration depth. This contradictory pattern reflects the findings observed in the literature review, which suggest that the behaviour of recycled concrete is strongly dependent on the quality of the recycled aggregates employed.

I-CC **I-RC-L(S)** **I-RC-M(S)** **I-RC-H(S)**

Figure 9.23: Examples of the water penetration zone in specimens pertaining to phase I

Table 9.8: Water penetration depths

	CC	RC-L(S)	RC-M(S)	RC-H(S)
Phase I				
Average depth (mm)	15.6	10.02	5.88	18.32
Variation (%)	-	-35.77	-62.31	17.44
Maximum depth (mm)	35.35	23.95	29.8	34.6
Variation (%)	-	-32.25	-15.70	-2.12
Phase II				
Maximum depth (mm)	56.06	33.35	24.88	55.71
Variation (%)	-	-40.51	-55.62	-0.62

The Spanish Code on structural concrete (Permanent Commission on Concrete, 2008) establish that the average and maximum penetration depth should be lower than 30 mm and 50 mm, respectively, for mass or reinforced concrete structures subjected to environmental classes IIIa, IIIb, IV, Qa, E, H, F and Qb or 20 mm and 30 mm, respectively, for pre-stressed concrete elements subjected to environmental classes IIIc, Qc and Qb. Therefore, the pore structure of the recycled concretes guarantees impermeability and sufficient durability throughout their service life for all concretes in phase I when both the limits are assessed for environmental classes IIIa, IIIb, IV, Qa, E, H, F and Qb (Figure 9.24). However, the conventional concrete and the recycled II-RC-H(S) mixture pertaining to phase II investigations, exceeded the limit for environmental classes IIIa, IIIb, IV, Qa, E, H, F and Qb (Figure 9.24). Hence, if these mixtures are to be used in reinforced concretes, the cover of the reinforcements should be increased. Regarding to the suitability of these mixtures in the production of pre-stressed concrete elements, the limit of average was not surpassed by any concrete in phase I but the restriction in terms of maximum penetration depth was not fulfilled by the conventional concrete and the recycled II-RC-H(S) mixture. Similarly, the results of phase II showed that only the II-RC-M(S) mixture exhibited a behaviour complying with the requirements for environmental classes IIIc, Qc and Qb (Figure 9.24).

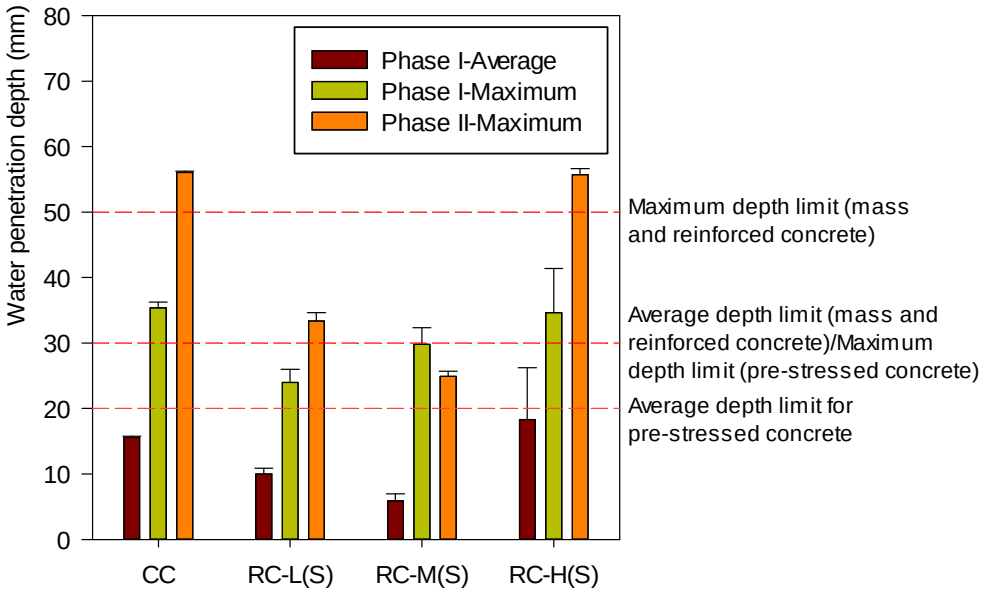

Figure 9.24: Water penetration depths

6.1. RELATIONSHIP BETWEEN THE WATER PENETRATION UNDER PRESSURE AND THE POROSITY BY MIP

The critical pore diameter, which represents the most frequently occurring pore size in interconnected pores, is a parameter often used to assess the transmissivity of the concrete. Figure 9.25 illustrates the relationship between the water penetration depth and the critical pore diameter of the concrete mixture determined by MIP. As can be observed, higher pore size values led to higher water permeability. Hence, the penetration of water in recycled mixtures also depends on the pore refinement of the concrete structure as stated by Bermejo et al. (2010) for conventional concretes.

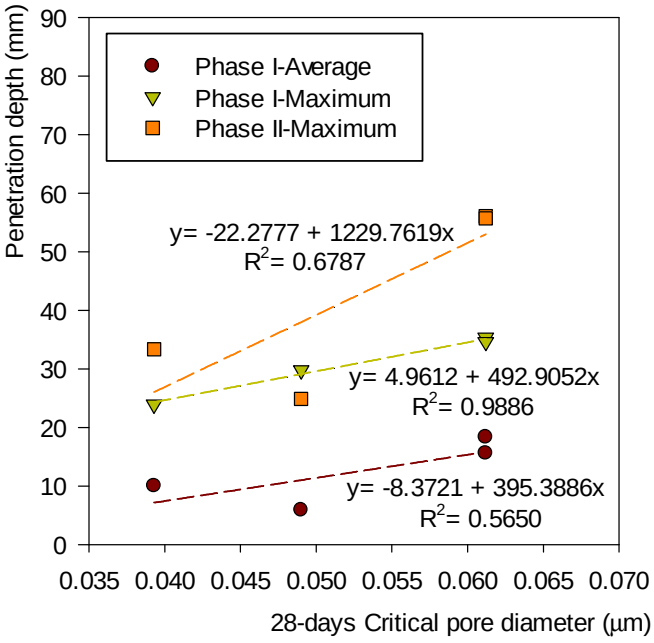

Figure 9.25: Relationship between the water penetration depth and the critical pore diameter

7. FROST-SALT RESISTANCE

The deterioration of concrete due to freeze-thaw cycles is one of the most important causes decreasing its life span in countries with a continental climate. Since the use of de-icing salts is a common practice used to de-ice concrete roadways and walkways, the superficial degradation is increased due to frost-salt scaling. However, it is agreed that the deterioration is mostly physical, whereas the chemical reactions between the salt and the hydration products play a secondary role in the damage (Malhotra, 2011). Moreover, as this deterioration is progressive, the concrete becomes exposed to the ingress of moisture and other aggressive species that further affect its durability.

Although the phenomenology that characterizes this damage is well known, the underlying mechanism is not fully understood yet. According to Wardeh et al. (2011), the formation of cracks is a result of the hydraulic pressure due to the 9% increase in volume caused by the ice formation, the osmotic pressure due to the movement of liquid water from small neighbouring pores towards large pores containing the first ice crystals in order to restore thermodynamic equilibrium and the pressure caused by the growth of crystals in the pore walls. Valenza II and Scherer (2007), who described and criticized most of the available theories (hydraulic pressure, crystallization pressure, thermal shock, precipitation and growth of salt, salt concentration, reduction in vapour pressure, osmotic pressure and glue spalling), stated that glue spalling seems to give the only plausible explanation. The cracking of the ice layer is caused by the tensile stresses induced by the differences in the coefficient of thermal expansion of ice and concrete. Those cracks penetrate the concrete and propagate into a parallel path to its surface causing the damage.

Several studies have compared the freeze-thaw durability of concrete incorporating recycled concrete aggregates with that of concrete made with natural coarse aggregates. Lower freeze-thaw performance has been reported for recycled concrete compared to conventional concrete (Kasai et al., 1988; Nishibayashi and Yamura, 1988; Zaharieva et al., 2004). In the manufacture of self-compacting recycled concrete, Tuyan et al. (2014) registered higher weight changes for concretes made with 20% to 60% recycled concrete aggregates. Despite that Nagataki and Lida (2001) also observed declines in the frost resistance of concrete made with recycled concrete aggregates, the authors reported that the recycled concretes still performed satisfactory after 300 freeze-thaw cycles. In addition, the frost durability of conventional and recycled concrete mixtures was comparable after 1 year of curing. In this line, Limbachiya et al. (2000) observed similar durability against the freeze-thaw deterioration between non air-entrained recycled concrete with replacements ratios ranging from 20% to 100% and air entrained conventional concrete of 30-50 MPa target strength. For testing intervals between 50 and 100 cycles, Hwang et al. (2013) detected comparable decreases in the relative dynamic modulus of elasticity (87%-96%) between conventional concretes and recycled mixtures containing 30% fly ash or 60% blast furnace slag. The declines were higher when Portland cement was employed in the recycled concretes resulting in failures after 250 cycles. For 50% and 100% replacement ratios, Yildirim et al. (2015) obtained comparable results for concrete containing recycled aggregates and conventional ones. Nonetheless, the authors observed improvements in the frost performance when the recycled aggregates were semi-saturated and fully saturated.

de Oliveira and Vazquez (1996) observed that concrete made with dry recycled aggregates had a higher resistance than that of mixtures with completely saturated recycled concrete aggregates. However, semi-saturated recycled aggregate displayed the highest frost durability, resisting more than 100 freeze-thaw cycles. By using the EMV proportioning method, Razaqpur et al. (2010) observed similar freeze-thaw resistance between 100% recycled concrete and that of a conventional mixture; whereas Abbas et al. (2009) registered better results due to the application of that technique. Similarly, Güneyisi et al. (2014) observed that the treatment of the recycled aggregates with HCl solution, water glass dispersion, the two mixing stage approach (TMSA) and cement-silica slurry resulted in an enhancement of the ultrasonic velocity pulse between 1.50% and 2.30% after 100 cycles. Finally, Gokce et al. (2004) reported that the use of recycled concrete aggregates derived from air-entrained concretes resulted in higher frost resistance for recycled concretes than that of a conventional mixture after 500 cycles of freeze-thaw. However, the presence of a small amount of recycled concrete aggregates obtained from parent concrete without air entraining agents led to poor frost performances. The authors stated that treatments to reduce the amount of adhered mortar content slightly improved the durability. The lack of consensus regarding the effect of recycled aggregates on the frost resistance of concrete can be explained by the different quality, particularly in terms of water absorption and fragmentation resistance (Kevern et al., 2009).

The investigation of the frost-salt resistance of concrete mixtures containing recycled aggregates is very limited. Dhir and Paine (2007) observed that concretes made with mixed recycled aggregates containing 80% ceramic materials exhibited lower frost resistance than that of a conventional mixture after 56 cycles of scaling. For mixed recycled aggregates containing 25% concrete rubble and 75% of ceramic bricks, Richardson et al. (2011) observed lower mass loss, a 42.06% improvement in the ultrasonic pulse velocity reduction and a 81.64% higher mean failure load after 56 freeze-thaw cycles due to the good quality of the recycled aggregates and the pre-soaking technique performed.

Some more research has been conducted on the effect of ceramic recycled aggregates in the resistance to freeze-thaw cycles. Topçu and Sengel (2004) observed marginal deterioration of concrete made with brick recycled aggregates subjected to -20ºC for 8 hours and 20ºC for 16 hours. However, when crushed tiles were used to replace 50% and 100% of the natural aggregates, Topçu and Canbaz (2007) registered an increase from 0.40% to 1.40% in the mass loss due freeze-thaw degradation compared to the conventional mixture. Bolouri Bazaz and Khayati (2011) noticed that concrete made with crushed brick aggregates was able to resist 50 cycles without experimenting cracks if the water/cement ratio was 0.45, whereas the recycled concrete mixtures exhibited a high degradation after the first cycle and fractured after 5 cycles for high water/cement ratios. For ceramic sanitary ware, Medina et al. (2013) registered a similar mass loss for the first 14 freeze-thaw cycles that turned to lower scaling damage in concretes with 20% and 25% replacements ratios. However, after 56 freeze-thaw cycles, the mass loss was around 0.08 kg/m^2 for the three mixtures, with 2.1% and 3.68% lower scaling in the recycled mixtures. Finally, Adamson et al. (2015) noticed an increase in the freeze-thaw resistance of the recycled concrete with 25% and 50% brick recycled aggregates, since the reduction of the modulus of elasticity reached 10% and 30% while the conventional concrete exhibited a decline around 40% after 300 freeze-thaw cycles.

Figure 9.26 displays the evolution of the ultrasonic pulse velocity (UPV) of conventional and recycled mixtures in phase I. The oscillating pattern observed throughout the test is due to the continuation of the hydration process during the freeze and thaw experiment, which partially compensates the reductions in UPV as consequence of the micro-cracks caused by the expansion of the freezing water. Al-Assadi et al. (2011) and Molero et al. (2012) also registered some increases in the ultrasonic velocity despite the deterioration suffered by the frost action.

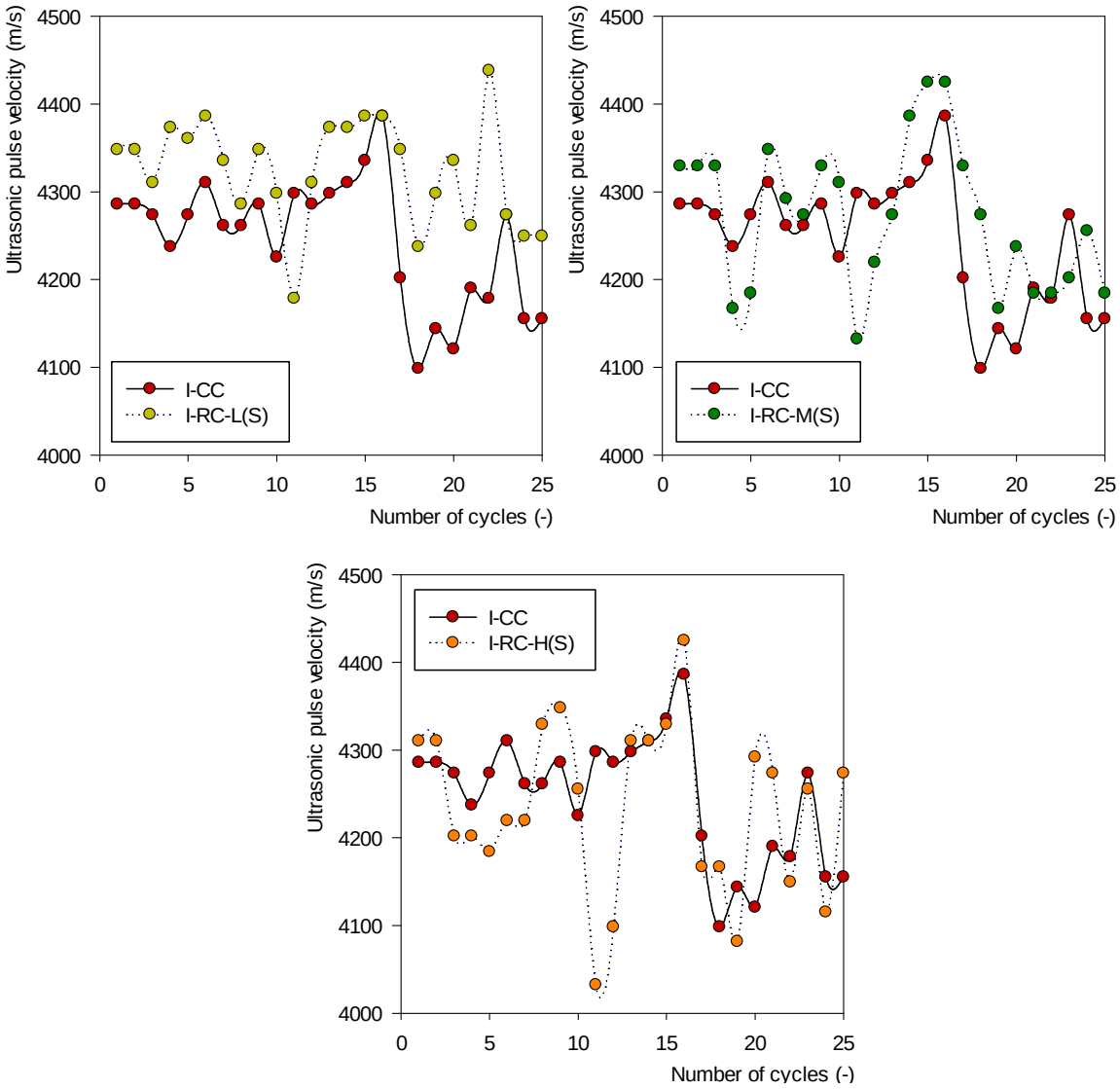

Figure 9.26: Comparison between the ultrasonic pulse evolution of the conventional and recycled concrete mixtures in phase I

Table 9.9: Frost resistance of the concrete mixtures in phase I after 25 freeze-thaw cycles

	Mass loss (%)	Variation (%)	UPV reduction (%)	Variation (%)
I-CC	2.26	-	3.05	-
I-RC-L(S)	2.13	-5.97	2.27	-25.62
I-RC-M(S)	2.53	11.80	3.35	9.85
I-H(S)	2.56	13.08	0.85	-71.95

The frost resistance parameters of the concrete mixtures in phase I are presented in Table 9.9 and Figure 9.27. In terms of mass loss, variations up to -5.97%, 11.80% and 13.08% were registered for low, medium and high ceramic content compared to the conventional concrete, respectively. Thus, a low correlation (R^2=0.41) exists between the weight loss and the amount of ceramic wastes incorporated in the concrete (Figure 9.27). Moreover, after 25 freeze-thaw cycles, only mixture I-RC-M(S) exhibited a decline up to 3.35% (9.85% more than the reference) in the ultrasonic velocity after 25 cycles. Meanwhile, mixtures I-RC-L(S) and I-RC-H(S) showed 25.62% and 71.95% lower UPV reductions than the conventional concrete. Consequently, a modest relationship (R^2=0.70) was found between the ultrasonic pulse velocity reduction and the ceramic content in the mixture (Figure 9.27). Nevertheless, the UPV values were above 4000 m/s for all concrete mixtures after the degradation experiment, which is indicative of a good quality concrete according to Malhotra and Carino (2003).

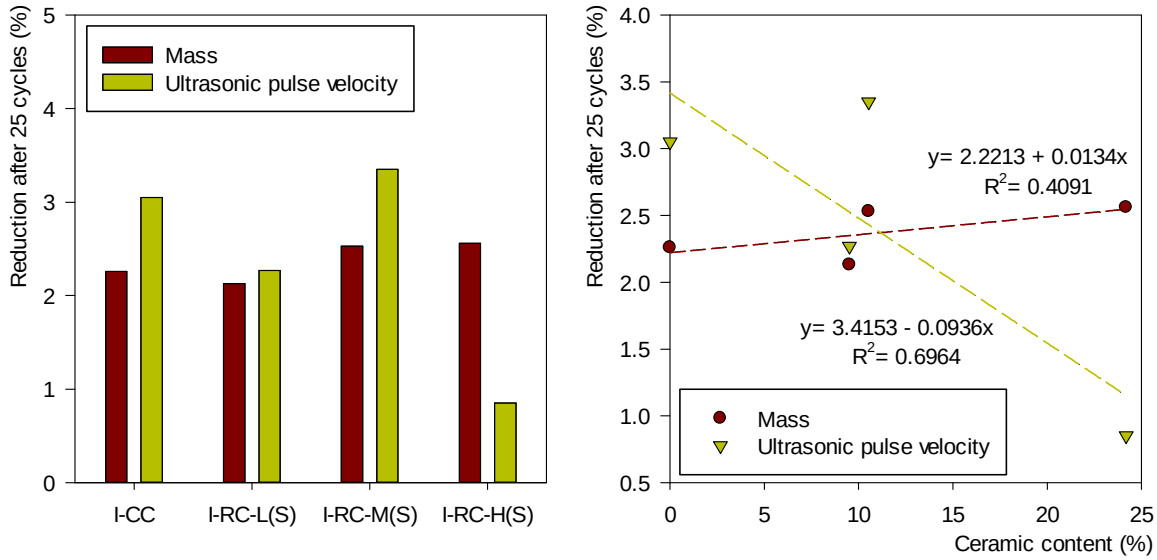

Figure 9.27: Reduction of the mass and ultrasonic pulse velocity in phase I after 25 freeze-thaw cycles and their relationship with the ceramic content in the total weight of aggregates

Figure 9.28 and Figure 9.29 illustrate the deterioration of the surface layer of concrete exposed to 7, 14, 21 and 28 freeze-thaw cycles. While the casting surface layer of mixture II-RC-H(S) was still pretty intact after the test, the rest of specimens exhibited a complete removal of the surface layer as consequence of a severe scaling. In addition, some aggregates pop-out to the concrete surface, especially in the trowelled faces. The pressure inside of the aggregate by the freezing of the water in its interior is responsible for the generation of a pressure able to separate it from the surrounding cement paste (Mehta and Monteiro, 2006). As a separate testing was carried out for casting and trowelled surfaces, the influence of the superficial finishing of the concrete on the mass loss per unit area was assessed. In general, casting surfaces exhibited a milder scaling than the trowelled surface of all concrete mixtures and particularly pronounced differences were registered between casting and trowelled surfaces of mixture II-RC-H(S). The findings of Van den Heede (2014) also suggest that trowelled faces have a worse performance when concretes are designed without air entraining agents.

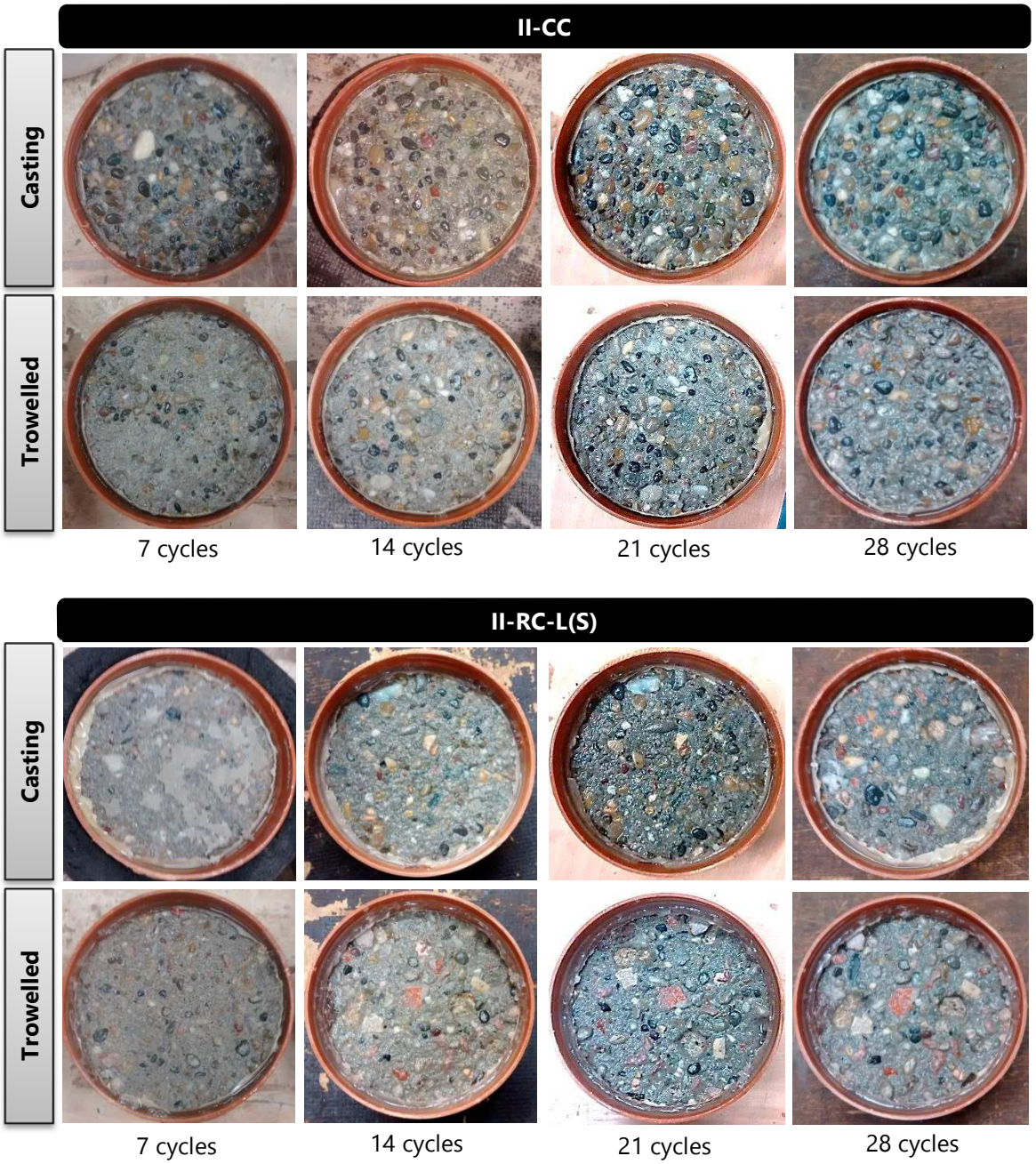

Figure 9.28: Examples of the evolution of the scaling in concrete mixtures II-CC and II-RC-L(S)

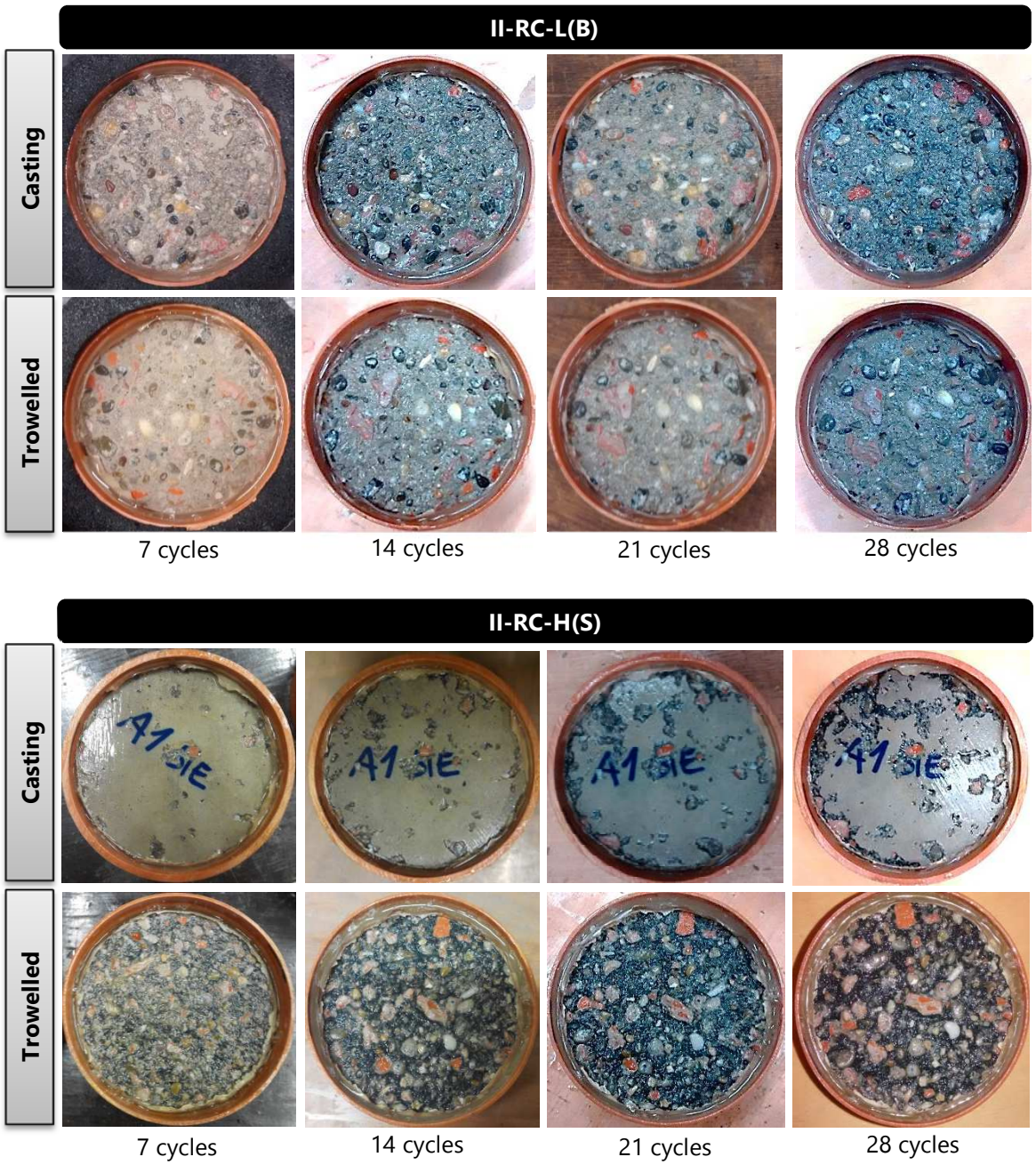

Figure 9.29: Examples of the evolution of the scaling in concrete mixtures II-RC-L(B) and II-RC-H(S)

Quantitatively, Figure 9.30 displays the evolution of the frost-salt scaling damage of the phase II concrete mixtures containing natural and recycled aggregates. For both casting and trowelled surfaces, the mass loss between cycles was lower as the test progressed, which suggests that the weakest surface layer is already removed after 1 cycle, and the underlying layers are stronger, reducing the amount of scaled material.

Table 9.10 and Figure 9.31 show the mass loss due to scaling after 28 freeze-thaw cycles. For all concrete mixtures, trowelled surfaces were more susceptible to the frost-salt action than the casting surfaces as observed through visual inspection (Figure 9.28 and Figure 9.29). The differences reached values up to 45.76%, 78.57%, 29.49% and 445.10% for the conventional and recycled concretes with low, medium and high ceramic contents, respectively. The high variability can be explained by the fact that some of the specimens lost both cement paste and aggregates, while others only loose cement paste flakes.

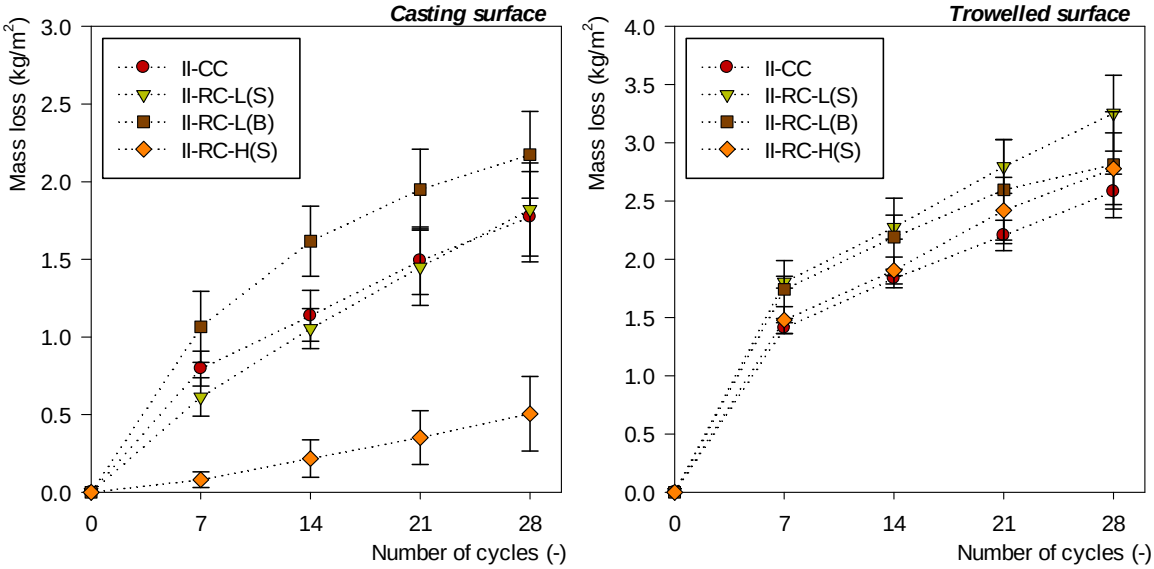

Figure 9.30: Cumulative mass loss due to scaling of concrete mixtures in phase II

Table 9.10: Frost resistance of the concrete mixtures in phase II after 28 freeze-thaw cycles

	Mass loss (%) Casting surface	Variation (%)	Mass loss (%) Trowelled surface	Variation (%)
II-CC	1.77		2.58	
II-RC-L(S)	1.82	2.71	3.25	26.12
II-RC-L(B)	2.17	22.55	2.81	8.97
II-H(S)	0.51	-71.51	2.78	7.63

Regarding the variation of the scaling of the recycled mixtures compared to the conventional concrete, in general, recycled concretes presented a worse performance and exhibited increases in the weight loss between 2.71% and 26.12% (Table 9.10). While no relationship (R^2=0.03) was found between the scaling behaviour of the trowelled surfaces and the ceramic content incorporated in the concrete mixtures, a modest correlation (R^2=0.60) between both variables was identified for casting surfaces (Figure 9.31).

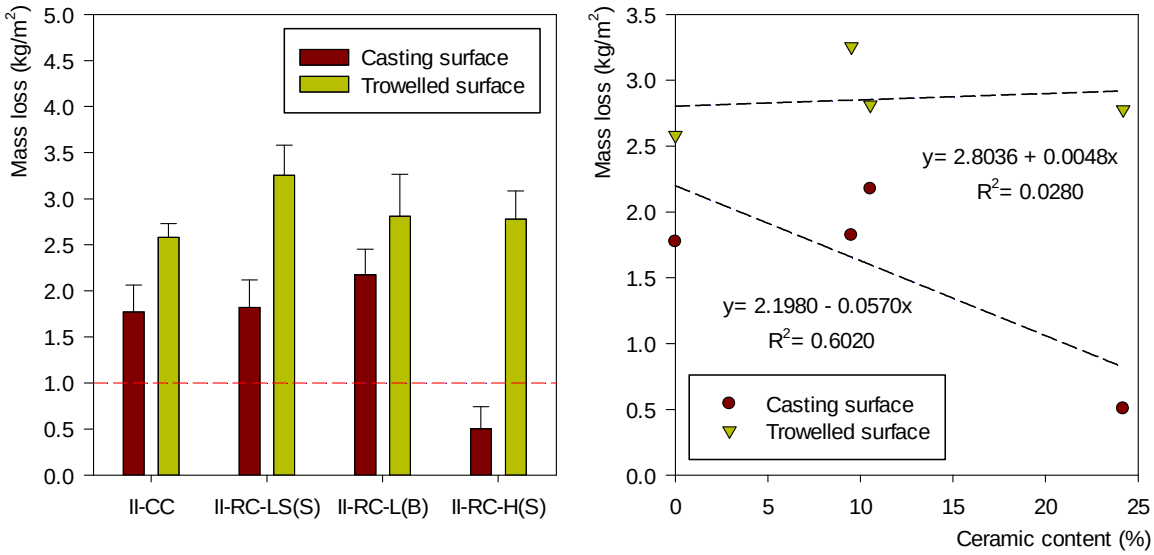

Figure 9.31: Mass loss due to salt-scaling after 28 freeze-thaw cycles and its relationship with the ceramic content incorporated in the total weight of aggregates

Although the porosity of CDW has been recognised to provide a level of protection from freeze-thaw damage (Richardson et al., 2011) due to the higher ease to dissipate the generated hydraulic pressures in the pore structure of concrete (Verbeck and Landgren, 1960), this effect was only observed in the casting surface of mixture II-RC-H(S). Except in that case, all specimens exhibited unacceptably high mass losses due to scaling and surpassed the limit of 1 kg/m^2 established in the UNE EN 1339 (2004). The lack of fulfilment of the standard requirement is in agreement with previous results, as none of the concrete mixtures satisfied the maximum spacing factor of 0.2 mm recommended by Mehta and Monteiro (2006) in order to prevent the freeze-thaw damage. Nevertheless, it is worth remarking that no air entrainment agent was employed in this research work. Hence, the use of such admixture will considerably increase the frost resistance of both conventional and recycled concrete mixtures, as Salem et al. (2003) proved that the use of air entrainment agent in recycled concrete significantly improves the freeze-thaw resistance.

8. CHLORIDE INGRESS

The high alkalinity of concrete is responsible for the passivation of the surface steel reinforcement bars, which protects them against corrosion. However, the penetration of chlorides mainly coming from seawater or de-icing salts by capillary suction or diffusion can trigger the corrosion process due to the decomposition of the passivity layer. It is worth mentioning that not all the chlorides that penetrate into concrete are liable for the corrosion of the rebar since some of them are bound to the hydration products (Yuan et al., 2009). Up to a certain amount of chlorides the corrosion phenomenon stays in an initiation stage which corresponds to the process of chloride transport to a steel surface and does not pose any damage to the steel, but there is a critical chloride content at the surface of the rebar at which the corrosion enters in the propagation stage (Angst et al., 2009).

The corrosion process in presence of chlorides is schematically shown in Figure 9.32. During this process, there is distinctive separation between anodic zone and cathodic zone that leads to the establishment of a macrocell. As the ferrous atoms in the steel become oxidized, a current circulates from the anode to the cathode, where water and oxygen atoms react to produce excess hydroxyl ions. The combination between ferrous and hydroxyl ions results in the formation of rust, which is an insoluble compound; whereas the bond between ferrous and chloride ions leads to the formation to a soluble compound that diffuses away from the steel which allows corrosion to continue.

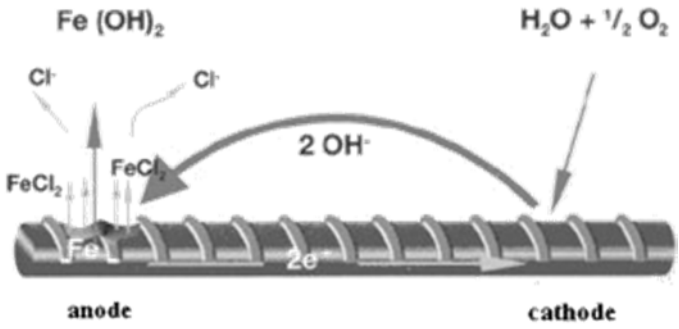

Figure 9.32: Chloride-induced corrosion of steel bar in concrete (Ji et al., 2013)

Due to the harmful effect of chlorides in the corrosion of reinforced concrete, a vast amount of research has been carried out about the influence of using recycled concrete aggregates on the resistance to chloride penetration, which is considered as an indicator of the durability of concrete. Limbachiya et al. (2000) observed a similar chloride performance among high-strength conventional and recycled concretes with partial or total replacement ratios. Similarly, Tu et al. (2006) reported comparable resistance to the chloride penetration for high-performance conventional and recycled concretes. According to Villagrán-Zaccardi et al. (2008), similar chloride penetration depths are to be expected for conventional and recycled mixtures with the same water/cement ratio since the extra chloride ingress in recycled concretes was compensated by the higher binding capacity of the recycled aggregates. When the EMV proportioning method was used in the design of the recycled concretes, comparable chloride resistances are observed between conventional concrete and concretes made with recycled concrete aggregates due to their coating with pozzolanic materials (Abbas et al., 2009; 2010; Razaqpur et al., 2010). In this line, Tam and Tam (2007) stated that the TMSA improved the chloride permeability of recycled concretes with complete replacement ratio up to a 29.98%. For replacement ratios below 30%, Amorim et al. (2012) concluded that a 20% substitution level did not cause significant performance losses, whereas Limbachiya et al. (2012) registered marginal differences in the chloride ingress of recycled mixtures with replacement ratios below 30% compared to the concrete made with conventional aggregates. By using pre-cast rejects, Soares et al. (2014) observed variations between 7% and -3% in the chloride diffusion coefficient of recycled mixtures with 25% and 100% of recycled concrete aggregates compared to the control concrete. The authors attributed the marginal differences to the good quality of the recycled aggregates.

However, the incorporation of recycled concrete aggregates in the concrete manufacture is liable for poorer performances regarding the resistance to chloride penetration with respect to the reference mixtures (Olorunsogo and Padayachee, 2002; Shayan and Xu, 2003; Gonçalves et al., 2004; Kou and Poon, 2006, 2013, 2015; Kou et al., 2007; Limbachiya et al., 2012; Hwang et al., 2013; Duan and Poon, 2014; Gonzalez and Etxeberria, 2014; Pedro et al., 2014b; Zhao et al., 2014; Lotfy and Al-Fayez, 2015; Zhang and Zhao, 2015). Generally, declines between 10% and 30% have been reported for replacement ratios up to 100% compared to conventional concretes (Berndt, 2009; Corral-Higuera et al., 2011; Kou et al., 2011a; Rao et al., 2011; Limbachiya et al., 2012; Wang et al., 2013; Tuyan et al., 2014). Olorunsogo and Padayachee (2002) reported that recycled concrete made with 100% recycled coarse concrete aggregates performed 73.2% worse than the conventional mixture. For a complete substitution, Kou and Poon (2009) found that chloride ions penetration of recycled concrete increased 53% and 47% compared to conventional concretes at 29 and 90 days respectively. Tuyan et al. (2014) observed a decrease in the resistance to chloride-ion permeability ranging from 26.9% to 43% for a 60% replacement of the natural coarse aggregates. Several authors have correlated these greater performance losses in the chloride resistance of recycled concretes with the lower quality of parent concrete from which the recycled aggregates are derived (Wang et al., 2013; Gonzalez and Etxeberria, 2014; Pedro et al., 2014b; Kou and Poon, 2015).

When mixed recycled aggregates are used in the replacement of the natural coarse aggregates, Gomes and de Brito (2009) observed an increase between 15.12% and 94.40% in the chloride penetration depth for 25% and 37.5% replacement ratios of ceramic coarse aggregates. However, the differences regarding the diffusion coefficient were up to 15.06% and 18.86%, respectively. For a 100% replacement, Beltrán et al. (2014a) found a 93% increase in the chloride penetration depth of concrete made with mixed recycled aggregates. Despite increasing the cement content with the rising replacement ratios, Beltrán et al. (2014b) observed average increases of 68.95%, 96.43% and 121.98% in the chloride penetration depth of recycled concretes for 20%, 50% and 100% substitution levels. For mixed recycled aggregates containing 67% of ceramic materials, González-Corominas and Etxeberria (2014) observed decreases in the resistance to the chloride penetration between 35% and 90%, approximately, as the recycled aggregate content increased. From CDW sourcing from Valnor and Retria, Bravo et al. (2015) registered average increases in the 28-days chloride diffusion coefficient up to 10.35%, 22.05%, 26.15% and 37.20% for 10%, 25%, 50% and 100% replacement ratios with mixed recycled aggregates. Contrarily, Corinaldesi and Morriconi (2009) observed improvements in the chloride penetration resistance of recycled concretes around 58% for full replacements of fine and coarse natural aggregates with mixed recycled aggregates containing 70% of concrete and 27% of ceramics wastes.

Regarding the influence of ceramic recycled aggregates on the resistance to chlorides, Kibriya and Speare (1996) observed increases between 46% and 129% in the chloride diffusion coefficients in concrete made with different types of crushed brick aggregates. By means of a salt spray fog experiment, Medina (2011) stated that conventional concretes displayed lower chloride penetration depth than recycled concretes made with 20% and 25% of ceramic sanitary ware. For recycled ceramic aggregates derived from electrical insulators, Senthamarai et al. (2011) observed decreases in the chloride resistance of the recycled concrete ranging from 23.33% to 115.26% for water/cement ratios between 0.35 and 0.60.

Compared to a reference concrete, Zhang and Zong (2014) observed comparable chloride penetration values for 30% substitution level but approximately increases of 28% and 21% for a 40% replacement ratio at 28 and 56 days. For a 50% replacement, Zong et al. (2014) registered a 63% higher chloride permeability in recycled concretes. Adamson et al. (2015) found that the chloride penetration increased by 16% and 24% for 25% and 50% brick content incorporations at six months of exposure due to the higher porosity of the ceramic materials. Contrarily, Pacheco-Torgal and Jalali (2010) reported improvements in the resistance to the chloride ingress of concretes made with 100% coarse ceramic aggregates compared to conventional concretes.

In any case, it has been reported that increasing curing periods decreased the differences between conventional and recycled concretes. Kou et al. (2007) and Kim et al. (2013) observed the same tendency for recycled concrete aggregates, González-Corominas and Etxeberria (2014) and Bravo et al. (2015) reported the same behaviour in concretes with mixed recycled aggregates and Zhang and Zong (2014) registered a similar pattern for recycled ceramic aggregates.

A separate assessment was carried out for casting and trowelled surfaces in order to study the influence of the superficial finishing of the concrete on the chloride ingress. Table 9.11 shows the non-steady migration coefficient for the conventional and recycled concretes calculated from the maximum penetration depths. In all cases, the trowelled surfaces led to higher penetration depths, ranging from 17.10% to 56.11%. Consequently, declines of 37.06%, 25.23% and 46.15% and variations of 3.33%, -18.80% and -36.95% were observed in the non-steady migration coefficient of II-RC-L(S), II-RC-L(B) and II-RC-M(S) for the casting and trowelled surfaces, respectively. As can be observed in Figure 9.33, acceptable correlations exist between the decrease in the chloride migration and the increasing ceramic incorporations (R^2=0.80 for the casting surface and R^2=0.74 for the trowelled face). Moreover, based on the criteria established by Sengul et al. (2014), the mixture II-RC-H(S) displayed a high resistance to the chloride penetration, while the rest of the mixtures exhibited a moderate chloride permeability.

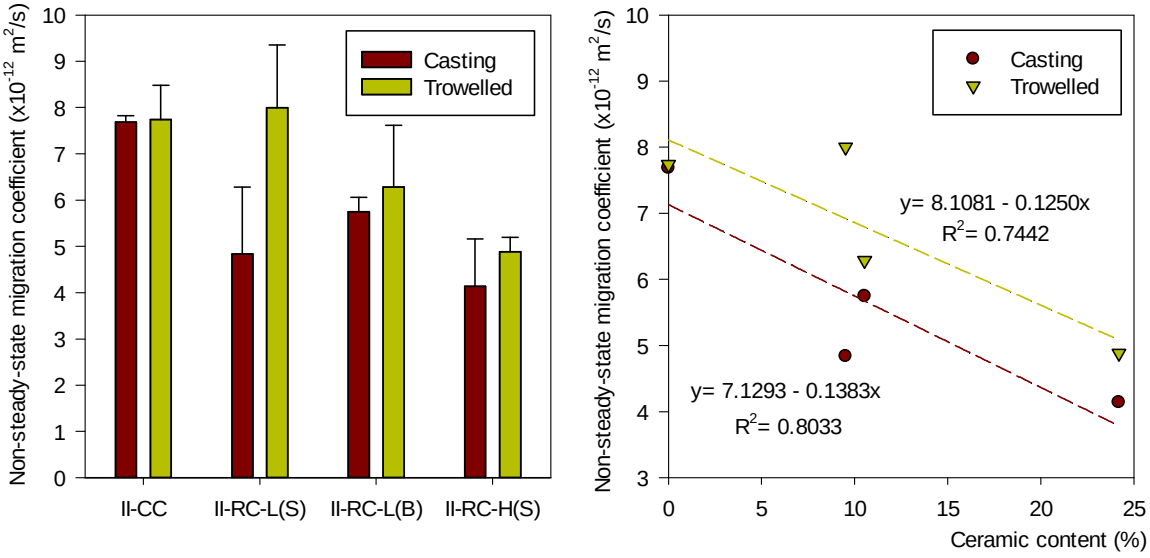

Figure 9.33: Non-steady migration coefficient for concretes in phase II and its relationship with the ceramic content incorporated in the total weight of aggregates

Table 9.11: Non-steady migration coefficient for concretes in phase II

	Non-steady migration coefficient (10^{-12} m^2/s)			
	Casting surface	**Variation (%)**	**Trowelled surface**	**Variation (%)**
II-CC	7.68	-	7.74	-
II-RC-L(S)	4.84	-37.06	8.00	3.33
II-RC-L(B)	5.74	-25.23	6.28	-18.80
II-RC-H(S)	4.14	-46.15	4.88	-36.95

The good performance exhibited by the recycled concretes containing a 50% replacement ratio of recycled aggregates from CDW with varying ceramic percentages is due to several factors. In the first place, the lower effective water/cement ratio of the recycled mixtures is responsible for higher chloride resistance since the concrete becomes more impermeable (Kou et al., 2007; Ann et al., 2008). It has been largely demonstrated that the use of pozzolanic or supplementary cementing materials enhances the resistance to the chloride ingress in recycled concrete due to the improvement of the microstructure and the higher binding capacity of the cement paste (Ann et al., 2008; Berndt, 2009; Qin et al., 2010; Corral-Higuera et al., 2011; Kou et al., 2011a; Hwang et al., 2013; Zhang and Zong, 2014). Hence, for the recycled mixtures, the pozzolanic nature of the CDW (Medina et al., 2014, 2015) exerts an additional beneficial effect to the resistance against chloride ingress. Moreover, several researchers have noticed that the combination of the recycled aggregates with the chloride ions was liable for a reduction in the rate of diffusion as consequence of an increased binding capacity to the cement matrix (Gonçalves et al., 2004; Villagrán-Zaccardi et al., 2008; Vázquez et al., 2014). Finally, as the quality of the cement paste of conventional and recycled mixtures is comparable (see chapter 7), the influence that the porous aggregates have on the chloride resistance is mitigated (Bogas and Gomes, 2013).

8.1. RELATIONSHIP BETWEEN THE CHLORIDE INGRESS AND THE WATER ABSORPTION BY CAPILLARITY

Acceptable correlation exist between the non-steady chloride migration coefficient and the primary sorptivity rate of concrete mixtures (R^2=0.70 and R^2=0.84), particularly for the ingress in through the troweled surface (Figure 9.34). For conventional concretes, Basheer et al. (2001) also observed the same tendency between those properties, and similar findings were reported by Medina (2011) and Senthamarai et al. (2011) for recycled concretes.

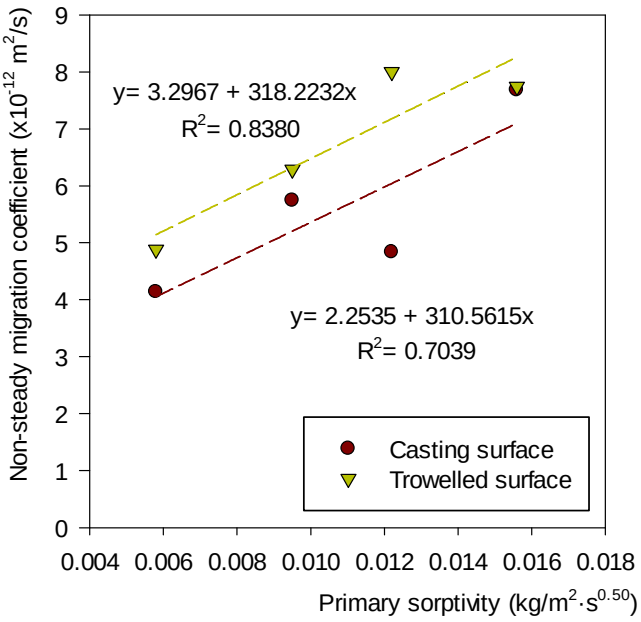

Figure 9.34: Relationship between the chloride ingress and the water absorption by capillarity of concrete mixtures in phase II

9. ELECTRICAL RESISTIVITY

The pore water of concrete is an electrolytic solution containing ions (mostly potassium, sodium, calcium, sulphates and hydroxides but also chlorides due to infiltration from the environment to which the concrete is exposed). For greater concentration of ions, the conductivity is higher and then the electrical resistivity is reduced. The electrical resistivity, i.e. the inverse of the conductivity, can be used to indirectly assess the interconnected porosity and the corrosion risk of a concrete mixture and consequently its durability. According to Whiting and Nagi (2003), changes in aggregate type and content influence the electrical resistivity of concrete so it is expected that the use of recycled aggregates would affect the response of the recycled concretes to this property.

Few experimental data are available on the electrical resistivity of recycled concrete mixtures. Dhir and Paine (2007) did not register any relationship between the content of any type of recycled aggregate and the resistivity displayed by the recycled concretes. The authors also noticed that concretes with recycled concrete aggregate substitutions showed lower resistivity than those made of ceramic brick aggregates. Arredondo-Rea et al. (2011) and Corral-Higuera et al. (2011), who employed electrochemical impedance spectroscopy to compare conventional and recycled concrete mixtures, observed that the use of recycled concrete aggregates reduced the electrical resistivity, which suggests that the corrosion would take place earlier in the recycled concretes than in the conventional mixture. In his PhD dissertation, Medina (2011) observed that recycled concrete mixtures with 20% and 25% replacement ratios of ceramic sanitary ware presented higher electrical resistivity values than those of the respective control concrete. The higher electrical resistivity exhibited by the ceramic sanitary ware when compared to the gravel was used to explain these differences.

Gonzalez and Etxeberria (2014) also registered a general tendency towards the reduction of the electrical resistivity values of the recycled concrete mixtures compared to the control concrete due to the higher porosity of the old adhered mortar. By using electrical impedance spectroscopy, Adamson et al. (2015) indicated that the control mixture presented the highest electrical resistivity and the recycled concrete containing 50% of brick aggregates displayed the lowest resistivity. The authors observed a good inverse relationship between these values and the porosity and chloride penetration results.

Since the concrete specimens were tested in a completely saturate state, the results shown in Table 9.12 correspond to the lowest possible electrical resistivity of the concrete mixtures studied in this research work. The results obtained for recycled mixtures are within the range of values (10-100 Ω·m) commonly reported for saturated conventional concrete (López and González, 1993; Whiting and Nagi, 2003; Newlands et al., 2008). While most research works on the electrical resistivity of recycled concrete mixtures with several replacement ratios of concrete and brick waste are within the aforementioned range (Dhir and Paine, 2007; Arredondo-Rea et al., 2011; Corral-Higuera et al., 2011; Adamson et al., 2015), González and Etxeberria (2014) registered values between 90 Ω·m and 330 Ω·m approximately, for recycled concrete made with 20%, 50% and 100% replacement ratios of recycled concrete aggregates which could be associated to the low effective water/cement ratio (0.29) of the mixtures.

Table 9.12: Electrical resistivity of the conventional and recycled concrete mixtures of phase I

	Electrical resistivity (Ω·m)	**Variation (%)**
I-CC	47.80	-
I-RC-L(S)	48.44	1.33
I-RC-M(S)	48.17	0.78
I-RC-H(S)	44.60	-6.68

Although aggregates do not usually release noticeable amounts of ions into pore solution (Shi, 2004), a study performed by Dhir et al. (2005) pointed out that brick recycled aggregates released higher percentages of alkalis than recycled concrete aggregates. Therefore, a higher concentration of ions is to be expected as the ceramic content increases, which lower the electrical resistivity values. The 6.68% decline in electrical resistivity exhibited by the recycled concrete containing the higher amount of ceramic materials is in good agreement with this explanation.

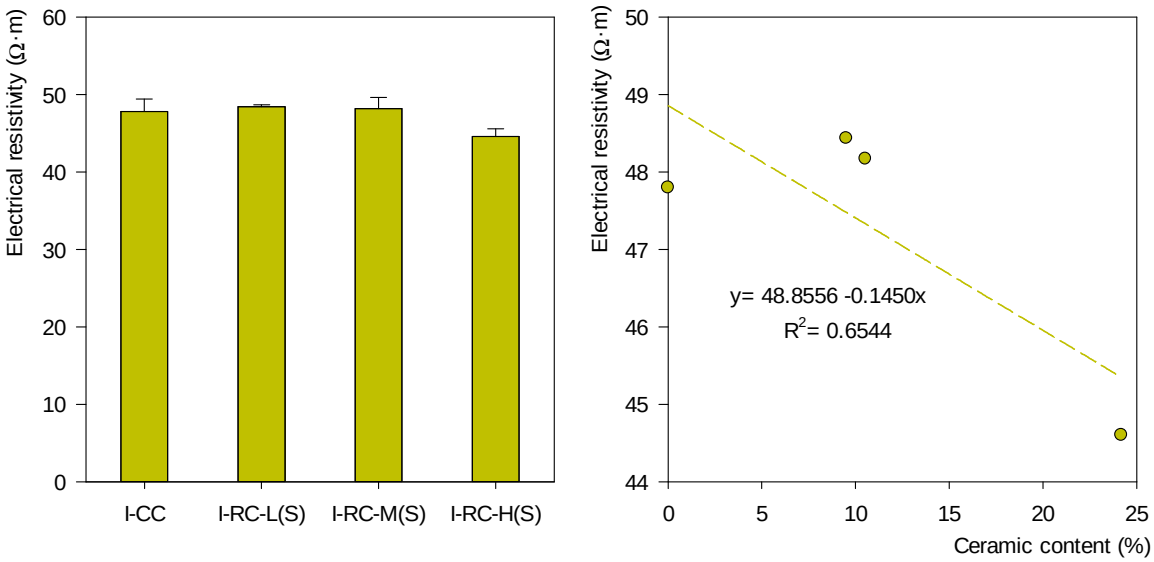

Figure 9.35: Electrical resistivity and its relationship with the ceramic content incorporated in the total weight of aggregates

The electrical resistivity decreased as the ceramic content employed in the recycled concrete increased (Figure 9.35). However, the relationship found between both variables presented a modest correlation factor (R^2= 0.65), since for I-RC-L(S) and I-RC-M(S) mixtures, the resistivity values are comparable to that of the conventional concrete. This can be explained by the fact that the reduction behaviour of the ceramic incorporation was overpowered by the positive effect that rising contents of aggregates (Hughes et al., 1985) and declines in the water/cement ratio (Hughes et al., 1985) have on the electrical resistivity of concrete.

9.1. RELATIONSHIP BETWEEN THE ELECTRICAL RESISTIVITY AND THE POROSITY BY MIP

Figure 9.36 shows the relationship between the electrical resistivity and some porosity parameters defining the concrete mixture. Albeit exhibiting low correlation factors ($R^2 \leq 0.31$), the experimental results presented a similar behaviour to the ones reported in the literature. Hence, the electrical resistivity decreased with the amount of macropores (Elkey and Sellevold, 1995) and increased with the amount of mesopores (Hunkeler, 1996; Newlands et al., 2008). The increase of the electrical resistivity with the total porosity of the concrete mixture was due to the increase in the fraction of smaller pores caused by the incorporation of recycled aggregates. Medina (2011) and Hunkeler et al. (1996) also observed this tendency. Regarding the pore size, decreases in mean pore diameter by were linked to increases in electrical resistivity by a modest correlation factor (R^2=0.57). This result was consistent with those obtained in other research works carried out by Hunkeler et al. (1996), McCarter et al. (2000), Whiting and Nagi (2003), Tumidajski (2005) and Arredondo-Rea et al. (2011), where the increase in electrical resistivity was related to the refinement of the porosity.

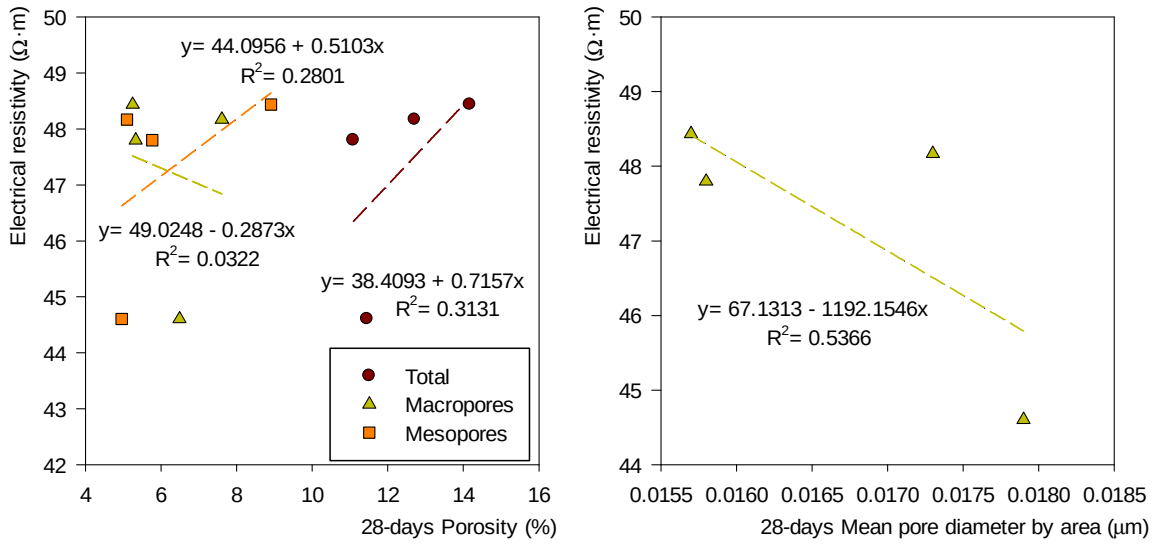

Figure 9.36: Relationship between the electrical resistivity and respectively the effective porosity and the mean pore diameter

9.2. PREDICTION OF THE CORROSION RATE THROUGH THE ELECTRICAL RESISTIVITY

Corrosion is an electro-chemical process and thus electrical resistivity plays an important role in the rate at which corrosion occurs. Thus, an inverse relationship exists between the corrosion rate and the electrical resistivity of concrete (Whiting and Nagi, 2003). Hence, higher resistivity suggests a slower deterioration rate and longer durability of concrete. Values greater than 2000 Ω·m are often linked to negligible corrosion rate (Feliu et al., 1996), whereas resistivity figures lower than 50 Ω·m can support a rapid corrosion of steel (Browne, 1980; Langford and Broomfield, 1987; Feliu et al., 1996). Hence, all the mixtures designed in this investigation are expected to exhibit the same poor performance against the corrosion if used in reinforced concrete. However, according to Andrade and Alonso (1996), electrical resistivity values below 100 Ω·m indicate that this property is not the controlling parameter the corrosion rate.

10. ALKALI-SILICA REACTION

Concrete can be deteriorated by the deleterious chemical reactions occurring between the sodium and potassium ions, usually from the cement, and some kinds of reactive aggregates. The alkali-silica reaction (ASR) is the most common of these reactions. However, three conditions must concur in order to generate ASR damage: available alkali hydroxides in the pore solution, reactive silica in the aggregate i.e. poorly crystallized or amorphous silica, and sufficient moisture. It has been also proposed that the concentration of calcium hydroxide is also an important factor due to its role as a source of hydroxyl ions (Chatterji et al., 1988; Davies and Oberholster, 1988).

As a result, a hydrophilic alkali-silica gel is produced around the aggregates and within the pores of the concrete, which swells due to the absorption of water from the surrounding pore solution producing expansion stress that can lead to the formation of cracks and the durability loss of the concrete. Nevertheless, the harmful consequences of this mechanism are associated to the presence of a pessimum concentration of reactive siliceous aggregates. Hence, the reaction is not destructive below that concentration, and no degradation is produced above that concentration either because the lack of sufficient alkali concentration (Vivian, 1947).

The ASR deterioration in recycled concrete is more complex than in conventional mixtures. Firstly, recycled aggregates from CDW are a supplementary source of alkalis (Shehata et al., 2010). For instance, Dhir et al. (2005) reported that masonry and concrete particles are able to release up to 0.60% and 0.20% Na_2O_{eq} respectively. Nevertheless, Dhir et al. (2005) did not find any correlation between the alkali released by the recycled aggregates and the ASR expansion suffered by the recycled concrete mixtures. In order to reduce the alkali contribution of the recycled aggregates, their washing was proposed as a preventive measure. However, the results of Shehata et al. (2010) showed that the alkali content was still considerable after 18 hours of the cleaning treatment. Moreover, these aggregates could contain reactive particles in their composition such as glass particles and old mortar adhered or concrete particles originating from concrete structures affected by ASR. In the issue of ASR reactivation, Gottfredsen and Thogersen (1993) indicated that the use of recycled concrete aggregates from a parent concrete severely damaged by ASR caused less expansion than that originating from partially ASR affected parent concrete since, in the latter case, a major fraction of unreacted silica was still present. Additionally, the swelling of already-formed ASR gel could occur and generate new potentially reactive fractured surfaces, i.e. parts that did not react during the service life of the old structure (Li and Gress, 2006).

Generally, ASR deterioration is assessed through length variations, visual inspection of the cracks and petrographic analysis. Despite it is widely accepted that the methods employed for conventional mixtures are also acceptable for recycled concretes, Gress and Kozikowski (2000) proposed some changes (different shape and preservation conditions, increase of the temperature or alkalis content, and use of microwave energy or ultra-sonic energy) in the methodology for testing recycled aggregates against ASR in order to accelerate the procedure. However, such modifications have not been employed in the practice by others.

Several studies have been focused on the concrete durability loss due to ASR caused by the use of recycled aggregates. The studies carried by Dhir et al. (2003, 2007; 2005) have demonstrated that recycled aggregates can be regarded as normal reactivity aggregate since the expansions registered were below the 0.10% limit specified for a 20-day Oberholster test. Special attention has received the influence of the use of ASR-affected recycled concrete aggregates. Desmyter and Blockmans (2000) observed expansion results below the limit of the concrete prism test for the use of ASR-affected recycled aggregates which was attributed to the depletion of reactive silica during the first life cycled of the concrete. Nevertheless, the use of this type of recycled aggregates generally caused significant length expansions (Stark, 1996; Li and Gress, 2006; Shehata et al., 2010), necessitating the use of appropriate preventive measures, such as the use of fly ash, silica fume or blast furnace slag.

The efficacy of the use of supplementary cementing materials responds to their ability to reduce the alkalinity of the pore solution through binding mechanisms (Xu et al., 1995; Shehata et al., 1999; Shehata and Thomas, 2000, 2002). Hence, higher amounts of supplementary cementing materials are required to decrease the alkalinity of recycled concrete mixtures (Scott IV and Gress, 2004; Li and Gress, 2006; Shehata et al., 2010). In this line, Carles-Gibergues et al. (2007) suggested that the fine fraction of the reactive aggregate produced a mitigation of the ASR deterioration due to the pozzolanic reaction of the powder. However, Shehata et al. (2010) did not observe a significant improvement in the expansion due to the fine fraction incorporated with the coarse recycled concrete aggregates. Moreover, no consensus exists on the consequences of using ground clay brick waste in the reduction of the ASR damage. While Turanli et al. (2003) reported a beneficial effect, Betkas et al. (2009) did not register any positive influence.

The changes in length due to alkali-silica reaction of the concrete specimens tested in this investigation are presented in Table 9.13. In all cases, the length change was lower than the 0.10% and 0.15% values established by Oberholster and Davies (1986) and Davies and Oberholster (1987) for non-reactive aggregates. Nonetheless, significant differences can be appreciated between the conventional and recycled aggregates (Figure 9.37). The conventional concrete exhibited shrinkage, while most of the recycled concretes presented an expansion of length. Thus, the results show a decrease in the resistance against ASR when recycled aggregates are used in the concrete manufacture. However, the relationship between the length change and the ceramic content in the concrete mixture showed a low correlation factor (R^2=0.49). According to Scott IV and Gress (2004), some of the enlargement could be caused by the water absorption and swelling of the aggregate due to the use of recycled aggregates without pre-saturation, which may explain the variability among the results.

Table 9.13: Length change due to alkali-silica reaction after 4 weeks of Oberholster test

	Change of length (%)	**Variation (%)**
II-CC	-0.031	-
II-RC-L(S)	-0.020	-35.48
II-RC-L(B)	0.020	-164.52
II-RC-M(S)	0.038	-222.58
II-RC-H(S)	0.011	-135.48

Moreover, no cracks or deterioration of the aggregates were appreciated by visual inspection of the concrete cylinders after the testing. Therefore, the use of recycled aggregates from CDW in the production of concrete did not entail an ASR risk. Nonetheless, it should be noted that these results occurred under the specific conditions propitiated by the use of slag blended cements, which are responsible for reducing the alkalinity of the pore solution and the concentration of $Ca(OH)_2$ which decreases the ASR risk (Fernández-Jiménez and Puertas, 2002).

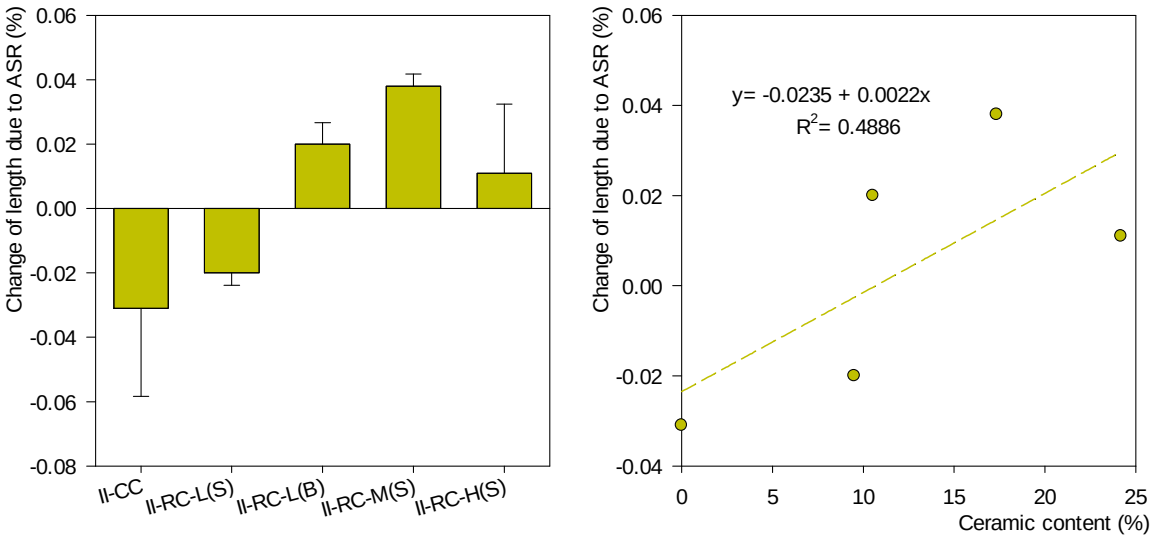

Figure 9.37: Length change due to alkali-silica reaction and its relationship with the ceramic content incorporated in the total weight of aggregates

11. RESISTANCE TO ORGANIC ACIDS

Farm environments are very demanding on concrete, especially regarding the exposure to organic compounds that may cause its degradation. For instance, concrete employed in floor of animal housing and silage structures is subjected to manure and silage effluents liable for organic acid attack. Silage produced and stored in horizontal concrete silos produces around 140 l/t of effluent containing acetic and lactic acids, which present a pH value around 4 (O'Donnell et al., 1995); while liquid manure, which contains a mix of volatile fatty acids such acetic, propionic, butyric and isobutyric, has a pH around 6-8 units (Williams, 1983). Besides the chemical deterioration, the mechanical abrasion produced by animals and machinery causes an important damage to concrete.

Whilst manure only affects the concrete elements in the animal housing (mainly floors), the silage effluent causes deterioration problems both in silage structures and the floor of animal housings by the effect of silage feeding and acidification of meal in contact with water. The investigation of Bertron et al. (2005a) suggested that the use of acetic acid is adequate to recreate the acid attack of liquid manure on concrete, whereas the solution causes milder effects than those produced by silage effluent. Hence, to simulate the deterioration of concrete in both farm environments, a mix of lactic-acetic acid solution (CH_3–CHOH–COOH and CH_3–COOH) was employed. Although the brushing procedure also led to a deterioration of the concrete specimens, the process only consisted of the removal of the loose material, which can be equated to the typical three-body wear abrasion caused by animals and machines (Hutchings, 2002).

The acid attack of concrete is based on its own alkaline nature. Portlandite (CH) is the most vulnerable hydration product against acid attacks and decomposes at pH below 12 units (Shi and Stegemann, 2000). Nevertheless, the attack may result in the total decomposition of the hydration products as a result of the decalcification, leaving silica, alumina and ferric hydrogels as final products. As a result, the attacked layer increases its porosity to a point of lower mechanical resistance that leads to its removal, thus, exposing the interior of the concrete to further deterioration.

The deterioration mechanism is based on the processes of decomposition and leaching of the constituents of the cement matrix (Zivica and Bajza, 2001). The solubility of the calcium salt produced by the organic acid reaction is an indicator for the aggressiveness of the attack and the extent of the deterioration as they are leached away fostering the progress of the reaction (De Belie et al., 1997a; Zivica and Bajza, 2001; Bertron et al., 2005b). For instance, calcium lactate and calcium acetate have a solubility in water of 1.05% and 52%, respectively (Zivica and Bajza, 2001).

Figure 9.38 displays the evolution of the pH in the lactic-acid solution throughout the accelerated degradation test. The regular adjustments to the pH pretended to better simulate the real conditions, where fresh spillages of silage effluents or manure replace the previous discharges that went partly neutralized or cleaned. The pH of the lactic-acetic acid solution varies from 2.1-2.3 at the beginning of the cycle to increase up to 4.4-5.2 units. Similar oscillations in pH were encountered in the investigation of Gruyaert (2011).

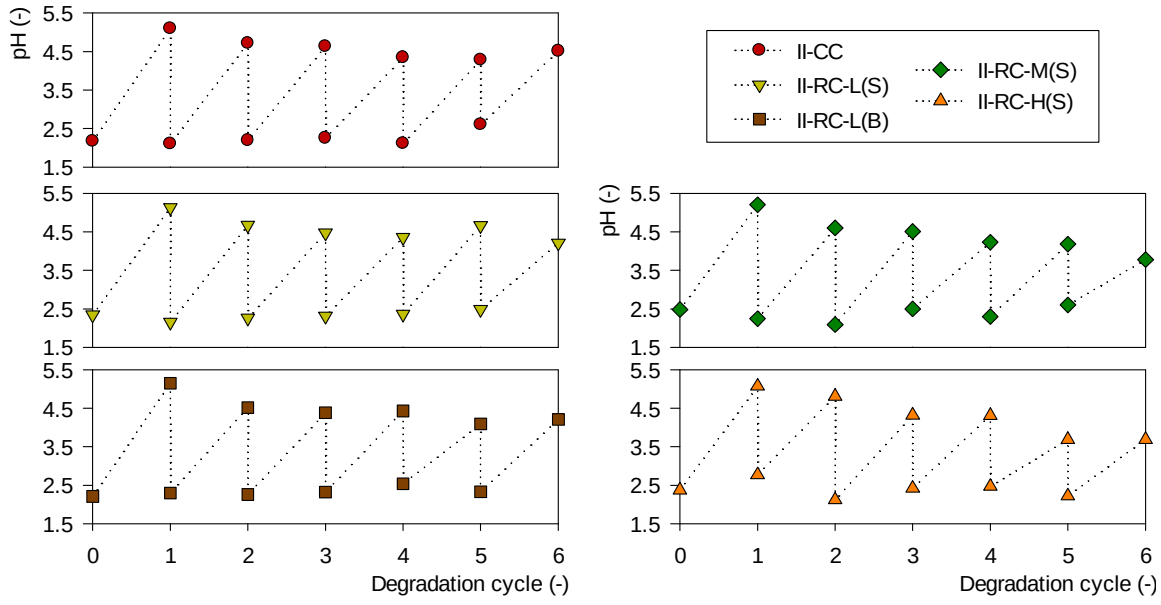

Figure 9.38: Evolution of the pH in the lactic-acid solution throughout the accelerated degradation test

On one hand, pH values around 2, which are considered highly aggressive for concrete (CEB, 1998), are lower to those reported in real conditions due to the lack of buffering feed ingredients (De Belie et al., 1997a). On the other hand, the general decrease of these values indicates an increasing decalcification of hydration products as the degradation test developed.

Moreover, two strong relationships were identified between the pH of the spent solution and the ceramic content in the concrete mixtures for cycles 3 and 6 (Figure 9.39). In both cases, the level of neutralization associated to recycled concrete was lower than that of the conventional mixture, which suggests a lower decalcification of the hydration products when recycled aggregates were employed.

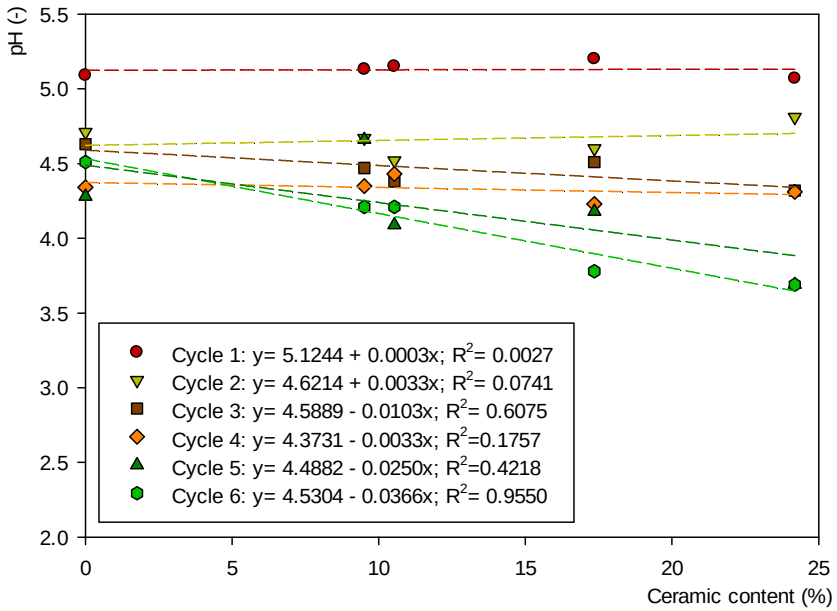

Figure 9.39: Relationship between the pH at the end of a degradation cycle and the ceramic content incorporated in the total weight of concrete mixtures in phase II

As the concrete disintegrates, the average accumulated reduction in radius after each degradation cycle was recorded and it is presented in Figure 9.40.

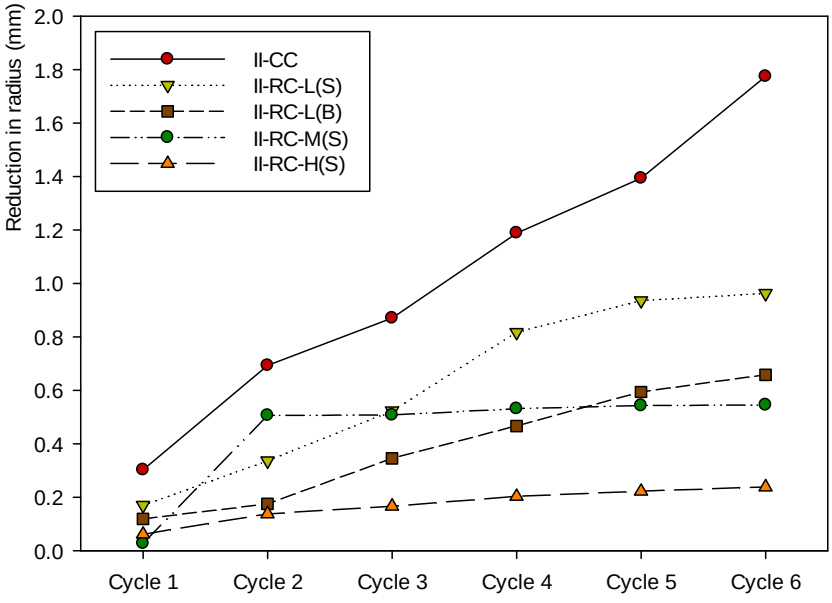

Figure 9.40: Evolution of the reduction in radius of the concrete mixtures pertaining to phase II

While the maximum reduction in radius was lower than 2 mm at the end of the test, none of the recycled mixtures presented a decline in radius higher than 1 mm. Regarding the evolution of the change in radius, different behaviour can be observed among mixtures. The conventional concrete showed a monotonous increase without a sign of a plateau phase within the 6 cycles carried out, whereas the recycled concrete mixtures exhibited a level of stabilization between cycles 5 and 6. However, different degradation patterns were displayed in the 3 first degradation cycles, as the deterioration was not according to the ceramic content in the mixtures, since the concrete with low ceramic content (II-RC-L(S) and II-RC-L(B)) performed better than the mixture with medium amount of ceramic materials (II-RC-M(S)). Nevertheless, this pattern was reversed as the test progressed. Hence, at the end of the test, the recycled mixtures performed 45.74%, 62.88%, 69.25% and 86.55% better in terms of reduction in radius for rising ceramic contents incorporated in the total weight of aggregates than the conventional concrete.

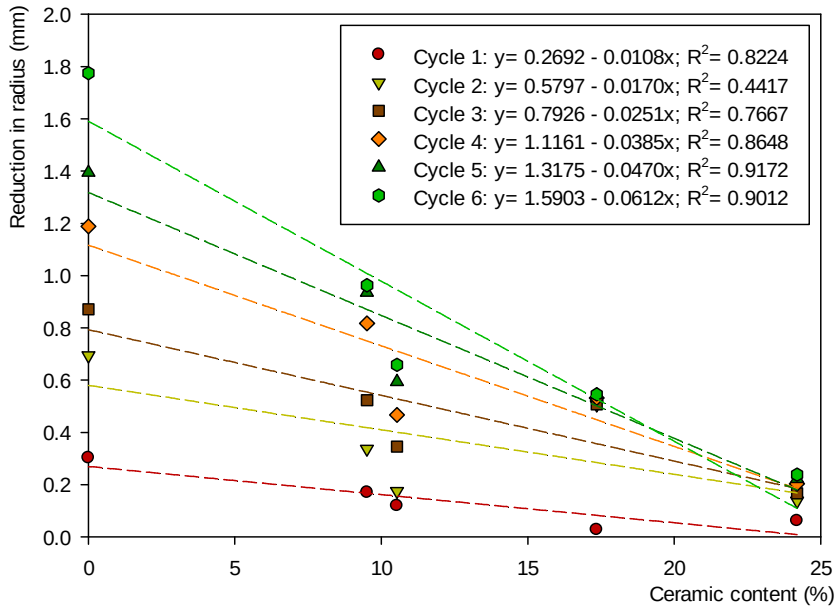

Figure 9.41: Relationship between the reduction in radius and the ceramic content incorporated in the total weight of concrete mixtures in phase II

The improved performance of the recycled concretes against acidic attack can be explained by the beneficial effect of pozzolanic materials in the CDW (O'Donnell et al., 1995), the presence of secondary elements such as Fe, Al, etc. in the cement matrix as consequence of the recycled aggregates incorporation (Bertron et al., 2004) that also caused differences in the in the hydrations products (Gruyaert, 2011), the lower effective water/cement ratio (De Belie et al., 1997a) as well as the refinement in the porous network (De Belie et al., 1996, 1997b; Bertron et al., 2004; Gruyaert, 2011) . Thus, the reduction in radius showed good levels of correlation with the ceramic content incorporated in the concrete mixture (Figure 9.41).

In addition to the degradation depth, the surface roughness was also evaluated (Figure 9.42). The results suggest that the damage of the concrete exterior layer increases monotonously with the exposure time. Thus, at the end of the test, the Ra values were 6.11, 1.32, 2.66, 1.24 and 1.13 times higher for CC, RC-L(S), RC-L(B), RC-M(S) and RC-H(S), respectively. Therefore, the use of recycled aggregates from CDW, in particular with high ceramic percentages, is a potential measure to reduce the deterioration of concrete floors in animal housing and consequently prevent health problems of the animals. It is interesting to mention that the conventional concrete displayed smaller Ra values than most of the recycled mixtures after the 3 first cycles of degradation. Nonetheless, from that point onwards, this behaviour shifted and thus recycled concrete mixtures exhibited better results of surface roughness until the end of the test. Note that the high standard deviation of the mean surface roughness values is a result of the variability of the change in radius throughout the circumference of the concrete specimen. In spite of these uncertainties, the Ra values clearly indicate that the replacement of natural coarse aggregates by recycled aggregates from CDW was positive. Therefore, after the 6 cycles, an improvement in the smoothness of the concrete surface of 41.19%, 40.45%, 73.96% and 65.65% was registered for RC-L(S), RC-L(B), RC-M(S) and RC-H(S), respectively. By studying the relationship between the surface roughness in each degradation cycle with the ceramic content incorporated in the concrete mixture (Figure 9.43), it is possible to observe the lack of any significant correlation during the 3 first degradation cycles ($R^2 \leq 0.10$), while the relationship between both variables progressively increased to show a strong correlation factor ($R^2 = 0.85$) at the end of the experiment.

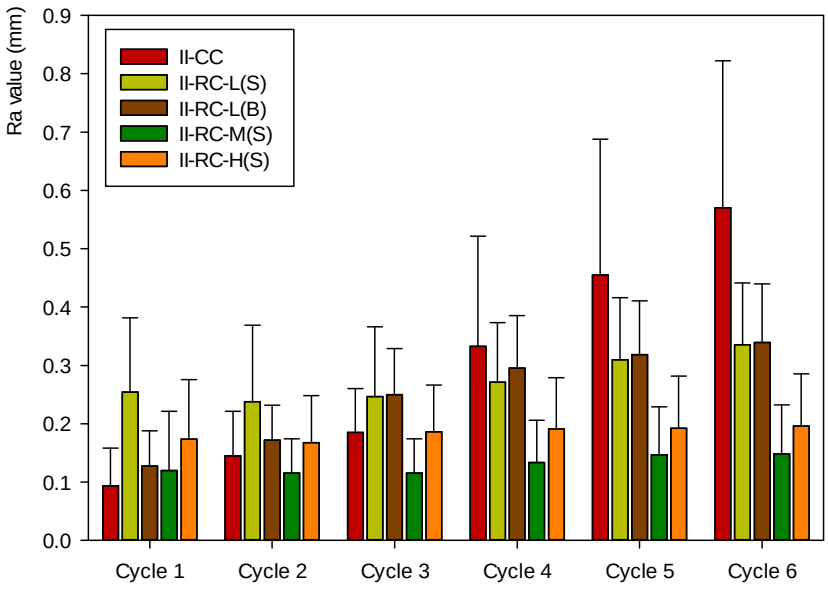

Figure 9.42: Evolution of the surface roughness of the concrete mixtures pertaining to phase II

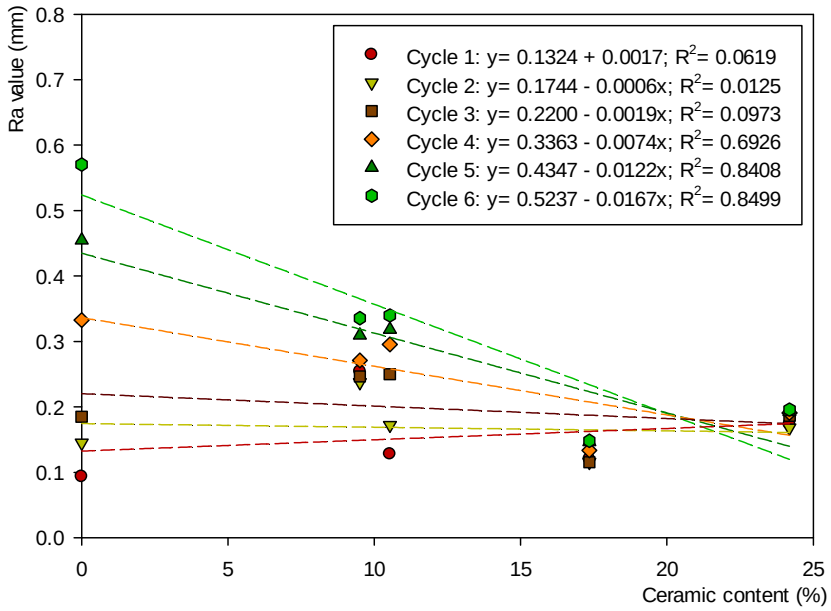

Figure 9.43: Relationship between the surface roughness and the ceramic content incorporated in the total weight of concrete mixtures in phase II

The findings regarding change in radius and surface roughness were also confirmed by visual inspection of the concrete specimens. Figure 9.44 shows some of the concrete specimens evaluated in a lactic-acetic acid solution at the beginning of the test and after 3 and 6 weeks of cyclical exposure. Experiments performed under the same conditions of aggressiveness showed that each of the degradation cycles corresponds to the damage at the most vulnerable place in animal houses, i.e. the concrete floors in front of the wet feeder, after one or two years of acid attack (De Belie et al., 1997a). A survey conducted in Flanders revealed that the coarse aggregates in the floor slats of 15% of the pigs farms were exposed within 2 years of use, which is detrimental for the engineering properties of concrete but also for the animal health (De Belie, 1997). However, as can be observed in Figure 9.44, none of the specimens showed signs of visible aggregates before the third degradation cycle. Moreover, the recycled concrete exhibited the lowest exposure level in this regard and a smoother surface was attained for recycled concretes with the rising of the ceramic content incorporated to the mixture. Nonetheless, the aggregates became visible for the conventional concrete and the recycled mixtures with low ceramic content (II-RC-L(S) and II-RC-L(B)) as the surface layer completely disappeared at the end of the 6 degradation cycles.

The parts of the test specimens that never came into direct contact with the lactic-acid solution, i.e. concrete around the rotational axle, were covered with soft and white/yellow crystals (Figure 9.45). However, the operating technique of the TAP apparatus did not allow the assessment of this kind of degradation and further research should be conducted on the resistance to the indirect exposure of recycled concrete to organic acids. Other researchers also reported the apparition of white (Bakharev et al., 2003) or yellow (Živica, 2006) deposits around concrete specimens exposed to acetic and lactic acids, respectively.

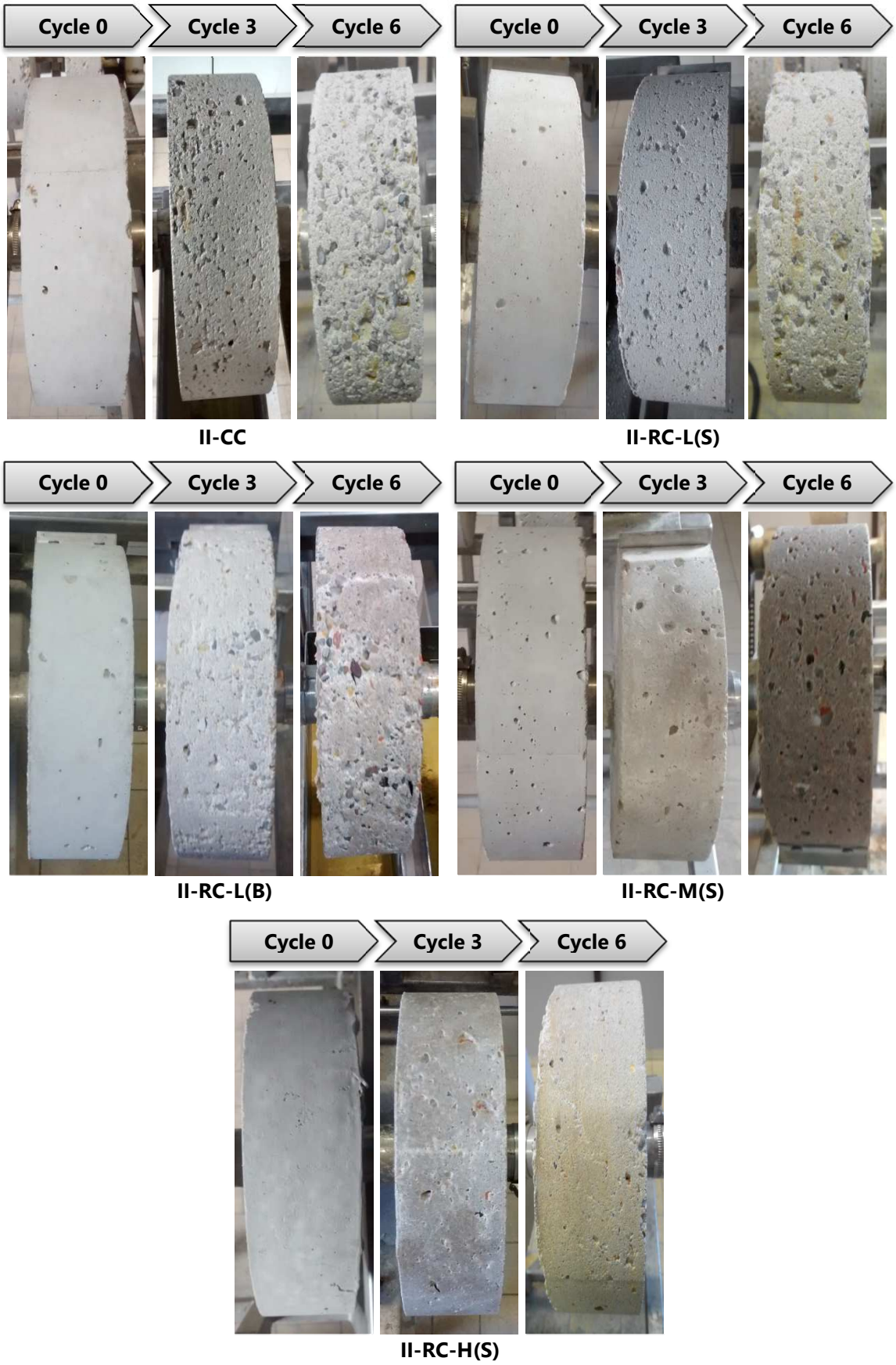

Figure 9.44: Superficial deterioration in the surface of the concrete mixtures pertaining to phase II before the test and after 3 and 6 degradation cycles.

Figure 9.45: Examples of the deposits on the lateral surface of the concrete specimens

11.1. RELATIONSHIP BETWEEN THE RESISTANCE TO ORGANIC ACIDS AND THE WATER ABSORPTION BY CAPILLARITY

The permeability of concrete to the acid penetration is a key factor in the extent of the chemical attack and the penetration of the lactic-acetic acid solution depends on the capillary sorptivity rate of the concrete mixture. Figure 9.46 illustrates the relationship of the water absorption by capillarity with the reduction in radius and the superficial roughness after 6 cycles of degradation. In both cases, strong correlation factors (R^2=0.96 and 0.85, respectively) were identified.

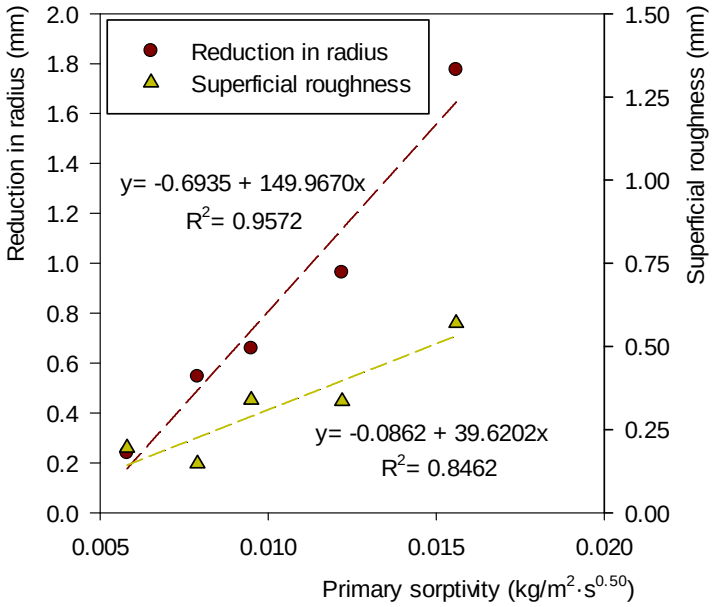

Figure 9.46: Relationship between the degradation due to organic acids and the sorptivity of concrete mixtures in phase II

12. DURABILITY INDEX

In summary, Figure 9.47 illustrates the general durability performance of the recycled mixtures in phase II with respect to the conventional concrete by the comparison of the results obtained for the different properties considered as indexes. First, all the values were adjusted to the assumption that higher figures of a determined property indicate a better performance. Hence, for those cases in which higher results convey the poorer performance of the recycled mixtures (i.e. except the results regarding to the gel open porosity), the index was constructed as the ratio between the result for a recycled concrete and the result of the conventional concrete for each considered property. In order to simplify the analysis, only the results for completely dry specimens were used for the gas permeability index; the frost-salt scaling and chloride penetration depth data were presented as the average value of the casting and troweled surfaces and the TAP data were evaluated using the degradation in the 6th cycle.

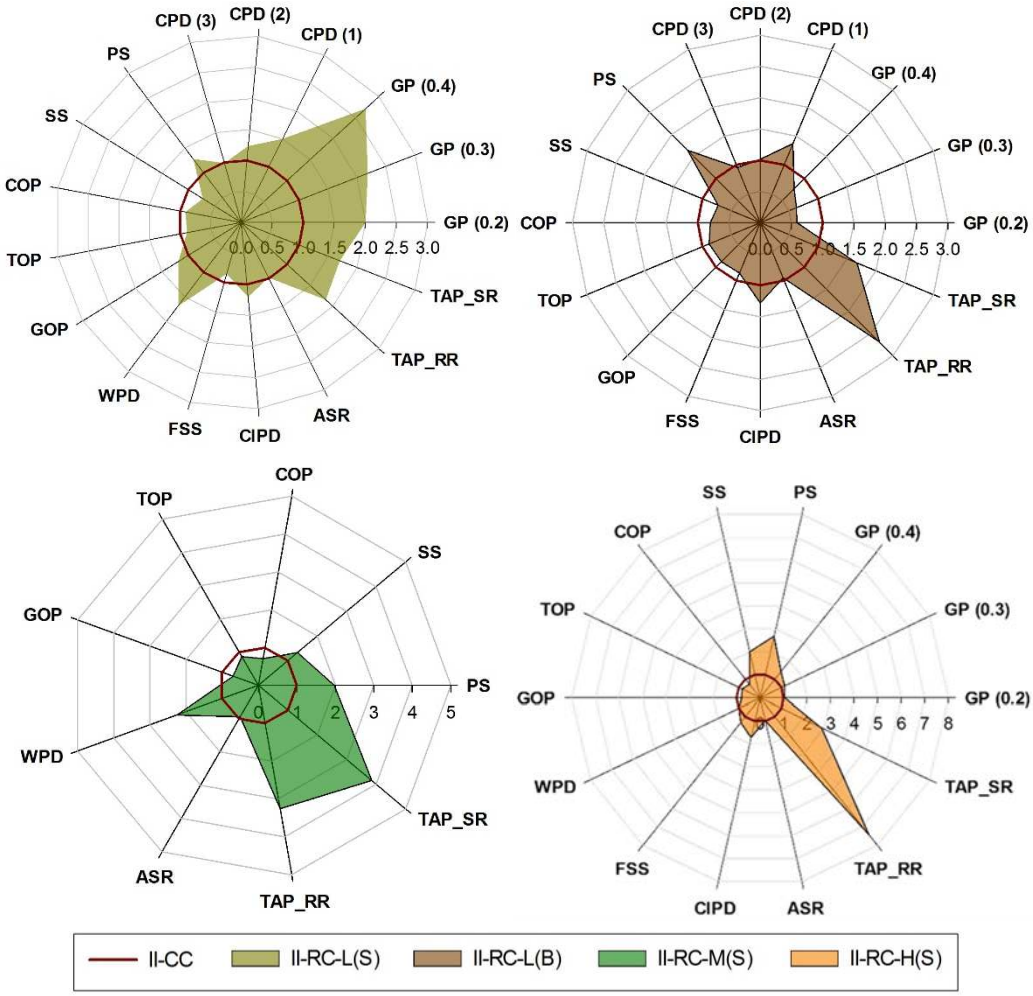

GP: Gas permeability at 0.20, 0.30 y 0.40 MPa
CDP: Carbonation depth at 1,2,3 months
PS: Primary sorptivity
SS: Secundary sorptivity
COP: Capillary open porosity
TOP: Total open porosity
GOP: Gel open porosity
WPD: Water penetration depth
FSS: Frost-salt scaling
ClPD: Chloride penetration depth
ASR: Alkali-silica reaction
TAP_RR: Reduction in radius due to organic acids
TAP_SR: Surface roughness due to organic acids

Figure 9.47: Durability indexes

13. REFERENCES

Abbas, A., Carcasses, M., Ollivier, J.P., 1999. Gas permeability of concrete in relation to its degree of saturation. *Materials and Structures* 32 (1): 3–8.

Abbas, A., Fathifazl, G., Isgor, O.B., Razaqpur, A.G., Fournier, B., Foo, S., 2009. Durability of recycled aggregate concrete designed with equivalent mortar volume method. *Cement and Concrete Composites* 31 (8): 555–563.

Adamson, M., Razmjoo, A., Poursaee, A., 2015. Durability of concrete incorporating crushed brick as coarse aggregate. *Construction and Building Materials* 94: 426–432.

Al-Assadi, G., Casati, M.J., Fernández, J., Gálvez, J. c., 2011. Effect of the curing conditions of concrete on the behaviour under freeze–thaw cycles*. *Fatigue & Fracture of Engineering Materials & Structures* 34 (7): 461–469.

Alexander, M., Mackechnie, J., Ballim, Y., 1999. Guide to the use of durability indexes for achieving durability in concrete structures, Research monograph 2. Universities of Cape Town and Witwatersrand, South Africa.

Amorim, P., De Brito, J., Evangelista, L., 2012. Concrete made with coarse concrete aggregate: influence of curing on durability. *ACI Materials Journal* 109 (2): 195–204.

Andrade, C., Alonso, C., 1996. Corrosion rate monitoring in the laboratory and on-site. *Construction and Building Materials*, Durability of Reinforced Concrete Structures 10 (5): 315–328.

Angst, U., Elsener, B., Larsen, C.K., Vennesland, Ø., 2009. Critical chloride content in reinforced concrete — A review. *Cement and Concrete Research* 39 (12): 1122–1138.

Ann, K.Y., Moon, H.Y., Kim, Y.B., Ryou, J., 2008. Durability of recycled aggregate concrete using pozzolanic materials. *Waste Management* 28 (6): 993–999.

Arredondo-Rea, S.P., Corral-Higuera, R., Neri-Flores, M., Gómez-Soberón, J., Almeraya-Calderón, F., Castorena-González, J., Almaral-Sánchez, J.L., others, 2011. Electrochemical corrosion and electrical resistivity of reinforced recycled aggregate concrete. *Int. J. Electrochem. Sci* 6: 475–483.

Audenaert, K., De Schutter, G., 2007. Relation between vacuum water absorption and porosity of self-compacting concrete, in: 5th International RILEM Symposium on Self-Compacting Concrete. RILEM Publications SARL, 701 – 706.

Bakharev, T., Sanjayan, J.G., Cheng, Y.-B., 2003. Resistance of alkali-activated slag concrete to acid attack. *Cement and Concrete Research* 33 (10): 1607–1611.

Barra de Oliveira, M., Vazquez, E., 1996. The influence of retained moisture in aggregates from recycling on the properties of new hardened concrete. *Waste Management* 16 (1–3): 113–117.

Basheer, L., Kropp, J., Cleland, D.J., 2001. Assessment of the durability of concrete from its permeation properties: a review. *Construction and Building Materials* 15 (2–3): 93–103.

Bektas, F., Wang, K., Ceylan, H., 2009. Effects of crushed clay brick aggregate on mortar durability. *Construction and Building Materials*, Compatibility of Plasters and Renders on Salt Loaded Substrates 23 (5): 1909–1914.

Beltrán, M.G., Agrela, F., Barbudo, A., Ayuso, J., Ramírez, A., 2014a. Mechanical and durability properties of concretes manufactured with biomass bottom ash and recycled coarse aggregates. *Construction and Building Materials* 72: 231–238.

Beltrán, M.G., Barbudo, A., Agrela, F., Galvín, A.P., Jiménez, J.R., 2014b. Effect of cement addition on the properties of recycled concretes to reach control concretes strengths. *Journal of Cleaner Production* 79: 124–133.

Bermejo, E.B., Moragues, A., Gálvez, J.C., Fernández Cánovas, M., 2010. Permeability and pore size distribution in medium strength self-compacting concrete. *Materiales de Construcción* 60 (299): 37–51.

Berndt, M.L., 2009. Properties of sustainable concrete containing fly ash, slag and recycled concrete aggregate. *Construction and Building Materials* 23 (7): 2606–2613.

Bertolini, L., Elsener, B., Pedeferri, P., Redaelli, E., Polder, R.B., 2013. Corrosion of steel in concrete: prevention, diagnosis, repair. John Wiley & Sons.

Bertron, A., Duchesne, J., Escadeillas, G., 2005a. Attack of cement pastes exposed to organic acids in manure. *Cement and Concrete Composites* 27 (9–10): 898–909.

Bertron, A., Duchesne, J., Escadeillas, G., 2005b. Accelerated tests of hardened cement pastes alteration by organic acids: analysis of the pH effect. *Cement and Concrete Research* 35 (1): 155–166.

Bertron, A., Escadeillas, G., Duchesne, J., 2004. Cement pastes alteration by liquid manure organic acids: chemical and mineralogical characterization. *Cement and Concrete Research* 34 (10): 1823–1835.

Boel, V., Audenaert, K., Schutter, G.D., 2007. Gas permeability and capillary porosity of self-compacting concrete. *Mater Struct* 41 (7): 1283–1290.

Bogas, J.A., Gomes, A., 2013. Compressive behavior and failure modes of structural lightweight aggregate concrete – Characterization and strength prediction. *Materials & Design* 46: 832–841.

Bolouri Bazaz, J., Khayati, M., 2011. Properties and performance of concrete made with recycled low-quality crushed brick. *Journal of Materials in Civil Engineering* 24 (4): 330–338.

Borges, P.H.R., Costa, J.O., Milestone, N.B., Lynsdale, C.J., Streatfield, R.E., 2010. Carbonation of CH and C–S–H in composite cement pastes containing high amounts of BFS. *Cement and Concrete Research* 40 (2): 284–292.

Bravo, M., de Brito, J., Pontes, J., Evangelista, L., 2015. Durability performance of concrete with recycled aggregates from construction and demolition waste plants. *Construction and Building Materials* 77: 357–369.

Browne, R.D., 1980. Mechanisms of corrosion of steel in concrete in relation to design, inspection, and repair of offshore and coastal structures. *ACI Special Publication* 65: 169–204.

Buyle-Bodin, F., Hadjieva-Zaharieva, R., 2002. Influence of industrially produced recycled aggregates on flow properties of concrete. *Mat. Struct.* 35 (8): 504–509.

Carcasses, M., Abbas, A., Ollivier, J.-P., Verdier, J., 2002. An optimised preconditioning procedure for gas permeability measurement. *Materials and Structures* 35 (1): 22–27.

Carles-Gibergues, A., Cyr, M., Moisson, M., Ringot, E., 2007. A simple way to mitigate alkali-silica reaction. *Mater Struct* 41 (1): 73–83.

CEB, 1998. Durable Concrete Structures: CEB Design Guide (CEB Bulletin 182). CEB, Switzerland.

Chatterji, S., Thaulow, N., Jensen, A., 1988. Studies of alkali-silica reaction, part 6. Practical implications of a proposed reaction mechanism. *Cement and Concrete Research* 18 (3): 363–366.

Cnudde, V., Cwirzen, A., Masschaele, B., Jacobs, P.J.S., 2009. Porosity and microstructure characterization of building stones and concretes. *Engineering Geology*, Applications of X-ray Computed Tomography in Engineering Geology 103 (3–4): 76–83.

Corinaldesi, V., Moriconi, G., 2009. Influence of mineral additions on the performance of 100% recycled aggregate concrete. *Construction and Building Materials* 23 (8): 2869–2876.

Corral-Higuera, R., Arredondo-Rea, S.P., Neri-Flores, M., Gomez-Soberon, J., Almaral-Sanchez, J.L., Castorena-Gonzalez, J., Martinez-Villafane, A., Almeraya-Calderón, F., others, 2011. Chloride ion penetrability and corrosion behavior of steel in concrete with sustainability characteristics. *Int. J. Electrochem. Sci* 6: 958–970.

Correia, J.R., Brito, J. de, Pereira, A.S., 2006. Effects on concrete durability of using recycled ceramic aggregates. *Materials and Structures* 39 (2): 169–177.

Davies, G., Oberholster, R., 1988. Alkali-silica reaction products and their development. *Cement and Concrete Research* 18 (4): 621–635.

Davies, G., Oberholster, R.E., 1987. An interlaboratory test programme on the NBRI accelerated test to determine the alkali reactivity of aggregates (Special Report No. BOU 92-1987). National Building Research Institute, Council for Scientific and Industrial Research, Pretoria.

De Belie, N., 1997. A Survey on Concrete Floors in Pig Houses and their Degradation. *Journal of Agricultural Engineering Research* 66 (3): 151–156.

De Belie, N., Debruyckere, M., Van Nieuwenburg, D., De Blaere, B., 1997a. Attack of Concrete Floors in Pig Houses by Feed Acids: Influence of Fly Ash Addition and Cement-bound Surface Layers. *Journal of Agricultural Engineering Research* 68 (2): 101–108.

De Belie, N., Debruyckere, M., Van Nieuwenburg, D., De Blaere, B., 1997b. Attack of Concrete Floors in Pig Houses by Feed Acids: Influence of Fly Ash Addition and Cement-bound Surface Layers. *Journal of Agricultural Engineering Research* 68 (2): 101–108.

De Belie, N., Verselder, H.J., De Blaere, B., Van Nieuwenburg, D., Verschoore, R., 1996. Influence of the cement type on the resistance of concrete to feed acids. *Cement and Concrete Research* 26 (11): 1717–1725.

Debieb, F., Courard, L., Kenai, S., Degeimbre, R., 2010. Mechanical and durability properties of concrete using contaminated recycled aggregates. *Cement and Concrete Composites* 32 (6): 421–426.

Debieb, F., Kenai, S., 2008. The use of coarse and fine crushed bricks as aggregate in concrete. *Construction and Building Materials* 22 (5): 886–893.

Desmyter, J., Blockmans, S., 2000. Evaluation of different measures to reduce the risk of alkali-silica reaction in recycled aggregate concrete, in: Proceedings of the 11th International Conference on Alkali-Aggregate Reaction in Concrete. Quebec, Canada, 603–612.

Dhir, R.K., Limbachiya, M.C., Leelawat, T., 1999. Suitability of recycled concrete aggregate for use in BS 5328 designated mixes. *Structures and Buildings* 134 (3): 257–274.

Dhir, R.K., Paine, K.A., 2003. Demonstration project utillising coarse recycled aggregates. (No. CTU/2403). Department of Trade and Industry.

Dhir, R.K., Paine, K.A., 2007. Performance related approach to use of recycled aggregates (AGG0074). WRAP.

Dhir, R.., McCarthy, M.., Halliday, J.., Tang, M.., 2005. ASR testing on recycled aggregates: Guidance on alkali limits and reactivity. (No. STBF 13/14C). WRAP.

Duan, Z.H., Poon, C.S., 2014. Properties of recycled aggregate concrete made with recycled aggregates with different amounts of old adhered mortars. *Materials & Design* 58: 19–29.

Eguchi, K., Teranishi, K., Nakagome, A., Kishimoto, H., Shinozaki, K., Narikawa, M., 2007. Application of recycled coarse aggregate by mixture to concrete construction. *Construction and Building Materials* 21 (7): 1542–1551.

Elkey, W., Sellevold, E.J., 1995. Electrical resistivity of concrete (Publication No. 80). Norwegian Road Research Laboratory, Oslo, Norway.

Elsharief, A., Cohen, M.D., Olek, J., 2005. Influence of lightweight aggregate on the microstructure and durability of mortar. *Cement and Concrete Research* 35 (7): 1368–1376.

Etxeberria, M., Vegas, I., 2015. Effect of fine ceramic recycled aggregate (RA) and mixed fine RA on hardened properties of concrete. *Magazine of Concrete Research* 67 (12): 645–655.

Fagerlund, G., 1982. On the capillarity of concrete. Nordic Concrete Research, Oslo.

Feliu, S., Andrade, C., Gonzalez, J., Alonso, C., 1996. A new method for in-situ measurement of electrical resistivity of reinforced concrete. *Materials and structures* 29 (6): 362–365.

Fernández-Jiménez, A., Puertas, F., 2002. The alkali–silica reaction in alkali-activated granulated slag mortars with reactive aggregate. *Cement and Concrete Research* 32 (7): 1019–1024.

Ferreira, L., de Brito, J., Barra, M., 2011. Influence of the pre-saturation of recycled coarse concrete aggregates on concrete properties. *Magazine of Concrete Research* 63 (8): 617–627.

Geraldes, V.L., 2013. Study on non-structural recycled concretes with mixed recycled aggregate: Mechanical properties and expansion due to sulphates [in Spanish]. Universidad Politécnica de Madrid, Madrid, Spain.

Gokce, A., Nagataki, S., Saeki, T., Hisada, M., 2004. Freezing and thawing resistance of air-entrained concrete incorporating recycled coarse aggregate: The role of air content in demolished concrete. *Cement and Concrete Research* 34 (5): 799–806.

Gokce, A., Nagataki, S., Saeki, T., Hisada, M., 2011. Identification of frost-susceptible recycled concrete aggregates for durability of concrete. *Construction and Building Materials* 25 (5): 2426–2431.

Gomes, M., Brito, J. de, 2009. Structural concrete with incorporation of coarse recycled concrete and ceramic aggregates: durability performance. *Materials and Structures* 42 (5): 663–675.

Gómez-Soberón, J.M.V., 2002. Porosity of recycled concrete with substitution of recycled concrete aggregate: An experimental study. *Cement and Concrete Research* 32 (8): 1301–1311.

Gonçalves, A., Esteves, A., Vieira, M., 2004. Influence of recycled concrete aggregates on concrete durability, in: International RILEM Conference on the Use of Recycled Materials in Building and Structures. Barcelona, Spain, 554–562.

Gonzalez, A., Etxeberria, M., 2014. Experimental analysis of properties of high performance recycled aggregate concrete. *Construction and Building Materials* 52: 227–235.

Gonzalez-Corominas, A., Etxeberria, M., 2014. Properties of high performance concrete made with recycled fine ceramic and coarse mixed aggregates. *Construction and Building Materials* 68: 618–626.

Gottfredsen, F., Thøgersen, F., 1993. Recycling of concrete in aggressive environment, in: Third International RILEM Symposium on Demolition and Reuse of Concrete and Masonry. RILEM Publications SARL, Odense, Denmark, 309–320.

Gress, D.L., Kozikowski, R.L., 2000. Accelerated ASR testing of concrete prisms incorporating recycled concrete aggregate, in: Proceedings of the 11th International Conference on Alkali-Aggregate Reaction in Concrete. Quebec, Canada, 1139–1148.

Gruyaert, E., 2011. Effect of blast-furnace slag as cement replacement on hydration, microstructure, strength and durability of concrete. Ghent University, Ghent, Belgium.

Güneyisi, E., Gesoğlu, M., Algın, Z., Yazıcı, H., 2014. Effect of surface treatment methods on the properties of self-compacting concrete with recycled aggregates. *Construction and Building Materials* 64: 172–183.

Güneyisi, E., Gesoğlu, M., Pürsünlü, Ö., Mermerdaş, K., 2013. Durability aspect of concretes composed of cold bonded and sintered fly ash lightweight aggregates. *Composites Part B: Engineering* 53: 258–266.

Hall, C., Hoff, W.D., Taylor, S.C., Wilson, M.A., Yoon, B.-G., Reinhardt, H.-W., Sosoro, M., Meredith, P., Donald, A.M., 1995. Water anomaly in capillary liquid absorption by cement-based materials. *J Mater Sci Lett* 14 (17): 1178–1181.

Heiyantuduwa, R., Alexander, M.G., Mackechnie, J.R., 2006. Performance of a penetrating corrosion inhibitor in concrete affected by carbonation-induced corrosion. *Journal of materials in civil engineering* 18 (6): 842–850.

Henry, M., Pardo, G., Nishimura, T., Kato, Y., 2011. Balancing durability and environmental impact in concrete combining low-grade recycled aggregates and mineral admixtures. *Resources, Conservation and Recycling* 55 (11): 1060–1069.

Hewlett, P. (Ed.), 2003. Lea's chemistry of cement and concrete. Butterworth-Heinemann.

Hilsdorf, H., Kropp, J. (Eds.), 2004. Performance criteria for concrete durability, RILEM Report. CRC Press.

Hoffmann, C., Schubert, S., Leemann, A., Motavalli, M., 2012. Recycled concrete and mixed rubble as aggregates: Influence of variations in composition on the concrete properties and their use as structural material. *Construction and Building Materials* 35: 701–709.

Hoseini, M., Bindiganavile, V., Banthia, N., 2009. The effect of mechanical stress on permeability of concrete: A review. *Cement and Concrete Composites* 31 (4): 213–220.

Hughes, B.P., Soleit, A.K.O., Brierley, R.W., 1985. New technique for determining the electrical resistivity of concrete. *Magazine of Concrete Research* 37 (133): 243–248.

Hunkeler, F., 1996. The resistivity of pore water solution—a decisive parameter of rebar corrosion and repair methods. *Construction and Building Materials*, Durability of Reinforced Concrete Structures 10 (5): 381–389.

Hutchings, I.M., 2002. Abrasion processes in wear and manufacturing. *Proceedings of the Institution of Mechanical Engineers, Part J: Journal of Engineering Tribology* 216 (2): 55–62.

Hwang, J.P., Shim, H.B., Lim, S., Ann, K.Y., 2013. Enhancing the durability properties of concrete containing recycled aggregate by the use of pozzolanic materials. *KSCE J Civ Eng* 17 (1): 155–163.

Jennings, H.M., 2000. A model for the microstructure of calcium silicate hydrate in cement paste. *Cement and Concrete Research* 30 (1): 101–116.

Jiménez, C., Barra, M., Valls, S., Aponte, D., Vázquez, E., 2014. Durability of recycled aggregate concrete designed with the Equivalent Mortar Volume (EMV) method: Validation under the Spanish context and its adaptation to Bolomey methodology. *Materiales de Construcción* 64 (313): e006.

Ji, Y., Zhao, W., Zhou, M., Ma, H., Zeng, P., 2013. Corrosion current distribution of macrocell and microcell of steel bar in concrete exposed to chloride environments. *Construction and Building Materials* 47: 104–110.

Kanellopoulos, A., Nicolaides, D., Petrou, M.F., 2014. Mechanical and durability properties of concretes containing recycled lime powder and recycled aggregates. *Construction and Building Materials* 53: 253–259.

Kasai, Y., Hisaka, M., Yanagi, K., 1988. Durability of concrete using recycled coarse aggregate, in: Proceedings of the Second International RILEM Symposium on Demolition and Reuse of Concrete and Masonry. Tokyo, Japan, 623–632.

Kearsley, E.P., Wainwright, P.J., 2001. Porosity and permeability of foamed concrete. *Cement and Concrete Research* 31 (5): 805–812.

Kevern, J.T., Wang, K., Schaefer, V.R., 2009. Effect of coarse aggregate on the freeze-thaw durability of pervious concrete. *Journal of Materials in Civil Engineering* 22 (5): 469–475.

Kibriya, T., Speare, P.R.S., 1996. The use of crushed brick coarse aggregate in concrete, in: International Congress on "Concrete in the Service of Mankind." Dundee, UK, 495–503.

Kim, K., Shin, M., Cha, S., 2013. Combined effects of recycled aggregate and fly ash towards concrete sustainability. *Construction and Building Materials* 48: 499–507.

Kong, D., Lei, T., Zheng, J., Ma, C., Jiang, J., Jiang, J., 2010. Effect and mechanism of surface-coating pozzalanics materials around aggregate on properties and ITZ microstructure of recycled aggregate concrete. *Construction and Building Materials* 24 (5): 701–708.

Kou, S.C., Poon, C.S., 2009. Properties of self-compacting concrete prepared with coarse and fine recycled concrete aggregates. *Cement and Concrete Composites* 31 (9): 622–627.

Kou, S.-C., Poon, C.-S., 2013. Long-term mechanical and durability properties of recycled aggregate concrete prepared with the incorporation of fly ash. *Cement and Concrete Composites* 37: 12–19.

Kou, S.C., Poon, C.S., Agrela, F., 2011a. Comparisons of natural and recycled aggregate concretes prepared with the addition of different mineral admixtures. *Cement and Concrete Composites* 33 (8): 788–795.

Kou, S.C., Poon, C.S., Chan, D., 2007. Influence of fly ash as cement replacement on the properties of recycled aggregate concrete. *Journal of Materials in Civil Engineering* 19 (9): 709–717.

Kou, S.C., Poon, C.S., Etxeberria, M., 2011b. Influence of recycled aggregates on long term mechanical properties and pore size distribution of concrete. *Cement and Concrete Composites* 33 (2): 286–291.

Kou, S., Poon, C., 2015. Effect of the quality of parent concrete on the properties of high performance recycled aggregate concrete. *Construction and Building Materials* 77: 501–508.

Kou, S.., Poon, C.S., 2006. Compressive strength, pore size distribution and chloride-ion penetration of recycled aggregate concrete incorporating class-F fly ash. *J. Wuhan Univ. Technol.-Mat. Sci. Edit.* 21 (4): 130–136.

Kwan, W.H., Ramli, M., Kam, K.J., Sulieman, M.Z., 2012. Influence of the amount of recycled coarse aggregate in concrete design and durability properties. *Construction and Building Materials* 26 (1): 565–573.

Langford, P., Broomfield, J., 1987. Monitoring the corrosion of reinforcing steel. *Construction Repair* 1 (2): 32–36.

Levy, S.M., Helene, P., 2004. Durability of recycled aggregates concrete: a safe way to sustainable development. *Cement and Concrete Research* 34 (11): 1975–1980.

Limbachiya, M.C., Leelawat, T., Dhir, R.K., 2000. Use of recycled concrete aggregate in high-strength concrete. *Materials and Structures* 33 (9): 574–580.

Limbachiya, M., Leelawat, T., Dhir, R., 1998. RCA concrete: a study of properties in the fresh state, strength development and durability, in: Proceedings of the International Symposium on Sustainable Construction: Use of Recycled Concrete Aggregate. London, UK.

Limbachiya, M., Meddah, M.S., Ouchagour, Y., 2012. Use of recycled concrete aggregate in fly-ash concrete. *Construction and Building Materials* 27 (1): 439–449.

Li, X., 2008. Recycling and reuse of waste concrete in China: Part I. Material behaviour of recycled aggregate concrete. *Resources, Conservation and Recycling* 53 (1–2): 36–44.

Li, X., Gress, D., 2006. Mitigating Alkali-Silica Reaction in Concrete Containing Recycled Concrete Aggregate. *Transportation Research Record: Journal of the Transportation Research Board* 1979: 30–35.

López-Gayarre, F., López-Colina, C., Serrano-López, M.A., García Taengua, E., López Martínez, A., 2011. Assessment of properties of recycled concrete by means of a highly fractioned factorial design of experiment. *Construction and Building Materials* 25 (10): 3802–3809.

López, W., González, J.A., 1993. Influence of the degree of pore saturation on the resistivity of concrete and the corrosion rate of steel reinforcement. *Cement and Concrete Research* 23 (2): 368–376.

Lotfy, A., Al-Fayez, M., 2015. Performance evaluation of structural concrete using controlled quality coarse and fine recycled concrete aggregate. *Cement and Concrete Composites* 61: 36–43.

Lothenbach, B., Matschei, T., Möschner, G., Glasser, F.P., 2008. Thermodynamic modelling of the effect of temperature on the hydration and porosity of Portland cement. *Cement and Concrete Research* 38 (1): 1–18.

Lydon, F.D., Broadley, D.K., 1994. Effects of coarse aggregate on relative permeability of concrete. *Construction and Building Materials* 8 (3): 185–189.

Malhotra, V.M., 2011. Durability of Concrete, in: Revie, R.W. (Ed.), Uhlig's Corrosion Handbook. John Wiley & Sons, Inc., 439–449.

Malhotra, V.M., Carino, N.J., 2003. Handbook on nondestructive testing of concrete. CRC press, New York, USA.

Martínez-Lage, I., Martínez-Abella, F., Vázquez-Herrero, C., Pérez-Ordóñez., J.L., 2012. Properties of plain concrete made with mixed recycled coarse aggregate. *Construction and Building Materials* 37: 171–176.

Martys, N.S., Ferraris, C.F., 1997. Capillary transport in mortars and concrete. *Cement and Concrete Research* 27 (5): 747–760.

Mas, B., Cladera, A., Bestard, J., Muntaner, D., López, C.E., Piña, S., Prades, J., 2012a. Concrete with mixed recycled aggregates: Influence of the type of cement. *Construction and Building Materials* 34: 430–441.

Mas, B., Cladera, A., Olmo, T. del, Pitarch, F., 2012b. Influence of the amount of mixed recycled aggregates on the properties of concrete for non-structural use. *Construction and Building Materials* 27 (1): 612–622.

McCarter, W.J., Starrs, G., Chrisp, T.M., 2000. Electrical conductivity, diffusion, and permeability of Portland cement-based mortars. *Cement and Concrete Research* 30 (9): 1395–1400.

Medina, C., Frías, M., Sánchez de Rojas, M.I., Thomas, C., Polanco, J.A., 2012. Gas permeability in concrete containing recycled ceramic sanitary ware aggregate. *Construction and Building Materials* 37: 597–605.

Medina, C., Sánchez de Rojas, M.I., Frías, M., 2013. Properties of recycled ceramic aggregate concretes: Water resistance. *Cement and Concrete Composites* 40: 21–29.

Medina, C., Sánchez de Rojas, M.I., Frías, M., 2013. Freeze-thaw durability of recycled concrete containing ceramic aggregate. *Journal of Cleaner Production* 40: 151–160.

Medina, C., Zhu, W., Howind, T., Frías, M., Sánchez de Rojas, M.I., 2015. Effect of the constituents (asphalt, clay materials, floating particles and fines) of construction and demolition waste on the properties of recycled concretes. *Construction and Building Materials* 79: 22–33.

Medina, C., Zhu, W., Howind, T., Sánchez de Rojas, M.I., Frías, M., 2014. Influence of mixed recycled aggregate on the physical – mechanical properties of recycled concrete. *Journal of Cleaner Production* 68: 216–225.

Medina Martínez, C., 2011. Behaviour of recycled concrete with ceramic aggregate: Physical, mechanical, microstructural and durability study [in Spanish]. Universidad de León, León, Spain.

Mehta, P.K., Monteiro, P.J., 2006. Concrete: microstructure, properties, and materials. McGraw-Hill New York.

Menendez, G., Bonavetti, V., Irassar, E., 2007. Ternary blend cements concrete. Part II: Transport mechanism. *Materiales de Construccion* 57 (285): 31–43.

Molero, M., Aparicio, S., Al-Assadi, G., Casati, M.J., Hernández, M.G., Anaya, J.J., 2012. Evaluation of freeze–thaw damage in concrete by ultrasonic imaging. *NDT & E International* 52: 86–94.

Nagataki, S., Lida, K., 2001. Recycling of Demolished Concrete. *ACI Special Publication* 200: 1–20.

Neville, A.M., 1995. Properties of concrete. Harlow, Essex: Longman.

Neville, A.M., Brooks, J.J., 2010. Concrete technology. Pearson, London, UK.

Newlands, M.D., Jones, M.R., Kandasami, S., Harrison, T.A., 2008. Sensitivity of electrode contact solutions and contact pressure in assessing electrical resistivity of concrete. *Materials and Structures* 41 (4): 621–632.

Nishibayashi, S., Yamura, K., 1988. Mechanical properties and durability of concrete from recycled coarse aggregate prepared by crushing concrete, in: Proceedings of the Second International RILEM Symposium on Demolition and Reuse of Concrete and Masonry. Tokyo, Japan, 652–659.

Oberholster, R.E., Davies, G., 1986. An accelerated method for testing the potential alkali reactivity of siliceous aggregates. *Cement and Concrete Research* 16 (2): 181–189.

O'Donnell, C., Dodd, V.A., O'Kiely, P., Richardson, M., 1995. A Study of the Effects of Silage Effluent on Concrete: Part 1, Significance of Concrete Characteristics. *Journal of Agricultural Engineering Research* 60 (2): 83–92.

Olorunsogo, F.T., Padayachee, N., 2002. Performance of recycled aggregate concrete monitored by durability indexes. *Cement and Concrete Research* 32 (2): 179–185.

Otsuki, N., Miyazato, S., Yodsudjai, W., 2003. Influence of recycled aggregate on interfacial transition zone, strength, chloride penetration and carbonation of concrete. *Journal of materials in civil engineering*.

Pacheco-Torgal, F., Jalali, S., 2010. Compressive strength and durability properties of ceramic wastes based concrete. *Materials and Structures* 44 (1): 155–167.

Paine, K.A., Collery, D.J., Dhir, R.K., 2009. Strength and deformation characteristics of concrete containing coarse recycled and manufactured aggregates, in: Proceedings of the 11th International Conference on Non-Conventional Materials and Technologies (NOCMAT 2009). Bath, UK, 1–9.

Parrott, L.J., 1994. Moisture conditioning and transport properties of concrete test specimens. *Materials and Structures* 27 (8): 460–468.

Parrott, L.J., 1996. Some effects of cement and curing upon carbonation and reinforcement corrosion in concrete. *Mat. Struct.* 29 (3): 164–173.

Pedro, D., Brito, J. de, Evangelista, L., 2014a. Performance of concrete made with aggregates recycled from precasting industry waste: influence of the crushing process. *Mater Struct* : 1–14.

Pedro, D., de Brito, J., Evangelista, L., 2014b. Influence of the use of recycled concrete aggregates from different sources on structural concrete. *Construction and Building Materials* 71: 141–151.

Pereira de Oliveira, L.A., Nepomuceno, M.C.S., Castro-Gomes, J.P., Vila, M.F.C., 2014. Permeability properties of self-compacting concrete with coarse recycled aggregates. *Construction and Building Materials* 51: 113–120.

Permanent Commission on Concrete, 2008. Code on structural concrete (EHE-08) [in Spanish]. Spanish Ministry of Public Works, Madrid.

Poon, C.S., Shui, Z.H., Lam, L., 2004. Effect of microstructure of ITZ on compressive strength of concrete prepared with recycled aggregates. *Construction and Building Materials* 18 (6): 461–468.

Punkki, J., Gjbrv, O.E., 1995. Effect of water absorption by aggregate on properties of high-strength lightweight concrete, in: International Symposium on Structural Lightweight Aggregate Concrete. Norwegian Concrete Association, Sandfjord, Norway, 604–616.

Punkki, J., Gjørv, O.., Monteiro, P.J.., 1996. Microstructure of high-strength lightweight aggregate concrete, in: 4th International Symposium on Utilization of High-Strength/high-Performance Concrete. F. Presses de 1'ENPC, Paris, France, 1281–1287.

Qin, H.Y., Zhao, Y.L., Luo, B.G., Chen, Y.H., 2010. Experimental Study on the Chloride Diffusivity of Recycled Aggregate Concrete. *Advanced Materials Research* 168-170: 1404–1408.

Rabehi, M., Mezghiche, B., Guettala, S., 2013. Correlation between initial absorption of the cover concrete, the compressive strength and carbonation depth. *Construction and Building Materials* 45: 123–129.

Rao, M.C., Bhattacharyya, S.K., Barai, S.V., 2011. Influence of field recycled coarse aggregate on properties of concrete. *Materials and Structures* 44 (1): 205–220.

Razaqpur, A.G., Fathifazl, G., Isgor, B., Abbas, A., Foo, S., Fournier, B., 2010. How to produce high quality concrete mixes with recycled concrete aggregate, in: Proceedings of the 2nd International Conference on Waste Engineering and Management - ICWEM 2010. RILEM Publications SARL, Shanghai, 11–35.

Richardson, A., Coventry, K., Bacon, J., 2011. Freeze/thaw durability of concrete with recycled demolition aggregate compared to virgin aggregate concrete. *Journal of Cleaner Production* 19 (2–3): 272–277.

Ridzuan, A.R.M., Ibrahim, A., Ismail, A.M.M., Diah, A.B.M., 2005. Durability performance of recycled aggregate concrete, in: Proceedings of International Conference on Global Construction: Ultimate Concrete Opportunities-Achieving Sustainability in Construction. Dundee, UK, 193–202.

RILEM TC 116-PCD, 1999. Permeability of concrete as a criterion of its durability. Recommendations. *Materials and Structures* 32: 174–179.

Ryu, J.S., 2002. An experimental study on the effect of recycled aggregate on concrete properties. *Magazine of Concrete Research* 54 (1): 7–12.

Safiuddin, M., Hearn, N., 2005. Comparison of ASTM saturation techniques for measuring the permeable porosity of concrete. *Cement and Concrete Research* 35 (5): 1008–1013.

Sagoe-Crentsil, K.K., Brown, T., Taylor, A.H., 2001. Performance of concrete made with commercially produced coarse recycled concrete aggregate. *Cement and Concrete Research* 31 (5): 707–712.

Salem, R.M., Burdette, E.G., Jackson, N.M., 2003. Resistance to freezing and thawing of recycled aggregate concrete. *ACI Materials Journal* 100 (3): 216–221.

Scott IV, H., Gress, D., 2004. Mitigating alkali silica reaction in recycled concrete. *ACI Special Publication* 219.

Sengul, O., 2014. Use of electrical resistivity as an indicator for durability. *Construction and Building Materials* 73: 434–441.

Senthamarai, R., Manoharan, P.D., Gobinath, D., 2011. Concrete made from ceramic industry waste: Durability properties. *Construction and Building Materials* 25 (5): 2413–2419.

Shayan, A., Xu, A., 2003. Performance and properties of structural concrete made with recycled concrete aggregate. *ACI Materials Journal* 100 (5): 371–380.

Shehata, M.H., Christidis, C., Mikhaiel, W., Rogers, C., Lachemi, M., 2010. Reactivity of reclaimed concrete aggregate produced from concrete affected by alkali–silica reaction. *Cement and Concrete Research*, Special Issue: ICAAR 13, Trondheim, Norway, June 16-20, 2008 40 (4): 575–582.

Shehata, M.H., Thomas, M.D.A., 2000. The effect of fly ash composition on the expansion of concrete due to alkali–silica reaction. *Cement and Concrete Research* 30 (7): 1063–1072.

Shehata, M.H., Thomas, M.D.A., 2002. Use of ternary blends containing silica fume and fly ash to suppress expansion due to alkali–silica reaction in concrete. *Cement and Concrete Research* 32 (3): 341–349.

Shehata, M.H., Thomas, M.D.A., Bleszynski, R.F., 1999. The effects of fly ash composition on the chemistry of pore solution in hydrated cement pastes. *Cement and Concrete Research* 29 (12): 1915–1920.

Shi, C., 2004. Effect of mixing proportions of concrete on its electrical conductivity and the rapid chloride permeability test (ASTM C1202 or ASSHTO T277) results. *Cement and Concrete Research* 34 (3): 537–545.

Shi, C., Stegemann, J.A., 2000. Acid corrosion resistance of different cementing materials. *Cement and Concrete Research* 30 (5): 803–808.

Silva, R.V., Neves, R., de Brito, J., Dhir, R.K., 2015. Carbonation behaviour of recycled aggregate concrete. *Cement and Concrete Composites* 62: 22–32.

Sim, J., Park, C., 2011. Compressive strength and resistance to chloride ion penetration and carbonation of recycled aggregate concrete with varying amount of fly ash and fine recycled aggregate. *Waste Management* 31 (11): 2352–2360.

Soares, D., de Brito, J., Ferreira, J., Pacheco, J., 2014. Use of coarse recycled aggregates from precast concrete rejects: Mechanical and durability performance. *Construction and Building Materials* 71: 263–272.

Sommerville, G., 1984. The interdependence of research, durability and structural design of concrete, in: Proceedings of Symposium on Design Life of Buildings. Thomas Telford, London, UK, 233–250.

Stark, D., 1996. The Use of Recycled-Concrete Aggregate from Concrete Exhibiting Alkali-Silica Reactivity (Research and Development Bulletin RD113). Portland Cement Association, Illinois, USA.

Tam, V.W.Y., Tam, C.M., 2007. Assessment of durability of recycled aggregate concrete produced by two-stage mixing approach. *J Mater Sci* 42 (10): 3592–3602.

Taylor, S.C., Hoff, W.D., Wilson, M.A., Green, K.M., 1999. Anomalous water transport properties of Portland and blended cement-based materials. *Journal of Materials Science Letters* 18 (23): 1925–1927.

Thiery, M., Villain, G., Dangla, P., Platret, G., 2007. Investigation of the carbonation front shape on cementitious materials: Effects of the chemical kinetics. *Cement and Concrete Research* 37 (7): 1047–1058.

Thomas, C., Setién, J., Polanco, J.A., Alaejos, P., Sánchez de Juan, M., 2013. Durability of recycled aggregate concrete. *Construction and Building Materials* 40: 1054–1065.

Topçu, İ.B., Şengel, S., 2004. Properties of concretes produced with waste concrete aggregate. *Cement and Concrete Research* 34 (8): 1307–1312.

Topçu, I., Canbaz, M., 2007. Utilization of crushed tile as aggregate in concrete. *Iranian Journal of Science and Technology* 31 (B5): 561.

Tumidajski, P.J., 2005. Relationship between resistivity, diffusivity and microstructural descriptors for mortars with silica fume. *Cement and Concrete Research* 35 (7): 1262–1268.

Turanli, L., Bektas, F., Monteiro, P.J.M., 2003. Use of ground clay brick as a pozzolanic material to reduce the alkali–silica reaction. *Cement and Concrete Research* 33 (10): 1539–1542.

Tu, T.-Y., Chen, Y.-Y., Hwang, C.-L., 2006. Properties of HPC with recycled aggregates. *Cement and Concrete Research* 36 (5): 943–950.

Tuyan, M., Mardani-Aghabaglou, A., Ramyar, K., 2014. Freeze–thaw resistance, mechanical and transport properties of self-consolidating concrete incorporating coarse recycled concrete aggregate. *Materials & Design* 53: 983–991.

Ulloa Mayorga, V.A., 2012. Durability of reinforced recycled concrete: assessment of the chloride corrosion on a marine environment [in Spanish]. Universitat Politècnica de València, Valencia, Spain.

UNE-83981, 2008. Concrete durability. Test methods. Determination to gas permeability of hardened concrete [in Spanish]. AENOR, Madrid.

UNE 83982, 2008. Concrete durability. Test methods. Determination of the capillar suction in hardened concrete. Fagerlund method [in Spanish]. AENOR, Madrid.

UNE EN 1339, 2004. Concrete paving flags - Requirements and test methods [in Spanish]. AENOR, Madrid.

Valenza II, J.J., Scherer, G.W., 2007. A review of salt scaling: II. Mechanisms. *Cement and Concrete Research* 37 (7): 1022–1034.

Van den Heede, P., 2014. Durability and sustainability of concrete with high volumes of fly ash. Ghent University, Ghent, Belgium.

Van den Heede, P., Gruyaert, E., De Belie, N., 2010. Transport properties of high-volume fly ash concrete: Capillary water sorption, water sorption under vacuum and gas permeability. *Cement and Concrete Composites* 32 (10): 749–756.

Van Genuchten, M.T., 1980. A closed-form equation for predicting the hydraulic conductivity of unsaturated soils. *Soil Science Society of America Journal* 44 (5): 892–898.

Vázquez, E., Barra, M., Aponte, D., Jiménez, C., Valls, S., 2014. Improvement of the durability of concrete with recycled aggregates in chloride exposed environment. *Construction and Building Materials* 67, Part A: 61–67.

Verbeck, G.J., Landgren, R., 1960. Influence of physical characteristics of aggregates on frost resistance of concrete (Research Department Bulletin No. 126). Portland Cement Association.

Verdier, J., Carcasses, M., 2004. Equivalent gas permeability of concrete samples subjected to drying. *Magazine of Concrete Research* 56 (4): 223–230.

Villagrán-Zaccardi, Y.A., Zega, C.J., Di Maio, A.A., 2008. Chloride Penetration and Binding in Recycled Concrete. *Journal of Materials in Civil Engineering* 20 (6): 449–455.

Vivian, H., 1947. The effects on mortar expansion of reactive component in the aggregate. Studies in cement-aggregate reactions, part 10 (CSIRO Bulletin No. 256). Commonwealth Scientific and Industrial Research Organisation (CSIRO), Australia.

Wainwright, P., Trevorrow, A., Yu, Y., Wang, Y., 1993. Modifying the performance of concrete made with coarse and fine recycled concrete aggregates, in: Proceedings of the Third International RILEM Symposium. RILEM Publications SARL, 319–330.

Wang, W., Kou, S., Xing, F., 2013. Deformation properties and direct shear of medium strength concrete prepared with 100% recycled coarse aggregates. *Construction and Building Materials* 48: 187–193.

Wardeh, G., Mohamed, M.A., Ghorbel, E., 2011. Analysis of concrete internal deterioration due to frost action. *Journal of Building Physics* 35 (1): 54–82.

Whiting, D.A., Nagi, M.A., 2003. Electrical resistivity of concrete-a literature review (R&D Serial No. 2457). Portland Cement Association, Illinois, USA.

Williams, A.G., 1983. Organic acids, biochemical oxygen demand and chemical oxygen demand in the soluble fraction of piggery slurry. *J. Sci. Food Agric.* 34 (3): 212–220.

Xiao, J., Li, L., Tam, V.W.Y., Li, H., 2014. The state of the art regarding the long-term properties of recycled aggregate concrete. *Structural Concrete* 15 (1): 3–12.

Xu, G.J.Z., Watt, D.F., Hudec, P.P., 1995. Effectiveness of mineral admixtures in reducing ASR expansion. *Cement and Concrete Research* 25 (6): 1225–1236.

Yanagi, K., Nakagawa, M., Hisaka, M., Kasai, Y., 1988. Effect of impurities in recycled coarse aggregate upon a few properties of the concrete produced with it, in: Proceedings of the Second International RILEM Symposium on Demolition and Reuse of Concrete and Masonry, Japan. 613–623.

Yang, K.-H., Chung, H.-S., Ashour, A.F., 2008. Influence of type and replacement level of recycled aggregates on concrete properties. *MJ* 105 (3): 289–296.

Yildirim, S.T., Meyer, C., Herfellner, S., 2015. Effects of internal curing on the strength, drying shrinkage and freeze–thaw resistance of concrete containing recycled concrete aggregates. *Construction and Building Materials* 91: 288–296.

Yuan, Q., Shi, C., De Schutter, G., Audenaert, K., Deng, D., 2009. Chloride binding of cement-based materials subjected to external chloride environment – A review. *Construction and Building Materials* 23 (1): 1–13.

Zaharieva, R., Buyle-Bodin, F., Skoczylas, F., Wirquin, E., 2003. Assessment of the surface permeation properties of recycled aggregate concrete. *Cement and Concrete Composites* 25 (2): 223–232.

Zaharieva, R., Buyle-Bodin, F., Wirquin, E., 2004. Frost resistance of recycled aggregate concrete. *Cement and Concrete Research* 34 (10): 1927–1932.

Zega, C.J., Di Maio, A.A., 2011. Recycled Concretes Made with Waste Ready-Mix Concrete as Coarse Aggregate. *Journal of Materials in Civil Engineering* 23 (3): 281–286.

Zhang, H., Zhao, Y., 2015. Integrated interface parameters of recycled aggregate concrete. *Construction and Building Materials* 101, Part 1: 861–877.

Zhang, S., Zong, L., 2014. Properties of concrete made with recycled coarse aggregate from waste brick. *Environ. Prog. Sustainable Energy* 33 (4): 1283–1289.

Zhao, Y., Dong, J., Wu, Y., Wang, H., Li, X., Xu, Q., 2014. Steel corrosion and corrosion-induced cracking in recycled aggregate concrete. *Corrosion Science* 85: 241–250.

Živica, V., 2006. Deterioration of cement-based materials due to the action of organic compounds. *Construction and Building Materials* 20 (9): 634–641.

Zivica, V., Bajza, A., 2001. Acidic attack of cement based materials — a review.: Part 1. Principle of acidic attack. *Construction and Building Materials* 15 (8): 331–340.

Zong, L., Fei, Z., Zhang, S., 2014. Permeability of recycled aggregate concrete containing fly ash and clay brick waste. *Journal of Cleaner Production* 70: 175–182.

Chapter 10

Environmental performance

1. INTRODUCTION

Although human activities have always had an impact on the environment, after the industrial revolution, the technological development achieved has not only meant that humans have a greater capacity for economic growth but also a greater negative impact on the environment. Since the first alarm voices rose up in the 1970s, the reconciliation of economic development with the preservation of the environment has been one of the major global challenges of the society.

Of the many environmental impacts of development, those caused by the construction industry have triggered considerable public and governmental concerns that have led to seek for ways to consume less energy and natural resources, and generate fewer wastes. The use of CDW as raw concrete materials for the production of eco-efficient concretes addresses the aforementioned environmental burdens; hence, it is considered among one of the best possibilities for the reduction of the environmental impacts of the concrete sector (Van den Heede and De Belie, 2012; Knoeri et al., 2013).

The aim of this chapter is to analyse the recycled concrete from an environmental point-of-view, using a life cycle approach in order to identify the environmental benefits associated to the use of recycled aggregates from construction and demolition wastes (CDW) when compared with conventional concrete mixtures.

2. ECOLOGICAL BACKGROUND OF THE CONCRETE SECTOR

Despite its high economic relevance, the construction sector is considered a major responsible of the environmental degradation due to the negative impacts generated by the extraction and consumption of raw materials, the intensive water and energy consumption and the elevated waste generation. The European construction industry exhausts more than 50% of European natural resources (Schultmann et al., 2010), is responsible for 40% of the total European energy consumption (Zabalza Bribián et al., 2009), and generates 34% of the waste produced annually (European Environment Agency, 2015). Since it is the most consumed building material of the planet, the sustainability of the concrete sector is especially important.

2.1. WATER USAGE

The concrete manufacture and the production of its raw materials (cement, sand and gravel) involve large amounts of water. The cement industry requires water for cooling equipment, in emission control systems and for preparing slurry in wet process kilns. Moreover, the production of aggregates entails important water consumption if wet screening and washing procedures are included. Finally, the manufacture of concrete also necessitates water for the production (hydration process) and curing and cleaning processes. These demands represent a high depletion potential of surface and groundwater resources; thus, these industries are trying to palliate the negative environmental impacts associated to the water consumption by using harvested rainwater and recycled water from manufacturing processes.

The impact posed by water consumption of concrete on water resources can be assessed by the determination of its water footprint (WF). According to Hoekstra et al. (2011) a product WF comprises the amount of water that is consumed and polluted in all processing stages of its production; hence, WF encompasses a direct and an indirect component, and it is measured in water volume per unit of production. For example, Holcim employs 185 litres of water to manufacture 1 tonne of cement, 282 litres of water for the production of 1 tonne of aggregates, and 283 litres of water to produce 1 m^3 of concrete (Holcim, 2014).

2.2. EMISSIONS FROM THE CEMENT PRODUCTION

Although it is estimated that the cement manufacture requires about 1.46 t of raw materials (limestone, clay, shale, marl, gypsum and mineral additions) per tonne of cement, the major impacts of its production fall onto the atmosphere as the generation of effluent is negligible (Schorcht et al., 2013).

It is estimated that the cement industry produces a 5% of the global manmade CO_2 emissions (Humphreys and Mahasenan, 2002; Damtoft et al., 2008), although it is only responsible for 3% of total anthropogenic greenhouse gas (GHG) emissions (Damtoft et al., 2008).

The majority of the CO_2 emissions of the cement industry are related to the clinker production, which can be derived from de-carbonation of the raw materials or the fuel burned in the kiln (Gartner, 2004), corresponding to a 62% and 38% of the total respectively (Schorcht et al., 2013). Furthermore, in the latter category, a distinction could be made between indirect emissions due to generation of electricity and direct emissions bound to fuel combustion in the kiln.

Humphreys and Mahasenan (2002) calculated that on average 0.87 kg of CO_2 are emitted for every kilogram of produced cement, and Damtoft et al (2008) estimated that CO_2 emissions ranged from 0.84 kg to 1.15 kg per kilogram of clinker production depending on the employed kiln. Process types and fuel shares differ considerably among regions modifying the actual CO_2 emissions figures. In 2013, the cement production in the European Union was responsible for the emission of 103 millions of tonnes of CO_2, excluding on-site power emission generation, which corresponds to 623 kg of gross CO_2 emissions (including those from use of wastes as fuel) per tonne of cement equivalent and 563 kg of net CO_2 emissions per tonne of cement equivalent (WBCSD/CSI, 2013).

In addition, exhaust gases in the cement production also contain SO_2, NO_x and dust, amongst others of minor entity. Most of the SO_2 emissions originate from the fuel combustion operations in the kiln or by vehicles and produce acidification. However, a high fraction of the SO_2 can be converted to calcium sulphate in the calcining zone, leaving the kiln absorbed within the clinker due to its high alkalinity (Schuhmacher et al., 2004). The NO_x values, which refer to both NO_2 and NO, are related to the fuel usage and also to the combustion during clinker production, thus varying according to the kiln used (Schorcht et al., 2013), but also during the energy consumption of other manufacture operations. Finally, cement kiln dust with a size range between 0.05 µm and 5 µm is also released from the burning and cooling processes, which may cause risks to the human health since these inhalable particulates, classified as PM_{10}, are caustic and irritant in nature (Schuhmacher et al., 2004). Nevertheless, according to Schuhmacher et al. (2004) these three pollutants turn out to cause low health risks.

The pressures for a sustainable cement industry have led to the recycling of wastes from other industrial branches in the cement production. The use of natural and artificial pozzolans is considered the most promising method to reduce the CO_2 emissions (Gartner, 2004). For instance, the use of blast furnace slag, which is a by-product form the steel production, generates an overall reduction of CO_2 emissions, since less amount of Portland cement clinker is required and the end-life management the waste is avoided, ranging from 29% to 46%; and furthermore, its use implies direct savings of about 4% to 15% in virgin raw materials (Prusinski et al., 2004). Another way to reduce emissions, as well as fossil fuel consumption, relies in the use of alternative fuels (Davies and Worthington, 2001; Damtoft et al., 2008). In 2030, 23.5 Mt of CO_2 emissions could be avoided if current trends in fuels substitutions are maintained (Joint Research Centre, 2014). The strategies for reducing the secondary emission consists of the use of lime hydrate (SO_2), flame cooling (NO_x), electrostatic precipitators and cascade impactors (PM_{10}).

2.3. SAND AND GRAVEL DEPLETION

Since concrete is the most used construction building material in the world, the consumption of sand and gravel, which represent around a 80% by mass in concrete, accounts for the largest volume of solid material extracted worldwide. According to Steinberger et al. (2010), sand and gravel account from 68% to 85% of the 47-59 billion tonnes of mined materials annually. The European Aggregates Association (UEPG, 2015) reported that the annual demand of aggregates in the European Union is up to 2.70 billion tonnes, of which 25% are required by the ready-mix concrete industry and 20% are destined to precast concrete and architectural concrete products.

To date, no signs of a worldwide shortage of natural aggregate has been perceived; however, note that, depending on the size of the studied territory, the depletion of bulk resources is perceived differently (Habert et al., 2010). Nonetheless, in 2014, the United Nations Environment Programme (UNEP, 2014) alerted of the actual depletion risk that a continued trend in the consumption of aggregates could cause.

Besides the resource depletion, the magnitude of the extracted volumes is bound to cause relevant environmental impacts (Sonak et al., 2006). Sand and gravel extraction affect the biodiversity of flora and fauna due to impacts on terrestrial, fluvial and coastal ecosystems and generate changes in the landscape. The aggregates also have a contribution in the CO_2 emissions of the concrete sector, ranging between 0.004 kg and 0.008 kg per kilogram of alluvial and crushed natural aggregate respectively (FIB, 2012), mainly due to the required energy for their production. Moreover, the mining operations are responsible for dust and noise generation and potential groundwater contamination (Krausmann et al., 2011).

Alternative sources of sand and gravel, such as the use of recycled aggregates arising from CDW, could substitute natural aggregates in concrete production, at least to reduce the industry dependence on natural resources. More environmental benefits are achieved by using wastes as secondary aggregates since the need for landfilling is reduced. However, nowadays, recycled aggregates only cover a 5% of the total production, while the remaining aggregates come from pits (39%), are crushed rock from quarries (53%) and are manufactured or sea dredged (3%) (UEPG, 2015).

2.4. ENERGY CONSUMPTION

In the production of concrete, the energy consumed from the mining and processing of natural resources to the manufacturing is commonly defined as embodied energy, and has been estimated between 0.89 MJ per kilogram (Struble and Godfrey, 2004) and 1.40 MJ per kilogram (Alcorn and Baird, 1996). Moreover, the embodied energy of reinforced concrete increases up to a 63% (Zabalza Bribián et al., 2011) because the energy demanded in the production of the steel rebar should be added.

Nonetheless, it is recognised that most of the embodied energy of concrete is used in the cement production for crushing, grinding, rotating the kiln, etc. Annually, at a European cement plant, the power consumption and the required thermal energy were, on average, 117 kWh per tonne of cement and 3.75 MJ per tonne of clinker, respectively (WBCSD/CSI, 2013). According to Taylor et al. (2006), these figures could be reduced if supplementary cementitious materials, dry processes and pre-calcination techniques are used. For instance, the use of blast furnace slag could produce energy savings ranging from 21.10% to 48.40% (Prusinski et al., 2004). In addition, the impacts associated to the energy demand in the cement production could be reduced by the use of alternative fuels, since the environmental impacts caused by energy consumption depend on the type of energy used (Sev, 2009). However, such use is below 5% in Spain, far behind the European average of 35%. (Zabalza Bribián et al., 2011).

Finally, besides the energy needed for the raw materials production, at the concrete plant electricity and fuel are required for mixing all the components. The energy consumption for the operations at a ready-mix concrete plant have been estimated as 4% of the embodied energy of concrete (Marceau et al., 2006)

2.5. WASTE

Solid wastes are generated during the raw material production and concrete processing. While dust is the principal waste in the cement and aggregate production, wastes derived from the concrete batching include mixer washout, sludge and returned excess of fresh concrete (Gursel et al., 2014). On average, the amount of waste generated by the ready-mix concrete sector is up to 0.45% of the total production, with maximum about 5-9% in times of great demand pressure (WBCSD/CSI, 2009). Regarding the precast concrete industry, the generation of concrete waste primarily happens due the rejection of constructive elements in the quality control procedure; a study suggested that the amount of waste is around 1-3% of gross production (Kaysser and Kott, 2002).

In order to improve the sustainability of the sector, the waste generated in the ready-mix and precast industries, as well as the concrete waste arising at the end of life of concrete buildings, could be recycled as secondary aggregate that, besides other low level applications, could be employed for the manufacture of new concrete. In Spain, secondary aggregates from crushed concrete represent the 15% and 30% of the recycled aggregates production and market (Güell-Ferré et al., 2012). As previously stated, the reutilization of CDW in the concrete sector is a symbiotic practice with twofold environmental advantages as it reduces the use of natural resources and avoids the landfilling.

3. LIFE CYCLE ASSESSMENT

Despite the numerous methods for the evaluation of the environmental impacts, the life cycle assessment (LCA) is one of the most widely employed due to its proficiency to calculate the potential effects that a product, process or service has on the environment over the entire period of its life cycle. Based upon the life phases considered, three types of LCA could be distinguished:

- Cradle to gate: This approach only considers the impact of raw material extraction, the production of materials and product parts until the end product leaves the gate of the factory. This assessment is the base for Environmental Product Declarations (EPD)

- Cradle to grave: In this approach, the transportation of the product until the service site, the use and repair stage and the final disposal at the end of its presumed lifespan are also included.

- Cradle to cradle: The end of life phase is considered in this approach in order to analyse the reuse, recovery and/or recycling potential of a product, good or service. This scenario is based on the notion that products should be designed in such a way that they could be recycled as raw material at the end of their life cycle, which represents the closed loop of production and circular economy.

The LCA framework and guidelines are described in UNE EN ISO 14040 (2006) and UNE EN ISO 14044 (2006). Briefly, the LCA methodology consists of four phases (Figure 10.1).

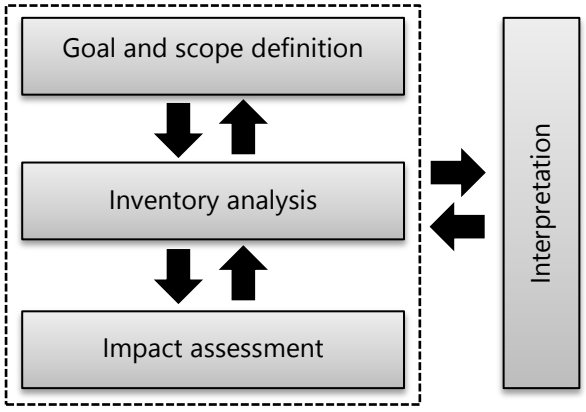

Figure 10.1: Phases on a life cycle assessment (LCA)

1. Goal and scope definition: This step identifies the purpose, functional unit, system boundaries, data quality, assumption and limitations of the study.

2. Inventory analysis: In this stage, information about the different unit processes is gathered in the form of inputs (primary raw materials, energy, etc.) and outputs (emissions to air, soil and water, waste, by-products, etc.) with respect to the environment. Great sources of information in this step are EPD and specific databases such as Ecoinvent (Frischknecht et al., 2005).

3. Impact assessment: To translate environmental measurements into ecological damage, several models have been developed such as Eco-indicator 99 (Goedkoop and Spriensma, 2001) or CML 2001 (Guinee, 2002) establishing different impact categories. In this phase, the potential environmental effects of the product, process or service during its lifecycle are quantified and characterized according to the relevant categories.

4. Interpretation: To conclude the analysis, the results are assessed in order to detect environmental issues and establish recommendations.

3.1. LITERATURE REVIEW: CONSTRUCTION AND DEMOLITION WASTES

Environmental protection has become an issue of global importance. Within the sustainable measures adopted by the construction industry, the CDW management and its recycling as secondary aggregates has been studied as a possible way to reduce the environmental burden on natural resources and to decrease the waste generation. To date, several authors have performed LCA to analyse the environmental benefits of CDW management practices.

Craighill and Powell (1999) applied a LCA methodology to evaluate the environmental, social and economic impacts of CDW management options. The authors concluded that CDW reuse has the lowest overall impact, followed by a combination of reuse and recycling, with landfill the least desirable option. However, the results have been questioned due to some methodological shortcomings (Tiruta-Barna et al., 2007).

Blengini (2009) conducted a cradle to grave LCA of the demolition of a building analysing different scenarios for the end-of-life management of CDW. Recycling aggregates achieved 19% energy savings and 10% greenhouse emissions savings. Later on, Blengini and Garbarino (2010) proved that the use of recycled aggregates from CDW resulted in an eco-efficient solution since the impacts of their production were lower than those avoided by their reutilization, and that the cost of treatment was covered by the avoidance of landfill taxes and the revenues of the recycled aggregates. Conjointly with the LCA, a GIS analysis on the transport distances was carried out in order to study the sensitivity of this factor. It was found that the transportation of recycled aggregates should experience a twofold or threefold increase before the CDW recycling loses the environmental gains.

Ortiz et al. (2010) compared three CDW management scenarios (landfilling, recycling and incineration). Because of the avoided impacts of the recovered materials, recycling was the most environmentally friendly scenario. Despite higher global warming potential impacts than landfilling, incineration was identified as the second best CDW management option. Kucukvar et al. (2014) also analysed the same three waste management options for different CDW fractions using an hybrid LCA model. Once again, recycling was recognized the better option for water, energy and carbon footprint reduction.

The results of Dahlbo et al. (2015) studying the potential climate change impacts of CDW management by means of an LCA showed that the recycling had an overall positive environmental effect, although the initial composition of the waste conditioned the actual benefit. Miscellaneous wastes, which correspond to the CDW studied in the present research, were considered among the fractions with a higher potential for reduction of climate change impacts.

Regarding the environmental effect in the generation of CDW, Coelho and de Brito (2012) performed an LCA comparing the environmental advantages that different deconstruction scenarios have over typical demolition. Full deconstruction was the most environmental friendly option regardless of the reuse/recycle ratio of the recovered materials. The deconstruction of non-structural elements was slightly better than the selective demolition of non-structural elements or soft-stripping, which in some impact categories performed worse than the typical demolition.

The LCA carried out by Mercante et al. (2012) on the CDW management as a function of the type of recycling plant showed that the type of plant affects the value of the impact indicators, the transportation stage plays a decisive role and recycling is not always beneficial. It was also found that the processing of concrete has a higher environmental impact than the processing of mixed CDW due to higher power requirements in the grinding stage. Continuing that research topic, Coelho and de Brito (2013a, 2013b) quantified basic environmental impact factors at a fixed large-scale CDW recycling facility in Portugal. They concluded that recycling CDW was environmentally beneficious in terms of energy consumption and CO_2 equivalent emissions (Coelho and de Brito, 2013a). From the sensitivity analysis (Coelho and de Brito, 2013b), environmental benefits can still be expected even if higher than expected transportation needs arise or separated input CDW mass (which reduces the environmental gains by means of metal recycling) are received for treatment.

Finally, facing the general lack of leaching emissions in the assessment of CDW as unbound material (Blengini, 2009; Blengini and Garbarino, 2010; Coelho and de Brito, 2012; Mercante et al., 2012; Kucukvar et al., 2014). Butera et al. (2015) included the leaching, as well as the carbonation of the concrete fraction, in their LCA model analysing the use of recycled aggregates from CDW in a road construction scenario. Except for non-carcinogenic human toxicity, freshwater ecotoxicity and freshwater eutrophication, the use of CDW in road constructions was a more environmentally favourable option than landfilling. Similar to other studies, transportation distances shorter than 40 km were recommended to ensure the environmental benefits. Previously, Collins (2010) also considered the CO_2 sequestered in the recycled aggregates due to the carbonation of the parent concrete in the LCA study of a bridge made with RCA, which could mean a reduction between 13% and 48% of the greenhouse gas emissions in function of the cement type and the application of the RCA.

3.2. LITERATURE REVIEW: RECYCLED CONCRETE AGGREGATES FROM CONSTRUCTION AND DEMOLITION WASTES

Contrarily, fewer studies focused on performing LCA evaluating the use of CDW as aggregates in the recycled concrete manufacture. Evangelista and de Brito (2007) studied the environmental gains achieved by the use of 30% and 100% fine recycled aggregates substitution in the manufacture of recycled concrete. The authors found that the benefits were obvious even considering the lower service life of recycled mixes. Chowdhury et al. (2010) found that recycled concrete pavement aggregates presented a higher impact in terms of energy demand, acidification potential and greenhouse warming potential, which was mainly due to the required production process. Once again, recycled aggregates were registered as environmentally beneficial if transport distances of recycled aggregates were at least one fourth shorter. Similarly, Marinković et al. (2010) reported slightly higher impacts in recycled concrete. Those results could be in part attributed to the use of a LCA attributional model and the fact that the proportioning of recycled mixtures had an additional 5% cement. Under these assumptions, recycled concrete was only environmentally beneficial if transport distances of recycled aggregates were approximately 7.5 times nearer.

Knoeri et al. (2013) compared conventional and recycled concrete mixtures with varying replacement percentages and concluded that the environmental impacts could be reduced up to 70% due to the iron recovery form the CDW and the avoidance of their transport and disposal in a landfill. They also stated that CDW composition has little effect on the results, while additional distances (about 15 km) in the transport of recycled aggregates shifted the positive environmental balance of RCA in terms of global warming potential. Lastly, Turk et al. (2015) performed a LCA analysis on recycled concrete made with partial substitution of reinforced waste concrete aggregates and obtained a reduction in the environmental impacts of 12% on average; nonetheless, the global warming indicator was only lowered with 4%. The reduction of landfilling is the main responsible for the improvement in the environmental performance, although the environmental benefits of the use of recycled aggregates depended on the delivery distances and was limited to a 100 km one-way distance.

4. CASE STUDY

4.1. GOAL AND SCOPE DEFINITION

The aim of the case study was to analyse the life cycle impacts of several recycled concrete types made with a 50% substitution of recycled aggregates from CDW with varying percentages of ceramic waste corresponding to the phase I of this investigation, and to compare the results with those of a conventional concrete mixture. The main purpose of the study was to evaluate the potential environmental benefits of recycling CDW as a sustainable measure for the concrete industry.

The phases of the life cycle of concrete are shown in Figure 10.2. However, the system boundaries of this case study were limited to a cradle to gate LCA, corresponding to the production of raw materials – i.e. extraction and processing of natural aggregate, processing of CDW into recycled aggregates, water exploitation and the production of cement - their transport to the concrete plant and the batching operations of the concrete plant, which are coloured in grey in Figure 10.2. The rest of the phases of the concrete life cycle were omitted from the analysis. Furthermore, similarly to Turk et al. (2015), the avoided impacts resulting from the recycling of CDW and reutilization of recycled aggregates are illustrated accordingly in black solid rectangles as a matter of account system expansion, and thus are both treated as environmental credits.

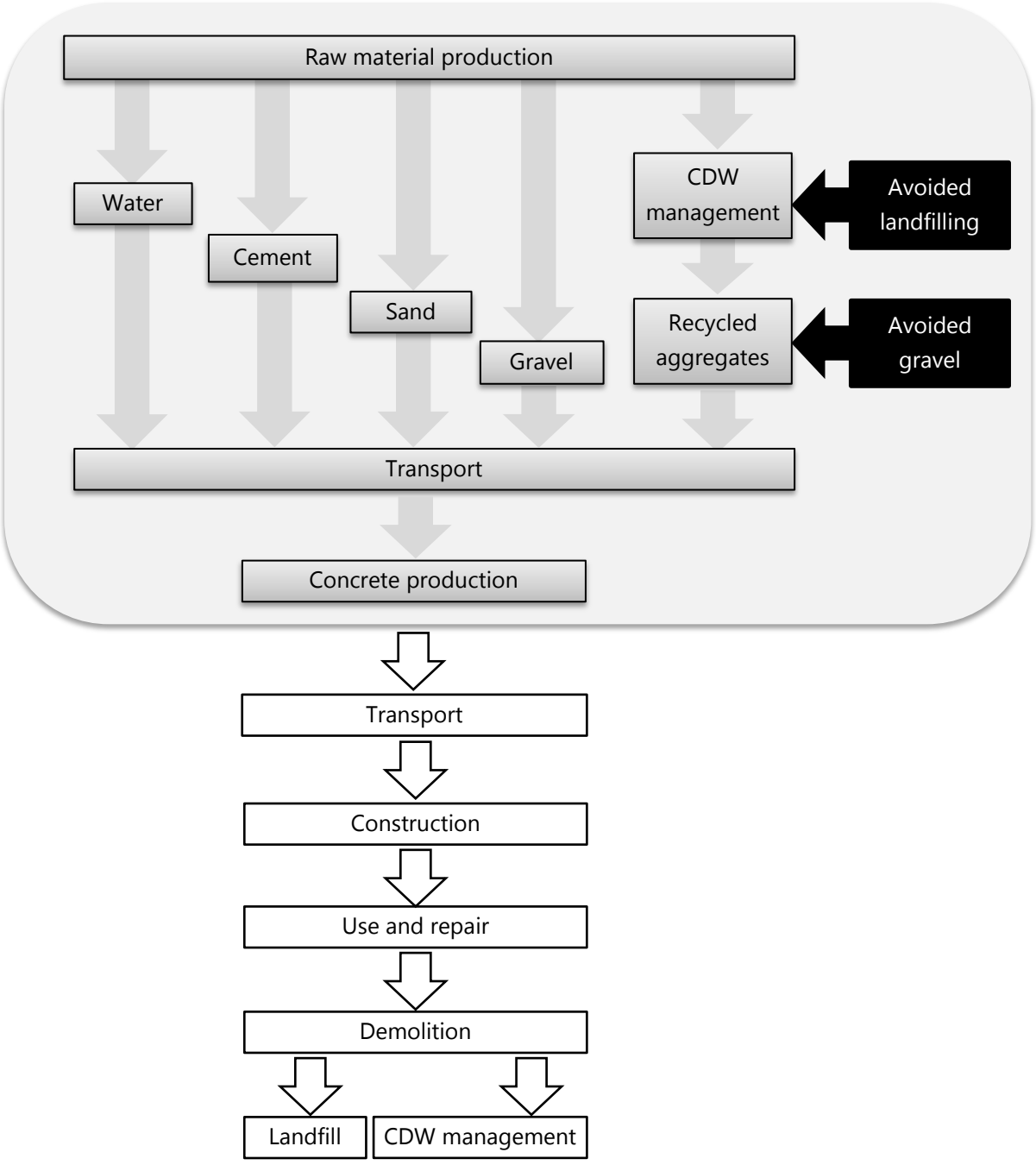

Figure 10.2: Life cycle of concrete and scope of the case study LCA

The selected functional unit or reference unit of the product system for which the environmental impact will be calculated (UNE EN ISO 14040, 2006), was the production of 1 m^3 of the conventional and recycled concrete mixtures pertaining to the first research phase. Provided that all mixtures comply with the design properties to be used in substitution of the conventional concrete, this functional unit was chosen in order to account only for the environmental differences due to the mixture proportioning caused by the incorporation of recycled aggregates.

4.2. INVENTORY ANALYSIS

The life cycle inventory was built based upon the data from the Ecoinvent 2.0 database (Frischknecht et al., 2005) and managed with the SimaPro LCA software (PRé Consultans bv, 2011). Provided that most of the data available in Ecoinvent is specific for Switzerland or, at best, a European average, the inventory data was revised and adaptations were made to take into account specific aspects of the Spanish scenario, such as the adoption of the Spanish energetic mix instead of the Swiss energetic mix.

4.2.1. WATER

Table 10.1: Ecoinvent inventory data for the production of 1 kg of tap water

	Amount	Unit
Resources		
Water, river	5.13×10^{-4}	m^3
Water, lake	2.05×10^{-4}	m^3
Water, well, in ground	4.10×10^{-4}	m^3
Materials/fuels		
Electricity, medium voltage, production UCTE, at grid/UCTE U*	3.90×10^{-4}	kWh
Chlorine, liquid, production mix, at plant/RER U	1.00×10^{-7}	kg
Hydrogen peroxide, 50% in H_2O, at plant/RER U	8.80×10^{-7}	kg
Ozone, liquid, at plant/RER U	3.33×10^{-6}	kg
Charcoal, at plant/GLO U	4.17×10^{-6}	kg
Aluminium sulphate, powder, at plant/RER U	6.33×10^{-6}	kg
Water supply network/CH/I U	3.14×10^{-10}	km
Pump station/CH/I U	2.06×10^{-11}	p
Water storage/CH/I U	2.06×10^{-11}	p
Water works/CH/I U	1.19×10^{-11}	p
Transport, freight, rail/RER U	8.89×10^{-6}	tkm
Transport, lorry >16t, fleet average/RER U	1.48×10^{-6}	tkm
Emissions to air		
Heat, waste	1.40×10^{-3}	MJ
Emissions to water		
Aluminium	1.29×10^{-6}	kg
Chlorine	1.00×10^{-7}	kg
Chloride	5.04×10^{-6}	kg
Waste to treatment		
Disposal, wood untreated, 20% water, to municipal incineration/CH U	4.17×10^{-6}	kg
Treatment, sewage, unpolluted, to wastewater treatment, class 3/CH U	1.77×10^{-5}	m^3

The Ecoinvent inventory data for 1 kg of tap water (Table 10.1) was employed as the mixing water used in all concrete mixtures, as the impacts related to this process could be considered an European average.

4.2.2. CEMENT

Table 10.2 gives an overview of the Ecoinvent inventory data for the production of 1 kg of blast furnace slag cement. This process includes the manufacturing operations as well as the transport and the specific infrastructure at the plant. Note that for blended cement, the clinker production is incorporated as a sub process, which contains data on raw material use and emission values for cement production (burning and milling).

Table 10.2: Ecoinvent inventory for 1 kg of blast furnace slag cement

	Amount	**Unit**
Materials/fuels		
Ethylene glycol, at plant/RER U	5.50×10^{-4}	kg
Clinker, at plant/CH U	4.60×10^{-1}	kg
Cement plant/CH/I U	5.36×10^{-11}	p
Electricity, medium voltage, at grid/ES U	7.83×10^{-2}	kWh
Steel, low-alloyed, at plant/RER U	1.10×10^{-4}	kg
Heavy fuel oil, burned in industrial furnace 1MW, non-modulating/CH U	1.03×10^{-1}	MJ
Transport, lorry 3.5-20t, fleet average/CH U	2.70×10^{-2}	tkm
Emissions to air		
Heat, waste	2.82×10^{-1}	MJ

4.2.3. NATURAL AGGREGATES

Sand and gravel are products of the natural disintegration of rocks, generally occurring in alluvial, subterranean or subaqueous deposits as poorly consolidated materials. Thus, extraction, screening and washing operations are the main part of their manufacture process. Besides the manufacturing operation, the process involves the land use, the future environmental recovery, the transport and the infrastructure for the operation. On the contrary, no dust was included since it is a wet treatment and the water employed is not considered polluted as no further treatment is required.

As round gravel and sand derive from the same process, the inventories of both products in the Ecoinvent database are identical, although the production mix is around 65% and 35% of gravel and sand respectively. Table 10.3 shows the modified Ecoinvent life cycle inventory of 1 kg of sand or gravel.

Table 10.3: Ecoinvent inventory for 1 kg of gravel or sand

	Amount	Unit
Resources		
Gravel, in ground	1.04	kg
Occupation, mineral extraction site	2.88×10^{-4}	m^2a
Occupation, water bodies, artificial	6.27×10^{-5}	m^2a
Transformation, to mineral extraction site	2.88×10^{-5}	m^2
Transformation, to water bodies, artificial	6.27×10^{-6}	m^2
Water, unspecified natural origin/m3	1.38×10^{-3}	m^3
Transformation, from unknown	3.50×10^{-5}	m^2
Materials/fuels		
Building, hall, steel construction/CH/I U	5.03×10^{-7}	m^2
Conveyor belt, at plant/RER/I U	9.51×10^{-8}	m
Diesel, burned in building machine/GLO U	1.47×10^{-2}	MJ
Electricity, medium voltage, at grid/ES U	2.72×10^{-3}	kWh
Heat, light fuel oil, at boiler 10kW, non-modulating/CH U	2.44×10^{-3}	MJ
Industrial machine, heavy, unspecified, at plant/RER/I U	1.12×10^{-5}	kg
Lubricating oil, at plant/RER U	1.85×10^{-6}	kg
Mine, gravel/sand/CH/I U	4.75×10^{-11}	p
Recultivation, limestone mine/CH U	8.48×10^{-6}	m^2
Steel, low-alloyed, at plant/RER U	1.30×10^{-5}	kg
Synthetic rubber, at plant/RER U	2.00×10^{-6}	kg
Tap water, at user/RER U	1.01×10^{-2}	kg
Transport, lorry 3.5-20t, fleet average/CH U	8.79×10^{-7}	tkm
Transport, lorry 20-28t, fleet average/CH U	1.72×10^{-5}	tkm
Transport, van <3.5t/CH U	1.55×10^{-5}	tkm
Emissions to air		
Heat, waste	9.77×10^{-3}	MJ
Waste to treatment		
Disposal, municipal solid waste, 22.9% water, to municipal incineration/CH U	2.77×10^{-6}	kg
Disposal, used mineral oil, 10% water, to hazardous waste incineration/CH U	1.85×10^{-6}	kg

4.2.4. RECYCLED AGGREGATES

Although the Ecoinvent database does not include the recycled aggregates production as a specific process, the inventory data for several unit processes were assembled in order to build a representative input-output model (Table 10.4). In the first place, the processes of "Disposal, building, brick, to sorting plant" and "Disposal, building, concrete, to sorting plant" were used as basis of the dismantling burdens (energy, emissions) of the generation of CDW and the sorting operation. Note that, the compositions of each final recycled aggregate - RA-L(S), RA-M(S) and RA-H(S) - (see chapter 4) were taken into account since the unit values sometimes depended on the type of material processed. In order to create the new unit process, a CDW management consisting of two crushing stages, several operations of sorting to recover different fractions of waste and screening to obtain different gradations was assumed. Hence, a crushing process was added, since the initial sorting operation corresponded to a CDW management plant with only one crushing stage. Finally, provided that the use of recycled aggregates conserves resources and avoids landfilling operations, both concepts were included as avoided products.

Table 10.4: Ecoinvent inventory for 1 kg of the different recycled aggregates

	Amount	Unit
Common for all recycled aggregates		
Avoided products		
Gravel, round, at mine/ES U	1.00	kg
Disposal, construction waste, to inert material landfill/CH U	1.00	kg
Materials/fuels		
Electricity, medium voltage, at grid/ES U	3.70×10^{-3}	kWh
Transport, lorry 20-28t, fleet average/CH U	2.18×10^{-2}	tkm
Crushing, rock/RER U	1.00	kg
Electricity/heat		
Sorting plant for construction waste/CH/I U	1.00×10^{-10}	p
Emissions to air		
Particulates, < 2.5 um	1.66×10^{-5}	kg
Particulates, > 2.5 um, and < 10um	6.34×10^{-5}	kg
Particulates, > 10 um	8.35×10^{-5}	kg
Heat, waste	1.33×10^{-2}	MJ
Recycled aggregate RA-L(S)		
Materials/fuels		
Diesel, burned in building machine/GLO U	4.11×10^{-2}	MJ
Excavation, hydraulic digger/RER U	6.02×10^{-4}	m^3
Recycled aggregate RA-M(S)		
Materials/fuels		
Diesel, burned in building machine/GLO U	3.85×10^{-2}	MJ
Excavation, hydraulic digger/RER U	6.48×10^{-4}	m^3
Recycled aggregate RA-H(S)		
Materials/fuels		
Diesel, burned in building machine/GLO U	3.59×10^{-2}	MJ
Excavation, hydraulic digger/RER U	6.94×10^{-4}	m^3

4.2.5. TRANSPORT

The transport of the different raw materials to the concrete plant was computed in tonne-kilometre, i.e. the load multiplied by the distance. Table 10.5 displays the inventory data for the transportation in a EURO4 type lorry with a nominal payload capacity ranging between 16 t and 32 t. The transportation of all raw materials to the concrete plant was assumed in this type of vehicle. Furthermore, one way distances were accounted in the LCA calculations, as the impacts of the transport should be shared among supplier and consumer since the common practice is that trucks do not return empty but with other goods after delivery. A transport distance for cement and natural aggregates of 100 km was assumed, while 50 km distances were considered for the transportation of the recycled aggregates since the market for this material is more local.

Table 10.5: Ecoinvent inventory for 1 tkm of transport in a EURO4 type lorry of 16-32 t

	Amount	Unit
Materials/fuels		
Operation, lorry 16-32t, EURO4/RER U	1.73 x10^{-1}	km
Lorry 28t/RER/I U	3.21 x10^{-7}	p
Maintenance, lorry 28t/CH/I U	3.21 x10^{-7}	p
Road/CH/I U	1.29 x10^{-3}	my
Operation, maintenance, road/CH/I U	2.03 x10^{-4}	my
Waste to treatment		
Disposal, lorry 28t/CH/I U	3.21 x10^{-7}	p
Disposal, road/RER/I U	1.29 x10^{-3}	my

4.2.6. CONCRETE PRODUCTION

The process "Concrete, normal, at plant" from the Ecoinvent database was adapted to the compositions (see chapter 5) of conventional and recycled concrete used in the first stage of this investigation (I-CC, I-RC-L(S), I-RC-M(S) and I-RC-H(S)). Table 10.6 displays the life cycle inventory of the production of 1 m^3 of concrete at plant. In the first part of the table, the inputs and outputs common for all concrete mixtures are listed (manufacturing operations, transport, infrastructure and waste treatment). Afterwards, the specific inputs for each composition, i.e. content of sand, gravel and recycled aggregates, as well as their transport to the concrete plant, are detailed.

Table 10.6: Ecoinvent inventory for 1 m^3 of the different concrete mixtures

	Amount	Unit
Common for all mixtures		
Materials/fuels		
Concrete mixing plant/CH/I U	4.57 x10^{-7}	p
Diesel, burned in building machine/GLO U	2.27 x10^{1}	MJ
Electricity, medium voltage, at grid/ES U	4.36	kWh
Heavy fuel oil, burned in industrial furnace 1MW, non-modulating/CH U	3.09	MJ
Light fuel oil, burned in industrial furnace 1MW, non-modulating/CH U	1.33 x10^{1}	MJ
Lubricating oil, at plant/RER U	1.19 x10^{-2}	kg
Natural gas, burned in industrial furnace low-NOx >100kW/RER U	1.16	MJ
Blast furnace slag cement, at plant/ES U	3.91 x10^{2}	kg
Steel, low-alloyed, at plant/RER U	2.38 x10^{-2}	kg
Synthetic rubber, at plant/RER U	7.13 x10^{-3}	kg
Tap water, at user/ES U	2.15 x10^{2}	kg
Emissions to air		
Heat, waste	1.57 x10^{1}	MJ
Waste to treatment		
Disposal, concrete, 5% water, to inert material landfill/CH U	1.69E x10^{1}	kg
Disposal, municipal solid waste, 22.9% water, to municipal incineration/CH U	9.51 x10^{-2}	kg
Wastewater treatment, concrete production effluent, class 3/CH U	1.43 x10^{-2}	m^3

Table 10.6: Ecoinvent inventory for 1 m^3 of the different concrete mixtures (continued)

Specific for I-CC mixture		
Materials/fuels		
Sand, at mine/ES U	6.50 $x10^2$	kg
Gravel, round, at mine/ES U	1.03 $x10^3$	kg
Transport, lorry 16-32t, EURO4/RER U	2.07 $x10^2$	tkm
Specific for I-RC-L(S) mixture		
Materials/fuels		
Sand, at mine/ES U	7.16 $x10^2$	kg
Gravel, round, at mine/ES U	4.47 $x10^2$	kg
Recycled aggregate, RA-L(S)	4.47 $x10^2$	kg
Transport, lorry 16-32t, EURO4/RER U	1.77 $x10^2$	tkm
Specific for I-RC-M(S) mixture		
Materials/fuels		
Sand, at mine/ES U	7.34 $x10^2$	kg
Gravel, round, at mine/ES U	4.26 $x10^2$	kg
Recycled aggregate, RA-M(S)	4.26 $x10^2$	kg
Transport, lorry 16-32t, EURO4/RER U	1.76 $x10^2$	tkm
Specific for I-RC-H(S) mixture		
Materials/fuels		
Sand, at mine/ES U	7.52 $x10^2$	kg
Gravel, round, at mine/ES U	4.06 $x10^2$	kg
Recycled aggregate, RA-H(S)	4.06 $x10^2$	kg
Transport, lorry 16-32t, EURO4/RER U	1.75 $x10^2$	tkm

4.3. IMPACT ASSESSMENT AND INTERPRETATION

LCA calculations were performed for all concrete compositions by means of SimaPro (PRé Consultans bv, 2011) since this software incorporates several impact assessment methods to be directly employed, of which CML 2001 and Eco-indicator 99 were selected.

Nonetheless, a custom method was first implemented in order to automatically collect elementary flows of Ecoinvent data on the principal emissions and energy and water demand in the different concrete compositions (Table 10.7). Except the emission of particulates, which increases almost a 50% when recycled aggregates are employed due to the dust generation in the CDW management (especially from the crushing stage), an environmental improvement could be observed in the production of recycled concrete. The most appreciable benefit is the saving in water (33.26% on average) because of the avoided consumption of gravel. In the same manner, the decrease in cumulative energy (8.25% on average) demand is due to the avoided operations of gravel production and landfilling of CDW. In terms of gas emissions, NO_x presents the higher reduction (10.16% on average) pointing to a reduction of fuel usage in the recycled concrete as a result of avoided impacts, and CO_2 emissions are the less affected (2.86%) since the principal responsible for this impact, i.e. cement production, remains constant for all concrete compositions.

Table 10.7: Emissions, energy and water demand of the concrete mixtures

	I-CC	I-RC-L(S)	I-RC-M(S)	I-RC-H(S)	Average improvement (%)
Energy (MJ)	1.94 x10^3	1.78 x10^3	1.78 x10^3	1.78 x10^3	8.25
Water (m^3)	4.50	2.98	3.00	3.03	33.26
Emissions (g)					
CO_2	2.33 x10^5	2.27 x10^5	2.26 x10^5	2.26 x10^5	2.86
CO	1.95 x10^2	1.84 x10^2	1.83 x10^2	1.82 x10^2	6.15
NO_x	2.46	2.22	2.21	2.20	10.16
SO_x	2.93 x10^2	2.78 x10^2	2.77 x10^2	2.77 x10^2	5.35
CH_4	2.34 x10^2	2.19 x10^2	2.19 x10^2	2.19 x10^2	6.41
NMVOC	8.31 x10^1	7.55 x10^1	7.52 x10^1	7.49 x10^1	9.51
Particulates	1.25 x10^2	1.91 x10^2	1.87 x10^2	1.84 x10^2	-49.87

4.3.1. CML 2001

Developed at Leiden University, the CML 2001 methodology organizes the results of the inventory according to the effect on environmental protection target (Guinee, 2002). Since the protection targets (Table 10.8) refer to environmental problems, this method is classified as problem-oriented according to its approach.

Table 10.8: Impact categories according to CML 2001

Impact category	Protection target	Unit
Abiotic depletion (ADP)	Human welfare, human health and ecosystem health	kg Sb_{eq}
Acidification (AP)	Soil, groundwater, surface water, organisms.	kg $SO_{2\ eq}$
Eutrophication (EP)	Air, water and soil	kg $PO_{4\ eq}$
Global warming (GWP100)	Ecosystem health, human health and material welfare	kg $CO_{2\ eq}$
Ozone layer depletion (ODP)	Human health, animal health, terrestrial and aquatic ecosystems, biochemical cycles and materials	kg CFC-11 $_{eq}$
Human toxicity (HTP)	Human environment	kg 1,4-DB $_{eq}$
Fresh water aquatic ecotoxicity (FAETP)	Fresh water ecosystems	kg 1,4-DB $_{eq}$
Marine aquatic ecotoxicity (MAETP)	Marine aquatic ecosystems	kg 1,4-DB $_{eq}$
Terrestrial ecotoxicity (TETP)	Terrestrial ecosystems	kg 1,4-DB $_{eq}$
Photochemical oxidation (POCP)	Human health and ecosystems	kg C_2H_4

Table 10.9 shows the CML 2001 impact indicators for 1 kg of the specified concrete raw materials and 1 tkm for the transport process. As expected, very low values were obtained for all impact categories of water, and the highest impacts corresponded to the cement production in most impacts categories, except ozone depletion potential which is highest for the transport operations. The negative impact values displayed by the recycled aggregates in some of the impact categories represent the environmental credit achieved by the avoidance of impacts associated to the gravel consumption and the waste landfilling.

Table 10.9: CML 2001 characterization factors per kg of the concrete raw materials and per 1 tkm for the transport

Impact category	Water	Cement	Sand/Gravel	Transport
ADP	2.04×10^{-6}	1.20×10^{-3}	2.39×10^{-5}	1.17×10^{-3}
AP	2.31×10^{-6}	1.07×10^{-3}	2.67×10^{-5}	6.34×10^{-4}
EP	5.47×10^{-7}	2.20×10^{-4}	6.18×10^{-6}	1.67×10^{-4}
GWP100	3.11×10^{-4}	4.75×10^{-1}	3.45×10^{-3}	1.65×10^{-1}
ODP	1.67×10^{-11}	1.67×10^{-8}	3.09×10^{-10}	2.61×10^{-8}
HTP	1.50×10^{-4}	5.71×10^{-2}	2.58×10^{-3}	3.89×10^{-2}
FAETP	1.18×10^{-4}	2.52×10^{-2}	8.82×10^{-4}	1.44×10^{-2}
MAETP	2.19×10^{-1}	5.87×10^{1}	1.71	3.13×10^{1}
TETP	1.81×10^{-6}	8.87×10^{-4}	1.39×10^{-5}	3.41×10^{-4}
POCP	1.29×10^{-7}	4.02×10^{-5}	9.67×10^{-7}	2.02×10^{-5}

Impact category	RA-L(S)	RA-M(S)	RA-H(S)
ADP	-2.05×10^{-5}	-2.19×10^{-5}	-2.33×10^{-5}
AP	2.30×10^{-5}	2.14×10^{-5}	1.97×10^{-5}
EP	4.80×10^{-6}	4.43×10^{-6}	4.04×10^{-6}
GWP100	2.34×10^{-3}	2.13×10^{-3}	1.91×10^{-3}
ODP	-8.13×10^{-10}	-8.40×10^{-10}	-8.66×10^{-10}
HTP	4.68×10^{-4}	3.30×10^{-4}	1.89×10^{-4}
FAETP	-1.88×10^{-4}	-1.97×10^{-4}	-2.07×10^{-4}
MAETP	-2.47×10^{-2}	-5.20×10^{-2}	-8.00×10^{-2}
TETP	-1.83×10^{-6}	-2.04×10^{-6}	-2.26×10^{-6}
POCP	2.81×10^{-7}	2.40×10^{-7}	1.98×10^{-7}

Figure 10.3 illustrates the environmental benefits of the use of recycled aggregates in comparison with the use of natural river gravel for the different impact categories of the CML 2001 methodology. The values displayed in the graph are the normalized version (CML 2001 under the West Europe 1995 criterion) of the figures in Table 10.9.

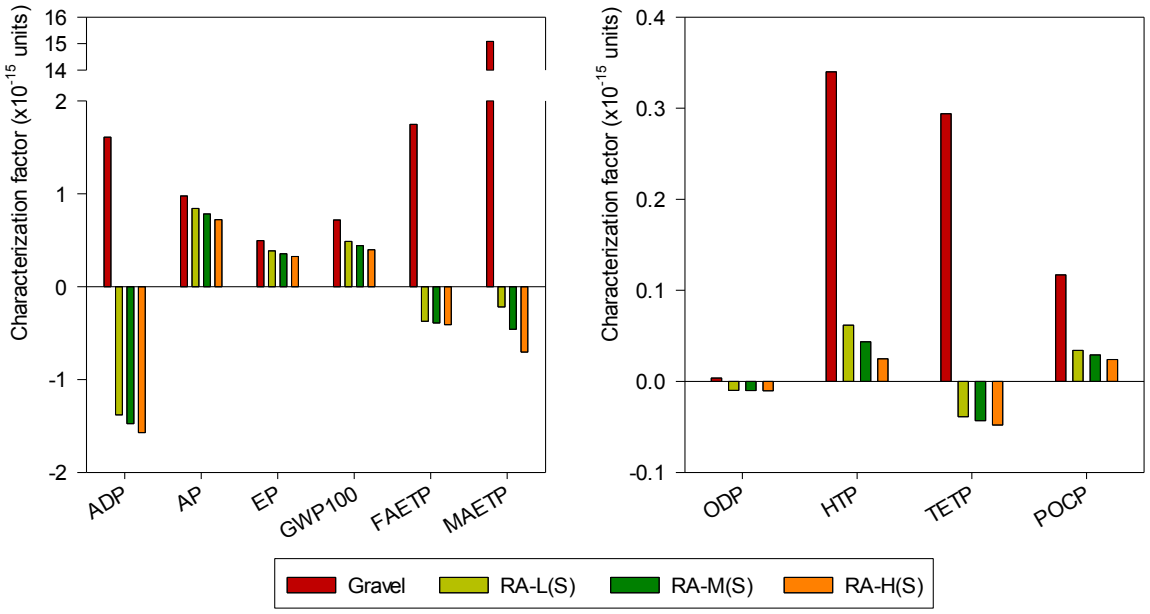

Figure 10.3: Comparison of the environmental impacts caused by the gravel and recycled aggregates production according to the CML 2001 methodology (see unit in Table 10.8)

It is clear that the environmental credits gained for the avoidance of gravel consumption and landfilling operations turn the recycled aggregates into the best environmental option for all impact categories. Nonetheless, while the impact in some categories is reduced (AP, EP, GWP100, HTP and POCP), the improvement for ADP, FAETP, MAETP, ODP and TETP categories shows a gaining balance (represented by negative figures) for the recycled aggregates. Since the use of recycled aggregates avoids the use of the same mass of natural resources, the benefit for ADP is obvious due to the reduction of the gravel extraction. Similarly, the mining of gravel and waste disposal are processes with a higher impact on the ecosystem (freshwater, marine and terrestrial) toxicity and thus the reduction. The ODP reduction is due to, principally, electricity and fuel savings in the gravel manufacture.

Table 10.10 displays the CML 2001 characterization factors for the different concrete mixtures showing the overall environmental benefits of the recycled concrete production, which perfectly reflect the environmental credit achieved by the substitution of 50% of the gravel. Thus, ADP, FAETP, MAETP, ODP and TETP are the impact categories with higher improvement.

Table 10.10: CML 2001 characterization factors for the concrete mixtures

Impact category	I-CC	I-RC-L(S)	I-RC-M(S)	I-RC-H(S)	Average improvement (%)
ADP	8.05×10^{-1}	7.38×10^{-1}	7.37×10^{-1}	7.36×10^{-1}	8.45
AP	6.4×10^{-1}	6.14×10^{-1}	6.12×10^{-1}	6.11×10^{-1}	4.32
EP	1.47×10^{-1}	1.38×10^{-1}	1.38×10^{-1}	1.37×10^{-1}	6.35
GWP100	2.33×10^{-2}	2.26×10^{-2}	2.26×10^{-2}	2.25×10^{-2}	3.15
ODP	1.32×10^{-5}	1.18×10^{-5}	1.17×10^{-5}	1.17×10^{-5}	11.11
HTP	4.50×10^{1}	4.15×10^{1}	4.15×10^{1}	4.14×10^{1}	7.85
FAETP	1.77×10^{1}	1.63×10^{1}	1.63×10^{1}	1.63×10^{1}	7.91
MAETP	3.91×10^{4}	3.65×10^{4}	3.65×10^{4}	3.65×10^{4}	6.65
TETP	4.84×10^{-1}	4.60×10^{-1}	4.59×10^{-1}	4.59×10^{-1}	5.10
POCP	2.36×10^{-2}	2.22×10^{-2}	2.22×10^{-2}	2.22×10^{-2}	5.93

Figure 10.4 illustrates the environmental improvement demonstrated by the recycled concrete made of recycled aggregates from CDW with varying percentages of ceramic waste as a function of the concrete constituents, their transport to the concrete plant and the batching operation of the concrete mixtures. In the figure, it is appreciable that operation percentage remains constant for all concrete mixtures within a specific impact category, but varies amongst them. The highest impacts are found in HTP (22.65%), FAETP (18.81%) and MAETP (17.25%), and the lowest impacts correspond to GWP100 (3.23%), ODP (5.68%) and ADP (6.45%). Provided the aim of this LCA, percentage values of both constituents and transport vary for each concrete mixture as the proportioning of sand, gravel and recycled aggregates is different and the use of recycled aggregates implies a change in the supply distance as previously stated. Nevertheless, the weight of the impact caused by the constituents is the highest for all categories. This predominance is especially noticeable in the GWP100 (around 80%) due to the major impact contribution of the cement production. Finally, transport impacts range between about 12% (TETP) and roughly 40% (ODP).

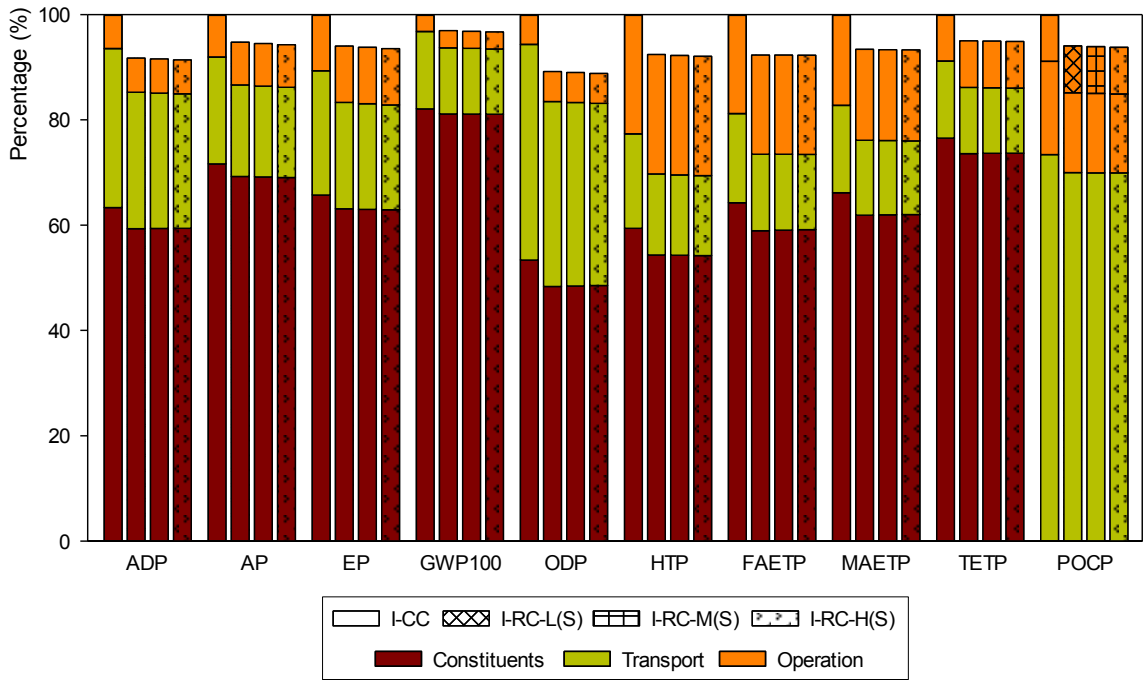

Figure 10.4: Environmental improvement of the use of recycled aggregates in concrete according to CML 1 characterization factors

The results of the life cycle impact assessment of the concrete production process for the different impact categories are presented in Figure 10.5, which displays in further detail the effect of the separate constituent materials and processes on each environmental category. Taking a first look at the results, it is seen how the environmental impact of the cement production process is the highest for all impact categories, which in a way will limit the environmental benefit achieved with the recycled concrete mixtures as all compositions were designed with the same amount of cement. The cement production process is characterized by its high CO_2 emissions, which is especially apparent in the GWP100 graph of Figure 10.5. To great extent (74.42%), the use of recycled aggregates reduces the emissions of CO_2 with respect to those in a conventional concrete; however, the required modifications in the sand content counteract somehow the effect, higher amounts in the recycled mixtures means that the CO_2 contribution of the fine aggregate is increased up to 13%. Also, an environmental credit is achieved due to the decrease in the transport distances of the recycled aggregates (14.87%).

The ODP is a measure of the destructive effects of gases on the ozone layer, and as so it is also strongly related to the CO_2 emissions of the cement production, but also to the impact of the material transport, which was reduced as the recycled aggregates required 50 km instead of 100 km. Moreover, the environmental credit of the recycled aggregates in this category was the highest due to electricity and fuels savings from the gravel manufacture, so the effect was translated to the concrete production.

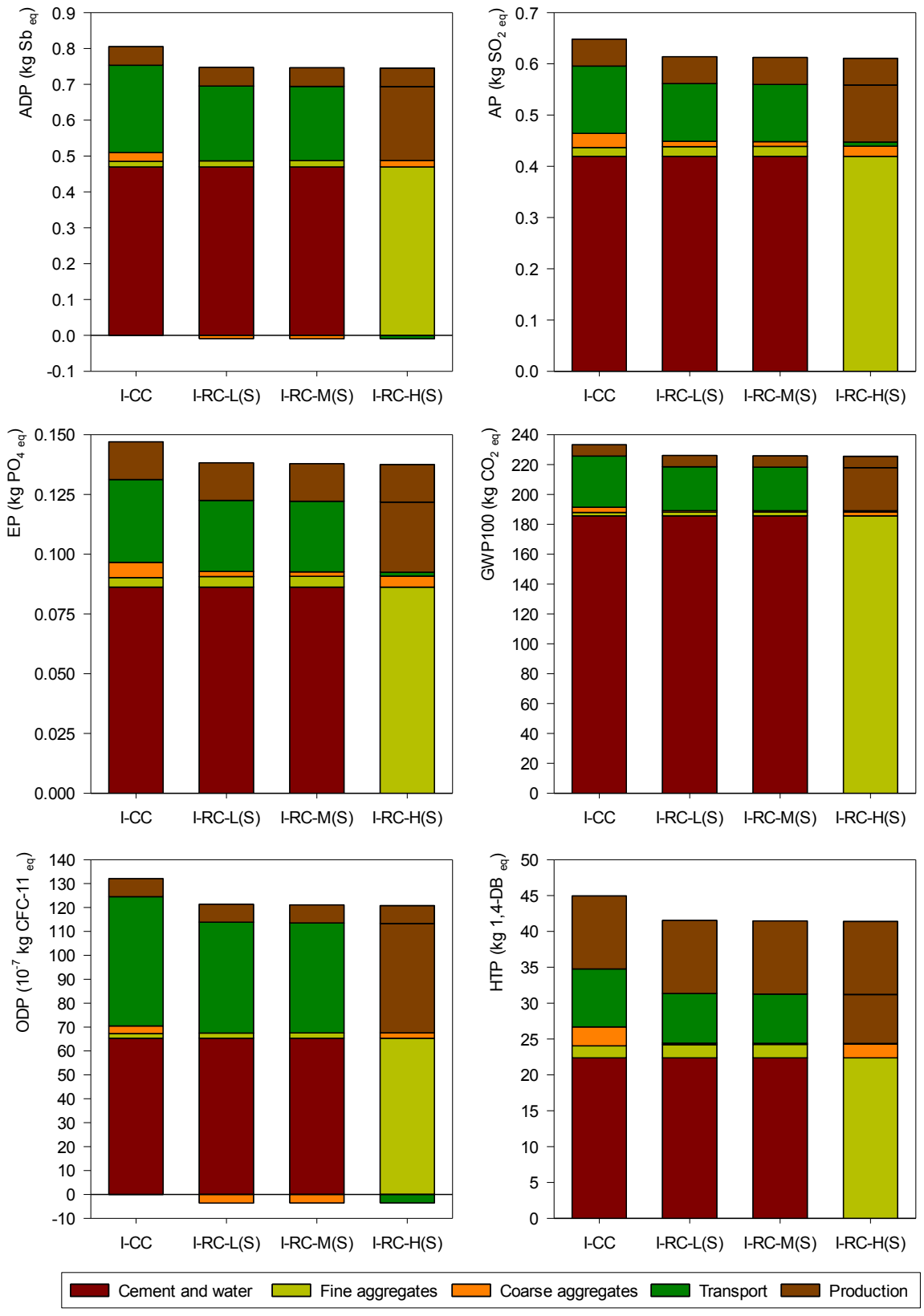

Figure 10.5: CML 2001 characterization factors for the concrete mixtures

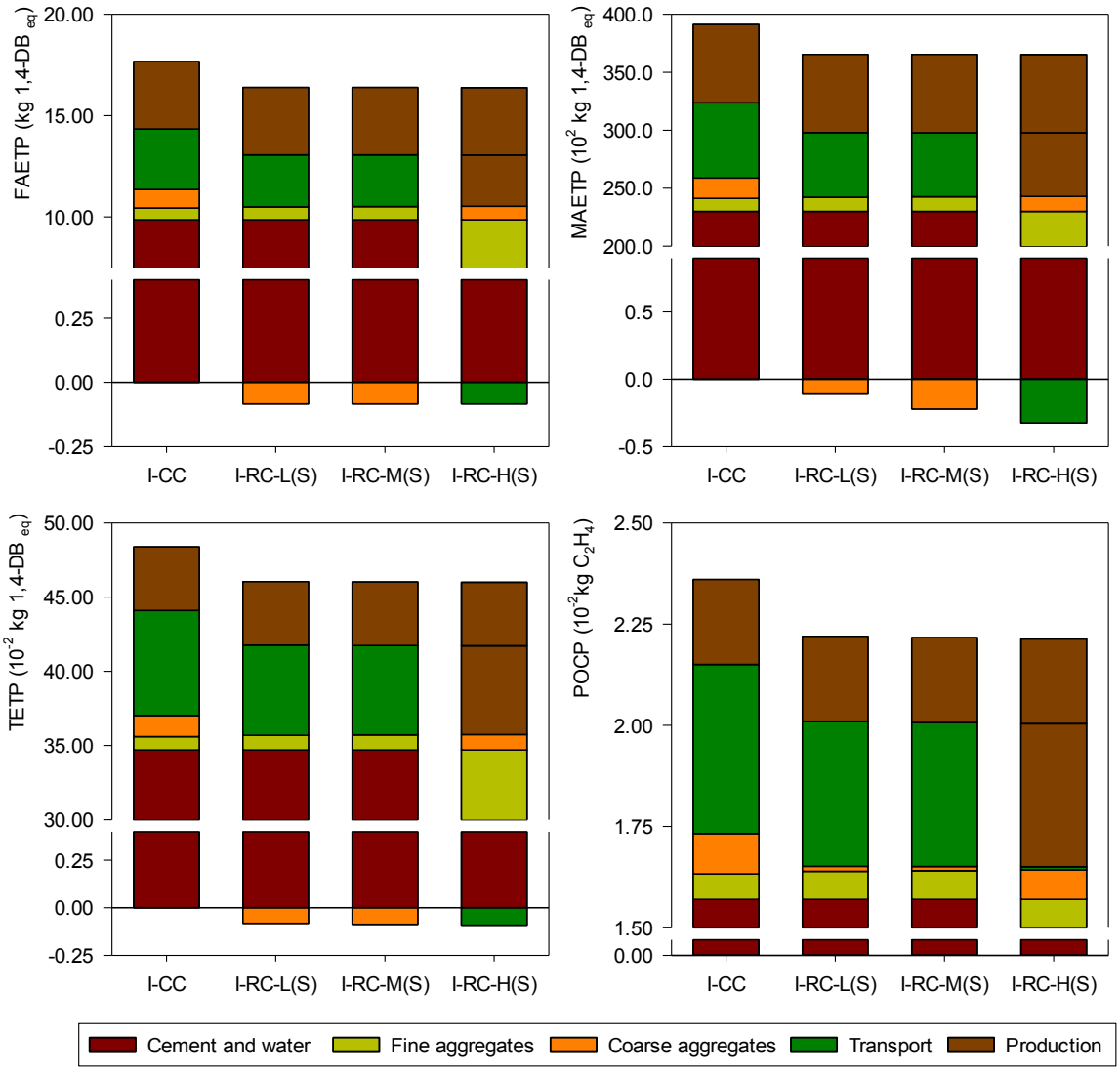

Figure 10.5: CML 2001 characterization factors for the concrete mixtures (continued)

Since ADP is related to the extraction of minerals and fossils fuels due to inputs in the life cycle inventory of each of the concrete mixtures, the environmental benefits in this category are the second highest due to the gravel substitution, which environmentally performs 2.6 times worse than the recycled aggregates in this category, but also due to the reduction in transport impacts, with an average 14.87% reduction of CO_2 emissions due to decrease in the fuel usage.

As indicated in the ecological background, the cement production and the transport are responsible for the emission of acidifying substances affecting the soil and water ecosystems, which could be appreciated in the AP graph of Figure 10.5. Nonetheless, the impact of the coarse aggregate in the recycled concretes is about 66% inferior that in the reference mixture.

The eutrophication phenomenon is due to excessive fertilization of soils and water sources, especially with phosphorous and nitrogen compounds. Mostly, these nutrients are released to the ecosystems during the manufacture of the concrete raw materials, and the use of recycled aggregates means up to 70.31% reduction in the contribution of the coarse aggregates.

In terms of toxicity, the production of recycled concrete represents an environmental benefit ranging from 5% to 8%, since the contribution of the cement production and the operation activities at the concrete plant (electricity and consumables) is far more prominent in the total impact. Nevertheless, as the impact resulting of the increase of sand amount almost counteracts the environmental gain achieved by the reduction of transport distances, the whole environmental credit is due to the lessening of the burdens represented by the coarse aggregates.

Finally, the summer smog potential, technically known as POCP, is a measure of harmful trace gases, such as NO_x, leading to detrimental impacts on human health and ecosystems by the formation of reactive substances, mainly ozone. Both the avoidance of gravel manufacture and the disposal of CDW play a similar role in the reduction of the impacts of the recycled aggregates in this category, as the use of gravel contributes 10 times more to the POCP.

4.3.2. ECO-INDICATOR 99

Also from Dutch origin, Eco-indicator 99 methodology follows a damage-oriented approach and expresses the damage to human health, ecosystem quality and resources by the weighed combination of the scores assigned to each environmental measurement by a panel of experts (Table 10.11) (Goedkoop and Spriensma, 2001).

Table 10.11: Impact categories according to Eco-indicator 99

Impact category	Combination of environmental measurements	Unit
Damage to human health	CO_2, hydrochlorofluorocarbons (HCFC); Hydrochlorofluorocarbons (HCFC); nuclides; suspended particulate matter (SPM), volatile organic compounds (VOC), NO_x, SO_x; polycyclic aromatic hydrocarbons (PAH)	Disability adjusted life years (DALY)
Damage to ecosystem quality	Pesticides, heavy metals; NO_x, SO_x, NH_3; occupation and transformation of land use	% vascular plant species x km^2 x year
Damage to mineral and fossil resources	Extraction of minerals and fossil fuels	MJ surplus energy

Figure 10.6 illustrates the underlying model in an Eco-indicator 99 evaluation. Being an end-point approach, the model starts by identifying the areas of environmental concern by means of a resource, land use and fate analysis of the LCA inventory data. Afterwards, an exposure and effect analysis considers the environmental cause-effect relations. Finally, the damage score is calculated by grouping all the impacts affecting a particular target (i.e. human health, ecosystem quality, and resources). If a single score for the indicator is required, further normalization and weighing of the damage factors should be applied to account for the different units of the categories and their relative importance, which is based on a specific area for one year and person. However, this final step was not applied in the investigation of the case study.

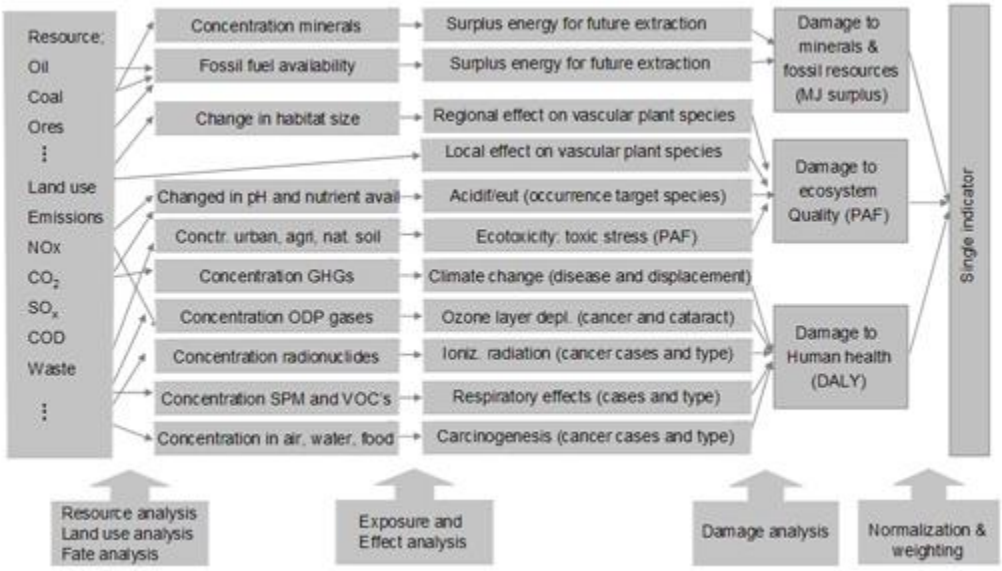

Figure 10.6: Schematic diagram for the Eco-indicator 99 approach (Goedkoop and Spriensma, 2001)

Table 10.12 shows the Eco-indicator 99 damage indicators for 1 kg of the specified concrete raw materials and 1 tkm for the transport process. As expected, very low values were obtained for all impact categories of water, and the highest impacts corresponded to the cement production in the category of damage to human health and to the transport in the categories of damage to the ecosystem quality and resources. Recycled aggregates resulted in negative impact values for these last two categories due to the environmental credit achieved by the avoidance of impacts associated to the gravel consumption and the waste landfilling. However, they present positive values in the damage to human health category due to the increase in particulate emissions resulting from their manufacture process.

Table 10.12: Eco-indicator 99 damage factors for the concrete raw materials

Impact category	**Water**	**Cement**	**Sand/Gravel**	**Transport**
Damage to human health	4.65×10^{-10}	2.77×10^{-7}	6.10×10^{-9}	1.67×10^{-7}
Damage to ecosystem quality	3.06×10^{-5}	1.05×10^{-2}	3.73×10^{-4}	1.33×10^{-2}
Damage to mineral and fossil resources	2.66×10^{-4}	2.04×10^{-1}	5.01×10^{-3}	3.33×10^{-1}
Impact category	**RA-L(S)**		**RA-M(S)**	**RA-H(S)**
Damage to human health	4.11×10^{-8}		4.07×10^{-8}	4.02×10^{-8}
Damage to ecosystem quality	-4.59×10^{-5}		-6.42×10^{-5}	-8.30×10^{-5}
Damage to mineral and fossil resources	-6.80×10^{-3}		-7.21×10^{-3}	-7.63×10^{-3}

Figure 10.7 illustrates the environmental benefits of the use of recycled aggregates in comparison with the use of natural river gravel for the different impact categories of the Eco-indicator 99 methodology. The values displayed in the graph are the Eco-indicator 99 normalized version of the figures in Table 10.12.

Taking a first look at the results, the environmental benefits of recycling CDW are limited to reduction in damages to the ecosystem quality and resource depletion. Under the Eco-indicator 99 assessment, the replacement of gravel causes higher damage to the human health.

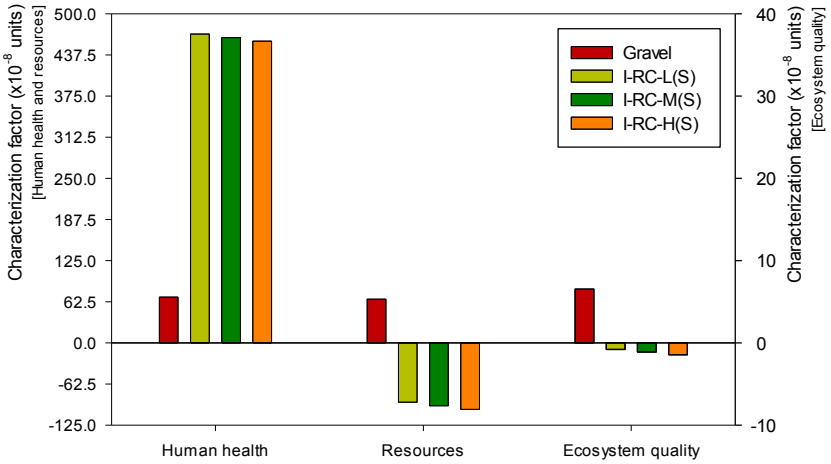

Figure 10.7: Comparison of the environmental impacts caused by the gravel and recycled aggregates production according to the Eco-indicator 99 methodology (see unit in Table 10.11)

Table 10.13 displays the Eco-indicator 99 characterization factors for the different concrete mixtures showing the overall environmental benefits of the recycled concrete production, which perfectly reflect the environmental credit achieved by the substitution of 50% of the gravel in the preservation of the ecosystem quality and the depletion of natural resources (fuels and minerals).

Table 10.13: Eco-indicator 99 damage factors for the concrete mixtures

Impact category	I-CC	I-RC-L(S)	I-RC-M(S)	I-RC-H(S)	Average improvement (%)
Damage to human health	1.69×10^{-4}	1.76×10^{-4}	1.75×10^{-4}	1.74×10^{-4}	-3.55
Damage to ecosystem quality	8.57	7.86	7.84	7.82	8.52
Damage to mineral and fossil resources	1.70×10^{2}	1.52×10^{2}	1.51×10^{2}	1.51×10^{2}	10.98

Figure 10.8 illustrates the environmental improvement demonstrated by the recycled concrete made of recycled aggregates from CDW with varying percentages of ceramic waste as a function of the concrete constituents, their transport to the concrete plant and the batching operation of the concrete mixtures. Once again, the operation percentage remains constant for all concrete mixtures within a specific impact category, but varies amongst them, from 7.24% (mineral and fossil resources) to 12.76% (ecosystem quality). The variation in the composition of the concrete mixtures represents an environmental gain up to 6.79% to the ecosystem quality and 8.85% to the mineral and fossil resources; on the contrary, it represents a 9.74% detriment regarding to the human health. Finally, a reduction (14.86%) could be observed for the transport process in all damage categories due to the decrease in the supply distance of recycled aggregate.

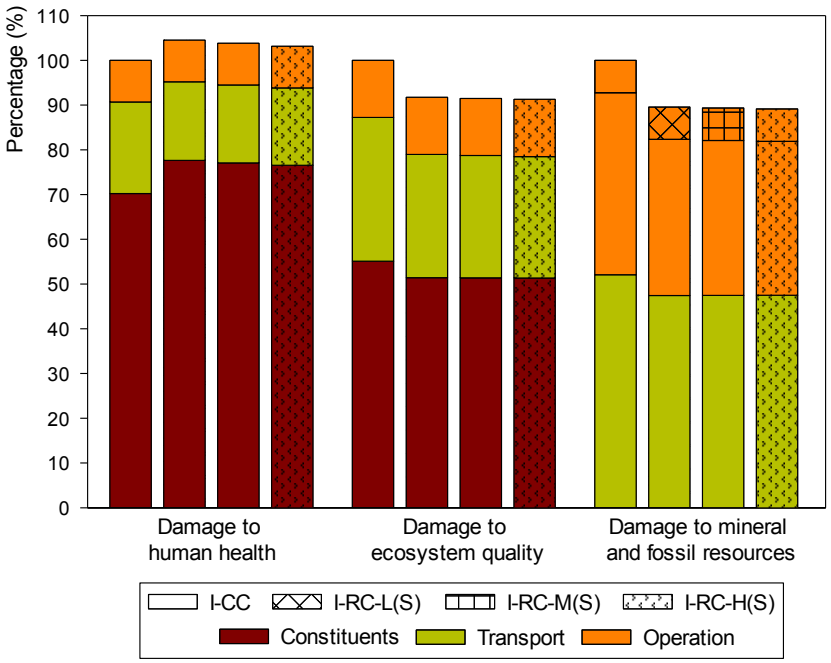

Figure 10.8: Environmental improvement of the use of recycled aggregates in concrete according to Eco-indicator 99 damage factors

A more detailed view of the results of the life cycle impact assessment of the concrete production process for the different impact categories of Eco-indicator 99 methodology are presented in Figure 10.9, which indicates the embodied environmental damage depending on the different constituent materials and processes of the concrete manufacture.

As expected, the major impacts affecting to the mineral and fossil resources are the cement production and the transport process respectively, while the recycled aggregates production represents an environmental credit (with an environmental performance 1.5 times better than the gravel), which is one pillar of environmental benefits of the use of recycled concretes. Similar behavior is appreciated for the damage to the ecosystem quality, with cement production and transport as principal responsible of the environmental impact, and virtually no impacts are attributed to the recycled aggregates production, that represents a 91.43% reduction when compared to the gravel manufacture contribution.

Despite the advantageous performance according to CML 2001 and the two aforementioned categories of the Eco-indicator 99, the bad performance of the recycled aggregates in the category of damage to the human health represent a evident downside in the recycling objective of CDW as secondary aggregates in the concrete manufacture. Nonetheless, since the generation of particulates is the driver of this environmental shortcoming, some technical measures could be applied in order to prevent or reduce the emissions.

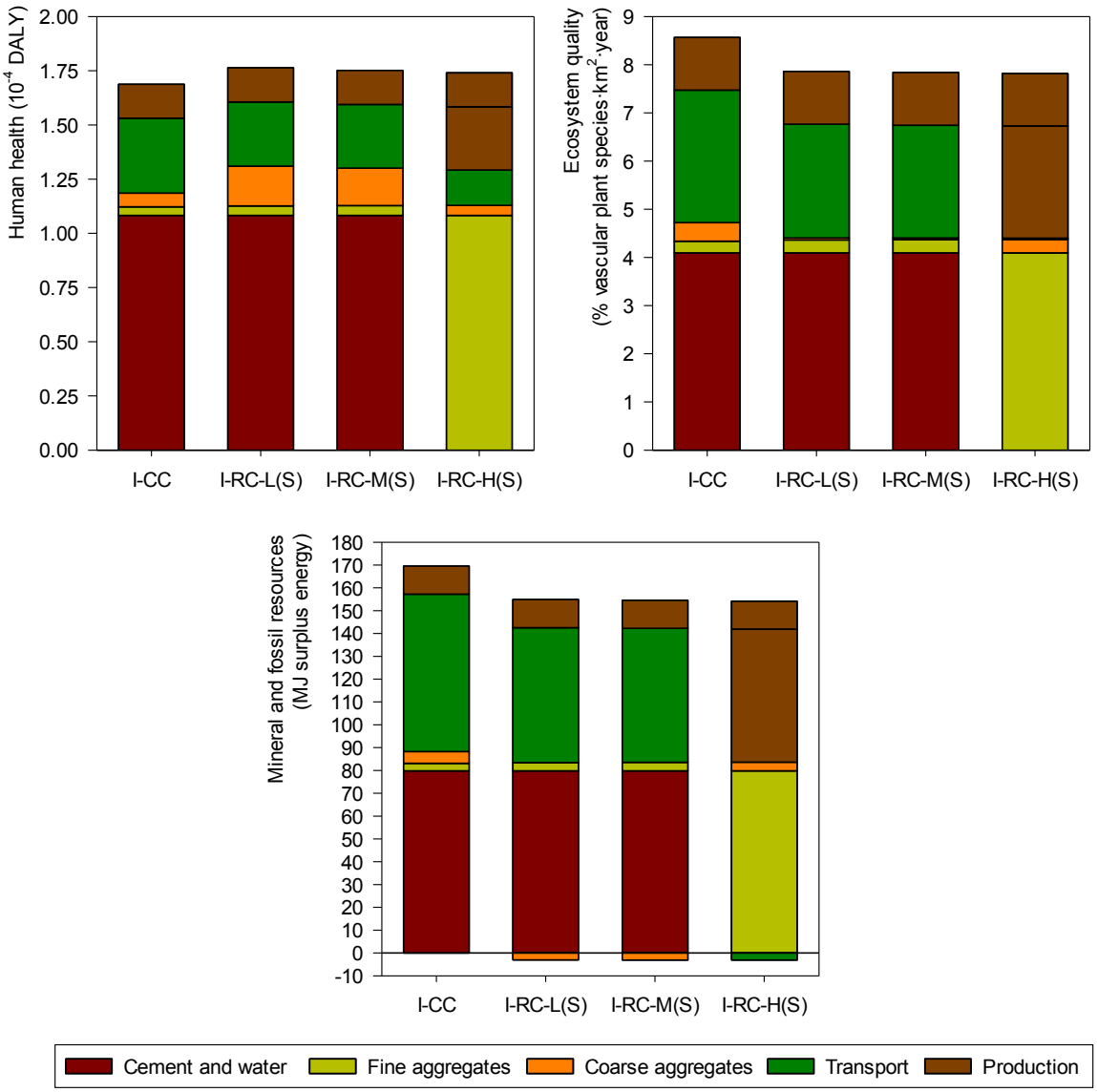

Figure 10.9: Eco-indicator 99 damage factors for the concrete mixtures

5. REFERENCES

Alcorn, J.A., Baird, G., 1996. Use of a hybrid energy analysis method for evaluating the embodied energy of building materials. *Renewable Energy*, Special Issue World Renewable Energy Congress Renewable Energy, Energy Efficiency and the Environment 8 (1–4): 319–322.

Blengini, G.A., 2009. Life cycle of buildings, demolition and recycling potential: A case study in Turin, Italy. *Building and Environment* 44 (2): 319–330.

Blengini, G.A., Garbarino, E., 2010. Resources and waste management in Turin (Italy): The role of recycled aggregates in the sustainable supply mix. *Journal of Cleaner Production* 18 (10-11): 1021–1030.

Butera, S., Christensen, T.H., Astrup, T.F., 2015. Life cycle assessment of construction and demolition waste management. *Waste Management* (In press): 10.1016/j.wasman.2015.07.011.

Cho, S.-W., 2012. Using mercury intrusion porosimetry to study the interfacial properties of cement-based materials. *Journal of Marine Science and Technology* 20 (3): 269–273.

Chowdhury, R., Apul, D., Fry, T., 2010. A life cycle based environmental impacts assessment of construction materials used in road construction. *Resources, Conservation and Recycling* 54 (4): 250–255.

Coelho, A., de Brito, J., 2012. Influence of construction and demolition waste management on the environmental impact of buildings. *Waste Management* 32 (3): 532–541.

Coelho, A., de Brito, J., 2013a. Environmental analysis of a construction and demolition waste recycling plant in Portugal – Part I: Energy consumption and CO2 emissions. *Waste Management* 33 (5): 1258–1267.

Coelho, A., de Brito, J., 2013b. Environmental analysis of a construction and demolition waste recycling plant in Portugal – Part II: Environmental sensitivity analysis. *Waste Management* 33 (1): 147–161.

Collins, F., 2010. Inclusion of carbonation during the life cycle of built and recycled concrete: influence on their carbon footprint. *The International Journal of Life Cycle Assessment* 15 (6): 549–556.

Craighill, A., Powell, J.C., 1999. A lifecycle assessment and evaluation of construction and demolition waste. Centre for Social and Economic Research on the Global Environment.

Dahlbo, H., Bachér, J., Lähtinen, K., Jouttijärvi, T., Suoheimo, P., Mattila, T., Sironen, S., Myllymaa, T., Saramäki, K., 2015. Construction and demolition waste management – a holistic evaluation of environmental performance. *Journal of Cleaner Production* (In press): 10.1016/j.jclepro.2015.02.073.

Damtoft, J.S., Lukasik, J., Herfort, D., Sorrentino, D., Gartner, E.M., 2008. Sustainable development and climate change initiatives. *Cement and Concrete Research*, Special Issue: The 12th International Congress on the Chemistry of Cement. Montreal, Canada, July 2007 38 (2): 115–127.

Davies, R., Worthington, G., 2001. Use of scrap tyre as a fuel in the cement manufacturing process, in: Recycling and Reuse of Used Tyres: Proceedings of an International Symposium Held at the University of Dundee. Dundee, UK, 93–106.

European Environment Agency, 2015. The European Environment. State and Outlook 2015 (SOER 2015). European Environment Agency, Copenhagen, Denmark.

Evangelista, L., de Brito, J., 2007. Environmental life cycle assessment of concrete made with fine recycled concrete aggregates, in: International Congress Sustainable Construction, Materials and Practices-Challenge of the Industry for the New Millennium. 978–1.

FIB, 2012. Guidelines for green concrete structures (FIB Bulletin No. 67), Guide to good practice. Fédération Internationale du Béton.

Frischknecht, R., Jungbluth, N., Althaus, H.-J., Doka, G., Dones, R., Heck, T., Hellweg, S., Hischier, R., Nemecek, T., Rebitzer, G., Spielmann, M., 2005. The Ecoinvent database: Overview and methodological framework. *The International Journal of Life Cycle Assessment* 10 (1): 3–9.

Galvín, A.P., Agrela, F., Ayuso, J., Beltrán, M.G., Barbudo, A., 2014. Leaching assessment of concrete made of recycled coarse aggregate: Physical and environmental characterisation of aggregates and hardened concrete. *Waste Management* 34 (9): 1693–1704.

Gartner, E., 2004. Industrially interesting approaches to "low-CO2" cements. *Cement and Concrete Research*, H. F. W. Taylor Commemorative Issue 34 (9): 1489–1498.

Goedkoop, M., Spriensma, R., 2001. The Eco-indicator99: a damage oriented method for life cycle impact assessment: methodology report. PRé Consultants, Amersfoort.

Güell-Ferré, A., Váquez-Ramonich, E., Varela-Pinto, E., Serna-Ros, P., Martínez-Abella, F., López-Gayarre, F., Barra-Bizinotto, M., Tirado-Alonso, A., Romero-Casado, A., Girbés-Clari, I., 2012. Spanish handbook on recycled aggregates from construction and demolition wastes (CDW) [in Spanish], Fueyo Editores. ed. Madrid, Spain.

Guinee, J.B., 2002. Handbook on life cycle assessment operational guide to the ISO standards. *The International Journal of Life Cycle Assessment* 7 (5): 311–313.

Gursel, A.P., Masanet, E., Horvath, A., Stadel, A., 2014. Life-cycle inventory analysis of concrete production: A critical review. *Cement and Concrete Composites* 51: 38–48.

Habert, G., Bouzidi, Y., Chen, C., Jullien, A., 2010. Development of a depletion indicator for natural resources used in concrete. *Resources, Conservation and Recycling* 54 (6): 364–376.

Hoekstra, A.Y., Chapagain, A.K., Aldaya, M.M., Mekonnen, M.M., 2011. The water footprint assessment manual: Setting the global standard. Earthscan, London.

Holcim, 2014. Building on ambition. Corporate Sustainable Development Report 2014. Holcim.

Humphreys, K., Mahasenan, M., 2002. Toward a sustainable cement industry. Sub-study 8: Climate change. World Business Council for Sustainable Development.

Joint Research Centre, 2014. 2013 Technology map of the European strategic energy technology plan, JRC Science and Policy Research. Joint Research Centre of the European Commission, Luxembourg.

Kaysser, D., Kott, M., 2002. Focusing on the future: Production-integrated environmental protection in the manufacture of concrete and reinforced concrete elements of building construction in the precast plant [in German]. *Betonwerk und Fertigteil-Technik* 68 (8): 52–57.

Knoeri, C., Sanyé-Mengual, E., Althaus, H.-J., 2013. Comparative LCA of recycled and conventional concrete for structural applications. *The International Journal of Life Cycle Assessment* 18 (5): 909–918.

Krausmann, F., Fischer-Kowalski, M., Schaffartzik, A., Steinberger, J.K.E.N., Eisenmenger, N., Weisz, B.U., 2011. Trends and developments of the use of natural resources in the European Union (No. 123), Social Ecology Working Paper. IFF Social Ecology (Universitaet Klagenfurt), Vienna, Austria.

Kucukvar, M., Egilmez, G., Tatari, O., 2014. Evaluating environmental impacts of alternative construction waste management approaches using supply-chain-linked life-cycle analysis. *Waste Management & Research* 32 (6): 500–508.

Marceau, M., Nisbet, M.A., Van Geem, M.G., 2006. Life cycle inventory of Portland cement manufacture (PCA R&D No. 2095b). Portland Cement Association, Illinois, USA.

Marinković, S., Radonjanin, V., Malešev, M., Ignjatović, I., 2010. Comparative environmental assessment of natural and recycled aggregate concrete. *Waste Management*, Special Thematic Section: Sanitary Landfilling 30 (11): 2255–2264.

Medina, C., Frías, M., Sánchez de Rojas, M.I., 2014. Leaching in concretes containing recycled ceramic aggregate from the sanitary ware industry. *Journal of Cleaner Production* 66: 85–91.

Mercante, I.T., Bovea, M.D., Ibáñez-Forés, V., Arena, A.P., 2012. Life cycle assessment of construction and demolition waste management systems: a Spanish case study. *The International Journal of Life Cycle Assessment* 17 (2): 232–241.

Ortiz, O., Pasqualino, J.C., Castells, F., 2010. Environmental performance of construction waste: Comparing three scenarios from a case study in Catalonia, Spain. *Waste Management* 30 (4): 646–654.

PRé Consultans bv, 2011. SimaPro Life Cycle Assessment Software Package.

Prusinski, J.R., Marceau, M.L., VanGeem, M.G., 2004. Life cycle inventory of slag cement concrete, in: Eighth CANMET/ACI International Conference on Fly Ash, Silica Fume, Slag and Natural Pozzolans in Concrete. 1–26.

Sani, D., Moriconi, G., Fava, G., Corinaldesi, V., 2005. Leaching and mechanical behaviour of concrete manufactured with recycled aggregates. *Waste Management* 25 (2): 177–182.

Schorcht, F., Kourti, I., Scalet, B.M., Roudier, S., Delgado Sancho, L., 2013. Best available techniques (BAT) reference document for the production of cement, lime and magnesium oxide. Industrial Emissions Directive 2010/75/EU (Integrated pollution prevention and control). (JRC Reference Reports). Joint Research Centre of the European Commission, Luxembourg.

Schuhmacher, M., Domingo, J.L., Garreta, J., 2004. Pollutants emitted by a cement plant: health risks for the population living in the neighborhood. *Environmental Research* 95 (2): 198–206.

Schultmann, F., Hiete, M., Kuehlen, A., Ludwig, J., Schulte Beerbuehl, S., Stengel, J., Vannieuwenhuyse, M., 2010. Collection of background information for the development of EMAS pilot reference sectoral documents: The construction sector. French-German Institute for Environmental Research (DFIU), Karlsruhe Institute of Technology (KIT), Karlsruhe, Germany.

Sev, A., 2009. How can the construction industry contribute to sustainable development? A conceptual framework. *Sustainable Development* 17 (3): 161–173.

Sonak, S., Pangam, P., Sonak, M., Mayekar, D., 2006. Impact of sand mining on local ecology, in: Multiple Dimensions of Global Environmental Change. Teri Press, New Delhi, India, 101–121.

Steinberger, J.K., Krausmann, F., Eisenmenger, N., 2010. Global patterns of materials use: A socioeconomic and geophysical analysis. *Ecological Economics* 69 (5): 1148–1158.

Struble, L., Godfrey, J., 2004. How sustainable is concrete?, in: International Workshop on Sustainable Development and Concrete Technology. 201–211.

Taylor, M., Tam, C., Gielen, D., 2006. Energy efficiency and CO2 emissions from the global cement industry, in: IEA-WBCSD Workshop on the Energy Efficiency and CO2 Emission Reduction Potentials and Policies in the Cement Industry. Paris, France, 1–12.

Tiruta-Barna, L., Benetto, E., Perrodin, Y., 2007. Environmental impact and risk assessment of mineral wastes reuse strategies: Review and critical analysis of approaches and applications. *Resources, Conservation and Recycling* 50 (4): 351–379.

Turk, J., Cotič, Z., Mladenovič, A., Šajna, A., 2015. Environmental evaluation of green concretes versus conventional concrete by means of LCA. *Waste Management* (In press): 10.1016/j.wasman.2015.06.035.

UEPG, 2015. A sustainable industry for a sustainable Europe (Annual Review 2013-2014). European Aggregates Association, Brussels, Belgium.

UNE EN ISO 14040, 2006. Environmental management. Life cycle assessment. Principles and framework. AENOR, Madrid.

UNE EN ISO 14044, 2006. Environmental management. Life cycle assessment. Requirements and guidelines. AENOR, Madrid.

UNEP, 2014. Sand, rarer than one thinks. UNEP Global Environmental Alert Service.

Van den Heede, P., De Belie, N., 2012. Environmental impact and life cycle assessment (LCA) of traditional and "green" concretes: Literature review and theoretical calculations. *Cement and Concrete Composites* 34 (4): 431–442.

WBCSD/CSI, 2009. Recycling concrete. World Business Council for Sustainable Development/Cement Sustainability Initiative.

WBCSD/CSI, 2013. Global Cement Database on CO2 and Energy Information – Getting the Numbers Right. World Business Council for Sustainable Development/Cement Sustainability Initiative.

Zabalza Bribián, I., Aranda Usón, A., Scarpellini, S., 2009. Life cycle assessment in buildings: State-of-the-art and simplified LCA methodology as a complement for building certification. *Building and Environment* 44 (12): 2510–2520.

Zabalza Bribián, I., Valero Capilla, A., Aranda Usón, A., 2011. Life cycle assessment of building materials: Comparative analysis of energy and environmental impacts and evaluation of the eco-efficiency improvement potential. *Building and Environment* 46 (5): 1133–1140.

Chapter 11
Capítulo

Conclusions
Conclusiones

1. CONCLUSIONS
CONCLUSIONES

In the following sections, the conclusions arising from each chapter of this dissertation are presented.

En las siguientes secciones, se presentan las conclusiones extraídas de cada uno de los capítulos de esta tesis.

1.1. CHARACTERIZATION OF THE RECYCLED AGGREGATES
CARACTERIZACIÓN DE LOS ÁRIDOS RECICLADOS

Four recycled aggregates samples were used in this investigation. Three of them (RA-L(S), RA-L(B) and RA-H(S)) corresponded with the commercialized material from an individual CDW management plant - TEC-REC, ARC and Bierzo Recicla respectively - while the forth sample (RA-M(S)) was artificially created by mixing the Spanish recycled aggregates to responded to the objectives of the investigation.

Cuatro muestras de áridos reciclados fueron utilizadas en la presente investigación. Mientras que tres de ellas (RA-L(S), RA-L(B) y RA-H(S)) fueron directamente obtenidas del material comercializado en una planta de gestión de RCD, -TEC-REC, ARC y Bierzo Recicla, respectivamente-, la cuarta muestra (RA-M(S)) fue creada artificialmente mediante la mezcla de los áridos reciclados españoles de acuerdo con los objetivos de la investigación.

The results showed that the predominant component was concrete (44% and 37% respectively) followed by materials of ceramic nature (34% and 38% respectively) in RA-L(S) and RA-L(B) samples, while in RA-M(S) the situation was reversed with a majoritarian ceramic component (66%) followed by the occurrence of cement based materials (17%). In regard to sample RA-H(S), the recycled aggregate was solely composed by ceramic materials (bricks and tiles principally). In terms of impurity content, sample RA-L(B) exceeded the 1% limit for asphalt in the Spanish standard, which is stricter than other Europeans standards, and RA-L(S) surpassed the 1% limit for other impurities (glass, metal, plastic and wood among others), which suggests a failure in the separation procedure at the management plant. For the organic matter content, all the recycled aggregates exhibited contents inferior to 0.80%, which prevents the deleterious effects of this component in the concrete manufacture. In addition, both the soaking in 1M hydrochloric acid and the frost damage approach reported similar contents of adhered mortar for RA-L(S), RA-L(B) and RA-H(S) of about 34%, 23% and 6%, respectively.

The grading of all recycled aggregates followed a continuous and non-uniform pattern and the the D/d ratio was greater than the limit stipulated of 1.40. Both the constituents and the management of the CDW resulted in a higher flakiness index for the recycled aggregates that, in all cases, complied with the 35% limit established in the EHE-08. Also dependent on the treatment procedure at the CDW management plant, the fines content of all samples was below the 1.50% limit. However, special attention must be paid to the generation of supplementary fines during the mixing procedure as consequence of self-attrition of the materials.

Los resultados mostraron una composición mayoritaria de hormigón (44% y 37%, respectivamente) seguida por materiales de naturaleza cerámica (34% y 38%, respectivamente) en las muestras RA-L(S) y RA-L(B), mientras que la situación se invirtió en la muestra RA-M(S), con un componente cerámico mayoritario (66%), seguido por la ocurrencia de materiales a base de cemento (17%). En la muestra RA-H(S), solo materiales cerámicos (ladrillos y azulejos principalmente) formaron parte del árido reciclado. En términos impurezas, RA-L(B) excedió el límite de 1% de asfalto, que es más estricto que en otros estándares europeos, y RA-L(S) superó el límite del 1% de otras impurezas (vidrio, metal, plástico y madera entre otros), lo que sugiere un cierto grado de fracaso en el procedimiento de separación en la planta de gestión. Respecto al contenido de materia orgánica, todos los áridos presentaron valores inferiores a 0,80%, evitando así los efectos nocivos en la fabricación de hormigón. Además, los resultados de los ensayos de remojo en ácido clorhídrico 1M y los daños por heladas indicaron contenidos similares de mortero adherido, 34%, 23% y 6% para RA-L(S), RA-L(B) y RA-H(S) respectivamente.

La granulometría de los áridos reciclados siguió una curva continua y no uniforme y presentó una relación D/d superior al límite estipulado de 1,40. Tanto los componentes como la gestión de los RCD resultaron en un índice de lajas más alto para los áridos reciclados que, en todos los casos, cumplió con el límite del 35% establecido en la EHE-08. También dependiente del tratamiento en la planta de gestión RCD, el contenido de finos de todas las muestras se mantuvo por debajo del límite de 1,50%. Sin embargo, se debe prestar especial atención a la generación de más finos durante el mezclado debido al auto-desgate de los materiales.

Despite the sand equivalent assessment indicated a questionable quality of the fines as none of the samples complied the 70-75% requirements, no expansive clays were detected by means of XRD that could negatively affect the recycled concrete performance or durability.

Notwithstanding that the EHE-08 does not lay down any limitation for the density of the aggregates to be used in concrete, the density of the recycled aggregates was significantly lower than that of the natural aggregates (between 18% and 29% for increasing ceramic contents). In contrast, water absorption is strictly limited to 7%, whereas higher leeway exists in the German standard or the RILEM recommendations. Hence, none of the recycled aggregates met the national specifications. Regarding the mechanical performance of the recycled aggregates, all of them were deemed suitable under the EHE-08 restrictions, but the sample RA-L(S) would only be apt for concrete with target strength up to 30 MPa since the Los Angeles coefficient was between 40% and 50%.

The chemical composition, mainly based on silicon oxide and aluminium oxide, was indicative of the occurrence of clay minerals and quartz in the recycled aggregates. Moreover, the alkali content of the recycled aggregates was about 23-34 times higher than the gravel. While the limit regarding chloride content (0.05 %) was not reached by any of the recycled aggregates, sample RA-L(S) surpassed the 0.80% limit for sulphate content, principally due to the high presence of gypsum.

The mineralogical composition of all samples was in good agreement with the chemical results arising from the X-ray fluorescence test performed.

A pesar de que el equivalente arena indicó una calidad cuestionable de los finos al no cumplir ninguna muestra los requisitos de 70-75%, la difracción de rayos X no detectó arcillas expansivas que pudieran afectar negativamente al hormigón reciclado.

Pese a que la EHE-08 no establece ninguna limitación para la densidad de los áridos de hormigón, los áridos reciclados presentaron una densidad significativamente menor que la de los áridos naturales (entre 18% y 29% para aumentos del contenido cerámico). Por el contrario, la absorción de agua está estrictamente limitada a 7%, mientras el estándar alemán o las recomendaciones RILEM son más permisivos. Por lo tanto, ninguno de los áridos reciclados cumplió las especificaciones nacionales. En cuanto a las prestaciones mecánicas de los áridos reciclados, todos ellos fueron considerados adecuados bajo las restricciones de la EHE-08, aunque la muestra RA-L(S) solo sería apta para hormigón hasta 30 MPa ya que el coeficiente de Los Ángeles estuvo entre 40% y 50%.

La composición química, principalmente óxido de silicio y óxido de aluminio, indicó la presencia de minerales de arcilla y cuarzo en los áridos reciclados. Además, el contenido de álcali de los áridos reciclados fue aproximadamente 23-34 veces mayor que la grava. Mientras que el límite de contenido de cloruro (0,05%) no fue alcanzado por ninguno de los áridos reciclados, la muestra de la RA-L(S) superó el límite de 0,80% de contenido en sulfatos, principalmente debido a la alta presencia de yeso.

La composición mineralógica de las muestras coincidió con los resultados químicos de fluorescencia de rayos X.

The main mineral in the ceramic recycled aggregate (RA-H(S)) was the quartz; while for mixed recycled aggregates (RA-L(S) and RA-M(S)), besides the quartz, the calcite was a major component due to the presence of concrete and mortar in the samples. The rest of detected components pointed to the relative ceramic content in the sample, e.g. feldspar minerals (anorthite, orthoclase), dolomite, hematite, muscovite, illite and cristobalite. Similarly, good correspondence was observed with the analysis carried out by scanning electron microscopy.

Nowadays, very little is known about the porosity of mixed and ceramic recycled aggregates, besides that it is a relatively high value, at least compared to that of natural aggregates. Although the results supported this fact (18%, 21% and 26% for RA-L(S), RA-M(S) and RA-H(S) samples respectively, which is an average of 23 times higher than for the natural gravel), they also provided a more complex insight in the pore structure of recycled aggregates. For example the ink-bottle porosity for the gravel (0.23%) was the minority component of the total porosity, whereas the contrary phenomenon occurs in the recycled aggregates (15% for RA-L(S), 15% for RA-M(S) and 19% for RA-H(S). These values are indicative of an elevated non-accessible porosity in the samples that translates in lower values of effective porosity, which suggests that the performance gap is not as obvious as initially considered.

Albeit that the use of mixed recycled aggregates or ceramic recycled aggregates has yet to be allowed by Spanish legislation, the results obtained in the physical, mechanical and microstructural characterization demonstrated that recycled aggregate samples with different ceramic contents showed a promising quality for their application in the concrete manufacture.

El principal mineral en el árido reciclado cerámico (RA-H(S)) fue el cuarzo; mientras que para los áridos reciclados mixtos (RA-L(S) y RA-M(S)), además del de cuarzo, el porcentaje de calcita también fue importante debido a la presencia de hormigón y mortero. El resto de los componentes apuntó al contenido relativo de cerámica, por ejemplo feldespato (anortita, ortoclasa), dolomita, hematita, moscovita, ilita y cristobalita. Del mismo modo, se observó una buena correspondencia con el análisis llevado a cabo por microscopía electrónica de barrido.

Hoy en día, se sabe muy poco acerca de la porosidad de los áridos reciclados mixtos y cerámicos, más allá de que es un valor relativamente alto en comparación con la de los áridos naturales. Aunque los resultados apoyaron este hecho (18 %, 21% y 26% para la RA-L(S), RA-M(S) y RA-H(S) respectivamente, es decir, alrededor de 23 veces mayores), también proporcionaron una visión más amplia de la estructura porosa de los áridos reciclados. Por ejemplo, la porosidad no efectiva para la grava (0,23%) es el componente minoritario de la porosidad total, mientras que lo contrario ocurre en los áridos reciclados (15% para RA-L(S), 15% para RA-M(S) y 19% para RA-H(S)). Estos valores son indicativos de una porosidad no accesible elevada que sugiere que las diferencias entre ambos áridos no son tan extremas como se consideró inicialmente.

Aunque que el uso de áridos reciclados mixtos o cerámicos aún no está permitido por la legislación española, los resultados obtenidos en la caracterización física, mecánica y microestructural realizada revelaron que las muestras de áridos reciclados con diferente contenido cerámico exhibieron prometedores resultados de calidad para su aplicación en la fabricación de hormigón.

Nonetheless, based on the experimental characterization, water absorption, Los Angeles abrasion loss and impurities are the main constraints for the use of these types of recycled aggregates in the concrete manufacture since they presented the largest deviation from the regulatory limits.

Sin embargo, basado en la caracterización experimental, la absorción de agua, pérdida por abrasión de Los Ángeles y las impurezas son las principales limitaciones para el uso de estos tipos de áridos reciclados en la fabricación de hormigón, ya que presentaron incumplimientos con respecto a los límites legales.

1.2. RECYCLED CONCRETE MIX DESIGN
DOSIFICACIÓN DEL HORMIGÓN RECICLADO

In this investigation, conventional and recycled concrete mixtures with different content of ceramic wastes were designed to assess the influence of a partial replacement (50%) of the natural coarse aggregate on the properties of concrete. For the proportioning, the De la Peña method was selected. The concrete mixtures were designed having in mind a structural concrete, which translates in a minimum 25 MPa characteristic compressive strength at 28 days. Other design parameters adopted were a maximum aggregate size of 20 mm and a S2 slump class for the conventional concrete as laid down in EHE-08. Since the proportioning of the aggregates was based upon the Fuller method and the density of the river gravel is higher than that of the recycled coarse aggregates, the recycled concrete mixtures contain higher amounts of sand for increasing ceramic incorporations. To satisfy durability requirements, the total water/cement ratio was set at 0.55. Therefore, the cement and water content were fixed in 391 kg/m^3 and 215 l/m^3. Since no additional water was added, the higher water absorption of the recycled aggregates is responsible for the absorption of part of the water during the mixing period? resulting in an effective water/cement ratio of 0.50 for all the recycled concrete mixtures.

En esta investigación, hormigones convencionales y reciclados con diferentes porcentajes cerámicos fueron dosificados para evaluar la influencia que un reemplazo parcial (50%) del árido grueso natural tiene en las propiedades del hormigón. Para la dosificación, se seleccionó el método De la Peña y se estableció una resistencia característica mínima a la compresión de 25 MPa a los 28 días, consistente con un uso estructural. Otros parámetros de diseño adoptados fueron un tamaño de árido máximo de 20 mm y asentamiento S2 para el hormigón convencional, según lo establecido en la EHE-08. Puesto que la dosificación de los áridos se basó en la parábola de Fuller y la densidad de la grava de río es mayor que la de los áridos gruesos reciclados, los hormigones reciclados contienen mayores cantidades de arena a medida que aumenta el contenido cerámico. Para cumplir con los requisitos de durabilidad, la relación total de agua/cemento se estableció en 0,55. Por lo tanto, el contenido de cemento y agua fue fijado en 391 kg/m^3 y 215 l/m^3. Dado que no se añadió agua adicional, la absorción por parte de los áridos reciclados causó que la relación efectiva de agua/cemento se redujera a 0,50 en los hormigones reciclados.

1.3. FRESH PROPERTIES OF RECYCLED CONCRETE
PROPIEDADES EN FRESCO DEL HORMIGÓN RECICLADO

Since no correction on the amount of water was carried out to the original proportioning method, the slump of the recycled concretes was lower than that of conventional mixtures. In the first phase, in a general more dry setting, the recycled concrete batches presented reductions of consistency, up to 28% for low ceramic content (I-RC-L(S)), around 41% for medium ceramic content (I-RC-M(S)) and roughly 69% for high ceramic content (I-RC-H(S)). In phase II, since the consistency of the conventional concrete is higher, the relative slump reductions were also higher, oscillating between 20% and 29% for the mixtures with low ceramic percentage (II-RC-L(S) and II-RC-L(B)), around 75% for medium ceramic content (II-RC-M(S)) and almost 91% for high ceramic content (II-RC-H(S)). However, no problems in workability were detected in any of the research phases.

Dado que la cantidad de agua respecto al método de dosificación original no fue corregida, el asentamiento de los hormigones reciclados fue menor. En la primera fase, el hormigón reciclado presentó reducciones inferiores de la consistencia, hasta un 28% para bajos contenidos de cerámica (I-RC-L(S)), alrededor de 41% para un contenido medio (I-RC-M (S)) y entorno al 69% para un contenido alto de cerámica (I-RC-H (S)). En la fase II, las reducciones de asentamiento fueron mayores ya que el hormigón convencional presentó una consistencia más alta, oscilando entre 20% y 29% para un bajo contenido cerámico (II-RC-L(S) y II-RC-L(B)), alrededor de 75% para un contenido medio (II-RC-M(S)) y casi 91% para un contenido alto de cerámica (II-RC-H (S)). Sin embargo, no se detectaron problemas en la trabajabilidad en ninguna de las fases de la investigación.

Due to the presence of adhered mortar and ceramic materials, the air content of the recycled concretes was higher and oscillated from 40% in II-RC-L(S) to 80% in II-RC-L(B), II-RC-M(S) and II-RC-H(S) since a higher porosity favours the occlusion of air in the pores. Furthermore, since the density of the mixed and ceramic recycled aggregates is lower than that of the natural aggregates, the fresh density of recycled concrete mixes was also lower, between 5% and 2%, than the conventional concrete for increasing ceramic incorporations.

Debido a la presencia de mortero y cerámica, el contenido de aire de los hormigones reciclados fue mayor y osciló entre un 40% en II-RC-L(S) y un 80% en II-RC-L(B), II-RC-M(S) y II-RC-H(S) pues mayores porosidades favorecen la oclusión de aire en los poros. Por el contrario, ya que la densidad de los áridos reciclados mixtos y cerámicos es menor que la de los áridos naturales, la densidad en fresco de los hormigones reciclados también fue inferior que en el hormigón convencional, entre 5% y 2%, para incorporaciones crecientes de cerámica.

Despite that all concrete raw materials were at the same ambient temperature before mixing, the recycled concrete mixtures presented lower initial temperature values (after no longer than 12 minutes after mixing).

A pesar de que todas las materias primas estuvieron a la misma temperatura ambiente, los hormigones reciclados presentaron valores de temperatura iniciales más bajas (tras periodos inferiores a 12 minutos después de la mezcla).

The values ranged from 9% (II-RC-L(S)) to 17% (II-RC-M(S)) with respect the conventional concrete. Contrarily, recycled concretes registered higher temperature values at the end of the semi-adiabatic measurements oscillating from 1% (II-RC-L(S)) to 4% (II-RC-H(S)). Hence, the recycled concretes showed 5% to 15%, higher total heat release than the conventional concrete for increasing ceramic contents incorporated in the total weight of aggregates. Notwithstanding a higher probability of early-age cracking, the lower coefficient of thermal expansion of ceramic materials is expected to counteract the effect of heat release during hydration.

Los valores oscilaron entre un 9% (II-RC-L (S)) y 17% (II-RC-M (S)) respecto al hormigón convencional. Por el contrario, se registraron valores de temperatura final más alta, oscilando entre un 1% (II-RC-L (S)) y un 4% (II-RC-H (S)). Por lo tanto, los hormigones reciclados mostraron una liberación total de calor entre el 5% y 15% superior que el hormigón convencional a medida que aumentaba el contenido de cerámica incorporado. A pesar de la mayor probabilidad en la formación de grietas a edad temprana, se espera que el menor coeficiente de expansión térmica de los materiales cerámicos contrarreste el mayor calor de hidratación.

In general, the use of recycled aggregates in the concrete manufacture was liable for the delay of both the initial and final setting times. However, some extreme results and the lack of coincidence between methods evidence the need for a greater number of investigations in order to ascertain the accuracy of some of the criteria proposed for conventional concretes. In any case, problems were not identified in the demoulding of specimens after 24 hours.

En general, el uso de áridos reciclados fue responsable del retraso de los tiempos iniciales y finales de fraguado. Sin embargo, algunos resultados extremos y la falta de coincidencia entre los métodos evidenciaron la necesidad de un mayor número de investigaciones que aseguren la exactitud de algunos de los criterios propuestos para hormigones convencionales. En cualquier caso, todas las muestras fueron desmoldadas tras 24 horas sin problemas.

1.4. MICROSTRUCTURE OF RECYCLED CONCRETE
MICROSTRUCTURA DEL HORMIGÓN RECICLADO

The microstructure study showed that recycled concretes presented fairly dense and continuous interfaces between concrete and ceramic recycled aggregates with the cement matrix. The good quality of ITZ was due to the lower effective water/cement ratio, the internal curing effect produced as the recycled aggregates return part of the water absorbed to the cement matrix, the use of a blended slag cement and the additional pozzolanic activity of the CDW, and the rough surface and sharper outlines of the recycled aggregates.

El estudio de la microestructura mostró que los hormigones reciclados presentan unas interfaces entre los áridos reciclados de hormigón y cerámicos con la matriz de cemento bastante densas y continuas. La buena calidad de ITZ fue debida a la menor relación efectiva agua/cemento, el efecto de curado interno producido por la devolución de parte del agua absorbida en los áridos reciclados, el uso de un cemento con escorias, la actividad puzolánica adicional de los RCD, y la superficie rugosa y contornos más nítidos de los áridos reciclados.

Moreover, the incorporation of recycled aggregates did not change the chemical composition of the cement paste (i.e. calcium and silicon as major elements, magnesium and aluminium as consequence of the slag particles and sulphur coming from the hydration retardant agent in the cement) nor the Ca/Si ratio.

Por otra parte, la incorporación de áridos reciclados no cambió la composición química de la pasta de cemento (es decir, calcio y silicio como elementos principales, magnesio y aluminio como consecuencia de las partículas de escoria, y azufre procedente del agente retardante del cemento) ni la relación Ca/Si.

The recycled concretes presented a higher total porosity than the conventional concrete at 28 days. In particular, higher differences were found for lower ceramic incorporations, ranging from 28% for low ceramic recycled concrete (I-RC-L(S)) and 15% for medium ceramic recycled concrete (I-RC-M(S)) to 3% for high ceramic recycled concretes, which suggest an inverse relationship between the total porosity of the recycled concretes and the percentage of ceramic waste included as aggregate. However, the situation is reversed after 56 days of curing and recycled mixtures presented a lower porosity than that of the conventional concrete, around 29% for I-RC-L(S), 11% for I-RC-M(S) and 17% for I-RC-H(S). Therefore, the recycled concretes acquired a significant decrease in porosity, up to 41% for I-RC-L(S), 26% for I-RC-M(S) and 31% for I-RC-H(S). Moreover, in general, recycled aggregates presented between 20% and 36% lower critical pore sizes than the respective conventional mixture which is indicative of finer pore structures.

Los hormigones reciclados presentaron una porosidad total mayor que el hormigón convencional a los 28 días. En particular, se encontraron diferencias más altas para incorporaciones de cerámica inferiores, que fueron desde 28% para bajo contenido cerámico (I-RC-L(S)) y 15% para contenido medio (I-RC-M(S)) a 3% para altos porcentajes de cerámica, lo que sugiere una relación inversa entre ambas variables. Sin embargo, la situación se invirtió después de 56 días de curado y hormigones reciclados presentaron una porosidad menor que la del hormigón convencional, alrededor de 29% para I-RC-L(S), 11% para I-RC-M(S) y 17% para I-RC-H(S). Por lo tanto, los hormigones reciclados experimentaron una disminución significativa en la porosidad, hasta de un 41% para I-RC-L(S), 26% para I-RC-M(S) y 31% para I-RC-H(S). Además, en general, los áridos reciclados presentan tamaños de poro crítico entre 20% y 36% inferiores al del hormigón convencional, lo que es indicativo de estructuras con poros más finos.

Analogously to the air content in fresh state, conventional concrete presented the lower amount of air voids (1%), whereas recycled concretes presented values between 1.6 and 2.5 times greater for increasing ceramic contents

Análogamente al contenido de aire en estado fresco, el hormigón convencional presentó la menor cantidad de aire ocluido (1%), mientras que los hormigones reciclados presentaron valores entre 1,6 y 2,5 veces mayores para contenidos de cerámica crecientes.

Nevertheless, recycled concrete mixtures displayed a worse distributed air void system compared to the conventional concrete with a decrease in the spacing factors ranging from 21% to 39% and average chord length between 1.7 and 2 times higher than that of the conventional concrete. However, none of the concretes fulfilled the recommendations for frost-resistant concrete in absence of air-entrainment agents.

Sin embargo, los hormigones reciclados mostraron una peor distribución del aire ocluido en comparación con el hormigón convencional, con una disminución del factor de separación entre un 21% y un 39%, y longitud media de cuerda entre 1,7 y 2 veces superior. Sin embargo, ninguno de los hormigones reciclados cumplió las recomendaciones establecidas para hormigones resistentes a heladas en ausencia de agentes incorporadores de aire.

1.5. MECHANICAL BEHAVIOUR OF RECYCLED CONCRETE
COMPORTAMIENTO MECÁNICO DEL HORMIGÓN RECICLADO

Similarly to the fresh state, the hardened density of recycled concrete is mainly influenced by the density of the aggregates employed and thus reductions between 2% and 8% were observed for increasing ceramic contents.

Al igual que en el estado fresco, la densidad del hormigón reciclado está principalmente influenciada por la densidad de los áridos empleadas y, por lo tanto, fueron observadas reducciones entre 2% y 8% para contenidos de cerámica crecientes.

In terms of compressive strength, all recycled concretes exhibited values over the 25 MPa targeted in the mixture dosage at 28 days. However, maximum reductions up to 22% for I-RC-L(S) at 7 days and 11% for I-RC-M(S) at 28 days were registered. It is noteworthy that the loss of compressive strength was more pronounced at 7 days and it is progressively reduced the older the concrete becomes. Therefore, the recycled mixtures displayed a higher strength development ratio than the conventional concrete due to the presence of unhydrated cement particles and ceramic fines that contributed to the resistance gain. Nevertheless, it is worth mentioning that the results obtained for the recycled concrete mixture containing the higher ceramic content (RC-H(S)) indicated a positive influence of the recycled aggregates on this property.

En cuanto a la resistencia a la compresión, todos los hormigones reciclados mostraron valores superiores a los 25 MPa establecidos en la dosificación para 28 días. Sin embargo, se registraron reducciones máximas de hasta 22% para I-RC-L(S) a los 7 días y 11% para I-RC-M(S) a los 28 días. Cabe destacar que la pérdida de resistencia fue más pronunciada a los 7 días y se redujo progresivamente con la edad del hormigón. Es decir, los hormigones reciclados desarrollaron más rápidamente su resistencia mecánica debido a la presencia de partículas de cemento no hidratadas y finos de cerámica que contribuyeron a la ganancia de resistencia. Sin embargo, vale la pena mencionar que los resultados obtenidos para los hormigones reciclados con alto contenido cerámico (I-RC-H(S) y II-RC-(S)) indicaron una influencia positiva de los áridos reciclados en esta propiedad.

Based on the compressive strength indexes, the replacement of natural by recycled aggregates had a favourable effect in mixture RC-H(S) at all curing ages and both research phases and in the specimens of II-RC-L(S) and II-RC-L(B) at 90 days of curing. Consequently, the adverse effect of the substitution was confirmed for the rest of the concrete mixtures as the contribution to strength is somewhat smaller than the amount of natural coarse aggregate replaced.

Similarly, the use of recycled aggregates caused a reduction of the flexural strength around 8% in phase I, whereas the decreases observed in phase II were in the 20% range for II-RC-L(S), II-RC-L(B) and II-RC-M(S) while II-RC-H(S) experienced a 13% decline. Regarding the splitting tensile strength, the declines with respect to the conventional concrete decreased for increasing ceramic concrete. Thus, on average, declines of 11%, 7% and 2% were registered when low, medium or high ceramic content recycled aggregates were employed. For both properties, the Eurocode-2 curve seemed an acceptable fit for the experimental results arising from cubic specimens and centre-point bending tests.

Regarding the toughness performance of the material, maximum 8% declines in the elastic modulus were observed compared to the conventional concrete when mixed or ceramic recycled aggregates were employed. For prediction purposes, the formula proposed by the ACI 318-14 led to the better approximations due to the incorporation of the density parameter. The analysis of the stress-strain curves showed that both conventional and recycled mixtures displayed a similar linear behaviour in the first part of the curve regardless of the ceramic content incorporated. However, differences were noticeable as the curve became parabolic.

En base a los índices de resistencia a la compresión, la sustitución de los áridos naturales con áridos reciclados tuvo un efecto favorable en I-RC-H(S) y II-RC-H(S) en todas las edades de curado y en las muestras II-RC-L(S) y II-RC-L(B) a los 90 días de curado. En consecuencia, se confirmó el efecto adverso de la sustitución para el resto de hormigones dado que la contribución a la resistencia es algo inferior que la cantidad de árido grueso natural reemplazado.

Del mismo modo, el uso de áridos reciclados causó una reducción de la resistencia a la flexión alrededor de 8% en la fase I, mientras que las disminuciones de la fase II estuvieron en el rango 20% para II-RC-L(S), II-RC-L(B) y II-RC-M(S), y 13% para II-RC-H(S). En cuanto a la resistencia a la tracción, las disminuciones respecto al hormigón convencional disminuyeron con el aumento de cerámica. En promedio, se registraron reducciones del 11%, 7% y el 2% para áridos reciclados con bajo, medio o alto contenido cerámico. Para ambas propiedades, la curva Eurocódigo-2 produjo un ajuste aceptable para especímenes cúbicos y el ensayo de punto central.

En cuanto a la tenacidad del material, cuando se emplean áridos reciclados mixtos o cerámicos, se observaron descensos máximos de un 8% en el módulo elástico en comparación con el hormigón convencional. En este caso, la fórmula propuesta por el ACI 318-14 produjo el mejor ajuste debido a la incorporación del parámetro de densidad a la predicción. El análisis de las curvas de tensión-deformación mostró que los hormigones convencionales y reciclados presentan un comportamiento lineal similar en la primera parte de la curva, independientemente del contenido de cerámica incorporado. Sin embargo, las diferencias fueron notables en la zona parabólica.

For the same relative stress units, the recycled mixtures with low ceramic content (I-RC-L(S), II-RC-L(S) and II-RC-L(B)) exhibited lower deformations than the conventional concrete, whereas the recycled mixtures with medium and high ceramic contents (I-RC-M(S), II-RC-M(S), I-RC-H(S) and II-RC-H(S)) displayed higher deformations than their respective reference mixtures. On average, the peak strains of recycled mixtures with low ceramic contents (I-RC-L(S), II-RC-L(S) and II-RC-L(B)) presented a deformation 3.95% lower than the reference concrete. Contrarily, the recycled mixtures with medium ceramic contents (I-RC-M(S), II-RC-M(S)) showed an increase up to 12% and the recycled mixtures with high ceramic contents (I-RC-H(S) and II-RC-H(S)) exhibited a mean rise of 6%.

In terms of the evolution of shrinkage with time, both the conventional and recycled mixtures presented parallel behaviours as hyperbolic curves that tend to an asymptotic value. Despite that the II-RC-M(S) concrete mixture displayed a lower shrinkage strain during the 10 first days of testing; the use of recycled aggregates generally produced an increase of the shrinkage strains compared to that of the conventional concrete regardless the type of recycled aggregate employed. Hence, recycled concretes presented total shrinkage strain after 91 days ranging from 12% to 75% higher than the conventional concrete. Analogously to the shrinkage deformations, it is possible to conclude that the recycled aggregates from CDW, both mixed and ceramic, resulted in parallel creep behaviour to that of a conventional concrete but with a general worse performance. Hence, recycled concretes exhibited total creep strains between 24% and 46% higher for decreasing ceramic contents.

Para un mismo nivel de esfuerzo, los hormigones con bajo contenido de cerámica (I-RC-L(S), II-RC-L(S) y II-RC-L(B)) exhibieron deformaciones más bajas que el hormigón convencional, mientras que aquellas muestras con contenido medio y alto (I-RC-M(S), II-RC-M(S), I-RC-H(S) y II-RC-H(S)) mostraron deformaciones superiores. En promedio, los hormigones reciclados con contenidos cerámicos bajos (I-RC-L(S), II-RC-L(S) y II-RC-L(B)) presentaron una deformación 3,95% inferior. Por el contrario, la deformación para contenidos de cerámica medios (I-RC-M(S) y II-RC-M(S)) y altos (I-RC-H(S) y II-RC-H(S)) fueron hasta 12% y 6% superiores respectivamente.

En cuanto a la evolución de la retracción con el tiempo, tanto los hormigones convencionales como los reciclados presentaron comportamientos paralelos como curvas hiperbólicas que tienden a un valor asintótico. A pesar de que el hormigón II-RC-M(S) experimentó una retracción inferior durante los 10 primeros días de ensayo, el uso de áridos reciclados produjo un aumento general de las deformaciones por retracción en comparación con la del hormigón convencional independientemente del tipo de árido reciclado empleado. Por lo tanto, después de 91 días, los hormigones reciclados presentaron deformaciones totales entre 12% y 75% superiores a las del hormigón convencional. Análogamente, es posible concluir que los áridos reciclados de RCD, tanto mixtos como cerámicos, ocasionaron un comportamiento de fluencia paralelo al de un hormigón convencional, aunque con un peor rendimiento general. Por ello, los hormigones reciclados exhibieron deformaciones de fluencia total entre 24% y 46% más altas, para contenidos cerámicos decrecientes.

Nevertheless, the mechanical performance exhibited by the recycled concretes can be considered as good and was explained by: the decrease of the aggregate/cement ratio with rising ceramic ratios, the use of recycled aggregates in in air-dried condition that reduced the effective water/cement ratio, the mixture procedure, the use of slag blended cement, the pozzolanic activity of the CDW fines, the superficial roughness of the recycled aggregates and their ability to return the water absorbed during the mixing to produce an internal curing effect enhancing the ITZ bond.

Pese a todo, el comportamiento mecánico exhibido por los hormigones reciclados puede ser considerado como bueno y se explica por la disminución de la relación de árido/cemento con el aumento de las proporciones de cerámica, el uso de áridos reciclados secados al aire que reduce la relación efectiva agua/cemento, el proceso de mezclado, el uso de cemento con escorias, la actividad puzolánica de los finos de RCD, la rugosidad superficial de los áridos reciclados y su capacidad para devolver parte del agua absorbida durante el mezclado, produciendo un efecto de curado interno que mejora el vínculo de la ITZ.

.

1.6. DURABILITY PERFORMANCE OF RECYCLED CONCRETE
DURABILIDAD DEL HORMIGÓN RECICLADO

In term of oxygen permeability, recycled concretes exhibited both lower (up to 15%) and higher (up to 71%) values than the conventional concrete with the porosity values being the main controlling factor instead of the ceramic content. However, the results obtained suggested a good performance regarding this property.

En términos de permeabilidad al oxígeno, los hormigones reciclados exhibieron valores inferiores (hasta 15%) y superiores (hasta 71%) a los del hormigón convencional, siendo la porosidad la principal responsable en lugar del contenido de cerámica. Sin embargo, los resultados de todas las muestras sugirieron un buen comportamiento.

The penetration of CO_2 was evaluated for a natural outdoor (0.06% CO_2) and an accelerated environment (10% CO_2) in phases I and II respectively. Recycled concretes in phase I exhibited a worse behaviour (around 70-75%) after 1 year of exposure due to the increase in the pore sizes higher than 0.067 µm. Despite that an average decline of 30% in the penetration depth was observed for 1 month of accelerated exposure due to the lower water/cement ratio and the higher alkalinity of recycled mixtures hindering the early penetration, the values progressively transformed in higher penetration values (up to 5% higher than II-CC) after 3 months of exposure.

La penetración de CO_2 fue evaluada para un ambiente natural exterior (0,06% CO_2) y uno acelerado (10% CO_2) en las fases I y II respectivamente. Los hormigones reciclados de la fase I exhibieron una peor durabilidad después de 1 año de exposición (alrededor de 70-75%) debido al aumento del tamaño de poro mayor que 0,067 micras. A pesar de observarse un descenso del 30% en la profundidad de penetración tras un 1 mes de exposición acelerada, ya que la menor relación agua/cemento y la mayor alcalinidad de los hormigones reciclados dificultaron la penetración, estos valores aumentaron progresivamente (hasta un 5% superior a II-CC) después de 3 meses.

Recycled concrete displayed a lower water capillary absorption than the conventional concrete due to the better quality of the cement matrix, i.e. lower effective water/cement ratio and porosity. Hence, primary sorptivity values were lower than that of the conventional concrete, with the reduction oscillating from 22% to 63% for increasing ceramic contents.

The test of water absorption under vacuum allowed the assessment of the open porosity. The results indicated that the capillary open porosity was greater, between 10% and 40%, for increasing ceramic contents, which suggested a worse performance of the recycled concretes.

For water penetration under pressure, recycled mixtures generally exhibited a better performance than the conventional concrete. Regarding the maximum penetration depth, reductions up to 32% and 56% were observed in phase I and II respectively. In terms of the average penetration depth, reductions of 36% and 62% were observed for I-RC-L(S) and I-RC-M(S), whereas I-RC-H(S) mixture showed a 17% higher penetration depth. Nonetheless, the results guaranteed a sufficient durability for environmental classes IIIa, IIIb, IV, Qa, E, H, F and Qb.

The deterioration of concrete due to freeze-thaw cycles in presence of de-icing salts showed that recycled concretes presented a worse performance than the conventional concrete. Nonetheless, the ultrasonic pulse velocity (UPV) results at the end of the test in phase I were indicative of a good quality concrete in spite of the up to 13% higher mass losses after 25 cycles.

El hormigón reciclado mostró una absorción de agua por capilaridad inferior al hormigón convencional debido a la mejor calidad de la matriz de cemento, es decir, menor relación agua/cemento y refinamiento poroso. Por lo tanto, los valores de absorción primarios fueron más bajos que los del hormigón convencional, oscilando entre 22% y 63% para contenidos de cerámica crecientes.

El ensayo de absorción de agua bajo vacío permitió la evaluación de la porosidad accesible. Los resultados indicaron que la porosidad capilar accesible fue mayor, entre 10% y 40%, en los hormigones reciclados en función del contenido de cerámica, lo que sugirió un peor rendimiento de los hormigones reciclados.

Respecto a la penetración de agua bajo presión, los hormigones reciclados generalmente exhibieron un mejor comportamiento que el convencional. La máxima profundidad se redujo un máximo de 32% y 56% en la fase I y II, respectivamente. En términos de profundidad media, se observaron reducciones de 36% y 62% para I-RC-L(S) y I-RC-M(S), mientras que la muestra I-RC-H(S) mostró un profundidad un 17% mayor. No obstante, los resultados garantizaron una durabilidad suficiente para clases ambientales IIIa, IIIb, IV, Qa, E, H, F y Qb.

El deterioro del hormigón debido a ciclos hielo-deshielo en presencia de sales de deshielo mostró que los hormigones reciclados se comportan peor que el hormigón convencional. Sin embargo, las velocidades de pulso ultrasónico (VPU) al final de la prueba en la fase I indicaron su buena calidad a pesar de que las pérdidas de masa fueron 13% superiores después de 25 ciclos.

In phase II, the relative mass losses due to freeze-thaw with de-icing salts increased up to 26% without correlation with the ceramic content but with a higher incidence in the trowelled surfaces. Nevertheless, it is worth remarking that the use of an air entrainment agent can improve the results.

Regarding the chloride ingress, the penetration depths in the migration test were also lower for the recycled concretes and thus the non-steady migration coefficient were 37%, 25% and 43% lower for the casting surfaces of II-RC-L(S), II-RC-L(B) and II-RC-H(S) and variations up to 3%, -19% and -37% existed for the trowelled surfaces of II-RC-L(S), II-RC-L(B) and II-RC-M(S) mixtures, respectively. Hence, the trowelled surfaces led to 17% to 56% higher penetration depths than the casting face. The improved performance exhibited is due to the lower effective water/cement ratio, the slag blended cement and the pozzolanic activity of CDW.

The electrical resistivity results were within the range of values (10-100 Ω·m) commonly reported for conventional concrete. Whereas mixed recycled aggregates exhibited an electrical resistivity comparable to that of a conventional mixture, the recycled concrete made with ceramic aggregates displayed a 7% lower value as consequence of a higher release of ions to the pore solution. Nonetheless, both conventional and recycled concretes exhibited electrical resistivity values associated with a poor performance against the corrosion.

As previously mentioned, recycled aggregates are susceptible to a supplementary release of alkalis that may increase the ASR risk.

En la fase II, la pérdida de masa relativa aumentó hasta un 26% sin correlación con el contenido de cerámica pero con una mayor incidencia en las superficies de fratasado. Sin embargo, vale la pena comentar que el uso de aditivos mejoraría estos resultados.

Respecto a la penetración de cloruros, las profundidades de migración fueron más bajas para los hormigones reciclados, lo que conllevó a que el coeficiente de la migración no estacionario fuera un 37%, 25% y 43% menor en las superficies de moldeo de las muestras II-RC-L(S), II-RC-L(B) y II-RC-H(S), y variase hasta un 3%, -19% y -37% en las caras de frasatado de los hormigones II-RC-L(S), II-RC-L(B) y II-RC-H(S), respectivamente. Es por ello que las superficies de fratasado mostraron valores más altos que la cara de acabado, entre 17% y 56%. El buen comportamiento exhibido se debió a la baja relación agua/cemento efectiva, el cemento con escorias y la actividad puzolánica de los RCD.

Los resultados de resistividad eléctrica se encontraron dentro del rango de los hormigones convencionales (10-100 Ω·m). Mientras que los áridos reciclados mixtos exhibieron una resistividad eléctrica comparable a un hormigón convencional, el hormigón reciclado hecho con áridos cerámicos mostró un valor 7% inferior como consecuencia de una mayor liberación de iones. No obstante, los hormigones convencionales y reciclados presentaron valores de resistividad eléctrica asociados a un mal desempeño contra la corrosión.

Como se mencionó anteriormente, los áridos reciclados son susceptibles de liberar álcalis y pueden aumentar el riesgo de ASR.

However, none of the recycled aggregates used in this dissertation was found to be reactive since the length variation of the recycled concrete prisms in a 20-day Oberholster test was lower than 0.10%. Moreover, no cracks or deterioration of the aggregates was appreciated by visual inspection of the concrete cylinders after the testing. Nonetheless, it should be noted that these results occurred under the specific conditions favoured by the use of slag blended cements.

Finally, the resistance to organic acids was tested by a mix of lactic-acetic acid solution simulating the typical environment on floors of animal housing and silage structures. While the maximum reduction in radius was lower than 2 mm at the end of the test for the conventional concrete, none of the recycled mixtures presented a decline in radius higher than 1 mm. The monotonous degradation throughput 6 cycles ended with the recycled mixtures performing 46%, 63%, 69% and 87% better than the conventional concrete in terms of reduction in radius for rising ceramic contents incorporated in the total weight of aggregates. Analogously, the surface roughness at the end of the test was between 40% and 74% smoother for rising ceramic content in the aggregates. The improved performance of concrete against acidic attack was explained by the beneficial effect of pozzolanic materials, the presence of secondary elements in the cement matrix, the lower effective cement/ratio as well as the refinement in the porous network that use of recycled aggregates causes.

Sin embargo, ninguno de los áridos reciclados utilizados en esta tesis fue identificado como reactivo pues la variación de la longitud del prisma de hormigón reciclado en una prueba Oberholster durante 20 días fue inferior a 0,10%. Por otra parte, no se apreciaron grietas en la inspección visual de los cilindros de hormigón tras el ensayo. No obstante, cabe señalar que estos resultados se produjeron favorecidos por el uso de cementos con escorias.

Por último, la resistencia a los ácidos orgánicos fue probada mediante una mezcla de solución de ácido láctico-acético simulando las condiciones típicas de un alojamiento de animales y/o silo. Mientras que la reducción máxima en el radio fue inferior a 2 mm para el hormigón convencional, ninguno de los hormigones reciclados presentó una disminución superior a 1 mm. La degradación fue progresiva durante los 6 ciclos y terminó con un comportamiento un 46 %, 63%, 69% y 87% mejor para porcentajes cerámicos crecientes. Análogamente, la rugosidad superficial al final del ensayo resultó ser entre un 40% y 74% más suave a medida que aumentó el contenido de cerámica incorporado en el peso total de los áridos. La mejora del rendimiento del hormigón frente a los ataques ácidos se explica por el efecto beneficioso de los materiales puzolánicos, la presencia de elementos secundarios en la matriz de cemento, la relación agua/cemento efectiva más baja, así como el refinamiento de la red porosa causada por el uso de áridos reciclados.

1.7. ENVIRONMENTAL PERFORMANCE OF RECYCLED CONCRETE
DESEMPEÑO MEDIOAMBIENTAL DEL HORMIGÓN RECICLADO

The system boundaries of this case study were limited to a cradle to gate LCA, corresponding to the production of raw materials – i.e. extraction and processing of natural aggregate, processing of CDW into recycled aggregates, water exploitation and the production of cement - their transport to the concrete plant and the batching operations of the concrete plant.

For both the inventory and analysis, the Ecoinvent database and the SimaPro LCA software were used, although precise modifications were made to take into account specific aspects of the Spanish scenario. However, specific inventories were created for the recycled aggregates production including both the environmental burdens of the generation and management of CDW and the environmental credits achieved by the avoidance of landfilling operations and the extraction of natural resources.

In general terms, except the emission of particulates, which increases almost a 50% when recycled aggregates were employed due to the dust generation in the CDW management, an environmental improvement could be observed in the production of recycled concrete. The most appreciable benefit is the saving in water (33% on average) and the decrease on cumulative energy (8% on average). In terms of gas emissions, NO_x presents the higher reduction (10% on average) pointing to a reduction of fuel usage in the recycled concrete as a result of avoided impacts, and CO_2 emissions are the least affected (3%) since the principal responsible for this impact, i.e. cement production, remains constant for all concrete compositions.

Los límites del estudio ACV se establecieron en la cuna y la puerta del proceso, lo que corresponde a la producción de materias primas -es decir, extracción y procesamiento de áridos naturales, el procesado de RCD en áridos reciclados, la explotación del agua y la producción de cemento-, su transporte a la planta de hormigón y las operaciones de transformación.

Tanto para el inventario como para el análisis, se emplearon la base de datos Ecoinvent y el software SimaPro LCA, aunque se hicieron las modificaciones precisas para la situación española. Sin embargo, inventarios específicos fueron creados para la producción de áridos reciclados incluyendo las cargas ambientales de la generación y gestión de los RCD y los créditos ambientales alcanzados al evitar las operaciones de vertido y la extracción de recursos naturales.

En términos generales, salvo la emisión de partículas que aumentó casi un 50% cuando se utilizaron los áridos reciclados debido a la generación de polvo en el manejo de los RCD, la producción de hormigón reciclado supone una mejora medioambiental. El beneficio más notable es el ahorro en agua (33% de media) y la disminución en la energía acumulada (8% de media). En términos de emisiones, el NOx presenta la reducción más alta (10% de media) debido a la reducción en el consumo de combustible como resultado de los impactos evitados, y las emisiones de CO_2 son las menos afectadas (3%) ya que el principal responsable de su generación, es decir, la producción de cemento, se mantuvo constante para todas las composiciones de hormigón.

The main advantage of using recycled concrete made of secondary aggregates from CDW was found in the reduction of the ozone depletion potential and the abiotic resource depletion in the CML 2001 assessment and the decrease in the damage to mineral and fossil resources in the Eco-indicator 99 evaluation. Despite these advantages, when Eco-indicator 99 is employed, recycled concrete presented a worse environmental performance in terms of damage to the human health. Nonetheless, since the generation of particulates is the driver of this environmental shortcoming, some technical measures could be applied in order to prevent or reduce the emissions.

La principal ventaja de utilizar hormigón reciclado hecho de áridos secundarios de RCD se encuentra en la reducción del potencial de agotamiento de ozono y el agotamiento de los recursos abiótico de acuerdo a la evaluación CML 2001 y la disminución en el daño a los recursos minerales y fósiles según el Eco-indicador 99. A pesar de estas ventajas, cuando se emplea Eco-indicador 99, el hormigón reciclado presentó un peor comportamiento ambiental en términos de daños a la salud humana. Sin embargo, dado que la generación de partículas es el parámetro responsable de esta deficiencia, podrían aplicarse algunas medidas técnicas con el fin de prevenir o reducir las emisiones.

APPENDIX A.

EQUIVALENCE OF ENVIRONMENTAL EXPOSURE CLASSES

Although as a general rule Spanish standards are mostly a translation of the European standards, the entry into effect of the EHE-08 (Permanent Commission on Concrete, 2008) forced to amend some national norms in order to provide a common nomenclature system.

One of the modifications imposed by EHE-08 (Permanent Commission on Concrete, 2008) relates to the classification of the environmental exposure classes. Table A. 1 portrays de equivalences between the Spanish (Permanent Commission on Concrete, 2008; UNE EN 206-1, 2008) and European system (EN 206-1, 2005).

Spanish classification	European classification
I Non-aggressive environment	**X0** No risk of corrosion or attack
IIa Normal environment with high humidity subjected to corrosion of origin different form chlorides	**XC1** Corrosion induced by carbonation in a dry or permanently wet environment **XC2** Corrosion induced by carbonation in a wet, rarely dry, environment **XC4** Corrosion induced by carbonation in a cyclic wet and dry environment
IIb Normal environment with average humidity subjected to corrosion of origin different form chlorides	**XC3** Corrosion induced by carbonation in a moderate humidity environment
IIIa Areas exposed to airborne salt but not in direct contact with sea water subjected to corrosion by chlorides from the marine environment	**XS1** Corrosion induced by chlorides from sea water of elements exposed to airborne salt but not in direct contact with sea water
IIIb Permanently submerged elements subjected to corrosion by chlorides from the marine environment	**XS2** Corrosion induced by chlorides from sea water in permanently submerged elements
IIIc Tidal, splash and spray zones subjected to corrosion by chlorides by chlorides from the marine environment	**XS3** Corrosion induced by chlorides from sea water of elements in tidal, splash and spray zones
IV Elements subjected to corrosion by chlorides other than from the marine environment	**XD1** Corrosion induced by chlorides other than from sea water in moderate humidity environment **XD2** Corrosion induced by chlorides other than from sea water in a wet, rarely dry, environment **XD3** Corrosion induced by chlorides other than from sea water in a cyclic wet and dry environment

Table A. 1: Equivalence between Spanish and European environmental exposure classes

Spanish classification	European classification
H Elements subjected to frost without de-icing salts	**XF1** Freeze-thaw attack without de-icing agents in elements under moderate water saturation **XF3** Freeze-thaw attack without de-icing agents in elements under high water saturation
F Elements subjected to frost with de-icing salts	**XF2** Freeze-thaw attack with de-icing agents in elements under moderate water saturation **XF4** Freeze-thaw attack with de-icing agents or sea water in elements under moderate high saturation
Qa Elements in an environment with a weak aggressive chemical attack	**XA1** Chemical attack in a slightly aggressive chemical environment
Qb Elements in an environment with an average aggressive chemical attack	**XA2** Chemical attack in a moderately aggressive chemical environment
Qc Elements in an environment with a strong aggressive chemical attack	**XA3** Chemical attack in a highly aggressive chemical environment
E Elements subjected to an erosive environment (abrasion or cavitation)	

Table A. 1: Equivalence between Spanish and European environmental exposure classes (continued)

REFERENCES

EN 206-1, 2005. Concrete. Part 1: Specification, performance, production and conformity. CEN, Brussels.

Permanent Commission on Concrete, 2008. Code on Structural Concrete (EHE-08) [in Spanish]. Spanish Ministry of Public Works, Madrid.

UNE EN 206-1, 2008. Concrete. Part 1: Specification, performance, production and conformity [in Spanish]. AENOR, Madrid.

APPENDIX B.

SELECTED POWDER DIFFRACTION FILES (PDF)

As described in chapter 3, the mineralogical phase identification was based on the comparison of the powder diffraction pattern of each sample with the patterns indexed on the Powder Diffraction Files (PDF) of the International Centre for Diffraction Data (ICDD, 2015) via the search-match DiffracPlus Evaluation software. Table B. 1 collects all the selected PDF used for each sample of natural and recycled aggregates analysed.

	Compound Name	Formula	PDF card
Sand and gravel	Quartz	SiO_2	01-079-1910 (C)
RA-L(S) S1	Anorthite	$Ca(Al_2Si_2O_8)$	01-086-1705 (C)
	Calcite	$Ca(CO_3)$	01-086-2339 (C)
	Corundum	Al_2O_3	01-075-0783 (C)
	Cristobalite	α-SiO_2	00-003-0272 (D)
	Dolomite	$CaMg_{0.77}Fe_{0.23}(CO_3)_2$	01-084-2065 (C)
	Feldspar potassian	$K_{.5}Na_{.5}AlSi_3O_8$	01-084-0710 (C)
	Hematite	α -Fe_2O_3	00-006-0502 (D)
	Quartz	SiO_2	01-079-1910 (C)
RA-L(S) S2	Anorthite	$Ca(Al_2Si_2O_8)$	01-073-0265 (C)
	Calcite	$Ca(CO_3)$	01-086-2339 (C)
	Cristobalite	α-SiO_2	00-003-0272 (D)
	Dolomite	$CaMg(CO_3)_2$	01-079-1343 (C)
	Dolomite, ferroan	$Ca(Mg,Fe)(CO_3)_2$	00-034-0517 (D)
	Gypsum	$Ca(SO_4)(H_2O)_2$	01-074-1433 (C)
	Hematite	Fe_2O_3	01-087-1166 (C)
	Muscovite 2M1	$(K_{0.82}Na_{0.18})(Fe_{0.03}Al_{1.97})(AlSi_3)O_{10}(OH)_2$	01-080-0742 (C)
	Orthoclase	KSi_3AlO_8	01-071-1540 (C)
	Quartz	SiO_2	01-079-1910 (C)
RA-L(S) S3	Anorthite	$Ca(Al_2Si_2O_8)$	01-073-0265 (C)
	Calcite	$Ca(CO_3)$	01-086-2339 (C)
	Cristobalite	α-SiO_2	00-003-0272 (D)
	Dolomite, ferroan	Ca(Mg,Fe)(CO3)2	00-034-0517 (D)
	Muscovite 2M1	$(K_{0.82}Na_{0.18})(Fe_{0.03}Al_{1.97})(AlSi_3)O_{10}(OH)_2$	01-080-0742 (C)
	Orthoclase	KSi_3AlO_8	01-071-1540 (C)
	Quartz	SiO_2	01-079-1910 (C)
RA-L(S) S4	Anorthite	$Ca(Al_2Si_2O_8)$	01-073-0265 (C)
	Calcite	$Ca(CO_3)$	01-086-2339 (C)
	Cristobalite	α-SiO_2	00-003-0272 (D)
	Dolomite, ferroan	Ca(Mg,Fe)(CO3)2	00-034-0517 (D)
	Muscovite 2M1	$(K_{0.82}Na_{0.18})(Fe_{0.03}Al_{1.97})(AlSi_3)O_{10}(OH)_2$	01-080-0742 (C)
	Orthoclase	KSi_3AlO_8	00-031-0966 (*)
	Quartz	SiO_2	01-079-1910 (C)

Table B. 1: Selected PDF to match the XRD aggregates patterns

	Compound Name	Formula	PDF
RA-M(S) S1	Anorthite	$Ca(Al_2Si_2O_8)$	01-073-0265 (C)
	Calcite	$Ca(CO_3)$	01-086-2339 (C)
	Cristobalite	α-SiO_2	00-003-0272 (D)
	Dolomite, ferroan	$Ca(Mg,Fe)(CO_3)_2$	00-034-0517 (D)
	Gypsum	$Ca(SO_4)(H_2O)_2$	01-074-1433 (C)
	Muscovite 2M1	$(K_{0.82}Na_{0.18})(Fe_{0.03}Al_{1.97})(AlSi_3)O_{10}(OH)_2$	01-080-0742 (C)
	Orthoclase	$KAlSi_3O_8$	00-031-0966 (*)
	Quartz	SiO_2	01-079-1910 (C)
RA-M(S) S2	Anorthite	$Ca(Al_2Si_2O_8)$	01-073-0265 (C)
	Calcite	$Ca(CO_3)$	01-086-2339 (C)
	Dolomite	$CaMg(CO_3)_2$	01-079-1344 (C)
	Hematite	F_e2O_3	01-087-1166 (C)
	Muscovite - 2M	$KAl_2(AlSi_3O_{10})(OH)_2$	01-079-2363 (C)
	Quartz	SiO_2	01-079-1910 (C)
RA-H(S)	Anorthite	$(Ca_{.94}Na_{.06})(Al_{1.94}Si_{2.06}O_8)$	01-084-0751 (C)
	Calcite	$CaCO_3$	00-047-1743 (C)
	Dolomite	$CaMg(CO3)_2$	01-079-1344 (C)
	Hematite	Fe_2O_3	00-002-0919 (D)
	Illite	$(Na,K)_{1-}x(Al,Mg,Fe)_2(Si,Al)_4O_{10}(OH)_2$	00-025-0001 (D)
	Orthoclase	$K_{.59}Ba_{.19}Na_{.22}(Al_{1.18}Si_{2.82}O_8)$	01-083-1324 (C)
	Quartz	SiO_2	01-079-1910 (C)

Table B. 1: Selected PDF to match the XRD aggregates patterns (continued)

REFERENCES

ICDD, 2015. International Centre for Diffraction Data [http://www.icdd.com/].

APPENDIX C.

BOX AND WHISKER PLOT

Throughout this thesis, box and whisker pots, created using Sigmaplot software (Systat Software, Inc, 2013), have been used as a means to statistically describe sets of data from the literature review. Figure C. 1 illustrates the meaning of the different common elements in this type of representations. The box plot indicates the values of the first and third quartile by means of its lower and upper boundaries respectively. In addition, the line within the box represents the median of the group of data. The whiskers, which extend as a delimited line from the top and bottom of the box plot, indicate the 10^{th} and 90^{th} percentiles. Finally, the outlying points are displayed as solid black points.

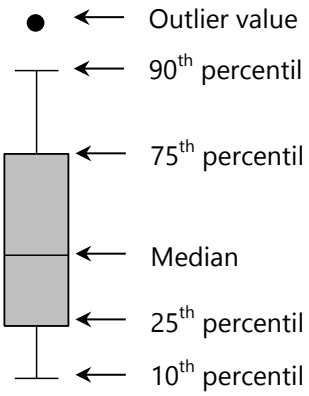

Figure C. 1: Box and whisker plot

REFERENCES

Systat Software, Inc, 2013. SigmaPlot. California, USA.




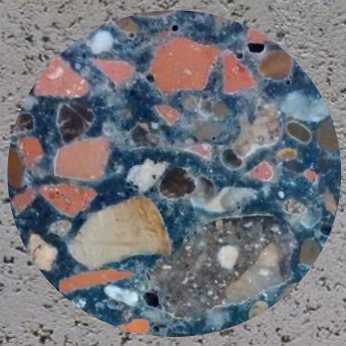


Doctorado en Ingeniería de Biosistemas
Escuela Superior y Técnica de Ingeniería Agraria
Departamento de Ingeniería y Ciencias Agrarias
Universidad de León

Doctoral Programme in Civil Engineering
Magnel Laboratory for Concrete Research
Department of Structural Engineering
Faculty of Engineering & Architecture
Ghent University